

Kasper Berg Skreien

# Comparison of different mixing methods in field and laboratory stabilized clay

Master's thesis in Civil and Environmental Engineering

Supervisor: Priscilla Paniagua, NTNU/NGI

Co-supervisor: Sølve Hov, NGI

June 2023



Kasper Berg Skreien

# **Comparison of different mixing methods in field and laboratory stabilized clay**

Master's thesis in Civil and Environmental Engineering  
Supervisor: Priscilla Paniagua, NTNU/NGI  
Co-supervisor: Sølve Hov, NGI  
June 2023

Norwegian University of Science and Technology  
Faculty of Engineering  
Department of Civil and Environmental Engineering





# Preface

This master's thesis was written in the spring semester of 2023 as a concluding part in my MSc in Civil and Environmental Engineering at the Norwegian University of Science and Technology (NTNU). The work is a continuation of my project thesis, written in the autumn semester of 2022, which was a literature review comparing deep mixing methods used in soil stabilization.

The aim of the master's thesis is to understand how strength, deformation properties and homogeneity of stabilized soil varies when using different mixing methods, both in the field and in the laboratory. The thesis is written in cooperation with the Norwegian Geotechnical Institute (NGI) as a supplement to their ongoing research on sustainable soil stabilization.

I want to thank my supervisors, Priscilla Paniagua and Sølve Hov, for giving great support and assistance throughout the semester. A special thanks is also given to PhD candidates Daniyal Younas and Mukul Jaiswal at the Department of Physics, NTNU for their help with  $\mu$ CT-analysis of the field samples. Finally, I want to thank Lee Thomas Champe and Espen Andersen for their assistance in the geotechnical laboratory.

Trondheim, 07.06.2023

A handwritten signature in black ink that reads "Kasper Berg Skreien". The signature is written in a cursive, flowing style.

Kasper Berg Skreien

# Abstract

Soil stabilization by deep mixing is a common way of improving soil properties while at the same time avoiding invasive excavation and filling. A machine with an attached drill-shaft stabilizes the soil by simultaneous mixing and binder injection. Binders can either be made from single components or be blends of different components. Cement and lime are the most frequently used binders today, even though their production emits large amounts of greenhouse gases. In recent years, deep mixing has gained in popularity, resulting in a greater focus on making the established procedures more sustainable. Alternative binders and methods are continuously being tested and implemented to optimize every aspect of the design and installation process.

In this thesis on deep stabilization, field samples from projects utilizing the wet deep mixing method (WDM) and the modified dry mixing method (MDM) were investigated. The aim was to assess the homogeneity and porosity of the samples by micro computed tomography ( $\mu$ CT-analysis). Further, a separate study of samples prepared in the laboratory aims to compare the wet and dry mixing method to find the optimal binder composition in sensitive clay. Samples with water to binder ratios (wbr) of 8 and 16 were prepared using cement (CEM I), ground granulated blast-furnace slag (GGBS), and paper sludge ash (PSA) as binders. After 28 days of curing, results from p-wave velocity and unconfined compression testing (UCT) were modelled as 3D response surfaces to efficiently evaluate performance and possible binder interaction. Additional laboratory samples were created using the MDM method adapted for the laboratory and the wet mixing method to study the effects of preparing identical samples with different methods.

The studied literature shows that the performance and homogeneity of field stabilized clay is largely influenced by the amount of mixing during installation. In the laboratory on the other hand, the quality is most influenced by the sample molding procedure. All of the tested samples were in this study molded with the rodding technique to examine the effects of altering the mixing method and binder composition. Other factors like curing temperature and curing stress were not varied to be able to compare the different binder compositions and mixing methods.

The field results showed that a very uniform texture with little to no entrapped air in the soil-binder mixture can be achieved with the WDM method. Porous areas were limited to brittle sections of unstabilized soil. In contrast, the MDM samples were less uniform, with a coarse texture, visible binder accumulation and a more even distribution of small pores and cracks.

The laboratory results showed that sample strength and deformation properties were affected by the mixing method. At a wbr of 8, wet mixing produces more consistent samples with less scatter between identical samples than the dry method. This results in response surface models with lower standard deviations and better prediction properties. When increasing the wbr to 16, findings are flipped, and the dry method is superior. To maximize strength and stiffness at 28 days of curing, an optimal binder composition of around 55 to 65 % CEM I and 35 to 45 % GGBS should be used regardless of mixing method and wbr. P-wave testing with the PUNDIT equipment is not currently suited for stabilized soils due to scatter and correlation inconsistencies. Finally, it was found that the wet mixing method and MDM method were not interchangeable when preparing samples in the laboratory.

# Sammendrag

Grunnforsterkning ved dypstabilisering er en vanlig måte å forbedre jordegenskaper samtidig som man unngår unødvendig grave- og fyllarbeid. En maskin med boretårn stabiliserer jorda ved å injisere et bindemiddel gjennom et roterende mikseverktøy. Bindemidler kan være enkeltkomponenter eller bestå av blandinger av forskjellige komponenter. Sement og kalk er de mest brukte bindemidlene i dag, selv om produksjonen slipper ut store mengder klimagasser. De siste årene har denne typen grunnforsterkning økt i popularitet, noe som har resultert i et større fokus på å gjøre eksisterende prosedyrer mer bærekraftige. Nye og alternative bindemidler og metoder blir kontinuerlig testet og implementert for å optimalisere alle aspekter av design- og installasjonsprosessen.

I denne oppgaven om dypstabilisering undersøkes feltprøver fra prosjekter som benytter installering med våt metode (WDM) og modifisert tørr metode (MDM). Målet er å vurdere homogeniteten og porøsiteten til prøvene ved hjelp av mikrocomputertomografi ( $\mu$ CT-analyse). En separat studie av laboratorieprøver har som mål å sammenligne en våt og tørr innblandingsmetode for å finne den optimale sammensetningen av bindemiddel i sensitiv leire. Prøver med vann-til-bindemiddel-forhold (wbr) på henholdsvis 8 og 16 ble blandet ved bruk av sement (CEM I), slagg (GGBS) og papiraske (PSA) som bindemiddel. Etter 28 dagers herding ble p-bølgehastighet og resultater fra en-aksial trykktesting (UCT) modellert som 3D-responsflater for å effektivt kunne evaluere ytelse og mulig bindemiddelinteraksjon. Ytterligere laboratorieprøver ble laget ved bruk av MDM-metoden tilpasset laboratoriet og våt innblandingsmetode for å studere effekten av å tilberede identiske prøver med ulike metoder.

Litteraturen viser at ytelsen og homogeniteten til feltstabilisert leire er i stor grad påvirket av blandingsarbeidet under installasjonen. I laboratoriet derimot, er kvaliteten mest påvirket av prepareringsmetoden brukt når prøvene tilvirkes. Her ble alle prøver tilvirket med metoden «rodding» for å isolere og undersøke effekten av å endre blandemetoden og sammensetningen av bindemidler. Andre faktorer som herdetemperatur og herdetrykk ble ikke justert mellom prøvene, selv om de også spiller en rolle i styrkeutviklingen.

Feltresultatene viste at WDM metoden gav en jevn tekstur med lite eller ingen porer i jorden som er stabilisert. Porøse områder var begrenset til skjøre biter av ustabilisert jord. MDM-prøvene var mer ujevne, med grovere tekstur, synlige spor av bindemiddel og jevnere fordeling av mindre porer og sprekker.

Laboratorieresultatene viste at prøvenes styrke- og deformasjonsegenskaper ble påvirket av blandingsmetoden. Ved en wbr på 8 gir våt metode mer konsistente prøver med mindre variasjon mellom identiske prøver enn den tørre metoden. Dette resulterer i responsflatemodeller med lavere standardavvik og bedre forutseende egenskaper. Om wbr økes til 16 gir tørr metode best egenskaper. For å maksimere styrke og stivhet ved 28 dagers herding, er den optimale sammensetningen av bindemiddel ca. 55 til 65 % CEM I og 35 til 45 % GGBS. Denne sammensetningen er uavhengig av blandemetode og wbr. Spredning i resultater og korrelasjonsproblemer gjør at PUNDIT-utstyret ikke er for øyeblikket egnet for måling av p-bølgehastighet i stabilisert jord. Til slutt ble det funnet at våt metode og MDM-metoden ikke gir prøver med tilsvarende egenskaper i laboratoriet.

# Contents

|  |           |
|--|-----------|
| Preface .....  | i         |
| Abstract.....  | ii        |
| Sammendrag.....                                      | iii       |
| List of Figures.....                                 | vii       |
| List of Tables .....                                 | x         |
| Acronyms and symbols .....                           | xii       |
| <b>1   Introduction.....</b>                         | <b>1</b>  |
| 1.1. Background.....                                 | 1         |
| 1.2. Objectives.....                                 | 2         |
| 1.3. Approach .....                                  | 2         |
| 1.4. Limitations .....                               | 3         |
| 1.5. Outline .....                                   | 3         |
| <b>2   Theory.....</b>                               | <b>5</b>  |
| 2.1 Deep stabilization .....                         | 5         |
| 2.1.1. Dry deep mixing (DDM).....                    | 5         |
| 2.1.2. Modified dry mixing (MDM).....                | 8         |
| 2.1.3. Wet deep mixing (WDM) .....                   | 10        |
| 2.1.4. Quality, cost, and sustainability.....        | 12        |
| 2.2 Binders.....                                     | 16        |
| 2.2.1. Cement.....                                   | 16        |
| 2.2.2. Fly ash (FA) and Paper sludge ash (PSA) ..... | 17        |
| 2.2.3. Slag (GGBS) .....                             | 18        |
| 2.2.4. Water to binder ratio (wbr).....              | 18        |
| 2.2.5. Reactions .....                               | 20        |
| 2.2.6. Blended binder interactions .....             | 21        |
| 2.3 Curing and sample preparation .....              | 23        |
| 2.3.1. Field curing.....                             | 23        |
| 2.3.2. Laboratory molding technique .....            | 27        |
| 2.3.3. Laboratory curing .....                       | 28        |
| <b>3   Method.....</b>                               | <b>30</b> |
| 3.1 Field samples .....                              | 30        |
| 3.1.1. Background information .....                  | 30        |
| 3.1.2. Field sampling and preparation .....          | 36        |
| 3.2 Laboratory samples.....                          | 39        |



|            |  |            |
|------------|--|------------|
| 3.2.1.     | Clay.....  | 39         |
| 3.2.2.     | Binders .....  | 44         |
| 3.2.3.     | Sample preparation .....                                       | 46         |
| 3.2.4.     | Laboratory molding technique .....                             | 53         |
| 3.3        | Test procedures.....   | 56         |
| 3.3.1.     | Visual inspection .....  | 56         |
| 3.3.2.     | Water content, corrected wbr, density, and entrapped air ..... | 56         |
| 3.3.3.     | P-wave measurements .....                                      | 57         |
| 3.3.4.     | Unconfined compression test (UCT) .....                        | 59         |
| 3.3.5.     | CT-analysis.....   | 61         |
| 3.4        | Data analysis .....  | 63         |
| 3.4.1.     | Response surface methodology (RSM).....                        | 63         |
| 3.4.2.     | Mixture design .....   | 64         |
| 3.4.3.     | Augmented simplex lattice.....                                 | 65         |
| 3.5        | Modeling software.....   | 67         |
| 3.5.1.     | Configuration .....  | 67         |
| 3.5.2.     | Model.....   | 67         |
| 3.5.3.     | Analysis of variance (ANOVA) and diagnostics.....              | 72         |
| <b>4  </b> | <b>Results .....</b>   | <b>75</b>  |
| 4.1        | Field samples .....  | 75         |
| 4.1.1.     | Visual inspection and sample quality .....                     | 75         |
| 4.1.2.     | Water content .....  | 75         |
| 4.1.3.     | P-wave velocity .....  | 76         |
| 4.1.4.     | CT-analysis.....   | 77         |
| 4.2        | Laboratory samples.....  | 83         |
| 4.2.1.     | Visual inspection and sample quality .....                     | 83         |
| 4.2.2.     | Water content, entrapped air and corrected wbr.....            | 84         |
| 4.2.3.     | Strength, stiffness and strain .....                           | 86         |
| 4.2.4.     | P-wave velocity .....  | 88         |
| 4.3        | Mixture design.....  | 88         |
| 4.3.1.     | Correlation, model and analysis of variance (ANOVA).....       | 89         |
| 4.3.2.     | Strength.....  | 99         |
| 4.3.3.     | Stiffness.....   | 102        |
| 4.3.4.     | Strain .....   | 104        |
| 4.3.5.     | P-wave velocity .....  | 106        |
| <b>5  </b> | <b>Discussion .....</b>  | <b>109</b> |
| 5.1        | Effect of binder composition on laboratory samples .....       | 109        |

|            |  |            |
|------------|--|------------|
| 5.1.1.     | Fracture patterns and sample quality .....   | 109        |
| 5.1.2.     | Strength.....  | 110        |
| 5.1.3.     | Stiffness.....   | 112        |
| 5.1.4.     | Strain at failure .....  | 113        |
| 5.1.5.     | P-wave velocity .....  | 114        |
| 5.2        | Homogeneity.....   | 114        |
| 5.2.1.     | Field samples .....  | 114        |
| 5.2.2.     | Laboratory samples .....   | 116        |
| 5.3        | Comparing mixing methods.....  | 116        |
| 5.3.1.     | Field samples .....  | 116        |
| 5.3.2.     | Laboratory samples .....   | 118        |
| 5.3.3.     | Single wet mixing method evaluation .....  | 119        |
| <b>6  </b> | <b>Conclusions and further work .....</b>  | <b>121</b> |
| 6.1        | Conclusions.....   | 121        |
| 6.1.1.     | Field study.....   | 121        |
| 6.1.2.     | Laboratory study .....   | 121        |
| 6.2        | Further work .....   | 122        |
| 6.2.1.     | Field .....  | 122        |
| 6.2.2.     | Laboratory.....  | 122        |
| <b>7  </b> | <b>Bibliography.....</b>   | <b>124</b> |
| <b>A  </b> | <b>FIELD DATA.....</b>   | <b>128</b> |
| A.1        | SAMPLE IMAGES .....  | 128        |
| A.2        | CT RESULTS.....  | 138        |
| <b>B  </b> | <b>LABORATORY DATA.....</b>  | <b>148</b> |
| B.1        | SAMPLE IMAGES AND UNCONFINED COMPRESSION TEST RESULTS .....                                    | 148        |
| B.2        | SAMPLE IMAGES AND UNCONFINED COMPRESSION TEST RESULTS FOR SINGLE MIXING METHOD EVALUATION..... | 189        |
| B.3        | LABORATORY RESULT OVERVIEW .....   | 194        |
| B.3.1.     | WATER CONTENT, ENTRAPPED AIR AND CORRECTED WBR.....  | 194        |
| B.3.2.     | STRENGTH, STIFFNESS AND STRAIN .....   | 199        |
| B.3.3.     | P-WAVE VELOCITY .....  | 204        |
| B.4        | DESIGN EXPERT RESULTS .....  | 207        |
| B.4.1.     | DRY AND WET MIXING METHOD WITH WBR=8 .....   | 207        |
| B.4.2.     | DRY AND WET MIXING METHOD WITH WBR=16 .....  | 233        |

# List of Figures

|  |    |
|--|----|
| Figure 1: DDM equipment and procedure.....   | 6  |
| Figure 2: Shape characteristics of deep mixing tools. Modified after (NGF, 2012). .....  | 7  |
| Figure 3: MDM equipment and procedure. ....  | 9  |
| Figure 4: WDM equipment and procedure. ....  | 11 |
| Figure 5: Flexural strength vs p-wave velocity for cementitious stabilized materials (Mandal et al., 2016). ....   | 14 |
| Figure 6: P-wave velocity of samples stabilized with decreased water to binder ratio (left) and increased water to binder ratio (right). Sample 1-6 has a cement/slag ratio of 70/30, sample 7-12 has 50/50 and sample 13-18 has 30/70 respectively (Lindh & Lemenkova, 2022)..... | 15 |
| Figure 7: Volumetric composition of cement paste at different water to cement ratios (Jacobsen et al., 2022). ....   | 19 |
| Figure 8: Water to binder ratio (wbr) vs shear strength ( $\tau_{max}$ ) for both wet (WM) and dry (NGF, NGF CE and NGF LT) mixing methods (Hov et al., 2022). ....  | 19 |
| Figure 9: UCS for silty clay till stabilized with cement, lime, and slag. Samples were vibrator-compacted and cured at 20 °C for 28 and 90 days. Modified after (Lindh, 2004). ....  | 22 |
| Figure 10: Interactions between GGBS, FGDG and CCS after 28 days of curing at 20 °C. Modified after (Wang et al., 2023). ....  | 22 |
| Figure 11: Stiffness at 50 % strength vs percent of binder. Modified after (Pakbaz & Farzi, 2015).....   | 23 |
| Figure 12: Common deep stabilization patterns. Modified after (NGF, 2012). ....  | 24 |
| Figure 13: Temperature development (°C) vs time (Days) in stabilized clay using different lime (kalk) and cement binders and patterns. Temperature is measured both inside and outside the finished columns (Åhnberg et al., 1995). ....   | 25 |
| Figure 14: Unconfined compressive strength (kPa) vs curing temperature (°C) at five different curing times (1 day to 28 days) (Enami et al., 1985, as cited in Kitazume & Terashi, 2013). ....   | 25 |
| Figure 15: Unconfined compressive strength increase (kPa) vs time (days) in two Swedish clays using (combinations of) cement (c), slag (s), lime (l) and fly ash (f). Modified after (Åhnberg, 2006).....  | 26 |
| Figure 16: Shear strength ( $\tau_{max}$ ) vs axial strain ( $\epsilon$ ) relation from samples cured at 0 kPa, 200 kPa and 400 kPa. Triaxial radial pressure set to 0 kPa. Modified after (Engeset, 2018). ....   | 27 |
| Figure 17: Typical concrete cylinder sample fracture pattern (Jacobsen et al., 2022). ...  | 28 |
| Figure 18: Processed $\mu$ CT images showing macro-porosity in field and laboratory mixed samples with a binder content of 50kg/m <sup>3</sup> . Modified after (Paniagua et al., 2022b).....  | 29 |
| Figure 19: Site overview showing geographical locations of where every sample and material was gathered (NVE, n.d.). ....  | 30 |
| Figure 20: Aerial photo of the area surrounding the Östrand WDM sampling site (Eniro, n.d.). ....  | 31 |
| Figure 21: Quaternary geology map of the area surrounding the Östrand WDM sampling site. Previous land reclamation is shown as a grey shaded area (SGU, n.d.).....   | 32 |
| Figure 22: Aerial photo of the area surrounding the Hjorthagen WDM sampling site. The yellow dotted line shows the recently developed area (Eniro, n.d.). ....   | 33 |
| Figure 23: Quaternary geology map of the area surrounding the Hjorthagen WDM sampling site. Previous land reclamation is shown as a grey shaded area (SGU, n.d.).....  | 34 |

|  |    |
|--|----|
| Figure 24: Aerial photo of the area surrounding the E6 Kvithammar-Åsen MDM sampling site. The yellow dotted line shows the approximate position of the updated highway (Kartverket, n.d.). | 35 |
| Figure 25: Quaternary geology map of the area surrounding the E6 Kvithammar-Åsen MDM sampling site. The grey shaded area is above the marine limit (NGU, n.d.).                            | 36 |
| Figure 26: Collecting MDM samples using an excavator.  | 37 |
| Figure 27: MDM sample before and after trimming.   | 37 |
| Figure 28: WDM sample before and after trimming.   | 38 |
| Figure 29: Aerial photo of the area surrounding the Tiller-Flotten research site (Kartverket, n.d.).   | 40 |
| Figure 30: Quaternary geology map of the Tiller-Flotten research site. The grey shaded area is above the marine limit (NGU, n.d.).   | 41 |
| Figure 31: Graphs of pore pressure measurements vs depth (left) and preconsolidation stress vs depth from 1D oedometer testing (right) (L'Heureux et al., 2019).                           | 42 |
| Figure 32: Chosen augmented simplex lattice design.  | 46 |
| Figure 33: Overview of lattice points and corresponding binder composition.  | 47 |
| Figure 34: Kitchen stand mixer (left) and k-type mixing tool (right) used to prepare batches of stabilized soil.   | 53 |
| Figure 35: Rodding technique equipment and setup.  | 54 |
| Figure 36: Laboratory batch sealed for curing.   | 55 |
| Figure 37: Hydraulic extrusion equipment for cylinder samples.   | 55 |
| Figure 38: PUNDIT PL-2 transmission methods.   | 57 |
| Figure 39: PUNDIT PL-2 p-wave equipment setup for calibrating (left) and testing cured samples (right).  | 58 |
| Figure 40: Pulse Velocity mode screen for testing p-wave velocity.   | 58 |
| Figure 41: Unconfined compression test equipment setup.  | 59 |
| Figure 42: Cylinder sample before (left) and after (right) UCT.  | 60 |
| Figure 43: Parameter determination from an axial strain ( $\epsilon$ ) vs axial stress ( $\sigma_1$ ) diagram.   | 61 |
| Figure 44: Principal sketch of a lab-based $\mu$ CT setup with a conical beam (Cnudde & Boone, 2013).  | 61 |
| Figure 45: X-ray source and rotating field sample (left). Nikon XT H 225 ST instrument (Right).  | 62 |
| Figure 46: Example of a response surface (left) and a contour plot (right). The strength is the response of the experiment, while depth and temperature are influential factors.           | 64 |
| Figure 47: Pure blend points on a standard box-type factorial design (Montgomery, 2013).   | 65 |
| Figure 48: Standard simplex lattice design with three components (Lindh, 2004).  | 66 |
| Figure 49: Trilinear coordinate system (Montgomery, 2013).   | 66 |
| Figure 50: Response information set in Design Expert.  | 67 |
| Figure 51: Mixture component information and constraints set in Design Expert.   | 67 |
| Figure 52: Deciding component interactions under model evaluation in Design Expert.  | 68 |
| Figure 53: Response surfaces from a single data set using the linear, modified (Only AB interaction), quadratic and special cubic models.  | 69 |
| Figure 54: FDS graph example in Design Expert.   | 70 |
| Figure 55: Data transformation options in Design Expert.   | 71 |
| Figure 56: Final model configuration window in Design expert with interaction settings.  | 71 |
| Figure 57: Model ANOVA summary window in Design Expert.  | 72 |
| Figure 58: Model fit statistics window in Design Expert.   | 73 |
| Figure 59: Model equation window in Design Expert.   | 73 |

|   |     |
|---|-----|
| Figure 60: Visible surface cracking in the upper section of the WDM.Hjorthagen.3 sample.<br>.....   | 75  |
| Figure 61: Sample water content after $\mu$ CT testing. ....  | 76  |
| Figure 62: Field sample p-wave velocity test results. ....  | 77  |
| Figure 63: Estimation of macro porosity along the z-axis (longitudinal direction) in the<br>Östrand samples (WDM). ....   | 78  |
| Figure 64: Estimation of macro porosity along the z-axis (longitudinal direction) in the<br>Hjorthagen samples (WDM). ....  | 79  |
| Figure 65: Estimation of macro porosity along the z-axis (longitudinal direction) in the E6<br>samples (MDM). ....  | 80  |
| Figure 66: 2D $\mu$ CT image (left) vs physical sample image (right) showing a small piece of<br>gravel as an inclusion in the WDM.Östrand.2 sample at slice 1072. ....                 | 82  |
| Figure 67: 2D $\mu$ CT image (left) vs physical sample image (right) showing seashell inclusions<br>in the WDM.Hjorthagen.1 sample at slice 1280. ....                                  | 82  |
| Figure 68: Sample weight deviation after curing. ....   | 83  |
| Figure 69: Binder accumulation in a dry mixed sample. ....  | 84  |
| Figure 70: Combination of a cone and longitudinal fracture pattern. ....  | 86  |
| Figure 71: Hourglass shaped fracture patterns. ....   | 87  |
| Figure 72: Mainly longitudinal fracture patterns. ....  | 87  |
| Figure 73: Chosen augmented simplex lattice design. ....  | 88  |
| Figure 74: Overview of lattice points and corresponding binder content. ....  | 89  |
| Figure 75: Contour plot and response surface model comparison. Ultimate compressive<br>strength for samples prepared with dry- (left) and wet mixing (right) with a wbr of 8. ..        | 99  |
| Figure 76: Contour plot and response surface model comparison. Ultimate compressive<br>strength for samples prepared with dry- (left) and wet mixing (right) with a wbr of 16.<br>..... | 100 |
| Figure 77: Contour plot and response surface model comparison. Undrained shear strength<br>for samples prepared with dry- (left) and wet mixing (right) with a wbr of 8. ....           | 101 |
| Figure 78: Contour plot and response surface model comparison. Undrained shear strength<br>for samples prepared with dry- (left) and wet mixing (right) with a wbr of 8. ....           | 102 |
| Figure 79: Contour plot and response surface model comparison. Estimated stiffness for<br>samples prepared with dry- (left) and wet mixing (right) with a wbr of 8. ....                | 103 |
| Figure 80: Contour plot and response surface model comparison. Estimated stiffness for<br>samples prepared with dry- (left) and wet mixing (right) with a wbr of 16. ....               | 104 |
| Figure 81: Contour plot and response surface model comparison. Failure strain for samples<br>prepared with dry- (left) and wet mixing (right) with a wbr of 8. ....                     | 105 |
| Figure 82: Contour plot and response surface model comparison. Failure strain for samples<br>prepared with dry- (left) and wet mixing (right) with a wbr of 16. ....                    | 106 |
| Figure 83: Contour plot and response surface model comparison. P-wave velocity for<br>samples prepared with dry- (left) and wet mixing (right) with a wbr of 8. ....                    | 107 |
| Figure 84: Contour plot and response surface model comparison. P-wave velocity for<br>samples prepared with dry- (left) and wet mixing (right) with a wbr of 16. ....                   | 108 |
| Figure 85: P-wave velocity vs ultimate compressive strength. ....   | 111 |
| Figure 86: Estimated stiffness vs ultimate compressive strength. ....   | 112 |

# List of Tables

|  |    |
|--|----|
| Table 1: DDM equipment specifications and common applications. Modified after (Skreien, 2022).....                                 | 8  |
| Table 2: MDM equipment specifications and common applications. Modified after (Skreien, 2022).....                                 | 10 |
| Table 3: WDM equipment specifications and common applications. Modified after (Skreien, 2022).....                                 | 12 |
| Table 4: Estimated deep mixing cost overview for 2022 from NGI experience (Skreien, 2022).....                                     | 15 |
| Table 5: Emissions from commonly used binders (Skreien, 2022). .....   | 16 |
| Table 6: Major clinker phases and typical composition in Portland clinker (Jacobsen et al., 2022).....                             | 17 |
| Table 7: Chemical notations of major components in slag and fly ash (Jacobsen et al., 2022).....                                   | 18 |
| Table 8: Binder reaction types and common timeframe of main strength increase (Janz & Johansson, 2002). .....                      | 21 |
| Table 9: Overview of installation parameters in the WDM projects. Data provided by NGI. ....                                       | 34 |
| Table 10: Overview of installation parameters in the MDM project. Data provided by NGI. ....                                       | 36 |
| Table 11: Trimmed field sample overview. ....  | 39 |
| Table 12: Approximate parameters for Tiller-Flotten quick clay at depths between 7.5 and 20 meters (L'Heureux et al., 2019). ..... | 43 |
| Table 13: Major elements in Tiller-Flotten quick clay from XRF analysis. ....  | 43 |
| Table 14: Overview of Tiller-Flotten quick clay collected for laboratory testing.....  | 44 |
| Table 15: Major elements from XRF analysis for NORCEM CEM I 52.5 R, Norske Skog Skogn PSA and Slagg Bremen GGBS.....               | 45 |
| Table 16: Batch mixing factors overview. ....  | 47 |
| Table 17: Overview of laboratory samples prepared with the dry mixing method and a water to binder ratio of 8.....                 | 49 |
| Table 18: Overview of laboratory samples prepared with the dry mixing method and a water to binder ratio of 16. ....               | 50 |
| Table 19: Overview of laboratory samples prepared with the wet mixing method and a water to binder ratio of 8.....                 | 51 |
| Table 20: Overview of laboratory samples prepared with the wet mixing method and a water to binder ratio of 16. ....               | 52 |
| Table 21: PUNDIT transducer specifications and test object limitations (Proceq SA, 2017). ....                                     | 57 |
| Table 22: Settings for the $\mu$ CT scans. ....  | 62 |
| Table 23: Issues with factorial designs for mixtures. ....   | 65 |
| Table 24: Interpretation of Pearson's $r$ (Zou et al., 2003). ....   | 70 |
| Table 25: Combinations of automatic model selections and criterions (Stat-Ease, 2020). ....  | 72 |
| Table 26: Overview of the main statistical evaluations in the ANOVA.....   | 73 |
| Table 27: Diagnostic plot evaluation (Stat-Ease, 2020). ....   | 74 |
| Table 28: Sample cutting information. ....   | 81 |
| Table 29: Assumed clay water content overview.....   | 85 |
| Table 30: Samples and values not included in response surface modelling. ....  | 90 |

|  |     |
|--|-----|
| Table 31: Correlation matrix for samples prepared with the dry mixing method and wbr of 8. ....                                | 91  |
| Table 32: Model information and ANOVA results for samples prepared with the dry mixing method and wbr of 8.....                | 92  |
| Table 33: Correlation matrix for samples prepared with the dry mixing method and wbr of 16. ....                               | 93  |
| Table 34: Model information and ANOVA results for samples prepared with the dry mixing method and wbr of 16.....               | 94  |
| Table 35: Correlation matrix for samples prepared with the wet mixing method and wbr of 8. ....                                | 95  |
| Table 36: Model information and ANOVA results for samples prepared with the wet mixing method and wbr of 8.....                | 96  |
| Table 37: Correlation matrix for samples prepared with the wet mixing method and wbr of 16. ....                               | 97  |
| Table 38: Model information and ANOVA results for samples prepared with the wet mixing method and wbr of 16.....               | 98  |
| Table 39: Summary of the field installation parameters. ....   | 116 |
| Table 40: Summary of the field sample results.....   | 117 |
| Table 41: Summary of mixing method findings.....   | 118 |
| Table 42: Average results for single wet mixing method evaluation.....   | 119 |
| Table 43: Corrected wbr, entrapped air and water content for samples prepared with the dry mixing method and a wbr of 8. ....  | 195 |
| Table 44: Corrected wbr, entrapped air and water content for samples prepared with the dry mixing method and a wbr of 16. .... | 196 |
| Table 45: Corrected wbr, entrapped air and water content for samples prepared with the wet mixing method and a wbr of 8.....   | 197 |
| Table 46: Corrected wbr, entrapped air and water content for samples prepared with the wet mixing method and a wbr of 16.....  | 198 |
| Table 47: UCT results for samples prepared with the dry mixing method and a wbr of 8. ....                                     | 200 |
| Table 48: UCT results for samples prepared with the dry mixing method and a wbr of 16. ....                                    | 201 |
| Table 49: UCT results for samples prepared with the wet mixing method and a wbr of 8. ....                                     | 202 |
| Table 50: UCT results for samples prepared with the wet mixing method and a wbr of 16. ....                                    | 203 |
| Table 51: P-wave test results for samples prepared with the dry mixing method. ....  | 205 |
| Table 52: P-wave test results for samples prepared with the wet mixing method. ....  | 206 |

# Acronyms and symbols

|        |  |
|--------|--|
| μCT    | Micro Computed Tomography  |
| AICc   | Akaike Information Criterion corrected for a small design                |
| BIC    | Bayesian Information Criterion   |
| BBD    | Box-Behnken Design   |
| CCS    | Calcium Carbide Slag   |
| CKD    | Cement Kiln Dust   |
| CDM    | Dement deep mixing   |
| DDM    | Dry deep mixing  |
| DJM    | Deep jet mixing  |
| DoE    | Design of Experiments  |
| EPD    | Environmental Product Declaration  |
| FA     | Fly Ash  |
| FGDG   | Flue Gas Desulfurization Gypsum  |
| FFR    | Free-Free Resonant   |
| FDS    | Fraction of Design Space   |
| GGBS   | Ground Granulated Blast-furnace Slag                                     |
| LKD    | Lime Kiln Dust   |
| LOI    | Loss On Ignition   |
| MDM    | Modified dry mixing  |
| NGI    | Norges Geotekniske Institutt (English: Norwegian Geotechnical Institute) |
| NTNU   | Norwegian University of Science and Technology                           |
| OCR    | Overconsolidation ratio  |
| PSA    | Paper Sludge Ash   |
| PUNDIT | Portable Ultrasonic Non-destructive Digital Indicating Tester            |
| RPMS   | Raw Paper Material Sludge  |
| RSM    | Response Surface Methodology   |
| SGI    | Statens Geotekniska Institut (English: Swedish Geotechnical Institute)   |
| UCS    | Unconfined Compressive Strength  |
| UCT    | Unconfined Compression Test  |
| wbr    | Water to binder ratio  |



|                |   |
|----------------|---|
| WDM            | Wet deep mixing                                 |
| XRF            | X-ray fluorescence                              |
| 3D             | Three-dimensional                               |
| $C_{Binder}$   | Cost of binder                                  |
| $C_{m-Pile}$   | Cost per meter pile                             |
| $C_{Pile}$     | Cost per pile                                   |
| $C_{Rig}$      | Cost of rigging up and down                     |
| $C_{Tot}$      | Total installation cost                         |
| $d_P$          | Pile diameter                                   |
| $D_P$          | Pile depth                                      |
| $E_{50}$       | Estimated stiffness at 50% compressive strength |
| $G_s$          | Specific gravity                                |
| $I_L$          | Liquidity index                                 |
| $I_P$          | Plasticity index                                |
| $m_b$          | Mass of added binder                            |
| $m_{CEMI}$     | Mass of CEMI                                    |
| $m_{cyl}$      | Empty plastic cylinder weight                   |
| $m_{cyl,full}$ | Full plastic cylinder weight                    |
| $m_{GGBS}$     | Mass of GGBS                                    |
| $m_{PSA}$      | Mass of PSA                                     |
| $m_{soil}$     | Mass of soil                                    |
| $m_{w,s}$      | Mass of naturally occurring water on the soil   |
| $m_{w,a}$      | Mass of added water                             |
| $n_{air}$      | Entrapped air                                   |
| $n_p$          | Number of piles                                 |
| $q_u$          | Ultimate compressive strength                   |
| $q_{u,28}$     | 28-day compressive strength                     |
| $r$            | Pearson's correlation coefficient               |
| $s_p$          | Penetration rate                                |
| $s_R$          | Retrieval rate                                  |
| $S_t$          | Sensitivity                                     |

|                 |  |
|-----------------|--|
| $S_u$           | Undrained shear strength                                   |
| $S_{ur}$        | Remolded undrained shear strength                          |
| $t$             | Time   |
| $T$             | Blade rotation number                                      |
| $V_p$           | P-wave velocity  |
| $w_s$           | Soil water content   |
| $w_{stab}$      | Soil water content of the homogenized soil                 |
| $w_L$           | Liquid limit   |
| $w_P$           | Plastic limit  |
| $w_{UCT}$       | Soil water content after unconfined compression testing    |
| $w_{\mu CT}$    | Soil water content after micro computed tomography testing |
| $wbr_{corr}$    | Corrected water to binder ratio                            |
| $\Sigma M$      | Number of micing tool blades/paddles                       |
| $\alpha$        | Binder content   |
| $\beta_i$       | Regression parameter                                       |
| $\gamma$        | Bulk/total unit weight                                     |
| $\bar{\gamma}$  | Average bulk/total unit weight                             |
| $\varepsilon$   | Axial strain   |
| $\varepsilon_v$ | Failure strain   |
| $\varepsilon_s$ | Statistical error  |
| $\rho_{stab}$   | Measured density   |
| $\rho_{theor.}$ | Theoretical density  |
| $\rho_w$        | Density of water (1 t/m <sup>3</sup> )                     |
| $\sigma_1$      | Axial stress   |
| $\tau_{max}$    | Shear strength   |

# 1 | Introduction

## 1.1. Background

Ground stabilization by deep mixing aims to improve existing soil properties. Stabilization is performed by mixing and injecting a chemical binder. The current methods have roots in the 1970s, where two main variations, the wet and the dry method, were developed in Japan and the Nordic countries respectively (Eggen, 2013; Kitazume & Terashi, 2013). In the following decades, technological improvements made both methods effective for specific conditions and projects. Still, interaction and exchange of knowledge remained insufficient for a long time, making it difficult and costly to implement new methods in the design process. This imbalance of knowledge and practice has most likely resulted in engineers choosing methods which are not optimal in the given conditions. Both efficiency and sustainability in construction projects may have been affected consequently. In recent years, ground improvement by deep mixing has gained popularity in the rest of the world, generating a need for further research to optimize all aspects of the design and installation process.

One such initiative is the research project GOAL; Green sOil stAbiLization; a research and development project started by the Norwegian Geotechnical Institute (NGI) (NGI, n.d.) together with academic (NTNU, University of California Berkeley, University College Dublin, Danmarks Tekniske Universitet) and industry (Keller Geoteknikk, Lindum, Bergene Holm, Celsa Armeringsstål, Norske Skog Skogn) partners, and financed by the Research Council of Norway (project number 328767). One of the main issues in the soil stabilization industry highlighted by the project, is the lack of implementation of sustainable binders in practice. Lime and cement, which have substantial carbon emissions associated with production, are almost exclusively used for deep stabilization today. Sustainable binder alternatives with potential to offset the emissions of lime and cement are industry by-products like blast furnace slag and fly ash. These binders not only help to reduce emissions but can in some cases improve soil properties beyond what is possible when solely using (combinations of) lime and cement (Lindh, 2001; Yong-Feng et al., 2017; Åhnberg, 2006). Further research can therefore be conducted in optimizing the binder composition using alternative binders in both the wet and dry mixing method.

The Nordic market of deep mixing is currently undergoing a change in the status quo due to the testing and implementation of the wet mixing method. Involvement from NGI in multiple projects creates an opportunity to examine the wet mixing method in comparison with other mixing methods. However, problems arise when trying to find measurable benefits which will be important for the wet method to take hold in a competitive market. Testing on field samples by for example CT-scanning and compression tests can give an understanding of quality and homogeneity of stabilized soil but comparing the results with laboratory mixed samples is proven difficult in many studies (Falle, 2021; Larsson, 2005; Larsson et al., 2005a). Comparing the field homogeneity achieved by using new and existing methods in Nordic conditions is an important topic of research to better understand which method is ideal for different applications.

## 1.2. Objectives

The main objective of this thesis is split in two sub-objectives:

- 1) Compare the wet and dry mixing method in the laboratory to find the optimal binder composition in sensitive clay using cement, ground granulated blast-furnace slag, and paper sludge ash. Soft sensitive clay is chosen because most Nordic deep stabilization projects are performed in this type of soil (Larsson, 2021). The comparison will be done from a quality, cost, and sustainability perspective.
- 2) Examine the structure and homogeneity in field stabilized clay samples by  $\mu$ CT-scanning and image analysis. Field samples from multiple deep stabilization projects utilizing the wet deep mixing method and the modified dry mixing method are to be used.

Both objectives aim to collectively answer the research questions listed below.

### Research questions:

- a) What are the distinguishable differences in internal structure and porosity of stabilized field samples when using the wet deep mixing method and modified dry mixing method?
- b) How do different binder compositions affect the strength and stiffness of laboratory stabilized clay samples when using wet and dry mixing methods?
- c) Can the modified dry mixing method be simulated in the laboratory by using a single wet mixing method?
- d) What type of deep mixing method should be chosen in the design process in terms of conditions, costs, quality, and sustainability?

## 1.3. Approach

The approach for this thesis is divided according to the two main studies conducted. The first part of the thesis is field sampling and testing. The field samples were gathered from ongoing projects in Norway and Sweden with NGI involvement. Modified dry mixing (MDM) samples were collected using an excavator from a Norwegian road project, while cylindrical wet deep mixing (WDM) samples were collected from two different construction projects in Sweden using a trifle tube sampler. The MDM samples were trimmed to match the WDM samples before they were handed off to the Physics Department at the Norwegian University of Science and Technology (NTNU). The Physics Department performed micro computed tomography ( $\mu$ CT) on the samples to analyse homogeneity and porosity. As an added measure, the field sample p-wave velocity was tested as well.

The second part of the work consists of laboratory sample mixing and testing, which was conducted over the same period as the study of field samples. Untreated quick clay from the Tiller-Flotten research site (L'Heureux et al., 2019) was provided by NTNU, while binders (i.e. cement, blast furnace slag and paper sludge ash) were provided by NGI industry partners. Batches were mixed using both the wet and the dry mixing methods. Two different water to binder ratios (wbr) were used for each method. Samples were molded using the rodding method which works well for creating high quality samples in

soft clays (Kitazume et al., 2015). The varying binder composition in the batches (recipes), correspond to set points on an augmented simplex lattice. Water content was measured in each batch to find the actual water to binder ratio. After curing for 28 days, an unconfined compression test (UCT) and p-wave test were performed to assess performance in terms of strength and deformation properties. Three runs were performed in each point to increase reliability. The results were modeled in Design-Expert, which is a design of experiments (DoE) software. Response surface methodology (RSM) was used for result-analysis. In addition to studying different binder compositions, identical samples at two different wbr were also prepared using the modified dry mixing method adapted for the laboratory and the wet mixing method. After curing for 28 days, UCT was conducted to evaluate if the modified mixing method and the wet mixing method are interchangeable in the laboratory.

## **1.4. Limitations**

The findings from the field study are limited to overall method variations because the samples are collected from three different projects in Norway and Sweden. This causes factors like binder type and amount, installation parameters, soil type and curing conditions to vary, which are known to affect quality. One set of samples is also collected with an excavator and trimmed to match the rest of the cylindrical samples, possibly impacting quality. The overall limited field data makes findings less reliable.

The findings from the laboratory study are limited to two water to binder ratios in each mixing method to make the number of samples manageable. Modeling of the variations in binder interaction across different binder contents is therefore excluded from the thesis. Percentages of pure binder components can vary according to the product declarations. These binder deviations are assumed to be negligible and not to affect the findings. Strength evolution over time is not evaluated because the samples are only tested after 28 days of curing.

## **1.5. Outline**

The thesis contains an introduction of the topic, with relevant information on the background, goals, and limitations of the work. The remaining five chapters are structured to include the following:

Chapter 2 covers relevant literature for describing the three main methods of deep stabilization. Theoretical and practical advantages and disadvantages are highlighted along with a description of quality control procedures. A thorough description of binders and curing conditions and their influence on deep mixing performance is also included.

Chapter 3 describes the methodology of the research. This includes information on the materials, as well as procedures applied during sampling, sample preparation, curing and testing. The methods and tools used for modeling and analysis of collected data are also described.

Chapter 4 presents complete results from the field and laboratory studies.

Chapter 5 discusses the findings from Chapter 4 both individually and as a whole with limitations.

Chapter 6 presents the conclusion of the study and contains recommendations for further work.

## 2 | Theory

Part of the theory chapter in this thesis is condensed from the project thesis performed in the fall semester of 2022. The project thesis was a literature review, where the main objective was comparing three deep mixing methods for soil stabilization in terms of practical applications, quality of results, installation costs and sustainability (Skreien, 2022). The remaining theory sections explain central remaining definitions and factors which influence obtained strength and quality in deep stabilization projects. This includes effects of curing in different conditions, sample preparation and interactions between binders.

### 2.1 Deep stabilization

Deep stabilization, or deep mixing, is a collective term for soil improvement by injecting a binder during insertion and/or retrieval of a rotating mixing tool. The installation equipment, binder type and composition, as well as general methodology varies greatly across regions. There are also different adaptations developed to excel in certain conditions and project types. Three main deep mixing methods are described in the following sections. The methods are chosen based on their current relevancy and future possibilities of implementation in Nordic projects. Furthermore, understanding the variations between the methods is crucial when discussing which method is optimal based off laboratory results in varying conditions.

#### 2.1.1. Dry deep mixing (DDM)

Dry deep mixing, referred to as DDM, is the standard deep mixing method in the Nordic countries. A schematic of the basic DDM set-up and procedure is shown in Figure 1. The machines are equipped with a tall drill shaft which uses force and rotation to insert a mixing tool into the soil. During the retrieval phase, compressed air is used to inject a dry binder while simultaneous rotation homogenizes the soil-binder mixture. The type of binder greatly affects both the strength development and final strength of the stabilized soil. Cost, emissions, and heat development are also affected by the binder composition. When trying to meet design values and project requirements, it is important to balance these factors. This is done by optimizing binder content and composition. Binder content is often referred to as  $\alpha$  when referring to kg of binder added per cubic meter of soil. The most common binders are lime, cement, pozzolanic materials and industry by-products like for example lime kiln dust (LKD) or cement kiln dust (CKD). A detailed overview of selected binders, reactions and their interactions is described in section 2.2. Unique to DDM is the fact that only the natural water content of the soil is used to hydrate the binder. From NGIs experience, DDM is also more flexible when it comes to using alternative binders. Clogging risk is reduced because the dry binders do not react until it is mixed and hydrated with the soil water content. This is especially important for fast reacting binders like quicklime.

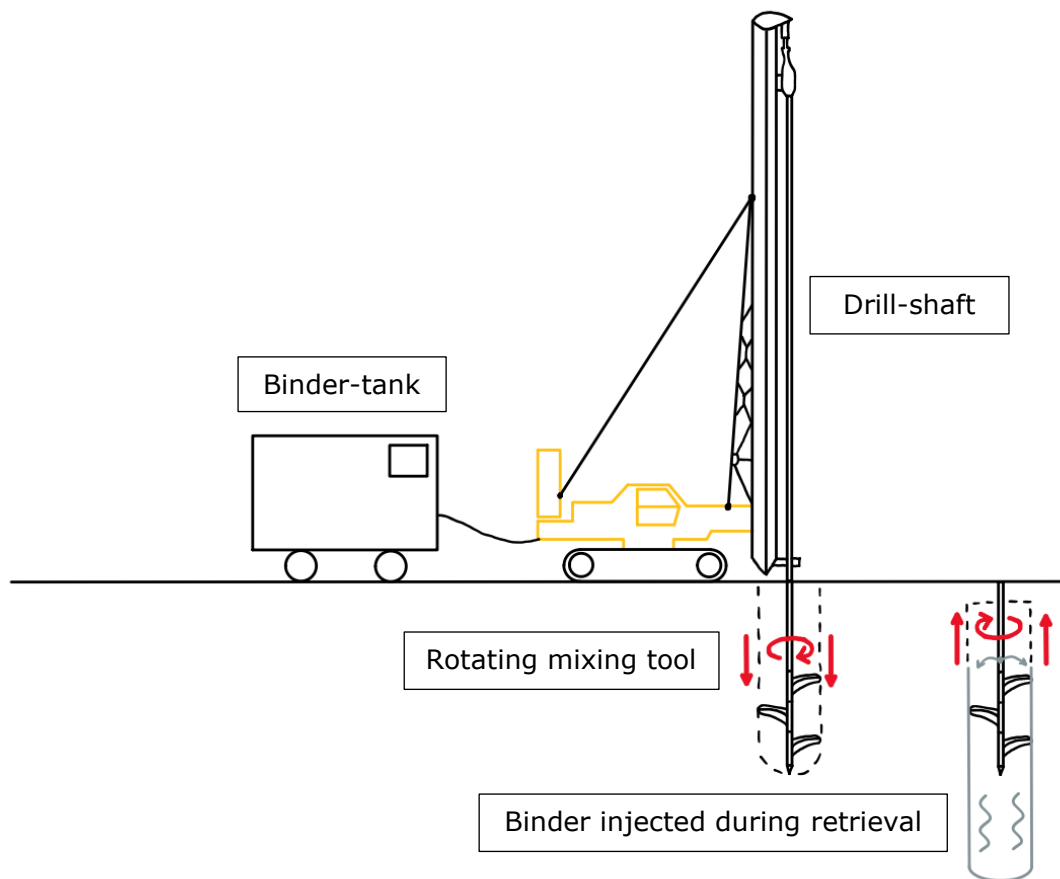


Figure 1: DDM equipment and procedure.

Mixing tools are in general not standardized and vary between contractors. Besides, different sizes and configurations can be utilized to fit varying conditions. The most common mixing tools have a hook shape or consist of single paddles, while combined tools also exist. Examples of different types of mixing tools are shown in Figure 2. Dry drilling limits the penetration ability of the mixing tools when performing DDM. The method can therefore only be applied to softer soils which have a minimum water content to hydrate the binder.



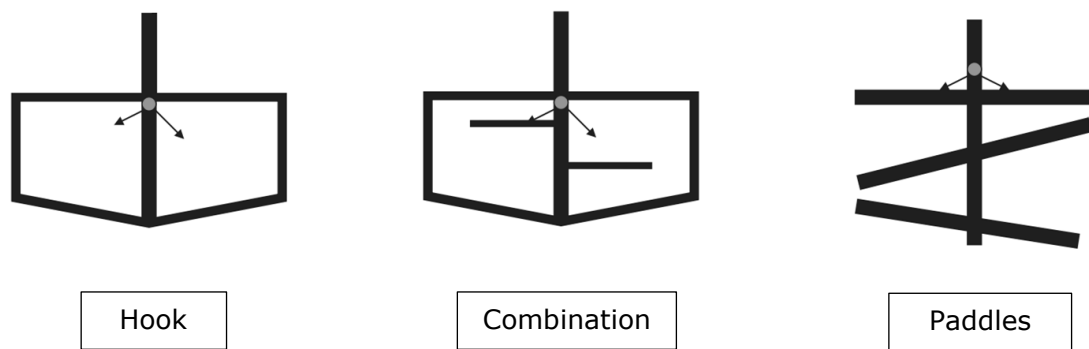


Figure 2: Shape characteristics of deep mixing tools. Modified after (NGF, 2012).

The development of DDM was initiated in the 1970s, where smaller machines primarily injected lime into the soil as a binder (Eggen, 2013; Larsson, 2021). The Nordic method is used as a basis for this thesis, but an equivalent method used in the Japanese market exists, and is often referred to as dry jet mixing or DJM (Kitazume & Terashi, 2013). Despite the DDM method remaining much the same today, modern machines are capable of reaching greater depths, while better monitoring technology has allowed for installation parameters to be tailored to specific conditions.

Adjacent structures and general stability of the surrounding soil can be affected during installation. These responses, often seen as deformations, are caused by increased excess pore pressure during the injection of binder and compressed air (Larsson, 2021). Finished DDM columns are usually cut off from the surface because the method cannot stabilize through dry crust. The main advantages of DDM is good performance in undrained soft and clayey soil, effective and flexible equipment, and the wide binder selection.

Specifics regarding equipment can all be altered within a practical range. An overview of DDM equipment specifications and common applications collected during the project thesis literature review is presented in Table 1 (Skreien, 2022).

Table 1: DDM equipment specifications and common applications. Modified after (Skreien, 2022).

| Parameters                            | DDM - Nordic                        | Applications  |
|---------------------------------------|-------------------------------------|---|
| Max stabilization depth               | 15-25 m                             | <ul style="list-style-type: none"> <li>- Stabilization of cuts, embankments, and natural slopes</li> <li>- Deep excavation bracing</li> <li>- Construction pit bracing</li> <li>- Securing utility trenches</li> <li>- Vibration reduction</li> <li>- Settlement reduction</li> <li>- Seabed stabilization</li> <li>- Soil bracing</li> <li>- Stabilization of contaminated soil</li> </ul> |
| Mixing tool diameter                  | 0.5 m, 0.6 m, 0.8 m, 1.0 m          |   |
| Number of mixing tools (shafts)       | 1                                   |   |
| Retrieval rate                        | 10-35 mm/rev                        |   |
| Rotational speed                      | 50-210 revolutions/min              |   |
| Installation pressure (feed pressure) | 3-4 bar at 10 m<br>6-10 bar at 20 m |   |
| Max inclination machine               | 15°                                 |   |
| Max install inclination               | 45°                                 |   |
| Machine weight                        | 30-55 tons                          |   |
| Ground pressure machine               | 24-50 kN/m <sup>2</sup>             |   |
| Ground pressure binder wagon          | 40-60 kN/m <sup>2</sup>             |   |

### 2.1.2. Modified dry mixing (MDM)

Modified dry mixing, referred to as MDM, is a deep stabilization method which alters the drilling procedure of standard DDM. The modified procedure, shown in Figure 3, introduces water during insertion of the mixing tool (Eriksson et al., 2005). The water is pumped into the soil from a separate water tank and makes the method applicable to conditions DDM is not suited for. A binder, usually with a very high cement content, is injected into the soil by compressed air during retrieval of the mixing tool. The method is usually performed in firm clay, silt, and sand (drained or undrained).

The mixing tool used for MDM is usually a hook type tool (see Figure 2). Due to the geometry, the tool is stiffer than the paddle tools, which in turn increases penetration ability. The added water also facilitates drilling conditions.

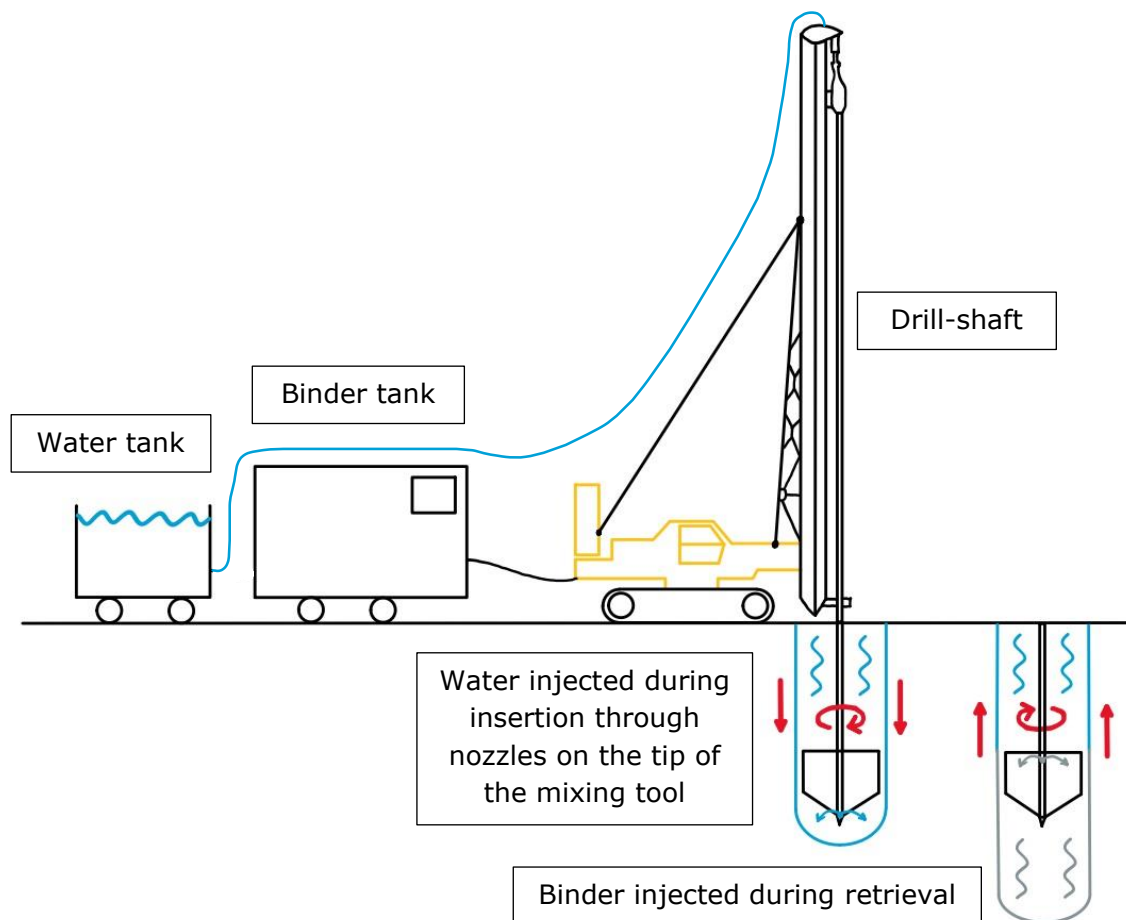


Figure 3: MDM equipment and procedure.

MDM was developed as a collaborative project between LCT technology, LLC, Hercules Grundläggning AB and the Swedish Geotechnical Institute (SGI) and introduced in 2004 (Gunther et al., 2004). From NGI's experience, the use of the method remains limited despite the benefits over traditional DDM. Besides the shared disadvantages, the limited selection of contractors is the main disadvantage of the MDM method.

By controlling the water content of the soil during insertion, layered soil can be stabilized appropriately based on inherent properties. Columns with very high strength can also be made through dry crust because large amounts of binder can be hydrated. Another advantage of the MDM method is the ability to perform DDM with the same equipment (Gunther et al., 2004). This makes it a flexible and cost-effective solution in projects with varying conditions.

An overview of MDM equipment specifications and common applications collected during the project thesis literature review is presented in Table 2 (Skreien, 2022). Due to the limited implementation and public research, most of the observed applications and benefits is found in the papers by Gunther et al. (2004) and Eriksson et al. (2005). These describe the technology and initial field testing of the MDM method.

Table 2: MDM equipment specifications and common applications. Modified after (Skreien, 2022).

| Parameters                            | MDM (Nordic DDM)   | Applications   |
|---------------------------------------|--|--|
| Max stabilization depth               | 15-25 m  | <ul style="list-style-type: none"> <li>- All applications of the dry mixing method</li> <li>- Stabilizing dry soils with insufficient water content for traditional dry mixing.</li> <li>- High strength and stiffness columns with low permeability by hydration of large amounts of binder</li> <li>- Stabilization through harder layers (both crust and embedded layers) which traditional dry mixing cannot penetrate.</li> </ul> |
| Mixing tool diameter                  | 0.5 m, 0.6 m, 0.8 m, 1.0 m   |  |
| Number of mixing tools (shafts)       | 1  |  |
| Retrieval rate                        | 10-35 mm/rev   |  |
| Rotational speed                      | 50-210 revolutions/min   |  |
| Installation pressure (feed pressure) | 3-4 bar at 10 m<br>6-10 bar at 20 m  |  |
| Max inclination machine               | 15°  |  |
| Max install inclination               | 45°  |  |
| Machine weight                        | 30-55 tons   |  |
| Ground pressure machine               | 24-50 kN/m <sup>2</sup>  |  |
| Ground pressure binder wagon          | 40-60 kN/m <sup>2</sup>  |  |
| Ground pressure water tank            | Usually neglected because a small water tank or a hose connection is usually sufficient. |  |

### 2.1.3. Wet deep mixing (WDM)

Wet deep mixing, referred to as WDM, is the most common deep stabilization method outside the Nordic countries (Chaumeny et al., 2018). The WDM equipment requires more allotted construction site space compared with DDM and MDM. Figure 4 shows the main WDM equipment and procedure used in Europe. The additional required space is mostly due to the addition of a separate binder plant which is not mobile. The plant requires a separate power and water source to mix binder and water into a slurry. The water fully hydrates the binder before it is injected into the soil. In WDM, the binder is usually made from cement to prevent premature curing of the slurry, but a combination of cement and ground granulated blast-furnace slag (GGBS) is also commonly used.

The ability to inject a mixed cement slurry from the binder plant both during insertion and retrieval is unique to WDM. The most typically used mixing tool for WDM is the paddle type, with separate nozzles for injecting binder during insertion and retrieval (Kitazume & Terashi, 2013). To increase homogeneity of the finished columns, the drilling process can also be repeated, with or without injecting additional binder. After installing columns with a high binder content, steel reinforcement is often added instead of casting a traditional concrete foundation.

Even though the added water gives good penetration abilities, added water also introduces some limitations to the conditions in which WDM can be applied. Soils with a high natural water content need more binder to achieve the same water to binder ratio as dry

installation methods. Common conditions where the wet deep mixing method is used includes soft to medium firm clay, medium density sand, organic material, and stratified soils (Kirsch & Bell (Eds.), 2012; Kitazume & Terashi, 2013).

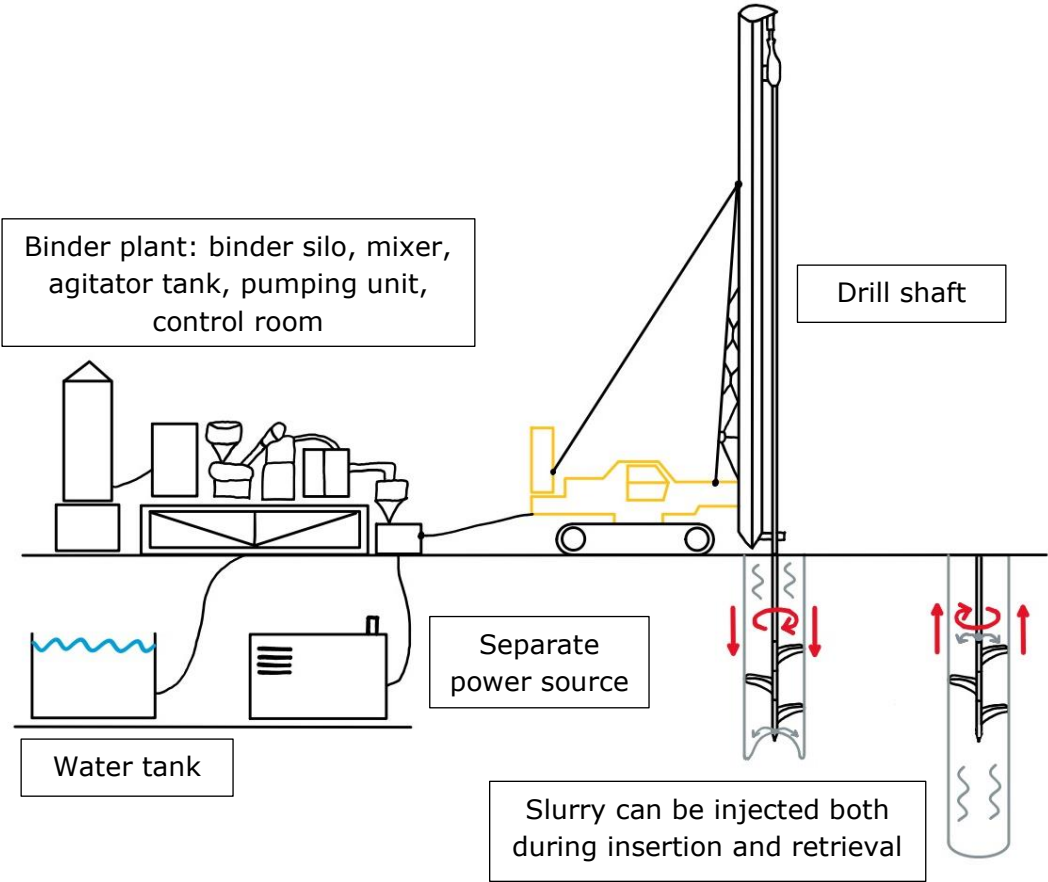


Figure 4: WDM equipment and procedure.

The first wet deep mixing method to be developed was cement deep mixing, referred to as CDM. CDM was developed in Japan in the late 1960s and implemented in the early to mid-'70s (Kirsch & Bell (Eds.), 2012; Kitazume & Terashi, 2013). The main difference between the European method described in this section, and the Japanese method, is the design of the equipment. CDM machines are usually equipped with multiple drill shafts to increase efficiency in large projects (Eggen, 2013). An overview of the differences is shown in Table 3. Few efforts have been made to implement WDM in the Nordic countries, where only pilot projects have been performed according to NGI.

Adjacent structures and general stability are affected by the same factors as described for DDM and MDM. The main advantage of WDM is the ability to efficiently create large, homogenous columns with high strength (Kirsch & Bell (Eds.), 2012; Kitazume & Terashi, 2013).

An overview of Japanese CDM and European WDM equipment specifications, along with common applications collected during the project thesis literature review, is presented in Table 3 (Skreien, 2022).

Table 3: WDM equipment specifications and common applications. Modified after (Skreien, 2022).

| Parameters                                    | WDM – CDM<br>(WDM - European method)  | Applications   |
|---|---|--|
| Max stabilization depth                       | 10-40 m<br>(15-30 m)  | <ul style="list-style-type: none"> <li>- Road and railway embankments</li> <li>- Retention systems and excavation support</li> <li>- Foundation support</li> <li>- Liquefaction mitigation</li> <li>- Hydraulic cut-off walls</li> <li>- Environmental remediation (Block contaminated groundwater etc.)</li> <li>- Slope stabilization</li> </ul> |
| Mixing tool diameter                          | 1.0-1.3 m<br>(1.0–2.5 m)  |  |
| Number of mixing tools (shafts)               | 2<br>(1)  |  |
| Penetration rate                              | 25-50 mm/rev<br>(15-40 mm/rev)  |  |
| Retrieval rate                                | 17.5-25 mm/rev<br>(25-33.3 mm/rev)  |  |
| Rotational speed - Penetration                | 20 revolutions/min<br>(20-25 revolutions/min)   |  |
| Rotational speed – Retrieval                  | 40 revolutions/min<br>(40-60 revolutions/min)   |  |
| Binder pressure (pumping pressure from plant) | 25 bar  |  |
| Installation capacity – Delivery rate         | 20 m <sup>3</sup> /hr.<br>(5-15 m <sup>3</sup> /hr.)  |  |
| Max inclination machine                       | -   |  |
| Max install inclination                       | -   |  |
| Machine weight                                | 40-120 tons   |  |
| Binder plant ground pressure                  | Plants vary in size meaning the required bearing capacity should be checked depending on the equipment used. The binder plant usually requires about 200 m <sup>2</sup> of area with a maximum silo capacity of 300 kN. |  |

#### 2.1.4. Quality, cost, and sustainability

The chosen method also has implications on column quality, cost, and sustainability in deep mixing projects. Cost and sustainability, which are somewhat easier to quantify from installation parameters, are only described in brief because they are usually not the main focus in deep mixing research. The main installation parameters are listed below.

- Retrieval/penetration rate (mm/rev): The vertical distance the mixing tool travels per revolution. This is also used to control binder amount.

- Rotational speed (revolutions/min): Number of mixing tool revolutions per minute.
- Installation pressure/feed pressure (bars): Pressure of the air used to inject the binder.

Quality is an especially important factor which can be estimated by using different practices. It is recommended to perform initial laboratory testing on field material to get an idea of stabilized soil properties (Kitazume & Terashi, 2013; NGF, 2012). However, multiple studies show the difficulties of accurately determining field properties by testing of field and laboratory samples (Hov et al., 2022; Kitazume, 2005). Section 2.3 further describes how the results are influenced by both sample preparation and curing conditions.

The Norwegian guidelines operates with standard minimum binder amounts found empirically through laboratory testing to achieve sufficient quality (NGF, 2012). The guideline also mentions the importance of adapting installation parameters to specific soil conditions, which has been studied in detail by Larsson et al. (2005a, 2005b). They concluded that only the retrieval rate and number of mixing tool blades/paddles significantly affected column quality. The two factors were then condensed into an expression named the "Blade rotation number" ( $T$ ), which can be defined as the total number of blades passing through the soil per meter. The study found that a value of 400 per meter or more is an indication of good field quality when using DDM. Even with sufficient mixing, some binder accumulation is found when inspecting field samples from DDM projects (Larsson et al., 2005a). The expression shown in *Eq.1* is altered to fit the varying installation rates of WDM (Kitazume & Terashi, 2013).

$$T = \sum M * \left( \frac{1}{s_p} + \frac{1}{s_R} \right) \quad \text{Eq.1}$$

An important note is that the quality criterion expressed as a blade rotation number is not equal throughout regions. In Japan, values between 300 and 360 per meter are mentioned for reaching sufficient quality in WDM columns (Kirsch & Bell (Eds.), 2012; Kitazume & Terashi, 2013).

Primary waves, here referred to as p-waves, are another way to assess quality in stabilized material. The p-waves are compression waves in the longitudinal direction of the material. Measuring the p-waves can be done without destroying the material (non-destructive). It can therefore easily be used to assess the evolution in mechanical and physical properties over time (Lindh & Lemenkova, 2022).

Multiple studies have been performed on stabilized soil to correlate p-wave velocity and strength properties. Mandal et al. (2016) found that p-wave velocity increased with curing time and binder content when using PUNDIT (Portable Ultrasonic Non-destructive Digital Indicating Tester) equipment. Good correlations between p-wave velocity and flexural strength were also found for various soil types stabilized with different binders (see Figure 5).

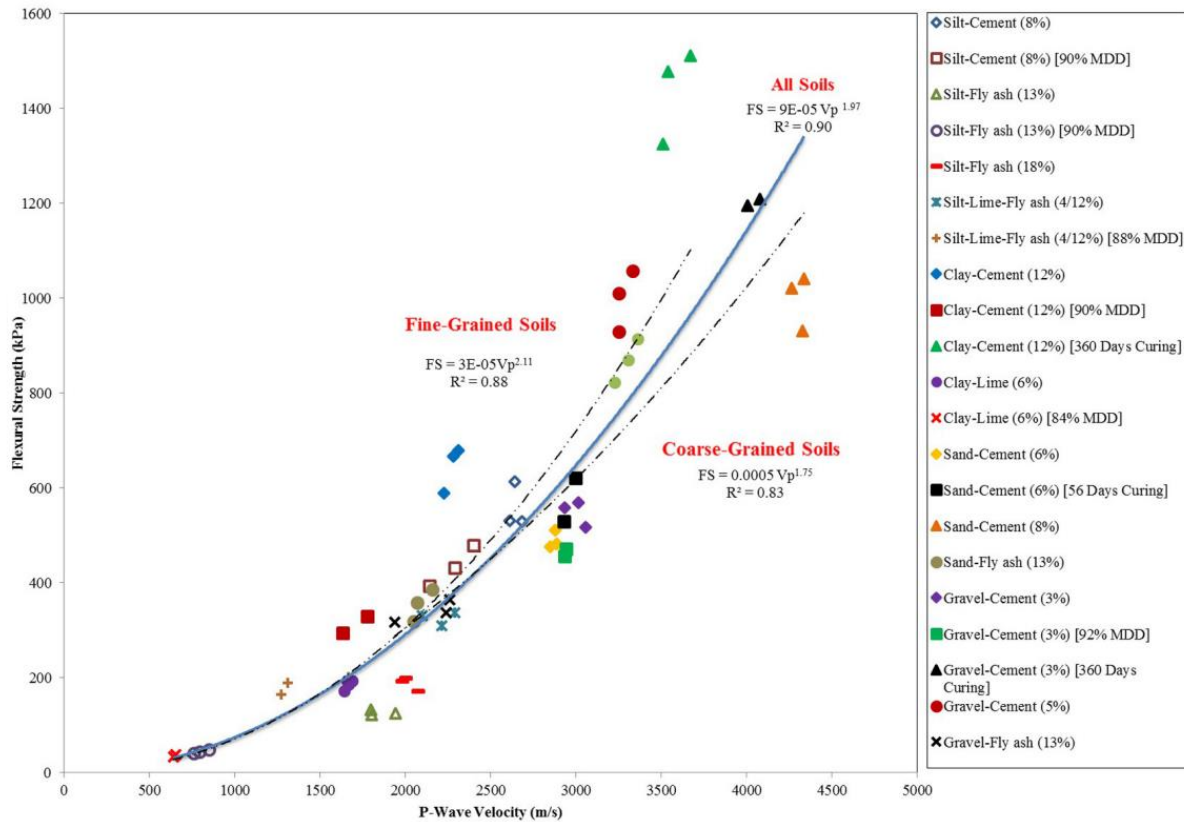


Figure 5: Flexural strength vs p-wave velocity for cementitious stabilized materials (Mandal et al., 2016).

A Swedish study by Lindh & Lemenkova (2022) found good correlations between the compressive strength of stabilized soft silty and clayey soil and p-wave velocity when using the Free-Free Resonant (FFR) test method. Included in the test was different ratios of binder and water. Results showed higher p-wave velocities in samples stabilized with low water content ( $L_w$ ) and high binder content ( $H_B$ ) (see Figure 6). The p-wave velocities at 28 days of curing varied between about 250 and 950 m/s depending on the binder ratio, amount of water and curing time. For reference, the p-wave velocity in water is 1450 m/s (McDowell et al., 2002).



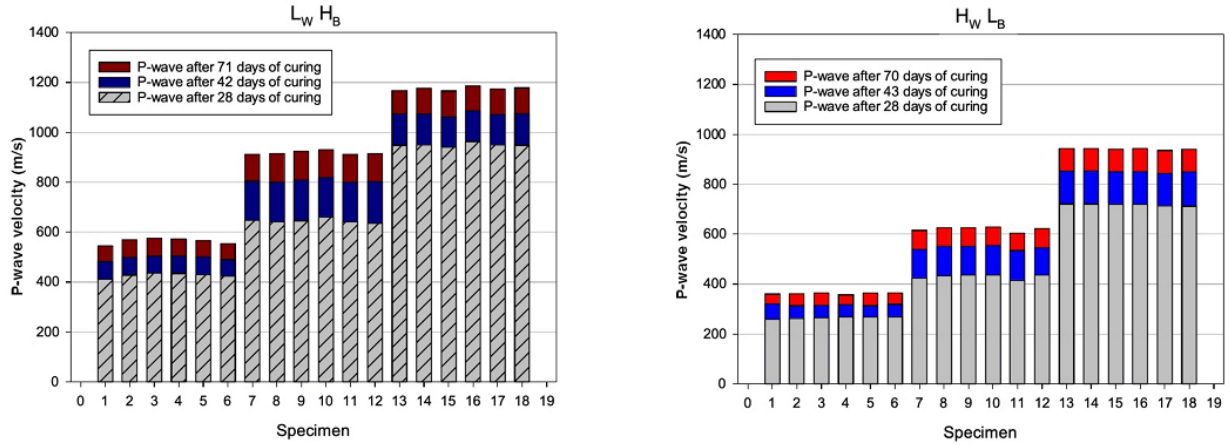


Figure 6: P-wave velocity of samples stabilized with decreased water to binder ratio (left) and increased water to binder ratio (right). Sample 1-6 has a cement/slag ratio of 70/30, sample 7-12 has 50/50 and sample 13-18 has 30/70 respectively (Lindh & Lemenkova, 2022).

Total cost is difficult to quantify because it depends on many varying factors including size of the project, geographical location, and accessibility. Table 4 shows an overview of the estimated cost of the three methods based off NGI experience in 2022 (Skreien, 2022). Wet deep mixing is much more costly due to the extra rigging costs and larger machines but can still be economical in large projects. Eq. 2 shows how total installation costs ( $C_{Tot}$ ) can be estimated. The cost of each pile ( $C_{Pile}$ ) is usually excluded from the expression when using WDM.

Table 4: Estimated deep mixing cost overview for 2022 from NGI experience (Skreien, 2022).

|     | Rigging cost [kNOK] | Cost per meter pile [NOK/m] |
|-----|---------------------|-----------------------------|
| DDM | ≈75-250             | ≈59-251                     |
| MDM | ≈75-250             | ≈88-251                     |
| WDM | ≈500-1000           | ≈200-2945                   |

$$C_{Tot} = C_{Rig} + n_p \left( C_{Pile} + D_p * \left( \pi * \left( \frac{d_p}{2} \right)^2 * \alpha * C_{Binder} + C_{m-Pile} \right) \right) \quad Eq. 2$$

Sustainability in deep mixing projects is mostly dependent on the binder amount and type of binder used. For that reason, research efforts are being made to monitor and efficiently stabilize soil using low binder contents and alternative binders (NGI, n.d.). A rundown of specific greenhouse gas emissions of common binders is shown in Table 5 (Skreien, 2022). An Environmental Product Declaration (EPD) is not available for paper sludge ash specifically, but it is assumed to be like standard fly ash.

Table 5: Emissions from commonly used binders (Skreien, 2022).

| Product<br>(Norwegian/Nordic market)  | Equivalent CO <sub>2</sub> emissions<br>[kg CO <sub>2</sub> -eq/ton]                        |
|---|---|
| Industrisement<br>(CEM I 52,5 R)  | 716 (NORCEM AS, 2020a)  |
| Standardsement FA<br>(CEM II/B-M)   | 581 (NORCEM AS, 2020d)  |
| Quicklime CL90-Q /Stabila B100<br>100 % Quicklime, 0 % LKD  | 1035 (Bache et al., 2021; Franzefoss<br>Minerals AS, 2022)                                  |
| Quicklime CL80-Q/Stabila B80<br>80 % Quicklime, 20 % LKD  | 822 (Bache et al., 2021)  |
| Quicklime CL70-Q/Stabila B60<br>70 % Quicklime, 30 % LKD  | 719 (Bache et al., 2021)  |
| LKD<br>0 % Quicklime, 100 % LKD   | 0, because it follows the emissions given for<br>pure quicklime (CL90) (Bache et al., 2021) |
| Multicem<br>50 % Industrisement, 50 % CKD   | 358 (NORCEM AS, 2020b)  |
| Multicem<br>50 % Standardsement FA, 50 % CKD  | 291 (NORCEM AS, 2020c)  |
| Industry average ground granulated<br>blast-furnace slag<br>(~100 % GGBS)<br>(Not specifically Nordic market) | 60.21 (JSW Cement Limited, 2019)  |
| Emineral Fly ash<br>(100 % FA)  | 1.85 (Emineral A/S, 2020)   |

## 2.2 Binders

A binder is a material which can chemically react with soil to improve engineering properties (Kitazume & Terashi, 2013). The type of binder used in deep stabilization can either be made from single components or be mixed from multiple components. Typical binders are cement, lime and industry by-products like fly ash or blast furnace slag. However, the binder types are not interchangeable across the different methods of stabilization. DDM is more flexible when it comes to choosing a binder, while the wet methods are more limited due to clogging risk. The binder materials used in the laboratory experiments and how they react, both with each other and water, is described in the following sections.

### 2.2.1. Cement

Cement is made by heating ground limestone (>90 %) to a final temperature of around 1450 °C (Jacobsen et al., 2022). Other minor constituents (gypsum, quartz etc.) are added to the ground limestone before heating to produce a raw meal with the appropriate oxide composition. Once the final temperature is reached, nodules of cement clinker is formed.

The clinker is made up of four main components, called clinker phases, which are shown in Table 6. The hot and semi-solid clinker is then cooled and ground together with gypsum to a final cement powder. The gypsum (or other forms of calcium sulphate) helps prevent curing issues.

Table 6: Major clinker phases and typical composition in Portland clinker (Jacobsen et al., 2022).

| Major phase                 | Typical major phase content | “Mineralogical term” | Cement chemical notation (Oxide notation) | Shortened cement chemical notation |
|-----------------------------|-----------------------------|----------------------|---|------------------------------------|
| Tricalcium silicate         | 50-70 %                     | Alite                | $3CaO * SiO_2$                            | $C_3S$                             |
| Dicalcium silicate          | 15-30 %                     | Belite               | $2CaO * SiO_2$                            | $C_2S$                             |
| Tricalcium aluminate        | 5-10 %                      | Aluminate            | $3CaO * Al_2O_3$                          | $C_3A$                             |
| Tetracalcium aluminoferrite | 5-15 %                      | Ferrite              | $4CaO * Al_2O_3 * Fe_2O_3$                | $C_4AF$                            |

Cement is widely used in deep mixing projects due to its ability to gain strength quickly compared to other binders (Janz & Johansson, 2002). Many commercial cements with added pozzolanic materials are also available. The stabilizing process and mode of operation is described in section 2.2.5.

## 2.2.2. Fly ash (FA) and Paper sludge ash (PSA)

Fly ash, referred to as FA, is a by-product from coal-fired power plants. No such power plants exist in Norway, meaning all fly ash is imported from other countries (mainly Denmark) (Jacobsen et al., 2022). The properties and composition of fly ash can vary greatly depending on coal types and what filters are used to collect it etc. Fly ash is made up of two main reactive components, silicon dioxide ( $SiO_2$ ) and aluminium oxide ( $Al_2O_3$ ), usually in the range of 45-55 % and 20-30 % respectively (Jacobsen et al., 2022).

Fly ash is a pozzolanic material used as a replacement for cement and quicklime in deep mixing to primarily reduce emissions in construction projects. The stabilizing process and mode of operation is described in section 2.2.5.

Different types of fly ash can also be produced from other industries. Paper sludge ash, referred to as PSA, is a by-product from paper production and recycling. PSA is a type of fly ash which is produced when a semi-solid paper sludge is incinerated (Mavroulidou, 2018). In addition to a high amount of calcium oxide ( $CaO$ ), the main reactive components in PSA is silicon dioxide ( $SiO_2$ ) and aluminium oxide ( $Al_2O_3$ ). Exact composition is usually tested before use because how the composition varies between producers has not been thoroughly researched. This is because the material variations are less researched than fly ash from coal-fired power plants.

### 2.2.3. Slag (GGBS)

Ground granulated blast-furnace slag, referred to as GGBS or just slag, is a by-product from the iron and steel industry. It is made by rapidly cooling excess material to around 800 °C which creates a glassy, latent hydraulic cement (Lindh, 2004). GGBS made up of about 35-45 % calcium oxide ( $CaO$ ), 33-43 % silicon dioxide ( $SiO_2$ ), as well as 10-15 % aluminium oxide ( $Al_2O_3$ ). Table 7 shows the simplified chemical notations of the main components in slag and fly ash.

Table 7: Chemical notations of major components in slag and fly ash (Jacobsen et al., 2022).

| Major phase     | Cement chemical notation<br>(Oxide notation) | Shortened chemical notation |
|-----------------|--|-----------------------------|
| Calcium oxide   | $CaO$  | $C$                         |
| Silicon dioxide | $SiO_2$                                      | $S$                         |
| Aluminium oxide | $Al_2O_3$                                    | $A$                         |

Slag is also a pozzolanic material used as a replacement for cement and quicklime in deep mixing projects. It is primarily used for its delayed reaction properties and to reduce emissions. The stabilizing process and mode of operation is described in section 2.2.5.

### 2.2.4. Water to binder ratio (wbr)

The water content is an important parameter to control because it affects the water to binder ratio, referred to as wbr. Typical in-situ water content for clay is between 40 and 60 %, with the majority being between 30 and 45 % (NGF, 2012). Soil with lower water content and a low wbr is known to have high strength. This is because excess water creates pores which do not contribute to strength. It is also important to not have too low wbr, because pockets of unhydrated binder forms. Figure 7 shows how the porosity in cement paste is affected by wbr (here referred to as water to cement ratio). The component contributing to strength is the cement gel.

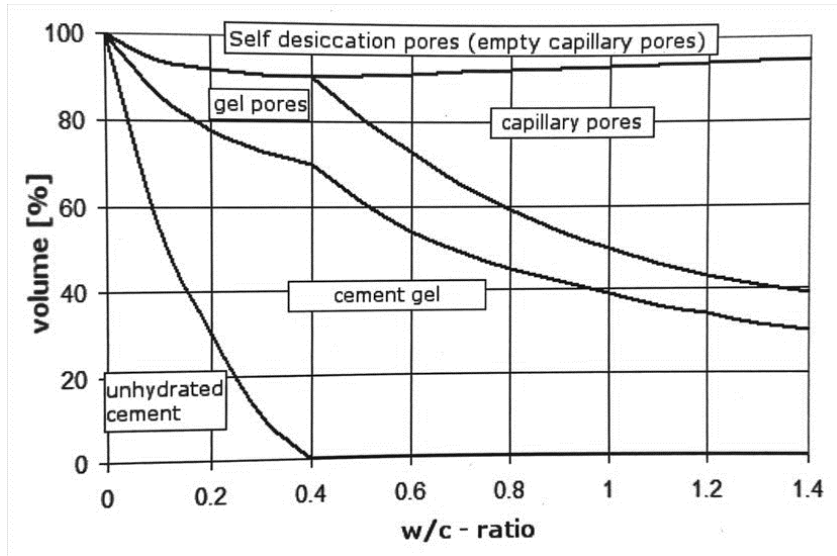


Figure 7: Volumetric composition of cement paste at different water to cement ratios (Jacobsen et al., 2022).

The effect of wbr on stabilized clay performance was visualized in a study by Paniagua et al. (2022a), where a large database of laboratory stabilized clay specimens was used. Samples stabilized with specific binders showed very large variations in strength with a small variation in wbr. A common formulation of the water to binder ratio is shown in Eq. 3.

$$wbr = \frac{m_{w,s} + m_{w,a}}{m_b} \quad Eq. 3$$

When looking at other studies with more controlled laboratory parameters, a relation can more clearly be shown. Figure 8 shows how strength relates to wbr when using different mixing and molding techniques.

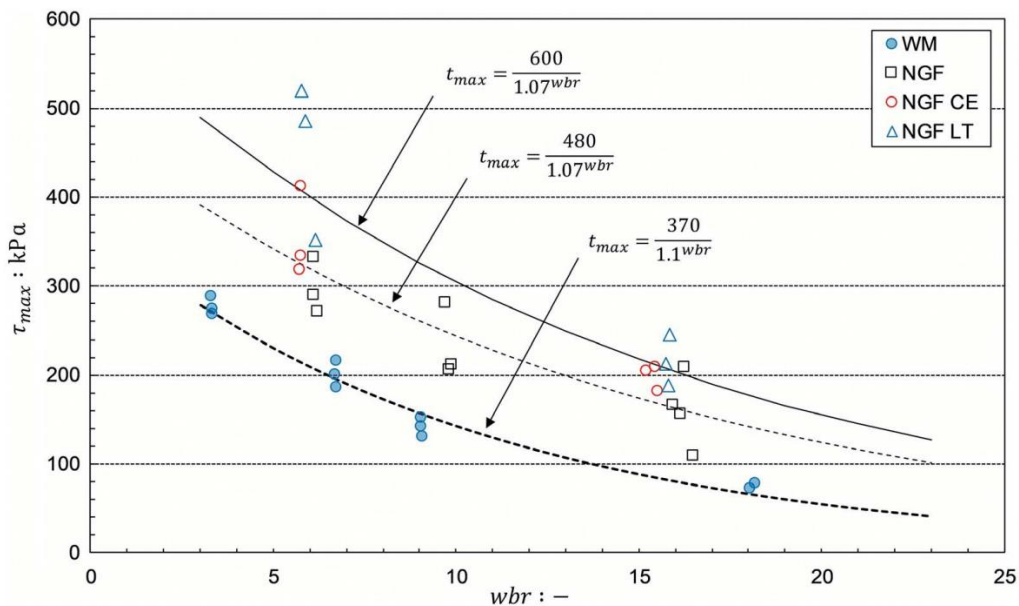


Figure 8: Water to binder ratio (wbr) vs shear strength ( $\tau_{max}$ ) for both wet (WM) and dry (NGF, NGF CE and NGF LT) mixing methods (Hov et al., 2022).

## 2.2.5. Reactions

Cement is a hydraulic binder, meaning it starts to cure when exposed to water alone (Jacobsen et al., 2022). Water ( $H_2O$ ) is referred to as  $H$  in the shortened chemical notations and can be pore water naturally occurring in the soil and/or added water in the wet mixing method. For the hydration of the cement, only the Alite ( $C_3S$ ) and Belite ( $C_2S$ ) reactions are shown (see Eq. 4 and Eq. 5). Aluminate and ferrite is excluded because they contribute much less to the increase in strength.



When the reactions are completed, calcium-silicate-hydrates ( $C_3S_2H_3$ ), mainly referred to as  $CSH$ , is produced.  $CSH$  ensures strength and stiffness, as well as durability properties to the stabilized soil. The residual  $CH$  ( $Ca(OH)_2$ ) from the cement hydration also contribute to forming more  $CSH$  through the pozzolanic reactions.

Pozzolanic materials are silicon- and aluminium containing amorphous and crystalline fine powders. They do not have binder abilities by themselves, but they can react with water and  $CH$  to create additional  $CSH$  (Jacobsen et al., 2022). PSA and GGBS are both pozzolanic materials, but they also contain a large amount of reactive calcium oxide  $CaO$ , often called lime/quicklime. Latent hydraulic binders can in addition to  $CH$  be activated by sulphate rich solutions (usually calcium sulphate) (Jacobsen et al., 2022). Eq. 6 shows the initial exothermic reaction of quicklime which is present in GGBS (Lindh, 2004). This is more similar to cement hydration than other pozzolanic materials without much  $CaO$ . Eq. 7, Eq. 8 and Eq. 9 shows the simplified pozzolanic reactions (Jacobsen et al., 2022; Åhnberg, 2006). The amount of different reaction products can vary, but they are all variants of  $CSH$  with similar strength properties.



Pozzolanic reactions are also dependent on a high pH environment. A high pH (>10-11) ensures that both silica and alumina are soluble (Lindh, 2004). Clay can also contain silica and alumina, which contribute to additional pozzolanic reactions. Cement (or lime) is a good facilitator for pozzolanic reactions because a pH of around 13 is achieved from the created hydration products.

The presence of  $CaO$  also gives a stabilizing effect caused by ion exchange and subsequent flocculation (Bache et al., 2021; Lindh, 2004). This effect is most present in the first seconds to hours after mixing. A surplus of  $Ca^{2+}$  ions in the pore water results in an exchange of ions (mainly  $Na^+$  and  $K^+$ ) on the clay particle surface. The flocculation of the clay particles causes them to go from a plate-like structure to a needle-like structure with a much coarser texture.

Reaction speeds vary greatly between different binders. An overview of reaction types and typical timeframes for significant strength increase is shown in Table 8. Controlling the amount of water is important because of the “drying” effect hydration has on the soil. When performing DDM in soils with a low natural water content, it is also important to control the heat development. Too much heat can evaporate water required in the hydration reactions, resulting in lower final strength (Lindh, 2004).

Table 8: Binder reaction types and common timeframe of main strength increase (Janz & Johansson, 2002).

| Binder                                | Reaction type                    | Main strength increase timeframe |
|---------------------------------------|----------------------------------|----------------------------------|
| Cement                                | Hydraulic                        | Days                             |
| Quicklime                             | Pozzolanic                       | Months                           |
| GGBS<br>(PSA has similar composition) | Latent hydraulic<br>(Pozzolanic) | Weeks                            |
| Fly ash                               | Pozzolanic                       | Months                           |

### 2.2.6. Blended binder interactions

Using combinations of different binders can have benefits beyond being more cost effective and sustainable. Interactions between binder materials can actually give improved strength and stiffness compared with single binders. Interpolating values from single binder results is not viable, so to find the interactions, laboratory tests have to be performed with different combinations. It is well known that combining lime and cement gives high strength (Janz & Johansson, 2002), but other binders can also give good results from interactions.

Interactions between cement, lime and slag in fine-grained tills were studied as part of a doctoral thesis by Lindh (2004). A clear unconfined compressive strength (UCS) interaction between slag and lime was found, indicating that mixing of the two is beneficial. The tests were performed on silty clay till samples cured at 20 °C for 7, 28 and 90 days. RSM was used to visualize the results shown in Figure 9. The figure also shows single binder performance in which slag gives the lowest strength because a good activation condition was not achieved.

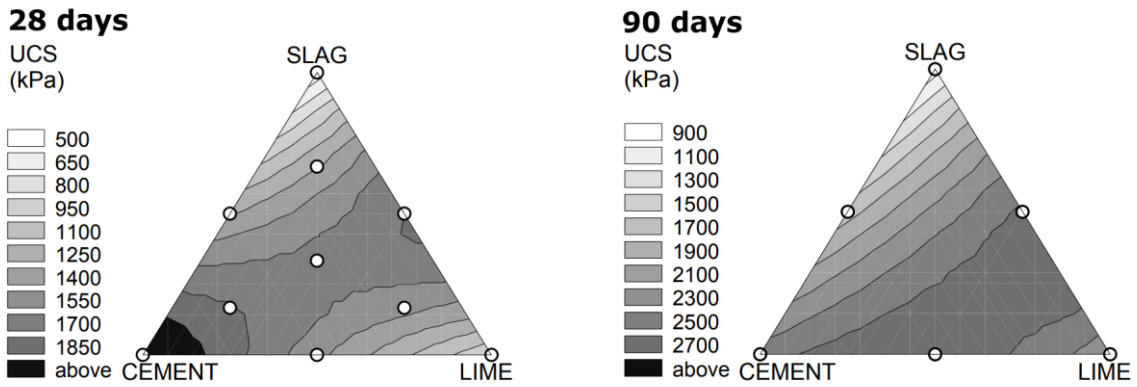


Figure 9: UCS for silty clay till stabilized with cement, lime, and slag. Samples were vibrator-compacted and cured at 20 °C for 28 and 90 days. Modified after (Lindh, 2004).

Interactions between other alternative binders were studied by Wang et al. (2023). Combinations of ground granulated blast furnace slag (GGBS), flue gas desulfurization gypsum (FGDG) and calcium carbide slag (CCS) were compared with the stabilizing effect of ordinary Portland cement. The soil was a soft marine clay which was prepared with a static compaction method. Samples were cured for 3, 7, 14 and 28 days at approximately 20 °C before UCS testing. RSM with a Box-Behnken design (BBD) was used to visualize and model the results. Figure 10 shows the interaction effect between two and two binders as curves in the 3D surfaces. The results showed that an optimal combination of the industry by-products gave a UCS of 25 % above ordinary Portland cement at 28 days of curing.

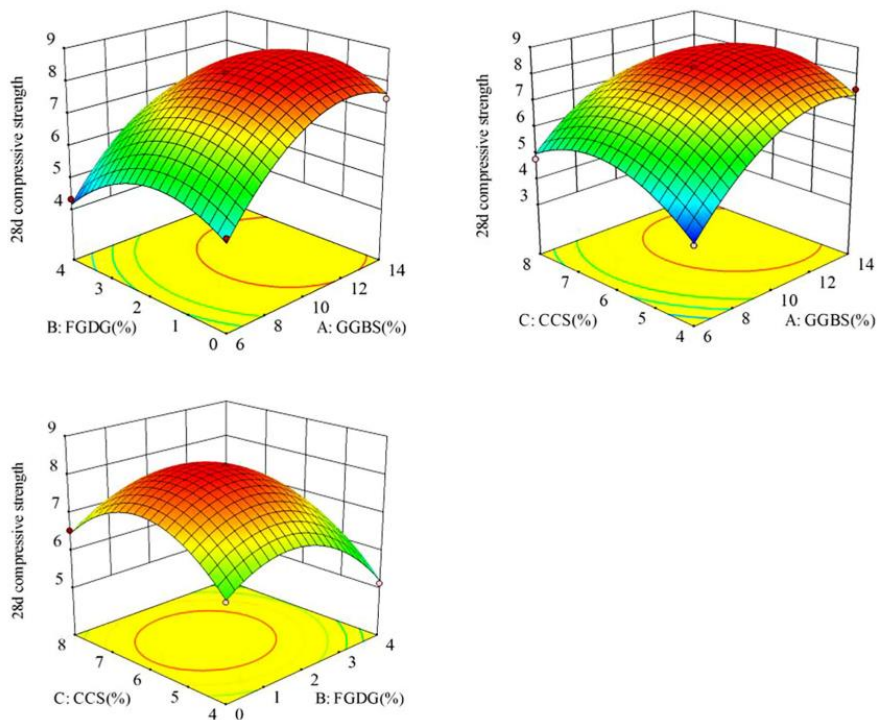


Figure 10: Interactions between GGBS, FGDG and CCS after 28 days of curing at 20 °C. Modified after (Wang et al., 2023).



Pakbaz & Farzi (2015) found diverging interactions between lime and cement depending on if the samples were prepared with the wet or dry mixing method. Figure 11 shows stiffness after 28 days of curing for lime, cement, and a mix of 50 % of each binder. An artificial soil made with 60 % commercial bentonite and 40 % windblown sand was used for the tests.

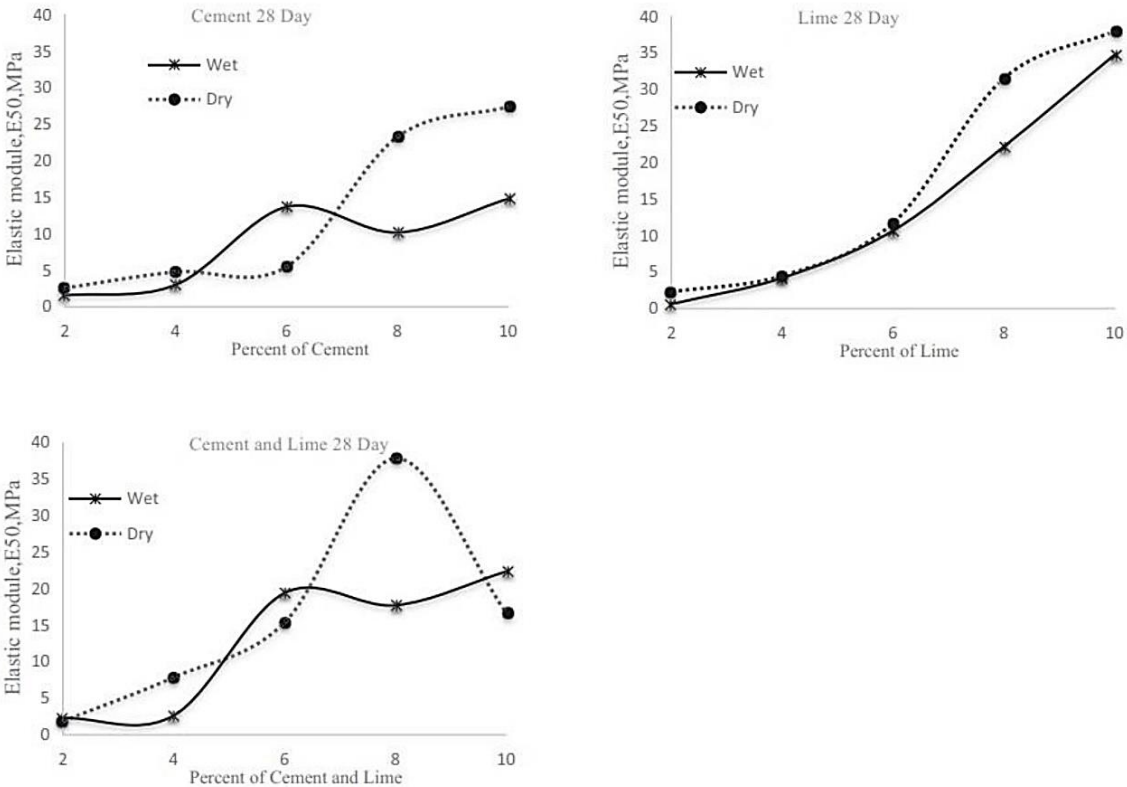


Figure 11: Stiffness at 50 % strength vs percent of binder. Modified after (Pakbaz & Farzi, 2015).

### 2.3 Curing and sample preparation

#### 2.3.1. Field curing

Final engineering properties are not only affected by soil and mixing conditions, binder type, and water to binder ratio. The curing conditions also play a large role when trying to achieve desired properties and quality of the stabilized soil. In the field, curing time and temperature, maturity, and stress conditions are the factors which influence the finished columns the most. Some of these curing factors, like the temperature, can somewhat be controlled during and after installation. Other factors cannot be adapted as easily. Specifics regarding laboratory curing and how it differs from field curing is described in section 2.3.3.

Changing the type of binder will affect both the peak temperature as well as temperature development in the soil, because the hydration reactions are exothermic. The amount of energy released from hydration is highest in quicklime, with a value of 1163 kJ/kg (Boynton, 1980, as cited in Janz & Johansson, 2002). This is over double the energy

released by standard Portland cement, which is around 400-500 kJ/kg (Jacobsen et al., 2022). Pozzolanic materials like blast furnace slag and fly ash both show signs of retarded heat development, making them better suited for situations when lower temperatures are desired (Jacobsen et al., 2022). The surrounding soil conditions also affect the reactions which are temperature sensitive. If the soil temperature is high, the reactions speed up, resulting in a faster temperature development (Janz & Johansson, 2002). To further control the curing temperature during and after installation, planning when the installation is performed, along with installing insulation and heating elements, can be done.

Multiple studies have looked into the described effects of temperature on strength increase in stabilized soil (Kitazume & Terashi, 2013). One study was performed in Sweden by Åhnberg et al. (1995). The study confirmed that a higher developed temperature is achieved when the amount of quicklime is increased. It also concludes that reaction speed increases with temperature which gives quicklime high initial strength development. Another important finding is how the temperature is affected by the chosen pattern of columns, and that the development is possible to model quite accurately. Besides single columns, the most common patterns used in deep stabilization are panels, blocks, and grids (Figure 12).

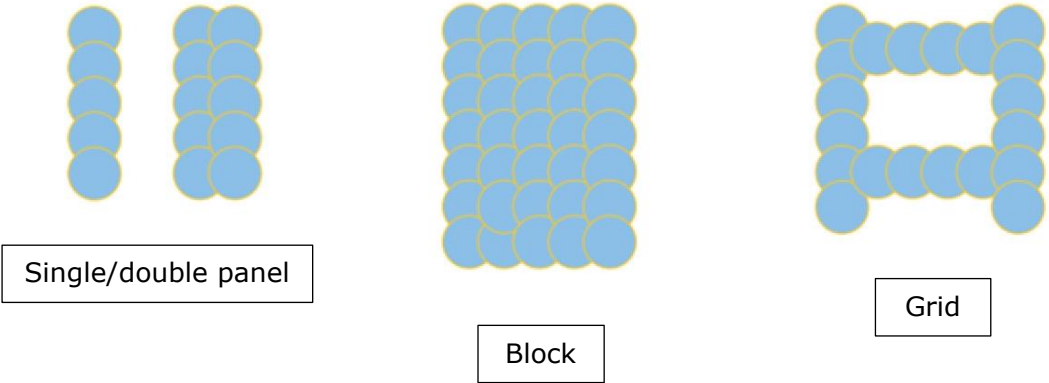


Figure 12: Common deep stabilization patterns. Modified after (NGF, 2012).

Figure 13 shows that the residual heat is preserved when piles are grouped, while the peak temperature is not affected as much. A master thesis by Wiersholm (2018) had the same conclusion regarding the high temperature dependency on strength increase.

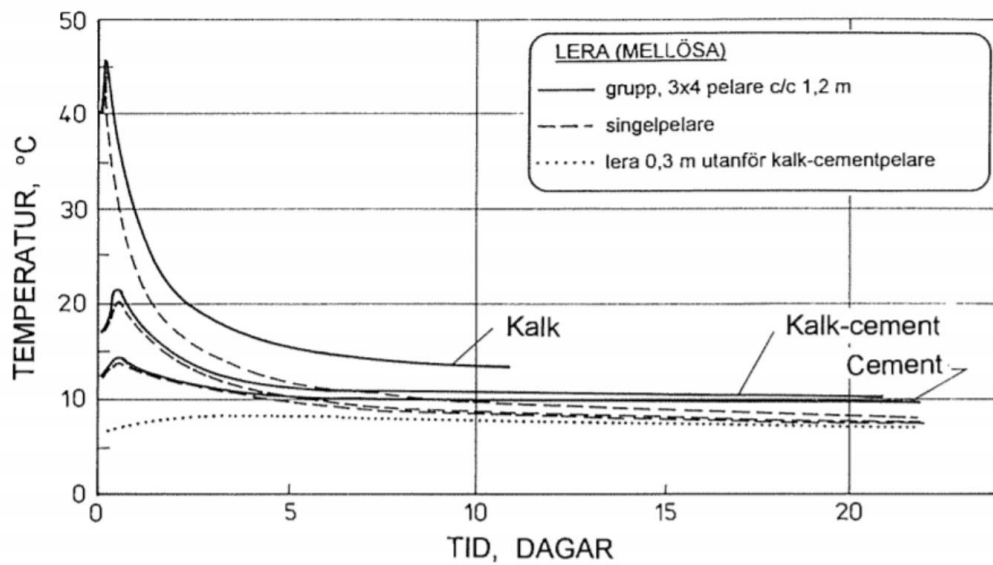


Figure 13: Temperature development (°C) vs time (Days) in stabilized clay using different lime (kalk) and cement binders and patterns. Temperature is measured both inside and outside the finished columns (Åhnberg et al., 1995).

The performance of stabilized soil is most commonly measured by the increase in compressive strength. Most samples are tested for compressive strength at a standard of 28 days. Figure 14 shows the influence of both temperature and time on compressive strength in Japanese silty soil. The interaction of the factors makes it difficult to compare values from field cured samples with laboratory samples exposed to vastly different mixing and curing conditions.

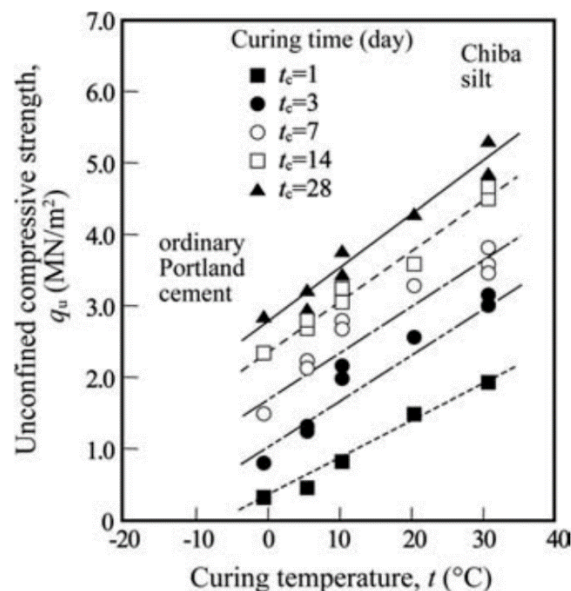


Figure 14: Unconfined compressive strength (kPa) vs curing temperature (°C) at five different curing times (1 day to 28 days) (Enami et al., 1985, as cited in Kitazume & Terashi, 2013).

Even though samples are mostly tested after 28 days, their strength is known to increase significantly in the following months and years. An effect which is not as present in concrete castings. Long term strength gain in laboratory mixed samples with a binder content of 100kg/m<sup>3</sup>, was researched as part of Helen Åhnbergs doctoral thesis (2006). Figure 15 shows how strength increases in two different Swedish clays stabilized with different binders. After an initial quick development, the strength increases mostly linearly after about three months of curing.

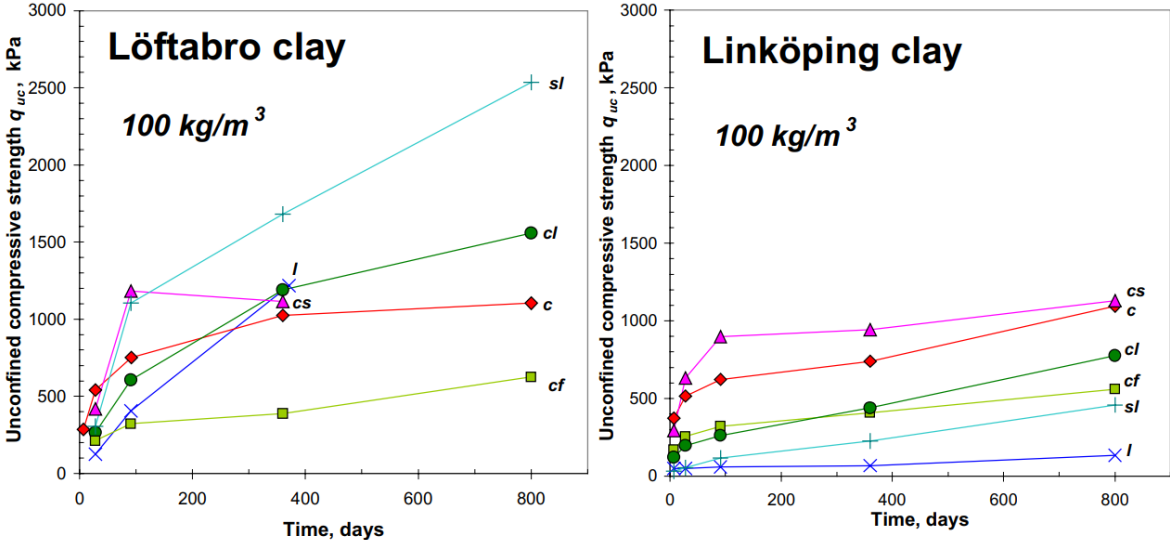


Figure 15: Unconfined compressive strength increase (kPa) vs time (days) in two Swedish clays using (combinations of) cement (c), slag (s), lime (l) and fly ash (f). Modified after (Åhnberg, 2006).

Often times, field samples cannot be transported and tested at exactly 28 days. To back calculate strength in samples cured at varying periods and temperatures, the concept of maturity is often used in concrete engineering. The maturity is a virtual age of the concrete equivalent to a 20 °C curing temperature (Jacobsen et al., 2022), but calculation parameters are difficult to measure and control in field samples. This makes it especially tough to calculate short term strength, while long term strength is more predictable. A relation between 28-day compressive strength ( $q_{u,28}$ ) and ultimate compressive strength ( $q_u$ ), which is only dependent on time ( $t$ ), can be found empirically. One such relation (Eq. 10) was suggested by Åhnberg (2006) for cement stabilized soil. The formula assumes curing at 7 °C and a curing time between 7 and 800 days.

$$\frac{q_u}{q_{u,28}} = 0.3 * \ln(t) \tag{Eq. 10}$$

The curing stress, which is mostly decided by the specific installation depth, also affects the obtained strength. This is also a main way field curing diverges from laboratory curing described in section 2.3.3. Stress dependency in laboratory samples was the focus of a master thesis by Engeset (2018). When increasing both the horizontal and vertical curing stress, the research showed increasing values of strength, density, and cohesion. Figure 16 shows the rising shear strength when increasing the curing stress up to 400 kPa. The test was performed in a triaxial apparatus with 0 kPa radial pressure, giving a test equivalent to that of a uniaxial compression test (UCT).

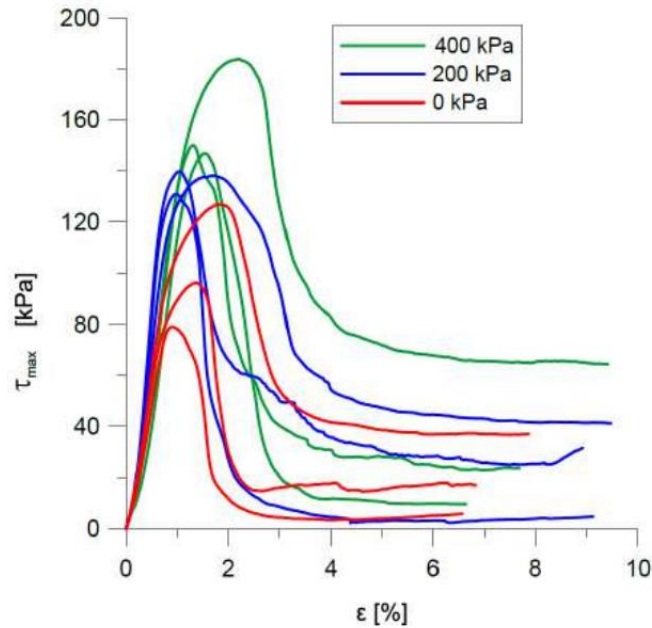


Figure 16: Shear strength ( $\tau_{max}$ ) vs axial strain ( $\epsilon$ ) relation from samples cured at 0 kPa, 200 kPa and 400 kPa. Triaxial radial pressure set to 0 kPa. Modified after (Engeset, 2018).

The curing stress can under some conditions be altered by an external load to achieve higher strength. This is especially effective in peat, shown as part of the thesis by Åhnberg (2006).

### 2.3.2. Laboratory molding technique

The laboratory molding technique describes how the finished, standardized test samples are made from batches of mixed clay. This is an important step in the quality control in deep stabilization projects. Guidelines in Norway and Japan describe the required test procedures with different descriptions of molding techniques (Kitazume & Terashi, 2013; NGF, 2012). Multiple studies prove the importance of molding technique and how it affects further testing. Still, there is a wide variety of different techniques in use depending on who executes the laboratory work.

In Norway, the most prevalent mixing method is dry mixing. This mixing method usually produces stiffer samples which can create difficulties in the molding process. A master thesis by Fredrik Falle (2021) tries to find the ideal molding technique for reproducing dry mixing field sample results. His findings resulted in recommending a dynamic compaction method (called the NGF-method) to produce samples with high strength, stiffness, and density. Still, he concluded that the laboratory results were not sufficiently accurate enough to be directly used as design values in the field.

Internationally, the wet mixing method is much more prevalent than dry mixing. This discrepancy also affects laboratory work. One of the most detailed studies on laboratory molding techniques internationally is by Kitazume et al. (2015), with a goal of finding the superior molding technique in varying conditions across geographical locations. Four

research groups in Asia and Europe conducted the experiments. The study lists the most common molding techniques as follows:

- Tapping (TP): The sample is tapped a set number of times directly against a hard surface for each layer used to fill the mold.
- Rodding (RD): Each layer used to fill the mold is slowly tamped down with a steel rod a set number of times. Excess material on the rod is pushed down into the mold if necessary.
- Dynamic compaction (DC): Each layer used to fill the mold is compacted by special equipment utilizing a falling weight. Both the fall height and number of blows is set in each compaction.
- Static compaction (SC): Each layer used to fill the mold is compacted by special equipment applying a set pressure on the surface for a set amount of time.
- No compaction (NC): Simply pouring or placing the finished mix into the mold and using no further agitation.

All participants followed similar methodology to prepare cylindrical samples with a two to one height to diameter ratio, but with varying binder and soil types. This resulted in two main soil characteristics (i.e. undrained shear strength and liquidity index) being considered as good for finding ideal molding technique. Across most conditions and situations, the method found to be most applicable for producing reliable samples was the rodding technique.

When doing unconfined compression testing, the cylindrical shape used during laboratory molding typically results in an hourglass shaped fracture pattern for concrete samples (Figure 17). Concrete expands laterally when compressed, which would in theory result in vertical failure planes. In practice however, the sample is prevented from expanding at the ends. This is caused by the friction between the sample and the steel load frame which creates an hourglass-shaped failure pattern (Jacobsen et al., 2022).



Figure 17: Typical concrete cylinder sample fracture pattern (Jacobsen et al., 2022).

### **2.3.3. Laboratory curing**

The performance of the laboratory cured samples are affected by the same factors as the field cured samples described in section 2.3.1. It is however not easy to match the field curing parameters in the laboratory. The field stress conditions are especially difficult and expensive to replicate, which causes, among other things, the samples to have lower

compressive shear strength. The standard laboratory procedure is to cure laboratory samples without applying a curing stress, but assuming a higher field strength will be achieved. This is in line with findings in most Nordic studies (Paniagua et al., 2022a). Some other countries have differing experiences, but this is possibly due to different laboratory procedures. In Japan for example, it is well known that a lower field strength is expected compared with laboratory mixed specimens (Kitazume & Terashi, 2013).

Due to these differences, studies often focus on researching which curing and mixing factors affect performance, and why. One study by Paniagua et al. (2022b) uses X-ray micro computed tomography to assess homogeneity in both field, and laboratory mixed samples. Dry mixing is used to prepare the laboratory samples. The results showed that the samples mixed in the laboratory had much higher values of porosity. Observed porosity values were 0.5 to 1.6 % in the field samples and 6.9 to 18.0 % in the laboratory samples. The porosity, which mostly is a result of entrained air during mixing, gave the laboratory samples lower strength and stiffness. Figure 18 shows  $\mu$ CT images of field and laboratory stabilized samples stabilized with a binder content of  $50\text{kg/m}^3$ . The grey binder is clearly denser in the field stabilized sample.

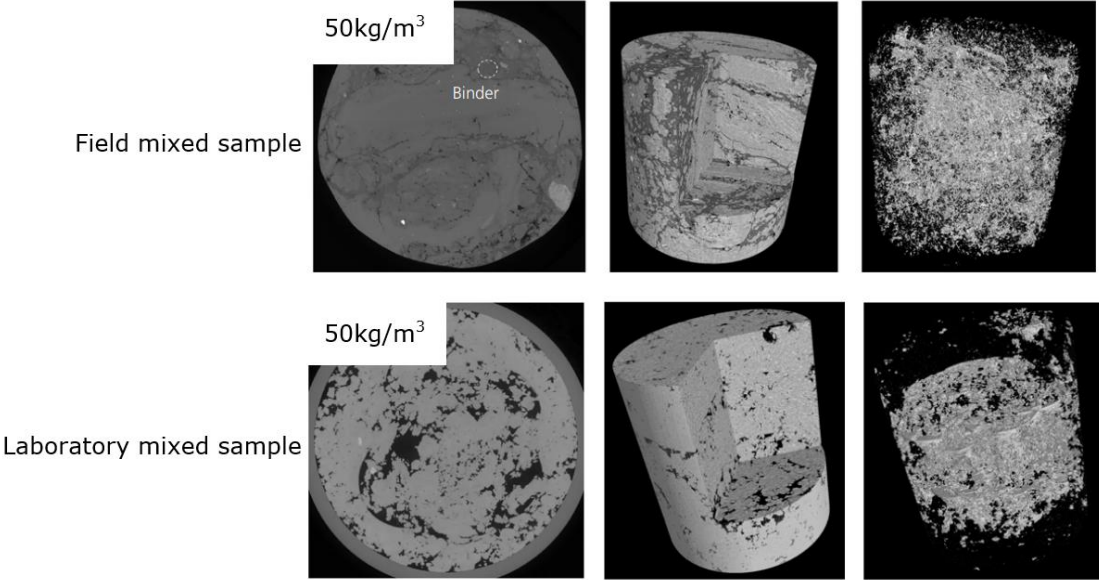


Figure 18: Processed  $\mu$ CT images showing macro-porosity in field and laboratory mixed samples with a binder content of  $50\text{kg/m}^3$ . Modified after (Paniagua et al., 2022b).

A destructive approach can also be used to create three dimensional reconstructions of stabilized samples. One study by Amrioui et al. (2023) shows that a suggested method of photographing sample slices before doing software reconstruction can capture soil inclusions which are otherwise invisible when using typical  $\mu$ CT. This gives an improved evaluation of sample homogeneity.





surrounding area is shown in Figure 20. The terrain is relatively flat, with forests lining most of the shoreline.

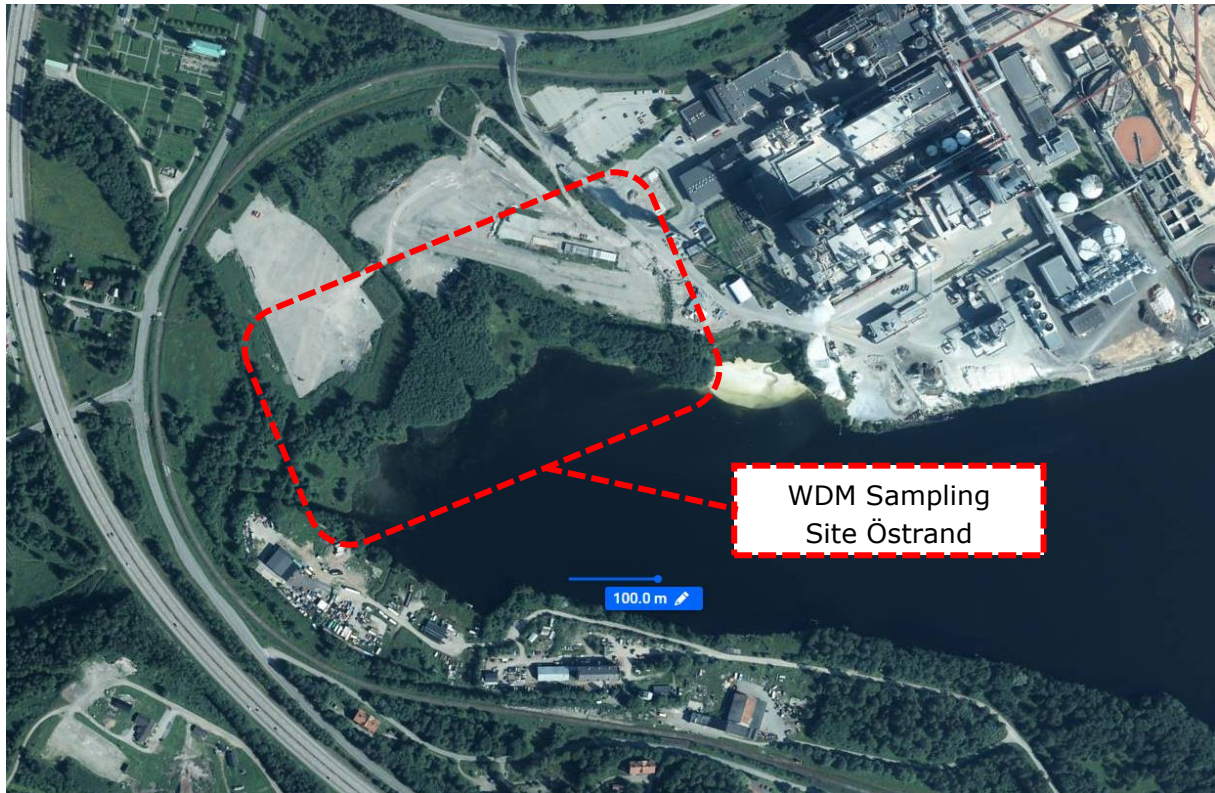


Figure 20: Aerial photo of the area surrounding the Östrand WDM sampling site (Eniro, n.d.).

Deposits at the Östrand site consists mostly of clay and silt, with some areas containing peat/bog/mud. The shoreline south of the site was formed during a previous land reclamation. An overview of the quaternary geology in the area is shown in Figure 21.

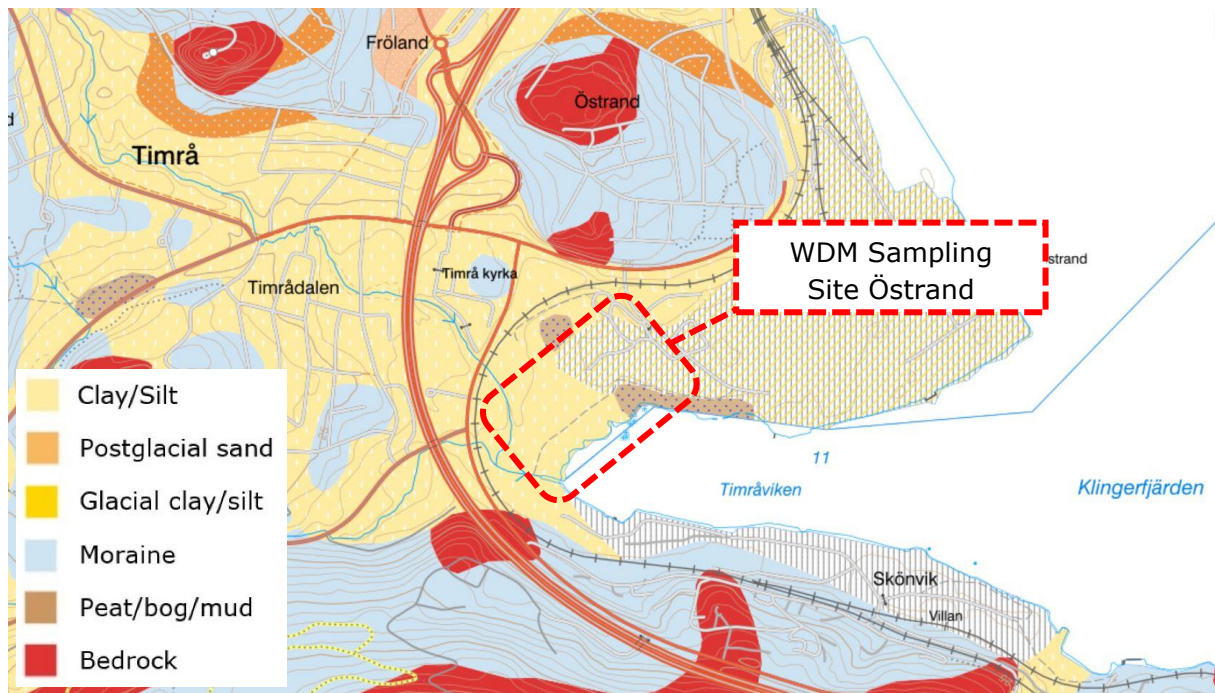


Figure 21: Quaternary geology map of the area surrounding the Östrand WDM sampling site. Previous land reclamation is shown as a grey shaded area (SGU, n.d.).

Ground improvement at the Hjorthagen site begun in 2022 (Stockholms stad, 2022). The project includes construction of 1500 new homes and is a collaboration between Stockholm municipality and 9 independent developers. The footprint of new construction is located next to a recently developed area and will cover part of the empty and undeveloped lot, as well as expanding into the water. An aerial photo of the surrounding area is shown in Figure 22. The terrain is slightly sloped from the developed residential area towards the water, with limited greenery.

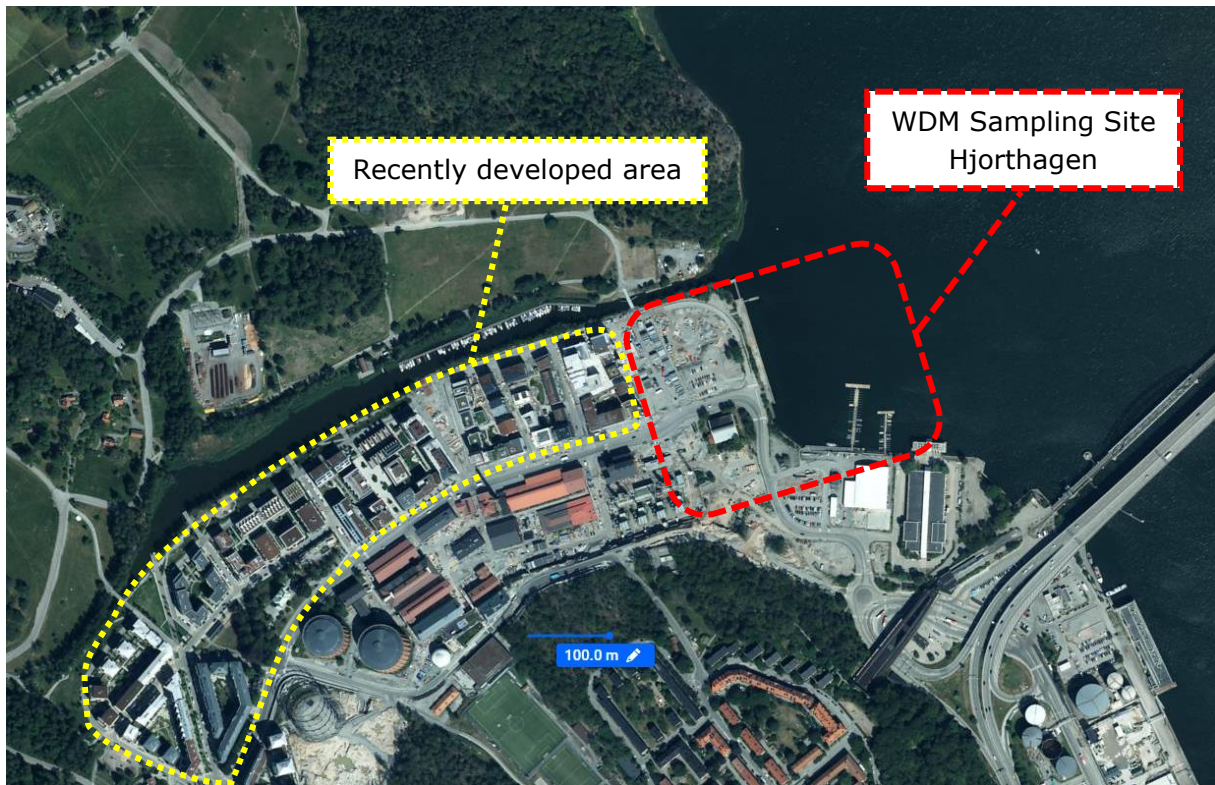


Figure 22: Aerial photo of the area surrounding the Hjørthagen WDM sampling site. The yellow dotted line shows the recently developed area (Eniro, n.d.).

From the quaternary geology map in Figure 22, it can be observed that the Hjørthagen project is purely a land reclamation project. Deposits in the surrounding area contain mostly glacial clay and silt, with some moraine. Sloping bedrock is present to the south of the site.

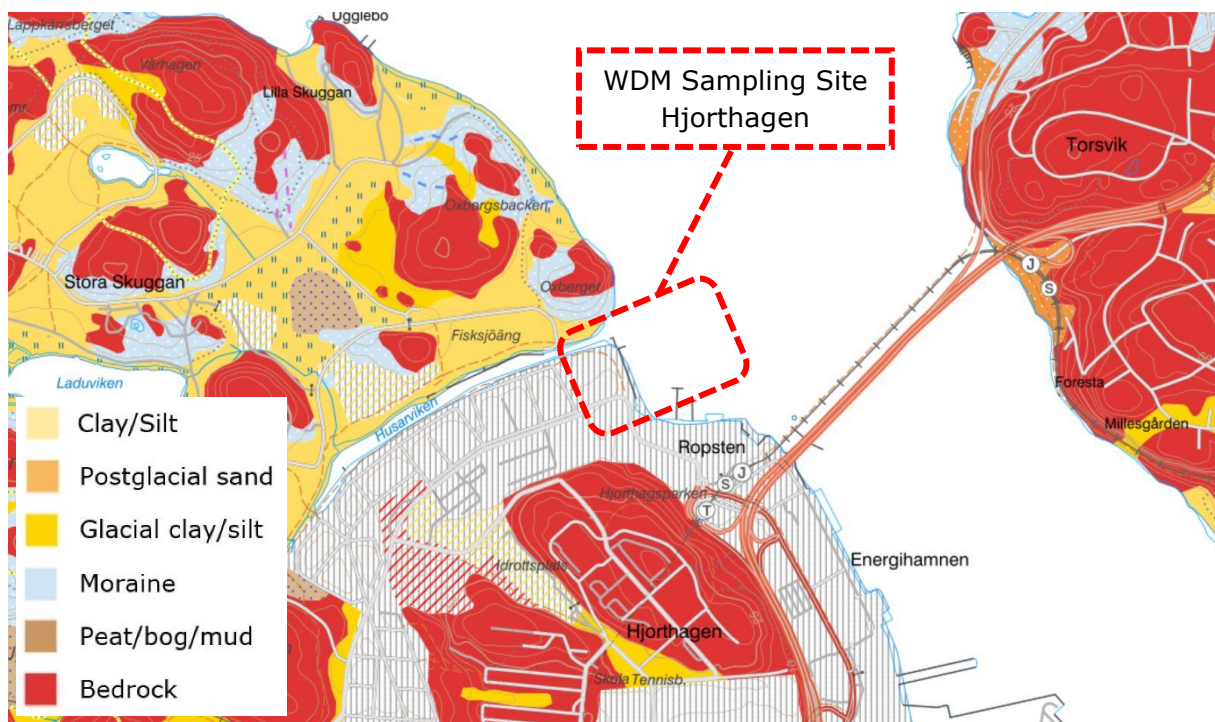


Figure 23: Quaternary geology map of the area surrounding the Hjorthagen WDM sampling site. Previous land reclamation is shown as a grey shaded area (SGU, n.d.).

The installation parameters of the WDM piles installed in the Östrand and Hjorthagen sites are presented in Table 9.

Table 9: Overview of installation parameters in the WDM projects. Data provided by NGI.

| Site       | Pile ID | Binder type  | Binder content, $\alpha$ [kg/m <sup>3</sup> ] | Blade rotation number, $T$ [n/m] | Installation period |
|------------|---------|--------------|---|----------------------------------|---------------------|
| Östrand    | P03.1   | 100 % cement | 200   | 666                              | December 2022       |
| Hjorthagen | D02.    | 100 % cement | 115   | 800                              | March 2022          |

The modified dry mixing samples were collected from an ongoing infrastructure project in the Stjørdal area, about 25 km northeast of Trondheim, Norway. The site is referred to as E6 Kvithammar-Åsen and can be seen on the overview in Figure 19. As part of the project, a bridge connecting the existing highway to a new tunnel is being constructed. NGI has the role of geotechnical sub-adviser in the bridge project (NGI, 2022). An aerial photo of the approximate position of the new highway and surrounding area is shown in Figure 24. The terrain is currently being used for agricultural purposes and is relatively flat. Some dips and ravines containing flowing water is also present in the area, the largest being Vollselva.

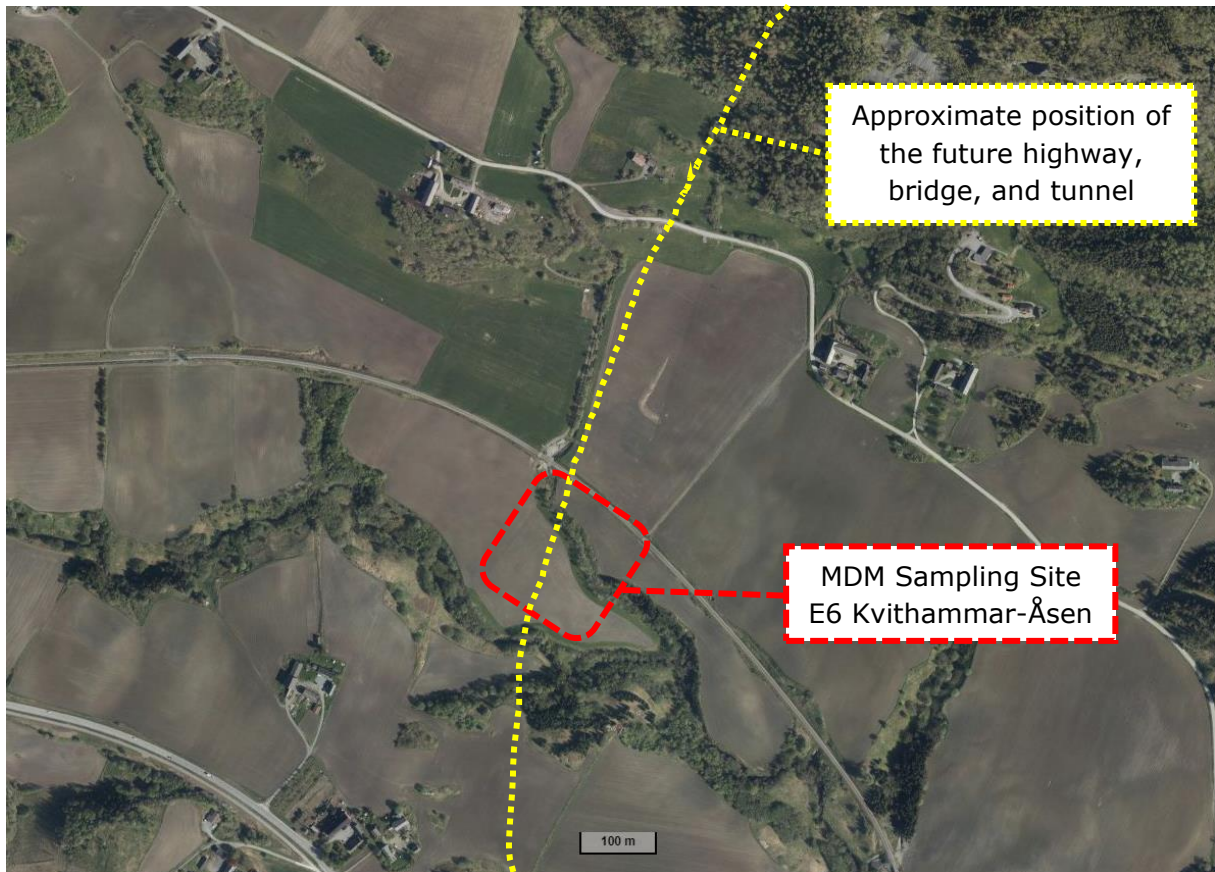


Figure 24: Aerial photo of the area surrounding the E6 Kvithammar-Åsen MDM sampling site. The yellow dotted line shows the approximate position of the updated highway (Kartverket, n.d.).

Deposits at the E6 Kvithammar-Åsen site mostly consist of marine sediments created after the increase in terrain elevation during the Holocene. The deposits in the surrounding area, along with the marine limit, can be seen on the quaternary geology map in Figure 25.

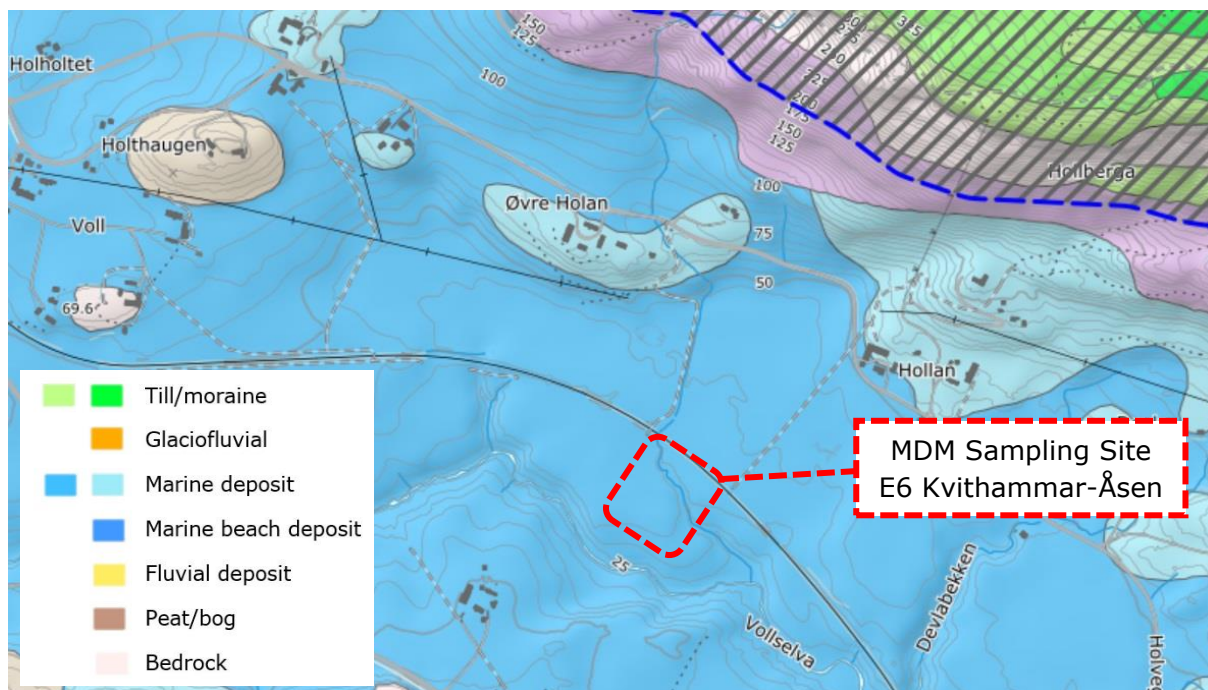


Figure 25: Quaternary geology map of the area surrounding the E6 Kvithammar-Åsen MDM sampling site. The grey shaded area is above the marine limit (NGU, n.d.).

The installation parameters of the MDM piles installed in the E6 Kvithammar-Åsen site is presented in Table 10. Water content in the soil varied between 50 and 80 l/m<sup>3</sup> during installation.

Table 10: Overview of installation parameters in the MDM project. Data provided by NGI.

| Site               | Pile ID | Binder type  | Binder content, $\alpha$ [kg/m <sup>3</sup> ] | Blade rotation number, $T$ [n/m] | Installation period |
|--------------------|---------|--------------|---|----------------------------------|---------------------|
| E6 Kvithammar-Åsen | Unknown | 100 % cement | 100   | 250                              | Summer 2022         |

### 3.1.2. Field sampling and preparation

The MDM samples from E6 Kvithammar-Åsen were collected on November 15<sup>th</sup>, 2022. An excavator was used to break off pieces of stabilized material, shown in Figure 26. Paint markings were used to indicate the vertical orientation of the pieces, which weighed between 5 and 15 kg.



Figure 26: Collecting MDM samples using an excavator.

A trifle tube sampler with a diameter of 100 mm was used to collect WDM samples from Östrand and Hjorthagen. The samples were sealed in plastic and carefully packaged before being shipped to the laboratory in Trondheim.

All field samples were sealed in at least two layers of plastic until February 23<sup>rd</sup>, when the samples were opened and trimmed. A core drill with an internal diameter of 102 mm was used to trim the blocks of MDM material to a cylinder shape. Due to limitations of the core drilling equipment, a maximum height of 100 mm was achieved for the finished MDM samples. Figure 27 and Figure 28 shows the field samples before and after trimming. Samples with excessive damage or cracking were discarded. Some imperfections in the samples were unavoidable due to the presence of larger stones in the clay.



Figure 27: MDM sample before and after trimming.



Figure 28: WDM sample before and after trimming.

An overview of the trimmed field samples and intended method of testing is presented in Table 11. Depth information is only available for the Östrand samples.



Table 11: Trimmed field sample overview.

| Sample ID <sup>[1]</sup>  | Height [mm] | Diameter [mm] | Project (depth information) | Testing method <sup>[2][3]</sup> |
|---|-------------|---------------|-----------------------------|----------------------------------|
| WDM.Östrand.1   | 150         | 100           | Östrand (≈3 m)              | μCT<br>PUNDIT                    |
| WDM.Östrand.2   | 150         | 100           | Östrand (≈6 m)              | μCT<br>PUNDIT                    |
| WDM.Östrand.3   | 150         | 100           | Östrand (≈6 m)              | μCT<br>PUNDIT                    |
| WDM.Hjorthagen.1  | 150         | 100           | Hjorthagen                  | μCT<br>PUNDIT                    |
| WDM.Hjorthagen.2  | 150         | 100           | Hjorthagen                  | μCT<br>PUNDIT                    |
| WDM.Hjorthagen.3  | 150         | 100           | Hjorthagen                  | μCT<br>PUNDIT                    |
| MDM.E6.1  | 100         | 102           | E6 Kvithammar-Åsen          | μCT<br>PUNDIT                    |
| MDM.E6.2  | 100         | 102           | E6 Kvithammar-Åsen          | μCT<br>PUNDIT                    |
| MDM.E6.3  | 100         | 102           | E6 Kvithammar-Åsen          | μCT<br>PUNDIT                    |
| <p>[1] Sample ID explanation: WDM. Östrand.1 = Installed with the WDM method, field sample from the Östrand site, sample number 1</p> <p>[2] μCT = Micro Computed Tomography</p> <p>[3] PUNDIT = P-wave testing using PUNDIT ultrasonic equipment</p> |             |               |                             |                                  |

## 3.2 Laboratory samples

### 3.2.1. Clay

The clay used to prepare the laboratory stabilized samples is very sensitive clay collected from the Tiller-Flotten research site. The site can be seen on the overview in Figure 19, and is located about 10km south of Trondheim. It was developed through the Norwegian GeoTest site (NGTS) project as one of five benchmark sites to improve our understanding of different soil types and conditions (L'Heureux et al., 2017). An aerial photo of the area surrounding the research site is shown in Figure 29. The terrain sits at an elevation of 125 m.a.s.l. and is mostly flat, consisting partly of agricultural land and part forest.



Figure 29: Aerial photo of the area surrounding the Tiller-Flotten research site (Kartverket, n.d.).

The map of quaternary geology in Figure 30 shows deposits of mainly marine sediments, with a thickness of about 50 meters (L'Heureux et al., 2019). Some peat/bog is present in the area covered by greenery. Elevation increases south of the site, where deposits of moraine /till follows the border of the marine limit. In the Trondheim region, the marine limit is around 175 m.a.s.l. (NVE, n.d.).

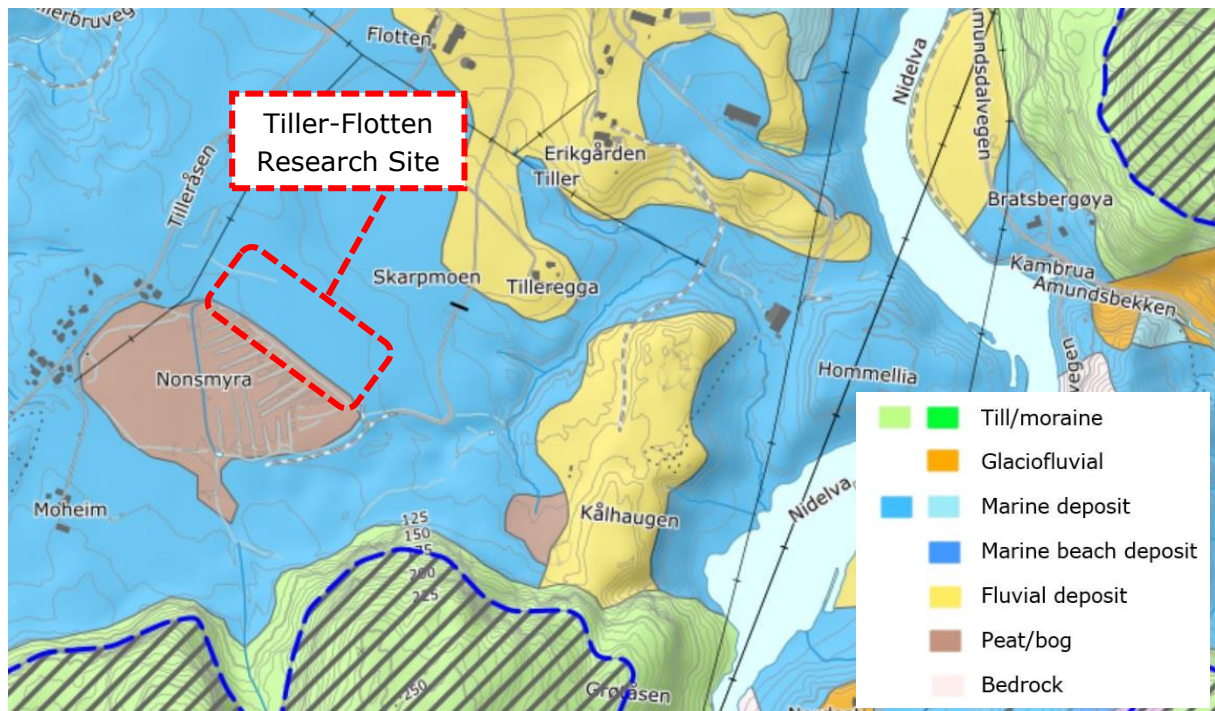


Figure 30: Quaternary geology map of the Tiller-Flotten research site. The grey shaded area is above the marine limit (NGU, n.d.).

The soil conditions were thoroughly tested and characterized in a study published as a research article in 2019 (L'Heureux et al.). Previous studies of conditions in the area were also included in the research. Due to the substantial deposit thickness, soil properties vary greatly in some areas. The first 7.5 meters below surface level consist of clay with low to medium sensitivity. The sensitivity ( $S_t$ ) increases to around 200 when reaching 20 meters below the surface. All of the Tiller-Flotten material collected and tested for this thesis is characterized as quick clay. Quick clay is a highly sensitive clay which can be found in large areas over Norway, Sweden, Finland and Canada (L'Heureux et al., 2017). The properties of the quick clay layer is therefore the main focus in the following paragraphs.

Previous geological history has given the sensitive clay an overconsolidation ratio (OCR) of 1.5-2.0 at depths exceeding 10 meters (L'Heureux et al., 2019). The groundwater table is observed from installed piezometers at 1-2 meters below surface level. The preconsolidation pressure which causes increased OCR, along with piezometer measurements, is shown in Figure 31. The clay content in the sensitive layer is observed to decrease with depth, from around 70 % at 7.5 m to around 50 % at 19 m. Still, this value greatly exceeds the defined clay classification limit of 30 % (NGF, 2011). Another indication of quick clay is low salt content in the pore water from ground water leeching. The salt content in sea water is around 35 g/l, while salt content in the sensitive clay is 2.1 g/l and 2.6 g/l at 8 and 15 meter depth, respectively.

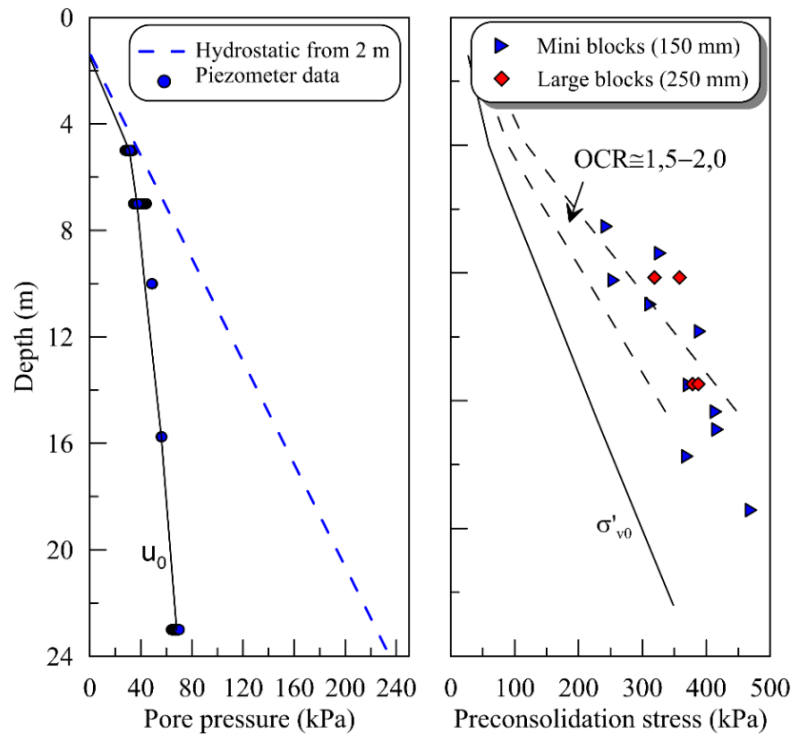


Figure 31: Graphs of pore pressure measurements vs depth (left) and preconsolidation stress vs depth from 1D oedometer testing (right) (L'Heureux et al., 2019).

The natural water content in the clay ( $w$ ) decreases slightly with depth, from around 50 % at 5 meters to 30-35 % at 20 meters (L'Heureux et al., 2019). Water content is corrected through further measurements during testing. Undrained remolded shear strength ( $S_{ur}$ ) falls below 0.5 kPa at depths exceeding 7.5 meters, while the undrained shear strength ( $S_u$ ) is above 30 kPa, making it a quick clay according to NGF (NGF, 2011).

The most relevant soil parameters for the sensitive clay layer at depths between 11 and 20 meters is shown in Table 12. These base values are further used for deciding optimal sample preparation technique as well as for calculating correct water to binder ratio and water content in each recipe. An undrained shear strength comparison can also be made after the stabilized material is tested.

Table 12: Approximate parameters for Tiller-Flotten quick clay at depths between 7.5 and 20 meters (L'Heureux et al., 2019).

| Parameter                         | Symbol   | Unit     | Value    |
|-----------------------------------|----------|----------|----------|
| Water content                     | $w$      | %        | 30-50    |
| Plastic limit                     | $w_p$    | %        | 21-22    |
| Liquid limit                      | $w_L$    | %        | 30-35    |
| Plasticity index                  | $I_p$    | %        | 8-15     |
| Liquidity index                   | $I_L$    | %        | 1.6-9.3  |
| Bulk/total unit weight            | $\gamma$ | $kN/m^3$ | 17-19    |
| Overconsolidation ratio           | $OCR$    | -        | 1.5-2.0  |
| Undrained shear strength          | $S_u$    | $kPa$    | 40-80    |
| Remolded undrained shear strength | $S_{ur}$ | $kPa$    | 0.15-0.5 |
| Sensitivity                       | $S_t$    | -        | 150-200  |
| Clay content                      | -        | %        | 50-75    |
| Salt content                      | -        | $g/l$    | 2.1-2.6  |

Results from an X-ray fluorescence (XRF) analysis of the Tiller-Flotten quick clay was provided by NGI. XRF is performed by exposing samples to high energy x-ray radiation and measuring the emitted fluorescent radiation which is characteristic for given elements (NGU, 2020). The results show accurate specific oxide composition of the tested material. An overview of the major elements found in the clay is shown in Table 13.

Table 13: Major elements in Tiller-Flotten quick clay from XRF analysis.

| Tiller-Flotten quick clay |                |
|---------------------------|----------------|
| Oxide                     | Composition[%] |
| $Na_2O$                   | 2.01           |
| $MgO$                     | 5.86           |
| $Al_2O_3$                 | 16.97          |
| $SiO_2$                   | 51.04          |
| $P_2O_5$                  | 0.13           |
| $SO_3$                    | 0.02           |
| $K_2O$                    | 4.05           |
| $CaO$                     | 3.22           |
| $TiO_2$                   | 0.75           |
| $Cr_2O_3$                 | 0.03           |
| $Mn_2O_3$                 | 0.15           |
| $Fe_2O_3$                 | 9.28           |
| $ZnO$                     | 0.02           |
| $BaO$                     | 0.10           |
| LOI (Loss On Ignition)    | 5.60           |

Sampling information for the specific material used during the laboratory work is shown in Table 14.

Table 14: Overview of Tiller-Flotten quick clay collected for laboratory testing.

| Sampling type                  | Diameter [mm] | Sampling date | Project number | Sample hole | Depth [m]   |
|--------------------------------|---------------|---------------|----------------|-------------|-------------|
| Steel cylinder piston sampling | 54            | 10.01.23      | 6623           | 6623#3      | 7.0-8.0     |
| Steel cylinder piston sampling | 54            | 25.01.23      | 6623           | 6623#7      | 7.0-8.0     |
| Steel cylinder piston sampling | 54            | 11.01.23      | 6623           | 6623#5      | 7.0-8.0     |
| Steel cylinder piston sampling | 54            | 30.01.23      | 6623           | 6623#8      | 7.0-8.0     |
| Steel cylinder piston sampling | 54            | 19.01.23      | 6623           | 6623#3      | 8.0-8.8     |
| Steel cylinder piston sampling | 54            | 10.01.23      | 6623           | 6623#3      | 8.0-9.0     |
| Steel cylinder piston sampling | 54            | 30.01.23      | 6623           | 6623#7      | 8.0-9.0     |
| Steel cylinder piston sampling | 54            | 11.01.23      | 6623           | 6623#5      | 9.0-10.0    |
| Steel cylinder piston sampling | 54            | 10.01.23      | 6623           | 6623#3      | 9.0-10.0    |
| Steel cylinder piston sampling | 54            | 30.01.23      | 6623           | 6623#7      | 10.0-11.0   |
| Steel cylinder piston sampling | 54            | 20.01.23      | 6623           | 6623#6      | 10.0-11.0   |
| Steel cylinder piston sampling | 54            | 20.01.23      | 6623           | 6623#6      | 11.0-12.0   |
| Steel cylinder piston sampling | 54            | 30.01.23      | 6623           | 6623#7      | 11.0-12.0   |
| Steel cylinder piston sampling | 54            | 30.01.23      | 6623           | 6623#7      | 13.0-14.0   |
| Steel cylinder piston sampling | 54            | 20.01.23      | 6623           | 6623#6      | 13.0-14.0   |
| Mini-block sampler             | 160           | 09.02.23      | MBEWH          | MBEWH       | 8.40-8.70   |
| Mini-block sampler             | 160           | 14.02.23      | MBEWH          | MBEWH       | 10.30-10.65 |

### 3.2.2. Binders

The specific European cement type used for laboratory mixing is NORCEM CEM I 52.5 R, which contains about 91 % clinker, 5 % gypsum and 4 % lime meal filler (NORCEM AS,

2020a). Results from an XRF analysis of the cement was provided by NGI. An overview of the major elements found in CEM I is shown in Table 15.

Table 15: Major elements from XRF analysis for NORCEM CEM I 52.5 R, Norske Skog Skogn PSA and Slagg Bremen GGBS.

| Oxide                     | Composition[%]         |                           |                       |
|---------------------------|------------------------|---------------------------|-----------------------|
|                           | NORCEM CEM I<br>52.5 R | Norske Skog Skogn,<br>PSA | Slagg Bremen,<br>GGBS |
| $Na_2O$                   | 0.34                   | 0.51                      | 0.39                  |
| $MgO$                     | 2.40                   | 2.28                      | 7.92                  |
| $Al_2O_3$                 | 4.58                   | 5.74                      | 12.20                 |
| $SiO_2$                   | 18.79                  | 22.90                     | 36.90                 |
| $P_2O_5$                  | 0.13                   | 0.95                      | <0.003                |
| $SO_3$                    | 3.94                   | 3.30                      | 1.92                  |
| $K_2O$                    | 0.87                   | 0.50                      | 0.58                  |
| $CaO$                     | 61.05                  | 40.90                     | 39.70                 |
| $TiO_2$                   | 0.30                   | 1.17                      | 0.76                  |
| $Cr_2O_3$                 | 0.02                   | 0.03                      | <0.005                |
| $Mn_2O_3$                 | 0.16                   | 0.11                      | Not measured          |
| $Fe_2O_3$                 | 3.30                   | 3.44                      | 0.35                  |
| $ZnO$                     | 0.03                   | 0.39                      | <0.002                |
| $BaO$                     | 0.06                   | 0.11                      | 0.10                  |
| $Mn_3O_4$                 | Not measured           | Not measured              | 0.17                  |
| $NiO$                     |                        |                           | <0.003                |
| $PbO$                     |                        |                           | <0.008                |
| $SrO$                     |                        |                           | 0.06                  |
| $V_2O_5$                  |                        |                           | 0.03                  |
| $ZrO_2$                   |                        |                           | 0.02                  |
| $CuO$                     |                        |                           | <0.004                |
| $HfO_2$                   |                        |                           | <0.004                |
| LOI<br>(Loss On Ignition) |                        |                           | 2.60                  |

The type of fly ash used for laboratory mixing is paper sludge ash (PSA) from Norske Skog Skogn, which is one of the largest newsprint mills in Europe (Norske Skog Skogn, n.d.). According to NGI data, the ash is made from incinerating ~58 % biofuel (demolition wood), ~25 % deinked pulp sludge, ~14 % bio sludge and ~3 % plastic/juice cartons etc. at 850 °C. PSA is sometimes referred to as raw paper material sludge ash (RPMS). Results from an XRF analysis of the paper sludge ash was provided by NGI. An overview of the major elements found in the PSA is shown in Table 15.

The type of ground granulated blast-furnace slag (GGBS) used for laboratory mixing is Slagg Bremen (Thomas Cement AB, 2018b). The slag is produced by Holcim AG in Bremen, Germany, and distributed to the Swedish market by Thomas Cement AB in Uddevalla (Thomas Cement AB, 2018a). XRF analysis of the slag was conducted with help from the Department of Geoscience and Petroleum at NTNU. The PANalytical Zetium 4 kW X-ray

spectrometer was used for analyzing oxide composition. An overview of the major elements found in Slagg Bremen is shown in Table 15.

### 3.2.3. Sample preparation

The recipes of the laboratory sample batches (Figure 33) correspond to the ten chosen lattice points shown in Figure 32. The concept behind the mixture design, called an augmented simplex lattice, is described in section 3.4.3. Binder contents of at least 80 % PSA or GGBS were chosen to ensure proper activation of the binders. Remaining lattice points were distributed evenly on the lattice to improve the reliability of the design.

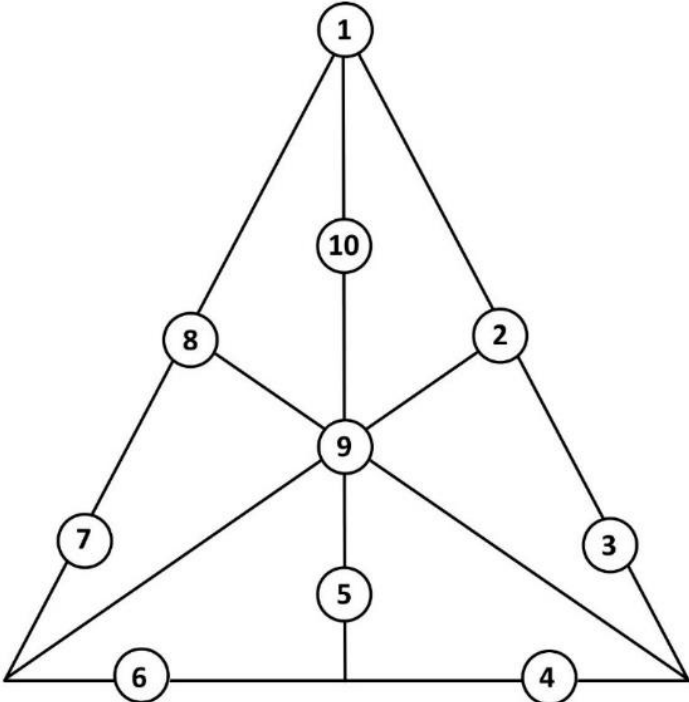


Figure 32: Chosen augmented simplex lattice design.



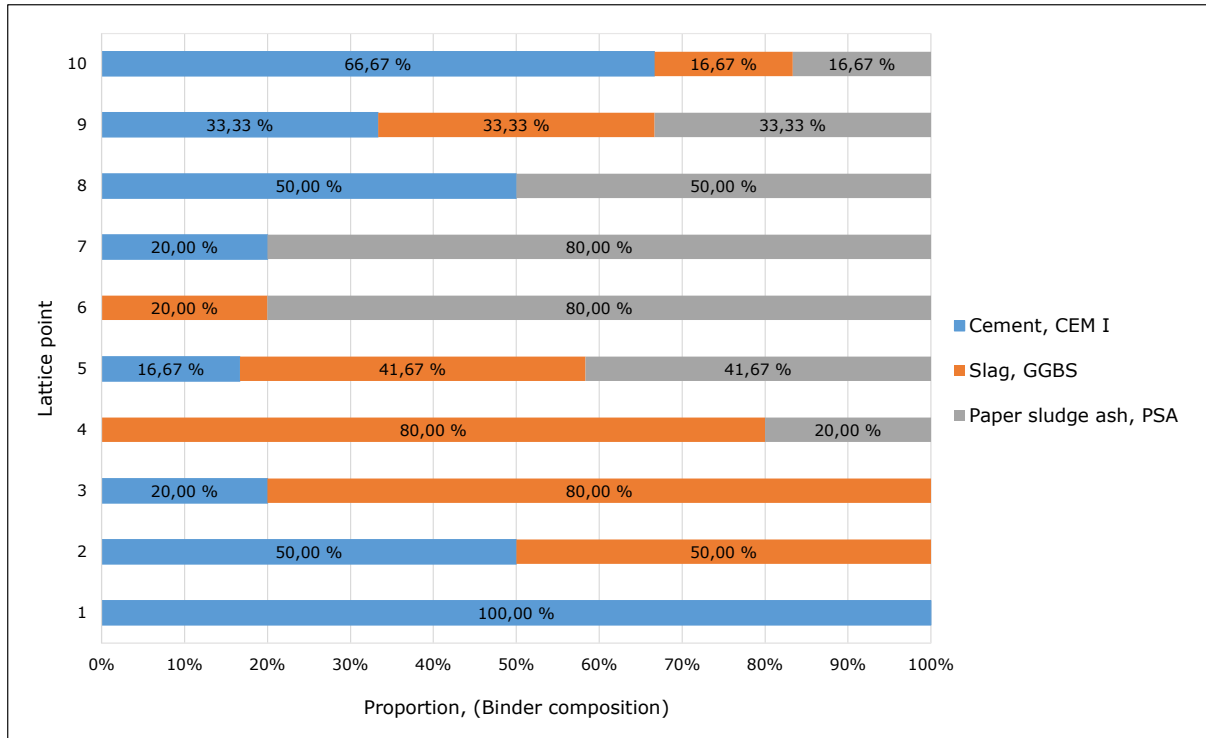


Figure 33: Overview of lattice points and corresponding binder composition.

The specific recipes used during batch preparation are based off known factors and assumptions of the Tiller-Flotten quick clay. An average soil water content ( $w_s$ ) was assumed for each batch, while an average bulk unit weight ( $\bar{\gamma}$ ) was assumed for the entire the layer (L'Heureux et al., 2019). The known factors include the water to binder ratio ( $wbr$ ), mass of soil ( $m_{soil}$ ), sample depth and sample dimensions. An overview of the known and assumed batch mixing factors is shown in Table 16.

Table 16: Batch mixing factors overview.

| Batch mixing factors                     | Value             | Unit                          |
|--|-------------------|-------------------------------|
| Soil water content, $w_s$                | 43-48             | [%]                           |
| Average bulk unit weight, $\bar{\gamma}$ | 18                | $\left[\frac{kN}{m^3}\right]$ |
| Mass of soil, $m_{soil}$                 | 1500              | [g]                           |
| Sample depth                             | 7-14 (Table 14)   | [m]                           |
| Sample height                            | 100               | [mm]                          |
| Sample diameter                          | 54                | [mm]                          |
| Sample volume                            | $\approx 2290.22$ | [mm <sup>3</sup> ]            |

For the batches prepared with the dry mixing method, each recipe includes mass of cement ( $m_{CEMI}$ ), mass of slag ( $m_{GGBS}$ ) and mass of paper sludge ash ( $m_{PSA}$ ). The recipes were calculated using the procedure in Eq. 11 to Eq. 15.

$$m_{w,s} = \frac{w_s * m_{soil}}{w_s + 1} \quad Eq. 11$$

$$m_b = \frac{m_{w,s}}{wbr} \quad Eq. 12$$

$$m_{CEMI} = m_b * CEM\ I\ Binder\ content\ [\%] \quad Eq. 13$$

$$m_{GGBS} = m_b * GGBS\ Binder\ content\ [\%] \quad Eq. 14$$

$$m_{PSA} = m_b * PSA\ Binder\ content\ [\%] \quad Eq. 15$$

When preparing batches using the wet mixing method, each recipe also include mass of added water ( $m_{w,a}$ ). The recipes were calculated using the partly altered formulas shown in Eq. 16 to Eq. 21.

$$m_{w,s} = \frac{w_s * m_{soil}}{w_s + 1} \quad Eq. 16$$

$$m_b = \frac{m_{w,s}}{wbr - 1} \quad Eq. 17$$

$$m_{CEMI} = m_b * CEM\ I\ Binder\ content\ [\%] \quad Eq. 18$$

$$m_{GGBS} = m_b * GGBS\ Binder\ content\ [\%] \quad Eq. 19$$

$$m_{PSA} = m_b * PSA\ Binder\ content\ [\%] \quad Eq. 20$$

$$m_{w,a} = m_b \quad Eq. 21$$

Eq. 22 shows how the standard binder content factor ( $\alpha$ ) can be estimated. The standard unit of  $\alpha$  is kg binder per m<sup>3</sup> soil.

$$\alpha = \left[ \frac{\left( \frac{\bar{y} * 1000}{10} \right)}{m_{soil}} \right] * m_b \quad Eq. 22$$

Three individual samples are prepared from each batch to increase reliability during further testing. An overview of the laboratory samples prepared with the dry mixing method is shown in Table 17 and Table 18.

Table 17: Overview of laboratory samples prepared with the dry mixing method and a water to binder ratio of 8.

| Sample ID <sup>[1]</sup> | Lattice point | Sample preparation Method | Curing time [Days] | Curing stress [kPa] | wbr | Curing temperature [°C] | Testing method <sup>[2][3]</sup> |
|--------------------------|---------------|---------------------------|--------------------|---------------------|-----|-------------------------|----------------------------------|
| DRY.8.1.1                | 1             | Rodding                   | 28                 | 0                   | 8   | 20                      | UCT<br>PUNDIT                    |
| DRY.8.1.2                |               |                           |                    |                     |     |                         |                                  |
| DRY.8.1.3                |               |                           |                    |                     |     |                         |                                  |
| DRY.8.2.1                | 2             | Rodding                   | 28                 | 0                   | 8   | 20                      | UCT<br>PUNDIT                    |
| DRY.8.2.2                |               |                           |                    |                     |     |                         |                                  |
| DRY.8.2.3                |               |                           |                    |                     |     |                         |                                  |
| DRY.8.3.1                | 3             | Rodding                   | 28                 | 0                   | 8   | 20                      | UCT<br>PUNDIT                    |
| DRY.8.3.2                |               |                           |                    |                     |     |                         |                                  |
| DRY.8.3.3                |               |                           |                    |                     |     |                         |                                  |
| DRY.8.4.1                | 4             | Rodding                   | 28                 | 0                   | 8   | 20                      | UCT<br>PUNDIT                    |
| DRY.8.4.2                |               |                           |                    |                     |     |                         |                                  |
| DRY.8.4.3                |               |                           |                    |                     |     |                         |                                  |
| DRY.8.5.1                | 5             | Rodding                   | 28                 | 0                   | 8   | 20                      | UCT<br>PUNDIT                    |
| DRY.8.5.2                |               |                           |                    |                     |     |                         |                                  |
| DRY.8.5.3                |               |                           |                    |                     |     |                         |                                  |
| DRY.8.6.1                | 6             | Rodding                   | 28                 | 0                   | 8   | 20                      | UCT<br>PUNDIT                    |
| DRY.8.6.2                |               |                           |                    |                     |     |                         |                                  |
| DRY.8.6.3                |               |                           |                    |                     |     |                         |                                  |
| DRY.8.7.1                | 7             | Rodding                   | 28                 | 0                   | 8   | 20                      | UCT<br>PUNDIT                    |
| DRY.8.7.2                |               |                           |                    |                     |     |                         |                                  |
| DRY.8.7.3                |               |                           |                    |                     |     |                         |                                  |
| DRY.8.8.1                | 8             | Rodding                   | 28                 | 0                   | 8   | 20                      | UCT<br>PUNDIT                    |
| DRY.8.8.2                |               |                           |                    |                     |     |                         |                                  |
| DRY.8.8.3                |               |                           |                    |                     |     |                         |                                  |
| DRY.8.9.1                | 9             | Rodding                   | 28                 | 0                   | 8   | 20                      | UCT<br>PUNDIT                    |
| DRY.8.9.2                |               |                           |                    |                     |     |                         |                                  |
| DRY.8.9.3                |               |                           |                    |                     |     |                         |                                  |
| DRY.8.10.1               | 10            | Rodding                   | 28                 | 0                   | 8   | 20                      | UCT<br>PUNDIT                    |
| DRY.8.10.2               |               |                           |                    |                     |     |                         |                                  |
| DRY.8.10.3               |               |                           |                    |                     |     |                         |                                  |

[1] Sample ID explanation: DRY.8.1.2 = Dry mixing method, water to binder ratio of 8, lattice point 1, sample number 2  
[2] UCT = Unconfined Compression Test  
[3] PUNDIT = P-wave testing using PUNDIT ultrasonic equipment

Table 18: Overview of laboratory samples prepared with the dry mixing method and a water to binder ratio of 16.

| Sample ID <sup>[1]</sup>   | Lattice point | Sample preparation Method             | Curing time [Days] | Curing stress [kPa] | wbr | Curing temperature [°C] | Testing method <sup>[2][3]</sup> |
|--|---------------|---------------------------------------|--------------------|---------------------|-----|-------------------------|----------------------------------|
| DRY.16.1.1   | 1             | Rodding                               | 28                 | 0                   | 16  | 20                      | UCT<br>PUNDIT                    |
| DRY.16.1.2   |               |                                       |                    |                     |     |                         |                                  |
| DRY.16.1.3   |               |                                       |                    |                     |     |                         |                                  |
| DRY.16.2.1   | 2             | Rodding                               | 28                 | 0                   | 16  | 20                      | UCT<br>PUNDIT                    |
| DRY.16.2.2   |               |                                       |                    |                     |     |                         |                                  |
| DRY.16.2.3   |               |                                       |                    |                     |     |                         |                                  |
| DRY.16.3.1   | 3             | Poured,<br>then stirred<br>and tapped | 28                 | 0                   | 16  | 20                      | UCT<br>PUNDIT                    |
| DRY.16.3.2   |               |                                       |                    |                     |     |                         |                                  |
| DRY.16.3.3   |               |                                       |                    |                     |     |                         |                                  |
| DRY.16.4.1   | 4             | Rodding                               | 28                 | 0                   | 16  | 20                      | UCT<br>PUNDIT                    |
| DRY.16.4.2   |               |                                       |                    |                     |     |                         |                                  |
| DRY.16.4.3   |               |                                       |                    |                     |     |                         |                                  |
| DRY.16.5.1   | 5             | Rodding                               | 28                 | 0                   | 16  | 20                      | UCT<br>PUNDIT                    |
| DRY.16.5.2   |               |                                       |                    |                     |     |                         |                                  |
| DRY.16.5.3   |               |                                       |                    |                     |     |                         |                                  |
| DRY.16.6.1   | 6             | Rodding                               | 28                 | 0                   | 16  | 20                      | UCT<br>PUNDIT                    |
| DRY.16.6.2   |               |                                       |                    |                     |     |                         |                                  |
| DRY.16.6.3   |               |                                       |                    |                     |     |                         |                                  |
| DRY.16.7.1   | 7             | Rodding                               | 28                 | 0                   | 16  | 20                      | UCT<br>PUNDIT                    |
| DRY.16.7.2   |               |                                       |                    |                     |     |                         |                                  |
| DRY.16.7.3   |               |                                       |                    |                     |     |                         |                                  |
| DRY.16.8.1   | 8             | Rodding                               | 28                 | 0                   | 16  | 20                      | UCT<br>PUNDIT                    |
| DRY.16.8.2   |               |                                       |                    |                     |     |                         |                                  |
| DRY.16.8.3   |               |                                       |                    |                     |     |                         |                                  |
| DRY.16.9.1   | 9             | Rodding                               | 28                 | 0                   | 16  | 20                      | UCT<br>PUNDIT                    |
| DRY.16.9.2   |               |                                       |                    |                     |     |                         |                                  |
| DRY.16.9.3   |               |                                       |                    |                     |     |                         |                                  |
| DRY.16.10.1  | 10            | Rodding                               | 28                 | 0                   | 16  | 20                      | UCT<br>PUNDIT                    |
| DRY.16.10.2  |               |                                       |                    |                     |     |                         |                                  |
| DRY.16.10.3  |               |                                       |                    |                     |     |                         |                                  |
| [1] Sample ID explanation: DRY.16.1.2 = Dry mixing method, water to binder ratio of 16, lattice point 1, sample number 2 |               |                                       |                    |                     |     |                         |                                  |
| [2] UCT = Unconfined Compression Test  |               |                                       |                    |                     |     |                         |                                  |
| [3] PUNDIT = P-wave testing using PUNDIT ultrasonic equipment  |               |                                       |                    |                     |     |                         |                                  |

An overview of the laboratory samples prepared with the wet mixing method is shown in Table 19 and Table 20. Additional points are included in the tables for the single wet mixing method testing. Recipes with 100 % CEM I as a single binder (lattice point 1) was used for preparing the four additional batches (two for a wbr of 8 and two for a wbr of 16).

Table 19: Overview of laboratory samples prepared with the wet mixing method and a water to binder ratio of 8.

| Sample ID <sup>[1]</sup> | Lattice point | Sample preparation Method | Curing time [Days] | Curing stress [kPa] | wbr | Curing temperature [°C] | Testing method <sup>[2][3]</sup> |
|--------------------------|---------------|---------------------------|--------------------|---------------------|-----|-------------------------|----------------------------------|
| WET.8.1.1                | 1             | Rodding                   | 28                 | 0                   | 8   | 20                      | UCT<br>PUNDIT                    |
| WET.8.1.2                |               |                           |                    |                     |     |                         |                                  |
| WET.8.1.3                |               |                           |                    |                     |     |                         |                                  |
| WET.8.1.4 <sup>[4]</sup> | 1             | Rodding                   | 28                 | 0                   | 8   | 20                      | UCT                              |
| WET.8.1.5 <sup>[4]</sup> |               |                           |                    |                     |     |                         |                                  |
| WET.8.1.6 <sup>[4]</sup> |               |                           |                    |                     |     |                         |                                  |
| MDM.8.1.1 <sup>[4]</sup> | 1             | Rodding                   | 28                 | 0                   | 8   | 20                      | UCT                              |
| MDM.8.1.2 <sup>[4]</sup> |               |                           |                    |                     |     |                         |                                  |
| MDM.8.1.3 <sup>[4]</sup> |               |                           |                    |                     |     |                         |                                  |
| WET.8.2.1                | 2             | Rodding                   | 28                 | 0                   | 8   | 20                      | UCT<br>PUNDIT                    |
| WET.8.2.2                |               |                           |                    |                     |     |                         |                                  |
| WET.8.2.3                |               |                           |                    |                     |     |                         |                                  |
| WET.8.3.1                | 3             | Rodding                   | 28                 | 0                   | 8   | 20                      | UCT<br>PUNDIT                    |
| WET.8.3.2                |               |                           |                    |                     |     |                         |                                  |
| WET.8.3.3                |               |                           |                    |                     |     |                         |                                  |
| WET.8.4.1                | 4             | Rodding                   | 28                 | 0                   | 8   | 20                      | UCT<br>PUNDIT                    |
| WET.8.4.2                |               |                           |                    |                     |     |                         |                                  |
| WET.8.4.3                |               |                           |                    |                     |     |                         |                                  |
| WET.8.5.1                | 5             | Rodding                   | 28                 | 0                   | 8   | 20                      | UCT<br>PUNDIT                    |
| WET.8.5.2                |               |                           |                    |                     |     |                         |                                  |
| WET.8.5.3                |               |                           |                    |                     |     |                         |                                  |
| WET.8.6.1                | 6             | Rodding                   | 28                 | 0                   | 8   | 20                      | UCT<br>PUNDIT                    |
| WET.8.6.2                |               |                           |                    |                     |     |                         |                                  |
| WET.8.6.3                |               |                           |                    |                     |     |                         |                                  |
| WET.8.7.1                | 7             | Rodding                   | 28                 | 0                   | 8   | 20                      | UCT<br>PUNDIT                    |
| WET.8.7.2                |               |                           |                    |                     |     |                         |                                  |
| WET.8.7.3                |               |                           |                    |                     |     |                         |                                  |
| WET.8.8.1                | 8             | Rodding                   | 28                 | 0                   | 8   | 20                      | UCT<br>PUNDIT                    |
| WET.8.8.2                |               |                           |                    |                     |     |                         |                                  |
| WET.8.8.3                |               |                           |                    |                     |     |                         |                                  |
| WET.8.9.1                | 9             | Rodding                   | 28                 | 0                   | 8   | 20                      | UCT<br>PUNDIT                    |
| WET.8.9.2                |               |                           |                    |                     |     |                         |                                  |
| WET.8.9.3                |               |                           |                    |                     |     |                         |                                  |
| WET.8.10.1               | 10            | Rodding                   | 28                 | 0                   | 8   | 20                      | UCT<br>PUNDIT                    |
| WET.8.10.2               |               |                           |                    |                     |     |                         |                                  |
| WET.8.10.3               |               |                           |                    |                     |     |                         |                                  |

[1] Sample ID explanation: WET.8.1.2 = Wet mixing method, MDM.8.1.2 = Modified dry mixing method, water to binder ratio of 8, lattice point 1, sample number 2

[2] UCT = Unconfined Compression Test

[3] PUNDIT = P-wave testing using PUNDIT ultrasonic equipment

[4] Additional points for single wet mixing method evaluation

Table 20: Overview of laboratory samples prepared with the wet mixing method and a water to binder ratio of 16.

| Sample ID <sup>[1]</sup>  | Lattice point | Sample preparation Method             | Curing time [Days] | Curing stress [kPa] | wbr | Curing temperature [°C] | Testing method <sup>[2][3]</sup> |
|---------------------------|---------------|---------------------------------------|--------------------|---------------------|-----|-------------------------|----------------------------------|
| WET.16.1.1                | 1             | Rodding                               | 28                 | 0                   | 16  | 20                      | UCT<br>PUNDIT                    |
| WET.16.1.2                |               |                                       |                    |                     |     |                         |                                  |
| WET.16.1.3                |               |                                       |                    |                     |     |                         |                                  |
| WET.16.1.4 <sup>[4]</sup> | 1             | Rodding                               | 28                 | 0                   | 16  | 20                      | UCT                              |
| WET.16.1.5 <sup>[4]</sup> |               |                                       |                    |                     |     |                         |                                  |
| WET.16.1.6 <sup>[4]</sup> |               |                                       |                    |                     |     |                         |                                  |
| MDM.16.1.1 <sup>[4]</sup> | 1             | Rodding                               | 28                 | 0                   | 16  | 20                      | UCT                              |
| MDM.16.1.2 <sup>[4]</sup> |               |                                       |                    |                     |     |                         |                                  |
| MDM.16.1.3 <sup>[4]</sup> |               |                                       |                    |                     |     |                         |                                  |
| WET.16.2.1                | 2             | Rodding                               | 28                 | 0                   | 16  | 20                      | UCT<br>PUNDIT                    |
| WET.16.2.2                |               |                                       |                    |                     |     |                         |                                  |
| WET.16.2.3                |               |                                       |                    |                     |     |                         |                                  |
| WET.16.3.1                | 3             | Poured,<br>then stirred<br>and tapped | 28                 | 0                   | 16  | 20                      | UCT<br>PUNDIT                    |
| WET.16.3.2                |               |                                       |                    |                     |     |                         |                                  |
| WET.16.3.3                |               |                                       |                    |                     |     |                         |                                  |
| WET.16.4.1                | 4             | Rodding                               | 28                 | 0                   | 16  | 20                      | UCT<br>PUNDIT                    |
| WET.16.4.2                |               |                                       |                    |                     |     |                         |                                  |
| WET.16.4.3                |               |                                       |                    |                     |     |                         |                                  |
| WET.16.5.1                | 5             | Poured,<br>then stirred<br>and tapped | 28                 | 0                   | 16  | 20                      | UCT<br>PUNDIT                    |
| WET.16.5.2                |               |                                       |                    |                     |     |                         |                                  |
| WET.16.5.3                |               |                                       |                    |                     |     |                         |                                  |
| WET.16.6.1                | 6             | Poured,<br>then stirred<br>and tapped | 28                 | 0                   | 16  | 20                      | UCT<br>PUNDIT                    |
| WET.16.6.2                |               |                                       |                    |                     |     |                         |                                  |
| WET.16.6.3                |               |                                       |                    |                     |     |                         |                                  |
| WET.16.7.1                | 7             | Poured,<br>then stirred<br>and tapped | 28                 | 0                   | 16  | 20                      | UCT<br>PUNDIT                    |
| WET.16.7.2                |               |                                       |                    |                     |     |                         |                                  |
| WET.16.7.3                |               |                                       |                    |                     |     |                         |                                  |
| WET.16.8.1                | 8             | Poured,<br>then stirred<br>and tapped | 28                 | 0                   | 16  | 20                      | UCT<br>PUNDIT                    |
| WET.16.8.2                |               |                                       |                    |                     |     |                         |                                  |
| WET.16.8.3                |               |                                       |                    |                     |     |                         |                                  |
| WET.16.9.1                | 9             | Poured,<br>then stirred<br>and tapped | 28                 | 0                   | 16  | 20                      | UCT<br>PUNDIT                    |
| WET.16.9.2                |               |                                       |                    |                     |     |                         |                                  |
| WET.16.9.3                |               |                                       |                    |                     |     |                         |                                  |
| WET.16.10.1               | 10            | Rodding                               | 28                 | 0                   | 16  | 20                      | UCT<br>PUNDIT                    |
| WET.16.10.2               |               |                                       |                    |                     |     |                         |                                  |
| WET.16.10.3               |               |                                       |                    |                     |     |                         |                                  |

[1] Sample ID explanation: WET.16.1.2 = Wet mixing method, MDM.16.1.2 = Modified dry mixing method, water to binder ratio of 16, lattice point 1, sample number 2

[2] UCT = Unconfined Compression Test

[3] PUNDIT = P-wave testing using PUNDIT ultrasonic equipment

[4] Additional points for single wet mixing method evaluation

A Kenwood Major Classic kitchen stand mixer with a k-type mixing tool (Figure 34) was used to prepare each batch of stabilized soil.



Figure 34: Kitchen stand mixer (left) and k-type mixing tool (right) used to prepare batches of stabilized soil.

The sample mixing procedure to prepare batches with the wet, dry, and modified dry mixing method (MDM) is described in the following steps (1-6). Procedure modified after (Statens vegvesen, 2016).

1. Measure out a set amount of clay ( $m_{soil}$ ) along with calculated amounts of cement ( $m_{CEMI}$ ), GGBS ( $m_{GGBS}$ ) and PSA ( $m_{PSA}$ ). In the wet method, a calculated amount of added water ( $m_{w,a}$ ) is also measured out.
2. Homogenize the clay for 5 minutes on medium speed in the kitchen stand mixer to break down the clay structure.
3. Take out a small sample of homogenized clay to test the water content.
4. If the wet method (WET) is used, mix the binder(s) and added water into a homogenous slurry.
5. If the modified dry method (MDM) is used, homogenize the added water and the clay for 15 seconds.
6. Add the dry binder(s) (DRY/MDM) or slurry (WET) to the homogenized soil and mix for an additional 5 minutes or until the clay stiffens enough to prevent further mixing. Manually homogenize by crushing/mixing if the machine mixing is unsatisfactory.

### 3.2.4. Laboratory molding technique

The rodding technique was chosen as the appropriate molding technique for the laboratory work. This is mainly due to good performance in varying soil conditions as described in section 2.3.2. It was also chosen because it is the preferred method by NGI and SGI, which are the Norwegian and Swedish geotechnical institutes respectively.

Figure 35 shows the rodding technique equipment and setup. The names and relevant specifications of each sample preparation component is listed below.

- Steel rod (25 mm diameter)
- Plastic cylinder (100 mm height, 54 mm inner diameter)
- Cylinder holder
- Plastic sheet liner

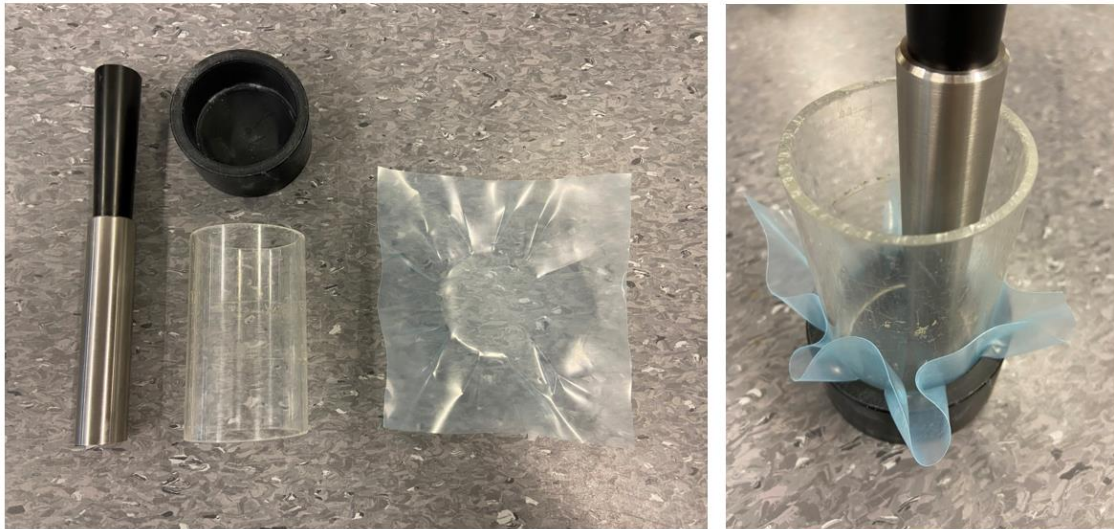


Figure 35: Rodding technique equipment and setup.

The rodding technique followed for sample preparation is described in the following steps (1-8). Procedure modified after (Kitazume et al., 2015).

1. Measure the weight of the empty plastic cylinder ( $m_{cyl}$ ).
2. Place the plastic sheet liner over the cylinder holder before firmly inserting the plastic cylinder.
3. Add a layer (2-3cm) of stabilized clay to the plastic cylinder.
4. Tamp down the stabilized clay until no visible air pockets are visible.
5. Repeat steps 3 and 4 until the top of the plastic cylinder is reached
6. Fill potential voids with stabilized clay after removing the plastic cylinder from the holder.
7. Carefully trim excess material to ensure an even base and top.
8. Measure the weight of the filled plastic cylinder ( $m_{cyl,full}$ ) to calculate the amount of entrapped air in the sample.

Batches which have insufficient stiffness to follow the procedure is poured directly into the mold and are stirred/tapped to remove as much air as possible.

Finished samples are wrapped in plastic and stored at 20 °C for 28 days before testing. Each batch is stored in a sealed plastic bag with a damp paper towel to minimize risk of drying (Figure 36). The sample weight deviation from before and after curing is measured to assess the curing conditions (see section 4.2.1).





Figure 36: Laboratory batch sealed for curing.

Demolding is performed either by hand or by mechanical extrusion if the sample is bonded to the plastic cylinder. A disk is placed on the back of the sample to distribute the applied force during extrusion. Figure 37 shows the equipment used for extrusion of the samples.



Figure 37: Hydraulic extrusion equipment for cylinder samples.

### 3.3 Test procedures

#### 3.3.1. Visual inspection

Samples prepared in the laboratory are all visually inspected and photographed before further testing to note any damage which could have occurred during molding and/or demolding. Deviations in the standard sample height is also checked because of the possible effects on p-wave and UCS measurements. For the field samples, only large cracks and surface deviations are noted.

#### 3.3.2. Water content, corrected wbr, density, and entrapped air

Water content was measured after the quick clay had been homogenized in the kitchen stand mixer ( $w_{stab}$ ). About 30 grams of material was used to get a representative measurement. The samples were dried for at least 24 hours at 105 °C to evaporate all of the water before measuring the weight deviation. Each batch of both laboratory and field samples were also tested with respect to water content after the UCT ( $w_{UCT}$ ) and  $\mu$ CT ( $w_{\mu CT}$ ) testing respectively.

The actual water content ( $w_{stab}$ ) was used to correct the assumed water to binder ratio ( $wbr_{corr}$ ) based off previous studies of the site.

The plastic cylinders used for preparing the laboratory samples were weighed both empty ( $m_{cyl}$ ) and full ( $m_{cyl,full}$ ). The formula in Eq. 23 was used to determine the measured density ( $\rho_{stab}$ ) in the samples.

$$\rho_{stab} = \frac{m_{cyl,full} - m_{cyl}}{\text{Cylinder volume}} \quad \text{Eq. 23}$$

To estimate the amount of entrapped air in the samples, a value of specific gravity ( $G_s$ ) in the clay was introduced. The specific gravity for the main clay minerals in Norwegian clays usually varies between 2.6 and 3.0 (Mitchell & Soga, 2005). An average value of 2.8 was used during testing, as the small amount of binder is assumed to have a negligible effect on the overall clay mineral density. Using an average value can make entrapped air values appear to be negative, which is not possible. This is not considered to be a problem because the amount of entrapped air is mainly used to check for large deviations when using the rodding technique. The density of water ( $\rho_w$ ) is assumed to be 1 t/m<sup>3</sup>.

Eq. 24 was used to estimate the theoretical density in a fully saturated condition. The Tiller-Flotten quick clay layer is assumed to be fully saturated because it sits well below the groundwater table (L'Heureux et al., 2019).

$$\rho_{theor.} = \frac{w_{stab} + 1}{\frac{w_{stab}}{\rho_w} + \frac{1}{G_s}} \quad \text{Eq. 24}$$

The expression in Eq. 25 was used to estimate the amount of entrapped air in the samples.

$$n_{air} = \frac{\rho_{theor.} - \rho_{stab}}{\rho_{theor.}} \quad \text{Eq. 25}$$

### 3.3.3. P-wave measurements

The Proceq PUNDIT PL-2 with 54kHz transducers was used to measure the p-wave velocities ( $V_p$ ) of the samples. The ultrasonic equipment is normally applied to concrete, wood, and rock materials, but the stabilized clay samples tested in the laboratory are within the test object limitations listed in Table 21. P-wave velocity values that fall within the expected ranges for stabilized soil described in section 2.1.4 is considered sufficiently reliable.

Table 21: PUNDIT transducer specifications and test object limitations (Proceq SA, 2017).

| P-wave transducer   | Frequency [kHz] | Test object limitations |                      |                             |
|---------------------|-----------------|-------------------------|----------------------|-----------------------------|
|                     |                 | Wavelength [mm]         | Max. grain size [mm] | Min. lateral dimension [mm] |
| Part No. 325 40 131 | 54.0            | 68.5                    | ≈34.0                | 69.0                        |

Three transmission methods are available when using the PUNDIT PL-2. The direct method where the transducers are directly in line with each other (Figure 38) is chosen.

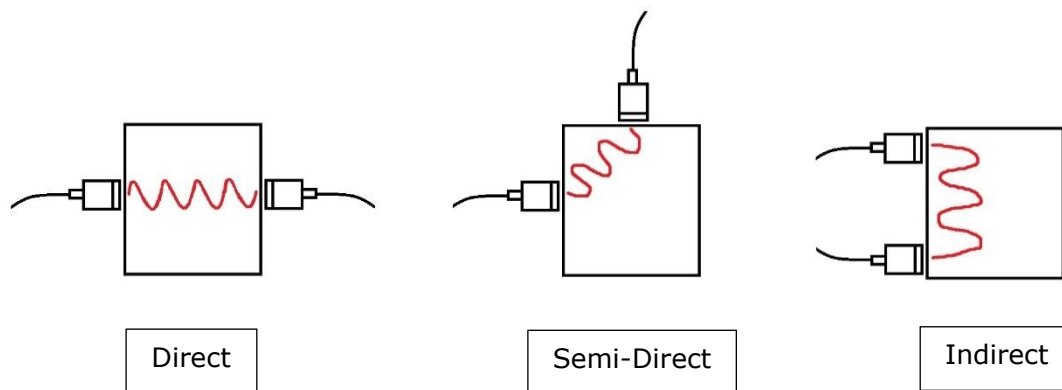


Figure 38: PUNDIT PL-2 transmission methods.

The p-wave test procedure is described in the following steps (1-10). Procedure modified after (Proceq SA, 2017).

1. Plug in the power cord, connect the 54 kHz transducers, and turn on the device.
2. Press the settings icon and set the Pulse Repetition Frequency to 10 Hz (10 measurements per second). Check also that the correct transducers are selected.
3. Press Pulse Velocity from the main menu to enter the p-wave velocity testing mode.
4. To calibrate the instrument, start by pressing the pencil icon shown in Figure 40 to set the length of the calibration rod (0.07 m). Go back to the settings menu and enter the calibration value (25.4  $\mu$ s) by pressing Zeroing Transducer. Hold the transducers firmly to each side of the calibration rod using the ultrasound couplant and press the play button to carry out the zeroing (Figure 39). "Zeroing succeeded" is displayed on the screen upon completion.
5. Return to Pulse Velocity mode after calibration.
6. Enter the length of the sample by pressing the pencil icon shown in Figure 40.

7. Hold the transducers firmly on each side of the sample and press the play button to start the measurement (Figure 39). An ultrasound couplant can be applied to the transducer ends if the signal is insufficient.
8. Increase the transmitter voltage from the lowest setting until a stable signal is achieved (Figure 40).
9. Receiver gain can also be increased until a desired signal curve amplitude is visible (Figure 40).
10. Note the measured p-wave velocity if the automatically determined time of arrival of the pulse corresponds well to the visible signal curve.

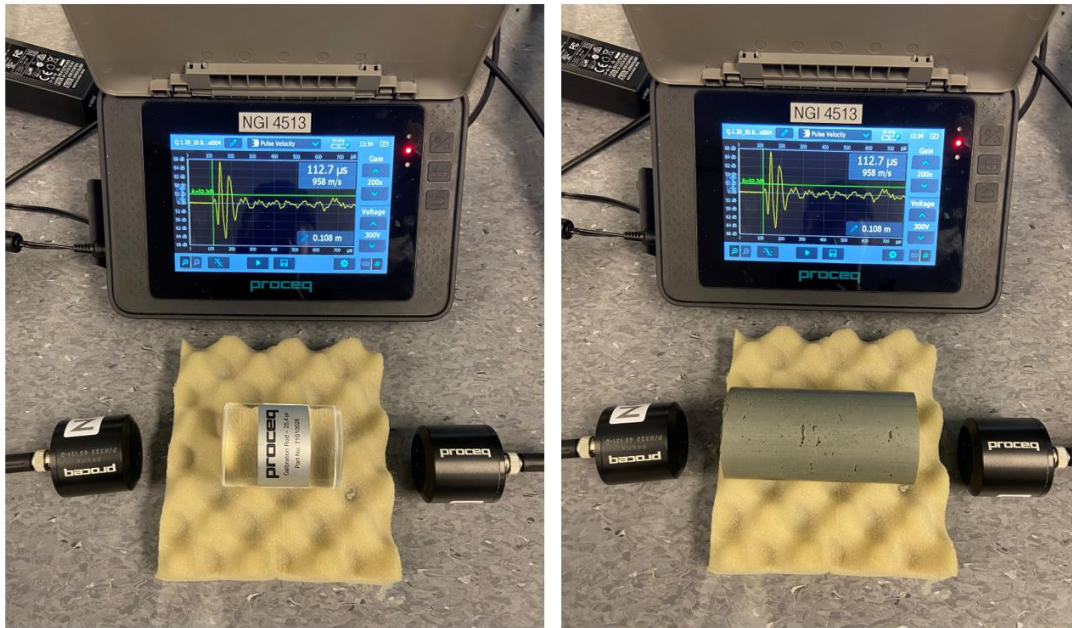


Figure 39: PUNDIT PL-2 p-wave equipment setup for calibrating (left) and testing cured samples (right).

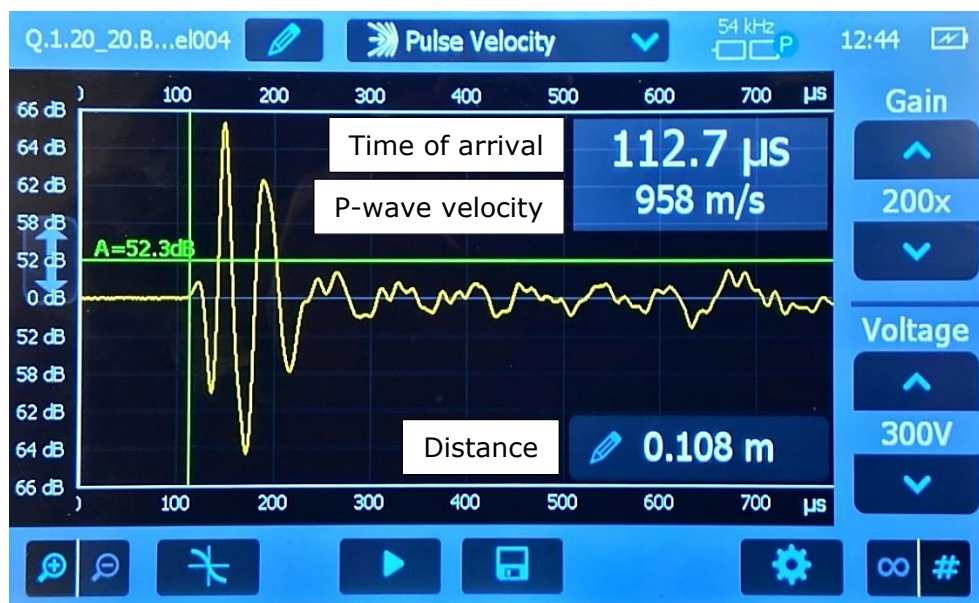


Figure 40: Pulse Velocity mode screen for testing p-wave velocity.

**3.3.4. Unconfined compression test (UCT)**

After testing p-wave velocity, unconfined compression testing (UCT) of the laboratory samples was performed according to the Norwegian guidelines for lime-cement stabilisation (NGF, 2012). A load frame with a HBM Typ. U2A 2-ton load cell was used for the UCT (Figure 41). The data from the tests were stored on a separate computer for further analysis. Figure 42 shows how a typical sample looks before and after UCT.



Figure 41: Unconfined compression test equipment setup.

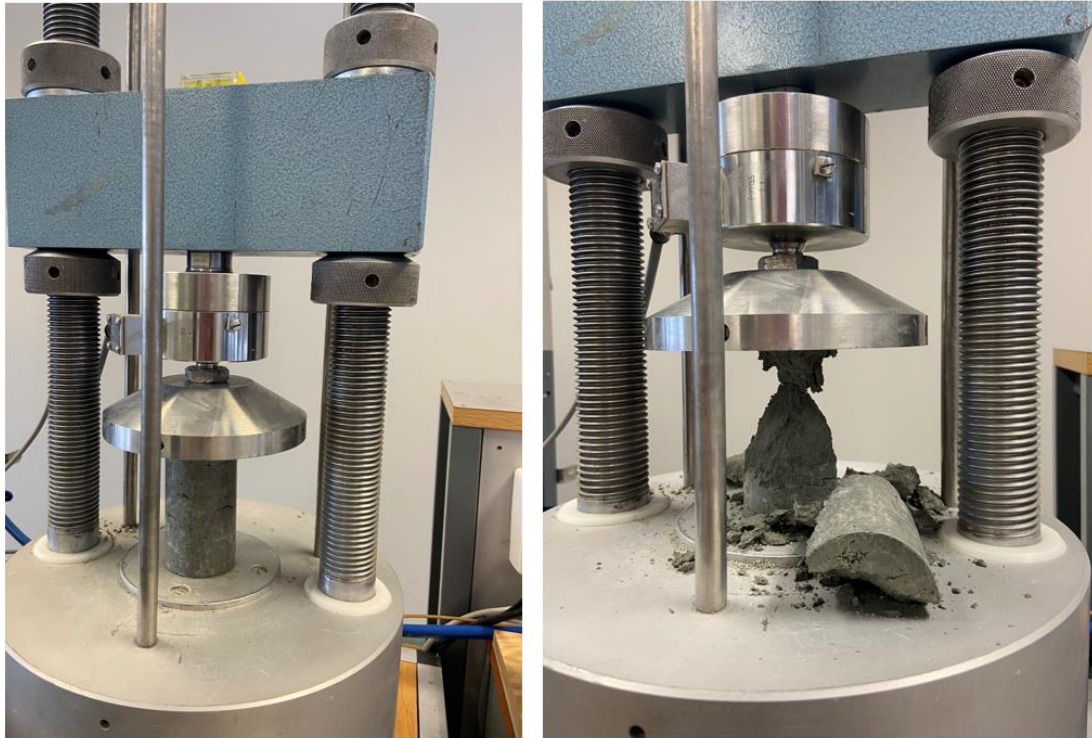


Figure 42: Cylinder sample before (left) and after (right) UCT.

The test procedure is described in the following steps (1-6). Procedure modified after (NGF, 2012).

1. Inspect the top and bottom of the sample. The ends should be flat to ensure good contact between the load cell plate and the sample.
2. Place the sample directly under the load cell plate in the uniaxial apparatus.
3. Manually adjust the height of the load cell until it is approximately in contact with the top of the sample.
4. Set the strain/deformation to zero, and the deformation rate to 1.5mm/min (1.5 %/min).
5. Start the test and run it until 10 % strain (or a full curve) is reached.
6. Photograph the samples after failure and take a water content measurement.
7. Export the data and analyze the results to determine the failure stress after 28 days of curing ( $q_{u,28}$ ), undrained shear strength ( $S_u$ ), failure strain ( $\varepsilon_v$ ) and estimated stiffness at 50 % compressive strength ( $E_{50}$ ).

The equipment registers both force and deformation over time. *Eq. 26* and *Eq. 27* shows how these parameters were used to find the axial stress ( $\sigma_1$ ) vs axial strain ( $\varepsilon$ ) in the samples. All of the samples have a height of 100 mm and a diameter of 54 mm, giving a cross sectional area of 2290.22 mm<sup>2</sup>.

$$\sigma_1 = \frac{\text{Force registered by the load cell} * (1 - \varepsilon)}{\text{Area of the sample}} \quad \text{Eq. 26}$$

$$\varepsilon = \frac{\text{Original sample height} - \text{Deformed sample height}}{\text{Original sample height}} * 100\% \quad \text{Eq. 27}$$

Figure 43 shows how failure stress after 28 days of curing ( $q_{u,28}$ ), undrained shear strength ( $S_u$ ), failure strain ( $\epsilon_v$ ) and estimated stiffness at 50 % compressive strength ( $E_{50}$ ) was determined. Determining the stiffness is often as important as determining strength because soil stabilization is often used for reducing settlements.

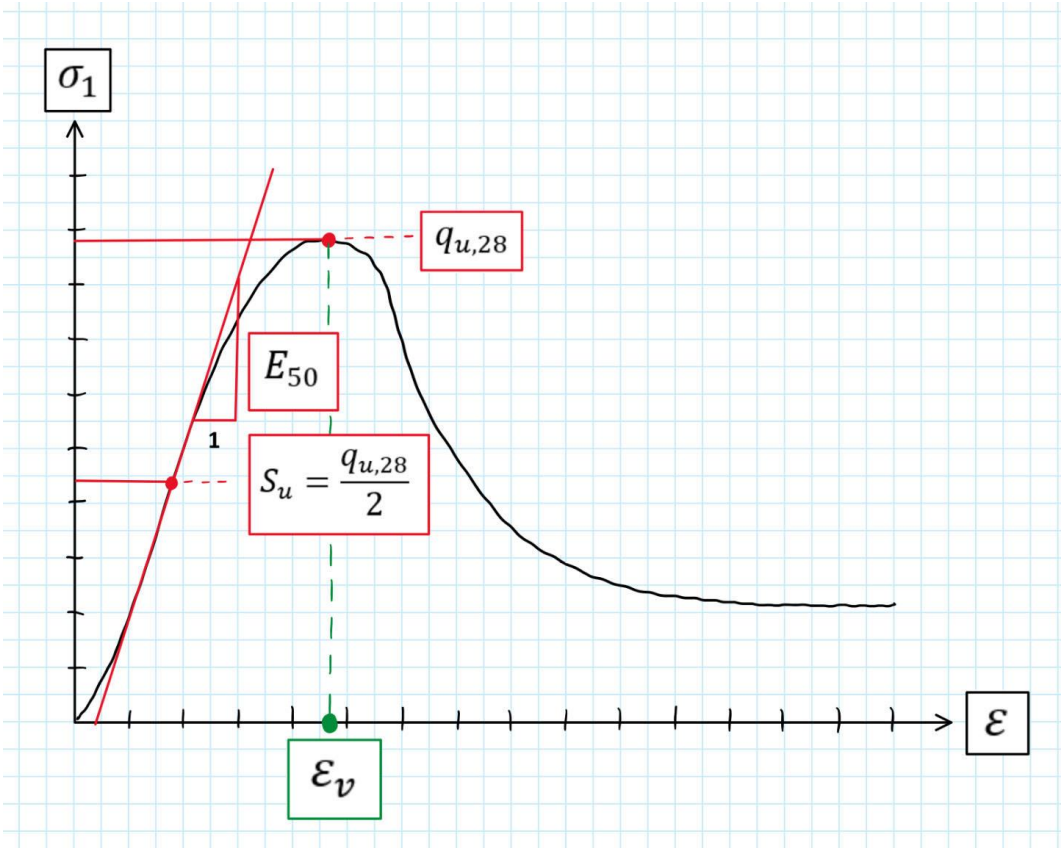


Figure 43: Parameter determination from an axial strain ( $\epsilon$ ) vs axial stress ( $\sigma_1$ ) diagram.

**3.3.5. CT-analysis**

Micro computed tomography ( $\mu$ CT) testing of the field samples was performed in collaboration with the Department of Physics at NTNU. A  $\mu$ CT scanner sends x-ray beams through a rotating sample into a detector that captures a shadow projection (image) of the sample (Figure 44).

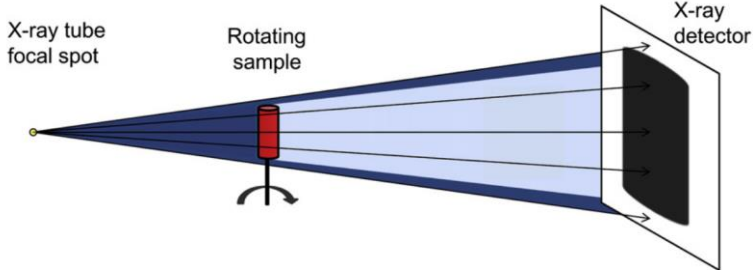


Figure 44: Principal sketch of a lab-based  $\mu$ CT setup with a conical beam (Cnudde & Boone, 2013).

Single images miss necessary depth information to create reliable interpretations, but stacking the images from different orientations allows for a reliable three-dimensional (3D) reconstruction to be made (Cnudde & Boone, 2013). Dedicated computer algorithms are used to reconstruct the data generated in each sample orientation. This is in principle made possible by exploiting the varying x-ray attenuation coefficient through the sample material.

By using this type of non-destructive testing, the macro porosity in the samples can be estimated. The images also show possible layering and binder accumulations in the samples.

A Nikon XT H 225 ST coupled with a 16-bit Perkin Elmer 1620 X-ray detector was used during testing of the field samples. The  $\mu$ CT-setup is shown in Figure 45. After initial testing, a pixel height of 1750 was chosen, which corresponds to about 100  $\mu$ m on the sample. The field of view width was also about 100 mm to match the sample diameter.

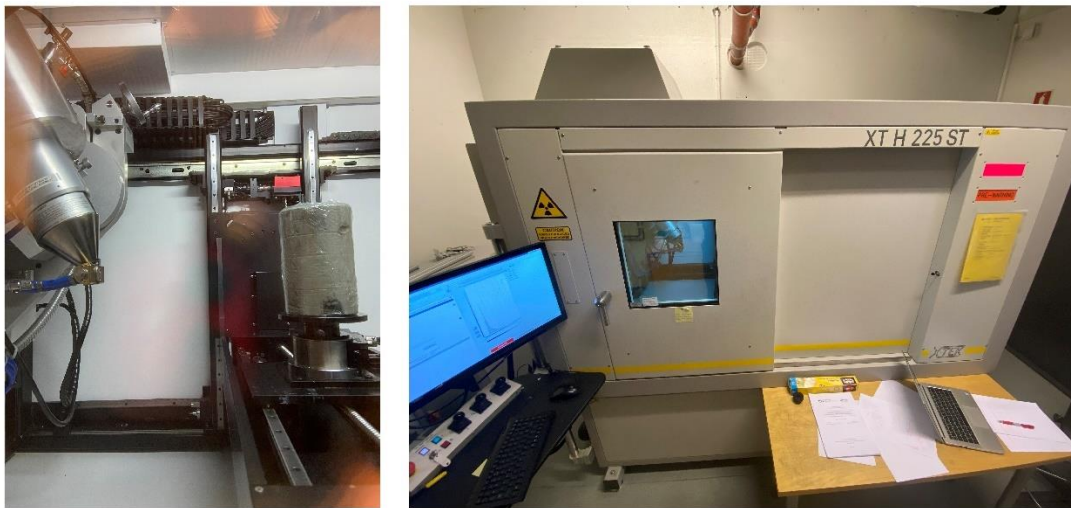


Figure 45: X-ray source and rotating field sample (left). Nikon XT H 225 ST instrument (Right).

An overview of the relevant  $\mu$ CT settings used during the scans is presented in Table 22.

Table 22: Settings for the  $\mu$ CT scans.

| Settings              | Field samples |
|-----------------------|---------------|
| Tube voltage [kV]     | 220-225       |
| Current [ $\mu$ A]    | 242-311       |
| Voxel size [ $\mu$ m] | 58-62         |
| Exposure time [s]     | 1.42-2.00     |
| Number of projections | 3141          |
| Filter                | 1.0 mm Ag     |

Each  $\mu$ CT scan can take over three hours to complete and it is important to not change the structure of the material during the process. At least two layers of plastic wrap were kept on during scanning to prevent the samples from drying, and thereby negatively influencing the gathered data.



After software reconstructions of 2D slices were created, the slice data was imported into 3D NumPy arrays. A 3D median filter (`nd.median` from SciPy) was applied before segmentation. Segmentation of the images was performed in three steps. This allows three sets of data (i.e. slice stacks of the full clay sample, porous regions, and inclusions) to be saved.

To segment the full clay sample, a threshold was chosen to locate the outer boundary of the sample. A new threshold value was then chosen to locate the porous regions inside the sample. To segment out the porous regions, the slices were inverted to get a stack of pores only. The macro porosity was estimated along the central axis of each sample, referred to as the z-axis. A porous shell around each sample was removed before calculating macro porosity. The calculation was done in each slice by converting the slices into a binary image. Finally, a threshold value was applied to locate and segment the inclusions in the sample. The inclusions are lumps of varying size and shape with high absorption compared with the rest of the sample.

## **3.4 Data analysis**

### **3.4.1. Response surface methodology (RSM)**

Response surface methodology, here referred to as RSM, is used for developing and improving processes through an assortment of statistical and mathematical tools (Myers et al., 2009). Optimizing already existing processes to meet specifications is also a main area of use for RSM. The performance of a process can often be measured through experimentation. The measure, which is called a response, is plotted with respect to multiple factors to visualize the resulting performance in three dimensions. These 3D-surfaces (and/or 2D contour graphs) have the advantage of being more concise and intuitive compared with multiple 2D-graphs. An example of a response surface along with a corresponding contour graph is shown in Figure 46.

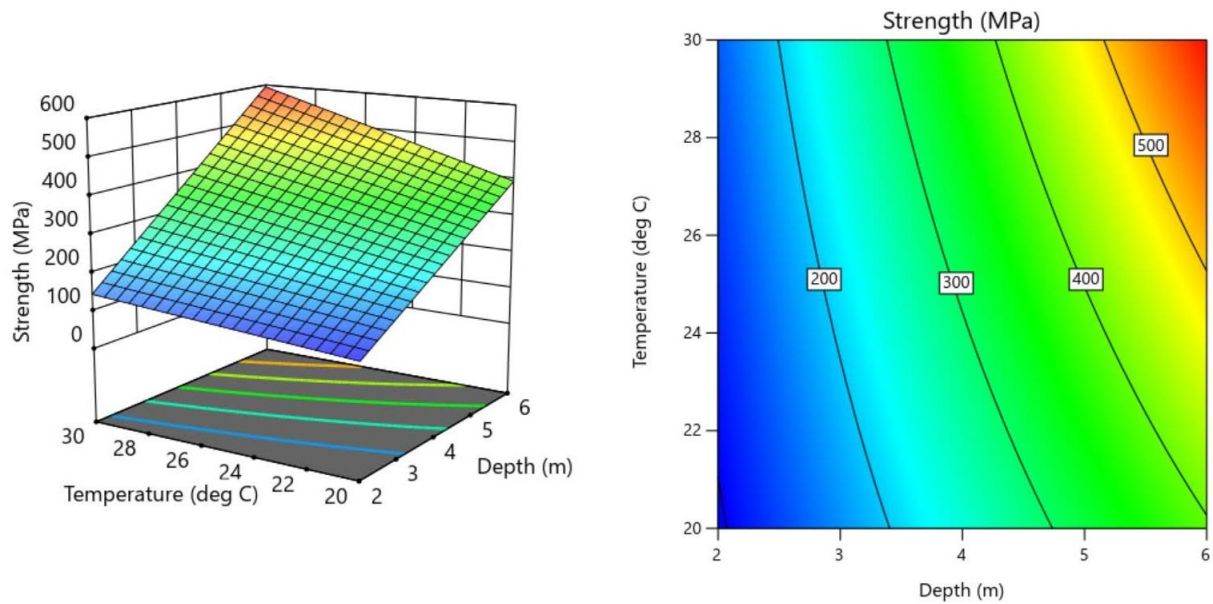


Figure 46: Example of a response surface (left) and a contour plot (right). The strength is the response of the experiment, while depth and temperature are influential factors.

Different methods are used when setting up and designing experiments to make them efficient and reliable. However, experimental design using RSM is difficult in geotechnical engineering. In the field, material properties are tough to accurately predict and can vary greatly over small areas. Even in a laboratory setting, the variables which occur when preparing and running a sample test are very high compared with man-made materials like steel. To achieve reliable results, the number of runs (tests where a measurement is collected) has to increase while at the same time limiting uncontrollable factors which can influence the results. In other words, the different variances have to be implemented and accounted for in the final design.

### 3.4.2. Mixture design

Three binder components are mixed and tested in the laboratory using varying recipes. To be able to measure the performance (i.e. strength and deformation properties) of different binder components, design of experiments (DoE) methodology was applied. DoE is more effective than traditional scientific methods, due to the fact that multiple factors can be changed in each run of the experiment. It also makes it possible to find the interactions between different binder components, which is an important aspect of this thesis. The type of designed experiment used in this thesis is called a mixture design.

The decision process used when setting up a mixture design diverges from other experiment designs, because all mixes have to add up to 100 percent. This makes each of the components dependent on each other (i.e. changing one factor influences other factors) (Montgomery, 2013). If this is not accounted for, unnecessary and redundant runs will reduce both accuracy and efficiency. An example of this is shown in Table 23, where a factorial design results in making two of the same exact mixtures, just in different volumes. The augmented simplex lattice design described in section 3.4.3 addresses this issue by introducing an expression where the response is a function of component proportions.

Table 23: Issues with factorial designs for mixtures.

|           |          | Cement (c)                           |                                      |
|-----------|----------|--------------------------------------|--------------------------------------|
|           |          | 1 liter                              | 2 liters                             |
| Water (w) | 1 liter  | Volume: 2 Liters<br>Ratio (w/c): 1.0 | Volume: 3 Liters<br>Ratio (w/c): 0.5 |
|           | 2 liters | Volume: 3 Liters<br>Ratio (w/c): 2.0 | Volume: 4 Liters<br>Ratio (w/c): 1.0 |

### 3.4.3. Augmented simplex lattice

Simplex designs are used to understand the effects of changing the proportions of components in a mixture (Montgomery, 2013). The effects are measured as changes in a selected response variable. A simplex lattice used for a mixture design with three components can be imagined as a triangular plane cut out of a standard box-type factorial design. Each corner of the triangle shown in Figure 47 corresponds to a single point along one of the three axes ( $x_1$ ,  $x_2$  and  $x_3$ ). These points are called pure blends (i.e. a blend containing a single binder).

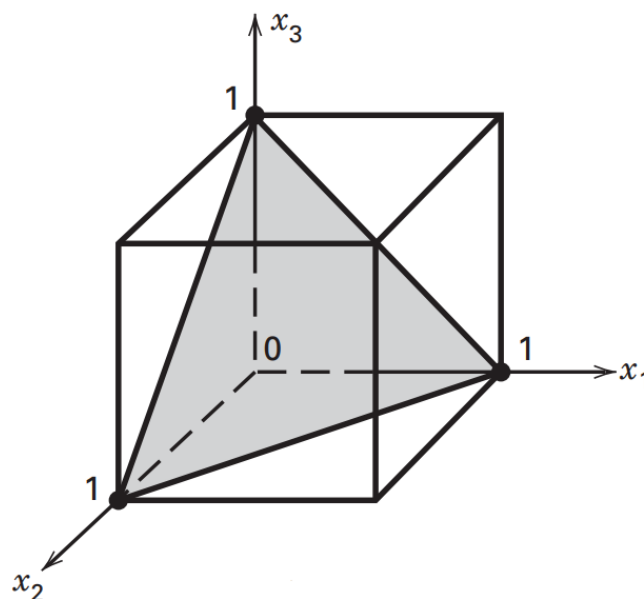


Figure 47: Pure blend points on a standard box-type factorial design (Montgomery, 2013).

The standard simplex lattice design uses the six points shown in Figure 48. The problem with this type of design is the fact that no mixtures contain all components. Only singular and binary mixtures (Lindh, 2004).

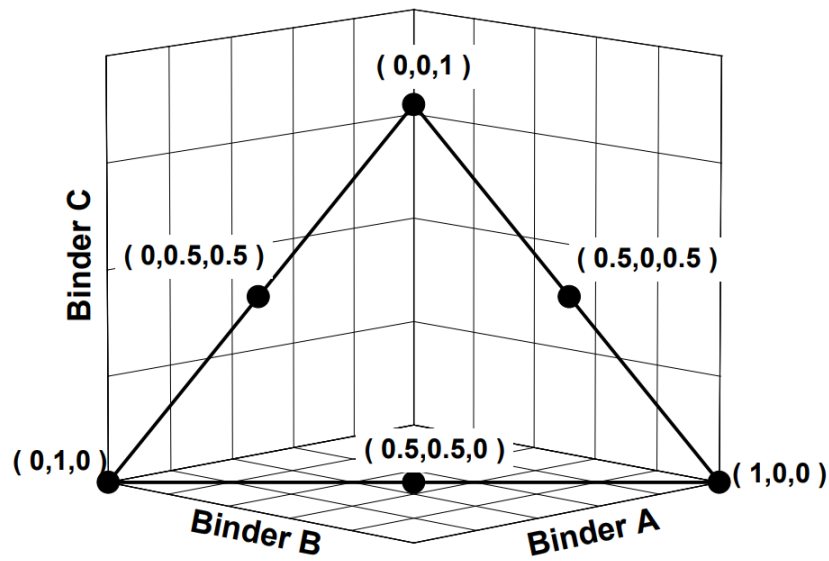


Figure 48: Standard simplex lattice design with three components (Lindh, 2004).

To understand the interactions between all three components, a desired number of interior points are added, resulting in what is called an augmented simplex lattice design. The coordinates of the interior points are based on the trilinear coordinate system shown in Figure 49. The three axes meet in the centroid of the triangle, which corresponds to a mixture with equal proportions of the components (1/3).

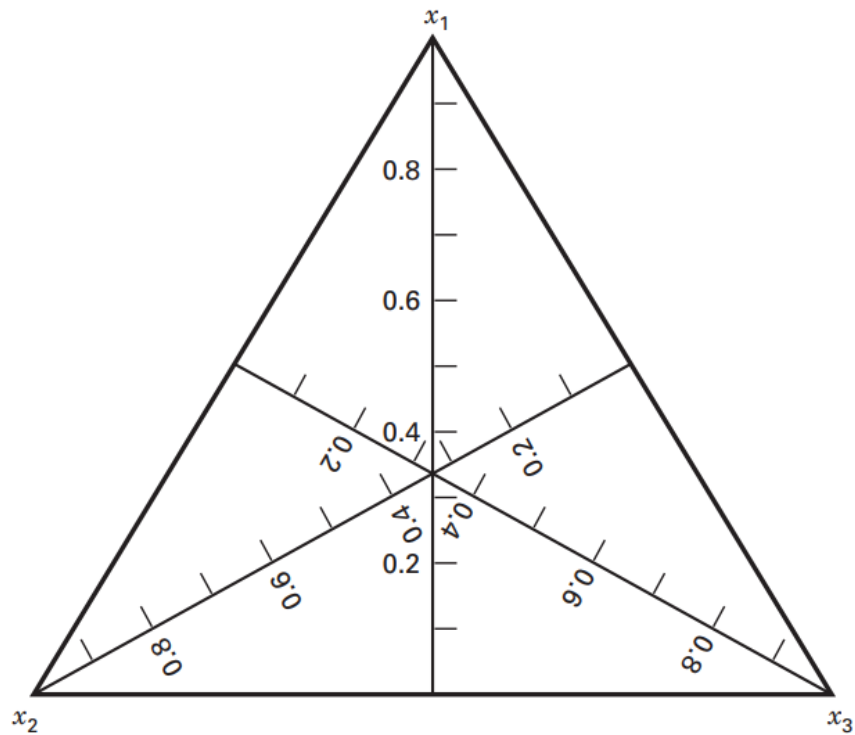


Figure 49: Trilinear coordinate system (Montgomery, 2013).

## 3.5 Modeling software

To analyze the results from the mixture design laboratory study, Design-Expert by Stat-Ease Inc. was chosen. Design-Expert is a statistical software which covers Design of Experiments (DoE) as well as data analysis and result visualization (Stat-Ease, n.d.-d). The setup and configuration of the included mixture design tools are described in the following sections.

### 3.5.1. Configuration

The first part of the software configuration is defining the objective of the experiment. In this case, the objective is to find the optimal binder composition in regard to various performance measures (responses). The five responses are shown in Figure 50. As mentioned in section 3.2.3, each lattice point is replicated three times to increase test reliability. This gives a total of 30 observations in a single augmented simplex lattice when 10 lattice points are used.

| Response | Name                          | Units | Observations |
|----------|-------------------------------|-------|--------------|
| R1       | Ultimate compressive strength | kPa   | 30,00        |
| R2       | Undrained shear strength      | kPa   | 30,00        |
| R3       | Failure strain                | %     | 30,00        |
| R4       | Estimated stiffness           | kPa   | 30,00        |
| R5       | P-wave velocity               | m/s   | 30,00        |

Figure 50: Response information set in Design Expert.

The augmented simplex lattice design (see section 3.2.3) was in this study chosen without using the software. For that reason, a custom mixture design containing the three binders shown in Figure 51 was used. The lattice constraints are also entered into the software.

| Component | Name  | Units | Type    | Minimum | Maximum |
|-----------|-------|-------|---------|---------|---------|
| A         | CEM I | %     | Mixture | 0       | 100     |
| B         | GGBS  | %     | Mixture | 0       | 80      |
| C         | PSA   | %     | Mixture | 0       | 80      |

Figure 51: Mixture component information and constraints set in Design Expert.

Samples which crack during extraction or deviate largely from its replicating runs are ignored to prevent the software from including unreliable points in the model.

### 3.5.2. Model

The Handbook for Experiments (Stat-Ease, 2020) provided with the software was used as a guide for choosing the appropriate response surface model. It can also be used for result analysis and evaluating the software output.

After the complete data set is added to the software, the evaluation tab was used to get an idea of the correct mixture order. The mixture order decides which expressions can be

included in the equation for the chosen response surface. By changing which interactions are included, expressions are either added or removed from the equation. The two most common models for mixture designs are the Quadratic model and the Special cubic model shown in Eq. 28 and Eq. 29 respectively (Lindh, 2004). The special cubic model is identical to the quadratic model except from an added term for testing interactions between all components ( $x_1 * x_2 * x_3$ ).

$$y = \beta_1 * x_1 + \beta_2 * x_2 + \beta_3 * x_3 + \beta_{1,2} * x_1 * x_2 + \beta_{1,3} * x_1 * x_3 + \beta_{2,3} * x_2 * x_3 + \varepsilon_s \quad \text{Eq. 28}$$

$$y = \beta_1 * x_1 + \beta_2 * x_2 + \beta_3 * x_3 + \beta_{1,2} * x_1 * x_2 + \beta_{1,3} * x_1 * x_3 + \beta_{2,3} * x_2 * x_3 + \beta_{1,2,3} * x_1 * x_2 * x_3 + \varepsilon_s \quad \text{Eq. 29}$$

Figure 52 shows the full list of possible interactions between the three mixture components labeled A, B and C.

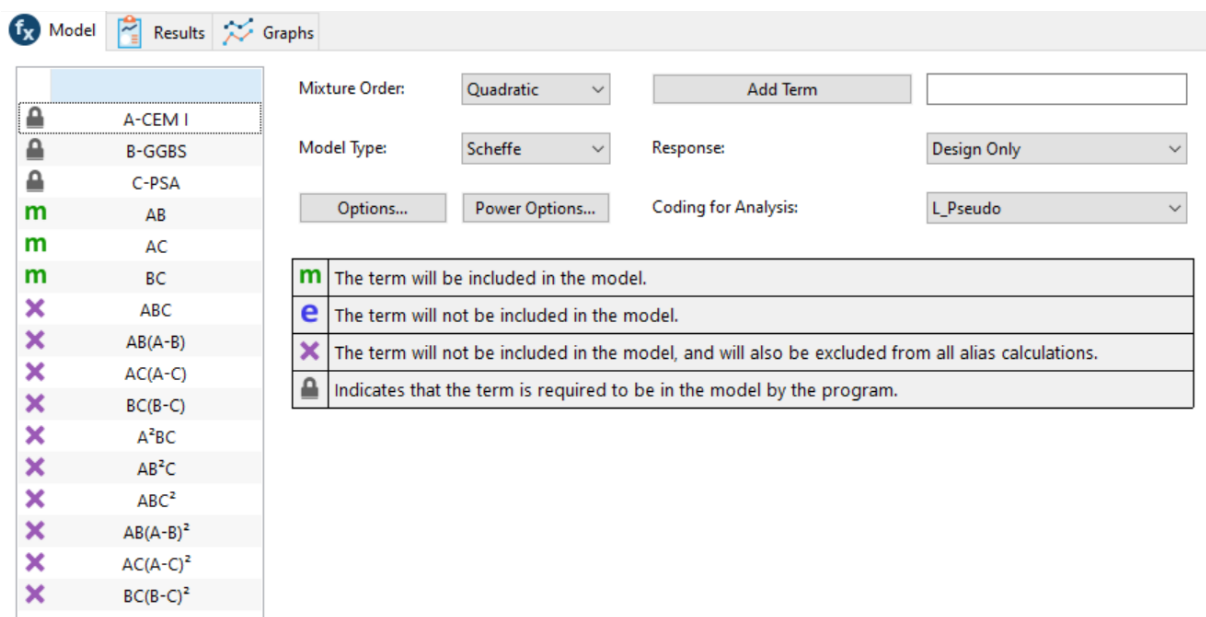


Figure 52: Deciding component interactions under model evaluation in Design Expert.

Altering the quadratic and special cubic models by excluding certain expressions, results in what Design Expert calls a modified or reduced mixture order. This is used to simplify the response surface equation when no interaction is observed. If no interaction between any components is observed, the mixture order is linear (Eq. 30). A linear model is a flat plane without curvature.

$$y = \beta_1 * x_1 + \beta_2 * x_2 + \beta_3 * x_3 + \varepsilon_s \quad \text{Eq. 30}$$

To visualize the different mixture design models, a single data set was used to create the response surfaces shown in Figure 53. When excluding interactions between two binders, the edge of the response surface gets a straight line (linear interaction) between the two binders.

Design-Expert® Software  
 Component Coding: Actual  
 Response: Ultimate compressive strength (kPa)  
 Design Points:  
 ● Above Surface  
 ○ Below Surface  
 136,86 1333,12

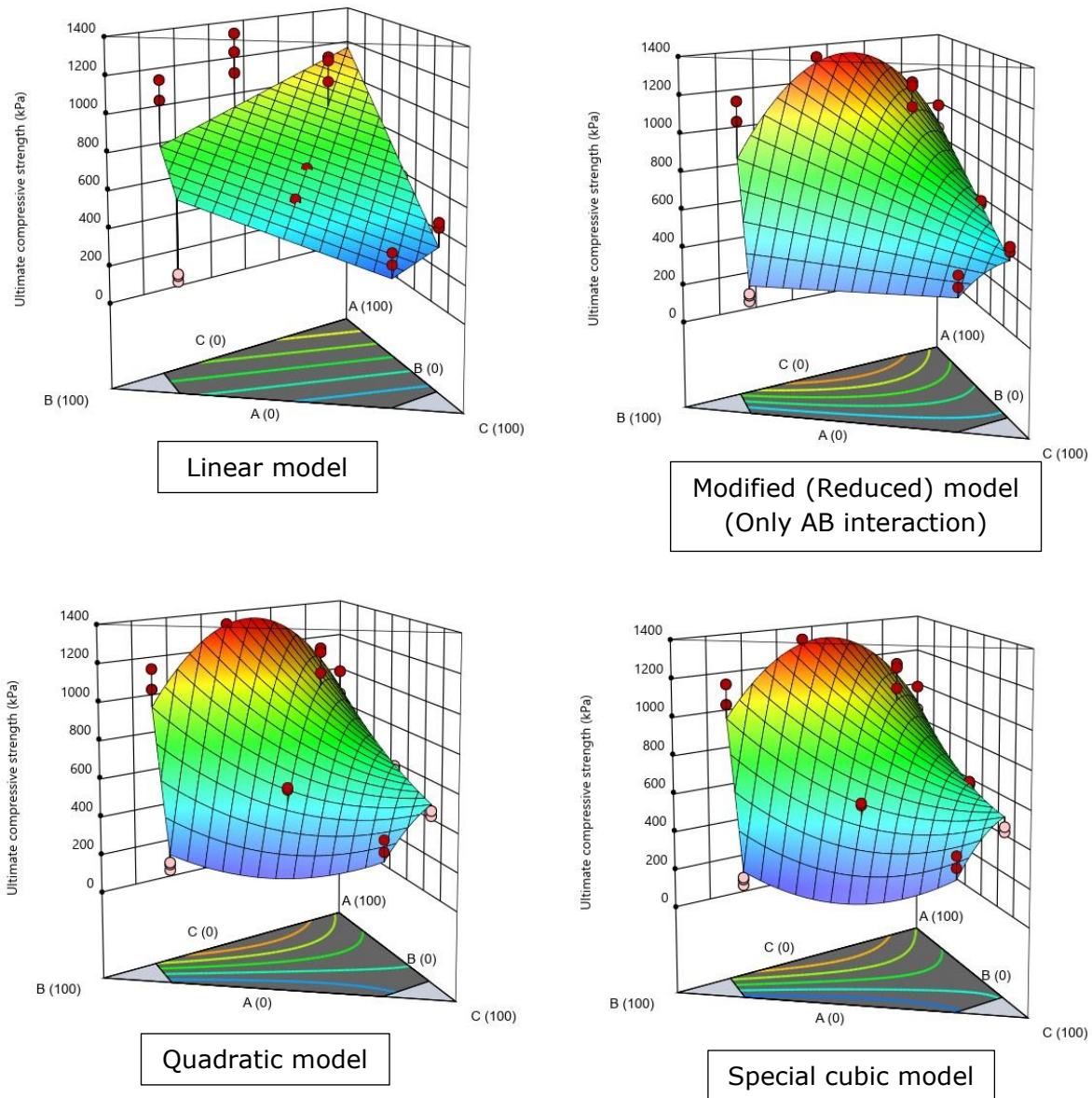


Figure 53: Response surfaces from a single data set using the linear, modified (Only AB interaction), quadratic and special cubic models.

After testing different combinations of interactions, models that are not aliased are considered for further analysis. Models are aliased if they have more terms than unique design points (Stat-Ease, n.d.-c). A Fraction of Design Space (FDS) graph (Figure 54) can also be used to evaluate different mixture design models. FDS is an alternative to power values in factorial designs and summarizes the model's prediction performance over the entire design space (Myers et al., 2009). The FDS curve should be relatively flat with low values of standard error.

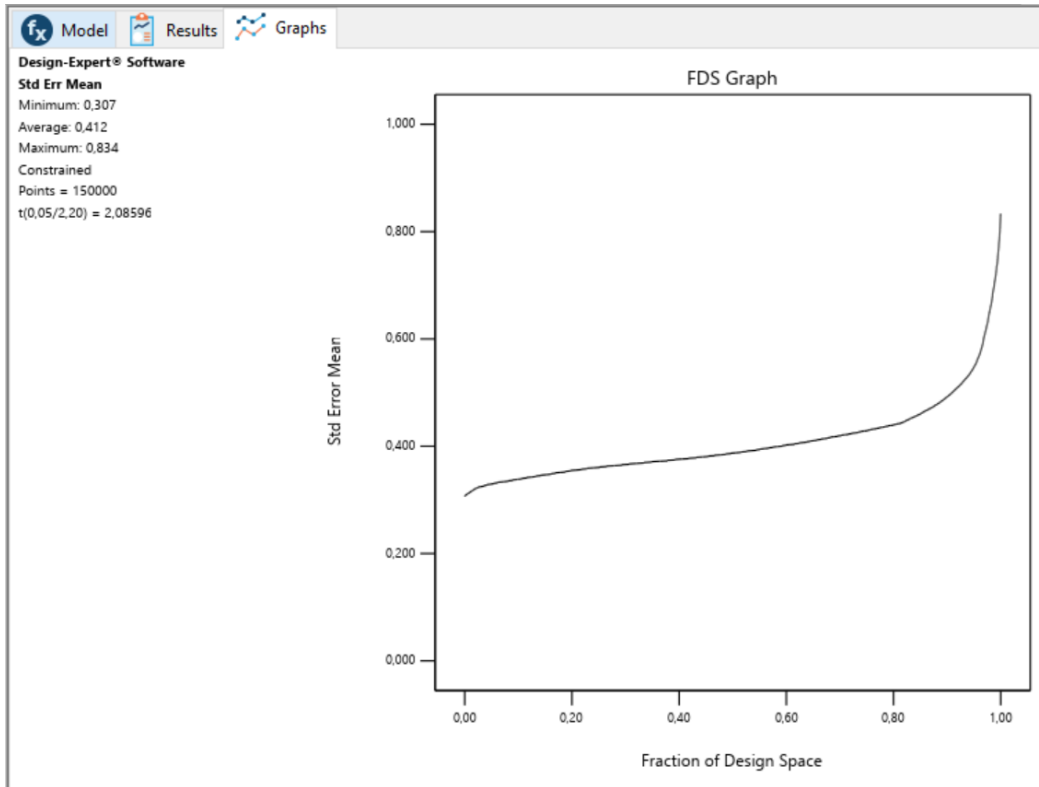


Figure 54: FDS graph example in Design Expert.

A correlation matrix is available to check for correlations between the responses in the raw data. The correlation coefficient (Pearson's  $r$ ) is here interpreted according to Table 24 (Stat-Ease, n.d.-e).

Table 24: Interpretation of Pearson's  $r$  (Zou et al., 2003).

| Pearson's correlation coefficient, $r$ | Direction and level of correlation |
|--|------------------------------------|
| -1.00                                  | Perfectly negative                 |
| -0.80                                  | Strongly negative                  |
| -0.50                                  | Moderately negative                |
| -0.20                                  | Weakly negative                    |
| 0.00                                   | No association                     |
| 0.20                                   | Weakly positive                    |
| 0.50                                   | Moderately positive                |
| 0.80                                   | Strongly positive                  |
| 1.00                                   | Perfectly positive                 |

To create the model in the analysis tab, a data transformation type was set in the configuration window. As a simplification, the "No transform" setting shown in Figure 55 was used for all models even if the diagnostics plots explicitly requires one.



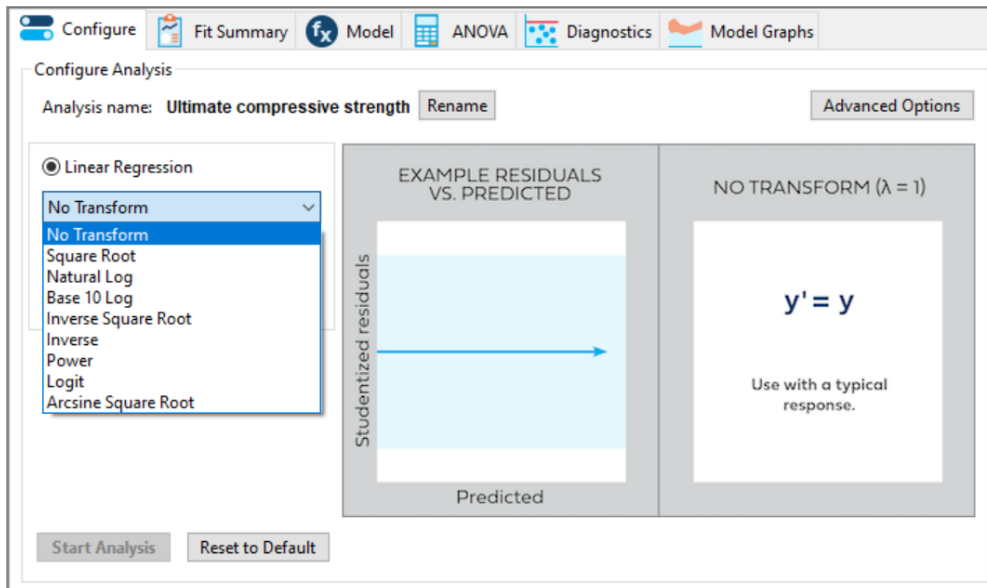


Figure 55: Data transformation options in Design Expert.

After pressing "Start Analysis", the fit summary window shows the suggested model type. The statistical parameters used by the software to determine the best model is described in section 3.5.3. The final step in choosing the model is deciding which interactions to include in the response surface equation. Aliased terms have a warning to prevent it from being included in the model (Figure 56).

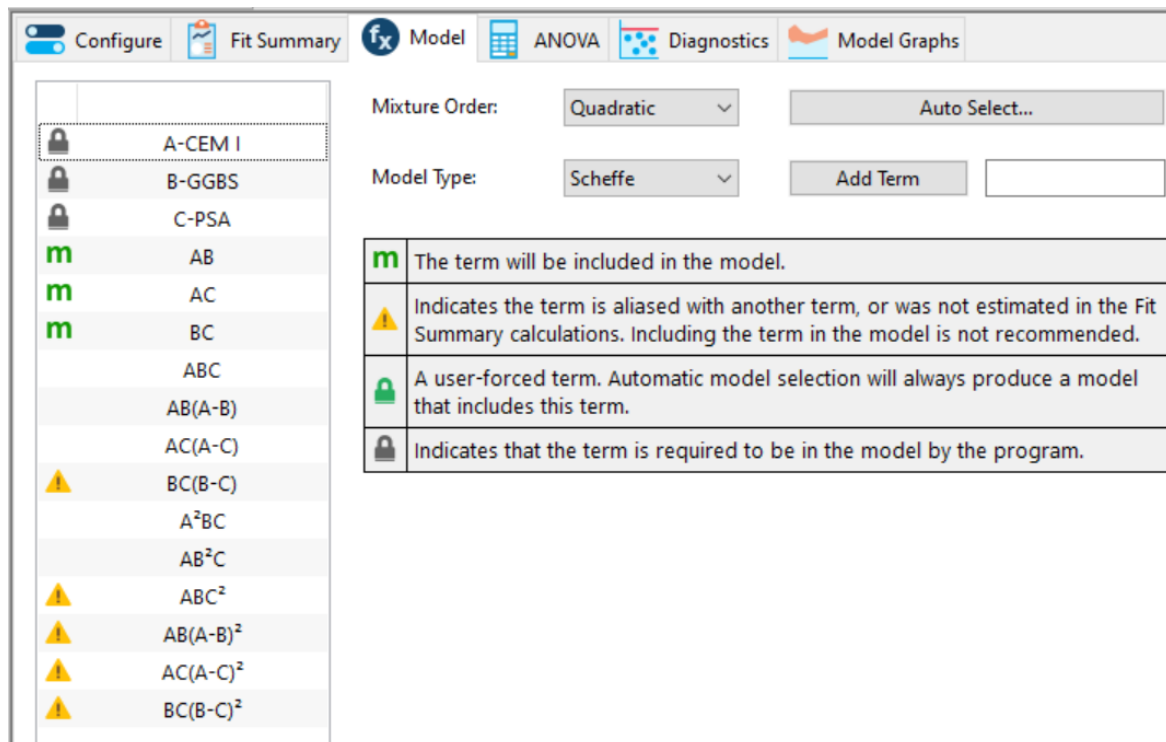


Figure 56: Final model configuration window in Design expert with interaction settings.

Interactions can also be chosen automatically by using the automatic model selection algorithms. Table 25 shows the possible combinations of automatic model selections and criteria. Only AICc (Akaike Information Criterion corrected for a small design) with forward selection was used because it chooses the best interactions based off goodness of

fit (Stat-Ease, 2020). Forward selection means that the model is initially empty before the algorithm incrementally adds each interaction. Each increment is tested for statistical significance. It is recommended to review the analysis of variance to confirm the automatic selection.

Table 25: Combinations of automatic model selections and criteria (Stat-Ease, 2020).

|           |                    | Selection |          |          |                  |
|-----------|--------------------|-----------|----------|----------|------------------|
|           |                    | Forward   | Backward | Stepwise | All Hierarchical |
| Criterion | AICc               | Yes*      | Yes*     | No       | No               |
|           | BIC                | Yes*      | Yes*     | No       | No               |
|           | p-value            | Yes       | Yes*     | Yes      | No               |
|           | Adjusted R-Squared | No        | No       | No       | Yes              |

*\*Best selection method for the given criterion*

### 3.5.3. Analysis of variance (ANOVA) and diagnostics

The Analysis of variance, referred to as ANOVA, is a collection of statistical tests and descriptive statistics (Stat-Ease, n.d.-a). Figure 57 shows the ANOVA window in Design Expert. Additionally, the Fit statistics shown in Figure 58 gives important information on the model precision.

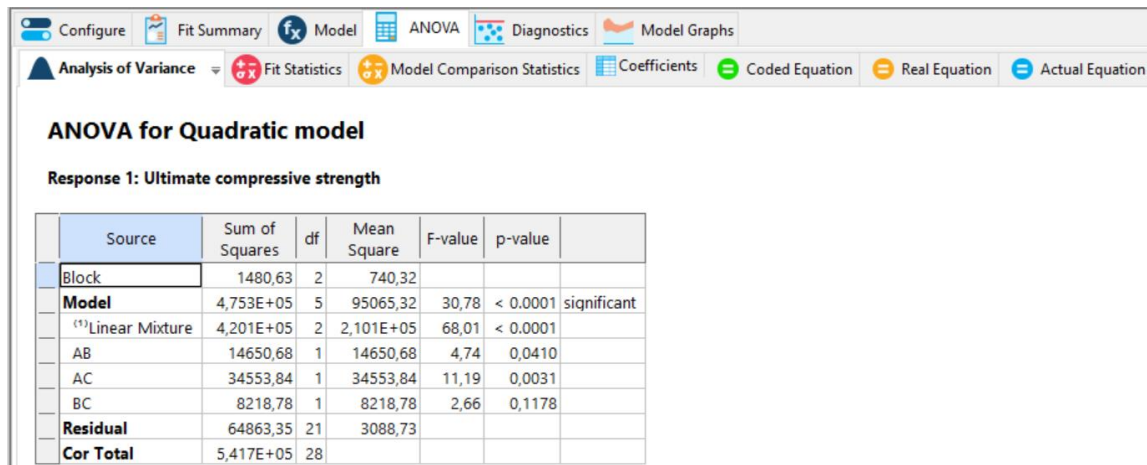


Figure 57: Model ANOVA summary window in Design Expert.

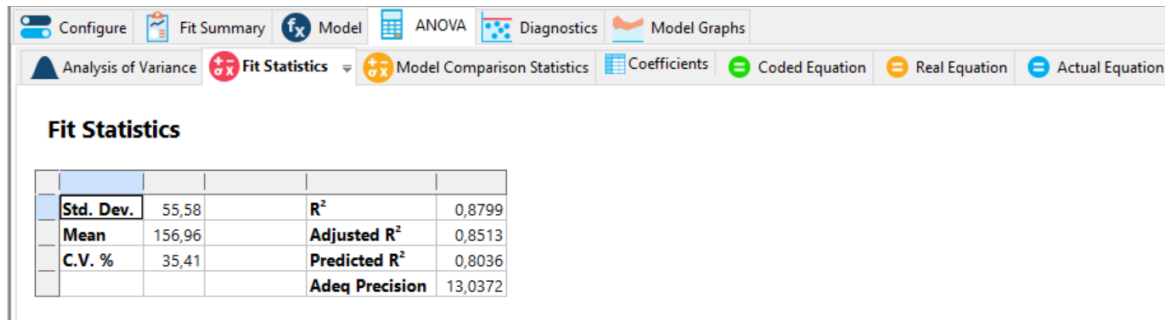


Figure 58: Model fit statistics window in Design Expert.

An overview of the main statistical tests and descriptive statistics, along with common criteria/evaluations, are shown in Table 26.

Table 26: Overview of the main statistical evaluations in the ANOVA.

| Statistical test/<br>Descriptive statistic          | Description   | Criterion/Evaluation   |
|---|---|--|
| p-value   | p-value is the lowest level of significance where the null hypothesis would be rejected (Montgomery, 2013).   | Significant if p-value is lower than 0.05. (Maximum 5 % probability of observing the same results in a scenario where the null hypothesis is true)                   |
| Adjusted R <sup>2</sup> vs Predicted R <sup>2</sup> | R <sup>2</sup> measures the level of variation around the mean decided by the model (Stat-Ease, n.d.-b). A value of 0 indicates no fit, while a value of 1 indicates a perfect fit. | Values should be as high as possible to ensure a good fit. The difference between Adjusted R <sup>2</sup> and Predicted R <sup>2</sup> should also be less than 0.2. |

Figure 59 shows the response surface model equation window. Depending on which interactions are chosen, the equation changes accordingly.

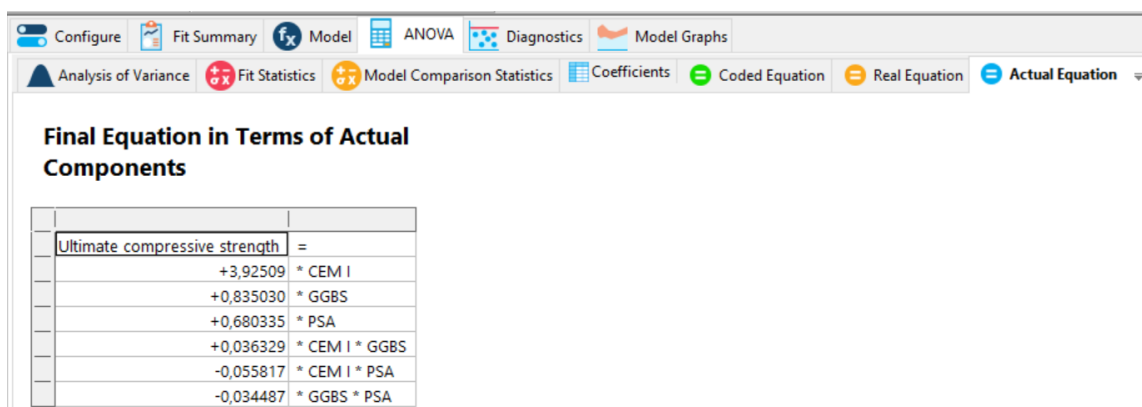


Figure 59: Model equation window in Design Expert.

After the ANOVA is reviewed and the best model is chosen, diagnostic plots are used to verify the model. An important definition in the diagnostic plots is Residuals. Residuals are

differences between the predicted and observed values of the response (Montgomery, 2013). An overview of general diagnostic plot evaluation is shown in Table 27.

Table 27: Diagnostic plot evaluation (Stat-Ease, 2020).

| Plot                   | Bad  | Good                                    |
|------------------------|--|---|
| Normal plot            | S shape  | Straight line                           |
| Residuals vs predicted | Megaphone shape  | Random scatter                          |
| Residuals vs run       | Trend, points outside limits   | No pattern                              |
| Predicted vs actual    | Groups of points away from the line which indicate areas of over or under prediction | Random scatter along the 45-degree line |
| Box-Cox plot           | Transformation recommended   | No transformation necessary             |
| Residuals vs factor    | Greater variation at one end (Watch only for very large differences)                 | Random scatter at both ends             |

The influence plots listed below can be reviewed if the diagnostic plots indicate problems in the model.

- Cook's Distance
- Leverage vs run
- DFFITS (Difference in fits)
- DFBETAS (Difference in beta coefficients)

# 4 | Results

## 4.1 Field samples

### 4.1.1. Visual inspection and sample quality

Images of the field samples are shown in appendix A.1. Each sample is photographed in two orientations and labeled as either exterior 1 or exterior 2. Some of the samples show light to medium surface cracking which was not present before  $\mu$ CT analysis. The cracking was most visible in the WDM.Hjorthagen.3 sample shown in Figure 60.



Figure 60: Visible surface cracking in the upper section of the WDM.Hjorthagen.3 sample.

The MDM.E6.1 sample has significant cracking which runs diagonally through most of the sample. However, this occurred during sampling and is assumed to not negatively affect  $\mu$ CT analysis.

Each sample is also cut to view the interior structure of the samples. The interior images are also shown in appendix A.1. A comparison of the  $\mu$ CT slices and the corresponding interior photos is showcased in section 4.1.4.

### 4.1.2. Water content

Water content measured from the field samples after micro computed tomography testing ( $w_{\mu CT}$ ) is shown in Figure 61. Variations in the water content is experienced due to visible drying in some samples.

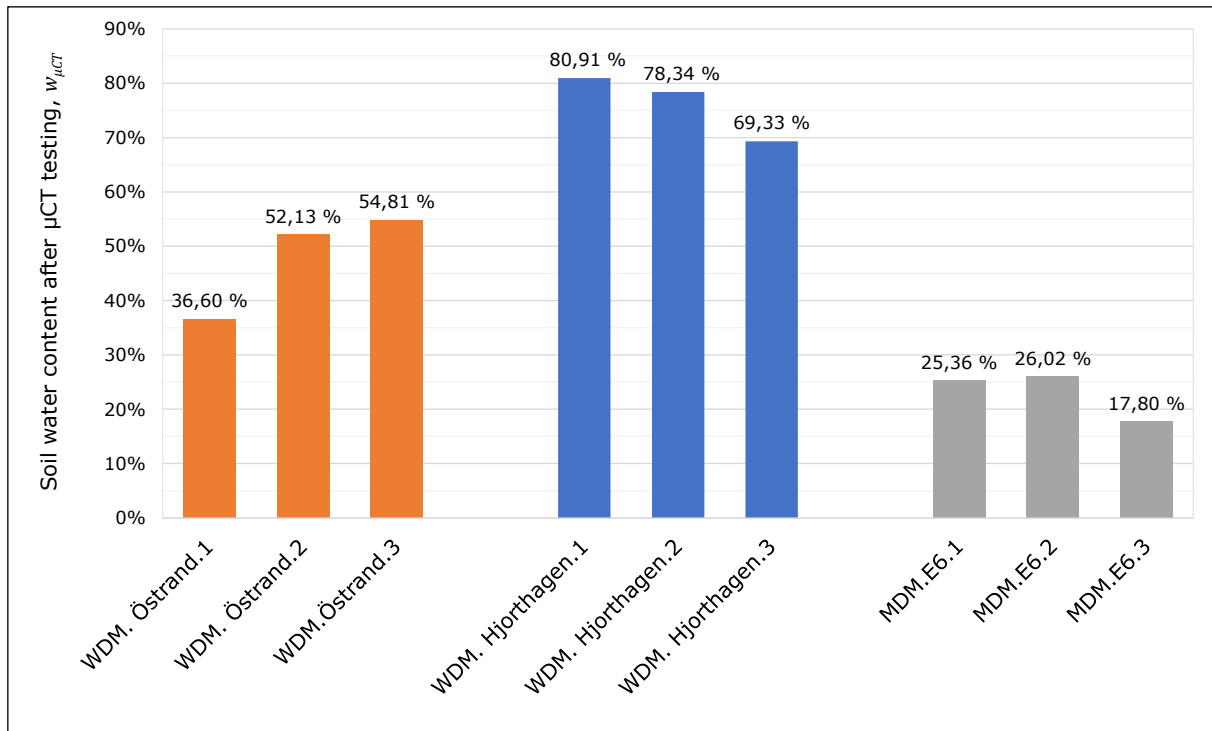


Figure 61: Sample water content after  $\mu$ CT testing.

#### 4.1.3. P-wave velocity

Results from the p-wave velocity measurements are presented in Figure 62. A voltage between 250 and 300 was set in the PUNDIT equipment during the measurements. The tops and bottoms of the field samples are not perfectly level and have rock shards lodged into the surfaces. These inconsistencies make compression testing and p-wave testing difficult. The p-wave velocities are here the only strength indication in the field samples.

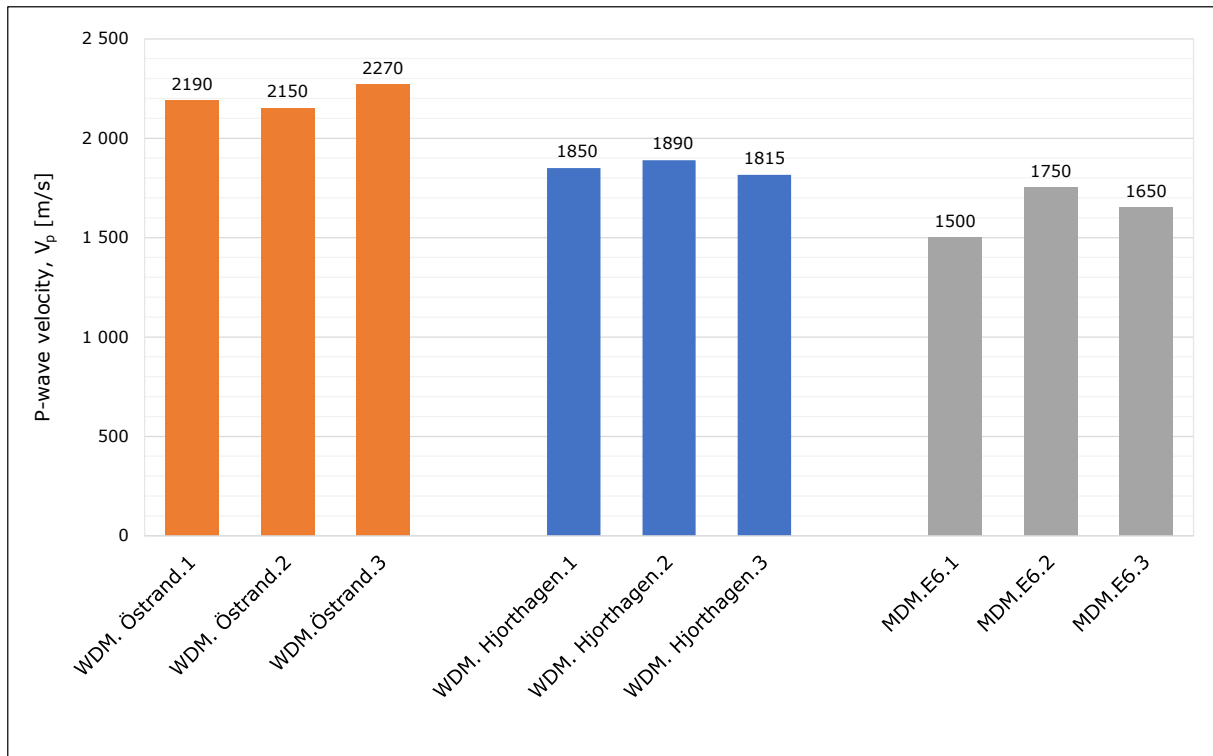


Figure 62: Field sample p-wave velocity test results.

#### 4.1.4. CT-analysis

Calculated macro porosity along the longitudinal axis of each sample (z-axis) is shown in Figure 63, Figure 64 and Figure 65. The large porosity values at the ends of the graphs are not included when calculating the average macro porosity shown in red. These larger values are caused by the conical x-ray beam (see Figure 44), which cuts off parts of the sample ends.

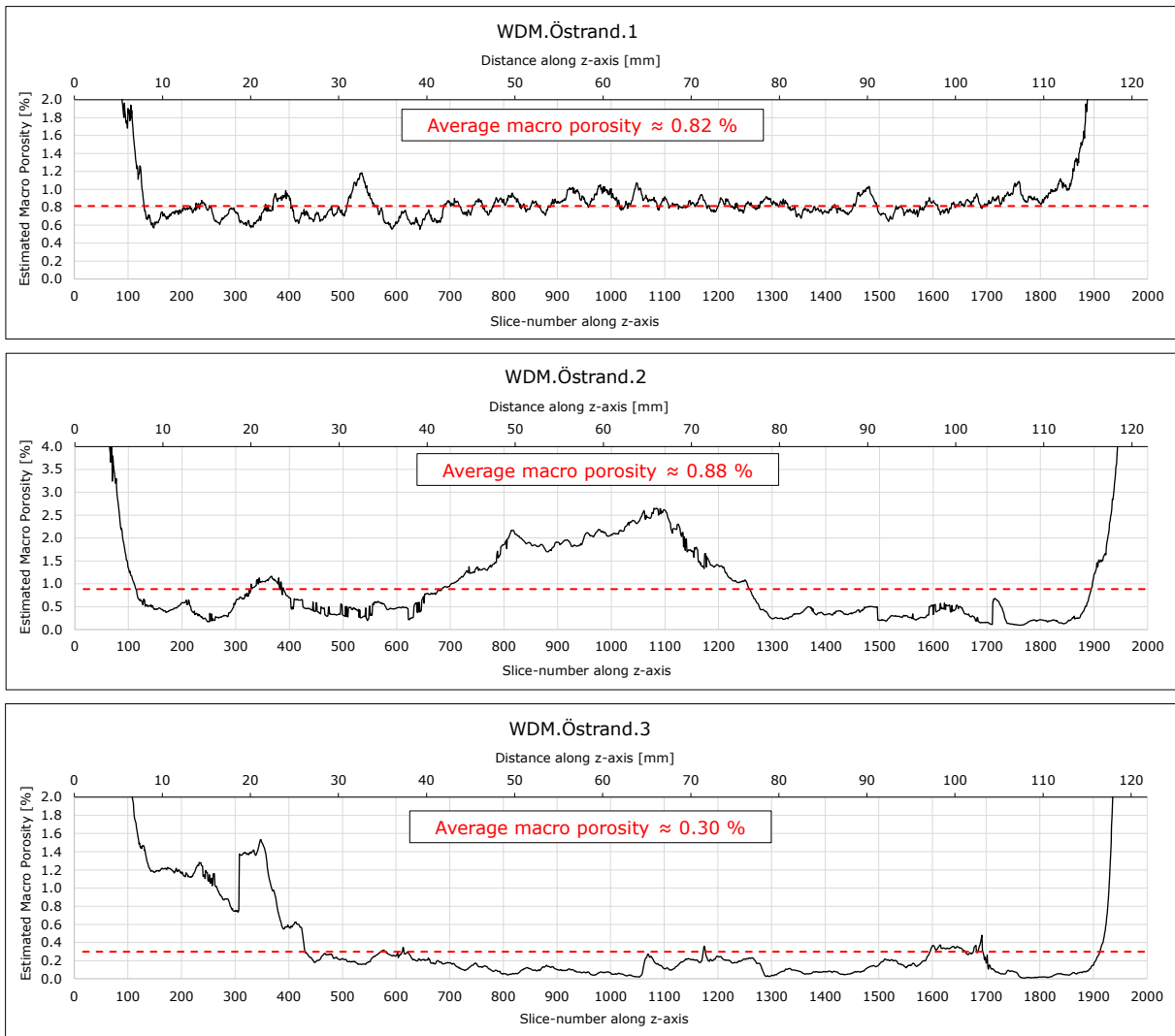


Figure 63: Estimation of macro porosity along the z-axis (longitudinal direction) in the Östrand samples (WDM).



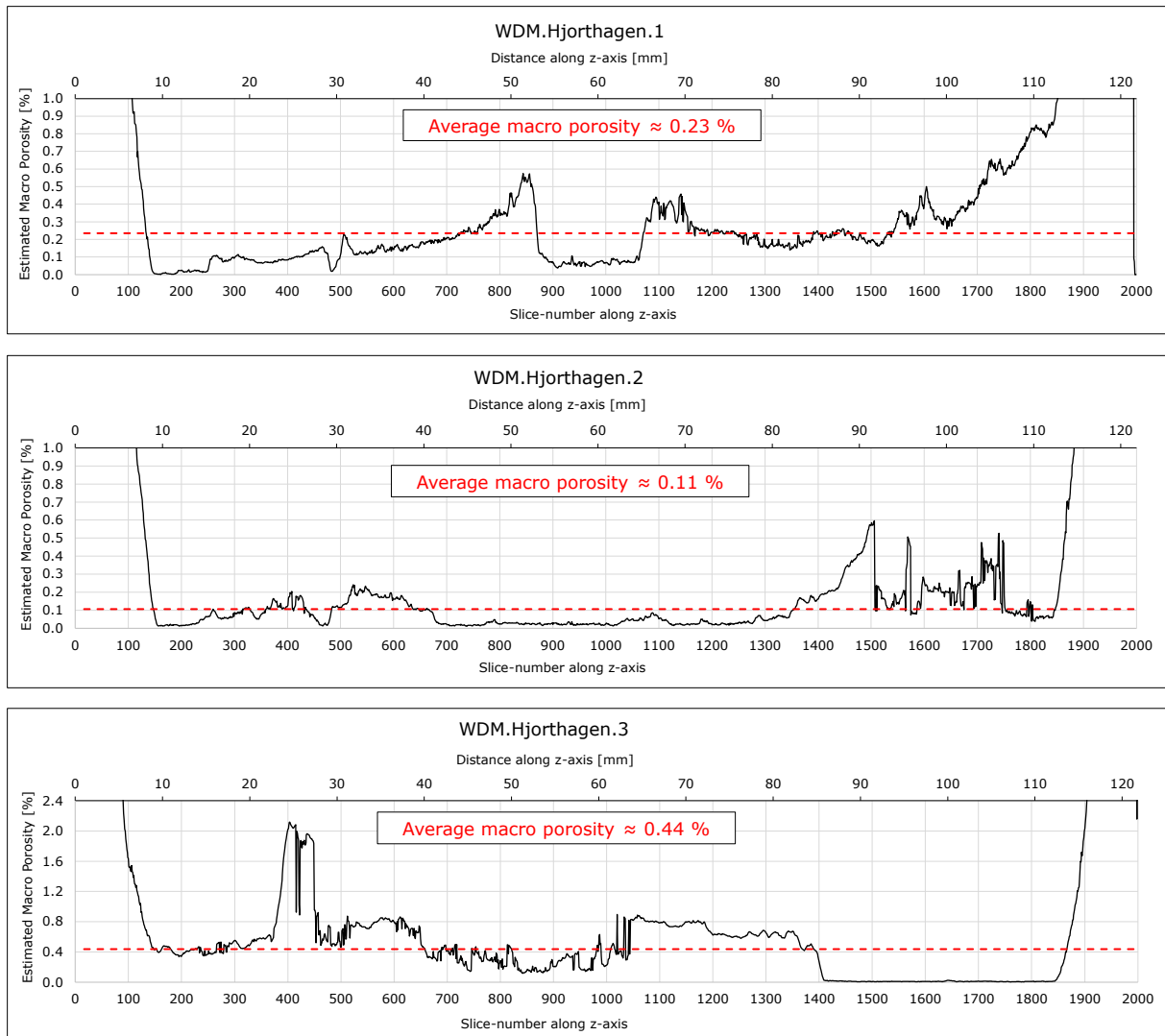


Figure 64: Estimation of macro porosity along the z-axis (longitudinal direction) in the Hjorthagen samples (WDM).

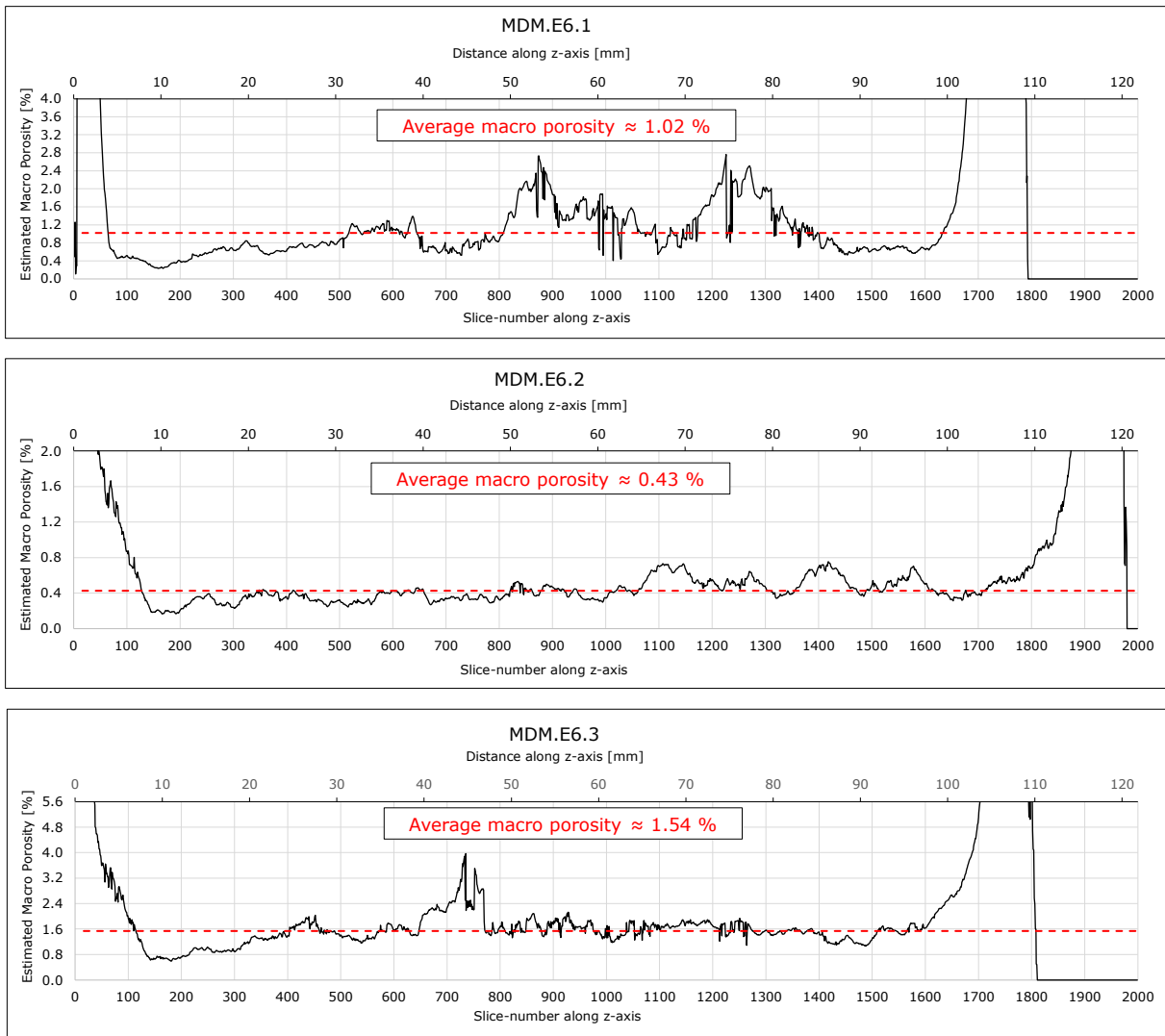


Figure 65: Estimation of macro porosity along the z-axis (longitudinal direction) in the E6 samples (MDM).

Each slice on the porosity graphs above correspond to a reconstructed  $\mu$ CT of the sample interior. To confirm the accuracy of the  $\mu$ CT images, a cut was made across the physical sample for an accurate comparison. The sample cutting information is shown in Table 28. Some samples did not split open evenly, so an estimated range of slices visible in the cut is given. Images of sample interiors at each specific slice (or range of slices) is given in appendix A.1.

Table 28: Sample cutting information.

| Sample ID <sup>[1]</sup> | Location of sample cut during inspection |                      |
|--------------------------|--|----------------------|
|                          | Slice-number                             | Z-axis location [mm] |
| WDM.Östrand.1            | 440-500                                  | ≈26.8-30.5           |
| WDM.Östrand.2            | 1072                                     | ≈65.3                |
| WDM.Östrand.3            | 284-380                                  | ≈17.3-23.1           |
| WDM.Hjorthagen.1         | 1280                                     | ≈78.0                |
| WDM.Hjorthagen.2         | 280-500                                  | ≈17.1-30.5           |
| WDM.Hjorthagen.3         | 804                                      | ≈49.0                |
| MDM.E6.1                 | 648-1540                                 | ≈39.5-93.8           |
| MDM.E6.2                 | 1320                                     | ≈80.4                |
| MDM.E6.3                 | 840                                      | ≈51.2                |

[1] Sample ID explanation: WDM. Östrand.1 = Installed with the WDM method, field sample from the Östrand site, sample number 1

The 2D  $\mu$ CT images of three representative slices, along with 3D reconstructions of the sample components are given in appendix A.2. The full sample along with pores, inclusions, and an overlay of all components cut in half is shown in the 3D reconstructions.

On the 2D  $\mu$ CT images, pores are black while the binder and soil can be seen as varying tones of dark to light grey. Inclusions is here referring to white lumps of varying size and shape with high absorption compared with the rest of the sample. After cutting the sample and comparing the images of the physical sample and the 2D  $\mu$ CT images, two main materials were discovered to have high absorption. Gravel of varying size were the main type of inclusion found in the samples from the Östrand site (Figure 66). Seashells and shell fragments were the main type of inclusion found in the samples from the Hjorthagen site (Figure 67).



Figure 66: 2D  $\mu$ CT image (left) vs physical sample image (right) showing a small piece of gravel as an inclusion in the WDM.Östrand.2 sample at slice 1072.

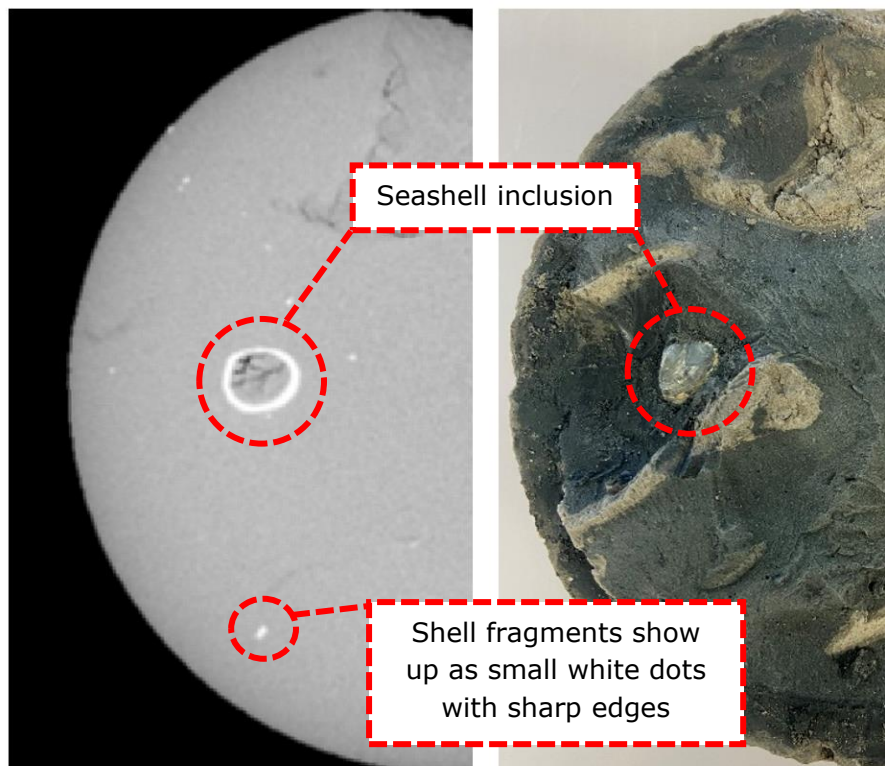


Figure 67: 2D  $\mu$ CT image (left) vs physical sample image (right) showing seashell inclusions in the WDM.Hjorthagen.1 sample at slice 1280.

## 4.2 Laboratory samples

### 4.2.1. Visual inspection and sample quality

The fresh consistency of laboratory mixed samples is greatly varying depending on binder type and wbr. In general, using the dry mixing method gives the samples a stiffer consistency compared with the wet mixing method for the same recipes. Wet mixed samples with a high wbr, low CEM I content and high PSA content results in a runny consistency after mixing. The PSA seems to form lumps in the slurry which the kitchen stand mixer cannot seem to break up.

After curing for 28 days, images of each sample were taken directly after extrusion (see appendix B.1 and B.2). The quality of the curing conditions is measured as sample weight deviation over the entire curing period. An overview of the sample weight deviation after curing is presented in Figure 68. Here, values are negative, because the sample weight deviation is defined as the weight after curing minus the initial weight, divided by the initial sample weight. Deviations are consistently low (around 0.5 % lower weight after curing) for most combinations of mixing method and wbr. The number of outliers in the plot is also low. Curing conditions are therefore considered to be satisfactory.

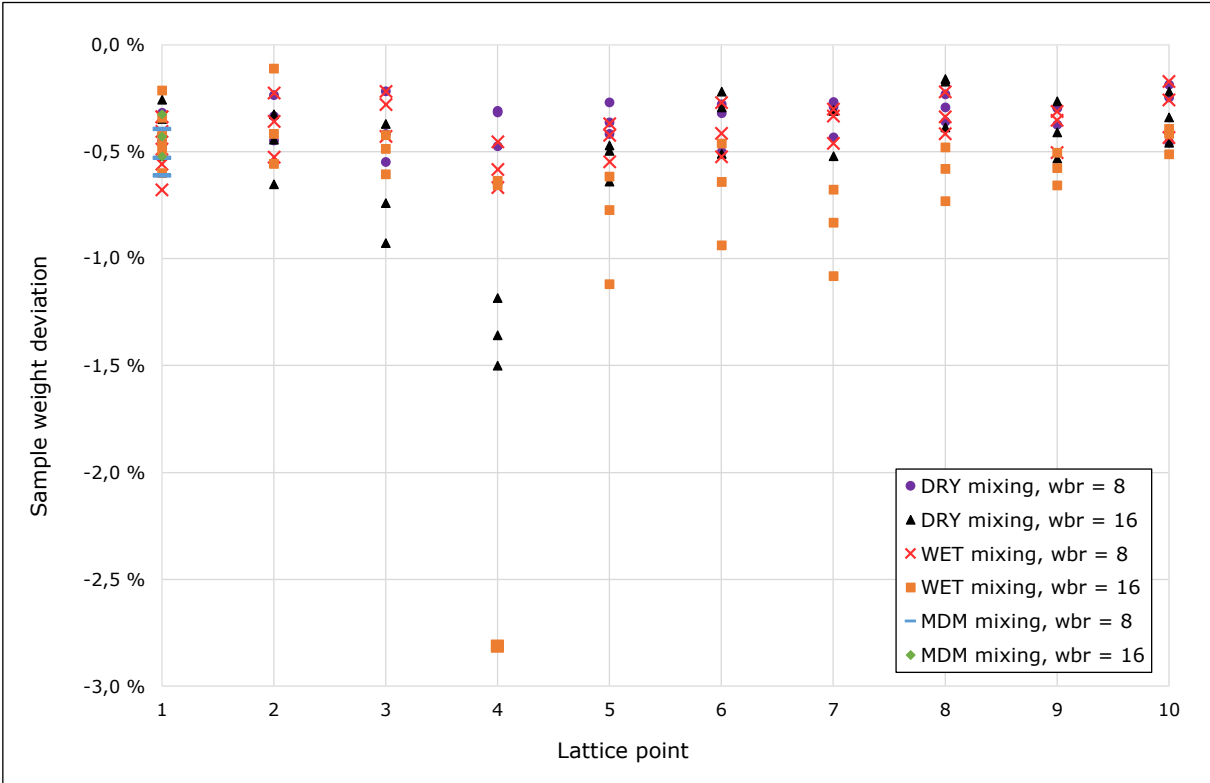


Figure 68: Sample weight deviation after curing.

After UCT, a visual inspection of the samples showed binder accumulation in some of the dry mixed samples. This is mainly noticeable in the samples with lower cement content. Figure 69 shows a dry mixed sample chunk with two clear accumulations of different colored binders. No visible binder accumulation is experienced in the wet mixed samples.



Figure 69: Binder accumulation in a dry mixed sample.

#### **4.2.2. Water content, entrapped air and corrected wbr**

Water content is assumed and measured in multiple phases of the laboratory testing. This is done to minimize the risk of errors and to have a good basis for discussion of the test results. An overview over the initial assumed soil water content in the samples is presented in Table 29.

Table 29: Assumed clay water content overview.

| wbr=8   |                                   | wbr=16                  |                                   |
|---|-----------------------------------|-------------------------|-----------------------------------|
| Batch ID <sup>[1]</sup>   | Assumed clay water content, $w_s$ | Batch ID                | Assumed clay water content, $w_s$ |
| DRY.8.1   | 45%                               | DRY.16.1                | 45%                               |
| DRY.8.2   | 45%                               | DRY.16.2                | 45%                               |
| DRY.8.3   | 45%                               | DRY.16.3                | 45%                               |
| DRY.8.4   | 45%                               | DRY.16.4                | 45%                               |
| DRY.8.5   | 45%                               | DRY.16.5                | 43%                               |
| DRY.8.6   | 45%                               | DRY.16.6                | 43%                               |
| DRY.8.7   | 45%                               | DRY.16.7                | 45%                               |
| DRY.8.8   | 45%                               | DRY.16.8                | 45%                               |
| DRY.8.9   | 45%                               | DRY.16.9                | 45%                               |
| DRY.8.10  | 45%                               | DRY.16.10               | 45%                               |
| WET.8.1   | 45%                               | WET.16.1                | 45%                               |
| WET.8.1 <sup>[2]</sup>  | 45%                               | WET.16.1 <sup>[2]</sup> | 45%                               |
| MDM.8.1 <sup>[2]</sup>  | 45%                               | MDM.16.1 <sup>[2]</sup> | 45%                               |
| WET.8.2   | 43%                               | WET.16.2                | 43%                               |
| WET.8.3   | 43%                               | WET.16.3                | 43%                               |
| WET.8.4   | 45%                               | WET.16.4                | 43%                               |
| WET.8.5   | 45%                               | WET.16.5                | 45%                               |
| WET.8.6   | 45%                               | WET.16.6                | 45%                               |
| WET.8.7   | 45%                               | WET.16.7                | 48%                               |
| WET.8.8   | 45%                               | WET.16.8                | 48%                               |
| WET.8.9   | 45%                               | WET.16.9                | 48%                               |
| WET.8.10  | 43%                               | WET.16.10               | 48%                               |
| [1] Batch ID explanation: DRY.8.1 = Dry mixing method, WET.8.1 = Wet mixing method, MDM.8.1 = Modified dry mixing method, water to binder ratio of 8, lattice point 1 |                                   |                         |                                   |
| [2] Additional points for single wet mixing method evaluation   |                                   |                         |                                   |

Result overviews for corrected wbr, entrapped air and water content in the samples are presented in appendix B.3.1. Most of the  $wbr_{corr}$  values are close to the set values of 8 and 16. Batches with high deviation in  $wbr_{corr}$  also have a large deviation between initial and assumed clay water content.

In general, the measured water content after UCT ( $w_{UCT}$ ) is lower than the measured initial clay water content ( $w_{stab}$ ). However, the results show that 14 out of 22 batches with a wbr of 8 increase in water content after UCT. For batches with a wbr of 16, only 4 out of 22 batches increase in water content after UCT.

Entrapped air is estimated to ensure that no samples have excessive air void content beyond what is visible on the sample images. Most of the  $n_{air}$  values are between 0 and 4 %. Negative  $n_{air}$  values are not possible to achieve in reality. They are caused by errors in the assumptions and/or measurements.

**4.2.3. Strength, stiffness and strain**

Sample deformation and fractures during unconfined compression testing clearly varied when changing binder content and amount. Medium to high CEM I content together with medium to high GGBS content gives high strength and low failure strain for a wbr of 8. When increasing the wbr to 16, then CEM I becomes the main contributor to strength development. The three main fracture patterns shown below occurred. An important note is that the patterns did not clearly match specific strengths. Figure 70 shows a combination of a cone and a longitudinal fracture pattern.



Figure 70: Combination of a cone and longitudinal fracture pattern.

Fracture patterns with clear hourglass shapes stretching from the top to the bottom of the sample is shown in Figure 71.



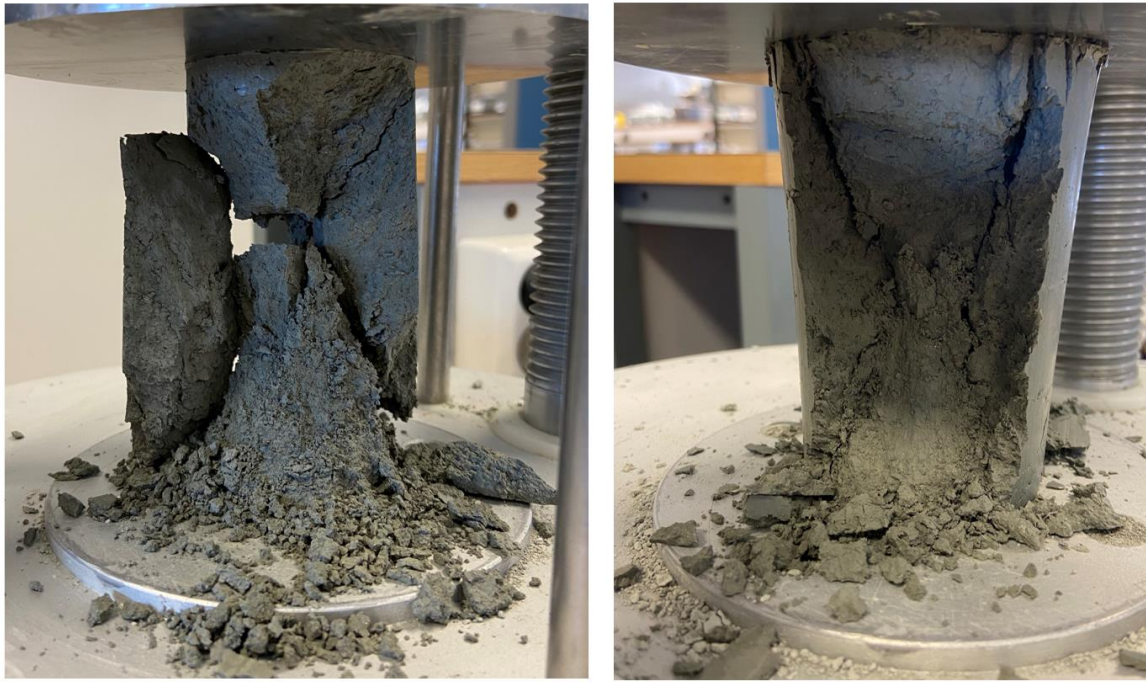


Figure 71: Hourglass shaped fracture patterns.

Mainly longitudinal sample fractures are shown in Figure 72.

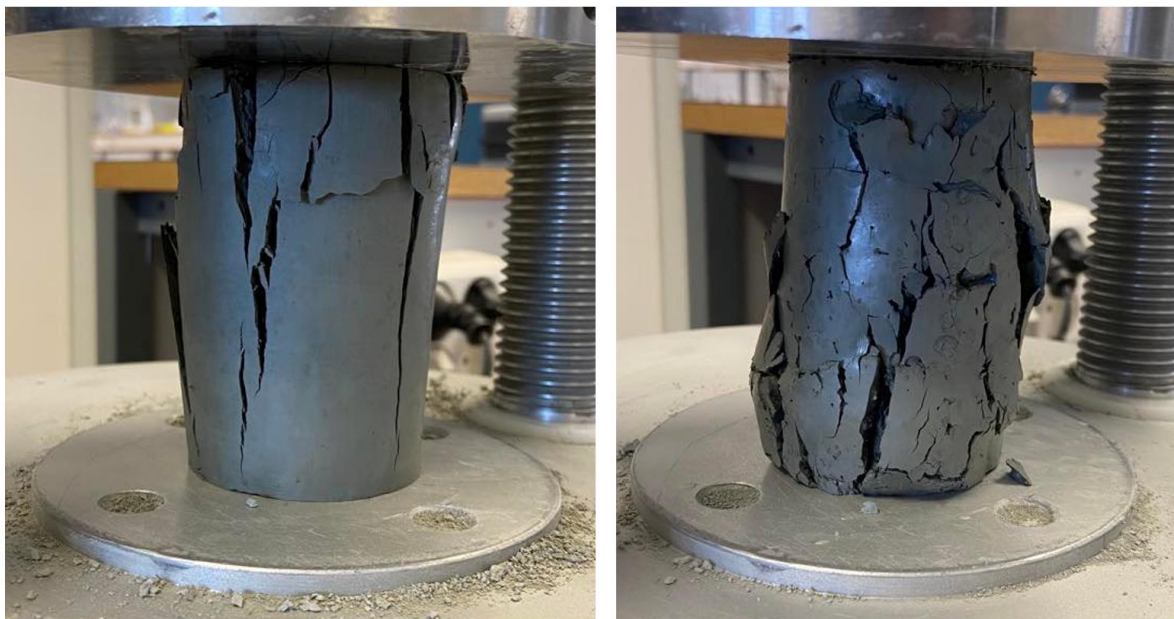


Figure 72: Mainly longitudinal fracture patterns.

A collection of the interpreted UCT parameters from the dry mixed samples is presented in Table 47 and Table 48 in appendix B.3.2. For complete UCT graphs, along with images and dry mixed sample information, see appendix B.1. All UCT graphs in the appendix are shifted to start when the load frame registers at least 0.5 to 2 Newtons of force. This causes the graphs to end slightly below 10 % strain (labeled as "Dotted line min." in appendix B.1 and B.2). The shift is necessary to get an accurate measurement of failure strain ( $\epsilon_v$ ).

A collection of the interpreted UCT parameters from the wet mixed samples is presented in Table 49 and Table 50 in appendix B.3.2. For complete UCT graphs, along with images and wet mixed sample information, see appendix B.1 and B.2. Appendix B.2 contains the full UCT results for the added sample points for single wet mixing method evaluation.

**4.2.4. P-wave velocity**

Results from the p-wave measurements are presented in Table 51 and Table 52 in appendix B.3.3 for the dry and wet mixed samples, respectively. P-wave velocities are consistent in most of the dry mixed batches, independent of wbr.

The p-wave results for wet mixed samples with a wbr of 8 are consistent in each batch. Voltage set in the PUNDIT equipment is consistent for most samples, independent of mixing method. When increasing wbr to 16 when using the wet method, some low strength samples show inconsistent and very high p-wave velocities ( $V_p$ ).

**4.3 Mixture design**

An overview of the lattice points and their corresponding binder contents (originally shown in section 3.2.3) is shown in Figure 73 and Figure 74.

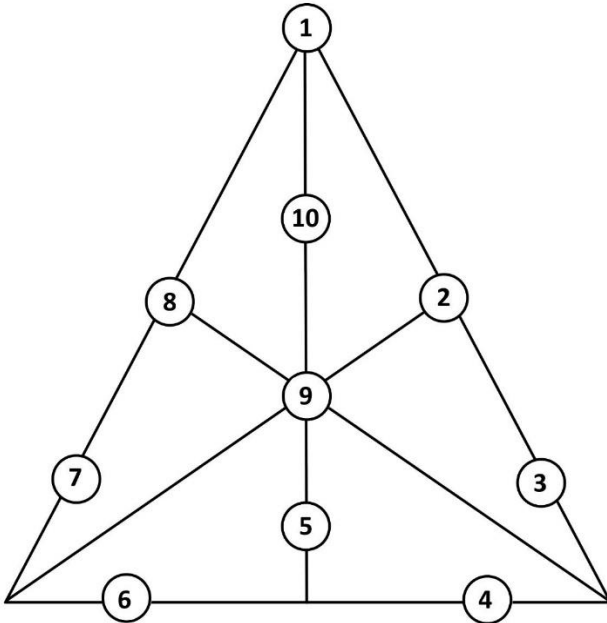


Figure 73: Chosen augmented simplex lattice design.

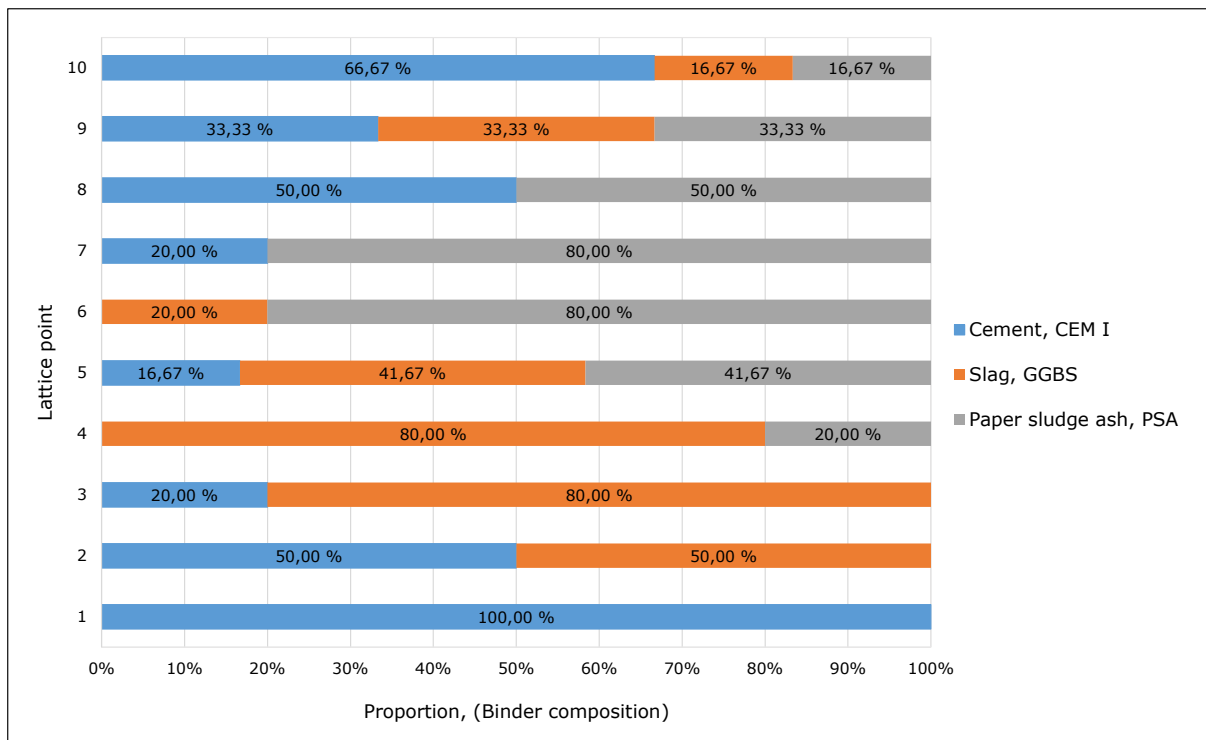


Figure 74: Overview of lattice points and corresponding binder content.

#### 4.3.1. Correlation, model and analysis of variance (ANOVA)

Samples which show clear signs of damage or other inconsistencies are ignored in the response surface modeling. The samples (and single values) which were not included in the response surface models due to cracking or performance inconsistencies is shown in Table 30. To avoid these values from being included in Design Expert, single cells or entire rows are ignored in the Design tab.

Table 30: Samples and values not included in response surface modelling.

| Sample ID   | Software Row (Cell) Status            | Comment   |
|-------------|---------------------------------------|---|
| DRY.8.3.3   | Ignored                               | Inconsistent strength due to sample damage (cracking) |
| DRY.8.6.3   | Ignored                               | Inconsistent strength                                 |
| DRY.8.7.3   | Ignored                               | Inconsistent strength due to sample damage (cracking) |
| WET.8.5.2   | Ignored                               | Inconsistent strength due to sample damage (cracking) |
| WET.16.7.3  | Ignored                               | Inconsistent strength                                 |
| DRY.8.1.2   | (Ignored single stiffness cell)       | Inconsistent stiffness                                |
| DRY.8.4.3   | (Ignored single stiffness cell)       | Inconsistent stiffness                                |
| DRY.16.10.3 | (Ignored single stiffness cell)       | Inconsistent stiffness                                |
| WET.8.1.3   | (Ignored single stiffness cell)       | Inconsistent stiffness                                |
| WET.8.2.3   | (Ignored single stiffness cell)       | Inconsistent stiffness                                |
| WET.16.1.1  | (Ignored single stiffness cell)       | Inconsistent stiffness                                |
| WET.8.7.1   | (Ignored single strain cell)          | Inconsistent strain                                   |
| WET.16.5.3  | (Ignored single strain cell)          | Inconsistent strain                                   |
| WET.16.6.2  | (Ignored single p-wave velocity cell) | Inconsistent p-wave velocity                          |

A correlation matrix for all five responses (R1 to R5) is shown in Table 31 for samples prepared with the dry mixing method and a wbr of 8. Interpretation of the direction and level of correlation by Pearson's  $r$  is also included in all of the correlation matrices (see section 3.5.2).

The full input and output of each Design Expert analysis, including diagnostic plots, is given in appendix B.4.1 and B.4.2. Every page has been labeled with either DRY.8 and WET.8, or DRY.16 and WET.16 to indicate which mixing method and wbr is compared. Five response surface models are created in each combination of mixing method and wbr. A total of 20 response surface models are therefore included. Model information and ANOVA results for samples prepared with the dry mixing method and a wbr of 8 is shown in Table 32.

Table 31: Correlation matrix for samples prepared with the dry mixing method and wbr of 8.

|   | R1:<br>Ultimate<br>compressive<br>strength, $q_u$ | R2:<br>Undrained<br>shear<br>strength, $S_u$ | R3:<br>Failure<br>strain, $\varepsilon_v$ | R4:<br>Estimated<br>stiffness, $E_{50}$ | R5:<br>P-wave<br>velocity, $V_p$ |
|---|---|--|---|---|----------------------------------|
| R1:<br>Ultimate<br>compressive<br>strength, $q_u$ | 1   | 1  | -0.73<br>Moderately<br>negative           | 0.93<br>Strongly<br>positive            | 0.92<br>Strongly<br>positive     |
| R2:<br>Undrained<br>shear<br>strength, $S_u$      | 1   | 1  | -0.73<br>Moderately<br>negative           | 0.93<br>Strongly<br>positive            | 0.92<br>Strongly<br>positive     |
| R3:<br>Failure<br>strain, $\varepsilon_v$         | -0.73<br>Moderately<br>negative                   | -0.73<br>Moderately<br>negative              | 1   | -0.87<br>Strongly<br>negative           | -0.88<br>Strongly<br>negative    |
| R4:<br>Estimated<br>stiffness, $E_{50}$           | 0.93<br>Strongly<br>positive                      | 0.93<br>Strongly<br>positive                 | -0.87<br>Strongly<br>negative             | 1                                       | 0.95<br>Strongly<br>positive     |
| R5:<br>P-wave<br>velocity, $V_p$                  | 0.92<br>Strongly<br>positive                      | 0.92<br>Strongly<br>positive                 | -0.88<br>Strongly<br>negative             | 0.95<br>Strongly<br>positive            | 1                                |

Table 32: Model information and ANOVA results for samples prepared with the dry mixing method and wbr of 8.

| Response   | Model characteristic                 | Result  |
|--|--------------------------------------|---|
| R1:<br>Ultimate compressive strength, $q_u$<br>(R2:<br>Undrained shear strength, $S_u$ ) | Selected interactions <sup>[1]</sup> | AB, BC  |
|  | Type                                 | Reduced quadratic   |
|  | Equation <sup>[1]</sup>              | $q_u = 878.201 * A + 398.832 * B + 361.473 * C + 2711.570 * AB - 1060.170 * BC$<br>$(S_u = 439.100 * A + 199.420 * B + 180.737 * C + 1355.784 * AB - 530.107 * BC)$ |
|  | p-value                              | <0.0001   |
|  | Standard deviation                   | 121.28 kPa (60.64 kPa)  |
|  | Mean                                 | 700.56 kPa (350.28 kPa)   |
|  | Adjusted R <sup>2</sup>              | 0.8942  |
|  | Predicted R <sup>2</sup>             | 0.8385  |
| R3:<br>Failure strain, $\varepsilon_v$   | Selected interactions <sup>[1]</sup> | AC, BC  |
|  | Type                                 | Reduced Quadratic   |
|  | Equation <sup>[1]</sup>              | $\varepsilon_v = 2.274 * A + 1.457 * B + 4.097 * C + 2.441 * AC + 8.547 * BC$   |
|  | p-value                              | <0.0001   |
|  | Standard deviation                   | 0.57 %  |
|  | Mean                                 | 3.29 %  |
|  | Adjusted R <sup>2</sup>              | 0.7672  |
|  | Predicted R <sup>2</sup>             | 0.6655  |
| R4:<br>Estimated stiffness, $E_{50}$   | Selected interactions <sup>[1]</sup> | AB, AC, BC  |
|  | Type                                 | Quadratic   |
|  | Equation <sup>[1]</sup>              | $E_{50} = 69252.991 * A + 58792.745 * B + 31052.325 * C + 190321.417 * AB - 110575.771 * AC - 251556.205 * BC$  |
|  | p-value                              | <0.0001   |
|  | Standard deviation                   | 17822.55 kPa  |
|  | Mean                                 | 44751.27 kPa  |
|  | Adjusted R <sup>2</sup>              | 0.8159  |
|  | Predicted R <sup>2</sup>             | 0.7176  |
| R5:<br>P-wave velocity, $V_p$  | Selected interactions <sup>[1]</sup> | AB, AC, BC  |
|  | Type                                 | Quadratic   |
|  | Equation <sup>[1]</sup>              | $V_p = 1264.128 * A + 878.220 * B + 620.974 * C + 2114.016 * AB - 1847.767 * AC - 3150.253 * BC$  |
|  | p-value                              | <0.0001   |
|  | Standard deviation                   | 135.66 m/s  |
|  | Mean                                 | 765.74 m/s  |
|  | Adjusted R <sup>2</sup>              | 0.9310  |
|  | Predicted R <sup>2</sup>             | 0.8968  |
| [1] A=CEM I, B=GGBS, C=PSA   |                                      |   |

A correlation matrix for all five responses (R1 to R5) is shown in Table 33 for samples prepared with the dry mixing method and a wbr of 16. Model information and ANOVA results for samples prepared with the dry mixing method and a wbr of 16 is shown in Table 34.

Table 33: Correlation matrix for samples prepared with the dry mixing method and wbr of 16.

|   | R1:<br>Ultimate<br>compressive<br>strength, $q_u$ | R2:<br>Undrained<br>shear<br>strength, $S_u$ | R3:<br>Failure<br>strain, $\varepsilon_p$ | R4:<br>Estimated<br>stiffness, $E_{50}$ | R5:<br>P-wave<br>velocity, $V_p$ |
|---|---|--|---|---|----------------------------------|
| R1:<br>Ultimate<br>compressive<br>strength, $q_u$ | 1   | 1  | -0.53<br>Moderately<br>negative           | 0.90<br>Strongly<br>positive            | 0.04<br>No<br>association        |
| R2:<br>Undrained<br>shear<br>strength, $S_u$      | 1   | 1  | -0.53<br>Moderately<br>negative           | 0.90<br>Strongly<br>positive            | 0.04<br>No<br>association        |
| R3:<br>Failure<br>strain, $\varepsilon_p$         | -0.53<br>Moderately<br>negative                   | -0.53<br>Moderately<br>negative              | 1   | -0.73<br>Moderately<br>negative         | -0.63<br>Moderately<br>negative  |
| R4:<br>Estimated<br>stiffness, $E_{50}$           | 0.90<br>Strongly<br>positive                      | 0.90<br>Strongly<br>positive                 | -0.73<br>Moderately<br>negative           | 1                                       | 0.32<br>Weakly<br>positive       |
| R5:<br>P-wave<br>velocity, $V_p$                  | 0.04<br>No<br>association                         | 0.04<br>No<br>association                    | -0.63<br>Moderately<br>negative           | 0.32<br>Weakly<br>positive              | 1                                |

Table 34: Model information and ANOVA results for samples prepared with the dry mixing method and wbr of 16.

| Response   | Model characteristic                 | Result   |
|--|--------------------------------------|--|
| R1:<br>Ultimate compressive strength, $q_u$<br>(R2:<br>Undrained shear strength, $S_u$ ) | Selected interactions <sup>[1]</sup> | AB, AC   |
|  | Type                                 | Reduced quadratic  |
|  | Equation <sup>[1]</sup>              | $q_u = 443.681 * A + 53.914 * B + 101.166 * C + 93.173 * AB - 142.024 * AC$<br>$(S_u = 221.841 * A + 26.957 * B + 50.583 * C + 46.587 * AB - 71.012 * AC)$ |
|  | p-value                              | <0.0001  |
|  | Standard deviation                   | 17.68 kPa (8.84 kPa)   |
|  | Mean                                 | 204.70 kPa (102.35 kPa)  |
|  | Adjusted R <sup>2</sup>              | 0.9769   |
|  | Predicted R <sup>2</sup>             | 0.9674   |
| R3:<br>Failure strain, $\varepsilon_v$   | Selected interactions <sup>[1]</sup> | AC, ABC  |
|  | Type                                 | Reduced special cubic  |
|  | Equation <sup>[1]</sup>              | $\varepsilon_v = 2.238 * A + 2.521 * B + 6.776 * C - 2.239 * AC - 16.734 * ABC$  |
|  | p-value                              | <0.0001  |
|  | Standard deviation                   | 0.45 %   |
|  | Mean                                 | 3.49 %   |
|  | Adjusted R <sup>2</sup>              | 0.8925   |
|  | Predicted R <sup>2</sup>             | 0.8396   |
| R4:<br>Estimated stiffness, $E_{50}$   | Selected interactions <sup>[1]</sup> | AB, AC   |
|  | Type                                 | Reduced quadratic  |
|  | Equation <sup>[1]</sup>              | $E_{50} = 32718.750 * A + 2962.630 * B + 3705.372 * C + 21510.070 * AB - 38470.194 * AC$   |
|  | p-value                              | <0.0001  |
|  | Standard deviation                   | 2077.80 kPa  |
|  | Mean                                 | 12354.31 kPa   |
|  | Adjusted R <sup>2</sup>              | 0.9584   |
|  | Predicted R <sup>2</sup>             | 0.9408   |
| R5:<br>P-wave velocity, $V_p$  | Selected interactions <sup>[1]</sup> | AB, AC, BC   |
|  | Type                                 | Quadratic  |
|  | Equation <sup>[1]</sup>              | $V_p = 1067.482 * A + 2084.408 * B + 261.778 * C - 2607.993 * AB - 1274.183 * AC - 2083.678 * BC$  |
|  | p-value                              | <0.0001  |
|  | Standard deviation                   | 137.45 m/s   |
|  | Mean                                 | 731.23 m/s   |
|  | Adjusted R <sup>2</sup>              | 0.9141   |
|  | Predicted R <sup>2</sup>             | 0.8824   |
| [1] A=CEM I, B=GGBS, C=PSA   |                                      |  |



A correlation matrix for all five responses (R1 to R5) is shown in Table 35 for samples prepared with the wet mixing method and a wbr of 8. Model information and ANOVA results for samples prepared with the wet mixing method and a wbr of 8 is shown in Table 36.

Table 35: Correlation matrix for samples prepared with the wet mixing method and wbr of 8.

|   | R1:<br>Ultimate<br>compressive<br>strength, $q_u$ | R2:<br>Undrained<br>shear<br>strength, $S_u$ | R3:<br>Failure<br>strain, $\epsilon_v$ | R4:<br>Estimated<br>stiffness, $E_{50}$ | R5:<br>P-wave<br>velocity, $V_p$ |
|---|---|--|--|---|----------------------------------|
| R1:<br>Ultimate<br>compressive<br>strength, $q_u$ | 1   | 1  | -0.79<br>Moderately<br>negative        | 0.94<br>Strongly<br>positive            | 0.89<br>Strongly<br>positive     |
| R2:<br>Undrained<br>shear<br>strength, $S_u$      | 1   | 1  | -0.79<br>Moderately<br>negative        | 0.94<br>Strongly<br>positive            | 0.89<br>Strongly<br>positive     |
| R3:<br>Failure<br>strain, $\epsilon_v$            | -0.79<br>Moderately<br>negative                   | -0.79<br>Moderately<br>negative              | 1                                      | -0.83<br>Strongly<br>negative           | -0.83<br>Strongly<br>negative    |
| R4:<br>Estimated<br>stiffness, $E_{50}$           | 0.94<br>Strongly<br>positive                      | 0.94<br>Strongly<br>positive                 | -0.83<br>Strongly<br>negative          | 1                                       | 0.94<br>Strongly<br>positive     |
| R5:<br>P-wave<br>velocity, $V_p$                  | 0.89<br>Strongly<br>positive                      | 0.89<br>Strongly<br>positive                 | -0.83<br>Strongly<br>negative          | 0.94<br>Strongly<br>positive            | 1                                |

Table 36: Model information and ANOVA results for samples prepared with the wet mixing method and wbr of 8.

| Response   | Model characteristic                 | Result  |
|--|--------------------------------------|---|
| R1:<br>Ultimate compressive strength, $q_u$<br>(R2:<br>Undrained shear strength, $S_u$ ) | Selected interactions <sup>[1]</sup> | AB, AC, BC  |
|  | Type                                 | Quadratic   |
|  | Equation <sup>[1]</sup>              | $q_u = 1048.465 * A + 382.999 * B + 443.700 * C + 2366.774 * AB - 712.015 * AC - 1311.203 * BC$<br>( $S_u = 524.232 * A + 191.496 * B + 221.850 * C + 1183.395 * AB - 356.020 * AC - 655.5794 * BC$ ) |
|  | p-value                              | <0.0001   |
|  | Standard deviation                   | 65.74 kPa (32.87 kPa)   |
|  | Mean                                 | 681.33 kPa (340.66 kPa)   |
|  | Adjusted R <sup>2</sup>              | 0.9704  |
|  | Predicted R <sup>2</sup>             | 0.9540  |
| R3:<br>Failure strain, $\epsilon_v$  | Selected interactions <sup>[1]</sup> | BC  |
|  | Type                                 | Reduced quadratic   |
|  | Equation <sup>[1]</sup>              | $\epsilon_v = 1.589 * A + 1.548 * B + 4.889 * C + 4.491 * BC$   |
|  | p-value                              | <0.0001   |
|  | Standard deviation                   | 0.30 %  |
|  | Mean                                 | 2.84 %  |
|  | Adjusted R <sup>2</sup>              | 0.9409  |
|  | Predicted R <sup>2</sup>             | 0.9107  |
| R4:<br>Estimated stiffness, $E_{50}$   | Selected interactions <sup>[1]</sup> | AB, AC, BC  |
|  | Type                                 | Quadratic   |
|  | Equation <sup>[1]</sup>              | $E_{50} = 116195.575 * A + 52622.490 * B + 40446.880 * C + 130715.010 * AB - 227090.064 * AC - 244914.046 * BC$   |
|  | p-value                              | <0.0001   |
|  | Standard deviation                   | 7170.20 kPa   |
|  | Mean                                 | 45667.64 kPa  |
|  | Adjusted R <sup>2</sup>              | 0.9710  |
|  | Predicted R <sup>2</sup>             | 0.9555  |
| R5:<br>P-wave velocity, $V_p$  | Selected interactions <sup>[1]</sup> | AB, AC, BC  |
|  | Type                                 | Quadratic   |
|  | Equation <sup>[1]</sup>              | $V_p = 1447.576 * A + 1191.290 * B + 873.118 * C + 1413.829 * AB - 3191.384 * AC - 4384.716 * BC$   |
|  | p-value                              | <0.0001   |
|  | Standard deviation                   | 107.35 m/s  |
|  | Mean                                 | 798.97 m/s  |
|  | Adjusted R <sup>2</sup>              | 0.9645  |
|  | Predicted R <sup>2</sup>             | 0.9457  |
| [1] A=CEM I, B=GGBS, C=PSA   |                                      |   |

A correlation matrix for all five responses (R1 to R5) is shown in Table 37 for samples prepared with the wet mixing method and a wbr of 16. Model information and ANOVA results for samples prepared with the wet mixing method and a wbr of 8 is shown in Table 38.

Table 37: Correlation matrix for samples prepared with the wet mixing method and wbr of 16.

|   | R1:<br>Ultimate<br>compressive<br>strength, $q_u$ | R2:<br>Undrained<br>shear<br>strength, $S_u$ | R3:<br>Failure<br>strain, $\varepsilon_v$ | R4:<br>Estimated<br>stiffness, $E_{50}$ | R5:<br>P-wave<br>velocity, $V_p$ |
|---|---|--|---|---|----------------------------------|
| R1:<br>Ultimate<br>compressive<br>strength, $q_u$ | 1   | 1  | -0.76<br>Moderately<br>negative           | 0.97<br>Strongly<br>positive            | 0.02<br>No<br>association        |
| R2:<br>Undrained<br>shear<br>strength, $S_u$      | 1   | 1  | -0.76<br>Moderately<br>negative           | 0.97<br>Strongly<br>positive            | 0.02<br>No<br>association        |
| R3:<br>Failure<br>strain, $\varepsilon_v$         | -0.76<br>Moderately<br>negative                   | -0.76<br>Moderately<br>negative              | 1   | -0.75<br>Moderately<br>negative         | 0.34<br>Weakly<br>positive       |
| R4:<br>Estimated<br>stiffness, $E_{50}$           | 0.97<br>Strongly<br>positive                      | 0.97<br>Strongly<br>positive                 | -0.75<br>Moderately<br>negative           | 1                                       | 0.10<br>No<br>association        |
| R5:<br>P-wave<br>velocity, $V_p$                  | 0.02<br>No<br>association                         | 0.02<br>No<br>association                    | 0.34<br>Weakly<br>positive                | 0.10<br>No<br>association               | 1                                |

Table 38: Model information and ANOVA results for samples prepared with the wet mixing method and wbr of 16.

| Response   | Model characteristic                 | Result  |
|--|--------------------------------------|---|
| R1:<br>Ultimate compressive strength, $q_u$<br>(R2:<br>Undrained shear strength, $S_u$ ) | Selected interactions <sup>[1]</sup> | AB, AC, BC  |
|  | Type                                 | Quadratic   |
|  | Equation <sup>[1]</sup>              | $q_u = 392.509 * A + 83.503 * B + 68.034 * C + 363.289 * AB - 558.1667 * AC - 344.873 * BC$<br>( $S_u = 196.255 * A + 41.752 * B + 34.013 * C + 181.654 * AB - 279.076 * AC - 172.436 * BC$ ) |
|  | p-value                              | <0.0001   |
|  | Standard deviation                   | 55.58 kPa (27.79 kPa)   |
|  | Mean                                 | 156.96 kPa (78.48 kPa)  |
|  | Adjusted R <sup>2</sup>              | 0.8513  |
|  | Predicted R <sup>2</sup>             | 0.8036  |
| R3:<br>Failure strain, $\varepsilon_v$   | Selected interactions <sup>[1]</sup> | AB, BC, ABC   |
|  | Type                                 | Reduced special cubic   |
|  | Equation <sup>[1]</sup>              | $\varepsilon_v = 1.940 * A + 2.502 * B + 3.154 * C - 0.173 * AB + 8.115 * BC - 15.754 * ABC$  |
|  | p-value                              | <0.0001   |
|  | Standard deviation                   | 0.32 %  |
|  | Mean                                 | 2.85 %  |
|  | Predicted R <sup>2</sup>             | 0.7918  |
| R4:<br>Estimated stiffness, $E_{50}$   | Selected interactions <sup>[1]</sup> | AC, BC  |
|  | Type                                 | Reduced quadratic   |
|  | Equation <sup>[1]</sup>              | $E_{50} = 35743.960 * A + 15352.934 * B + 6533.038 * C - 57783.981 * AC - 48408.519 * BC$   |
|  | p-value                              | <0.0001   |
|  | Standard deviation                   | 5232.23 kPa   |
|  | Mean                                 | 12193.29 kPa  |
|  | Predicted R <sup>2</sup>             | 0.7247  |
| R5:<br>P-wave velocity, $V_p$  | Selected interactions <sup>[1]</sup> | AB, AC  |
|  | Type                                 | Reduced quadratic   |
|  | Equation <sup>[1]</sup>              | $V_p = 1144.203 * A + 1564.201 * B + 1320.632 * C - 1518.829 * AB - 4582.970 * AC$  |
|  | p-value                              | <0.0001   |
|  | Standard deviation                   | 209.89 m/s  |
|  | Mean                                 | 904.46 m/s  |
|  | Predicted R <sup>2</sup>             | 0.7514  |
| [1] A=CEM I, B=GGBS, C=PSA   |                                      |   |

### 4.3.2. Strength

Figure 75 and Figure 76 shows contour plots and response surfaces of ultimate compressive strength ( $q_u$ ) for wet- and dry mixed samples with a wbr of 8 and 16 respectively. The 100 next to the binder's name indicates the binder content percentage at the maximum points on the trilinear coordinate system, as explained in section 3.4.3. Opposite from the 100, there is a 0, indicating a minimum for the binder on the opposite side. The red dots on the contour plot are the selected lattice points. The number next to each red dot is the number of samples included in the design for that specific batch (see Table 30). On the contour plots, the numbers in the white boxes indicate contour line values.

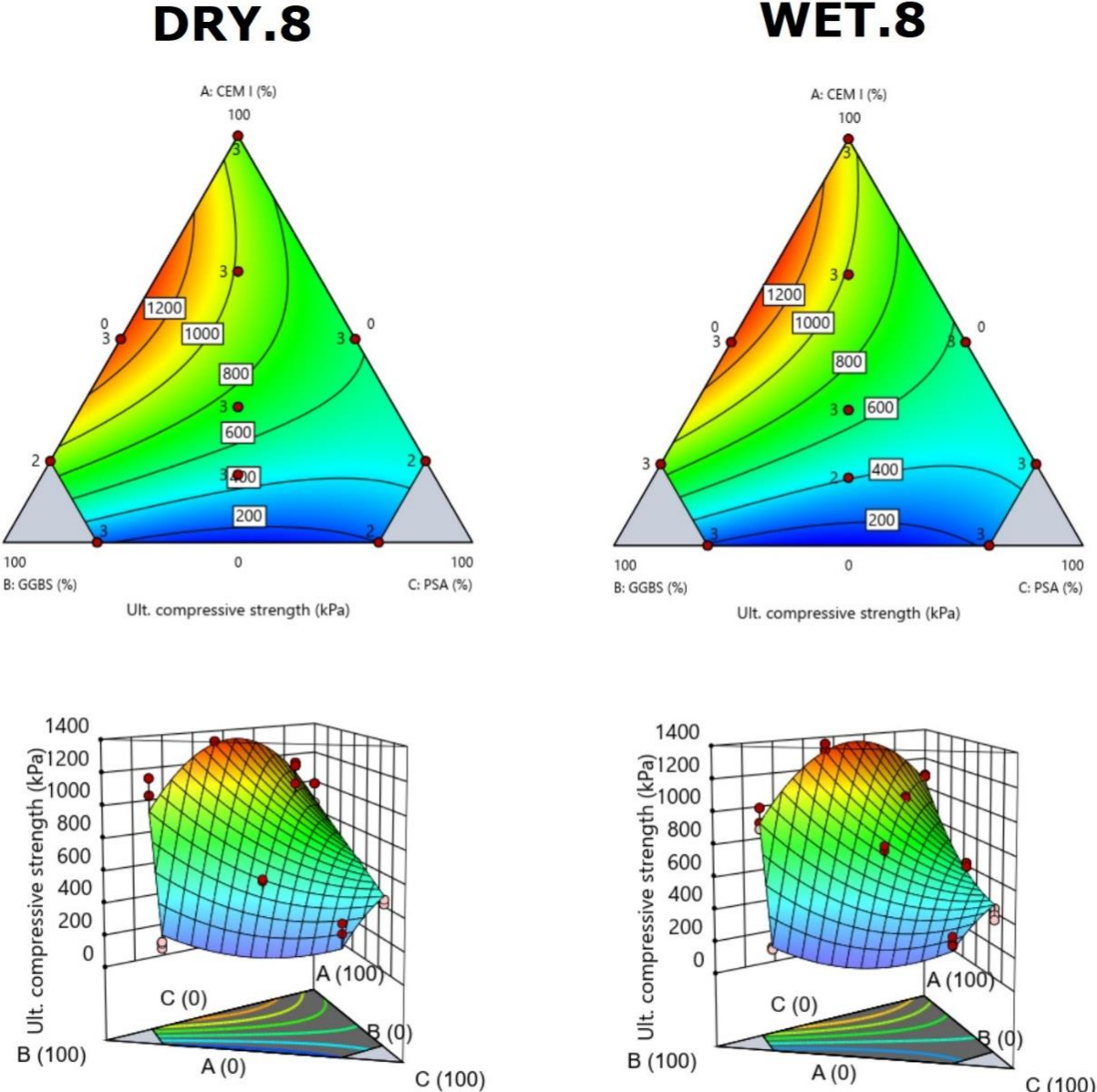
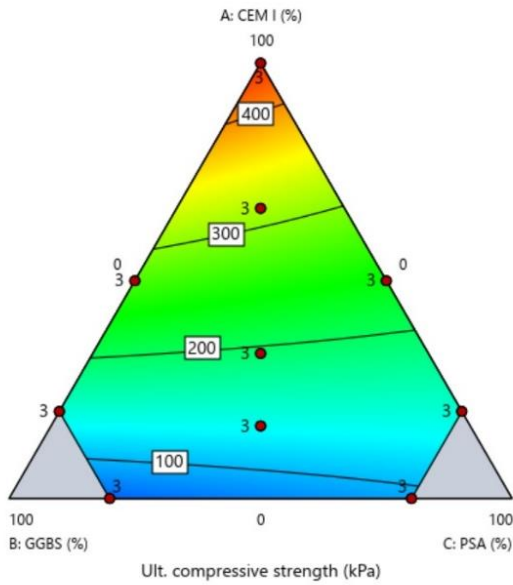


Figure 75: Contour plot and response surface model comparison. Ultimate compressive strength for samples prepared with dry- (left) and wet mixing (right) with a wbr of 8.

## DRY.16



## WET.16

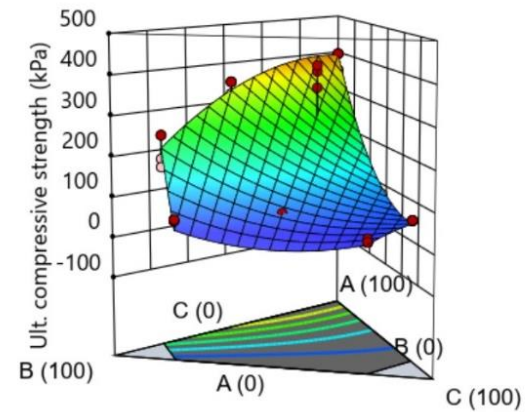
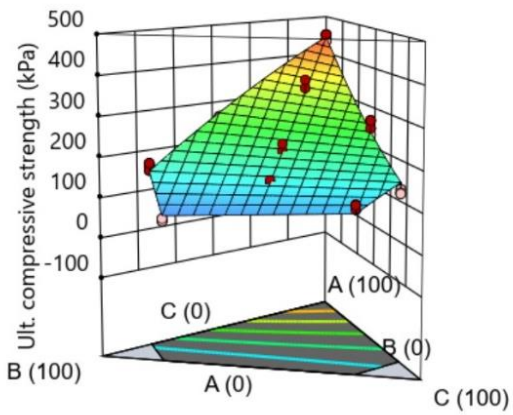
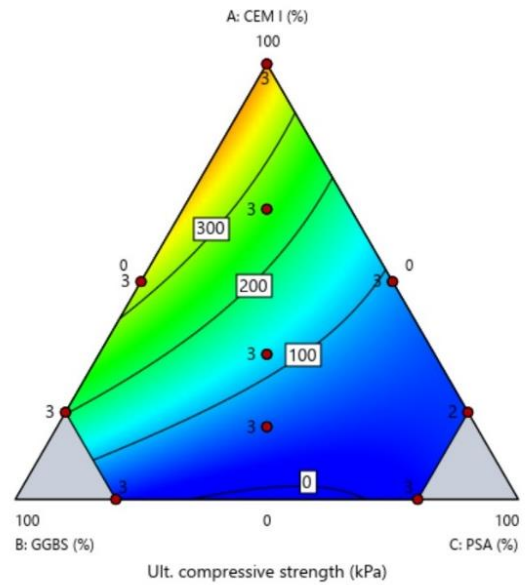
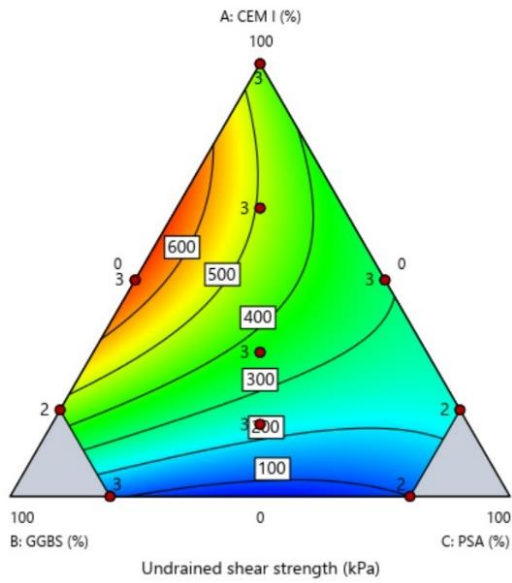


Figure 76: Contour plot and response surface model comparison. Ultimate compressive strength for samples prepared with dry- (left) and wet mixing (right) with a wbr of 16.

Figure 77 and Figure 78 shows contour plots and response surfaces of undrained shear strength ( $S_u$ ) for wet- and dry mixed samples with a wbr of 8 and 16 respectively. The values on the  $S_u$  plot are half the size compared with the  $q_u$  values. The plots are otherwise identical.

# DRY.8



# WET.8

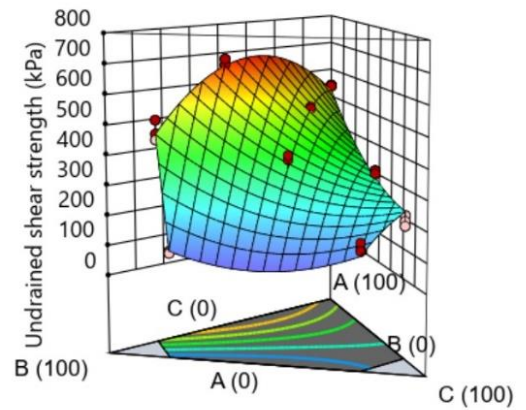
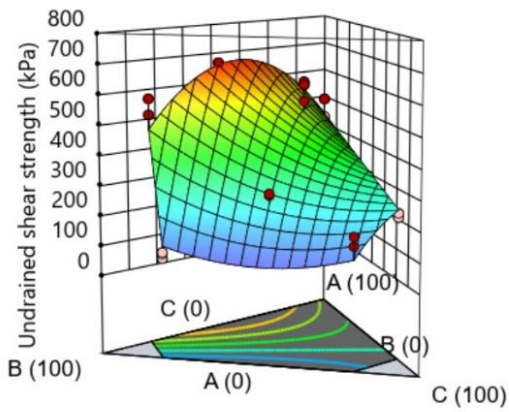
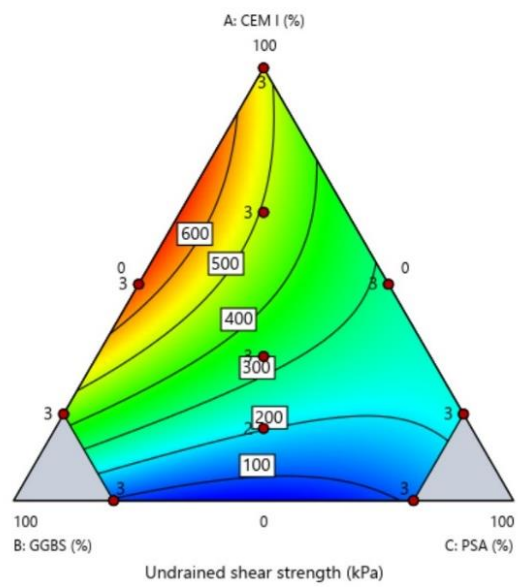
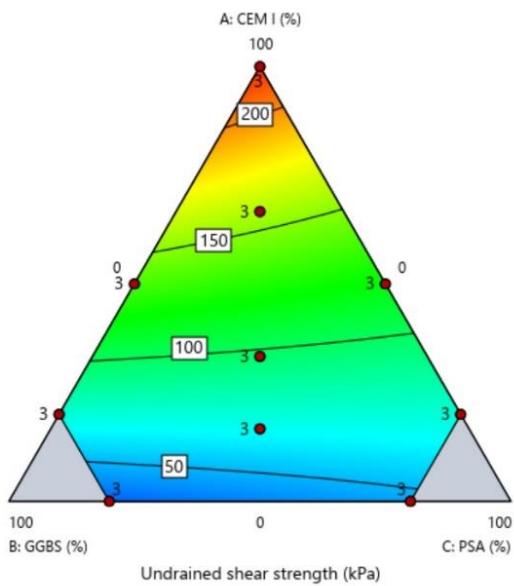


Figure 77: Contour plot and response surface model comparison. Undrained shear strength for samples prepared with dry- (left) and wet mixing (right) with a wbr of 8.

## DRY.16



## WET.16

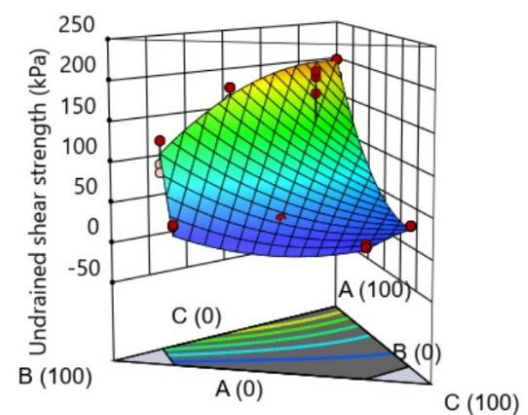
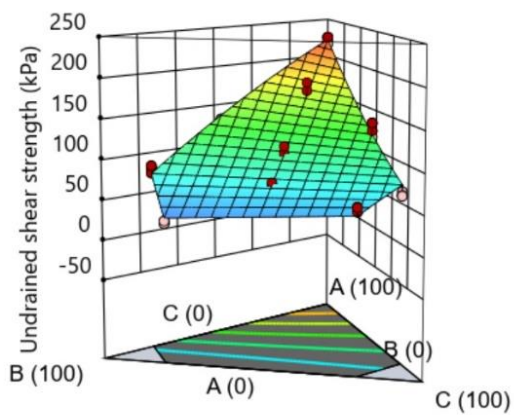
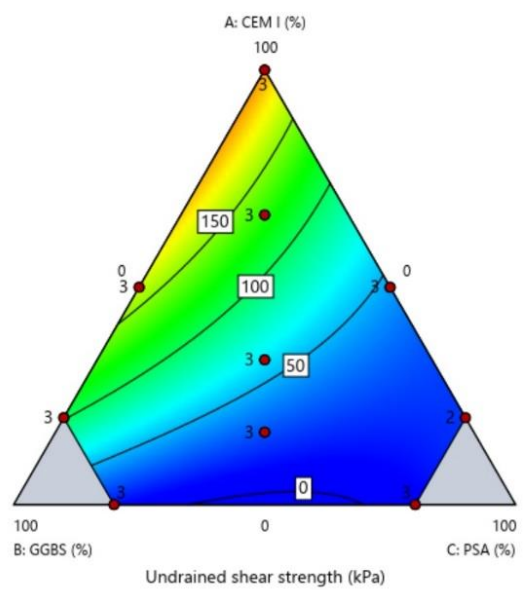


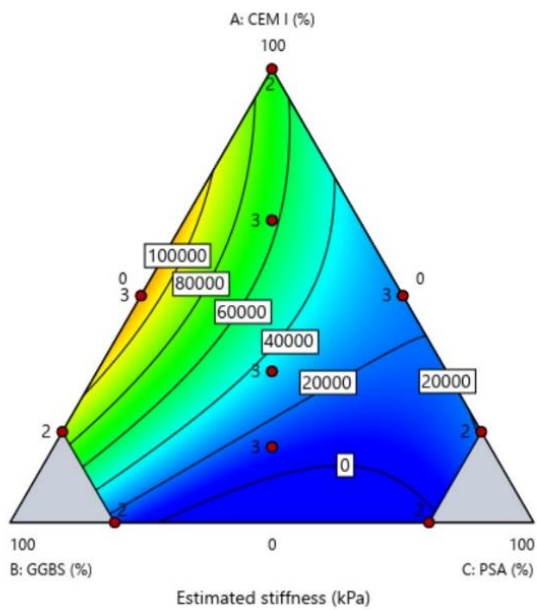
Figure 78: Contour plot and response surface model comparison. Undrained shear strength for samples prepared with dry- (left) and wet mixing (right) with a wbr of 8.

### 4.3.3. Stiffness

Figure 79 and Figure 80 shows contour plots and response surfaces of estimated stiffness ( $E_{50}$ ) for wet- and dry mixed samples with a wbr of 8 and 16 respectively.



# DRY.8



# WET.8

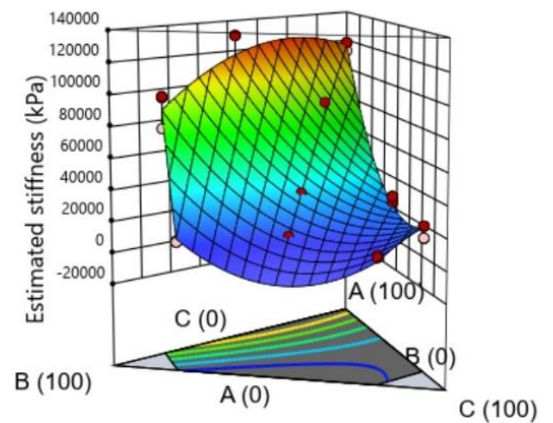
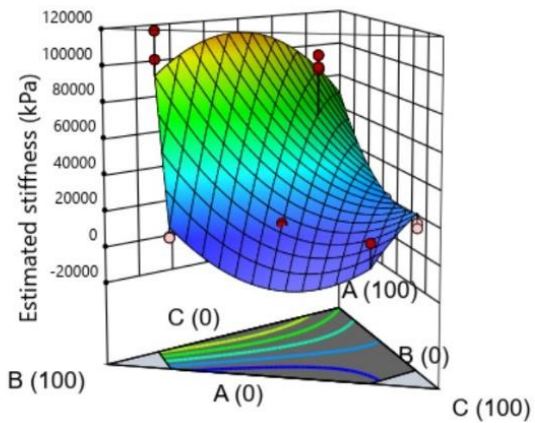
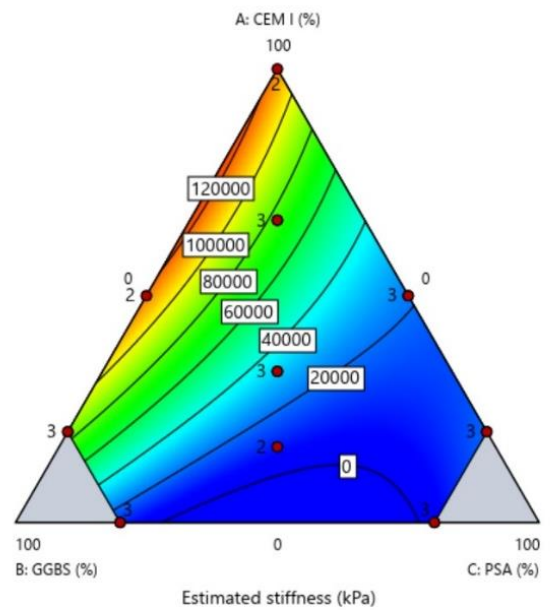
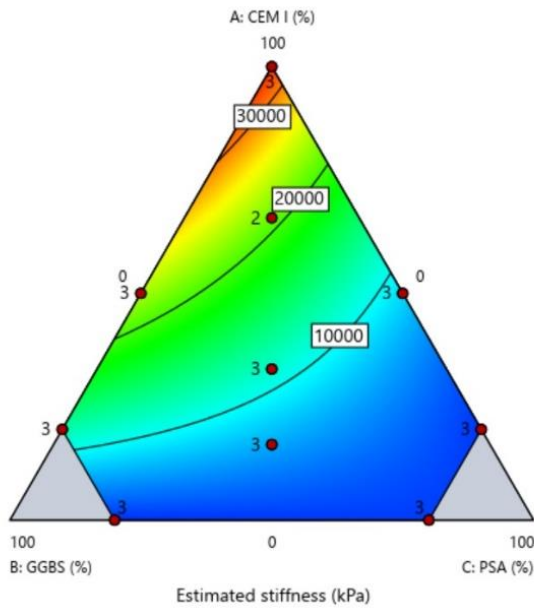


Figure 79: Contour plot and response surface model comparison. Estimated stiffness for samples prepared with dry- (left) and wet mixing (right) with a wbr of 8.

## DRY.16



## WET.16

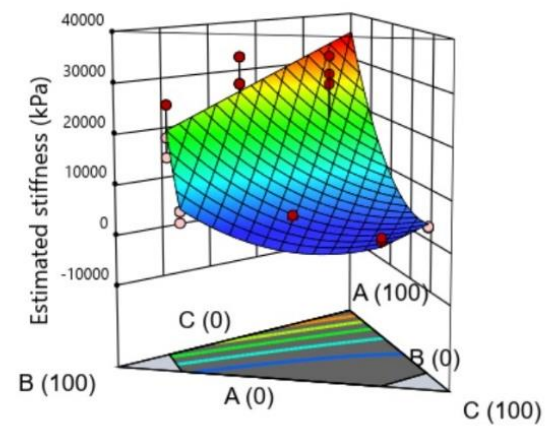
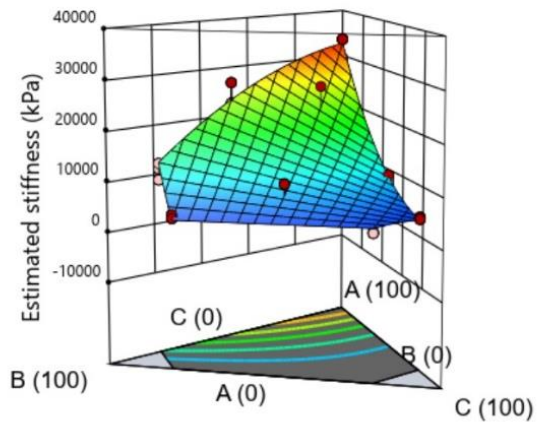
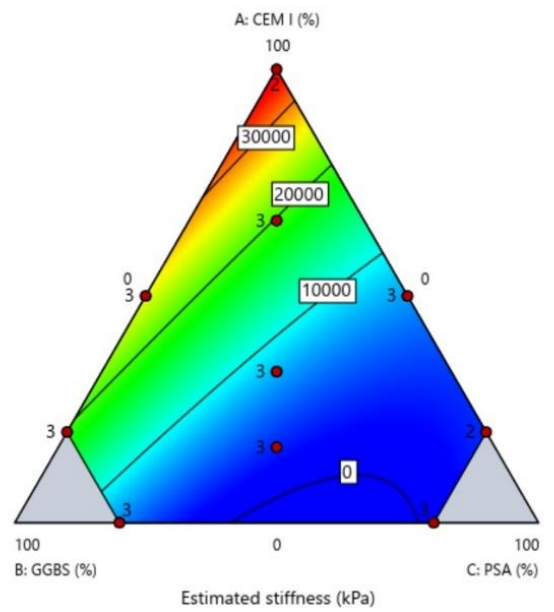
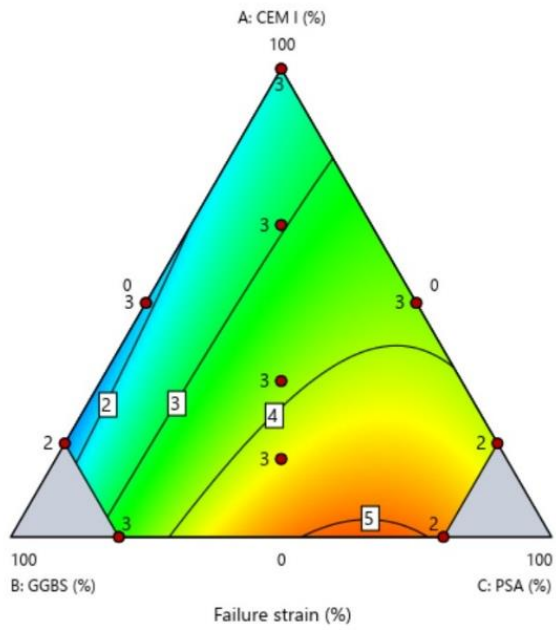


Figure 80: Contour plot and response surface model comparison. Estimated stiffness for samples prepared with dry- (left) and wet mixing (right) with a wbr of 16.

### 4.3.4. Strain

Figure 81 and Figure 82 shows contour plots and response surfaces of failure strain ( $\epsilon_f$ ) for wet- and dry mixed samples with a wbr of 8 and 16 respectively.

# DRY.8



# WET.8

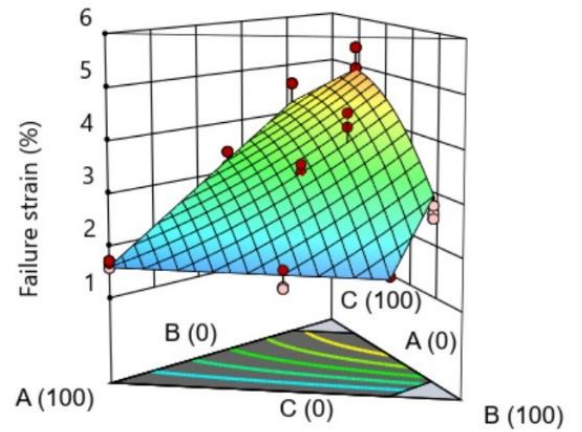
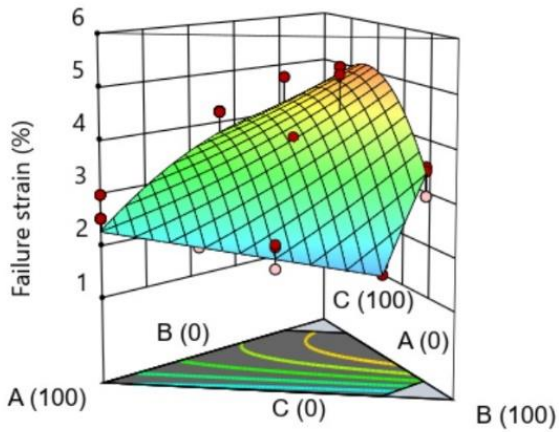
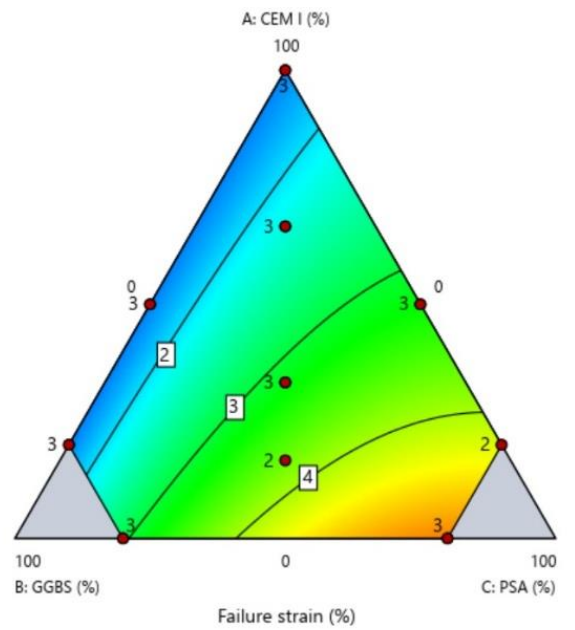
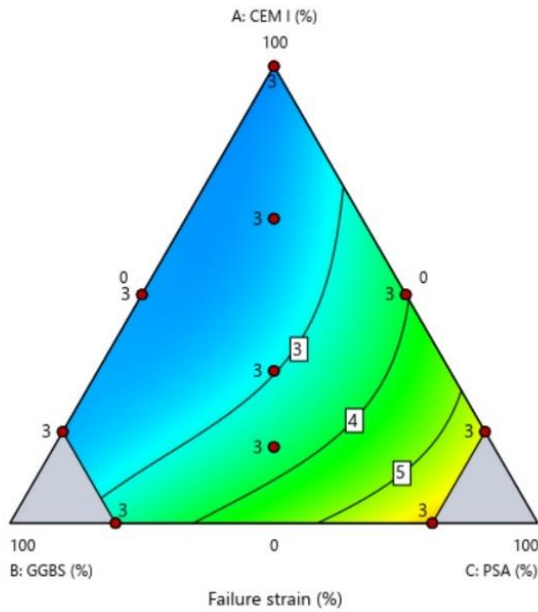


Figure 81: Contour plot and response surface model comparison. Failure strain for samples prepared with dry- (left) and wet mixing (right) with a wbr of 8.

## DRY.16



## WET.16

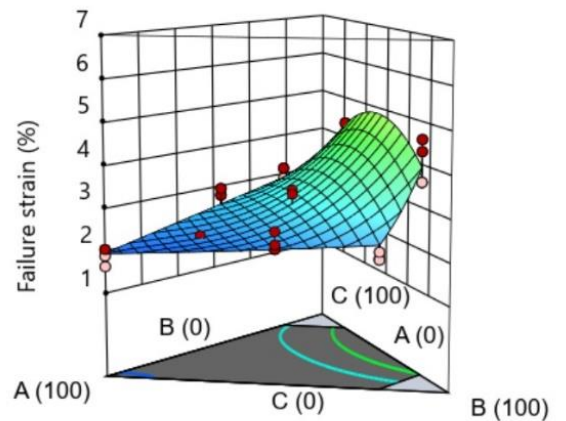
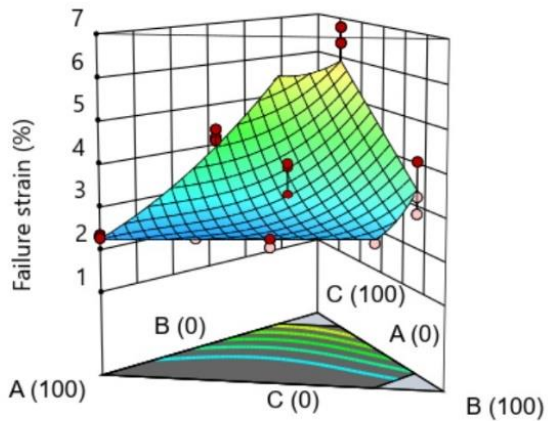
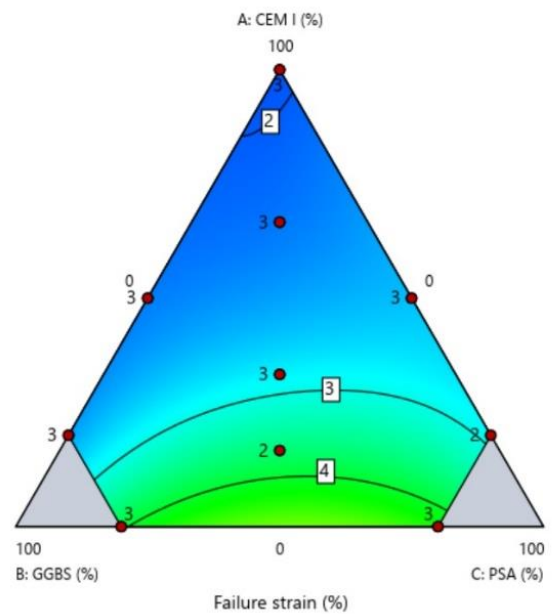
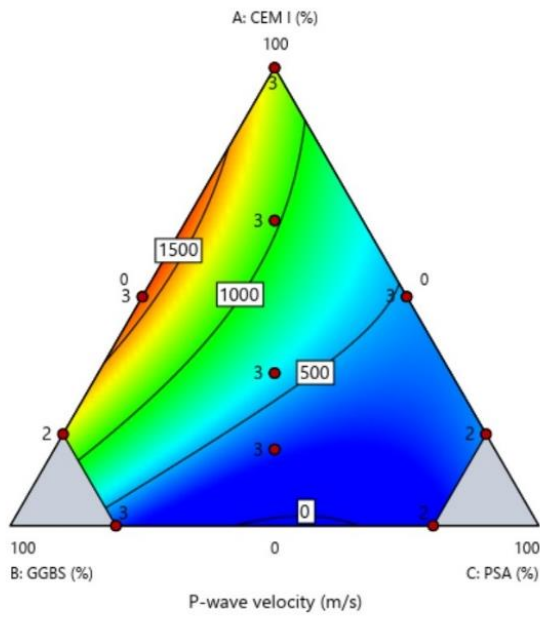


Figure 82: Contour plot and response surface model comparison. Failure strain for samples prepared with dry- (left) and wet mixing (right) with a wbr of 16.

### 4.3.5. P-wave velocity

Figure 83 and Figure 84 shows contour plots and response surfaces of p-wave velocity ( $V_p$ ) for wet- and dry mixed samples with a wbr of 8 and 16 respectively.

# DRY.8



# WET.8

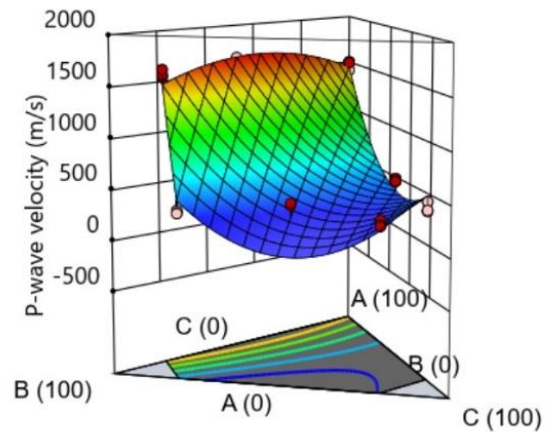
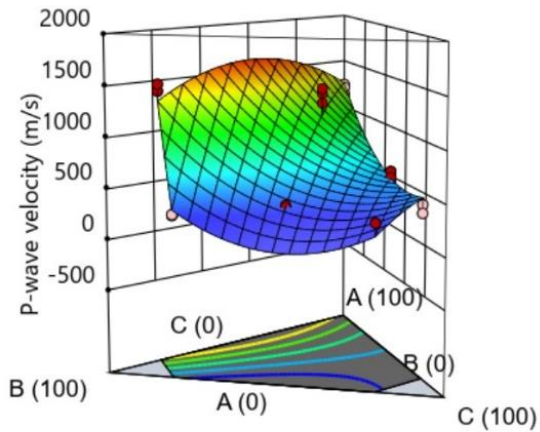
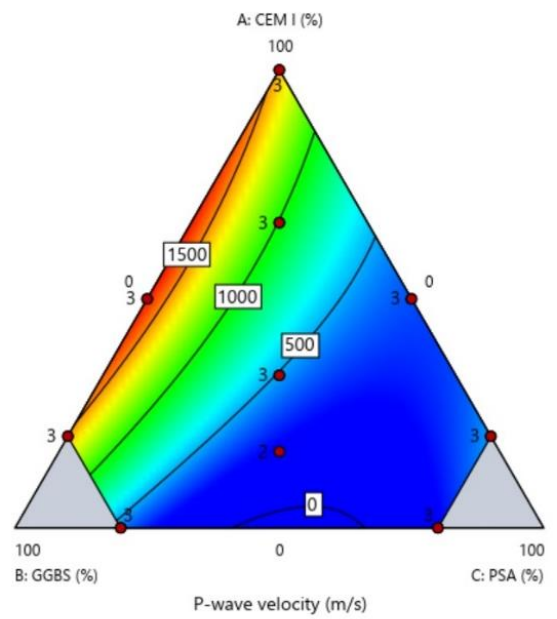
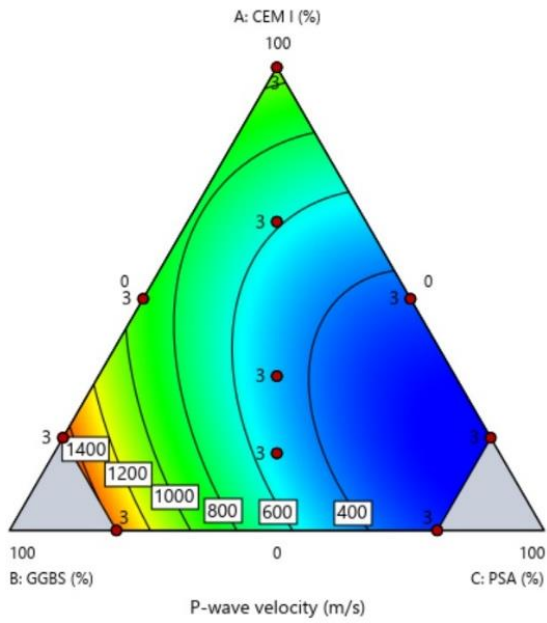


Figure 83: Contour plot and response surface model comparison. P-wave velocity for samples prepared with dry- (left) and wet mixing (right) with a wbr of 8.

# DRY.16



# WET.16

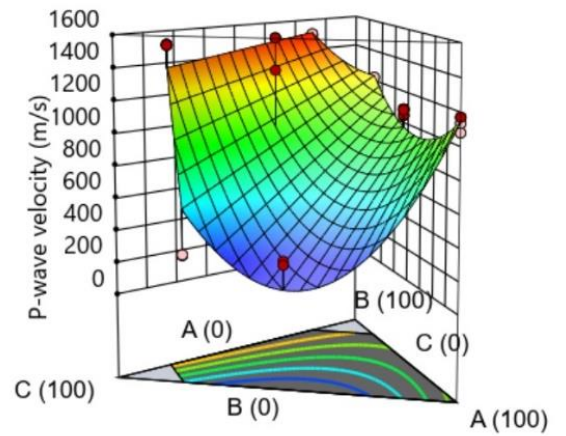
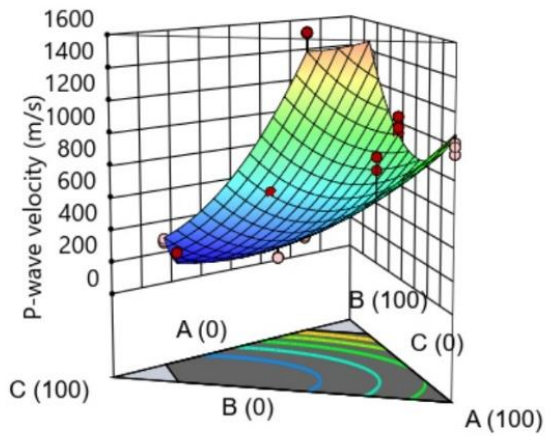
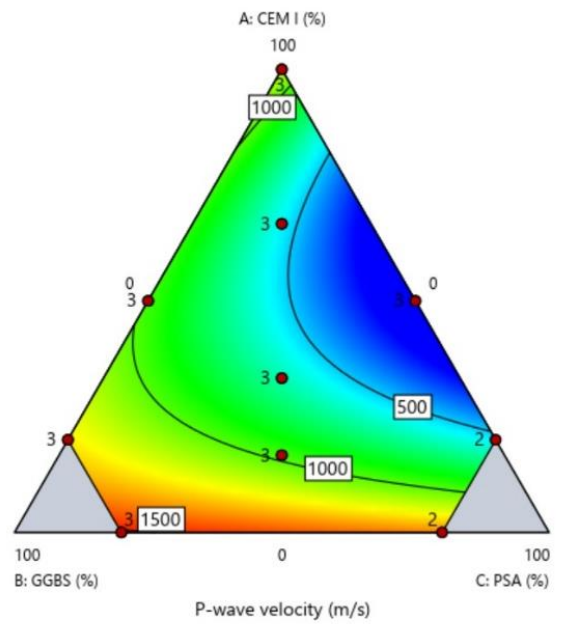


Figure 84: Contour plot and response surface model comparison. P-wave velocity for samples prepared with dry- (left) and wet mixing (right) with a wbr of 16.

# 5 | Discussion

## 5.1 Effect of binder composition on laboratory samples

### 5.1.1. Fracture patterns and sample quality

Before the effects of binder composition on strength and deformation properties is evaluated, it's important to assess the quality of the prepared samples and test procedures. When visually examining the samples in appendix B.1 and B.2, negligible differences is seen in air voids in the samples prepared with the rodding technique described in section 3.2.4. Three samples cracked during extrusion, but this is expected to be caused by errors during extrusion and not be indicative of issues with the sample preparation method. The visual difference is only clear in the samples which were poured directly into the cylinders. The poured samples have larger air voids and visible air bubbles. Out of all batches prepared with a wbr of 16, one dry mixed batch had to be poured (see Table 18), while six wet mixed batches had to be poured (see Table 20).

Most of the estimated amount of entrapped air ( $n_{air}$ ) in the samples range between 0 and 4 % (see appendix B.3.1). The tables show that the poured samples also have  $n_{air}$  values in the range of 0 and 4 %. This can be explained by either the estimation assumptions being wrong, or that the air voids were simply pushed towards the sample surface during pouring. As a consequence of there being quite a few samples with negative amounts of entrapped air, the assumptions being wrong is the most plausible cause. The value of specific gravity ( $G_s$ ) for example is assumed to be an average value of common minerals found in Norwegian clay. The entrapped air values are not discussed further, as they are mainly used to check for large deviations directly after molding each sample (see section 3.3.2).

Depth variation is also important to note when assessing quality. Samples were collected from different boreholes, at depths between 7.0 and 14.0 m (see Table 14). Perfectly comparable soil cannot be expected due to spatial variability described in section 3.2.1. The spatial variability was most noticeable in the water content measurements. Before testing, soil water content at each specific depth ( $w_s$ ) was assumed to fall between 43 and 48 % when looking at previous studies (L'Heureux et al., 2019). When mixing the initial batches, it was assumed that a single initial clay water content ( $w_{stab}$ ) value could be used for all samples with the same depth. Measurements taken after homogenizing the clay however, showed values of  $w_{stab}$  between 35.7 and 51.3 %. This proved that water content measurements had to be taken multiple times even when preparing samples with material from the same depth. Dry mixed samples with a  $w_{stab}$  of 38.1 % are only based off a single measurement (see Table 43). Such water content discrepancies cause the corrected wbr ( $wbr_{corr}$ ) to be off from the set values. The samples with a set wbr of 8 have a  $wbr_{corr}$  ranging from 6.55 to 8.98 (see Table 43 and Table 45), whereas the samples with a set wbr of 16 range between 13.54 and 16.54 (see Table 44 and Table 46). In theory, the samples with lower  $wbr_{corr}$  should be stronger as described in section 2.2.4. The varying  $wbr_{corr}$  was not included in the response modeling, because it is assumed that  $wbr_{corr}$  values are equally higher and lower than the set wbr.

The water content measured after UCT ( $w_{UCT}$ ) also showed some unexpected behavior seen in appendix B.3.1. Results show an increase in measured water content in the samples after UCT. This is most apparent in the samples prepared with a wbr of 8 (see Table 43

and Table 45), where over half of the samples show higher values of  $w_{UCT}$  than  $w_{stab}$ . The increase in water content range between 0.3 and 3.0 %, with one outlier of 7.9 %. Some variations are expected, as only a small chunk of material in each batch is removed to test for water content after UCT. In theory however, the water content should decrease due to hydration of the binder (see section 2.2.5). This binds the water from being able to evaporate, which in turn increases the solid mass and reduces mass of water. Negative values are most likely the result of poor scale calibration or a follow up error from the issues with  $w_{stab}$  mentioned in the paragraph above.

Still, some samples had unexpected compressive strength measurements in a single batch. This might be explained by the variation in fracture patterns across all strengths. The expected fracture pattern from theory is an hourglass shape (see section 2.3.2). However, many of the samples had longitudinal fracture patterns or a combination of a cone shape and longitudinal fracture pattern (see section 4.2.3). Different failure patterns are believed to be caused by the internal structure and microcracks in the samples created during preparation and curing. Variations in the failure patterns can also be caused by the varying friction between the steel load frame and the sample surface. The couplant gel, which is a lubricant, changes the friction between the steel load frame and the sample. These factors explain why some samples have very different fracture patterns in the same batch. The samples with visible cracks and performance inconsistencies are excluded from the response surface models (see Table 30). In future tests, the couplant gel should be fully removed to ensure equal boundary conditions during compression testing. This is expected to reduce the number of samples with performance inconsistencies.  $\mu$ CT analysis during UCT can also help determine how weak zones in the samples form and expand.

### 5.1.2. Strength

Expected model correlation from the initial test data is found by evaluating the correlation matrices shown in section 4.3.1. Samples prepared with a wbr of 8 show no clear differences in strength correlation between the dry and wet mixing method. The strength, either ultimate ( $q_u$ ) or undrained ( $S_u$ ), is moderately negatively correlated with failure strain ( $\epsilon_v$ ) and strongly positively correlated with both estimated stiffness ( $E_{50}$ ) and p-wave velocity ( $V_p$ ). This type of correlation is expected because higher p-wave velocity is proved to indicate higher strength (see section 2.1.4). Additionally, stronger samples tend to be less ductile (more brittle when compressed), which in turn increases stiffness and reduces failure strain. Unexpectedly, no correlation between strength and p-wave velocity is found for the samples prepared with a wbr of 16 (see Table 33 and Table 37). As described section 5.1.5, the assumed reason behind this discrepancy is the insufficient hydration of the binder. A visual representation of the correlations between strength and p-wave velocity for a wbr of 8 and 16 is shown in Figure 85. The large scatter and correlation issues shows that measuring p-wave velocity with the PUNDIT equipment is not reliable.



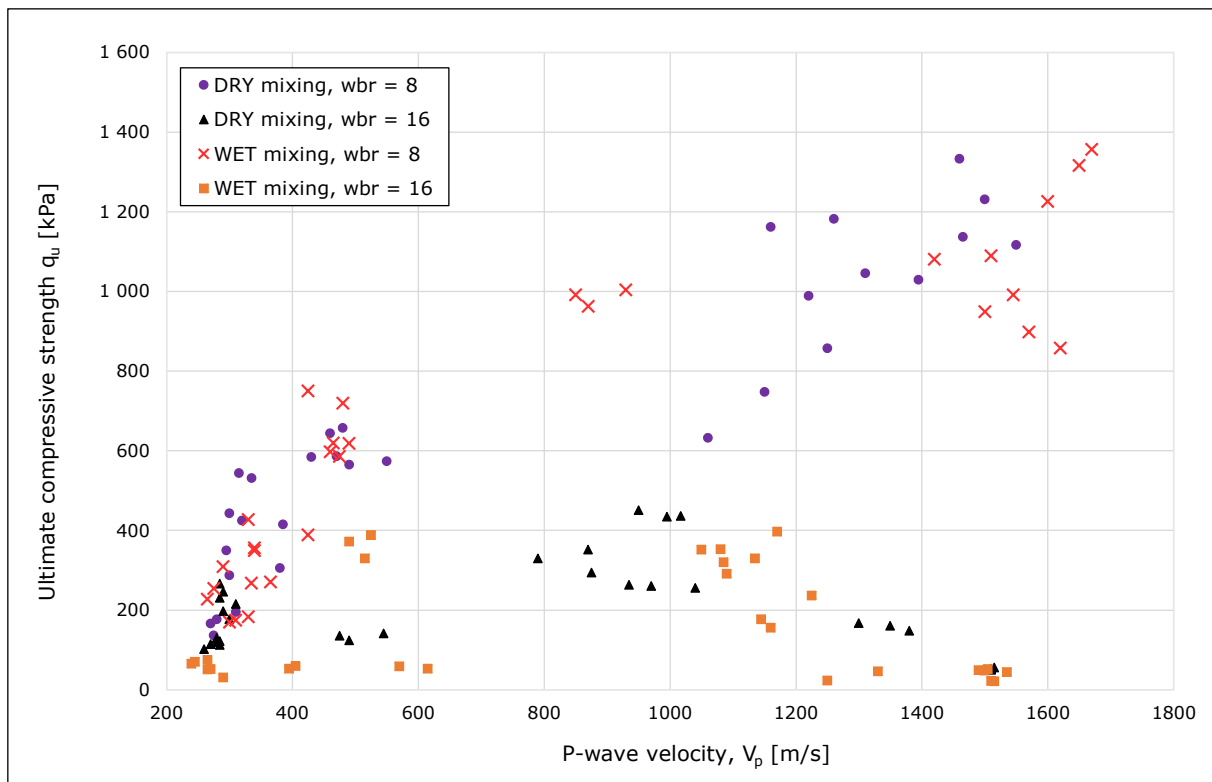


Figure 85: P-wave velocity vs ultimate compressive strength.

When looking at the model info and ANOVA results for samples prepared with a wbr of 8, there are some differences between the wet and dry mixing methods. Modeling the dry mixing data (Table 32) results in almost twice the standard deviation compared with the wet method data (Table 36). Modeling the wet method also results in a full quadratic model, whereas the dry model lacks significant interaction between CEM I and PSA. The values of predicted vs adjusted  $R^2$  are both sufficient according to Table 26. Wet and dry mixed samples with a wbr of 8 is labeled with DRY.8 and WET.8 in appendix B.4.1. A slight S shaped curve can be seen on both of the normal plot of residuals. The model is still assumed to be accurate since the other diagnostics plots show no clear issues (see Table 27).

The samples prepared with a wbr of 16 shows similarities in the model type and selected interactions between the dry and the wet mixing method. ANOVA results, however, are flipped, with exception of the values of predicted vs adjusted  $R^2$ , which are both sufficient. The dry method (Table 34) has about a third of the standard deviation compared with the wet method (Table 38). Residual plots in appendix B.4.2 shows an overall better fit for the samples prepared with the dry method.

For the samples prepared with a wbr of 8, Figure 75 and Figure 77 show an optimal binder composition of around 55 to 65 % CEM I and 35 to 45 % GGBS for maximum strength. According to NGI's experience, a mix of 70 % CEM I and 30 % GGBS is often used in the field when using DDM. As explained in section 2.2.5, GGBS takes a longer time than CEM I to react and give full effect. Curing further than the set 28 days might give an optimal binder content closer to what is used in the field.

For the dry mixed samples prepared with a wbr of 16, Figure 76 and Figure 78 show an optimal binder composition close to 100 % CEM I for maximum strength. Lines on the contour plot have little curvature, indicating low binder interaction in practice. GGBS

probably needs a higher CEM I content to be activated. The dry method shows a higher strength than the wet method.

Figure 76 and Figure 78 show that the wet mixed samples with a wbr of 16 have a clearer interaction between GGBS and CEM I. Binder composition for strength can include 10 to 15 % GGBS without losing much strength. An important note is that wet mixed batches with PSA have much less strength compared with the dry mixed batches. The lumps formed by the PSA in the slurry resulted in low strength for wet mixed batches with a wbr of 16 (see section 4.2.1). This limits the comparability of the wet and dry mixing method (DRY.16 and WET.16) because poor mixing must be avoided to compare the effects of different mixing methods on the soil-binder interactions. As the lumps could not be effectively homogenized by the kitchen stand mixer or by hand, a finer whisk would most likely solve this issue.

### 5.1.3. Stiffness

Estimated stiffness ( $E_{50}$ ) is strongly positively correlated with strength, either ultimate ( $q_u$ ) or undrained ( $S_u$ ). This correlation is visualized for both methods and wbr values in Figure 86.

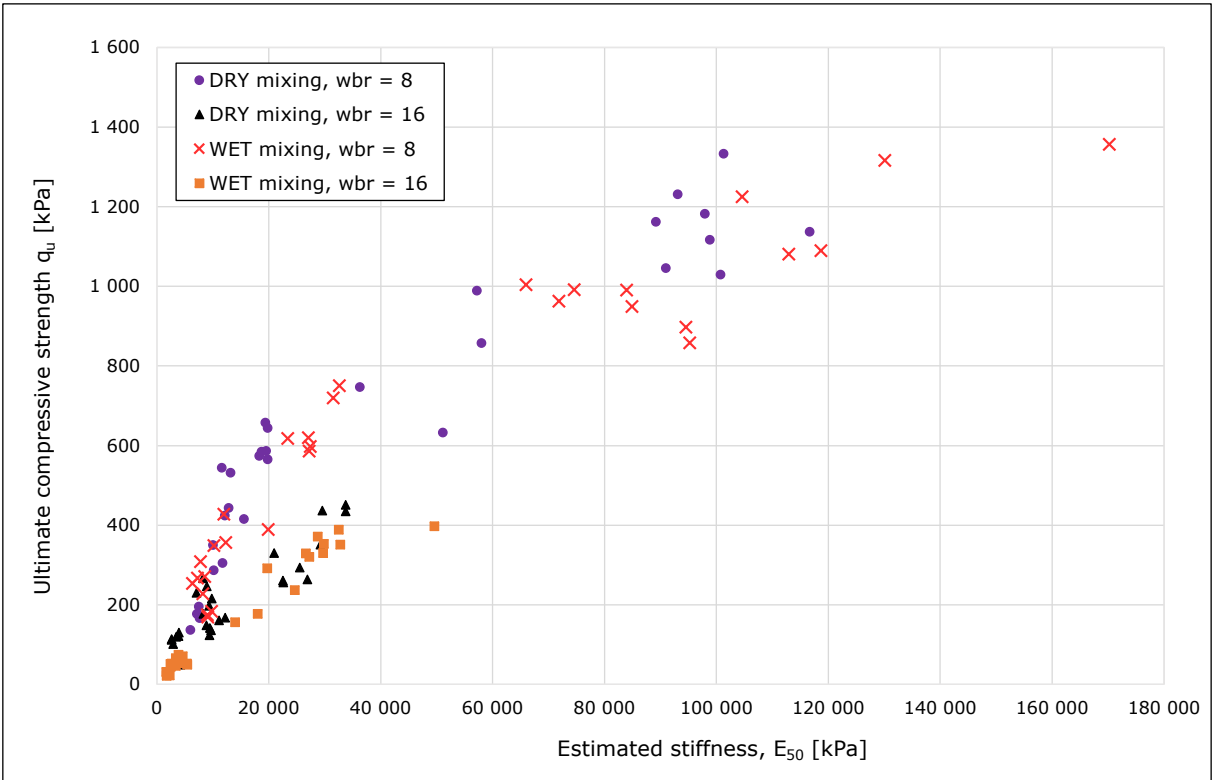


Figure 86: Estimated stiffness vs ultimate compressive strength.

In addition, correlation matrices shown in section 4.3.1 show that  $E_{50}$  in samples prepared with a wbr of 8 is strongly negatively correlated with  $\epsilon_v$  and strongly positively correlated with  $V_p$ . This is expected by the same reasoning used in the previous section. Although weaker, the samples prepared with a wbr of 16 show similar correlations. It must be noted that also here, the wet method shows no association between  $E_{50}$  and  $V_p$ , possibly due to the insufficient hydration of the binder explained in section 5.1.5.

The model info and ANOVA results for samples prepared with a wbr of 8 show that there are some differences between the wet and dry mixing methods. The model from the dry mixed samples (Table 32) has higher standard deviation and inferior prediction properties compared with the wet mixing model (Table 36). Differences are even clearer on the diagnostic plots in appendix B.4.1, where the dry model has a clear S shape on the normal plot of residuals. These differences are clear, even though both models are quadratic.

Samples prepared with a wbr of 16 have flipped ANOVA results which can easily be seen on the diagnostic plots in appendix B.4.2. The dry model (Table 34) has superior prediction properties and lower standard deviation compared with the wet model (Table 38). There is also a difference in interaction, where the dry model finds no significant interaction between GGBS and PSA and the wet model finds no significant interaction between CEM I and GGBS.

For all responses, ranges in the contour plots with negative sections are considered void. These negative areas are caused by the software outputting a response surface which can curve below zero in areas where there are no lattice points with realistic measurements. This limits the usable range in some of the contour plots, which is especially noticeable in the stiffness plots with a wbr of 8 (see Figure 79). To improve the model, batches with no/low CEM I content should be tested. The added lattice points should be between point number 4, 5 and 6 in Figure 73.

The optimal binder content to maximize  $E_{50}$  is essentially the same as for maximizing strength (see section 5.1.2). This is the case for both mixing methods and both wbr values (Figure 79 and Figure 80).

A clear difference in achieved maximum stiffness can be seen on Figure 79, where the wet method gives about 11.5 % higher maximum stiffness than the dry method. This is mainly due to the low stiffness measured in the dry mixed batch in lattice point 1. The wet method could be better suited for situations where 100 % CEM I is utilized.

#### **5.1.4. Strain at failure**

In addition to previously mentioned correlations, the matrices in section 4.3.1 show that  $\varepsilon_v$  is strongly negatively correlated  $V_p$  for samples prepared with a wbr of 8. Again, this is different for samples prepared with a wbr of 16, where the wet method shows weak positive correlation between  $\varepsilon_v$  and  $V_p$  (possibly caused by the insufficient hydration of the binder explained in section 5.1.5).

The model info and ANOVA results for samples prepared with a wbr of 8 show that the wet method (Table 36) is superior in terms of prediction and standard deviation. This is confirmed by the diagnostic plots in appendix B.4.1. The wet model only finds significant interaction between GGBS and PSA, while the dry model also finds significant interaction between CEM I and PSA (Table 32).

Unexpectedly, these results seem to be not affected by the wbr change as seen in the other responses. Samples prepared with a wbr of 16 have very similar ANOVA results and diagnostic plots (appendix B.4.2) to samples prepared with a wbr of 8. The main difference is the model type, which for wbr of 16 is a reduced special cubic model with an added expression for interaction between all three binder components (Table 34 and Table 38).

When looking at Figure 81 and Figure 82, the optimal binder content for maximizing  $\varepsilon_v$  is in the range of 70 to 80 % PSA and 20 to 30 % GGBS. This corresponds to the area of the contour plot with low values of  $q_u$ ,  $S_u$  and  $E_{50}$ . The low strength and stiffness in this area further indicates that the PSA has little a low stabilizing effect, especially at lower binder contents.

When maximizing strain and stiffness, the corresponding failure strain ranges between 1.55 to 2.00 % for a wbr of 8, and between 2.15 and 2.35 % for a wbr of 16. This value is important when designing and following up on projects where settlement is supposed to be mitigated.

### **5.1.5. P-wave velocity**

Previously discussed responses (i.e.  $q_u$ ,  $S_u$ ,  $E_{50}$  and  $\varepsilon_v$ ) show low amounts of correlation with  $V_p$  for samples prepared with a wbr of 16. The assumed reason behind this is insufficient hydration of the binders. In the dry mixed samples, this is most noticeable for samples with high GGBS content. When using wet mixing, the samples with high PSA content also show this behavior (see Figure 84). Measured  $V_p$  in these samples is around 1300 to 1500 m/s. This result stands out because it is close to 1450 m/s, which is the p-wave velocity for water (see section 2.1.4). The low activation of the pozzolanic binders, combined with a low total binder content, results in enough free water for the signal to pass through without indicating proper sample strength. Response surface models and contour plots for samples prepared with a wbr of 16 are not discussed further, as they are considered unusable for practical analysis.

The model info and ANOVA results for samples prepared with a wbr of 8 show that the wet method (Table 36) is slightly better than the dry method (Table 32) in terms of prediction and standard deviation. This is confirmed by the diagnostic plots in appendix B.4.1. Both methods find significant interaction between all binders, resulting in full quadratic models. The models are only considered accurate for a single wbr.

For a wbr of 8, the optimal binder content for maximizing  $V_p$  is essentially the same as for maximizing strength (see section 5.1.2). The  $V_p$  values in Figure 83 are in line with findings from previous studies (see Figure 5 and Figure 6). This confirms that the PUNDIT ultrasonic equipment can be used as a non-destructive test indicator for strength in stabilized soil. With this being said, field samples cannot be returned to the site after testing which makes destructive strength testing as viable as non-destructive testing. The p-wave velocity is still less reliable than UCT (see section 5.1.2) which in conclusion makes the PUNDIT equipment currently not suitable for stabilized soil.

## **5.2 Homogeneity**

### **5.2.1. Field samples**

The field homogeneity is assessed by comparing the sample images in appendix A.1 with the CT results in appendix A.2. Samples installed with the wet deep mixing method are

reviewed separately from the samples installed with the modified dry mixing method in this section. The mixing methods are compared in section 5.3.1.

On the exterior, the Östrand samples are similar in color, with varying amounts of pores and visible unstabilized clay. The sections of unstabilized clay can be recognized on the exterior of the samples as having a porous ring around the edge. An example of this can be seen on the lower half of the image labeled as exterior 2 on the WDM.Östrand.2 sample. These unstabilized areas are dry, brittle, and porous when inspected. On the interior images, as well as the 2D  $\mu$ CT images, it becomes clear that these areas of the samples are the main source of sample porosity. The only visible porosity in the stabilized areas are very small bubbles. Cracking and empty pores in the unstabilized clay sections are most likely caused by the surrounding clay-binder mixture, which pulls moisture from the unstabilized clay to feed the hydration of the binder (see section 2.2.5).

As mentioned in section 4.1.4, it is difficult to determine which material(s) make up the high absorption inclusions in the field samples. In the Östrand samples, the inclusions are made up from gravel of varying size (see Figure 66). The larger pieces of gravel is likely to have been pushed down from the surface level during insertion of the mixing tool. This is evident by the large pieces of gravel visible in the WDM.Östrand.1 sample which was retrieved from around 3 meters depth (see Table 11). On the other hand, WDM.Östrand.2 and WDM.Östrand.3 were both retrieved from around 6 meters depth and have almost no inclusions (see 3D reconstructions in appendix A.2).

The samples from the Hjorthagen site are very much the same as the ones from Östrand when visually inspecting them. A slight difference in the color can be seen, but the overall texture is very similar. The real difference is in the inclusions. A mostly even distribution of small inclusions can be seen on the 3D reconstructions of the Hjorthagen samples in appendix A.2. The larger inclusions are distinctly seashells. This is confirmed by inspecting the cut sample (see Figure 67). When looking at the 2D  $\mu$ CT images, most of the smaller inclusions have sharp edges, which indicate that they are mostly fragments of broken shell.

The MDM samples from the E6 site all have a much coarser texture than the WDM samples. White traces of binder can be seen on the interior images in appendix A.1, which suggests that the amount of mixing was insufficient. Binder accumulation is common in deep stabilization by DDM, which uses the same injection procedure as MDM (see section 2.1.4). Pores and cracks seem to not be limited to the sections of unstabilized clay in the E6 samples. The more even distribution of pores in the 2D  $\mu$ CT slices (see appendix A.2) indicates that air is more likely entrapped during dry binder injection.

Characterization of the homogeneity produced by the different mixing methods is limited to three samples from each site. The low number of samples, together with a rough sampling procedure for the MDM samples, may result in findings that are not representative of the method. Additionally, the uneven surface of the cut samples is difficult to compare with exact 2D  $\mu$ CT slices (see Table 28). In future studies, the photograph-reconstruction method applied by Amrioui et al. (2023) can be used to better evaluate sample homogeneity. This method can also notice inclusions which are otherwise invisible when only using  $\mu$ CT.

## 5.2.2. Laboratory samples

Variation in homogeneity of laboratory samples is difficult to assess without specific testing. The visual inspection of the samples both during preparation and testing is used to assess homogeneity along with performance characteristics. In general, sample homogeneity is affected by mixing method. Wet mixed samples with a wbr of 16, high PSA content and low CEM I content have the lowest homogeneity in terms of performance. These samples had a runny/lumpy consistency after mixing as described in section 5.1.1. It is unsure if this is due to the kitchen stand mixer or the mixing method because the dry method produced solid and uniform batches with higher viscosity. After UCT, the lumps were still present in the samples as they had higher strength compared with the rest of the sample.

During UCT, samples prepared with the dry method showed some binder accumulations which could not be seen in the wet mixed samples (see Figure 69). This is not considered to be indicative of poor homogeneity because of the low variation in performance between the wet and dry mixing methods (wbr of 8).

The results are limited to a single mixing time during sample preparation. In many cases, the mixing time also had to be cut short due to rapid strength development. Future studies can be conducted to compare the effects of different mixing times on stabilized samples.

## 5.3 Comparing mixing methods

### 5.3.1. Field samples

When comparing the mixing methods in terms of practical application, the limitations remain the same as in section 5.2.1. Too few samples were examined to properly evaluate and compare the WDM and MDM methods. Installation parameters like binder content and blade rotation number also vary greatly between the three sites. However, the results still show some characteristics of each mixing method which should be considered in the design process. A summary of the field installation parameters is shown in Table 39 (see section 3.1.1), while a summary of the field sample results is shown in Table 40 (see section 4.1).

Table 39: Summary of the field installation parameters.

| Site               | Binder type  | Binder content, $\alpha$ [kg/m <sup>3</sup> ] | Blade rotation number, $T$ [n/m] | Installation period |
|--------------------|--------------|---|----------------------------------|---------------------|
| Östrand            | 100 % cement | 200   | 666                              | December 2022       |
| Hjorthagen         | 100 % cement | 115   | 800                              | March 2022          |
| E6 Kvithammar-Åsen | 100 % cement | 100   | 250                              | Summer 2022         |

Table 40: Summary of the field sample results.

| Sample ID <sup>[1]</sup> | Soil water content after $\mu$ CT testing, $w_{\mu CT}$ | P-wave velocity, $V_p$ [m/s] | Average macro porosity |
|--------------------------|---|------------------------------|------------------------|
| WDM.Östrand.1            | 36.6 %  | 2190                         | 0.8 %                  |
| WDM.Östrand.2            | 52.1 %  | 2150                         | 0.9 %                  |
| WDM.Östrand.3            | 54.8 %  | 2270                         | 0.3 %                  |
| WDM.Hjorthagen.1         | 80.9 %  | 1850                         | 0.2 %                  |
| WDM.Hjorthagen.2         | 78.3 %  | 1890                         | 0.1 %                  |
| WDM.Hjorthagen.3         | 69.3 %  | 1815                         | 0.4 %                  |
| MDM.E6.1                 | 25.4 %  | 1500                         | 1.0 %                  |
| MDM.E6.2                 | 26.0 %  | 1750                         | 0.4 %                  |
| MDM.E6.3                 | 17.8 %  | 1650                         | 1.5 %                  |

[1] Sample ID explanation: WDM. Östrand.1 = Installed with the WDM method, field sample from the Östrand site, sample number 1

Results show that the WDM method produces samples with very low average macro porosity ( $\approx 0.1$  to  $0.9$  %). The Hjorthagen samples have lower porosity values than the Östrand samples. A possible cause for this is the higher blade rotation number in the Hjorthagen samples, which should in theory improve homogeneity and reduce the amount of unstabilized clay. Despite this, a clear conclusion cannot be made because the porosity might also be affected by the longer curing time and lower binder amount in the Hjorthagen samples. The average porosity in the MDM samples are higher ( $\approx 0.4$  to  $1.5$  %) and more scattered than in the WDM samples. This result is somewhat expected because the MDM method uses compressed air to inject a dry binder into the soil. Additionally, a low blade rotation number of 250 per meter was used during installation of the MDM piles. This value is much lower than the recommended lower limit of 400 per meter for DDM (see section 2.1.4), which might have worsened the result inconsistencies. Previously studied DDM field samples have higher porosity values ( $\approx 0.5$  to  $1.6$  %) than the WDM samples as well (see section 2.3.3). These porosity values for DDM are closer to what is observed in the MDM samples, indicating that there is a quality advantage in choosing the WDM method.

Water content also plays a role in the mixing process but getting an idea of its effect(s) on the stabilized soil is difficult because an initial water content was not provided for any of the three sites. The soil is assumed to be fully saturated in both WDM sites. However, the measured water content in the Hjorthagen samples is much higher than in the Östrand samples. This is most likely due to the higher cement content in the Östrand samples which needs more water to fully hydrate (see section 2.2.5). An interesting note is that there could also be a higher number of capillary pores from the higher water content in the Hjorthagen samples (see Figure 7). These pores can be very small and might not be included in the macro porosity estimation, linking this to the low average porosity mentioned in the paragraph above. The water content in the MDM samples is much lower than any of the WDM samples. This, along with the low blade rotation number might be a cause for the binder accumulations mentioned in section 5.2.1.

In the design process, strength is often the deciding factor when choosing a mixing method and installation parameters. Porosity and water content both influence strength (see section 2.2.4 and 2.3.3), along with many other factors. Examples of these other factors include curing temperature (see Figure 13 and Figure 14) and curing stress (see Figure

16). Due to many such unknown factors in the field samples, the strength is only indicated by the measured p-wave velocity. From theory, higher p-wave velocity equates to higher strength (see section 2.1.4). The p-wave velocity is highest in the Östrand WDM samples, which also has the highest binder content. As expected, the lower binder content in the Hjorthagen samples results in lower p-wave velocity. The MDM samples have a slightly lower binder content than the Hjorthagen samples, but a large decrease in p-wave velocity. This large drop in p-wave velocity is most likely due to insufficient mixing and the higher porosity in the MDM samples, and not the slight drop in binder content.

### 5.3.2. Laboratory samples

In general, results and findings from the laboratory cannot be used to directly estimate field properties. However, the obtained results can be indicative of the performance of the two mixing methods relative to each other. Table 41 shows a summary of the mixing method findings from the response discussion (see section 5.1).

Table 41: Summary of mixing method findings.

| Response  | Mixing method findings         |   |   |                          | Comment           |
|---|--------------------------------|---|---|--------------------------|-------------------|
|   | DRY.8 <sup>[1]</sup>           | WET.8 <sup>[2]</sup>  | DRY.16  | WET.16                   |                   |
| Ultimate compressive strength, $q_u$  | -                              | Lower standard deviation and superior prediction properties                                   | Lower standard deviation and superior prediction properties, higher maximum $q_u$ and $S_u$ | -                        | See section 5.1.2 |
| Undrained shear strength, $S_u$   |                                |   |   |                          | See section 5.1.2 |
| Failure strain, $\varepsilon_v$   | Higher overall $\varepsilon_v$ | Lower standard deviation and superior prediction properties                                   | Superior prediction properties, higher overall $\varepsilon_v$                              | Lower standard deviation | See section 5.1.3 |
| Estimated stiffness, $E_{50}$   | -                              | Lower standard deviation and superior prediction properties, higher observed maximum $E_{50}$ | Lower standard deviation and superior prediction properties                                 | -                        | See section 5.1.4 |
| P-wave velocity, $V_p$  | -                              | Lower standard deviation and superior prediction properties                                   | Not evaluated due to correlation inconsistencies  |                          | See section 5.1.5 |
| <p>[1] DRY.8 = Dry mixing method, water to binder ratio of 8</p> <p>[2] WET.8 = Wet mixing method, water to binder ratio of 8</p> |                                |   |   |                          |                   |



Table 41 clearly shows that strength and deformation properties are affected by water to binder ratio. At a wbr of 8, the wet method gives more consistent results compared with the dry method. The wet method response surface models also have a lower standard deviation and better prediction properties. Increasing the wbr to 16 flips most of the results, making the dry method appear to give better strength and deformation properties.

Field equivalent methods to the wet and dry laboratory mixing methods are DDM and WDM, respectively. WDM is much more expensive than the dry method (see section 2.1.4), which makes it most viable in projects which require higher binder content and high quality. In most other projects, which do not require high binder content and as much consistency, DDM is much more cost effective. This generalization is somewhat limited, as other factors like project size, soil conditions and geography greatly influence the chosen deep mixing method as well. It is important to note that the laboratory findings are only indicative of performance in soil which is similar to the tested quick clay (see 3.2.1).

The overall performance of samples made with the wet and dry mixing methods vary little in the laboratory. As a result, none of the methods show clear sustainability advantages from the laboratory testing. In deep mixing projects, DDM and MDM is best in terms of sustainability due to the smaller machinery their ability to use alternative, more environmentally friendly binders. Table 5 shows an overview of emissions from commonly used binders.

### 5.3.3. Single wet mixing method evaluation

Recipes with the exact same binder- and added water content was prepared using the wet mixing method and the modified dry mixing method to see if they are interchangeable when preparing laboratory samples. If so, studies using either mixing method can be compared more accurately. An overview of the result averages is presented in Table 42 (see section 4.2.3 and appendix B.3.2).

Table 42: Average results for single wet mixing method evaluation.

| Sample ID <sup>[1]</sup> | Ultimate compressive strength, $q_u$ [kPa] |                    | Failure strain, $\epsilon_v$ |                    | Estimated stiffness, $E_{50}$ [kPa] |                    |
|--------------------------|--|--------------------|------------------------------|--------------------|-------------------------------------|--------------------|
|                          | Average value                              | Standard deviation | Average value                | Standard deviation | Average value                       | Standard deviation |
| WET.8.1<br>(Sample 4-6)  | 1208                                       | 64                 | 1.31 %                       | 0.07 %             | 163 983                             | 6 229              |
| MDM.8.1                  | 1187                                       | 62                 | 1.06 %                       | 0.01 %             | 184 853                             | 15 794             |
| WET.16.1<br>(Sample 4-6) | 447  | 11                 | 1.31 %                       | 0.08 %             | 64 336                              | 2 793              |
| MDM.16.1                 | 569  | 14                 | 1.25 %                       | 0.09 %             | 87 638                              | 2 488              |

[1] Sample ID explanation: WET.8.1 = Wet mixing method, MDM.8.1 = Modified dry mixing method, water to binder ratio of 8, lattice point 1

The samples prepared with a wbr of 8 show very little variation in strength, but interestingly enough, the samples prepared with the MDM method have higher stiffness. This gives the MDM samples a considerably lower failure strain as seen in the other laboratory samples (see section 5.1.2).

Differences are even more clear in the samples with a wbr of 16, where the MDM samples are almost 30 % stronger than the wet mixed samples. Even though failure strain remains similar, the stiffness increases when using MDM method is also larger when using a wbr of 16.

The large differences suggest that a single wet mixing method cannot be used in the laboratory when making stabilized clay samples. Some differences are to be expected due to spatial variability in the soil and possible preparation errors. However, the limitations are assumed to not influence the overall conclusion because the results are reasonably similar across both wbr values.

# 6 | Conclusions and further work

## 6.1 Conclusions

### 6.1.1. Field study

The findings from the field study are summarized in the following conclusions:

1. Homogeneity in stabilized clay samples using WDM can be characterized as having little to no entrapped air in the soil-binder mixture, with pores only being visible in brittle sections of unstabilized clay. Color and texture are very consistent in the stabilized clay.
2. Homogeneity in stabilized clay samples using MDM can be characterized as having an even distribution of smaller pores and cracks. Varying amounts of visible binder accumulation, a coarse texture and uneven coloring is most likely caused by insufficient mixing and dry binder injection.
3. Soil stabilization with the WDM method results in lower average porosity ( $\approx 0.1$  to  $0.9$  %) compared with MDM ( $\approx 0.4$  to  $1.5$  %) and DDM ( $\approx 0.5$  to  $1.6$  %).

### 6.1.2. Laboratory study

The findings from the laboratory study are summarized in the following conclusions:

1. To maximize strength and stiffness at 28 days of curing, an optimal binder composition of around 55 to 65 % CEM I and 35 to 45 % GGBS should be used regardless of mixing method and wbr. This binder composition results in a failure strain between 1.55 and 2.00 % for a wbr of 8, and between 2.15 and 2.35 % for a wbr of 16.
2. Lower viscosity is achieved when preparing samples with the wet mixing method when compared with the dry mixing method. This is most noticeable in batches with a high wbr and low CEM I content.
3. Sample strength and deformation properties are affected by mixing method when using the rodding technique for sample molding. Dry mixed samples have small visible binder accumulations which do not seem to affect strength gain. The lowest performance in terms of strength and deformation properties was observed in wet mixed samples with a high content of pozzolanic binders and a wbr of 16. Inconsistent areas of higher strength (lumps) were observed inside these samples after UCT.
4. P-wave testing with the PUNDIT equipment is not currently suitable for stabilized soil even if the measurements are somewhat reliable for indicating strength and stiffness for samples prepared with a wbr of 8, regardless of mixing method. When increasing wbr to 16, p-wave velocities close to that of water is measured in low strength samples after 28 days of curing. Results are expected to change after longer curing periods, as the low strength samples are stabilized with mainly pozzolanic binders, which react slower than CEM I.
5. At a wbr of 8, wet mixing produces more consistent samples with less scatter between identical samples than the dry method. This results in response surface

models with a lower standard deviation and better prediction properties. When increasing the wbr to 16, findings are flipped, and the dry method is superior.

6. Preparing stabilized clay samples by adding a slurry containing binder and water do not equal adding the same amounts of water and dry binder separately. Adding the components separately improves strength and stiffness when CEM I is used as a binder.
7. When designing for quick clay conditions, the dry mixing method should in most deep stabilization projects be chosen to limit costs and environmental impact. This is mainly due to the smaller machinery and lower rigging- and installation costs compared with the wet deep mixing method. However, each site is different, and the final stabilization solution should be adapted to the specific needs of individual projects.

## **6.2 Further work**

### **6.2.1. Field**

It is difficult to properly evaluate the homogeneity of stabilized clay samples. Further research can focus on how qualitative data can be analyzed to measure homogeneity. Improved images of the sample interiors can be obtained by destructive testing. The suggested destructive testing consists of reconstructing samples from photos of physically sliced samples (Amrioui et al., 2023). This method can be used to find mixing characteristics and inclusions which are invisible on  $\mu$ CT images (2D and 3D).

Many factors influence the obtained strength in stabilized soil. Measurements can be done both destructive through unconfined compression testing and non-destructive with p-wave velocity measurements. Future studies can investigate larger scale testing of field and laboratory stabilized material with different mixing methods to increase the accuracy and reliability of p-wave velocity measurements.

As more alternative mixing methods and binders are being introduced, additional research can be done on recreating these field properties in the laboratory. Previous research has shown the difficulties in recreating field samples in the laboratory (Falle, 2021). However, many possibilities still exist in improving the current sample preparation techniques and curing conditions.

### **6.2.2. Laboratory**

The findings in this thesis are limited to Norwegian quick clay. Even if only one site was used (Tiller-Flotten), a high spatial variability regarding water content and remolded consistency was very much present. Future studies can evaluate the viability of wet and dry mixing methods in other materials.

Samples prepared with GGBS and PSA had lower strength compared with what is expected from pozzolanic binders. Future studies can cure stabilized samples for at least 90 days when pozzolanic binders are used. This can be done to improve the current understanding of interaction between alternative binders.

An expression for predicting the strength from p-wave velocity could not be made from the measurements in this thesis. For further research, the testing can be done by systematically varying the binder content when mixing samples with a set binder composition. These additional tests can also be used to find the binder content limit where the signal starts to pass through free water in the samples. This can be researched to avoid high p-wave velocity measurements in low strength samples (here observed in samples prepared with a wbr of 16).

The high performance of the MDM method in the laboratory samples can be researched further. It is unclear why mixing water into clay before adding a dry binder can result in improved strength and stiffness as opposed to just adding a premixed slurry of water and binder.

## 7 | Bibliography

- Amrioui, J., Duc, M., Le Kouby, A., Guedon, J.-S., Saussaye, L., Hemmati, S., Willot, F., & Dokladal, P. (2023). Characterization by image analysis of materials heterogeneities produced by the Deep Soil Mixing technique. *Materials Today: Proceedings*.
- Bache, B. K., Hov, S., & Mengede, M. (2021). Laboratorieforsøk med ulike typer kalkbaserte bindemidler med hensikt å optimalisere bindemiddeltipe, innblandingmengde og påvirkning på klima og miljø. *Referat fra Fjellsprengningsdagen, Bergmekanikkdagen, Geoteknikkdagen 2021, Oslo, Norge*. [In Norwegian]
- Chaumeny, J. L., Kanty, P., & Reitmeier, T. (2018). Remarks on wet deep soil mixing quality control. *ce/papers*, 2(2-3), pp. 427-432.
- Cnudde, V., & Boone, M. N. (2013). High-resolution X-ray computed tomography in geosciences: A review of the current technology and applications. *Earth-Science Reviews*, 123, pp. 1-17.
- Enggen, A. (2013). *Skånsomme installasjonsmetoder for kalksementpeler og bruk av slurry* (37). Naturfareprosjektet: Delprosjekt 6 Kvikkleire, Issue. Norges vassdrags- og energidirektorat, Statens vegvesen, & Jernbaneverket. [In Norwegian]
- Emineral A/S. (2020). Emineral Fly Ash. *ENVIRONMENTAL PRODUCT DECLARATION*. [In Danish]
- Engeset, I. (2018). *Betydning av spenningsnivå under herding av kalksementstabilisert leire* [Master's thesis, Norwegian University of Science and Technology]. Trondheim. [In Norwegian]
- Eniro. (n.d.). *Eniro Kartor*. Eniro AB. Retrieved 25.01.23 from <https://kartor.eniro.se/> [In Swedish]
- Eriksson, H., Gunther, J., & Ruin, M. (2005). MDM combines the advantages of dry and wet mixing. *Proceedings of the International Conference on Deep Mixing: Best Practice and Recent Advance*, 1, pp. 509-520.
- Falle, F. Å. (2021). *Comparing laboratory and field stabilised clay* [Master's thesis, Norwegian University of Science and Technology]. Trondheim. <https://hdl.handle.net/11250/2787267>
- Franzefoss Minerals AS. (2022). Brentkalk NFK (CL 90-Q). *ENVIRONMENTAL PRODUCT DECLARATION*. [In Norwegian]
- Gunther, J., Holm, G., Westberg, G., & Eriksson, H. (2004). Modified Dry Mixing (MDM) - A New Possibility in Deep Mixing. In *Geotechnical Engineering for Transportation Projects* (pp. 1375-1384). [https://doi.org/doi:10.1061/40744\(154\)127](https://doi.org/doi:10.1061/40744(154)127)
- Hov, S., Falle, F., & Paniagua, P. (2022). Optimization of Laboratory Molding Techniques for Nordic Dry Deep Mixing. *Geotechnical Testing Journal*, 45, p. 20210245. <https://doi.org/10.1520/GTJ20210245>
- Jacobsen, S., Maage, M., Smeplass, S., Kjellsen, K. O., Sellevold, E. J., Lindgård, J., Cepuritis, R., Myrdal, R., Bjøntegaard, Ø., Geiker, M., & m.fl. (2022). *Concrete Technology*. Department of Structural Engineering.
- Janz, M., & Johansson, S. (2002). Olika bindemedels funktion vid djupstabilisering (The fuction of different ammendments used for solidification). *Svensk Djupstabilisering (Swedish Deep Stabilization Research Centre), Linköping, Sweden*. [In Swedish]
- JSW Cement Limited. (2019). Average Ground Granulated Blast- Furnace Slag. *ENVIRONMENTAL PRODUCT DECLARATION*.
- Kartverket. (n.d.). *Norgeskart*. Statens kartverk. Retrieved 25.01.23 from <https://www.norgeskart.no/> [In Norwegian]
- Kirsch, K., & Bell (Eds.), A. (2012). *Ground Improvement* (3 ed.). CRC Press. <https://doi.org/https://doi.org/10.1201/b13678>

- Kitazume, M. (2005). *State of practice report–Field and laboratory investigations, properties of binders and stabilized soil*. Proceedings of the International Conference on Deep Mixing Best Practice and Recent Advances, (pp. 660-684).
- Kitazume, M., Grisolia, M., Leder, E., Marzano, I. P., Correia, A. A. S., Oliveira, P. J. V., Åhnberg, H., & Andersson, M. (2015). Applicability of molding procedures in laboratory mix tests for quality control and assurance of the deep mixing method. *Soils and Foundations*, 55(4), pp. 761-777.  
<https://doi.org/https://doi.org/10.1016/j.sandf.2015.06.009>
- Kitazume, M., & Terashi, M. (2013). *The Deep mixing method* (Vol. 21). CRC Press.
- L'Heureux, J.-S., Lunne, T., Lacasse, S., Carroll, R., Strandvik, S. O., Instanes, A., Sinitsyn, A., Degago, S. A., & Nordal, S. (2017). *Norway's national geotest site research infrastructure (NGTS)*. Unearth the Future, Connect beyond. Proceedings of the 19th International Conference on Soil Mechanics and Geotechnical Engineering,
- L'Heureux, J.-S., Lindgård, A., & Emdal, A. (2019). The Tiller-Flotten research site: Geotechnical characterization of a very sensitive clay deposit. *AIMS Geosciences*, 5, pp. 831-867. <https://doi.org/10.3934/geosci.2019.4.831>
- Larsson, S. (2005). State of Practice Report - Execution, monitoring and quality control. *Deep Mixing*, 5, pp. 732-785.
- Larsson, S. (2021). The Nordic dry deep mixing method: Best practice and lessons learned. *Proceedings in Deep Mixing-An Online Conference*.
- Larsson, S., Dahlström, M., & Nilsson, B. (2005a). A complementary field study on the uniformity of lime-cement columns for deep mixing. *Proceedings of the Institution of Civil Engineers - Ground Improvement*, 9(2), pp. 67-77.  
<https://doi.org/10.1680/grim.2005.9.2.67>
- Larsson, S., Dahlström, M., & Nilsson, B. (2005b). Uniformity of lime-cement columns for deep mixing: a field study. *Proceedings of the Institution of Civil Engineers - Ground Improvement*, 9(1), pp. 1-15. <https://doi.org/10.1680/grim.2005.9.1.1>
- Lindh, P. (2001). Optimising binder blends for shallow stabilisation of fine-grained soils. *Proceedings of the Institution of Civil Engineers - Ground Improvement*, 5(1), pp. 23-34. <https://doi.org/10.1680/grim.2001.5.1.23>
- Lindh, P. (2004). *Compaction and strength properties of stabilised and unstabilised fine-grained tills* [Doctoral dissertation, Lund University].
- Lindh, P., & Lemenkova, P. (2022). Seismic velocity of P-waves to evaluate strength of stabilized soil for Svenska Cellulosa Aktiebolaget Biorefinery Östrand AB, Timrå. *Bulletin of the Polish Academy of Sciences: Technical Sciences*, 70(4), p. e141593.
- Mandal, T., Tinjum, J. M., & Edil, T. B. (2016). Non-destructive testing of cementitiously stabilized materials using ultrasonic pulse velocity test. *Transportation Geotechnics*, 6, pp. 97-107.
- Mavroulidou, M. (2018). Use of waste paper sludge ash as a calcium-based stabiliser for clay soils. *Waste Management & Research*, 36(11), pp. 1066-1072.
- McDowell, P., Barker, R. D., Butcher, A., Culshaw, M., Jackson, P., McCann, D., Skipp, B., Matthews, S., & Arthur, J. (2002). *Geophysics in engineering investigations* (Vol. 19). Ciria London.
- Mitchell, J. K., & Soga, K. (2005). *Fundamentals of soil behavior* (Vol. 3). John Wiley & Sons New York.
- Montgomery, D. C. (2013). *Design and Analysis of Experiments* (8th ed.). John Wiley & Sons.
- Myers, R. H., Montgomery, D. C., & Anderson-Cook, C. M. (2009). *Response surface methodology: process and product optimization using designed experiments* (3rd ed.). John Wiley & Sons.
- NGF. (2011). *Veiledning for symboler og definisjoner i geoteknikk: Identifisering og klassifisering av jord*. Norwegian Geotechnical Association. [In Norwegian]
- NGF. (2012). *Veiledning for grunnforsterkning med kalksementpeler*. Norwegian Geotechnical Association. [In Norwegian]

- NGI. (2022). *E6 Kvithammar - Åsen: GEOTEKNISK PROSJEKTERINGSRAPPORT K101 OG K102 VOLLSELVBRUENE* (R1-GEOT-23). [In Norwegian]
- NGI. (n.d.). *R&D program| GOAL - Green sOIl stAbiLisation*. Norwegian Geotechnical Association. Retrieved 19.01.23 from <https://www.ngi.no/eng/Projects/GOAL-Green-sOil-stAbiLisation>
- NGU. (2020). *XRF*. Norges geologiske undersøkelse. Retrieved 13.03.23 from <https://www.ngu.no/fagomrade/xrf> [In Norwegian]
- NGU. (n.d.). *Løsmasser - Nasjonal løsmassedatabase*. Norges geologiske undersøkelse. Retrieved 24.01.23 from [https://geo.ngu.no/kart/losmasse\\_mobil/](https://geo.ngu.no/kart/losmasse_mobil/) [In Norwegian]
- NORCEM AS. (2020a). Norcem Industrisement, Brevik - CEM I 52,5 R. *ENVIRONMENTAL PRODUCT DECLARATION*. [In Norwegian]
- NORCEM AS. (2020b). Norcem Multicem 50/50 (CKD/IND). *ENVIRONMENTAL PRODUCT DECLARATION*. [In Norwegian]
- NORCEM AS. (2020c). Norcem Multicem 50/50 (CKD/STD FA). *ENVIRONMENTAL PRODUCT DECLARATION*. [In Norwegian]
- NORCEM AS. (2020d). Norcem Standardsement FA justert, Brevik - CEM II/ B-M 42,5 R. *ENVIRONMENTAL PRODUCT DECLARATION*. [In Norwegian]
- Norske Skog Skogn. (n.d.). *About Norske Skog Skogn*. Norske Skog ASA. <https://www.norskeskog.com/about-norske-skog/business-units/europe/norske-skog-skogn>
- NVE. (n.d.). *NVE Atlas*. Norges vassdrags- og energidirektorat. Retrieved 24.01.23 from <https://atlas.nve.no/Html5Viewer/index.html?viewer=nveatlas#>
- Pakbaz, M. S., & Farzi, M. (2015). Comparison of the effect of mixing methods (dry vs. wet) on mechanical and hydraulic properties of treated soil with cement or lime. *Applied Clay Science*, 105, pp. 156-169.
- Paniagua, P., Bache, B. K., Karlsrud, K., & Lund, A. K. (2022a). Strength and stiffness of laboratory-mixed specimens of stabilised Norwegian clays. *Proceedings of the Institution of Civil Engineers - Ground Improvement*, 175(2), pp. 150-163. <https://doi.org/10.1680/jgrim.19.00051>
- Paniagua, P., Falle, F. Å., Hov, S., Tekseth, K. R., Mirzaei, F., & Breiby, D. W. (2022b). Comparing laboratory and field samples of lime-cement-improved Norwegian clay. *Géotechnique Letters*, 12(4), pp. 265-271. <https://doi.org/10.1680/jgele.22.00067>
- Proceq SA. (2017). *PUNDIT PL-2 Operating Instructions*. Proceq SA.
- SCA. (2022). *Land Reclamation Östrand*. Svenska Cellulosa Aktiebolaget SCA. <https://www.sca.com/en/renewable-energy/liquid-biofuels/land-reclamation-ostrand/>
- SGU. (n.d.). *Jordarter 1:25000 - 1:100000*. Sveriges geologiska undersökning. Retrieved 24.01.23 from <https://apps.sgu.se/kartvisare/kartvisare-jordarter-25-100.html> [In Swedish]
- Skreien, K. B. (2022). *Comparing methods of deep stabilization* [Project thesis, Norwegian University of Science and Technology]. Trondheim.
- Stat-Ease. (2020). *A concise collection of handy tips to help you set up and analyze your designed experiments*. Stat-Ease Inc.
- Stat-Ease. (n.d.-a). *ANOVA*. Stat-Ease Inc. Retrieved 18.04.23 from <https://www.statease.com/docs/v11/navigation/anova-rsm/>
- Stat-Ease. (n.d.-b). *ANOVA Output*. Stat-Ease Inc. Retrieved 18.04.23 from <https://www.statease.com/docs/v11/contents/analysis/anova-output/>
- Stat-Ease. (n.d.-c). *Dealing with Aliased Models*. Stat-Ease Inc. Retrieved 17.04.23 from <https://www.statease.com/docs/v11/contents/analysis/dealing-with-aliased-models/>
- Stat-Ease. (n.d.-d). *Design-Expert*. Stat-Ease Inc. Retrieved 22.03.23 from <https://www.statease.com/software/design-expert/>
- Stat-Ease. (n.d.-e). *Evaluation Results*. Stat-Ease Inc. Retrieved 20.04.23 from <https://www.statease.com/docs/v11/navigation/evaluation-results/>
- Statens vegvesen. (2016). *Håndbok R210: Laboratorieundersøkelser*. [In Norwegian]



- Stockholms stad. (2022). *Bostäder, förskolor och handel i Kolkajen*. Stockholms stad. <https://vaxer.stockholm/projekt/kolkajen/> [In Swedish]
- Thomas Cement AB. (2018a). Slagg Bremen. *TEKNISK INFORMATION*. [In Swedish]
- Thomas Cement AB. (2018b). Slagg Bremen. *PRODUCT DATA SHEET*. [In Swedish]
- Wang, X., Kim, S., Wu, Y., Liu, Y., Liu, T., & Wang, Y. (2023). Study on the optimization and performance of GFC soil stabilizer based on response surface methodology in soft soil stabilization. *Soils and Foundations*, 63(2), p. 101278.
- Wiersholm, P. (2018). *Temperatureffekter i kalksementstabilisert leire* [Master's thesis, Norwegian University of Science and Technology]. Trondheim. [In Norwegian]
- Yong-Feng, D., Tong-Wei, Z., Yu, Z., Qian-Wen, L., & Qiong, W. (2017). Mechanical behaviour and microstructure of steel slag-based composite and its application for soft clay stabilisation. *European Journal of Environmental and Civil Engineering*, pp. 1-16. <https://doi.org/10.1080/19648189.2017.1357787>
- Zou, K. H., Tuncali, K., & Silverman, S. G. (2003). Correlation and simple linear regression. *Radiology*, 227(3), pp. 617-628.
- Åhnberg, H. (2006). *Strength of Stabilised Soil-A Laboratory Study on Clays and Organic Soils Stabilised with different Types of Binder* [Doctoral dissertation, Lund University].
- Åhnberg, H., Johansson, S.-E., Retelius, A., Ljungkrantz, C., Holmqvist, L., & Holm, G. (1995). *Cement och kalk för djupstabilisering av jord. En kemisk-fysikalisk studie av stabiliseringseffekter*. Statens geotekniska institut.

# **A | FIELD DATA**

## **A.1 SAMPLE IMAGES**

**WDM.Östrand.1**



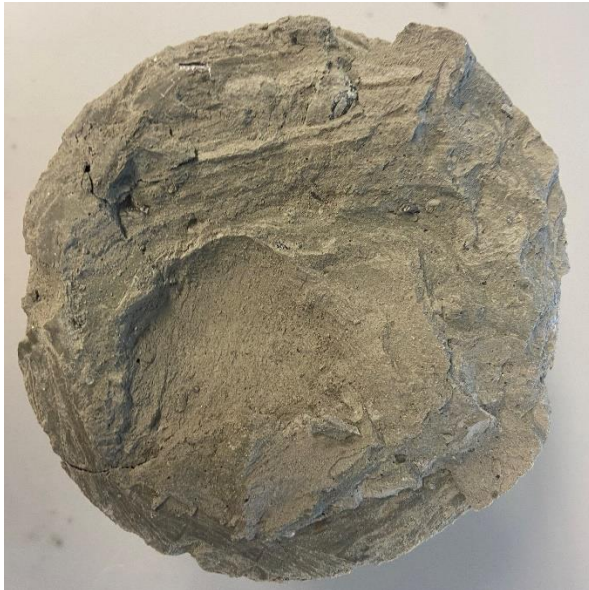
Exterior 1



Exterior 2



Interior 1 (Corresponding slice: 440-500)



Interior 2 (Corresponding slice: 440-500)  
(Flipped to match CT slice orientation)

**WDM.Östrand.2**



Exterior 1



Exterior 2



Interior 1 (Corresponding slice: 1072)



Interior 2 (Corresponding slice: 1072)  
(Flipped to match CT slice orientation)

**WDM.Östrand.3**



Exterior 1



Exterior 2



Interior 1 (Corresponding slice: 284-380)



Interior 2 (Corresponding slice: 284-380)  
(Flipped to match CT slice orientation)

**WDM.Hjorthagen.1**



Exterior 1



Exterior 2



Interior 1 (Corresponding slice: 1280)



Interior 2 (Corresponding slice: 1280)  
(Flipped to match CT slice orientation)

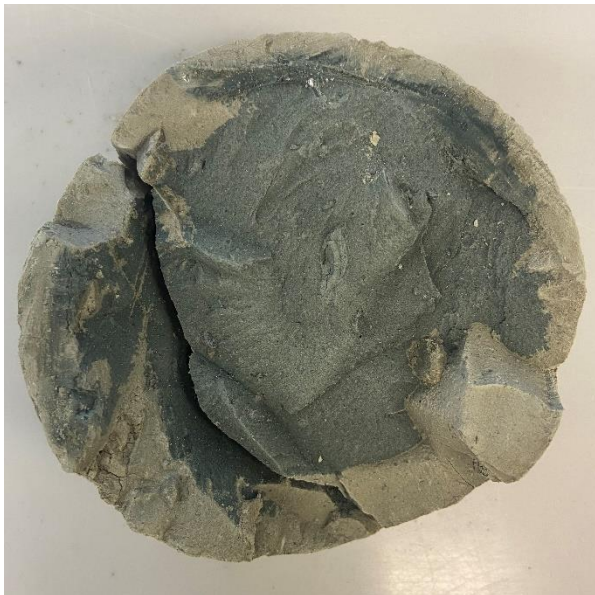
**WDM.Hjorthagen.2**



Exterior 1



Exterior 2



Interior 1 (Corresponding slice: 280-500)



Interior 2 (Corresponding slice: 280-500)  
(Flipped to match CT slice orientation)

**WDM.Hjorthagen.3**



Exterior 1



Exterior 2



Interior 1 (Corresponding slice: 804)



Interior 2 (Corresponding slice: 804)  
(Flipped to match CT slice orientation)



**MDM.E6.1**



Exterior 1



Exterior 2



Interior 1 (Corresponding slice: 648-1540)



Interior 2 (Corresponding slice: 648-1540)  
(Flipped to match CT slice orientation)

**MDM.E6.2**



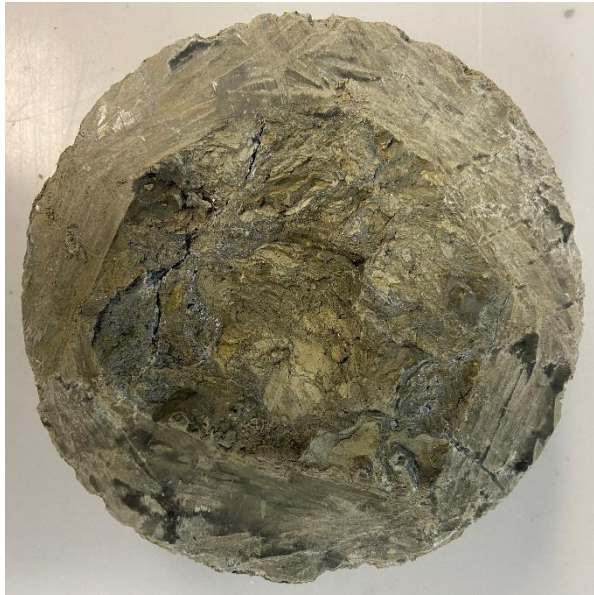
Exterior 1



Exterior 2



Interior 1 (Corresponding slice: 1320)



Interior 2 (Corresponding slice: 1320)  
(Flipped to match CT slice orientation)

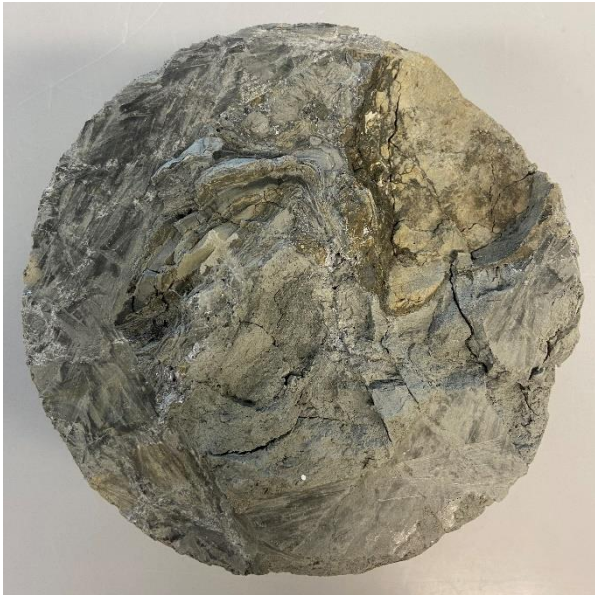
**MDM.E6.3**



Exterior 1



Exterior 2



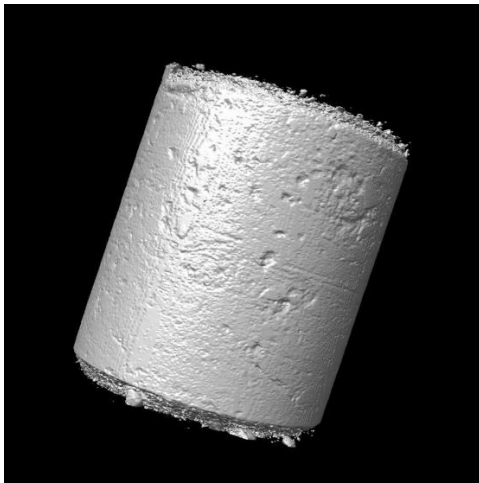
Interior 1 (Corresponding slice: 840)



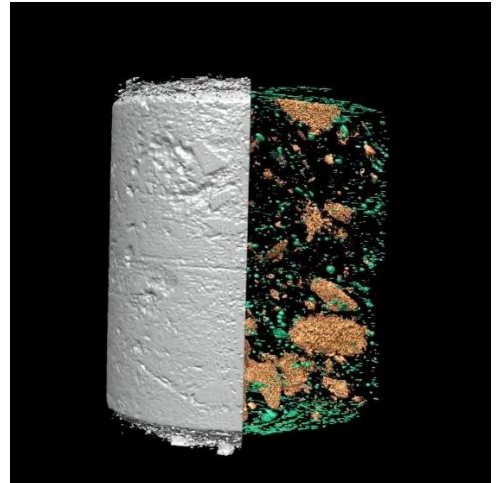
Interior 2 (Corresponding slice: 840)  
(Flipped to match CT slice orientation)

## **A.2 CT RESULTS**

**WDM.Östrand.1**



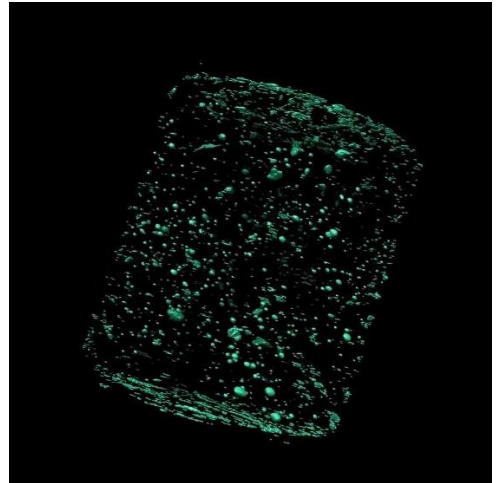
3D reconstruction: Full sample



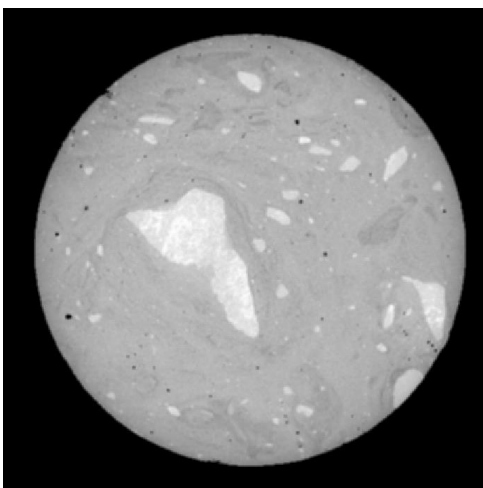
3D reconstruction: Half of sample + Inclusions + Pores



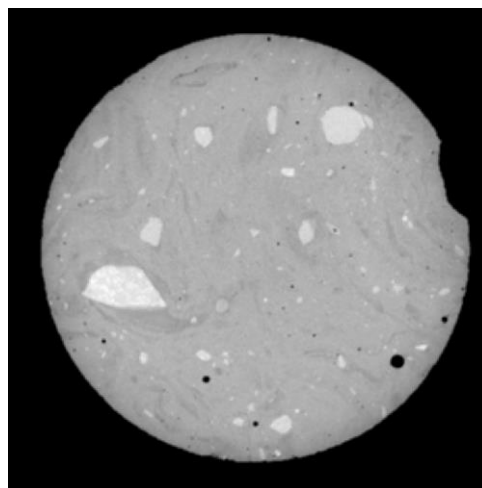
3D reconstruction: Inclusions



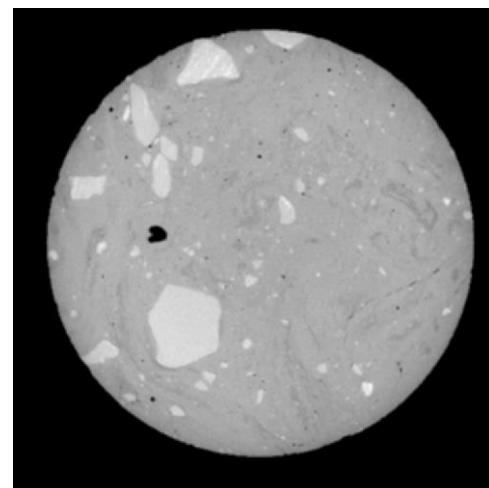
3D reconstruction: Pores



μCT Slice-number-number 440  
(Taken at inspection cut, see A.1)

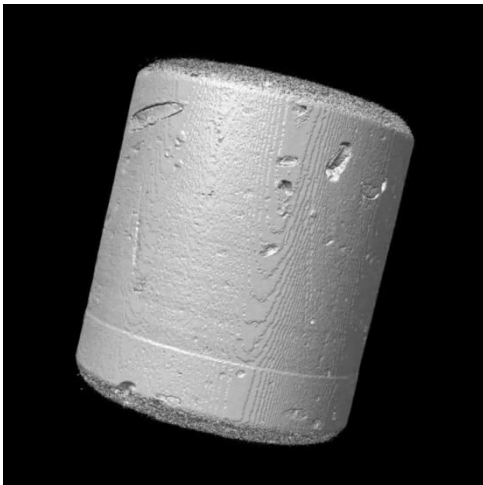


μCT Slice-number 920

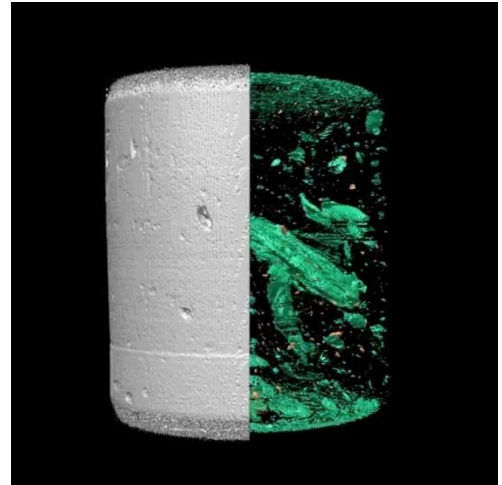


μCT Slice-number 1488

**WDM.Östrand.2**



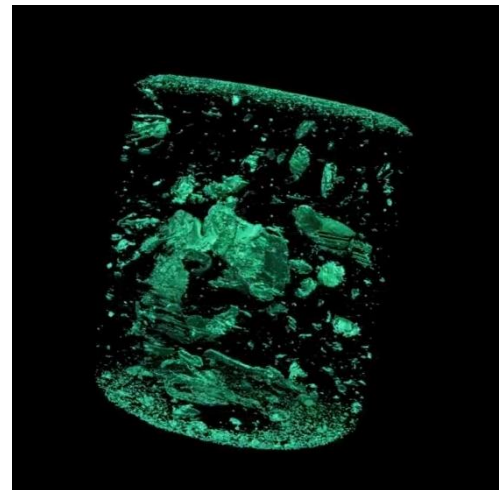
3D reconstruction: Full sample



3D reconstruction: Half of sample + Inclusions + Pores



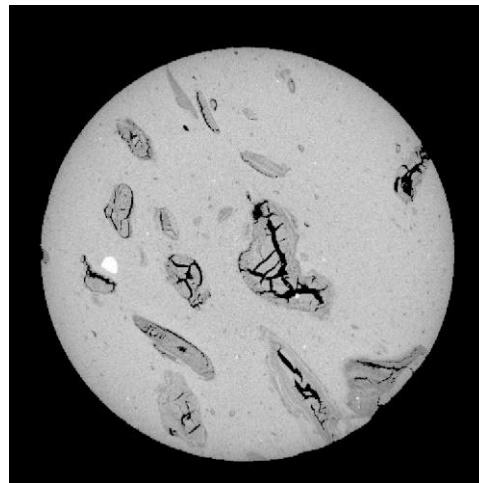
3D reconstruction: Inclusions



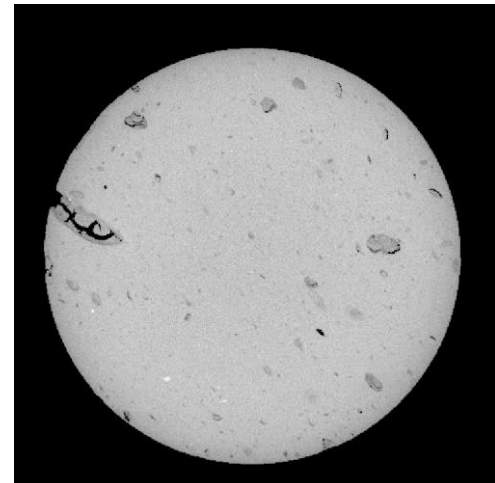
3D reconstruction: Pores



μCT Slice-number 360

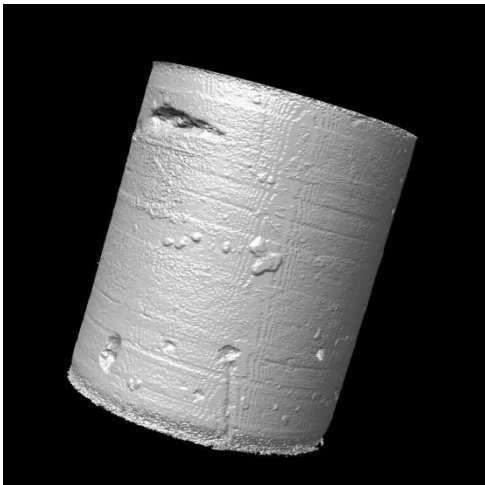


μCT Slice-number 1072  
(Taken at inspection cut, see A.1)

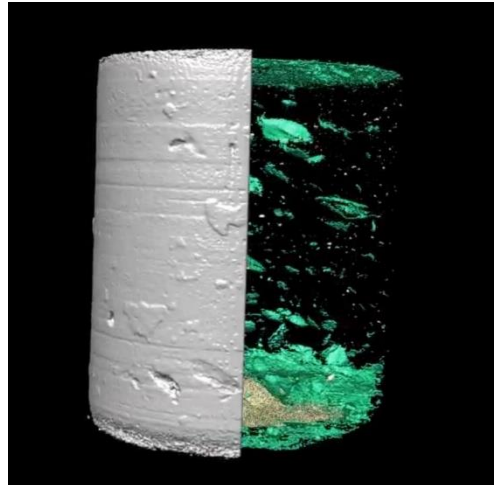


μCT Slice-number 1520

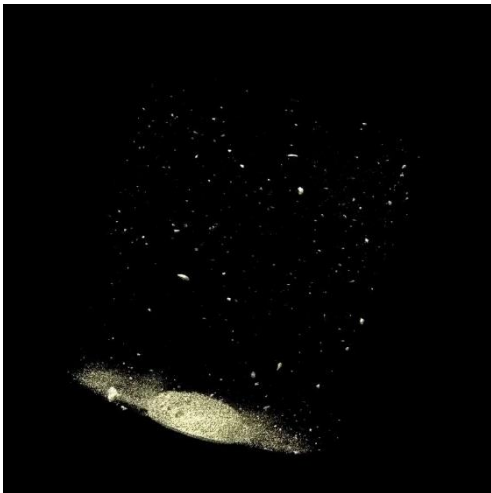
**WDM.Östrand.3**



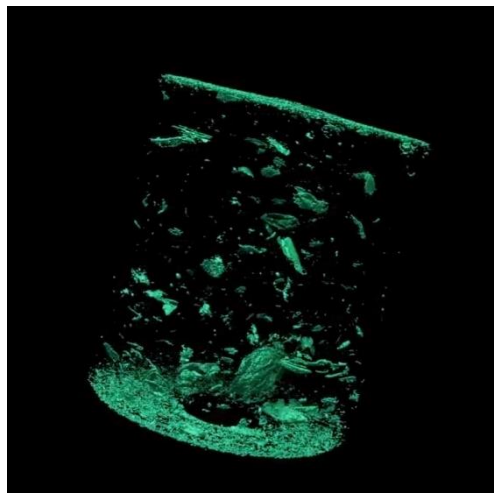
3D reconstruction: Full sample



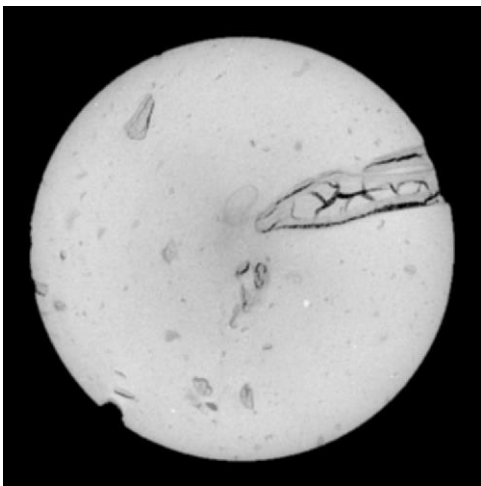
3D reconstruction: Half of sample + Inclusions + Pores



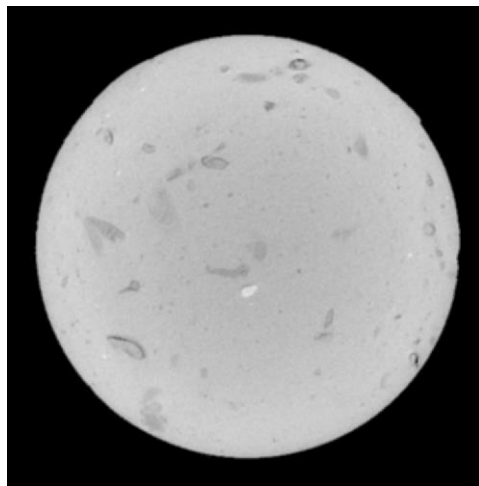
3D reconstruction: Inclusions



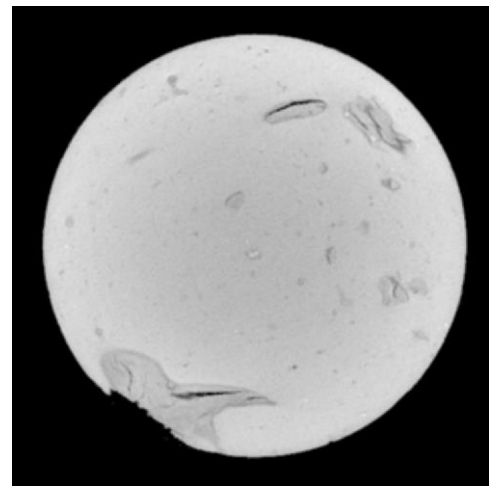
3D reconstruction: Pores



μCT Slice-number 284  
(Taken at inspection cut, see A.1)

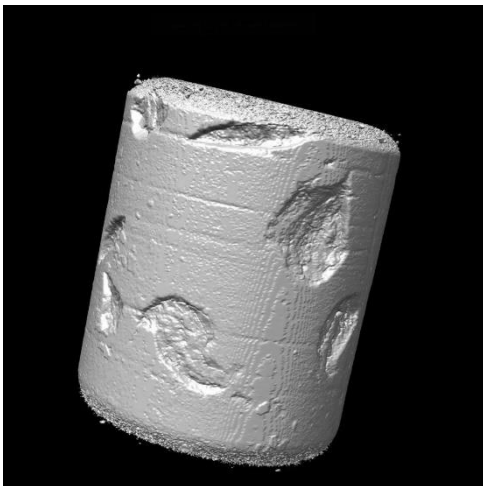


μCT Slice-number 720

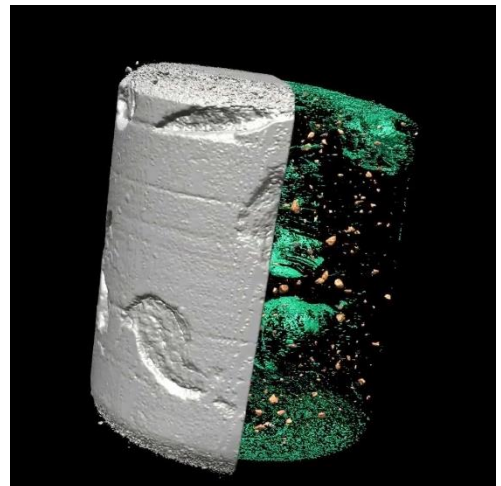


μCT Slice-number 1640

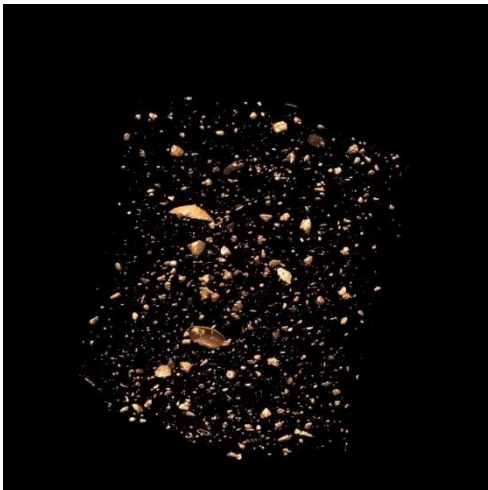
**WDM.Hjorthagen.1**



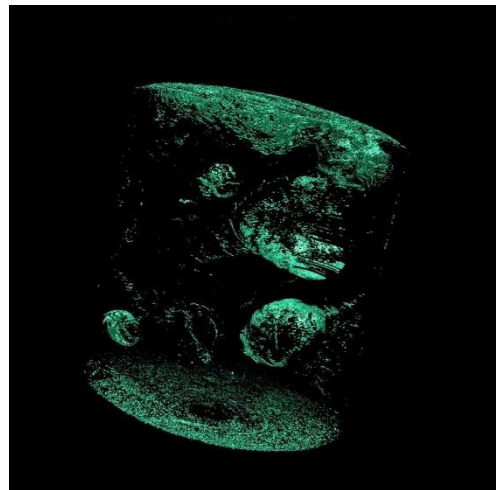
3D reconstruction: Full sample



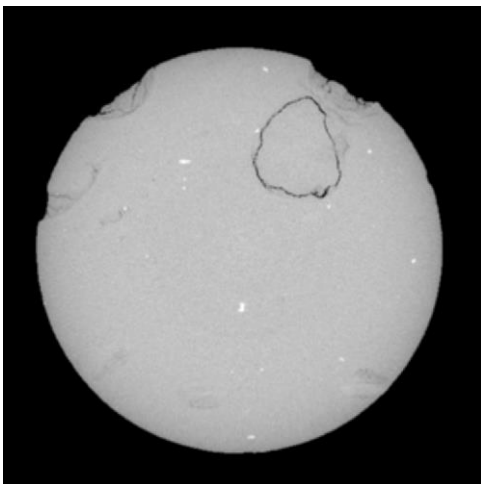
3D reconstruction: Half of sample + Inclusions + Pores



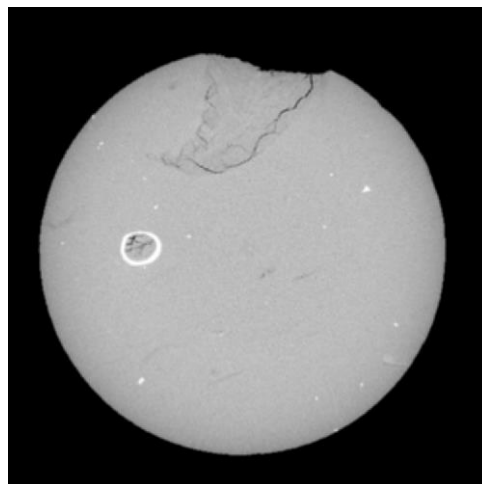
3D reconstruction: Inclusions



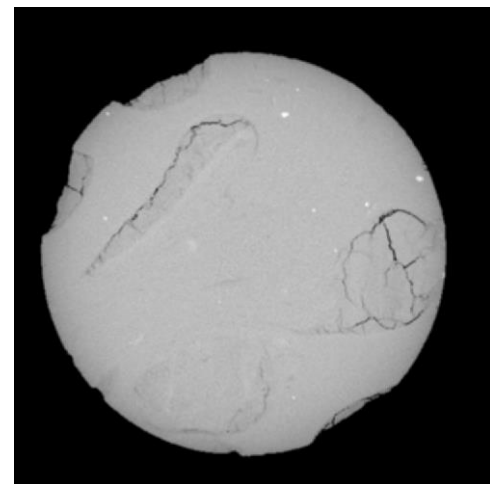
3D reconstruction: Pores



μCT Slice-number 800



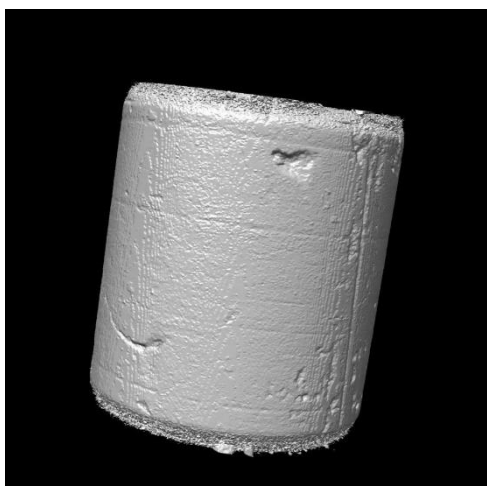
μCT Slice-number 1280  
(Taken at inspection cut, see A.1)



μCT Slice-number 1780



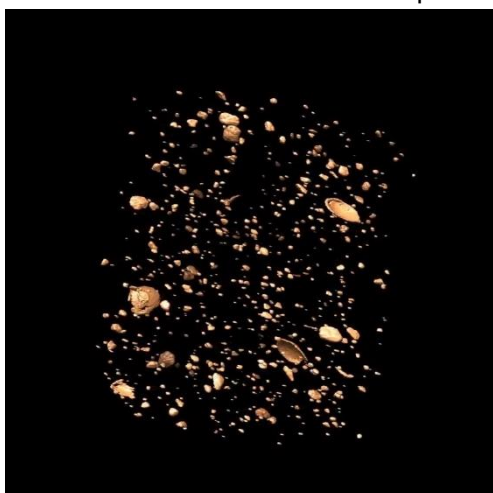
**WDM.Hjorthagen.2**



3D reconstruction: Full sample



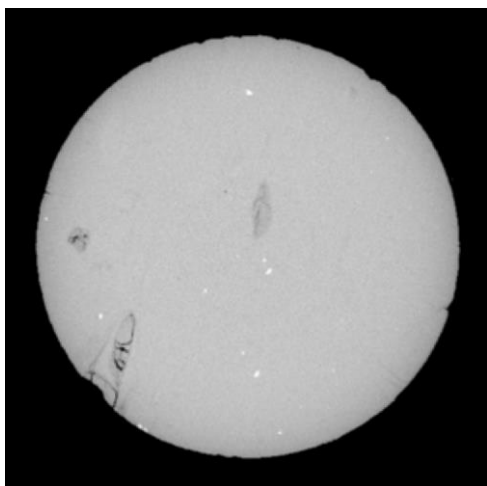
3D reconstruction: Half of sample + Inclusions + Pores



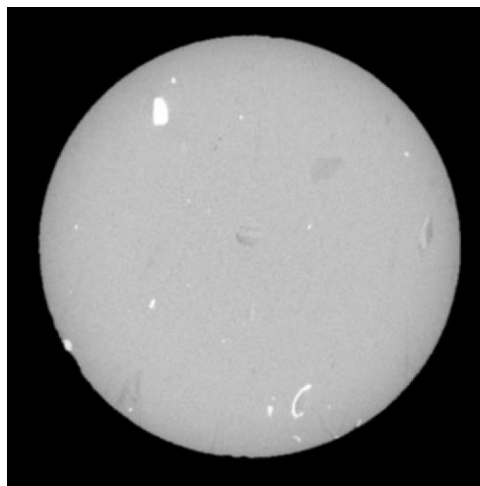
3D reconstruction: Inclusions



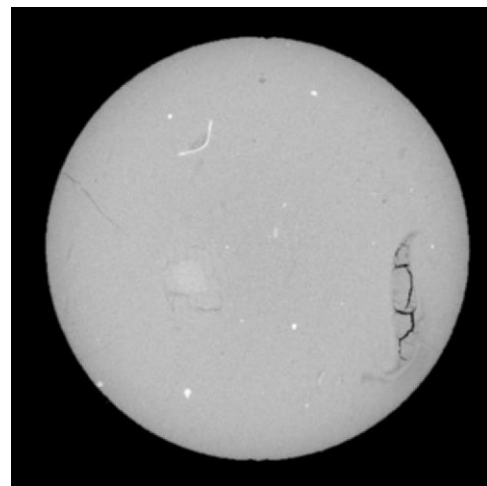
3D reconstruction: Pores



μCT Slice-number 380  
(Taken at inspection cut, see A.1)

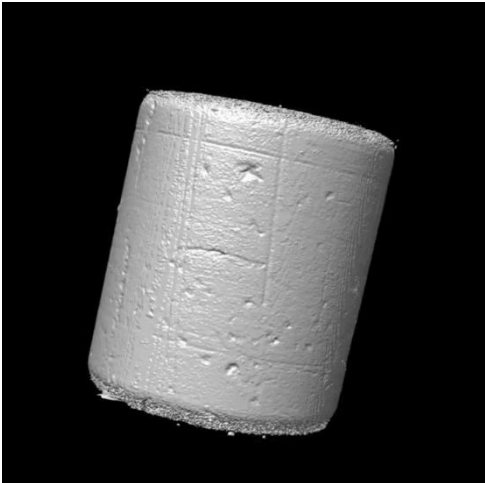


μCT Slice-number 720



μCT Slice-number 1440

**WDM.Hjorthagen.3**



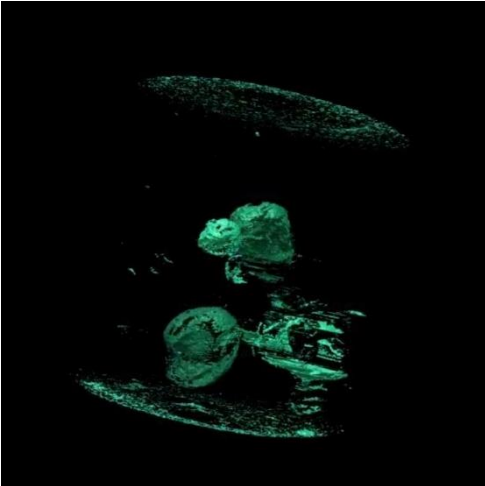
3D reconstruction: Full sample



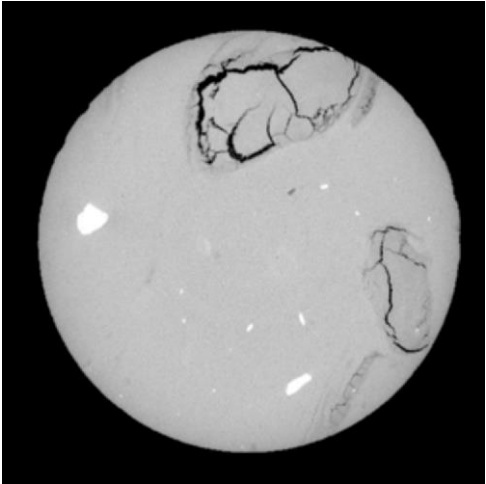
3D reconstruction: Half of sample + Inclusions + Pores



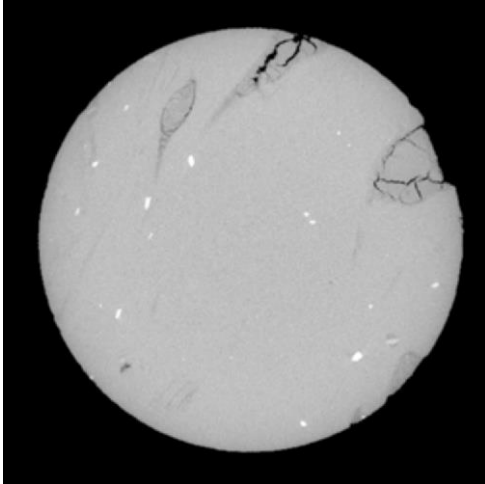
3D reconstruction: Inclusions



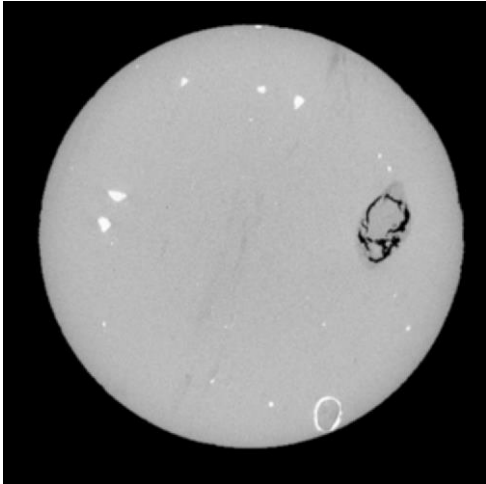
3D reconstruction: Pores



μCT Slice-number 440

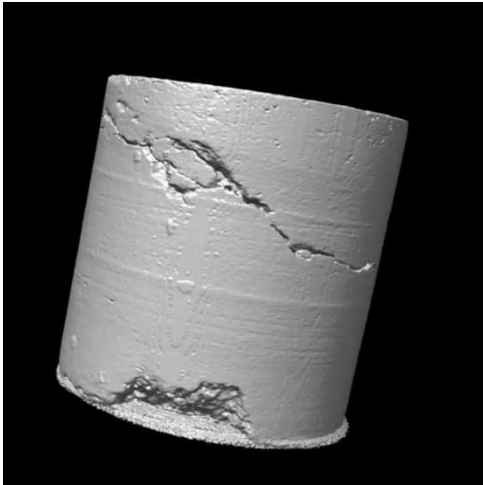


μCT Slice-number 804  
(Taken at inspection cut, see A.1)



μCT Slice-number 1360

**MDM.E6.1**



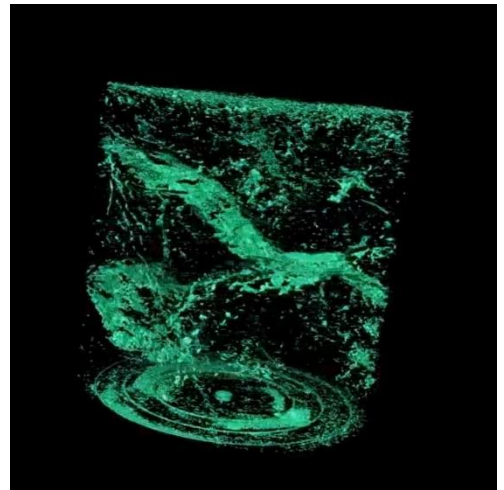
3D reconstruction: Full sample



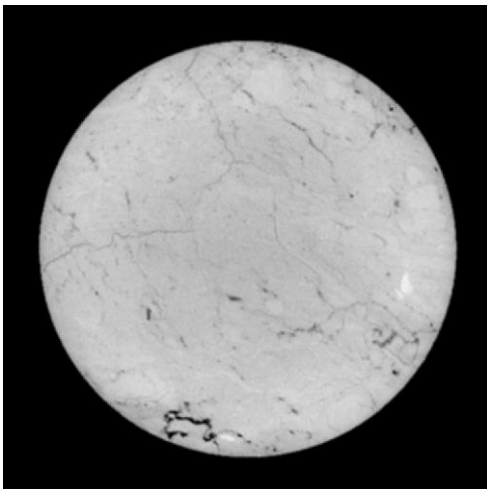
3D reconstruction: Half of sample + Inclusions + Pores



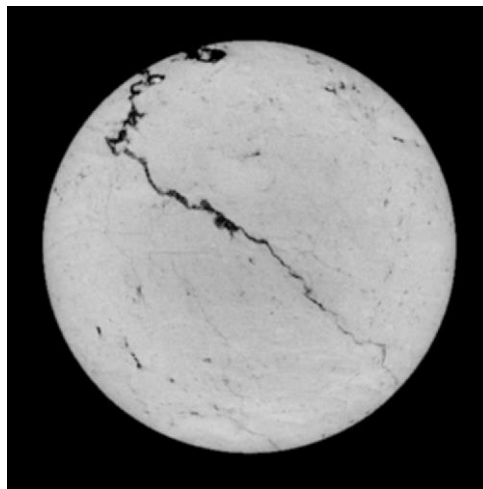
3D reconstruction: Inclusions



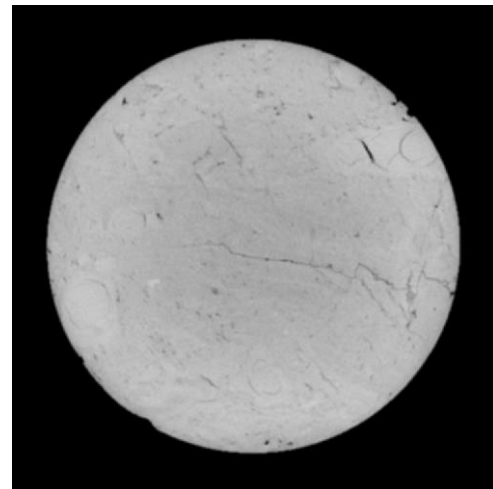
3D reconstruction: Pores



μCT Slice-number 648  
(Taken at inspection cut, see A.1)

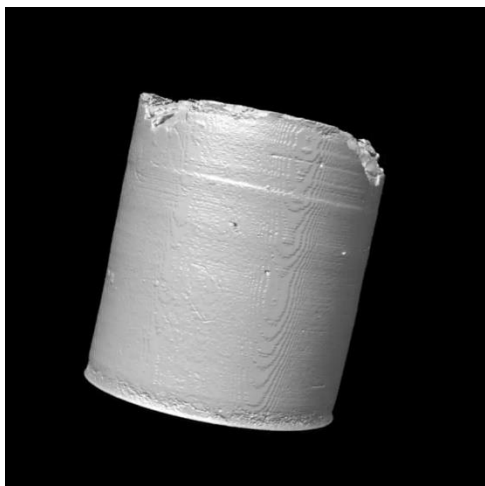


μCT Slice-number 1000  
(Taken at inspection cut, see A.1)

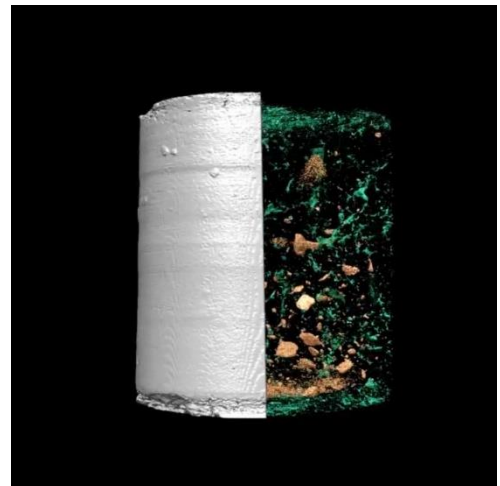


μCT Slice-number 1540  
(Taken at inspection cut, see A.1)

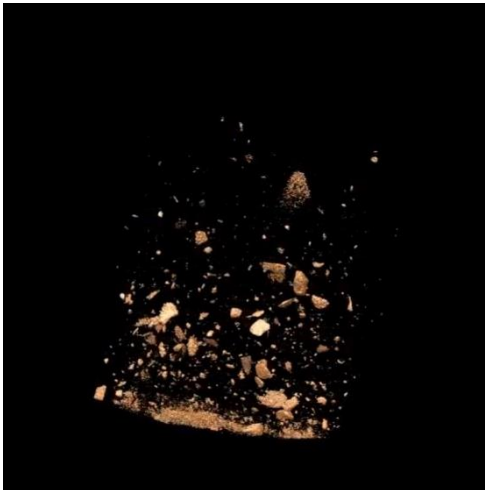
**MDM.E6.2**



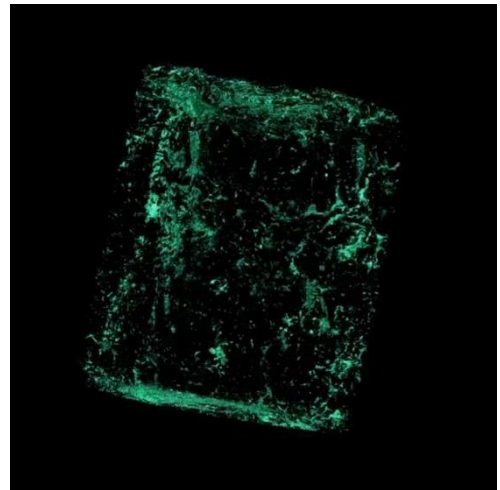
3D reconstruction: Full sample



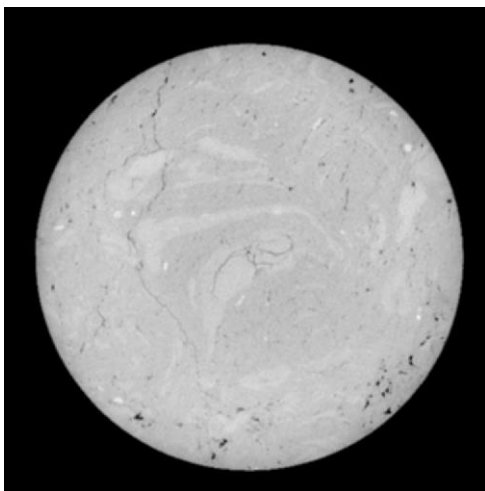
3D reconstruction: Half of sample + Inclusions + Pores



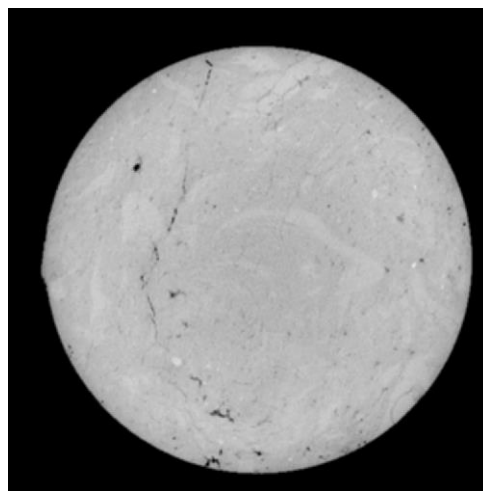
3D reconstruction: Inclusions



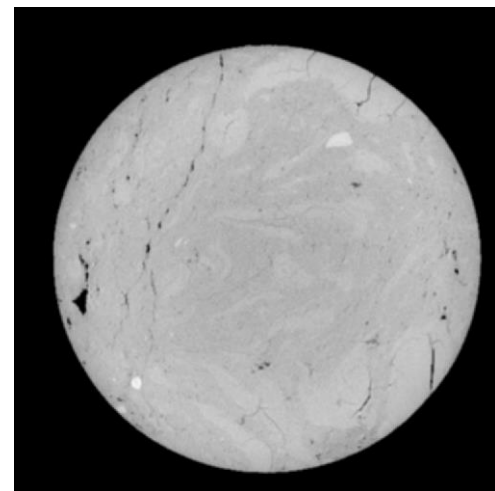
3D reconstruction: Pores



μCT Slice-number 400

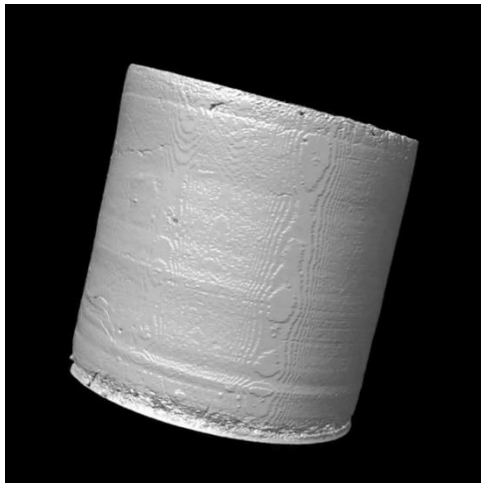


μCT Slice-number 1320  
(Taken at inspection cut, see A.1)



μCT Slice-number 1620

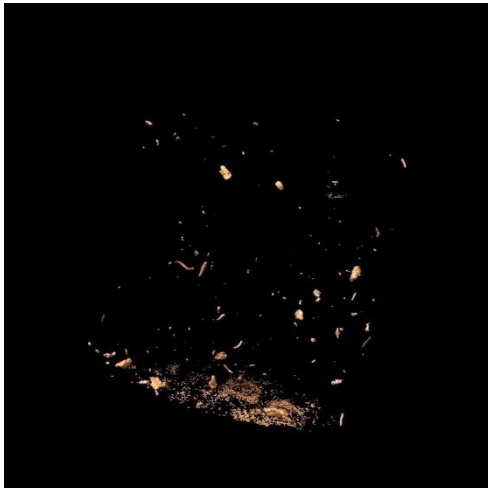
**MDM.E6.3**



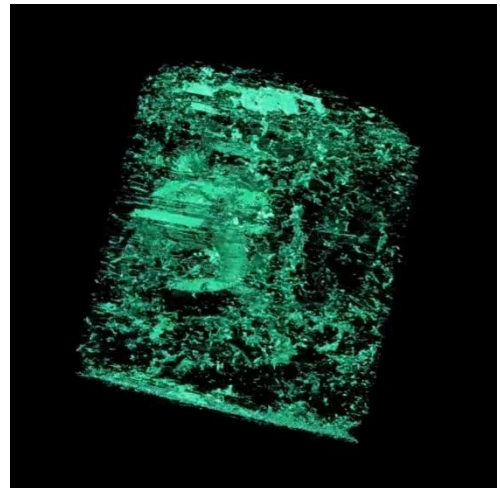
3D reconstruction: Full sample



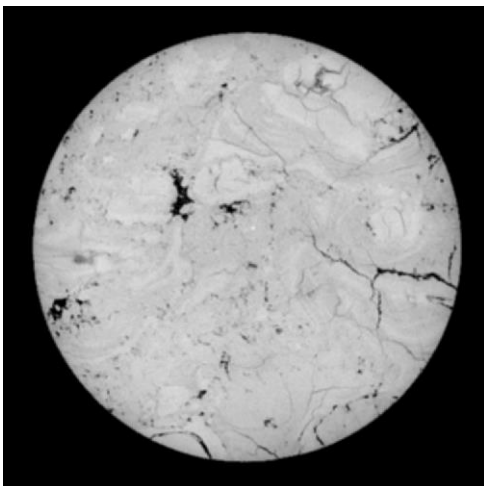
3D reconstruction: Half of sample + Inclusions + Pores



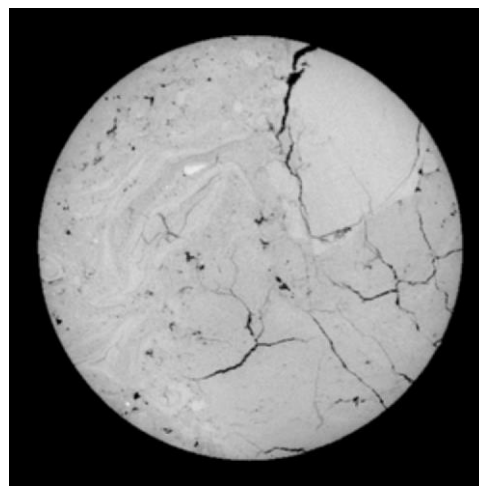
3D reconstruction: Inclusions



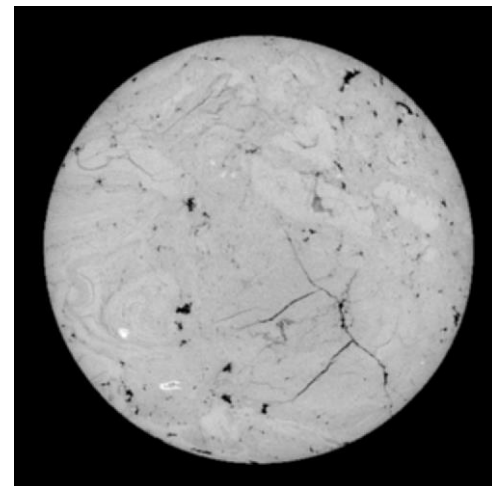
3D reconstruction: Pores



μCT Slice-number 440



μCT Slice-number 210  
(Taken at inspection cut, see A.1)

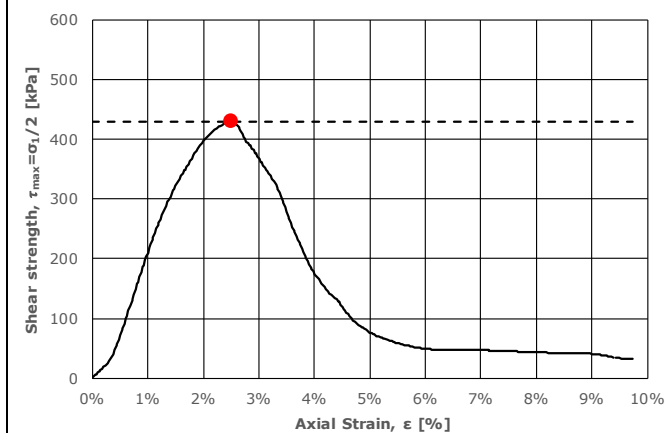
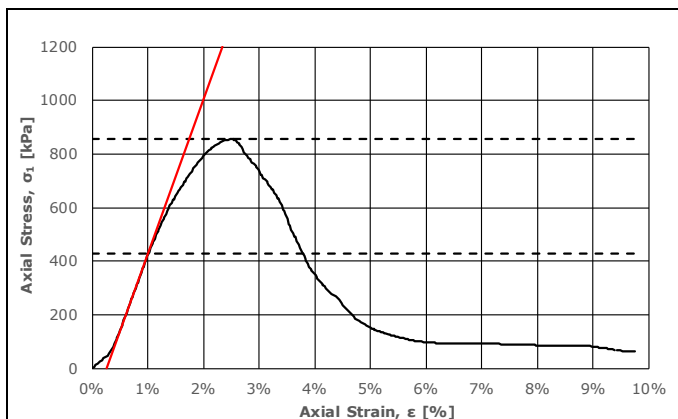


μCT Slice-number 1360

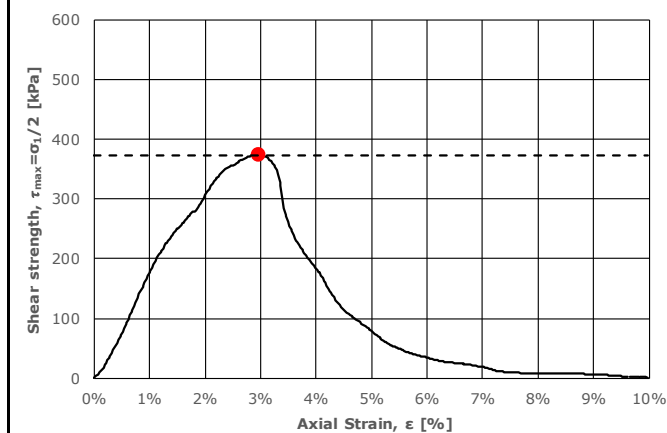
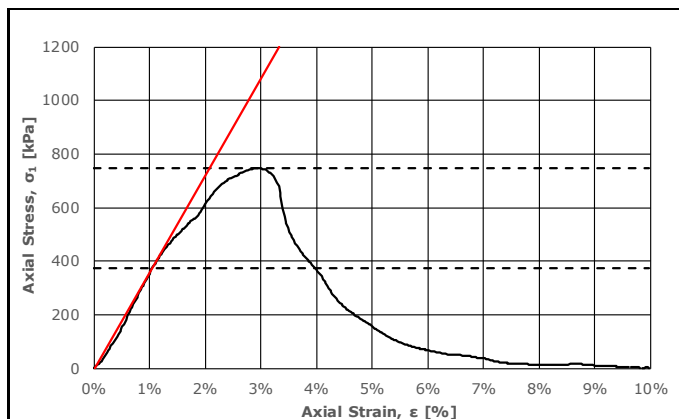
## **B | LABORATORY DATA**

### **B.1 SAMPLE IMAGES AND UNCONFINED COMPRESSION TEST RESULTS**

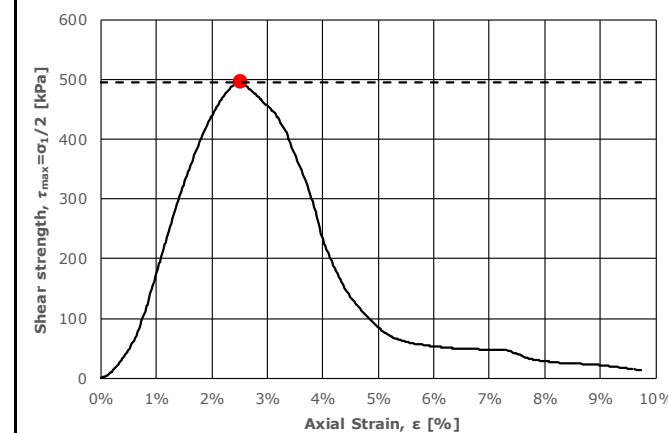
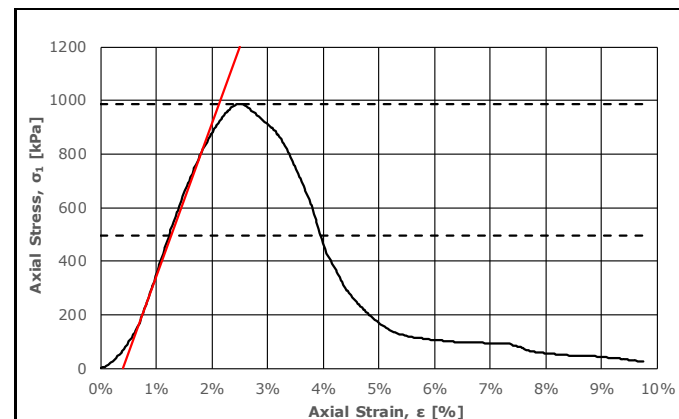
# APPENDIX B.1 SAMPLE IMAGES AND UNCONFINED COMPRESSION TEST RESULTS



| Sample ID                           | Curing time | Test date  |
|-------------------------------------|-------------|------------|
| DRY.8.1.1                           | 28 Days     | 15.03.2023 |
| Sample height                       | 100,00      | [mm]       |
| Sample diameter                     | 54,00       | [mm]       |
| Ultimate compressive strength $q_u$ | 856,95      | [kPa]      |
| Undrained shear strength $S_u$      | 428,47      | [kPa]      |
| Failure strain $\epsilon_v$         | 2,51        | [%]        |
| Estimated stiffness $E_{50}$        | 57971,01    | [kPa]      |
| Dotted line max.                    | 0,00        | [%]        |
| Dotted line min.                    | 9,74        | [%]        |

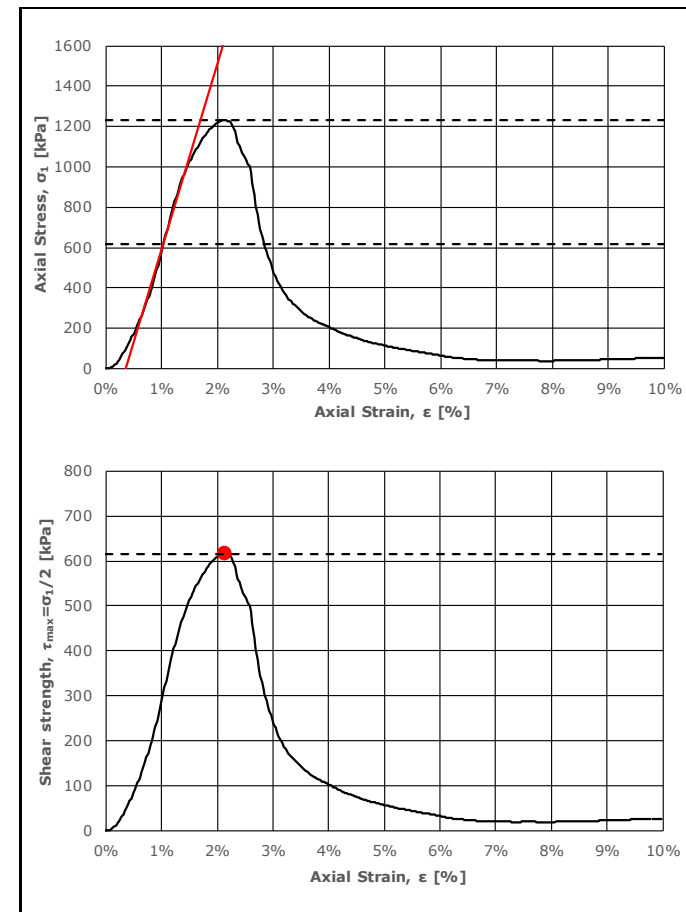
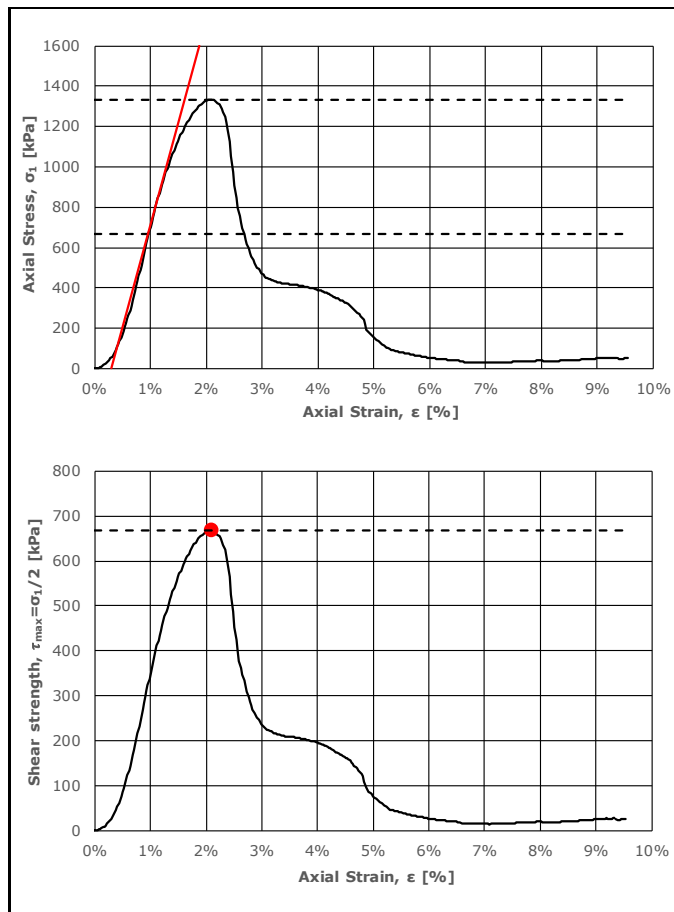
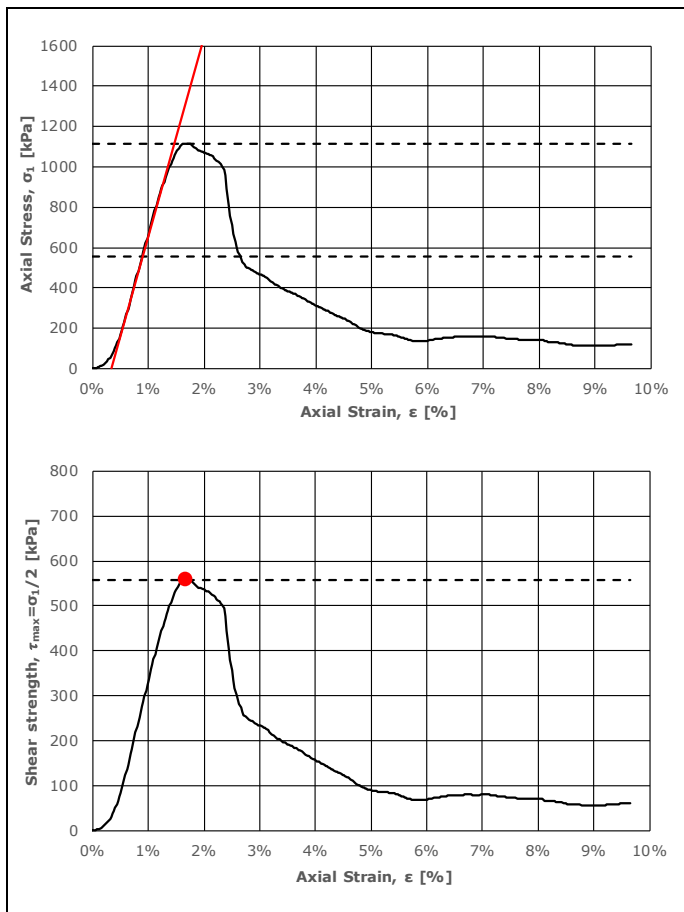



| Sample ID                           | Curing time | Test date  |
|-------------------------------------|-------------|------------|
| DRY.8.1.2                           | 28 Days     | 15.03.2023 |
| Sample height                       | 100,00      | [mm]       |
| Sample diameter                     | 54,00       | [mm]       |
| Ultimate compressive strength $q_u$ | 747,23      | [kPa]      |
| Undrained shear strength $S_u$      | 373,62      | [kPa]      |
| Failure strain $\epsilon_v$         | 2,97        | [%]        |
| Estimated stiffness $E_{50}$        | 36253,78    | [kPa]      |
| Dotted line max.                    | 0,00        | [%]        |
| Dotted line min.                    | 9,98        | [%]        |





| Sample ID                           | Curing time | Test date  |
|-------------------------------------|-------------|------------|
| DRY.8.1.3                           | 28 Days     | 15.03.2023 |
| Sample height                       | 100,00      | [mm]       |
| Sample diameter                     | 54,00       | [mm]       |
| Ultimate compressive strength $q_u$ | 988,71      | [kPa]      |
| Undrained shear strength $S_u$      | 494,35      | [kPa]      |
| Failure strain $\epsilon_v$         | 2,52        | [%]        |
| Estimated stiffness $E_{50}$        | 57142,86    | [kPa]      |
| Dotted line max.                    | 0,00        | [%]        |
| Dotted line min.                    | 9,74        | [%]        |

# APPENDIX B.1 SAMPLE IMAGES AND UNCONFINED COMPRESSION TEST RESULTS



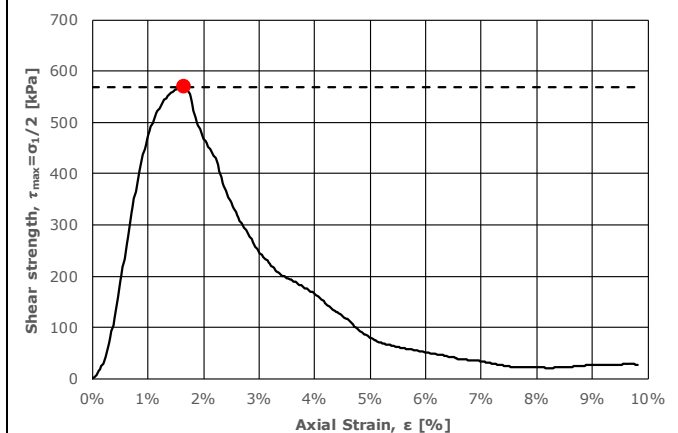
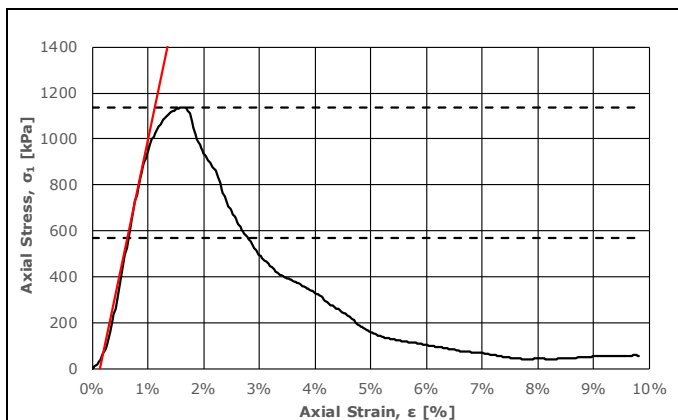
|   |                                     |             |            |
|---|-------------------------------------|-------------|------------|
|  | Sample ID                           | Curing time | Test date  |
|   | DRY.8.2.1                           | 28 Days     | 15.03.2023 |
|   | Sample height                       | 100,00      | [mm]       |
|   | Sample diameter                     | 54,00       | [mm]       |
|   | Ultimate compressive strength $q_u$ | 1116,59     | [kPa]      |
|   | Undrained shear strength $S_u$      | 558,30      | [kPa]      |
|   | Failure strain $\epsilon_v$         | 1,67        | [%]        |
|   | Estimated stiffness $E_{50}$        | 98765,43    | [kPa]      |
|   | Dotted line max.                    | 0,00        | [%]        |
|   | Dotted line min.                    | 9,65        | [%]        |

|   |                                     |             |            |
|---|-------------------------------------|-------------|------------|
|  | Sample ID                           | Curing time | Test date  |
|   | DRY.8.2.2                           | 28 Days     | 15.03.2023 |
|   | Sample height                       | 100,00      | [mm]       |
|   | Sample diameter                     | 54,00       | [mm]       |
|   | Ultimate compressive strength $q_u$ | 1333,12     | [kPa]      |
|   | Undrained shear strength $S_u$      | 666,56      | [kPa]      |
|   | Failure strain $\epsilon_v$         | 2,08        | [%]        |
|   | Estimated stiffness $E_{50}$        | 101265,82   | [kPa]      |
|   | Dotted line max.                    | 0,00        | [%]        |
|   | Dotted line min.                    | 9,54        | [%]        |

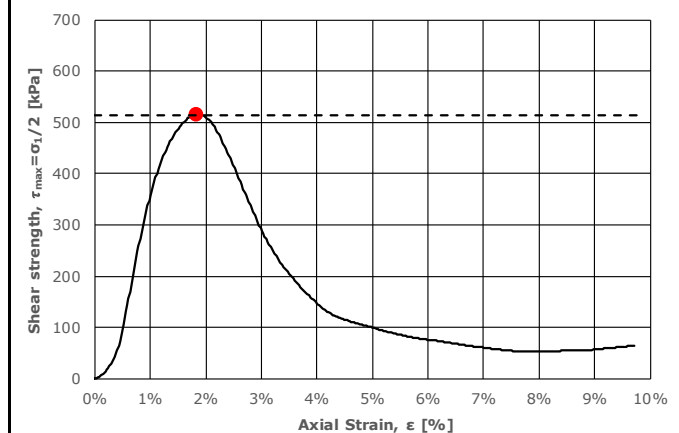
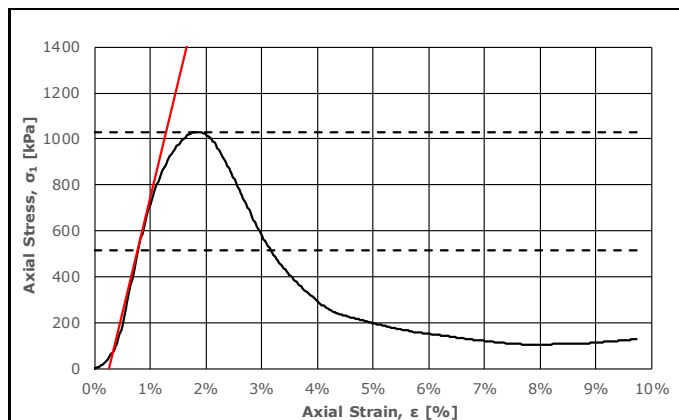
|   |                                     |             |            |
|---|-------------------------------------|-------------|------------|
|  | Sample ID                           | Curing time | Test date  |
|   | DRY.8.2.3                           | 28 Days     | 15.03.2023 |
|   | Sample height                       | 100,00      | [mm]       |
|   | Sample diameter                     | 54,00       | [mm]       |
|   | Ultimate compressive strength $q_u$ | 1231,30     | [kPa]      |
|   | Undrained shear strength $S_u$      | 615,65      | [kPa]      |
|   | Failure strain $\epsilon_v$         | 2,14        | [%]        |
|   | Estimated stiffness $E_{50}$        | 93023,26    | [kPa]      |
|   | Dotted line max.                    | 0,00        | [%]        |
|   | Dotted line min.                    | 9,98        | [%]        |



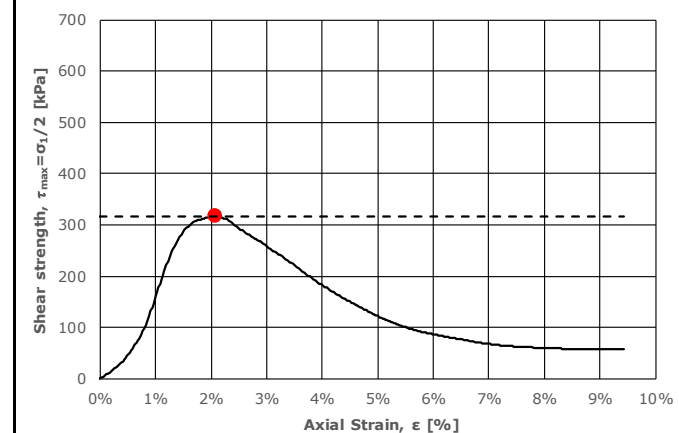
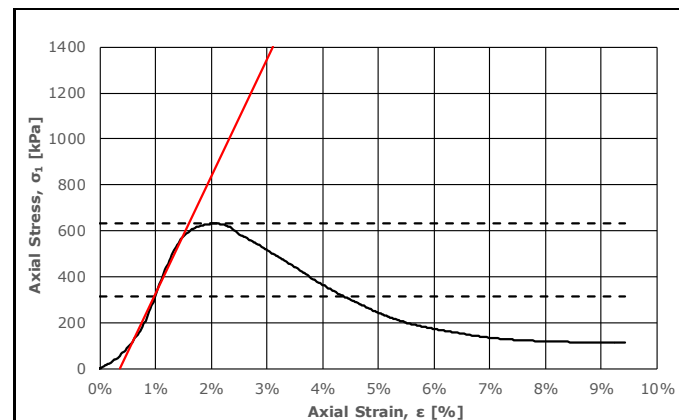
# APPENDIX B.1 SAMPLE IMAGES AND UNCONFINED COMPRESSION TEST RESULTS



| Sample ID                           | Curing time     | Test date  |
|-------------------------------------|-----------------|------------|
| DRY.8.3.1                           | 28 Days         | 17.03.2023 |
| Sample height                       | 100,00 [mm]     |            |
| Sample diameter                     | 54,00 [mm]      |            |
| Ultimate compressive strength $q_u$ | 1137,08 [kPa]   |            |
| Undrained shear strength $S_u$      | 568,54 [kPa]    |            |
| Failure strain $\epsilon_v$         | 1,64 [%]        |            |
| Estimated stiffness $E_{50}$        | 116666,67 [kPa] |            |
| Dotted line max.                    | 0,00 [%]        |            |
| Dotted line min.                    | 9,81 [%]        |            |

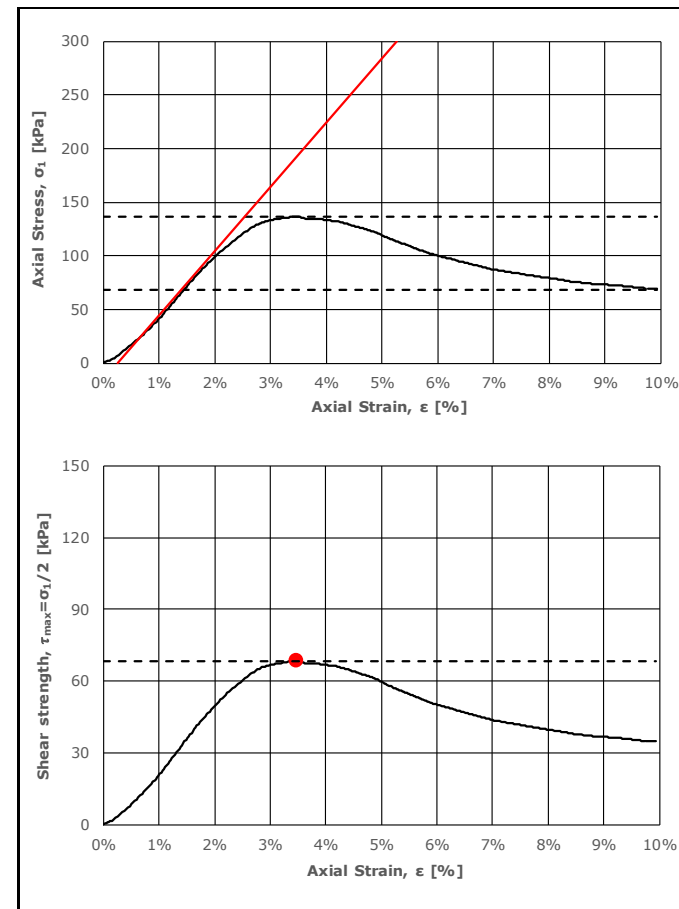
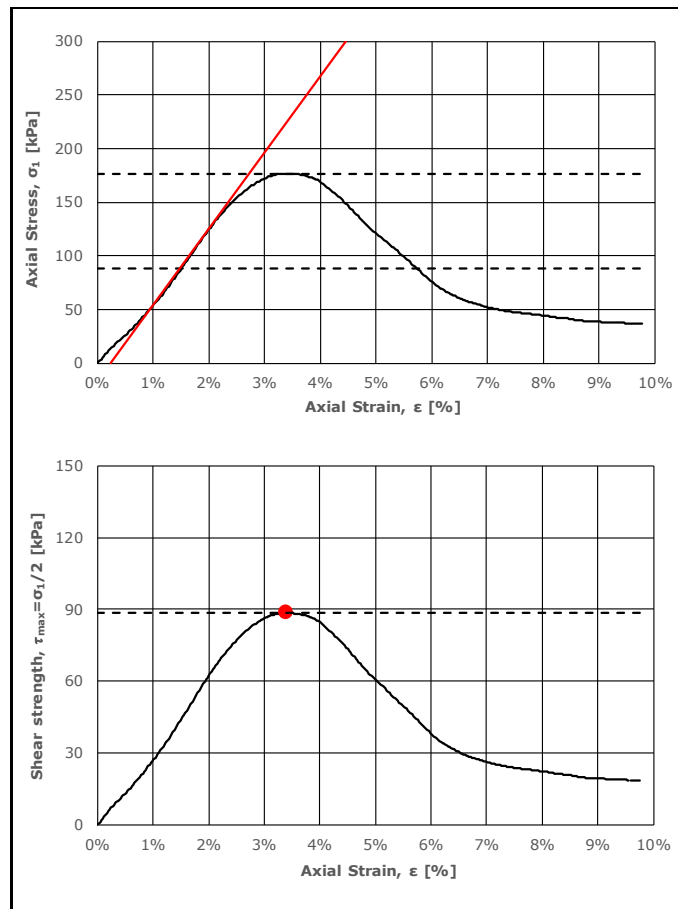
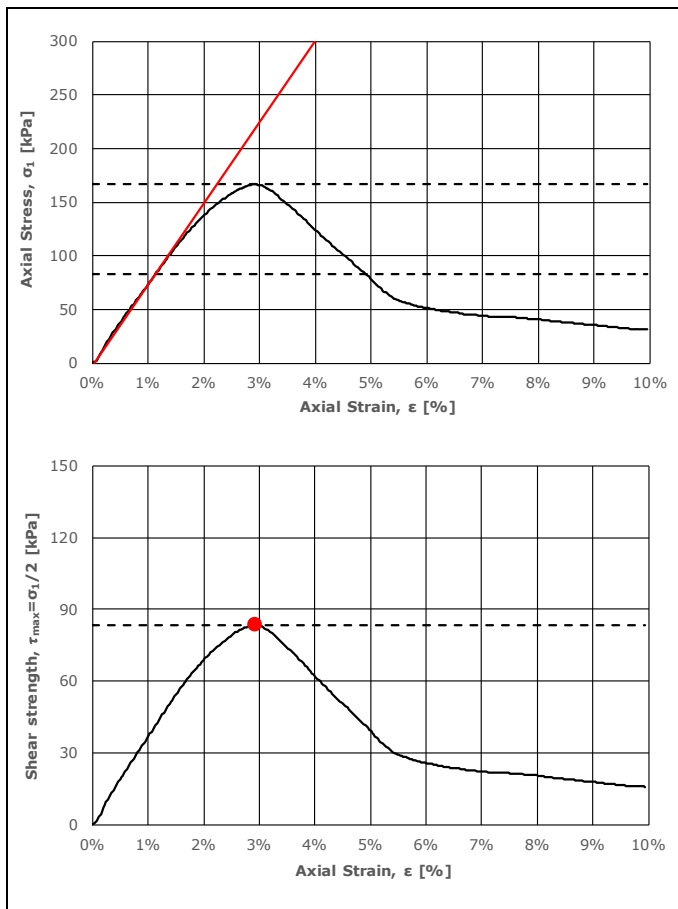


| Sample ID                           | Curing time     | Test date  |
|-------------------------------------|-----------------|------------|
| DRY.8.3.2                           | 28 Days         | 17.03.2023 |
| Sample height                       | 100,00 [mm]     |            |
| Sample diameter                     | 54,00 [mm]      |            |
| Ultimate compressive strength $q_u$ | 1029,07 [kPa]   |            |
| Undrained shear strength $S_u$      | 514,54 [kPa]    |            |
| Failure strain $\epsilon_v$         | 1,83 [%]        |            |
| Estimated stiffness $E_{50}$        | 100719,42 [kPa] |            |
| Dotted line max.                    | 0,00 [%]        |            |
| Dotted line min.                    | 9,75 [%]        |            |



| Sample ID                           | Curing time    | Test date  |
|-------------------------------------|----------------|------------|
| DRY.8.3.3                           | 28 Days        | 17.03.2023 |
| Sample height                       | 100,00 [mm]    |            |
| Sample diameter                     | 54,00 [mm]     |            |
| Ultimate compressive strength $q_u$ | 632,08 [kPa]   |            |
| Undrained shear strength $S_u$      | 316,04 [kPa]   |            |
| Failure strain $\epsilon_v$         | 2,08 [%]       |            |
| Estimated stiffness $E_{50}$        | 51094,89 [kPa] |            |
| Dotted line max.                    | 0,00 [%]       |            |
| Dotted line min.                    | 9,43 [%]       |            |

## APPENDIX B.1 SAMPLE IMAGES AND UNCONFINED COMPRESSION TEST RESULTS



| Sample ID                           | Curing time   | Test date  |
|-------------------------------------|---------------|------------|
| DRY.8.4.1                           | 28 Days       | 27.03.2023 |
| Sample height                       | 100,00 [mm]   |            |
| Sample diameter                     | 54,00 [mm]    |            |
| Ultimate compressive strength $q_u$ | 166,72 [kPa]  |            |
| Undrained shear strength $S_u$      | 83,36 [kPa]   |            |
| Failure strain $\epsilon_v$         | 2,92 [%]      |            |
| Estimated stiffness $E_{50}$        | 7575,76 [kPa] |            |
| Dotted line max.                    | 0,00 [%]      |            |
| Dotted line min.                    | 9,94 [%]      |            |

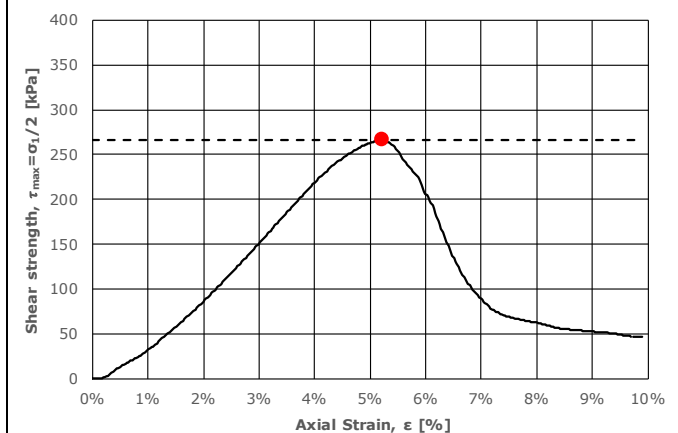
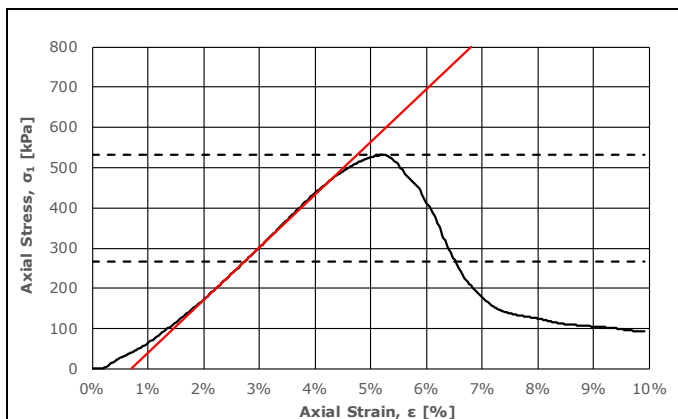


| Sample ID                           | Curing time   | Test date  |
|-------------------------------------|---------------|------------|
| DRY.8.4.2                           | 28 Days       | 27.03.2023 |
| Sample height                       | 100,00 [mm]   |            |
| Sample diameter                     | 54,00 [mm]    |            |
| Ultimate compressive strength $q_u$ | 177,00 [kPa]  |            |
| Undrained shear strength $S_u$      | 88,50 [kPa]   |            |
| Failure strain $\epsilon_v$         | 3,40 [%]      |            |
| Estimated stiffness $E_{50}$        | 7109,00 [kPa] |            |
| Dotted line max.                    | 0,00 [%]      |            |
| Dotted line min.                    | 9,76 [%]      |            |

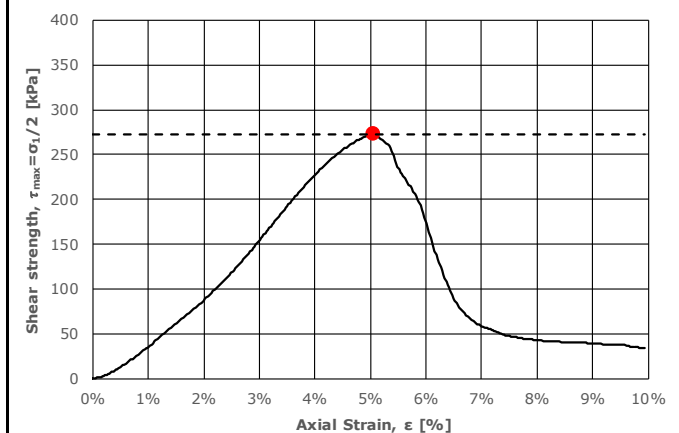
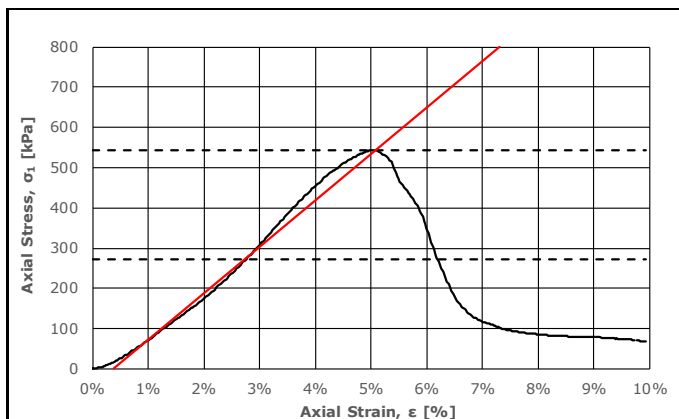


| Sample ID                           | Curing time   | Test date  |
|-------------------------------------|---------------|------------|
| DRY.8.4.3                           | 28 Days       | 27.03.2023 |
| Sample height                       | 100,00 [mm]   |            |
| Sample diameter                     | 54,00 [mm]    |            |
| Ultimate compressive strength $q_u$ | 136,86 [kPa]  |            |
| Undrained shear strength $S_u$      | 68,43 [kPa]   |            |
| Failure strain $\epsilon_v$         | 3,48 [%]      |            |
| Estimated stiffness $E_{50}$        | 5988,02 [kPa] |            |
| Dotted line max.                    | 0,00 [%]      |            |
| Dotted line min.                    | 9,93 [%]      |            |

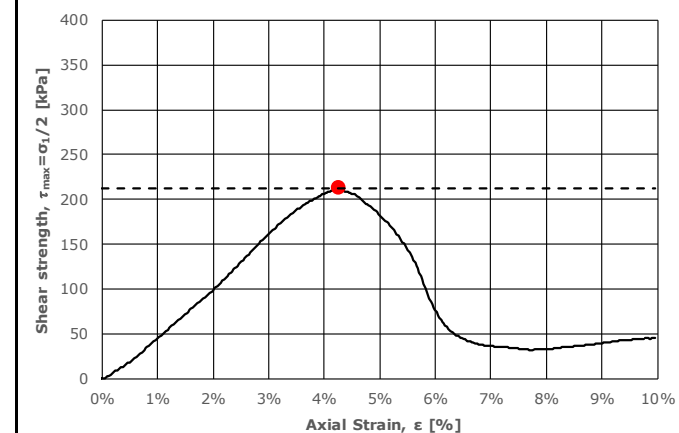
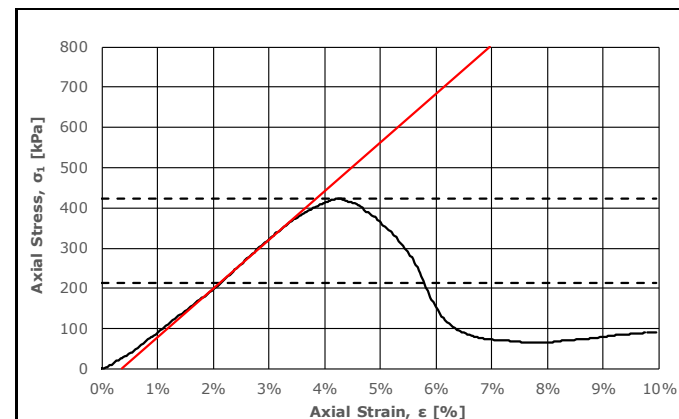
# APPENDIX B.1 SAMPLE IMAGES AND UNCONFINED COMPRESSION TEST RESULTS



| Sample ID                           | Curing time | Test date  |
|-------------------------------------|-------------|------------|
| DRY.8.5.1                           | 28 Days     | 27.03.2023 |
| Sample height                       | 100,00      | [mm]       |
| Sample diameter                     | 54,00       | [mm]       |
| Ultimate compressive strength $q_u$ | 531,68      | [kPa]      |
| Undrained shear strength $S_u$      | 265,84      | [kPa]      |
| Failure strain $\epsilon_v$         | 5,21        | [%]        |
| Estimated stiffness $E_{50}$        | 13114,75    | [kPa]      |
| Dotted line max.                    | 0,00        | [%]        |
| Dotted line min.                    | 9,90        | [%]        |

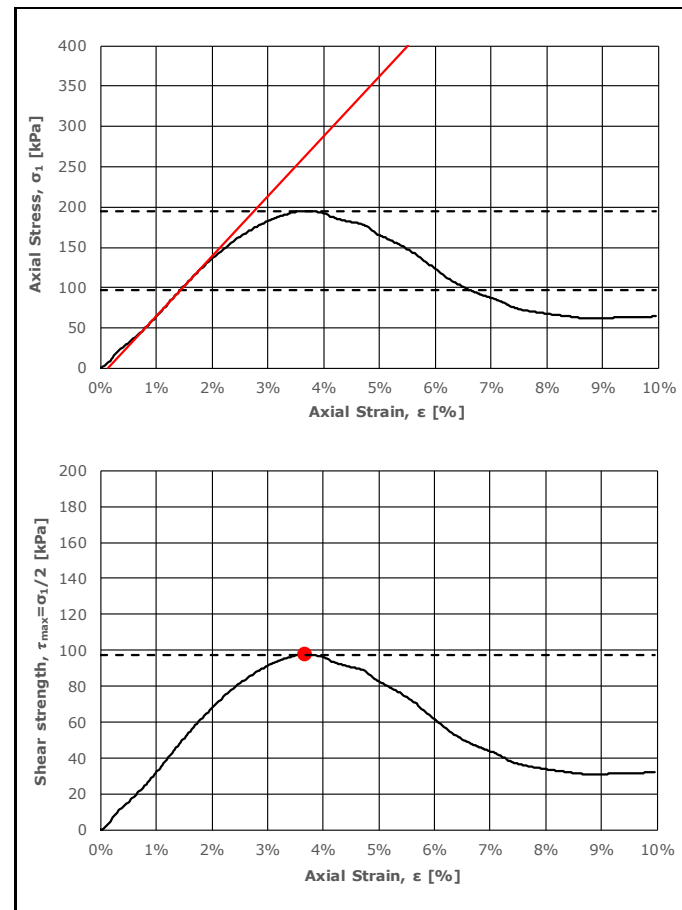
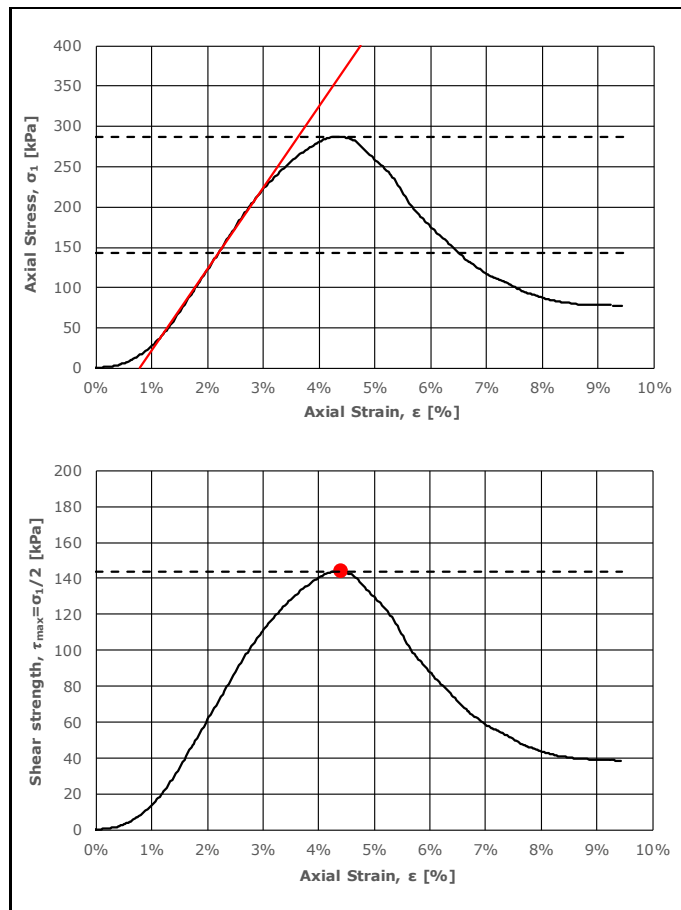
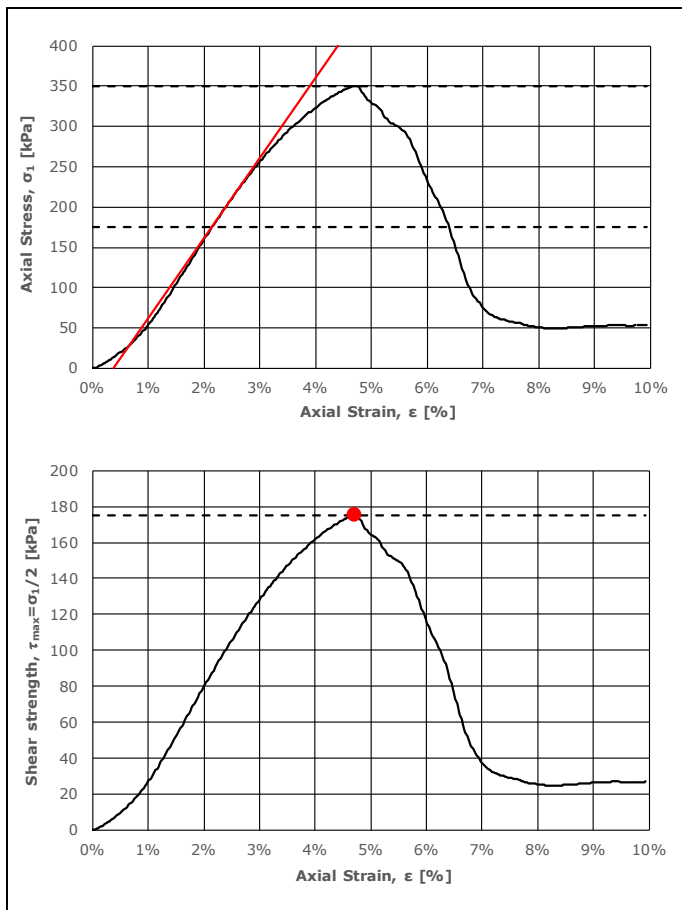


| Sample ID                           | Curing time | Test date  |
|-------------------------------------|-------------|------------|
| DRY.8.5.2                           | 28 Days     | 27.03.2023 |
| Sample height                       | 100,00      | [mm]       |
| Sample diameter                     | 54,00       | [mm]       |
| Ultimate compressive strength $q_u$ | 543,96      | [kPa]      |
| Undrained shear strength $S_u$      | 271,98      | [kPa]      |
| Failure strain $\epsilon_v$         | 5,06        | [%]        |
| Estimated stiffness $E_{50}$        | 11560,69    | [kPa]      |
| Dotted line max.                    | 0,00        | [%]        |
| Dotted line min.                    | 9,93        | [%]        |



| Sample ID                           | Curing time | Test date  |
|-------------------------------------|-------------|------------|
| DRY.8.5.3                           | 28 Days     | 27.03.2023 |
| Sample height                       | 100,00      | [mm]       |
| Sample diameter                     | 54,00       | [mm]       |
| Ultimate compressive strength $q_u$ | 424,37      | [kPa]      |
| Undrained shear strength $S_u$      | 212,18      | [kPa]      |
| Failure strain $\epsilon_v$         | 4,27        | [%]        |
| Estimated stiffness $E_{50}$        | 12139,61    | [kPa]      |
| Dotted line max.                    | 0,00        | [%]        |
| Dotted line min.                    | 9,96        | [%]        |

# APPENDIX B.1 SAMPLE IMAGES AND UNCONFINED COMPRESSION TEST RESULTS

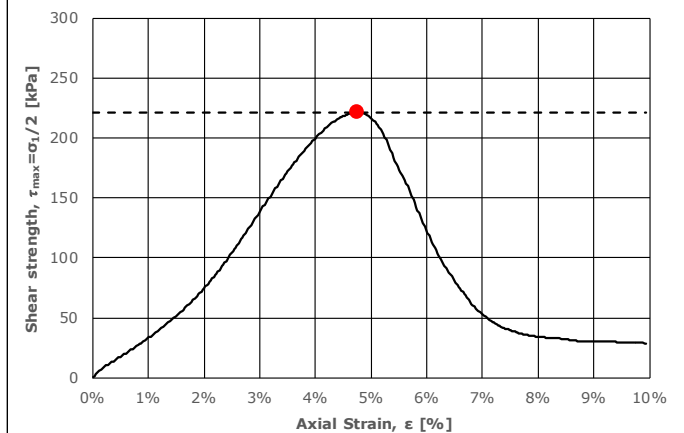
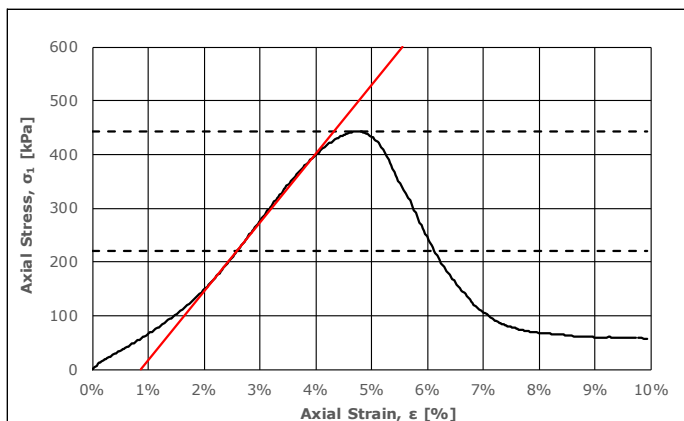


|  |                                     |           |             |         |           |            |
|--|-------------------------------------|-----------|-------------|---------|-----------|------------|
|  | Sample ID                           | DRY.8.6.1 | Curing time | 28 Days | Test date | 27.03.2023 |
|  | Sample height                       | 100,00    | [mm]        |         |           |            |
|  | Sample diameter                     | 54,00     | [mm]        |         |           |            |
|  | Ultimate compressive strength $q_u$ | 349,92    | [kPa]       |         |           |            |
|  | Undrained shear strength $S_u$      | 174,96    | [kPa]       |         |           |            |
|  | Failure strain $\epsilon_v$         | 4,70      | [%]         |         |           |            |
|  | Estimated stiffness $E_{50}$        | 9975,06   | [kPa]       |         |           |            |
|  | Dotted line max.                    | 0,00      | [%]         |         |           |            |
|  | Dotted line min.                    | 9,94      | [%]         |         |           |            |

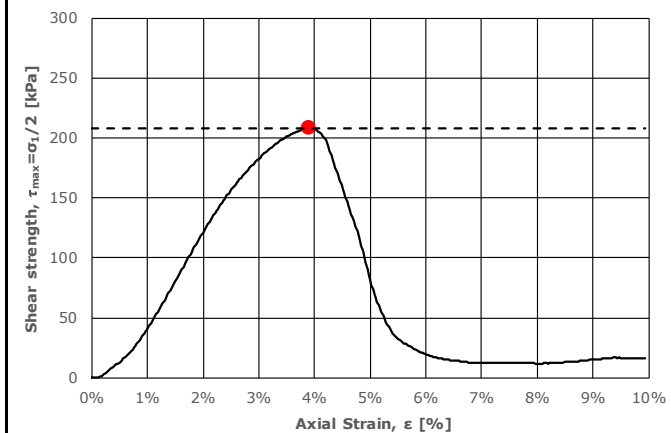
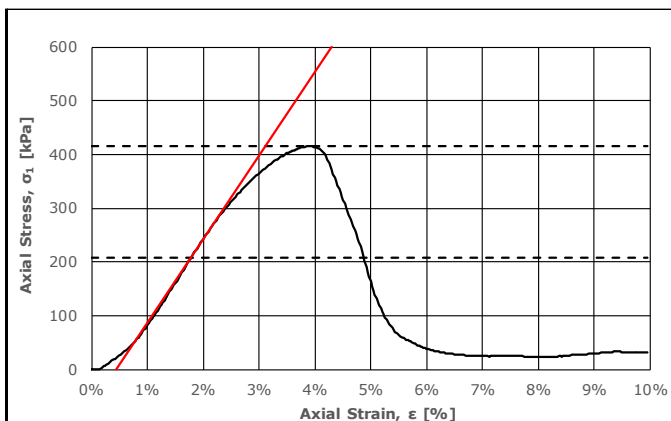
|  |                                     |           |             |         |           |            |
|--|-------------------------------------|-----------|-------------|---------|-----------|------------|
|  | Sample ID                           | DRY.8.6.2 | Curing time | 28 Days | Test date | 27.03.2023 |
|  | Sample height                       | 100,00    | [mm]        |         |           |            |
|  | Sample diameter                     | 54,00     | [mm]        |         |           |            |
|  | Ultimate compressive strength $q_u$ | 287,05    | [kPa]       |         |           |            |
|  | Undrained shear strength $S_u$      | 143,52    | [kPa]       |         |           |            |
|  | Failure strain $\epsilon_v$         | 4,41      | [%]         |         |           |            |
|  | Estimated stiffness $E_{50}$        | 10101,01  | [kPa]       |         |           |            |
|  | Dotted line max.                    | 0,00      | [%]         |         |           |            |
|  | Dotted line min.                    | 9,46      | [%]         |         |           |            |

|  |                                     |           |             |         |           |            |
|--|-------------------------------------|-----------|-------------|---------|-----------|------------|
|  | Sample ID                           | DRY.8.6.3 | Curing time | 28 Days | Test date | 27.03.2023 |
|  | Sample height                       | 100,00    | [mm]        |         |           |            |
|  | Sample diameter                     | 54,00     | [mm]        |         |           |            |
|  | Ultimate compressive strength $q_u$ | 195,12    | [kPa]       |         |           |            |
|  | Undrained shear strength $S_u$      | 97,56     | [kPa]       |         |           |            |
|  | Failure strain $\epsilon_v$         | 3,67      | [%]         |         |           |            |
|  | Estimated stiffness $E_{50}$        | 7476,64   | [kPa]       |         |           |            |
|  | Dotted line max.                    | 0,00      | [%]         |         |           |            |
|  | Dotted line min.                    | 9,96      | [%]         |         |           |            |

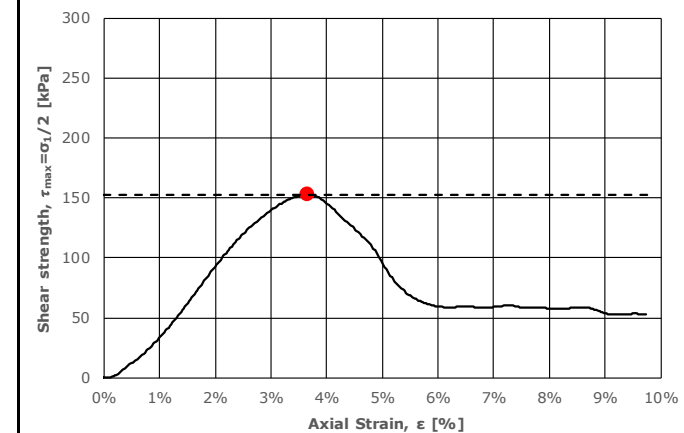
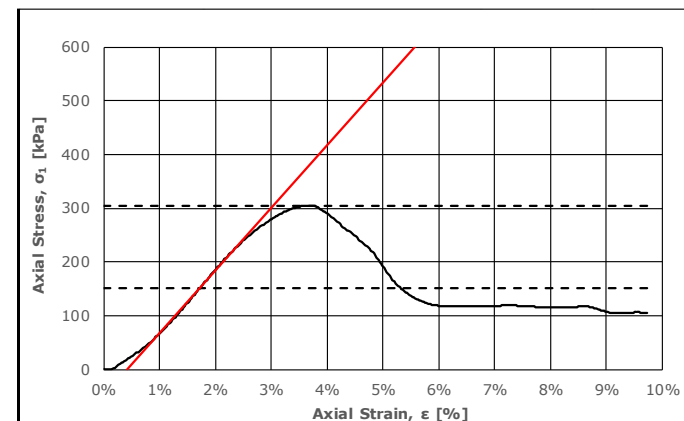
# APPENDIX B.1 SAMPLE IMAGES AND UNCONFINED COMPRESSION TEST RESULTS



| Sample ID                           | Curing time    | Test date  |
|-------------------------------------|----------------|------------|
| DRY.8.7.1                           | 28 Days        | 27.03.2023 |
| Sample height                       | 100,00 [mm]    |            |
| Sample diameter                     | 54,00 [mm]     |            |
| Ultimate compressive strength $q_u$ | 443,00 [kPa]   |            |
| Undrained shear strength $S_u$      | 221,50 [kPa]   |            |
| Failure strain $\epsilon_v$         | 4,75 %         |            |
| Estimated stiffness $E_{50}$        | 12820,51 [kPa] |            |
| Dotted line max.                    | 0,00 %         |            |
| Dotted line min.                    | 9,94 %         |            |

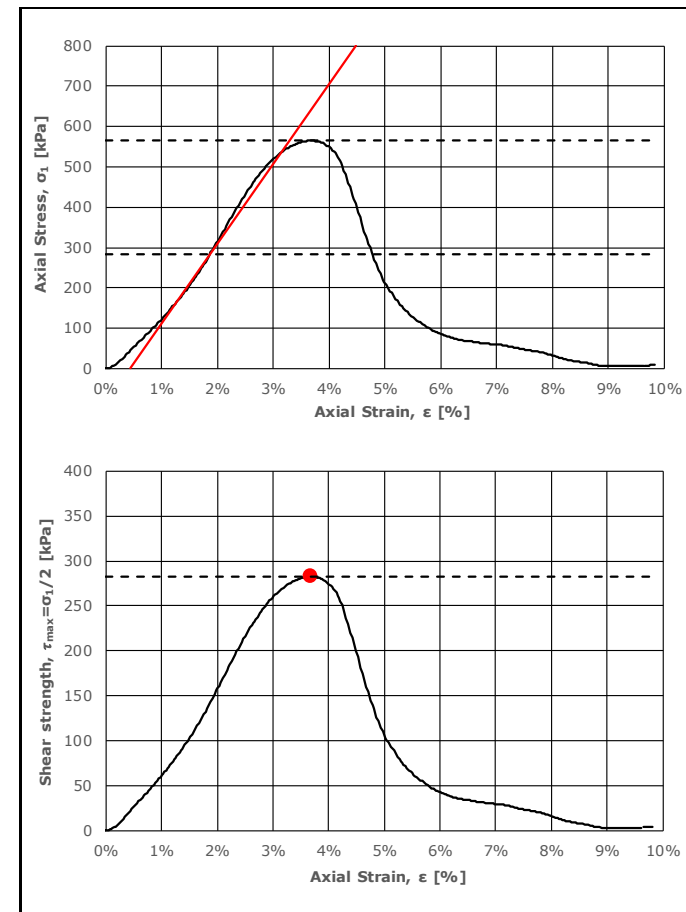
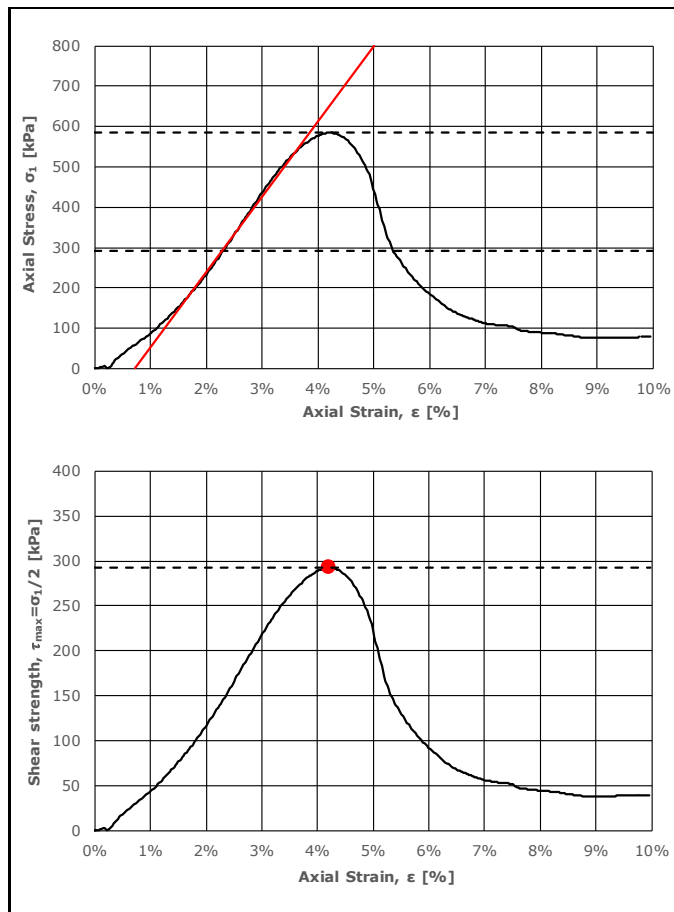
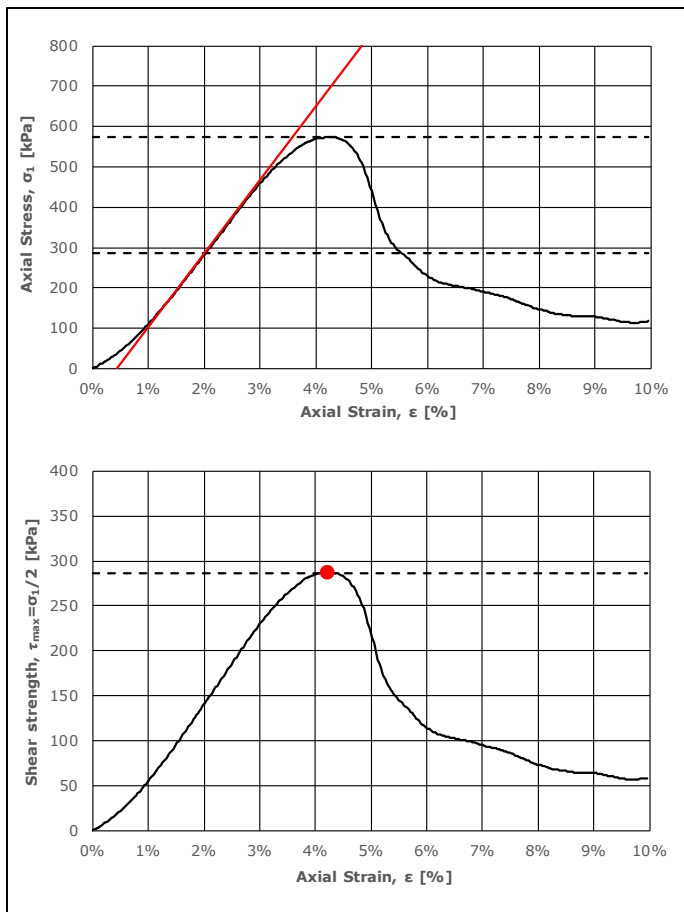



| Sample ID                           | Curing time    | Test date  |
|-------------------------------------|----------------|------------|
| DRY.8.7.2                           | 28 Days        | 27.03.2023 |
| Sample height                       | 100,00 [mm]    |            |
| Sample diameter                     | 54,00 [mm]     |            |
| Ultimate compressive strength $q_u$ | 415,49 [kPa]   |            |
| Undrained shear strength $S_u$      | 207,74 [kPa]   |            |
| Failure strain $\epsilon_v$         | 3,90 %         |            |
| Estimated stiffness $E_{50}$        | 15544,04 [kPa] |            |
| Dotted line max.                    | 0,00 %         |            |
| Dotted line min.                    | 9,94 %         |            |





| Sample ID                           | Curing time    | Test date  |
|-------------------------------------|----------------|------------|
| DRY.8.7.3                           | 28 Days        | 27.03.2023 |
| Sample height                       | 100,00 [mm]    |            |
| Sample diameter                     | 54,00 [mm]     |            |
| Ultimate compressive strength $q_u$ | 305,23 [kPa]   |            |
| Undrained shear strength $S_u$      | 152,62 [kPa]   |            |
| Failure strain $\epsilon_v$         | 3,66 %         |            |
| Estimated stiffness $E_{50}$        | 11673,15 [kPa] |            |
| Dotted line max.                    | 0,00 %         |            |
| Dotted line min.                    | 9,75 %         |            |

# APPENDIX B.1 SAMPLE IMAGES AND UNCONFINED COMPRESSION TEST RESULTS

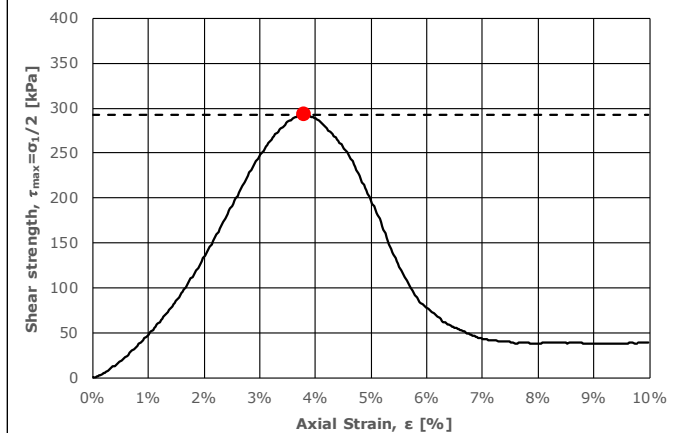
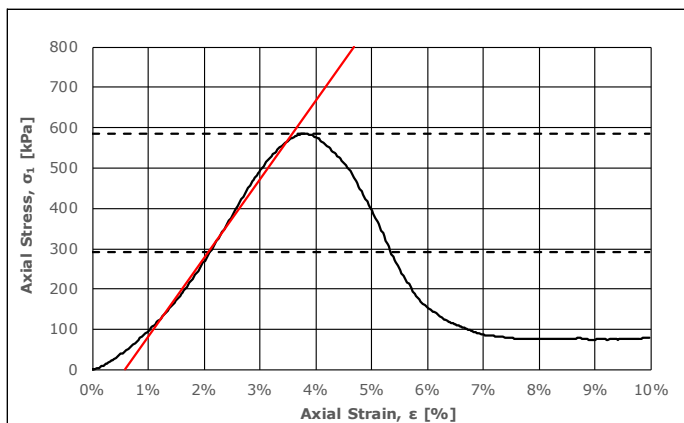


|   |                                     |             |            |
|---|-------------------------------------|-------------|------------|
|  | Sample ID                           | Curing time | Test date  |
|   | DRY.8.8.1                           | 28 Days     | 27.03.2023 |
|   | Sample height                       | 100,00      | [mm]       |
|   | Sample diameter                     | 54,00       | [mm]       |
|   | Ultimate compressive strength $q_u$ | 573,61      | [kPa]      |
|   | Undrained shear strength $S_u$      | 286,81      | [kPa]      |
|   | Failure strain $\epsilon_v$         | 4,23        | [%]        |
|   | Estimated stiffness $E_{50}$        | 18264,84    | [kPa]      |
|   | Dotted line max.                    | 0,00        | [%]        |
|   | Dotted line min.                    | 9,95        | [%]        |

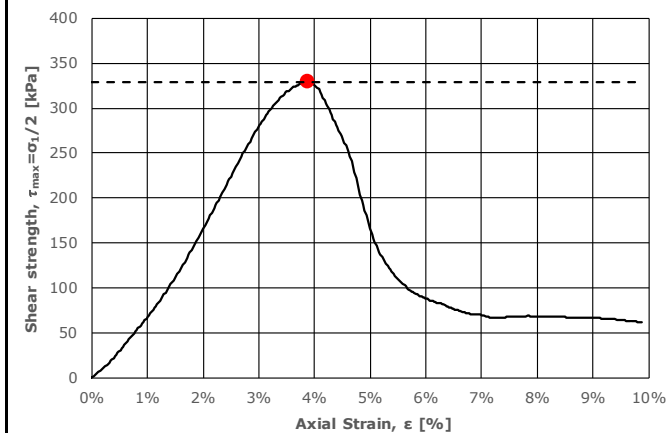
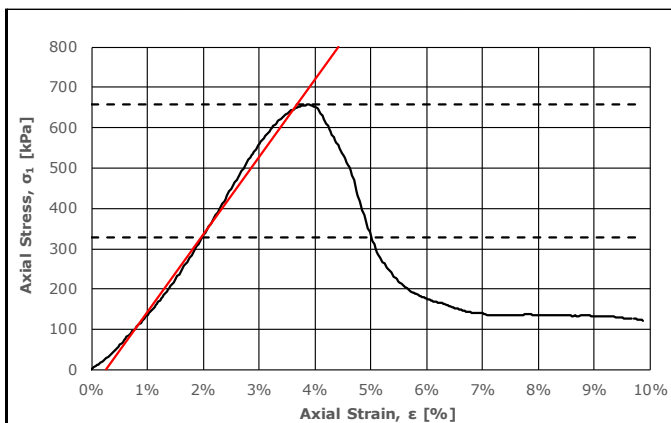
|   |                                     |             |            |
|---|-------------------------------------|-------------|------------|
|  | Sample ID                           | Curing time | Test date  |
|   | DRY.8.8.2                           | 28 Days     | 27.03.2023 |
|   | Sample height                       | 100,00      | [mm]       |
|   | Sample diameter                     | 54,00       | [mm]       |
|   | Ultimate compressive strength $q_u$ | 584,60      | [kPa]      |
|   | Undrained shear strength $S_u$      | 292,30      | [kPa]      |
|   | Failure strain $\epsilon_v$         | 4,21        | [%]        |
|   | Estimated stiffness $E_{50}$        | 18648,02    | [kPa]      |
|   | Dotted line max.                    | 0,00        | [%]        |
|   | Dotted line min.                    | 9,98        | [%]        |

|   |                                     |             |            |
|---|-------------------------------------|-------------|------------|
|  | Sample ID                           | Curing time | Test date  |
|   | DRY.8.8.3                           | 28 Days     | 27.03.2023 |
|   | Sample height                       | 100,00      | [mm]       |
|   | Sample diameter                     | 54,00       | [mm]       |
|   | Ultimate compressive strength $q_u$ | 565,01      | [kPa]      |
|   | Undrained shear strength $S_u$      | 282,51      | [kPa]      |
|   | Failure strain $\epsilon_v$         | 3,68        | [%]        |
|   | Estimated stiffness $E_{50}$        | 19801,98    | [kPa]      |
|   | Dotted line max.                    | 0,00        | [%]        |
|   | Dotted line min.                    | 9,82        | [%]        |

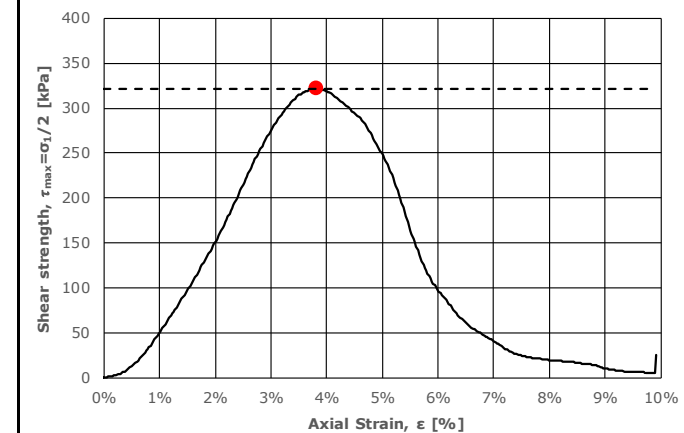
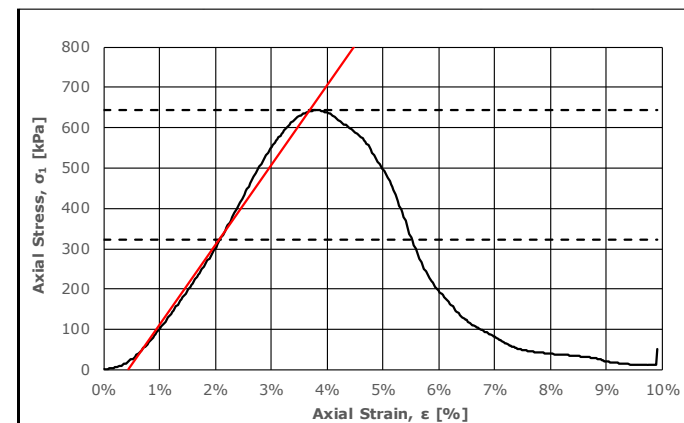
# APPENDIX B.1 SAMPLE IMAGES AND UNCONFINED COMPRESSION TEST RESULTS



| Sample ID                           | Curing time    | Test date  |
|-------------------------------------|----------------|------------|
| DRY.8.9.1                           | 28 Days        | 27.03.2023 |
| Sample height                       | 100,00 [mm]    |            |
| Sample diameter                     | 54,00 [mm]     |            |
| Ultimate compressive strength $q_u$ | 586,03 [kPa]   |            |
| Undrained shear strength $S_u$      | 293,01 [kPa]   |            |
| Failure strain $\epsilon_v$         | 3,81 [%]       |            |
| Estimated stiffness $E_{50}$        | 19512,20 [kPa] |            |
| Dotted line max.                    | 0,00 [%]       |            |
| Dotted line min.                    | 9,98 [%]       |            |

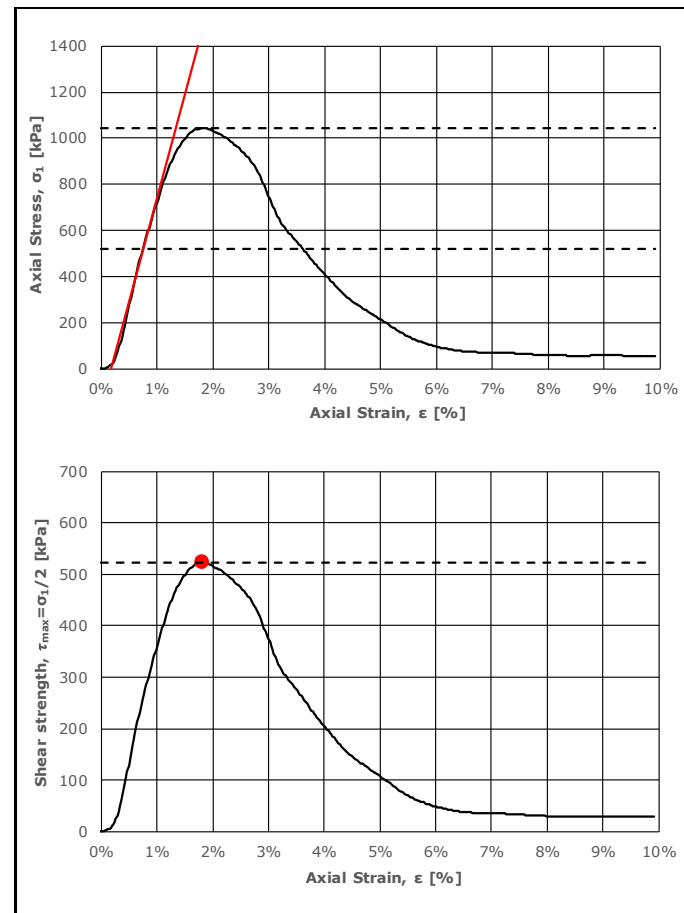
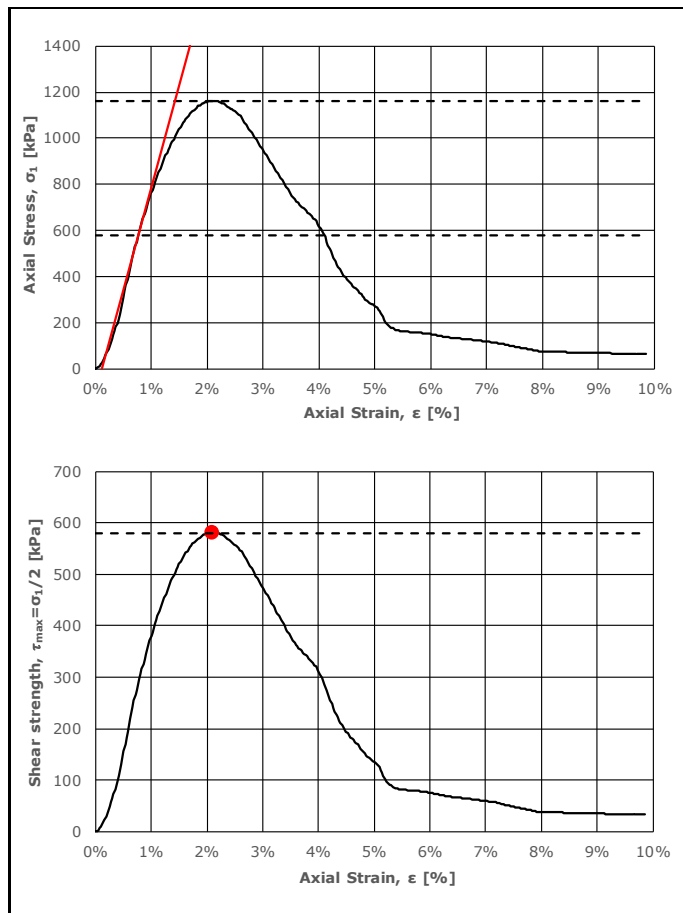
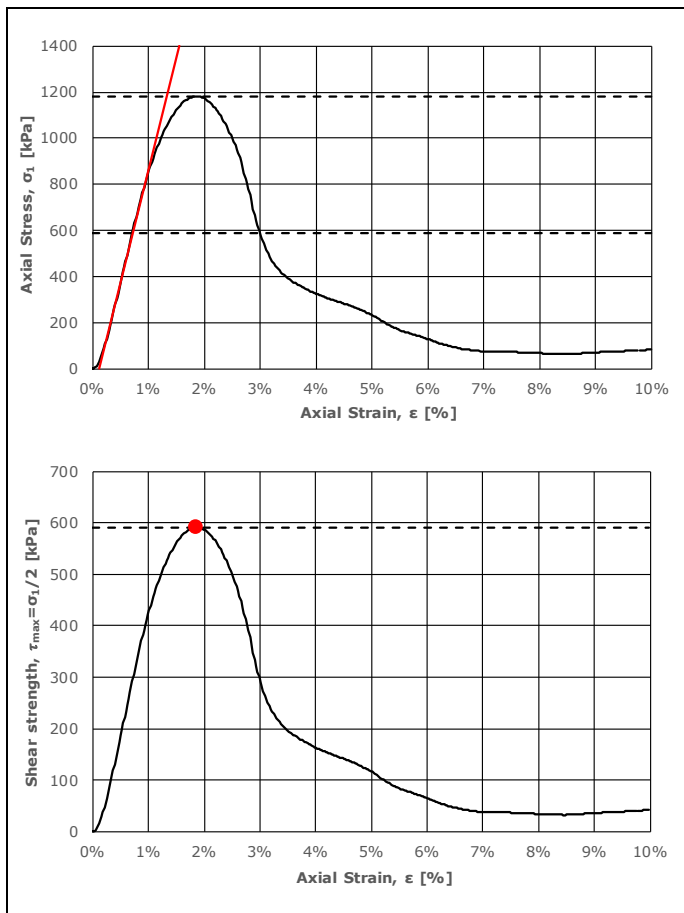


| Sample ID                           | Curing time    | Test date  |
|-------------------------------------|----------------|------------|
| DRY.8.9.2                           | 28 Days        | 27.03.2023 |
| Sample height                       | 100,00 [mm]    |            |
| Sample diameter                     | 54,00 [mm]     |            |
| Ultimate compressive strength $q_u$ | 657,12 [kPa]   |            |
| Undrained shear strength $S_u$      | 328,56 [kPa]   |            |
| Failure strain $\epsilon_v$         | 3,88 [%]       |            |
| Estimated stiffness $E_{50}$        | 19323,67 [kPa] |            |
| Dotted line max.                    | 0,00 [%]       |            |
| Dotted line min.                    | 9,88 [%]       |            |



| Sample ID                           | Curing time    | Test date  |
|-------------------------------------|----------------|------------|
| DRY.8.9.3                           | 28 Days        | 27.03.2023 |
| Sample height                       | 100,00 [mm]    |            |
| Sample diameter                     | 54,00 [mm]     |            |
| Ultimate compressive strength $q_u$ | 643,92 [kPa]   |            |
| Undrained shear strength $S_u$      | 321,96 [kPa]   |            |
| Failure strain $\epsilon_v$         | 3,83 [%]       |            |
| Estimated stiffness $E_{50}$        | 19753,09 [kPa] |            |
| Dotted line max.                    | 0,00 [%]       |            |
| Dotted line min.                    | 9,91 [%]       |            |

# APPENDIX B.1 SAMPLE IMAGES AND UNCONFINED COMPRESSION TEST RESULTS



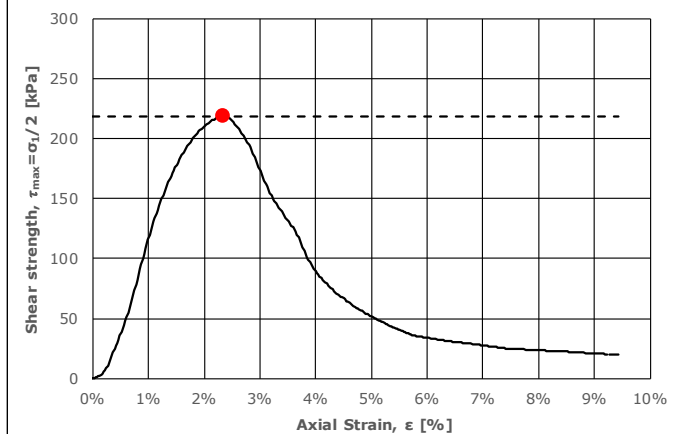
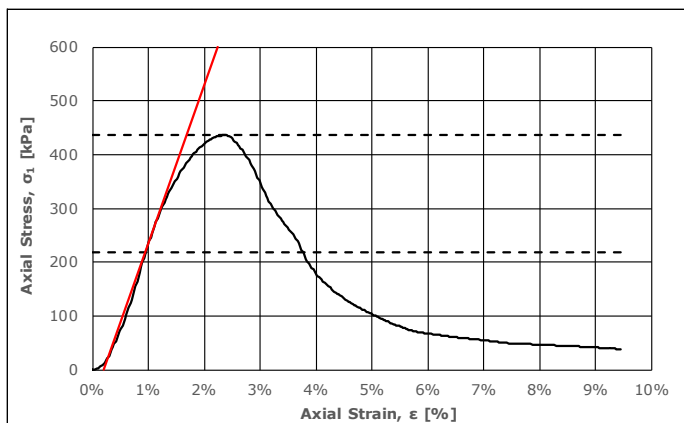
|  |                                     |            |             |         |           |            |
|--|-------------------------------------|------------|-------------|---------|-----------|------------|
|  | Sample ID                           | DRY.8.10.1 | Curing time | 28 Days | Test date | 27.03.2023 |
|  | Sample height                       | 100,00     | [mm]        |         |           |            |
|  | Sample diameter                     | 54,00      | [mm]        |         |           |            |
|  | Ultimate compressive strength $q_u$ | 1181,92    | [kPa]       |         |           |            |
|  | Undrained shear strength $S_u$      | 590,96     | [kPa]       |         |           |            |
|  | Failure strain $\epsilon_v$         | 1,87       | [%]         |         |           |            |
|  | Estimated stiffness $E_{50}$        | 97902,10   | [kPa]       |         |           |            |
|  | Dotted line max.                    | 0,00       | [%]         |         |           |            |
|  | Dotted line min.                    | 9,98       | [%]         |         |           |            |

|  |                                     |            |             |         |           |            |
|--|-------------------------------------|------------|-------------|---------|-----------|------------|
|  | Sample ID                           | DRY.8.10.2 | Curing time | 28 Days | Test date | 27.03.2023 |
|  | Sample height                       | 100,00     | [mm]        |         |           |            |
|  | Sample diameter                     | 54,00      | [mm]        |         |           |            |
|  | Ultimate compressive strength $q_u$ | 1161,61    | [kPa]       |         |           |            |
|  | Undrained shear strength $S_u$      | 580,80     | [kPa]       |         |           |            |
|  | Failure strain $\epsilon_v$         | 2,09       | [%]         |         |           |            |
|  | Estimated stiffness $E_{50}$        | 89171,97   | [kPa]       |         |           |            |
|  | Dotted line max.                    | 0,00       | [%]         |         |           |            |
|  | Dotted line min.                    | 9,88       | [%]         |         |           |            |

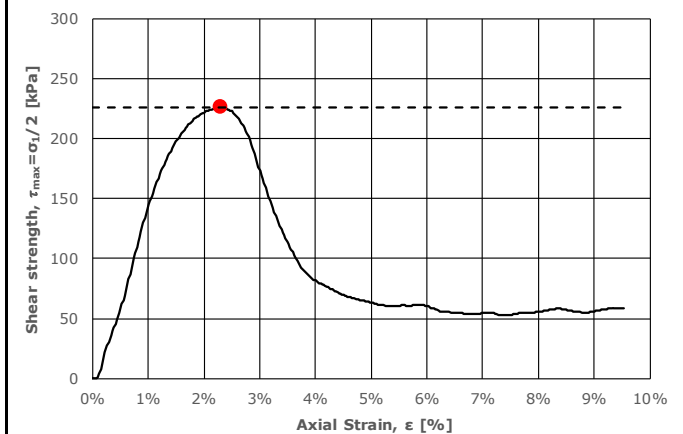
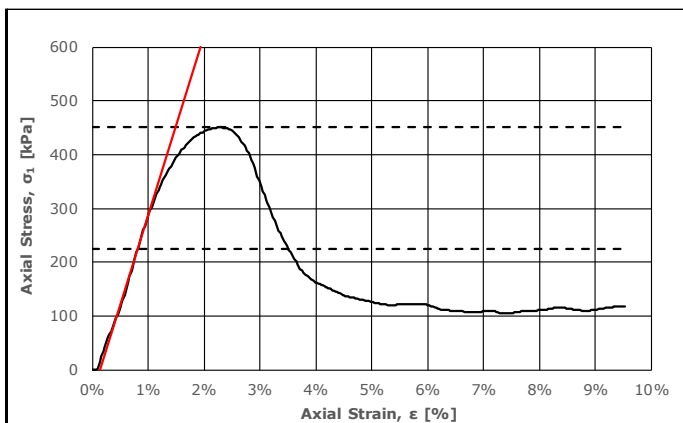
|  |                                     |            |             |         |           |            |
|--|-------------------------------------|------------|-------------|---------|-----------|------------|
|  | Sample ID                           | DRY.8.10.3 | Curing time | 28 Days | Test date | 27.03.2023 |
|  | Sample height                       | 100,00     | [mm]        |         |           |            |
|  | Sample diameter                     | 54,00      | [mm]        |         |           |            |
|  | Ultimate compressive strength $q_u$ | 1045,21    | [kPa]       |         |           |            |
|  | Undrained shear strength $S_u$      | 522,61     | [kPa]       |         |           |            |
|  | Failure strain $\epsilon_v$         | 1,83       | [%]         |         |           |            |
|  | Estimated stiffness $E_{50}$        | 90909,09   | [kPa]       |         |           |            |
|  | Dotted line max.                    | 0,00       | [%]         |         |           |            |
|  | Dotted line min.                    | 9,91       | [%]         |         |           |            |



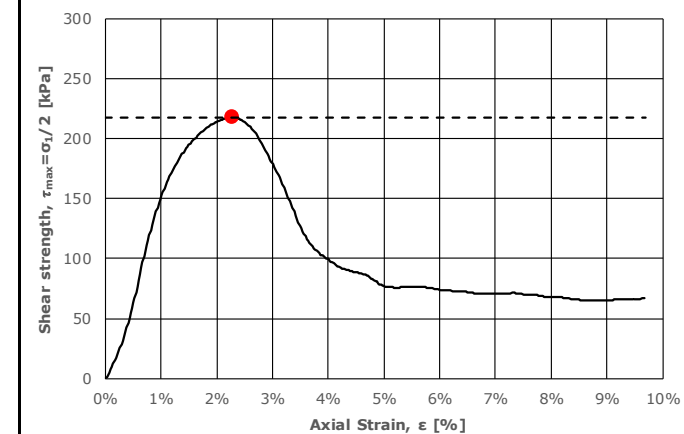
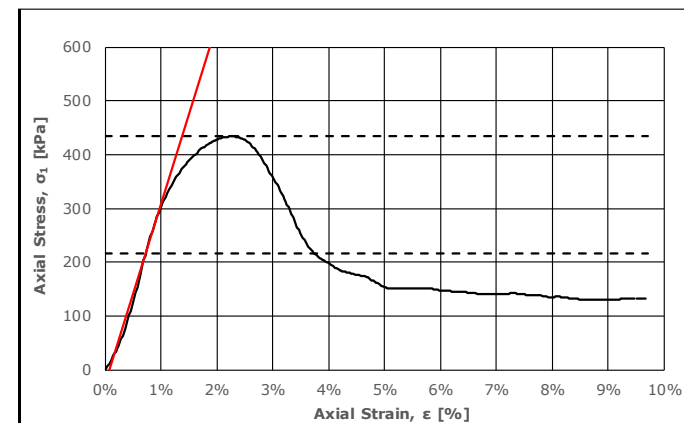
# APPENDIX B.1 SAMPLE IMAGES AND UNCONFINED COMPRESSION TEST RESULTS



| Sample ID                           | Curing time    | Test date  |
|-------------------------------------|----------------|------------|
| DRY.16.1.1                          | 28 Days        | 15.03.2023 |
| Sample height                       | 100,00 [mm]    |            |
| Sample diameter                     | 54,00 [mm]     |            |
| Ultimate compressive strength $q_u$ | 436,26 [kPa]   |            |
| Undrained shear strength $S_u$      | 218,13 [kPa]   |            |
| Failure strain $\epsilon_v$         | 2,35 [%]       |            |
| Estimated stiffness $E_{50}$        | 29556,65 [kPa] |            |
| Dotted line max.                    | 0,00 [%]       |            |
| Dotted line min.                    | 9,44 [%]       |            |

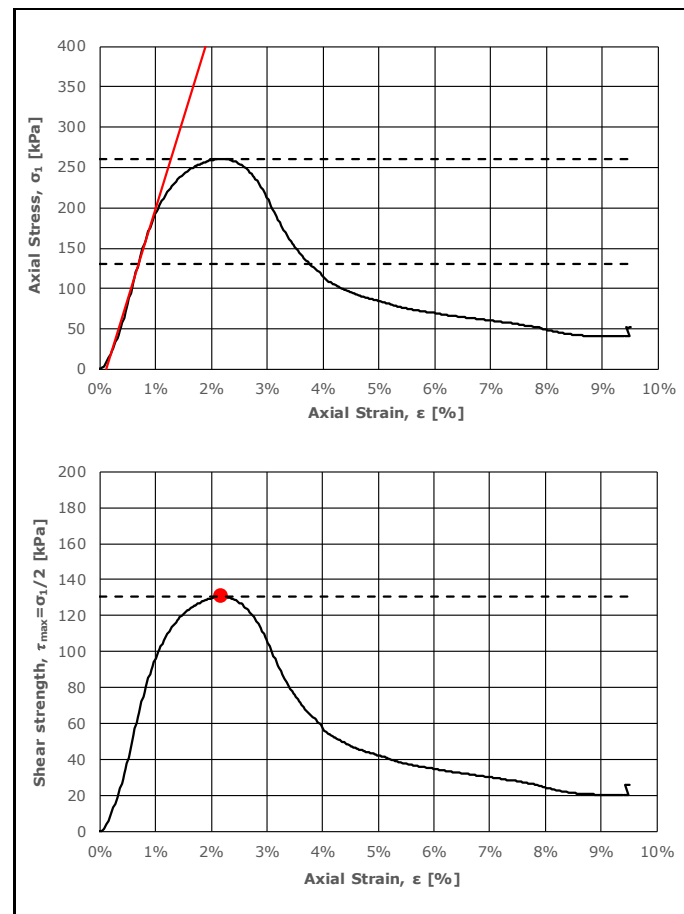
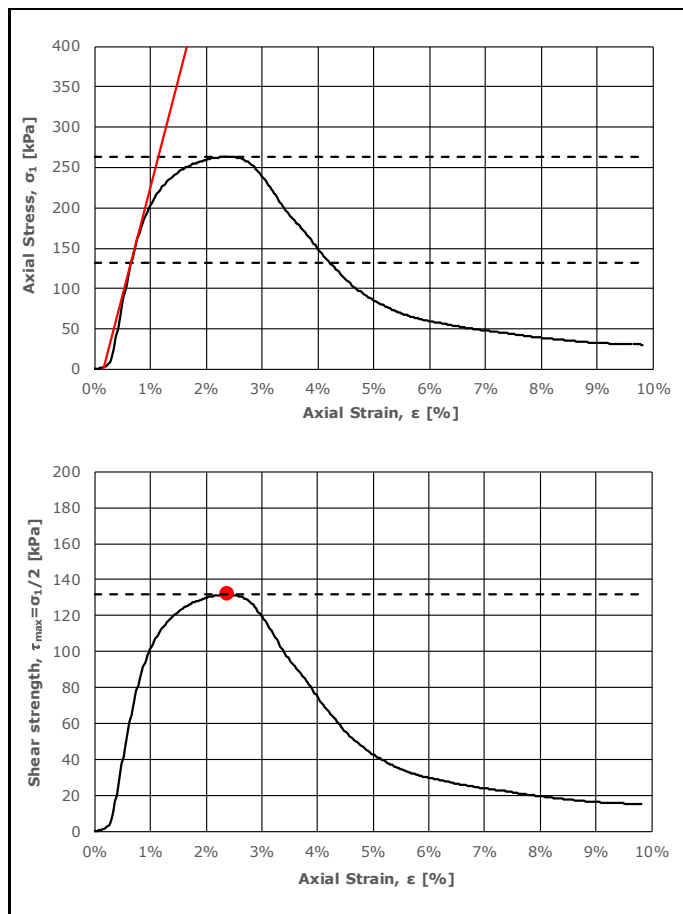
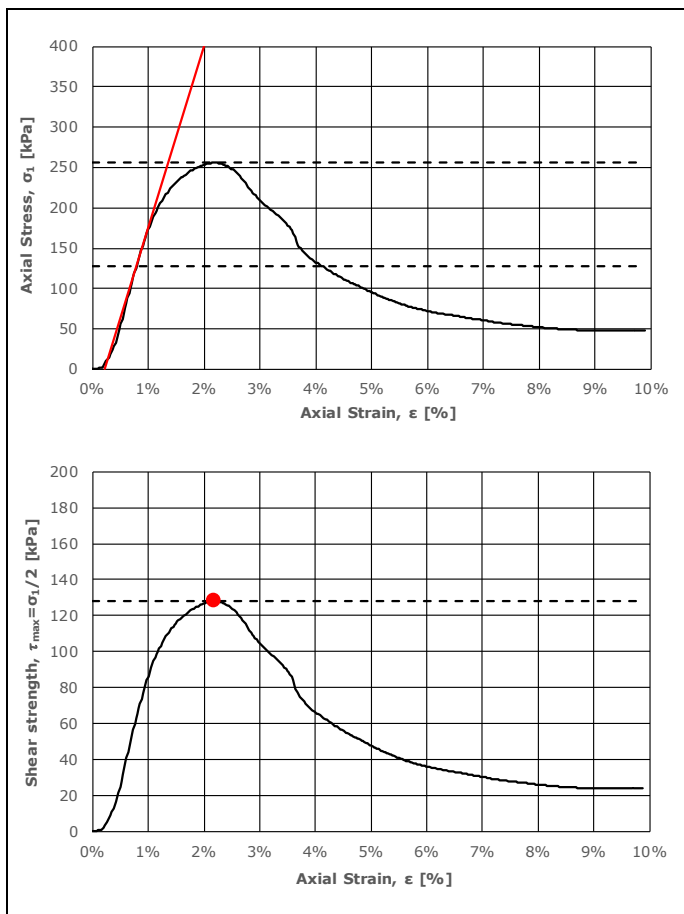


| Sample ID                           | Curing time    | Test date  |
|-------------------------------------|----------------|------------|
| DRY.16.1.2                          | 28 Days        | 15.03.2023 |
| Sample height                       | 100,00 [mm]    |            |
| Sample diameter                     | 54,00 [mm]     |            |
| Ultimate compressive strength $q_u$ | 451,00 [kPa]   |            |
| Undrained shear strength $S_u$      | 225,50 [kPa]   |            |
| Failure strain $\epsilon_v$         | 2,30 [%]       |            |
| Estimated stiffness $E_{50}$        | 33707,87 [kPa] |            |
| Dotted line max.                    | 0,00 [%]       |            |
| Dotted line min.                    | 9,53 [%]       |            |



| Sample ID                           | Curing time    | Test date  |
|-------------------------------------|----------------|------------|
| DRY.16.1.3                          | 28 Days        | 15.03.2023 |
| Sample height                       | 100,00 [mm]    |            |
| Sample diameter                     | 54,00 [mm]     |            |
| Ultimate compressive strength $q_u$ | 434,20 [kPa]   |            |
| Undrained shear strength $S_u$      | 217,10 [kPa]   |            |
| Failure strain $\epsilon_v$         | 2,27 [%]       |            |
| Estimated stiffness $E_{50}$        | 33707,87 [kPa] |            |
| Dotted line max.                    | 0,00 [%]       |            |
| Dotted line min.                    | 9,70 [%]       |            |

# APPENDIX B.1 SAMPLE IMAGES AND UNCONFINED COMPRESSION TEST RESULTS

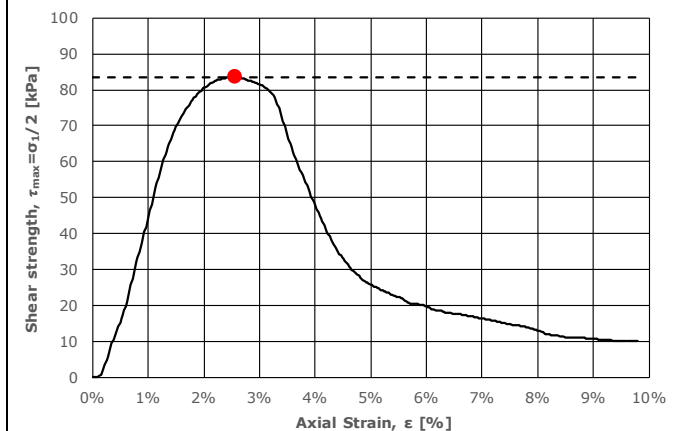
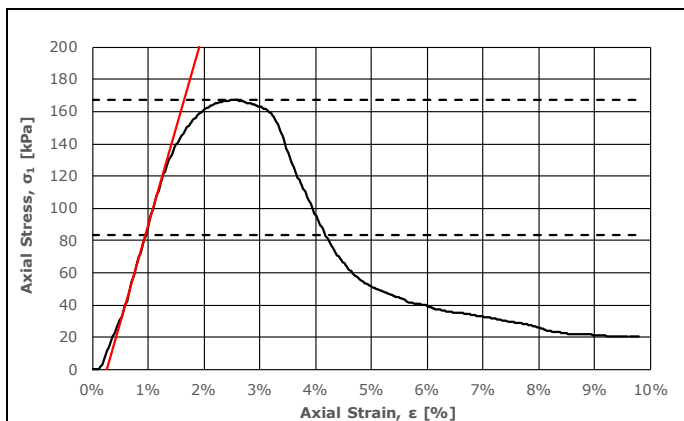


|  |                                     |            |             |         |           |            |
|--|-------------------------------------|------------|-------------|---------|-----------|------------|
|  | Sample ID                           | DRY.16.2.1 | Curing time | 28 Days | Test date | 15.03.2023 |
|  | Sample height                       | 100,00     | [mm]        |         |           |            |
|  | Sample diameter                     | 54,00      | [mm]        |         |           |            |
|  | Ultimate compressive strength $q_u$ | 255,90     | [kPa]       |         |           |            |
|  | Undrained shear strength $S_u$      | 127,95     | [kPa]       |         |           |            |
|  | Failure strain $\epsilon_v$         | 2,19       | [%]         |         |           |            |
|  | Estimated stiffness $E_{50}$        | 22598,87   | [kPa]       |         |           |            |
|  | Dotted line max.                    | 0,00       | [%]         |         |           |            |
|  | Dotted line min.                    | 9,89       | [%]         |         |           |            |

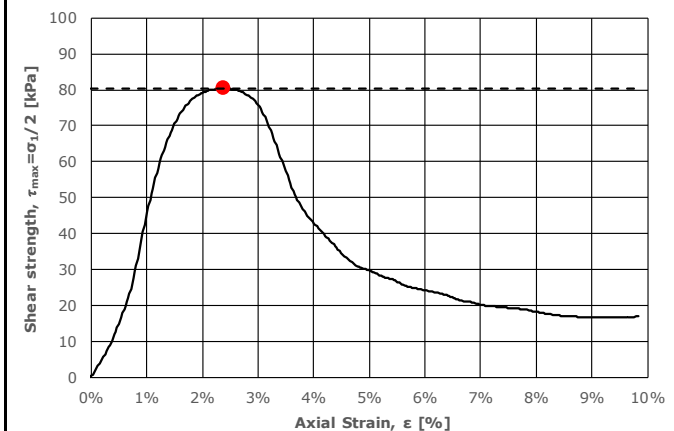
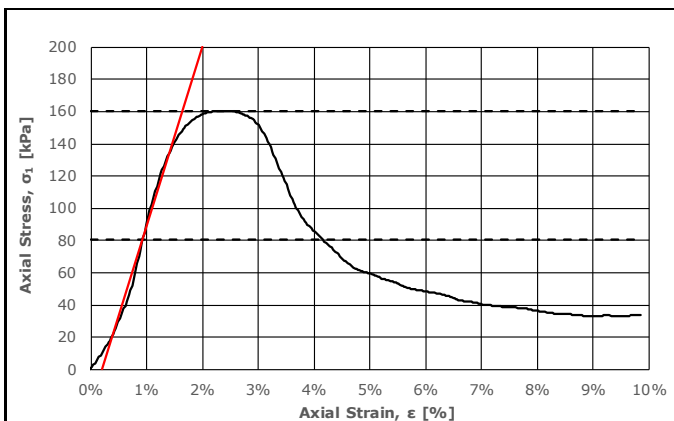
|  |                                     |            |             |         |           |            |
|--|-------------------------------------|------------|-------------|---------|-----------|------------|
|  | Sample ID                           | DRY.16.2.2 | Curing time | 28 Days | Test date | 15.03.2023 |
|  | Sample height                       | 100,00     | [mm]        |         |           |            |
|  | Sample diameter                     | 54,00      | [mm]        |         |           |            |
|  | Ultimate compressive strength $q_u$ | 263,29     | [kPa]       |         |           |            |
|  | Undrained shear strength $S_u$      | 131,65     | [kPa]       |         |           |            |
|  | Failure strain $\epsilon_v$         | 2,39       | [%]         |         |           |            |
|  | Estimated stiffness $E_{50}$        | 26845,64   | [kPa]       |         |           |            |
|  | Dotted line max.                    | 0,00       | [%]         |         |           |            |
|  | Dotted line min.                    | 9,82       | [%]         |         |           |            |

|  |                                     |            |             |         |           |            |
|--|-------------------------------------|------------|-------------|---------|-----------|------------|
|  | Sample ID                           | DRY.16.2.3 | Curing time | 28 Days | Test date | 15.03.2023 |
|  | Sample height                       | 100,00     | [mm]        |         |           |            |
|  | Sample diameter                     | 54,00      | [mm]        |         |           |            |
|  | Ultimate compressive strength $q_u$ | 260,77     | [kPa]       |         |           |            |
|  | Undrained shear strength $S_u$      | 130,39     | [kPa]       |         |           |            |
|  | Failure strain $\epsilon_v$         | 2,19       | [%]         |         |           |            |
|  | Estimated stiffness $E_{50}$        | 22471,91   | [kPa]       |         |           |            |
|  | Dotted line max.                    | 0,00       | [%]         |         |           |            |
|  | Dotted line min.                    | 9,51       | [%]         |         |           |            |

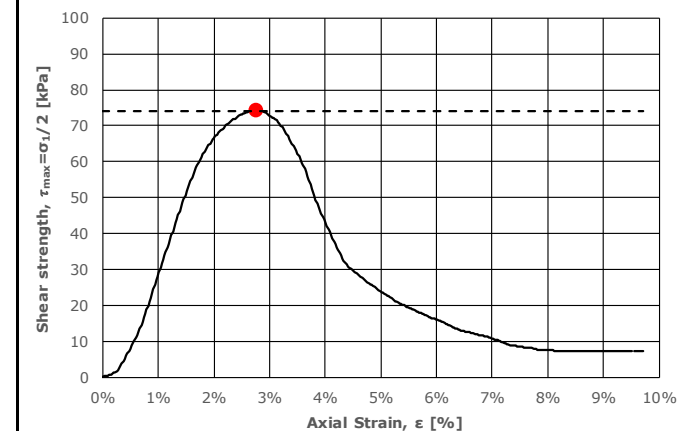
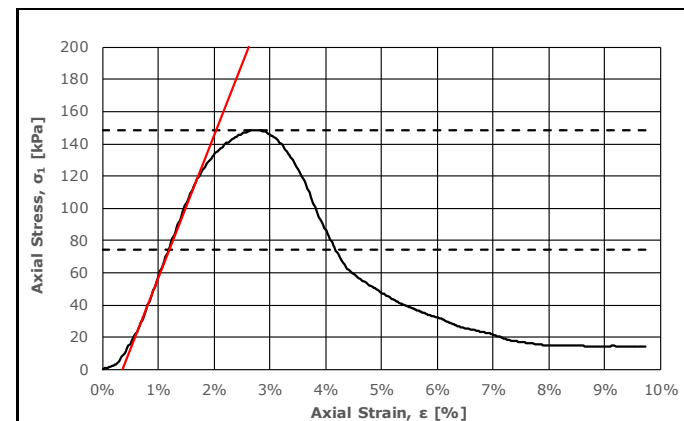
# APPENDIX B.1 SAMPLE IMAGES AND UNCONFINED COMPRESSION TEST RESULTS



| Sample ID                           | Curing time    | Test date  |
|-------------------------------------|----------------|------------|
| DRY.16.3.1                          | 28 Days        | 17.03.2023 |
| Sample height                       | 100,00 [mm]    |            |
| Sample diameter                     | 54,00 [mm]     |            |
| Ultimate compressive strength $q_u$ | 167,11 [kPa]   |            |
| Undrained shear strength $S_u$      | 83,55 [kPa]    |            |
| Failure strain $\epsilon_v$         | 2,57 [%]       |            |
| Estimated stiffness $E_{50}$        | 12195,12 [kPa] |            |
| Dotted line max.                    | 0,00 [%]       |            |
| Dotted line min.                    | 9,79 [%]       |            |

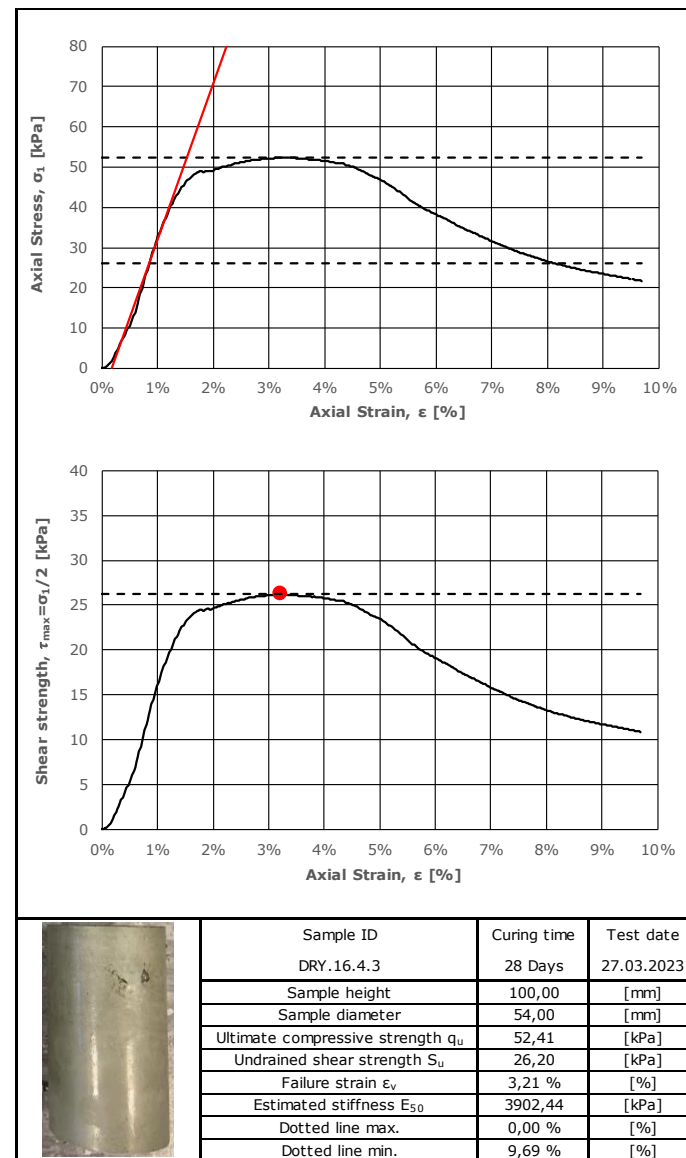
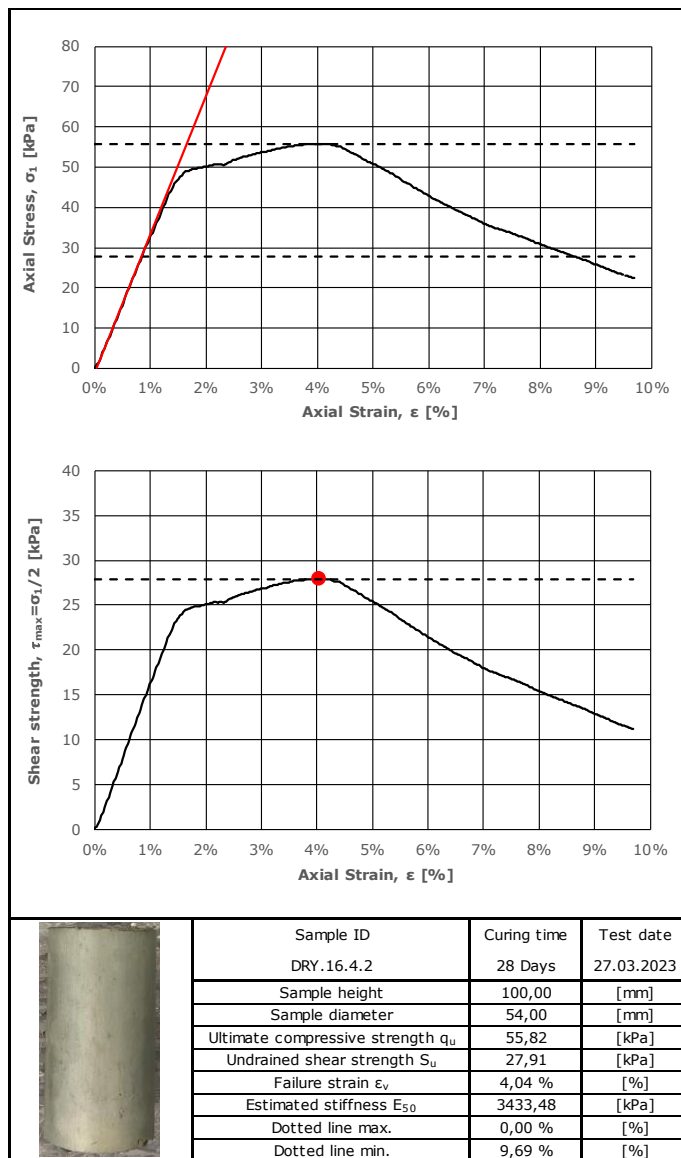
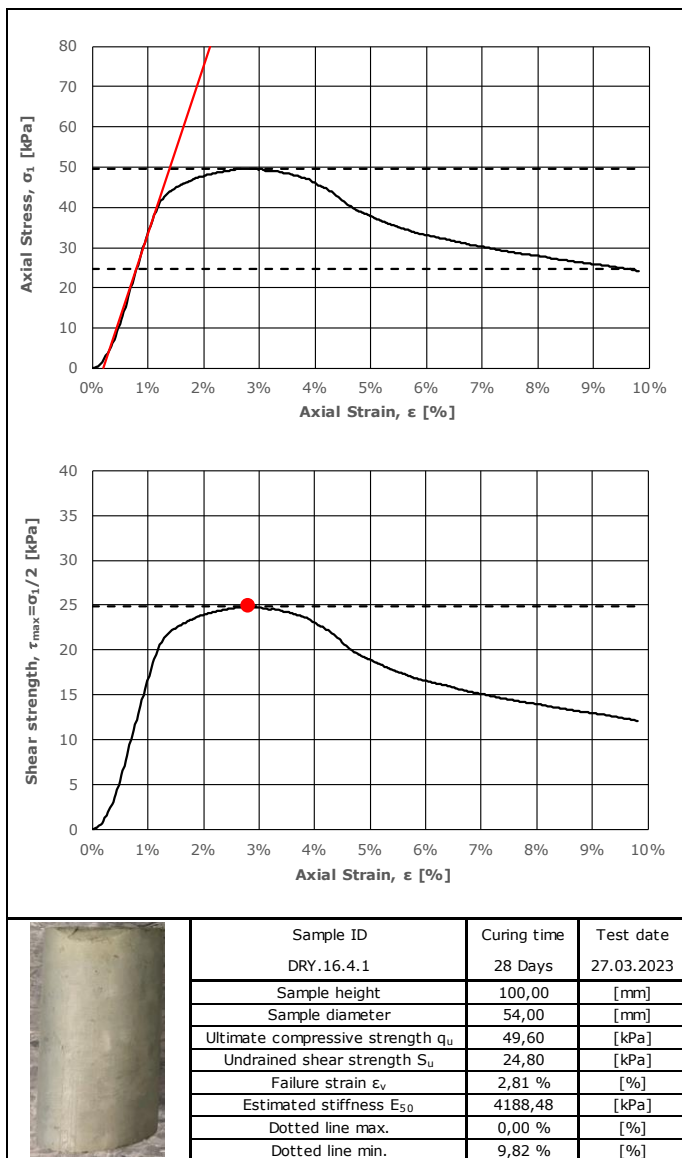


| Sample ID                           | Curing time    | Test date  |
|-------------------------------------|----------------|------------|
| DRY.16.3.2                          | 28 Days        | 17.03.2023 |
| Sample height                       | 100,00 [mm]    |            |
| Sample diameter                     | 54,00 [mm]     |            |
| Ultimate compressive strength $q_u$ | 160,65 [kPa]   |            |
| Undrained shear strength $S_u$      | 80,33 [kPa]    |            |
| Failure strain $\epsilon_v$         | 2,37 [%]       |            |
| Estimated stiffness $E_{50}$        | 11111,11 [kPa] |            |
| Dotted line max.                    | 0,00 [%]       |            |
| Dotted line min.                    | 9,84 [%]       |            |

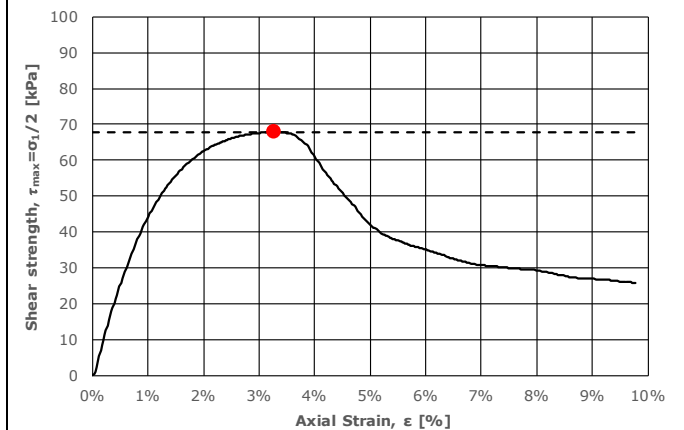
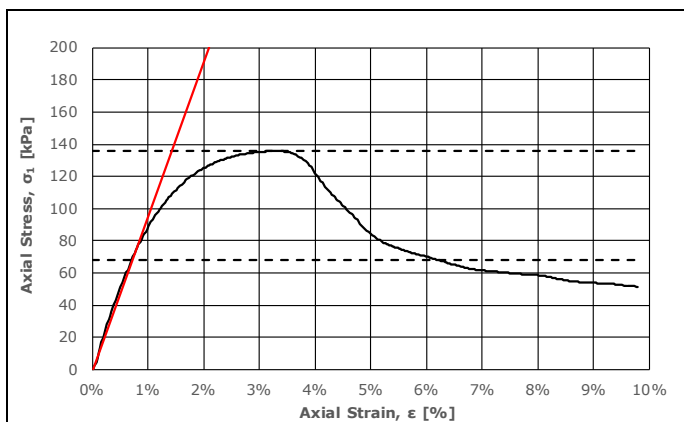


| Sample ID                           | Curing time   | Test date  |
|-------------------------------------|---------------|------------|
| DRY.16.3.3                          | 28 Days       | 17.03.2023 |
| Sample height                       | 100,00 [mm]   |            |
| Sample diameter                     | 54,00 [mm]    |            |
| Ultimate compressive strength $q_u$ | 148,44 [kPa]  |            |
| Undrained shear strength $S_u$      | 74,22 [kPa]   |            |
| Failure strain $\epsilon_v$         | 2,78 [%]      |            |
| Estimated stiffness $E_{50}$        | 8849,56 [kPa] |            |
| Dotted line max.                    | 0,00 [%]      |            |
| Dotted line min.                    | 9,72 [%]      |            |

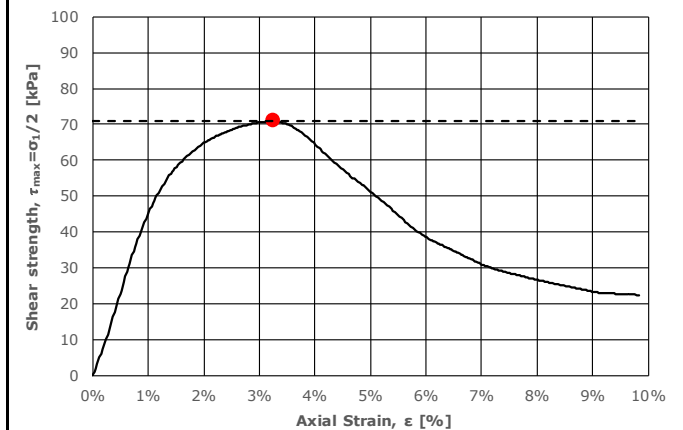
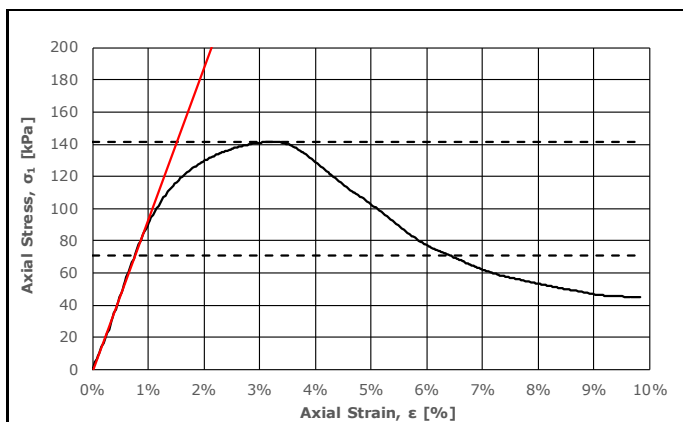
# APPENDIX B.1 SAMPLE IMAGES AND UNCONFINED COMPRESSION TEST RESULTS



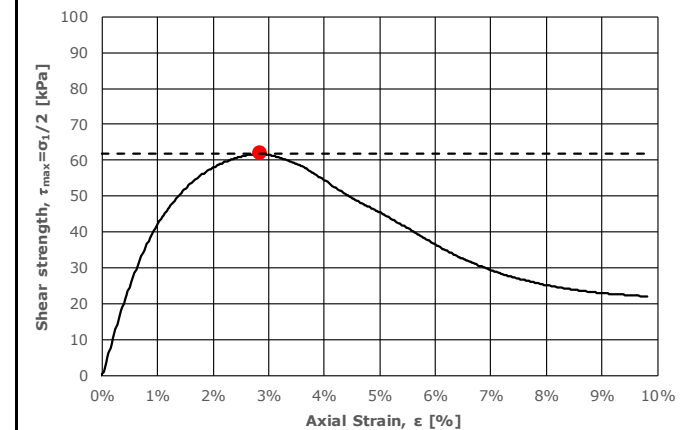
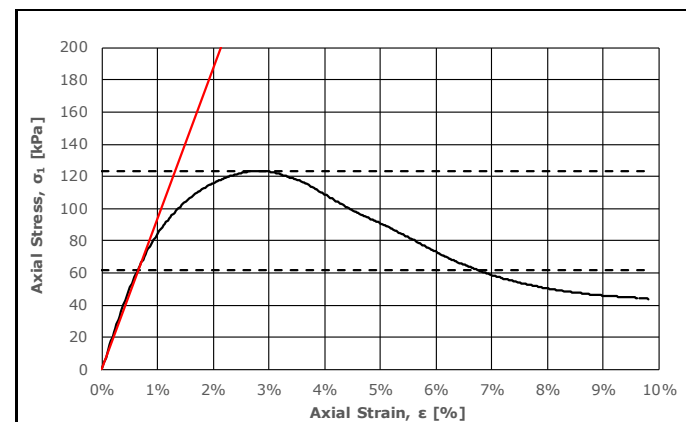
# APPENDIX B.1 SAMPLE IMAGES AND UNCONFINED COMPRESSION TEST RESULTS



| Sample ID                           | Curing time | Test date  |
|-------------------------------------|-------------|------------|
| DRY.16.5.1                          | 28 Days     | 28.03.2023 |
| Sample height                       | 100,00      | [mm]       |
| Sample diameter                     | 54,00       | [mm]       |
| Ultimate compressive strength $q_u$ | 135,82      | [kPa]      |
| Undrained shear strength $S_u$      | 67,91       | [kPa]      |
| Failure strain $\epsilon_v$         | 3,28 %      | [%]        |
| Estimated stiffness $E_{50}$        | 9661,84     | [kPa]      |
| Dotted line max.                    | 0,00 %      | [%]        |
| Dotted line min.                    | 9,79 %      | [%]        |

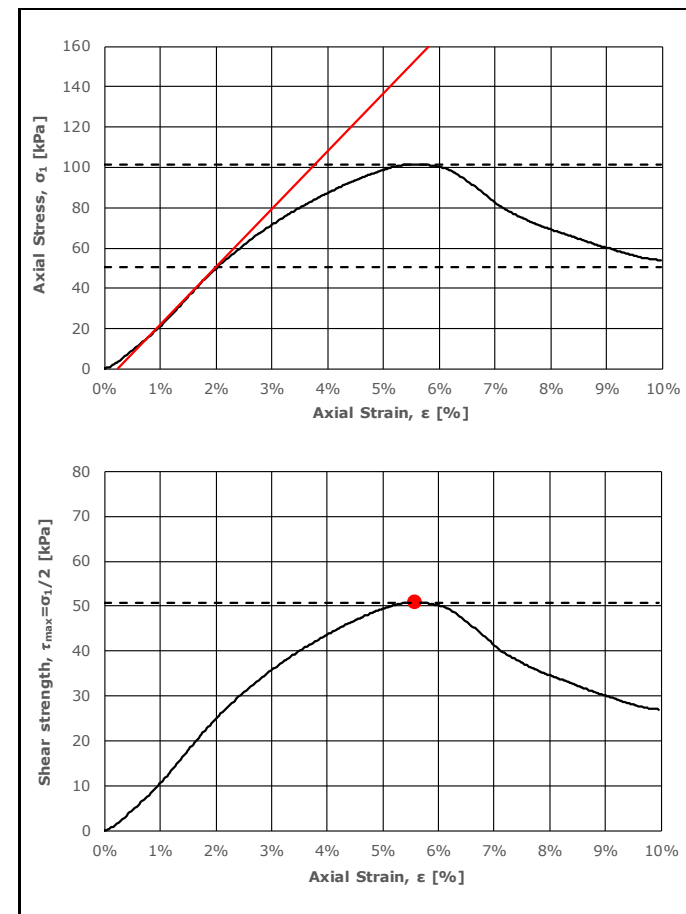
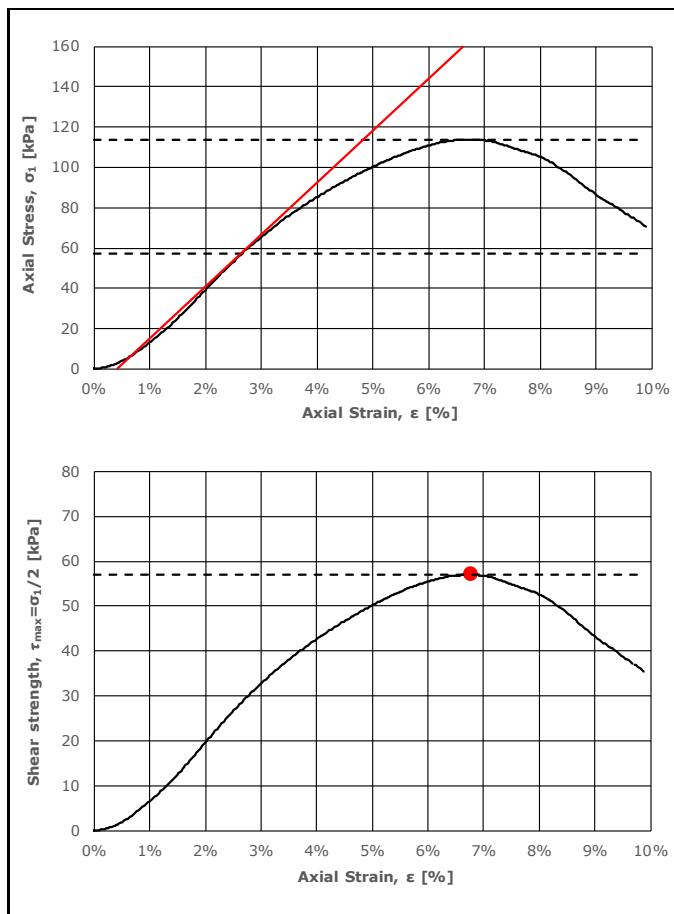
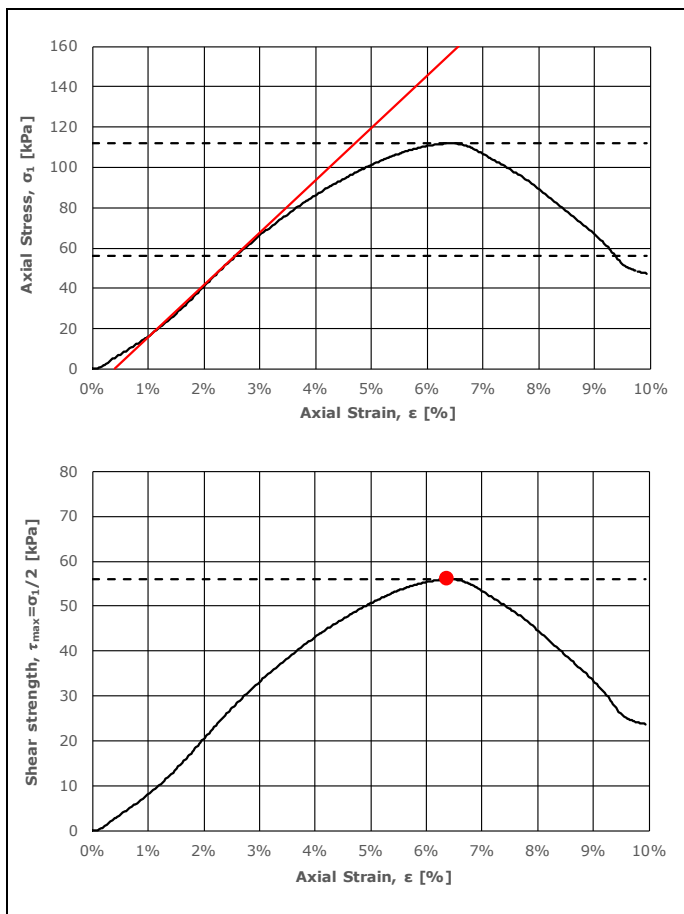



| Sample ID                           | Curing time | Test date  |
|-------------------------------------|-------------|------------|
| DRY.16.5.2                          | 28 Days     | 28.03.2023 |
| Sample height                       | 100,00      | [mm]       |
| Sample diameter                     | 54,00       | [mm]       |
| Ultimate compressive strength $q_u$ | 141,67      | [kPa]      |
| Undrained shear strength $S_u$      | 70,83       | [kPa]      |
| Failure strain $\epsilon_v$         | 3,25 %      | [%]        |
| Estimated stiffness $E_{50}$        | 9478,67     | [kPa]      |
| Dotted line max.                    | 0,00 %      | [%]        |
| Dotted line min.                    | 9,84 %      | [%]        |





| Sample ID                           | Curing time | Test date  |
|-------------------------------------|-------------|------------|
| DRY.16.5.3                          | 28 Days     | 28.03.2023 |
| Sample height                       | 100,00      | [mm]       |
| Sample diameter                     | 54,00       | [mm]       |
| Ultimate compressive strength $q_u$ | 123,58      | [kPa]      |
| Undrained shear strength $S_u$      | 61,79       | [kPa]      |
| Failure strain $\epsilon_v$         | 2,85 %      | [%]        |
| Estimated stiffness $E_{50}$        | 9389,67     | [kPa]      |
| Dotted line max.                    | 0,00 %      | [%]        |
| Dotted line min.                    | 9,81 %      | [%]        |

# APPENDIX B.1 SAMPLE IMAGES AND UNCONFINED COMPRESSION TEST RESULTS

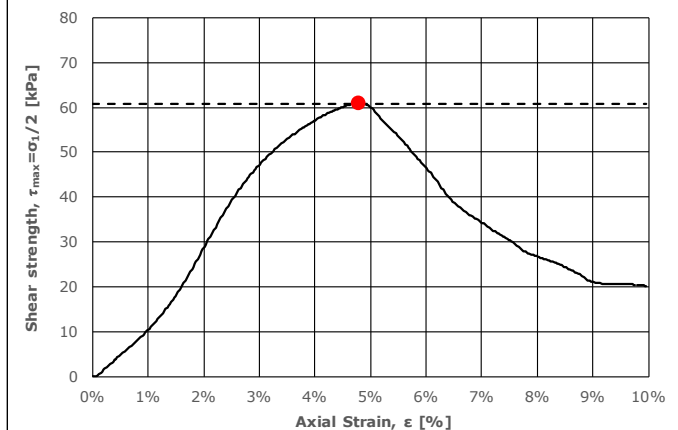
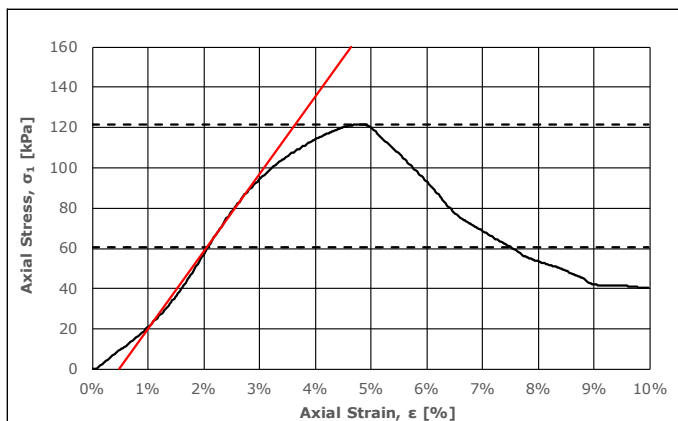


|   |                                     |             |            |
|---|-------------------------------------|-------------|------------|
|  | Sample ID                           | Curing time | Test date  |
|   | DRY.16.6.1                          | 28 Days     | 28.03.2023 |
|   | Sample height                       | 100,00      | [mm]       |
|   | Sample diameter                     | 54,00       | [mm]       |
|   | Ultimate compressive strength $q_u$ | 112,02      | [kPa]      |
|   | Undrained shear strength $S_u$      | 56,01       | [kPa]      |
|   | Failure strain $\epsilon_v$         | 6,38        | [%]        |
|   | Estimated stiffness $E_{50}$        | 2597,40     | [kPa]      |
|   | Dotted line max.                    | 0,00        | [%]        |
|   | Dotted line min.                    | 9,94        | [%]        |

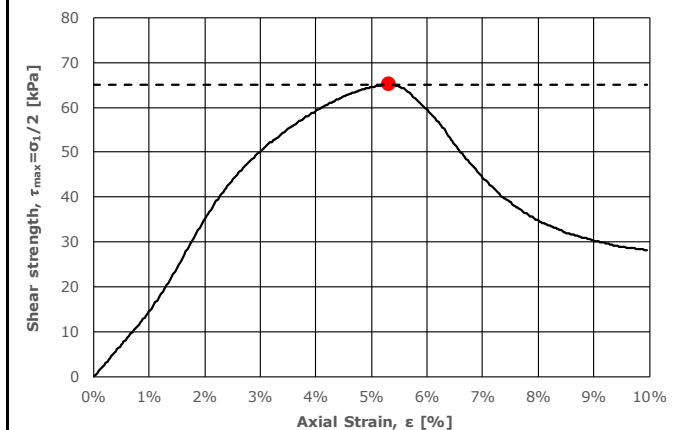
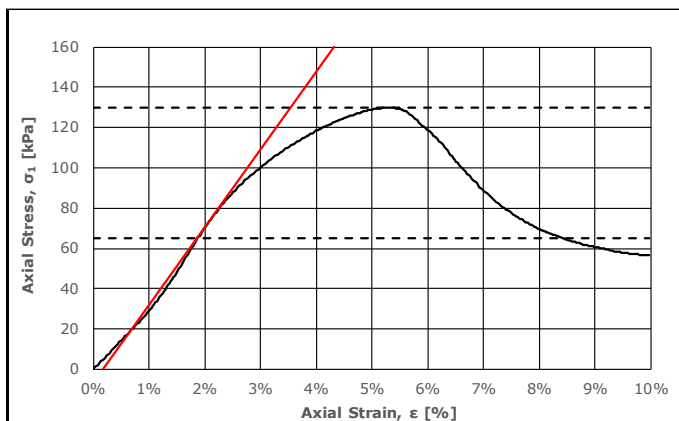
|   |                                     |             |            |
|---|-------------------------------------|-------------|------------|
|  | Sample ID                           | Curing time | Test date  |
|   | DRY.16.6.2                          | 28 Days     | 28.03.2023 |
|   | Sample height                       | 100,00      | [mm]       |
|   | Sample diameter                     | 54,00       | [mm]       |
|   | Ultimate compressive strength $q_u$ | 113,98      | [kPa]      |
|   | Undrained shear strength $S_u$      | 56,99       | [kPa]      |
|   | Failure strain $\epsilon_v$         | 6,78        | [%]        |
|   | Estimated stiffness $E_{50}$        | 2580,65     | [kPa]      |
|   | Dotted line max.                    | 0,00        | [%]        |
|   | Dotted line min.                    | 9,88        | [%]        |

|   |                                     |             |            |
|---|-------------------------------------|-------------|------------|
|  | Sample ID                           | Curing time | Test date  |
|   | DRY.16.6.3                          | 28 Days     | 28.03.2023 |
|   | Sample height                       | 100,00      | [mm]       |
|   | Sample diameter                     | 54,00       | [mm]       |
|   | Ultimate compressive strength $q_u$ | 101,62      | [kPa]      |
|   | Undrained shear strength $S_u$      | 50,81       | [kPa]      |
|   | Failure strain $\epsilon_v$         | 5,58        | [%]        |
|   | Estimated stiffness $E_{50}$        | 2872,53     | [kPa]      |
|   | Dotted line max.                    | 0,00        | [%]        |
|   | Dotted line min.                    | 9,96        | [%]        |

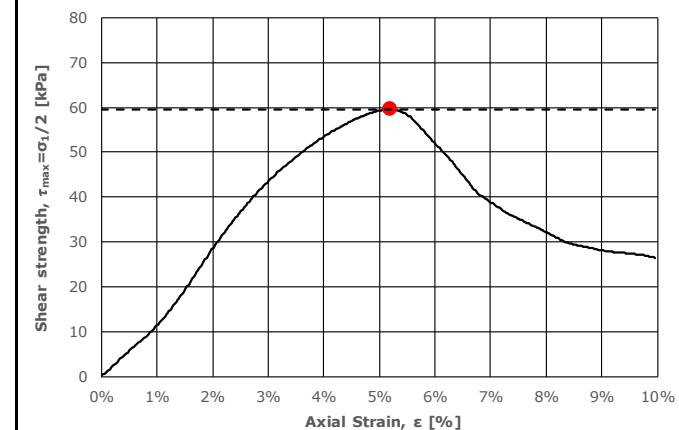
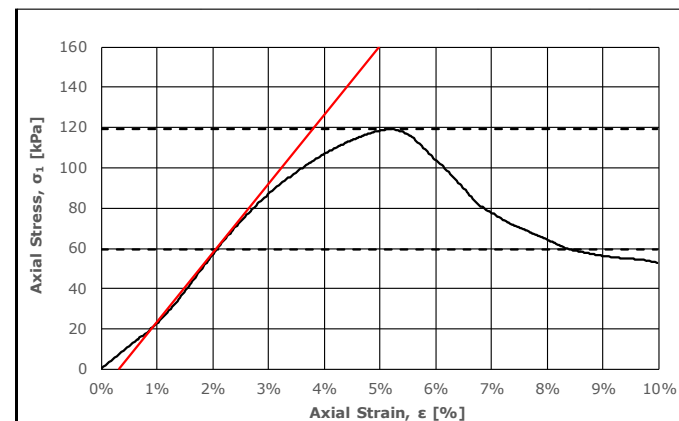
# APPENDIX B.1 SAMPLE IMAGES AND UNCONFINED COMPRESSION TEST RESULTS



| Sample ID                           | Curing time   | Test date  |
|-------------------------------------|---------------|------------|
| DRY.16.7.1                          | 28 Days       | 28.03.2023 |
| Sample height                       | 100,00 [mm]   |            |
| Sample diameter                     | 54,00 [mm]    |            |
| Ultimate compressive strength $q_u$ | 121,69 [kPa]  |            |
| Undrained shear strength $S_u$      | 60,84 [kPa]   |            |
| Failure strain $\epsilon_v$         | 4,80 [%]      |            |
| Estimated stiffness $E_{50}$        | 3836,93 [kPa] |            |
| Dotted line max.                    | 0,00 [%]      |            |
| Dotted line min.                    | 9,96 [%]      |            |

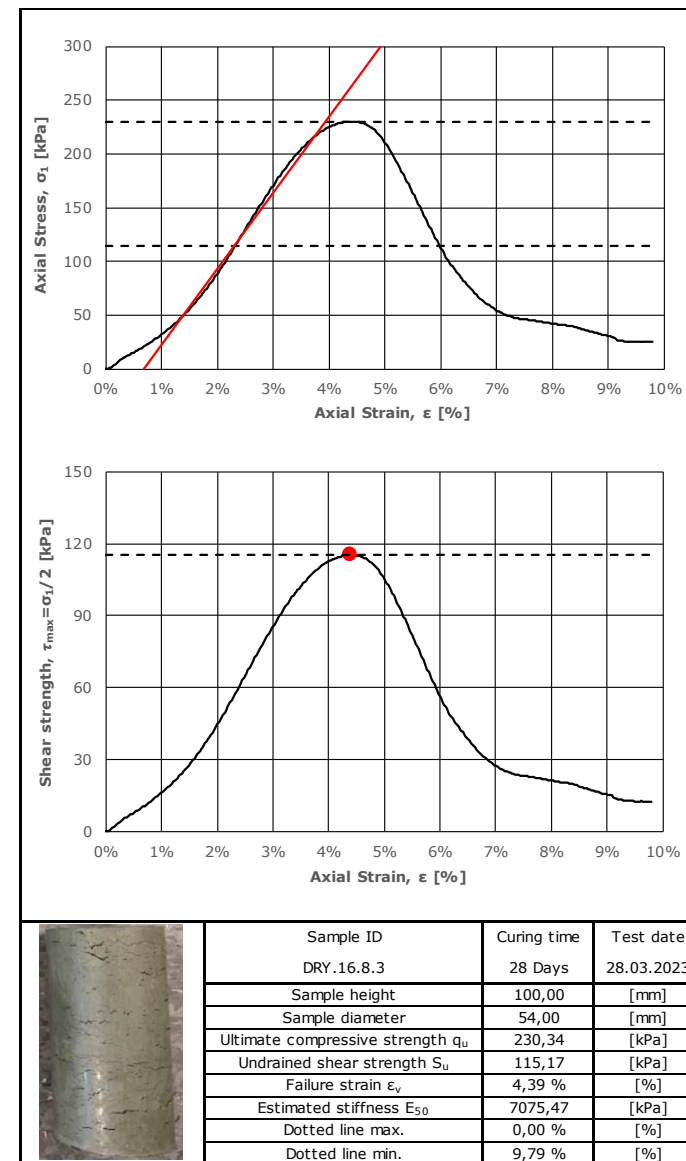
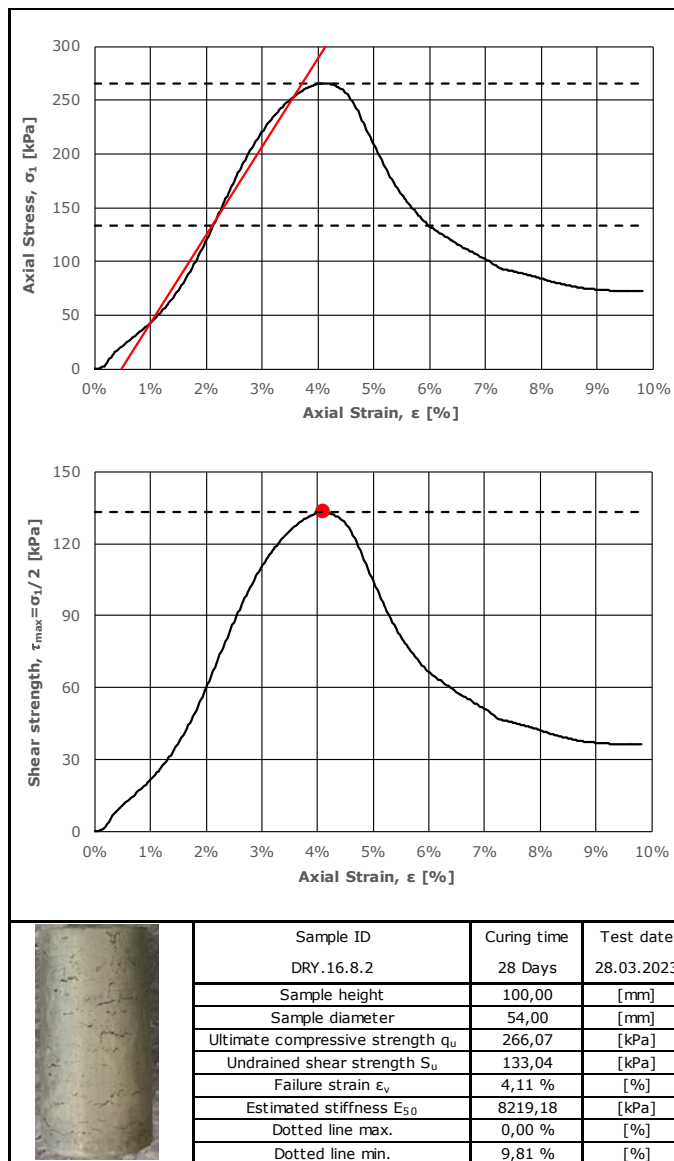
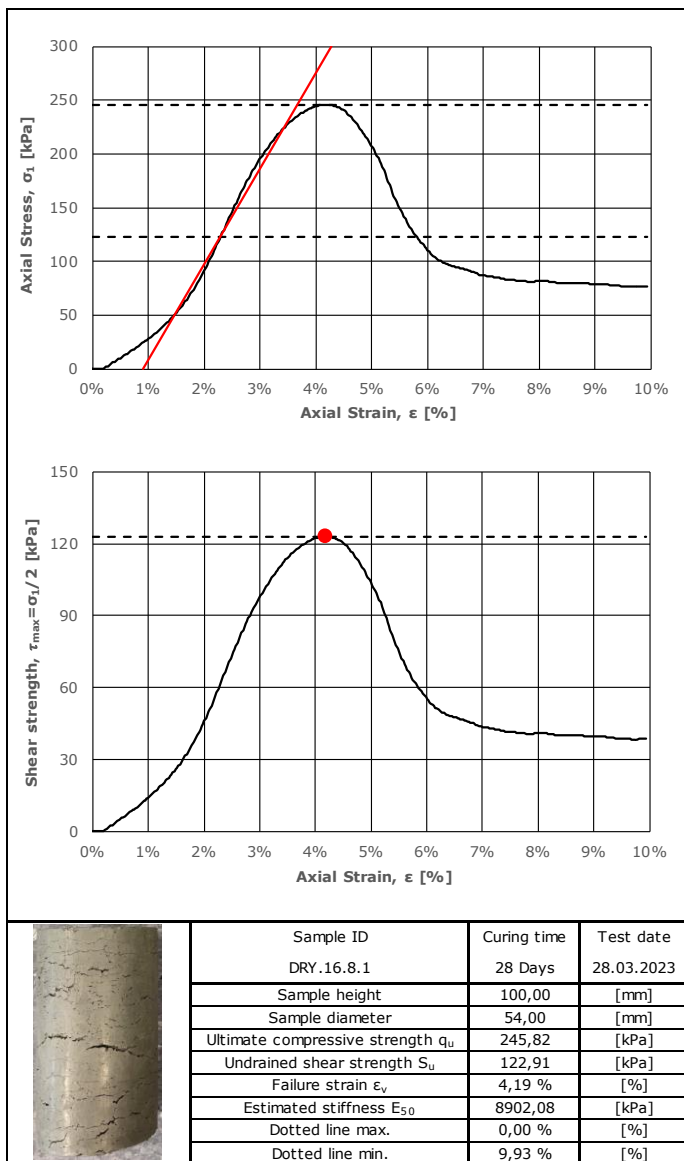


| Sample ID                           | Curing time   | Test date  |
|-------------------------------------|---------------|------------|
| DRY.16.7.2                          | 28 Days       | 28.03.2023 |
| Sample height                       | 100,00 [mm]   |            |
| Sample diameter                     | 54,00 [mm]    |            |
| Ultimate compressive strength $q_u$ | 129,88 [kPa]  |            |
| Undrained shear strength $S_u$      | 64,94 [kPa]   |            |
| Failure strain $\epsilon_v$         | 5,33 [%]      |            |
| Estimated stiffness $E_{50}$        | 3883,50 [kPa] |            |
| Dotted line max.                    | 0,00 [%]      |            |
| Dotted line min.                    | 9,96 [%]      |            |



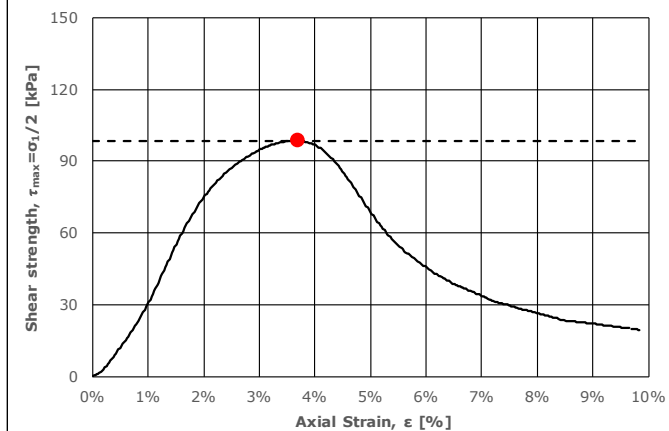
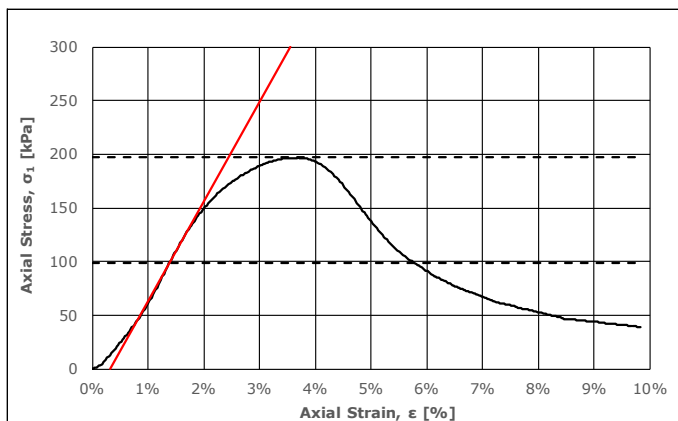
| Sample ID                           | Curing time   | Test date  |
|-------------------------------------|---------------|------------|
| DRY.16.7.3                          | 28 Days       | 28.03.2023 |
| Sample height                       | 100,00 [mm]   |            |
| Sample diameter                     | 54,00 [mm]    |            |
| Ultimate compressive strength $q_u$ | 119,22 [kPa]  |            |
| Undrained shear strength $S_u$      | 59,61 [kPa]   |            |
| Failure strain $\epsilon_v$         | 5,20 [%]      |            |
| Estimated stiffness $E_{50}$        | 3440,86 [kPa] |            |
| Dotted line max.                    | 0,00 [%]      |            |
| Dotted line min.                    | 9,96 [%]      |            |

# APPENDIX B.1 SAMPLE IMAGES AND UNCONFINED COMPRESSION TEST RESULTS

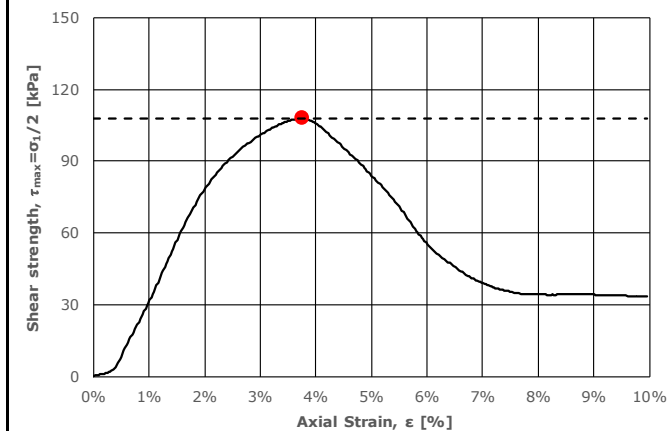
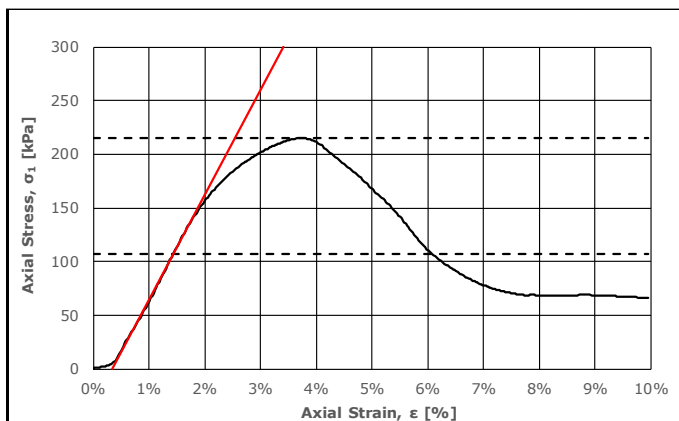




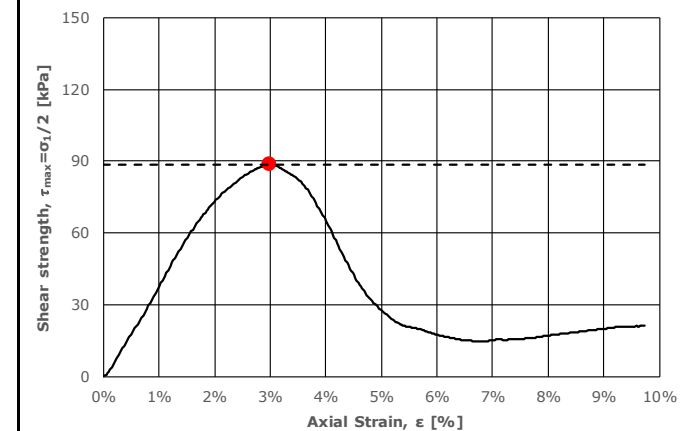
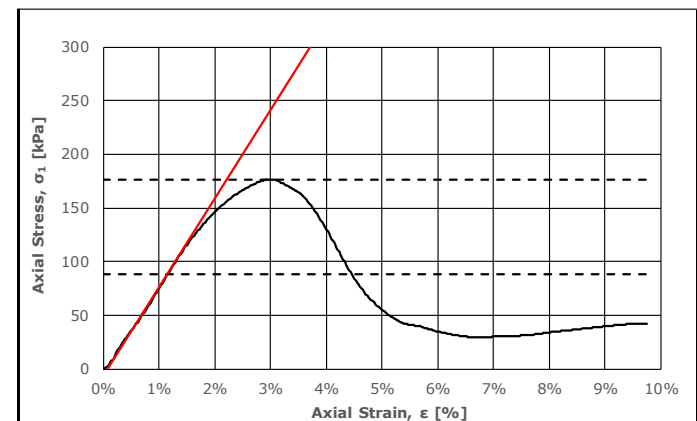
## APPENDIX B.1 SAMPLE IMAGES AND UNCONFINED COMPRESSION TEST RESULTS



| Sample ID                           | Curing time   | Test date  |
|-------------------------------------|---------------|------------|
| DRY.16.9.1                          | 28 Days       | 28.03.2023 |
| Sample height                       | 100,00 [mm]   |            |
| Sample diameter                     | 54,00 [mm]    |            |
| Ultimate compressive strength $q_u$ | 196,99 [kPa]  |            |
| Undrained shear strength $S_u$      | 98,50 [kPa]   |            |
| Failure strain $\epsilon_v$         | 3,69 [%]      |            |
| Estimated stiffness $E_{50}$        | 9287,93 [kPa] |            |
| Dotted line max.                    | 0,00 [%]      |            |
| Dotted line min.                    | 9,84 [%]      |            |

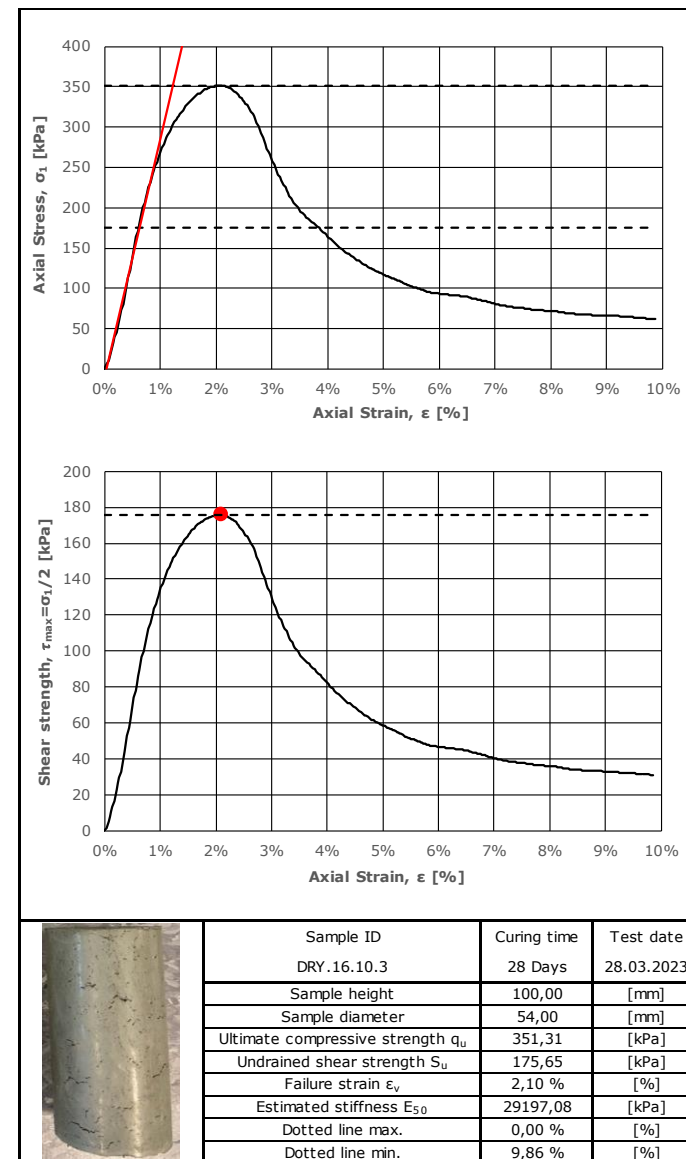
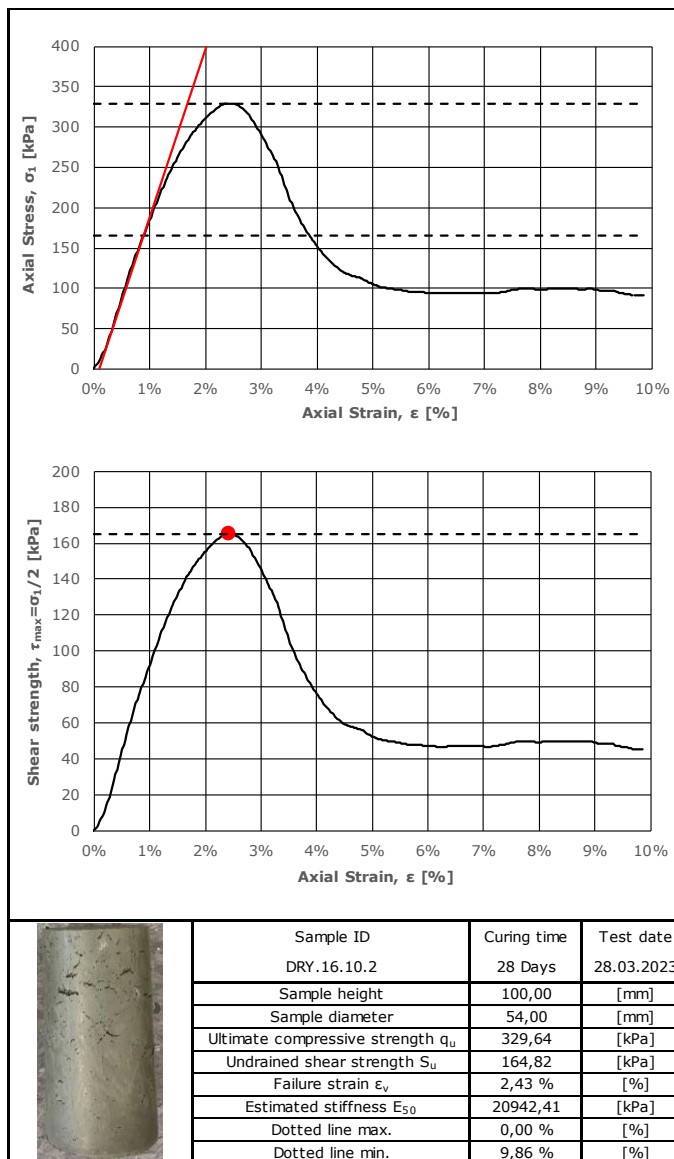
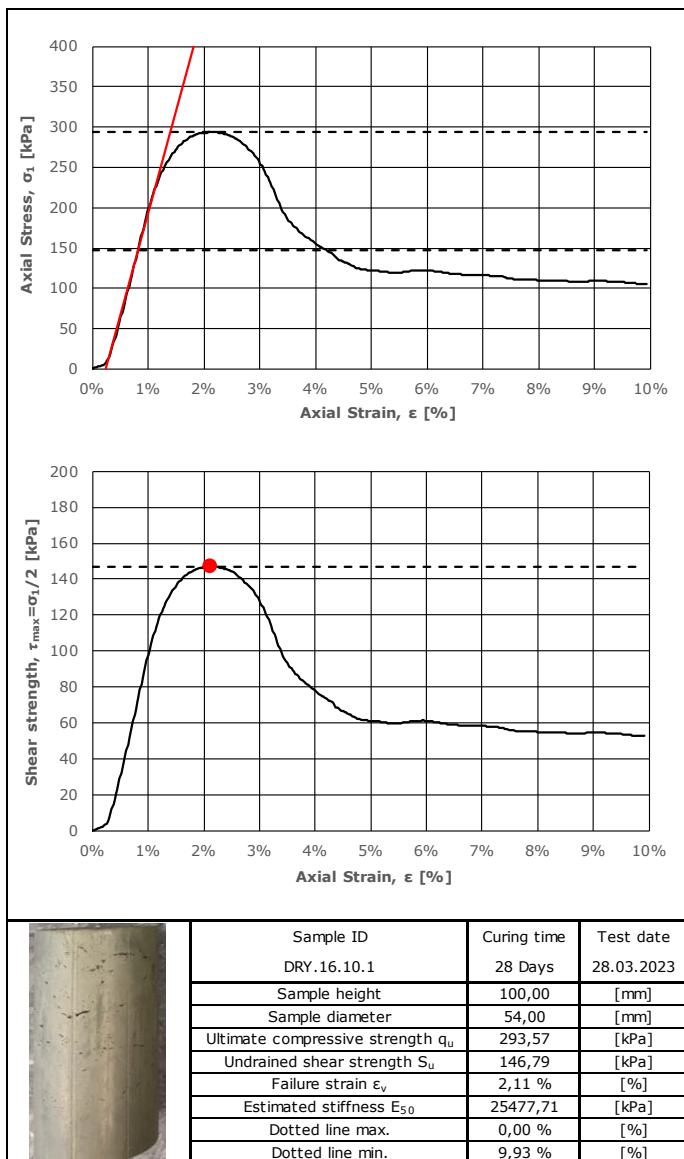


| Sample ID                           | Curing time   | Test date  |
|-------------------------------------|---------------|------------|
| DRY.16.9.2                          | 28 Days       | 28.03.2023 |
| Sample height                       | 100,00 [mm]   |            |
| Sample diameter                     | 54,00 [mm]    |            |
| Ultimate compressive strength $q_u$ | 215,35 [kPa]  |            |
| Undrained shear strength $S_u$      | 107,67 [kPa]  |            |
| Failure strain $\epsilon_v$         | 3,77 [%]      |            |
| Estimated stiffness $E_{50}$        | 9771,99 [kPa] |            |
| Dotted line max.                    | 0,00 [%]      |            |
| Dotted line min.                    | 9,96 [%]      |            |

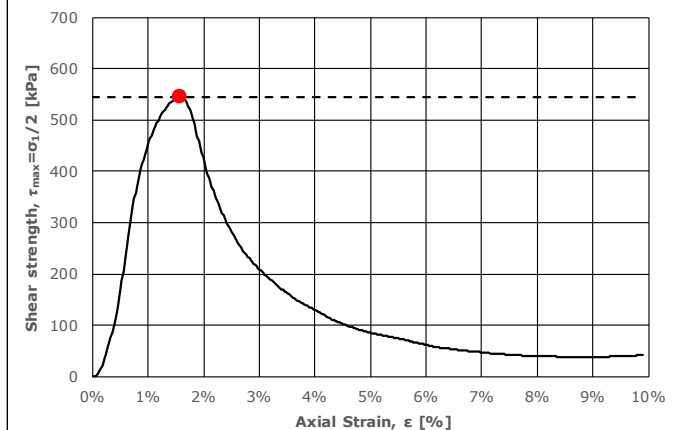
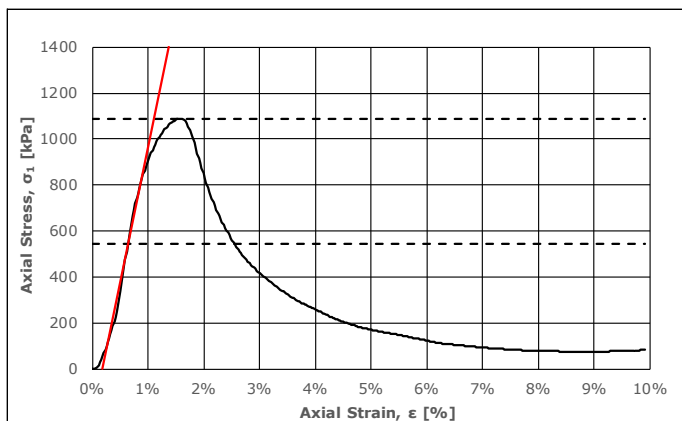


| Sample ID                           | Curing time   | Test date  |
|-------------------------------------|---------------|------------|
| DRY.16.9.3                          | 28 Days       | 28.03.2023 |
| Sample height                       | 100,00 [mm]   |            |
| Sample diameter                     | 54,00 [mm]    |            |
| Ultimate compressive strength $q_u$ | 177,05 [kPa]  |            |
| Undrained shear strength $S_u$      | 88,53 [kPa]   |            |
| Failure strain $\epsilon_v$         | 3,00 [%]      |            |
| Estimated stiffness $E_{50}$        | 8287,29 [kPa] |            |
| Dotted line max.                    | 0,00 [%]      |            |
| Dotted line min.                    | 9,74 [%]      |            |

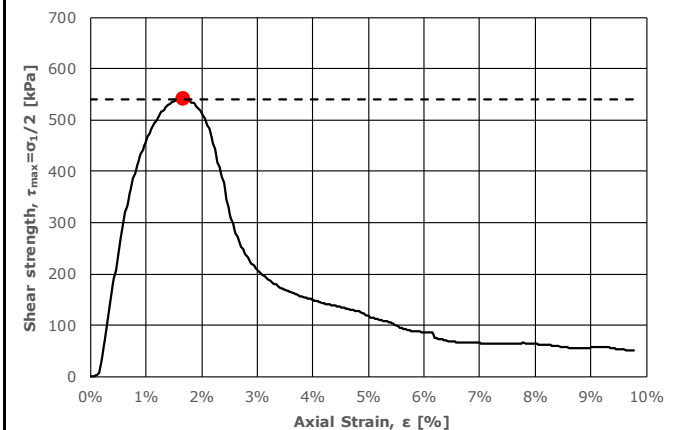
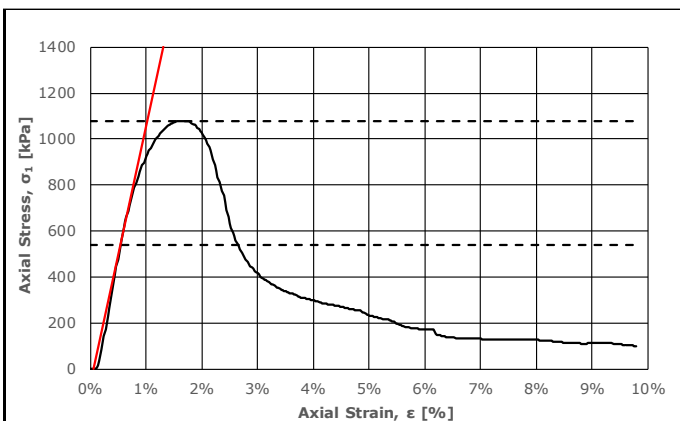
# APPENDIX B.1 SAMPLE IMAGES AND UNCONFINED COMPRESSION TEST RESULTS



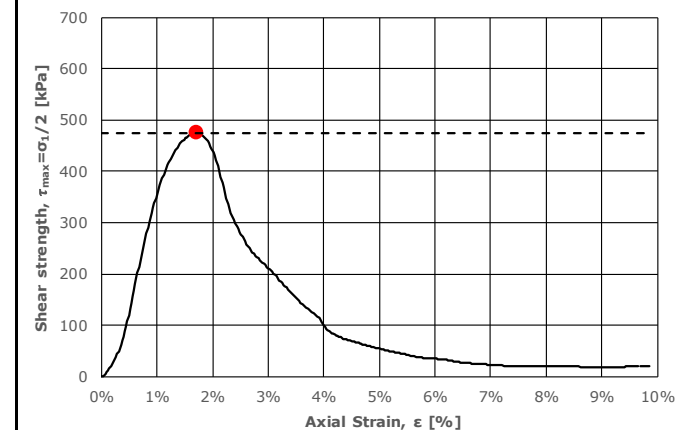
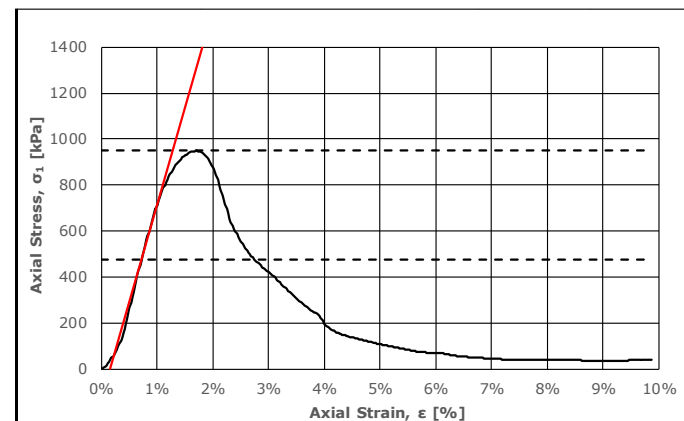
# APPENDIX B.1 SAMPLE IMAGES AND UNCONFINED COMPRESSION TEST RESULTS



| Sample ID                           | Curing time     | Test date  |
|-------------------------------------|-----------------|------------|
| WET.8.1.1                           | 28 Days         | 16.03.2023 |
| Sample height                       | 100,00 [mm]     |            |
| Sample diameter                     | 54,00 [mm]      |            |
| Ultimate compressive strength $q_u$ | 1089,52 [kPa]   |            |
| Undrained shear strength $S_u$      | 544,76 [kPa]    |            |
| Failure strain $\epsilon_v$         | 1,57 [%]        |            |
| Estimated stiffness $E_{50}$        | 118644,07 [kPa] |            |
| Dotted line max.                    | 0,00 [%]        |            |
| Dotted line min.                    | 9,91 [%]        |            |

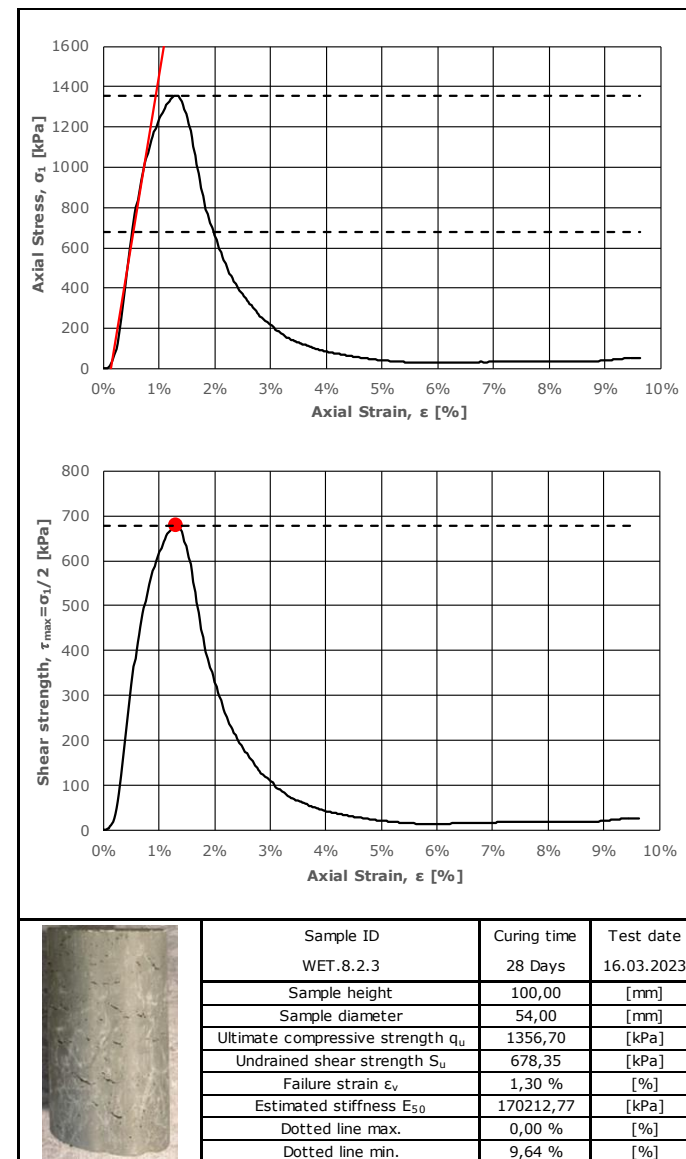
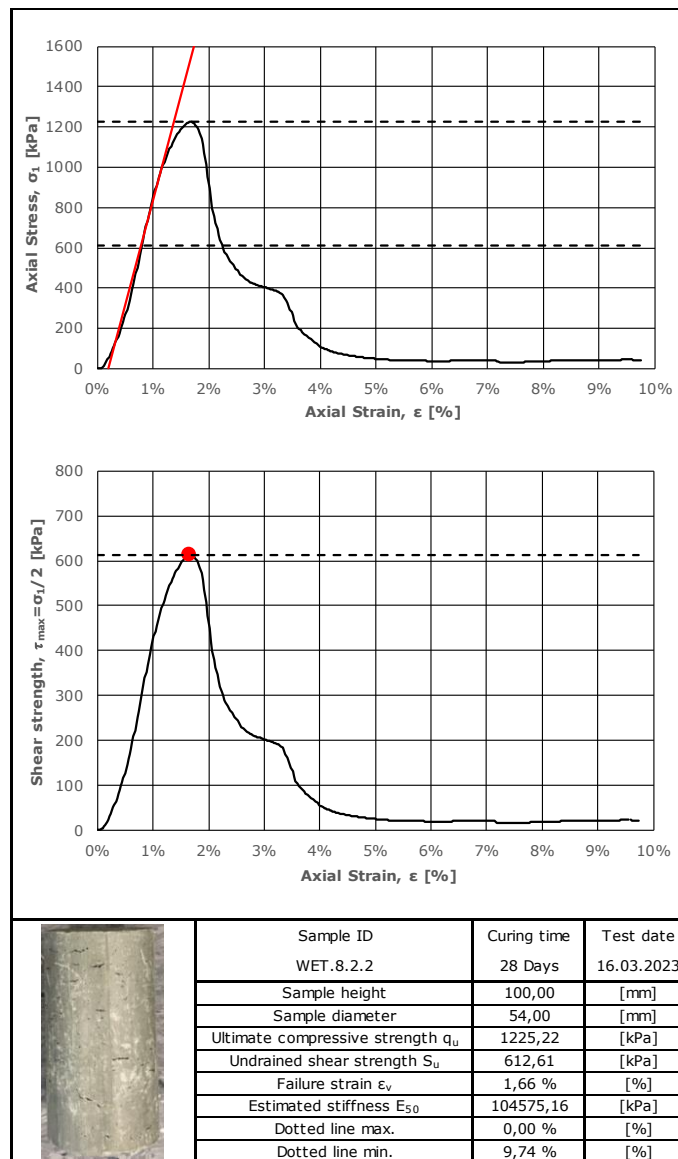
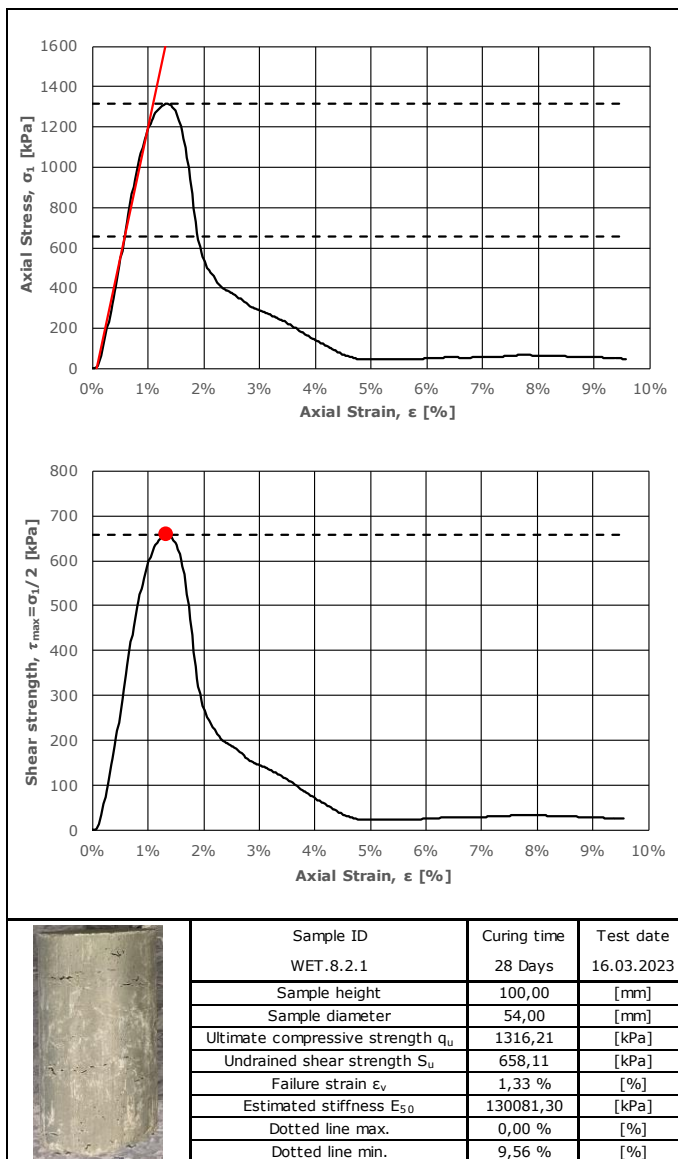


| Sample ID                           | Curing time     | Test date  |
|-------------------------------------|-----------------|------------|
| WET.8.1.2                           | 28 Days         | 16.03.2023 |
| Sample height                       | 100,00 [mm]     |            |
| Sample diameter                     | 54,00 [mm]      |            |
| Ultimate compressive strength $q_u$ | 1080,58 [kPa]   |            |
| Undrained shear strength $S_u$      | 540,29 [kPa]    |            |
| Failure strain $\epsilon_v$         | 1,67 [%]        |            |
| Estimated stiffness $E_{50}$        | 112903,23 [kPa] |            |
| Dotted line max.                    | 0,00 [%]        |            |
| Dotted line min.                    | 9,78 [%]        |            |

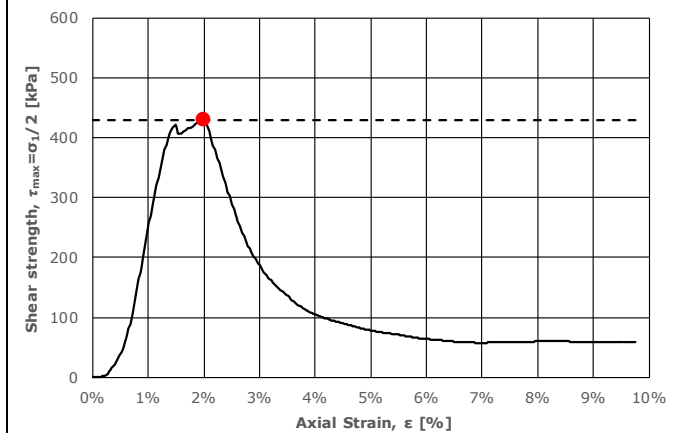
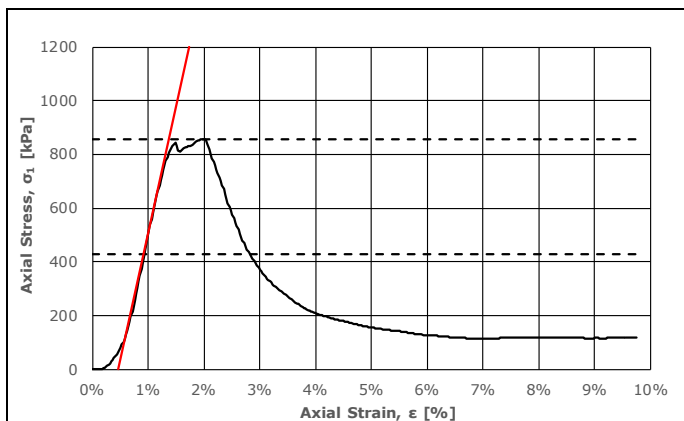


| Sample ID                           | Curing time    | Test date  |
|-------------------------------------|----------------|------------|
| WET.8.1.3                           | 28 Days        | 16.03.2023 |
| Sample height                       | 100,00 [mm]    |            |
| Sample diameter                     | 54,00 [mm]     |            |
| Ultimate compressive strength $q_u$ | 948,88 [kPa]   |            |
| Undrained shear strength $S_u$      | 474,44 [kPa]   |            |
| Failure strain $\epsilon_v$         | 1,71 [%]       |            |
| Estimated stiffness $E_{50}$        | 84848,48 [kPa] |            |
| Dotted line max.                    | 0,00 [%]       |            |
| Dotted line min.                    | 9,86 [%]       |            |

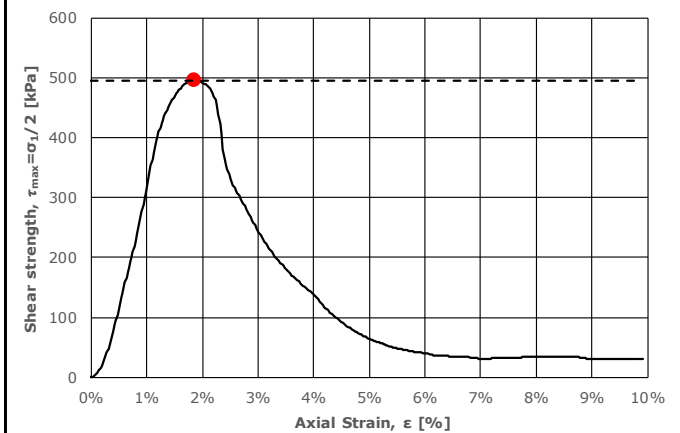
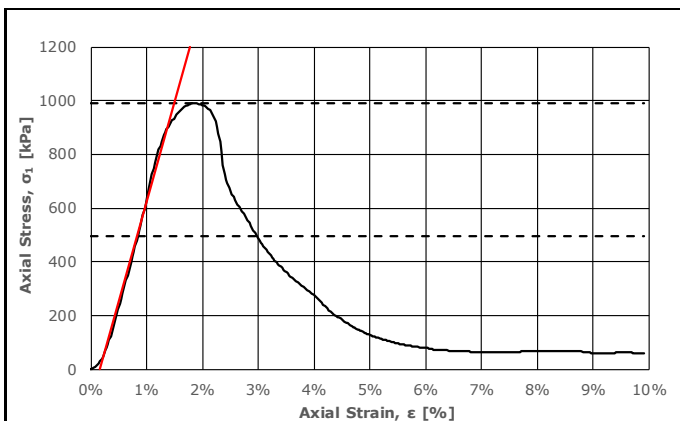
# APPENDIX B.1 SAMPLE IMAGES AND UNCONFINED COMPRESSION TEST RESULTS



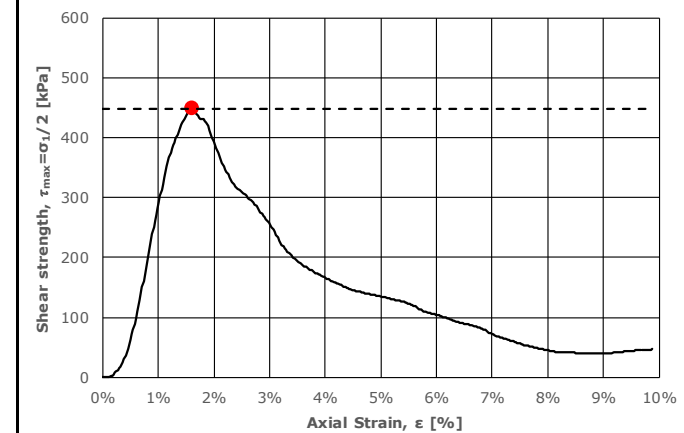
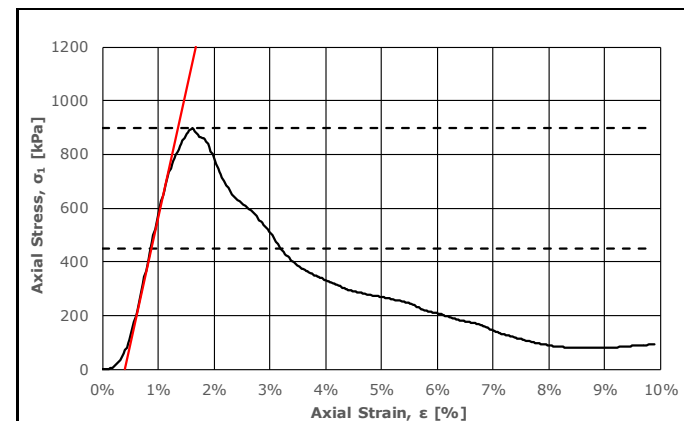
# APPENDIX B.1 SAMPLE IMAGES AND UNCONFINED COMPRESSION TEST RESULTS



| Sample ID                           | Curing time    | Test date  |
|-------------------------------------|----------------|------------|
| WET.8.3.1                           | 28 Days        | 17.03.2023 |
| Sample height                       | 100,00 [mm]    |            |
| Sample diameter                     | 54,00 [mm]     |            |
| Ultimate compressive strength $q_u$ | 857,41 [kPa]   |            |
| Undrained shear strength $S_u$      | 428,70 [kPa]   |            |
| Failure strain $\epsilon_v$         | 1,99 [%]       |            |
| Estimated stiffness $E_{50}$        | 95238,10 [kPa] |            |
| Dotted line max.                    | 0,00 [%]       |            |
| Dotted line min.                    | 9,75 [%]       |            |

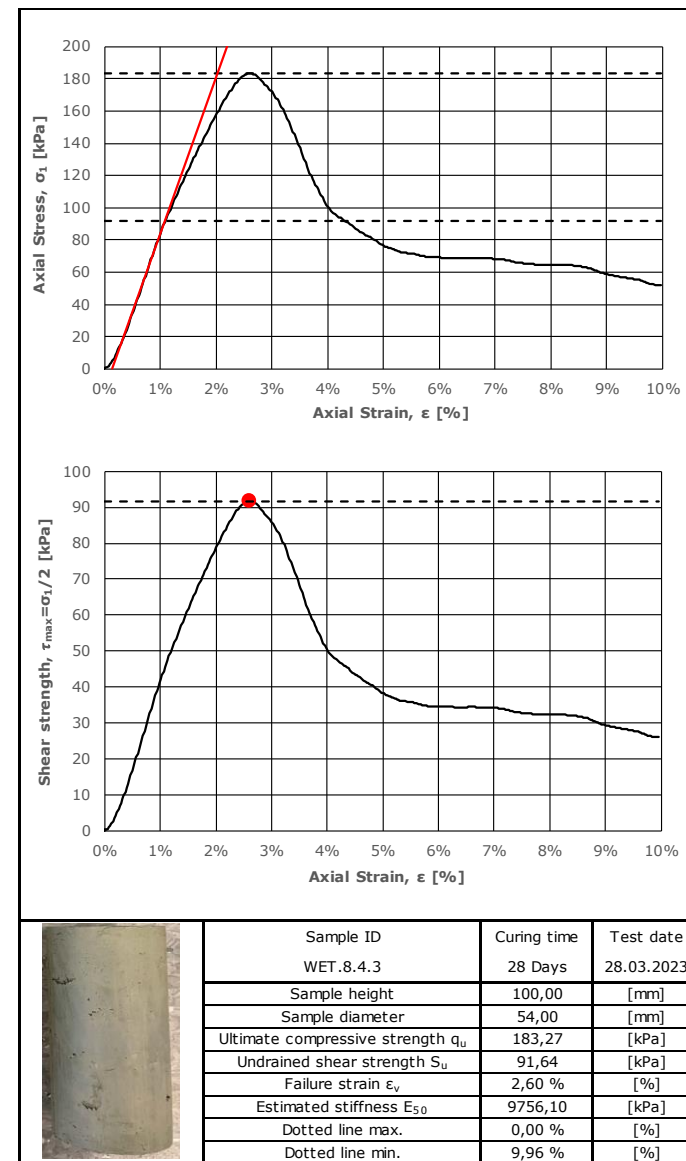
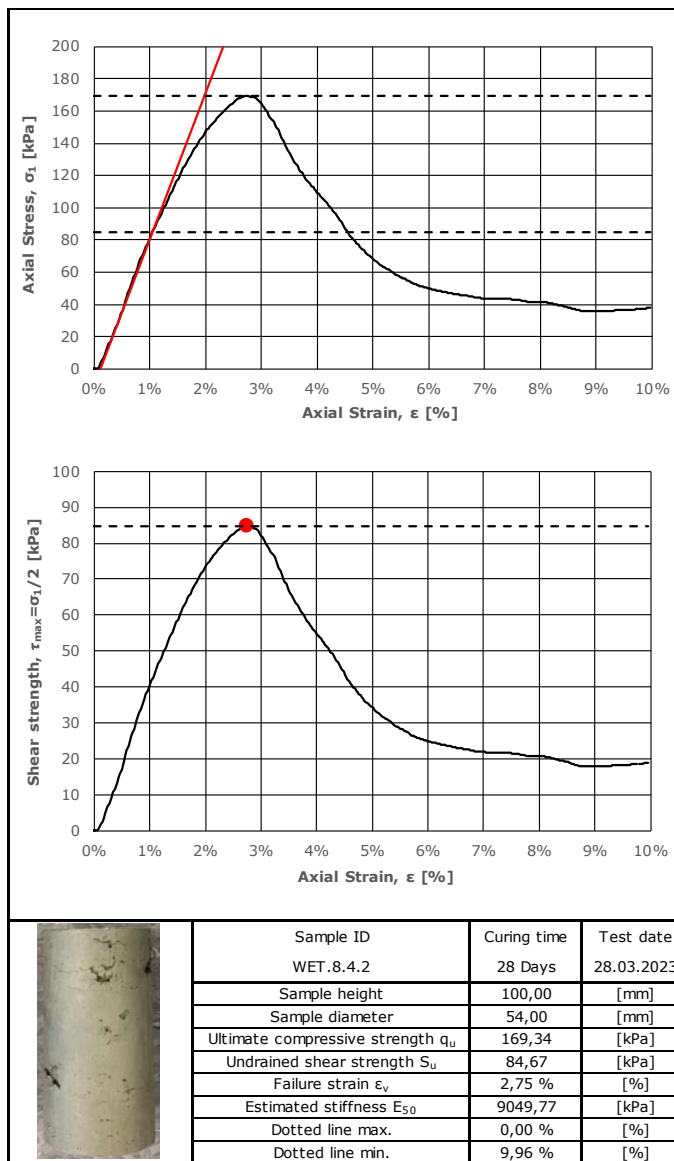
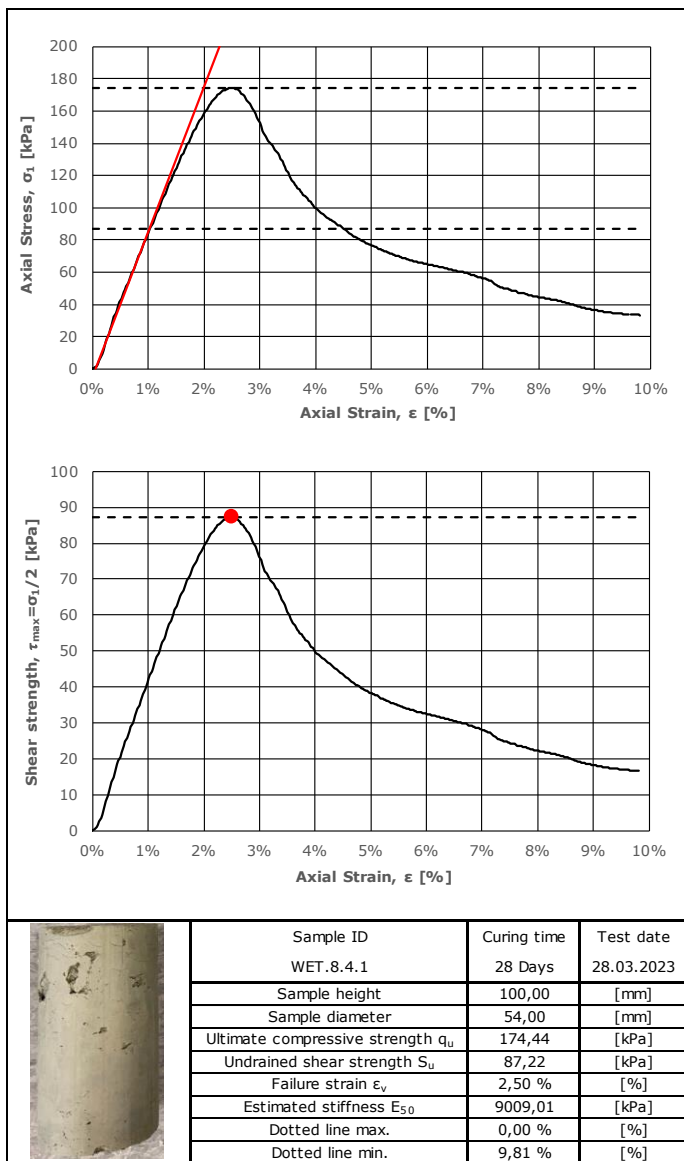


| Sample ID                           | Curing time    | Test date  |
|-------------------------------------|----------------|------------|
| WET.8.3.2                           | 28 Days        | 17.03.2023 |
| Sample height                       | 100,00 [mm]    |            |
| Sample diameter                     | 54,00 [mm]     |            |
| Ultimate compressive strength $q_u$ | 991,36 [kPa]   |            |
| Undrained shear strength $S_u$      | 495,68 [kPa]   |            |
| Failure strain $\epsilon_v$         | 1,85 [%]       |            |
| Estimated stiffness $E_{50}$        | 74534,16 [kPa] |            |
| Dotted line max.                    | 0,00 [%]       |            |
| Dotted line min.                    | 9,91 [%]       |            |

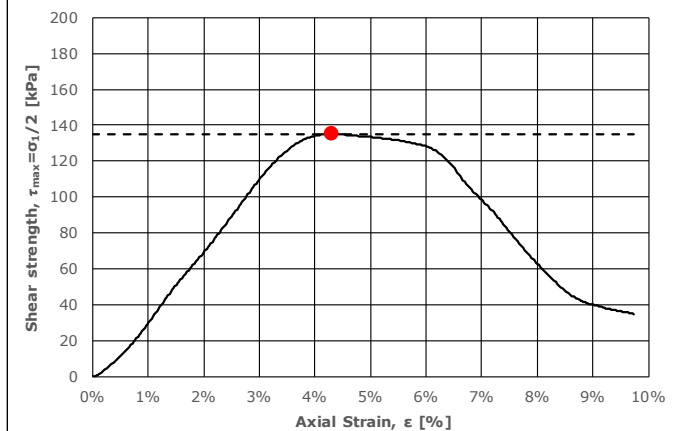
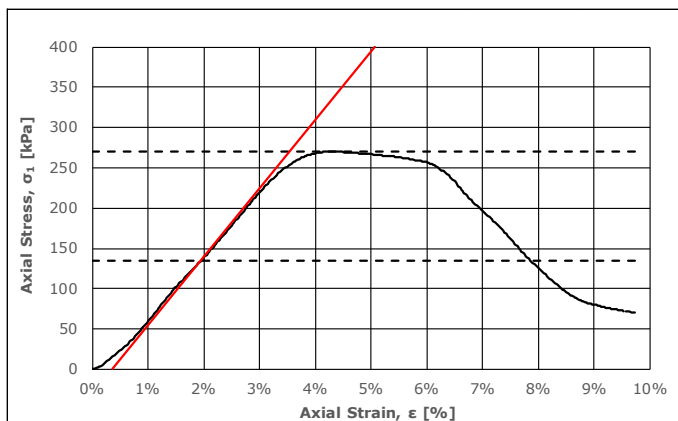


| Sample ID                           | Curing time    | Test date  |
|-------------------------------------|----------------|------------|
| WET.8.3.2                           | 28 Days        | 17.03.2023 |
| Sample height                       | 100,00 [mm]    |            |
| Sample diameter                     | 54,00 [mm]     |            |
| Ultimate compressive strength $q_u$ | 897,55 [kPa]   |            |
| Undrained shear strength $S_u$      | 448,77 [kPa]   |            |
| Failure strain $\epsilon_v$         | 1,61 [%]       |            |
| Estimated stiffness $E_{50}$        | 94488,19 [kPa] |            |
| Dotted line max.                    | 0,00 [%]       |            |
| Dotted line min.                    | 9,88 [%]       |            |

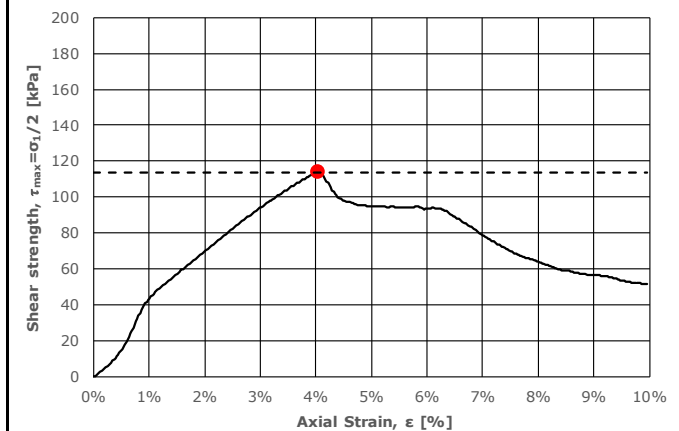
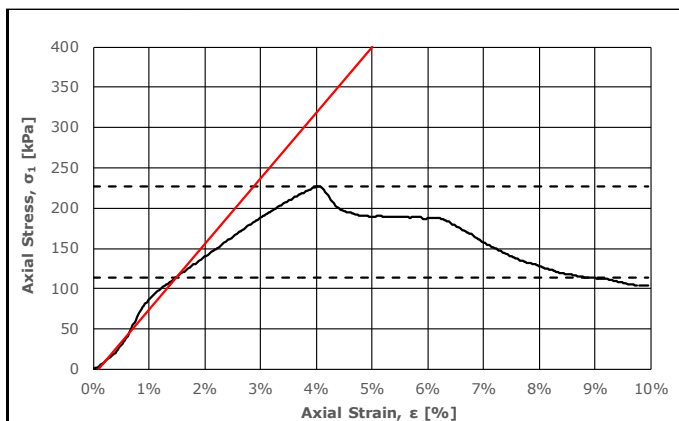
# APPENDIX B.1 SAMPLE IMAGES AND UNCONFINED COMPRESSION TEST RESULTS



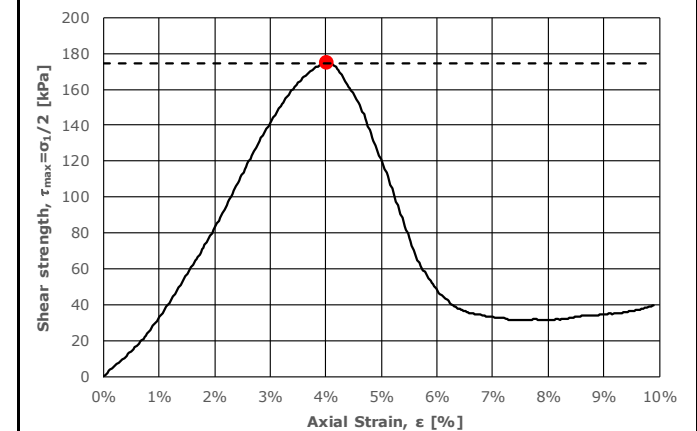
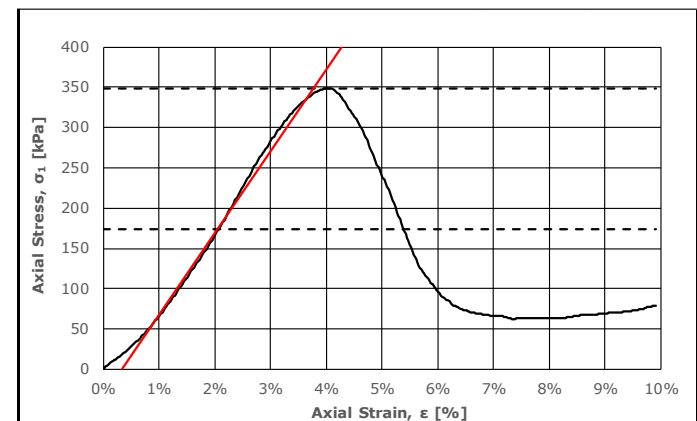
# APPENDIX B.1 SAMPLE IMAGES AND UNCONFINED COMPRESSION TEST RESULTS



| Sample ID                           | Curing time   | Test date  |
|-------------------------------------|---------------|------------|
| WET.8.5.1                           | 28 Days       | 28.03.2023 |
| Sample height                       | 100,00 [mm]   |            |
| Sample diameter                     | 54,00 [mm]    |            |
| Ultimate compressive strength $q_u$ | 270,28 [kPa]  |            |
| Undrained shear strength $S_u$      | 135,14 [kPa]  |            |
| Failure strain $\epsilon_v$         | 4,31 [%]      |            |
| Estimated stiffness $E_{50}$        | 8528,78 [kPa] |            |
| Dotted line max.                    | 0,00 [%]      |            |
| Dotted line min.                    | 9,73 [%]      |            |

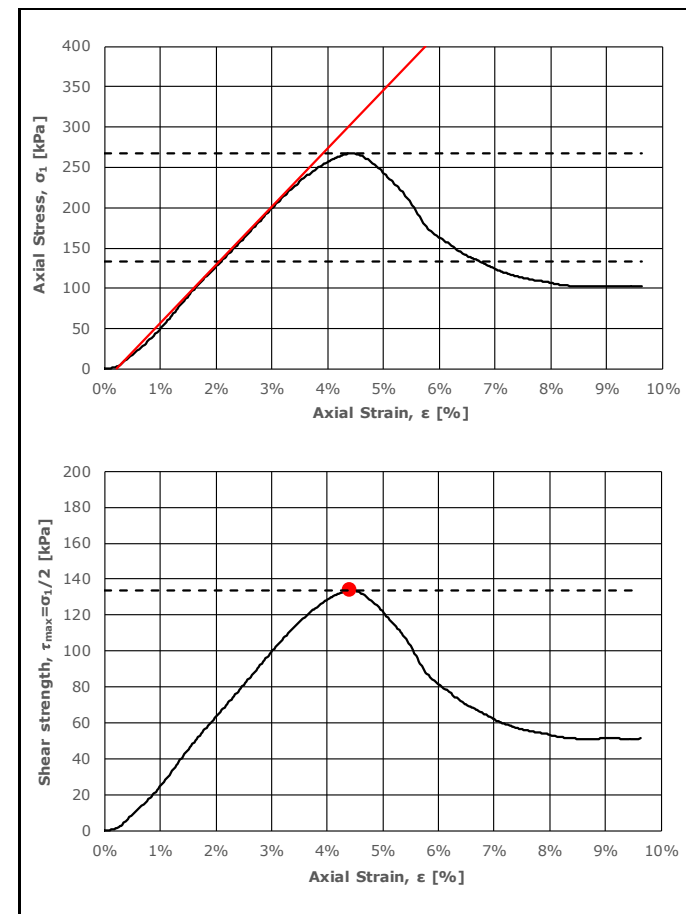
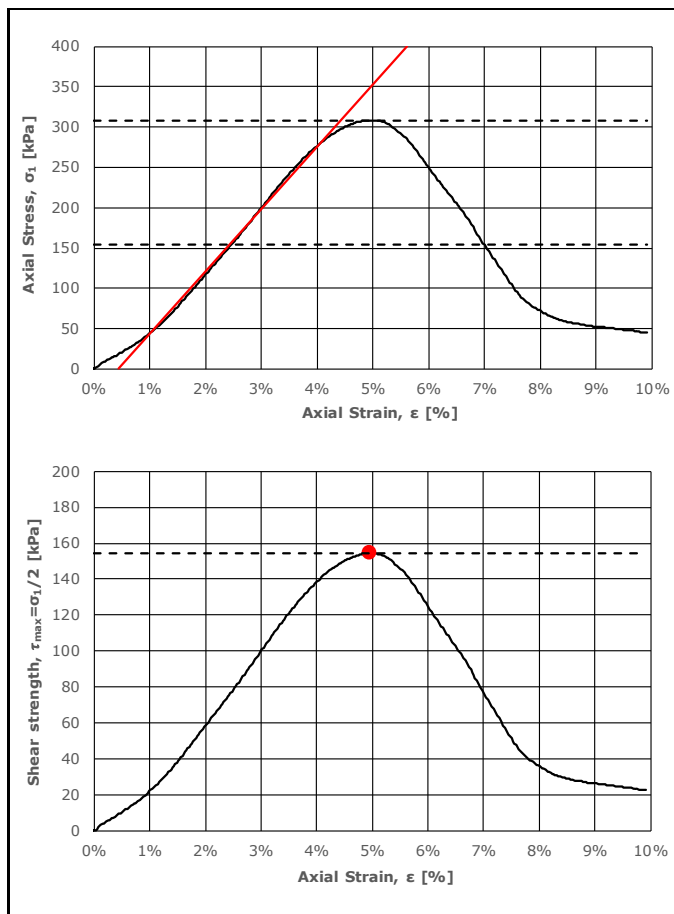
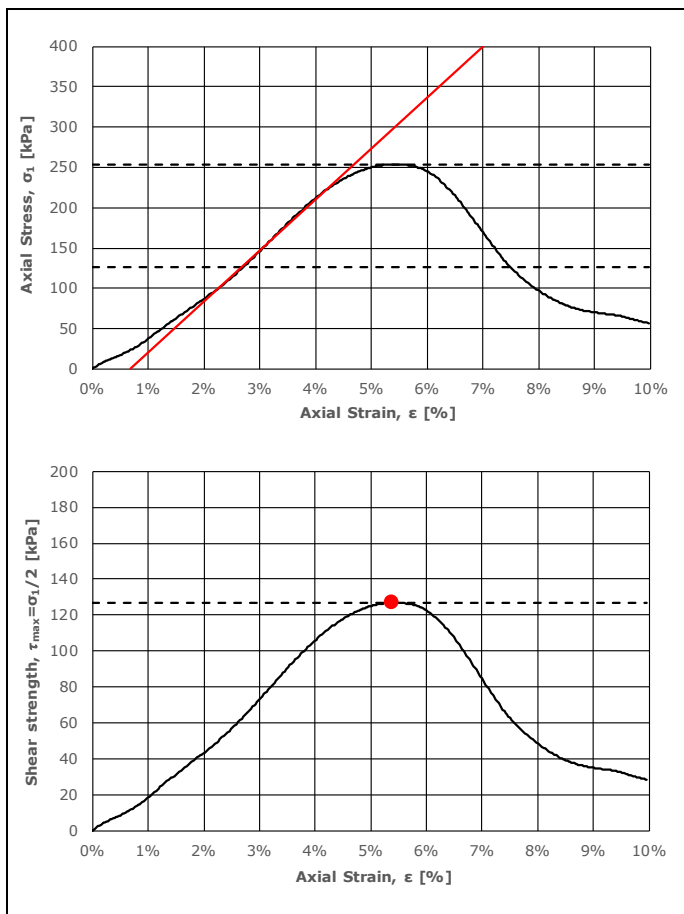



| Sample ID                           | Curing time   | Test date  |
|-------------------------------------|---------------|------------|
| WET.8.5.2                           | 28 Days       | 28.03.2023 |
| Sample height                       | 100,00 [mm]   |            |
| Sample diameter                     | 54,00 [mm]    |            |
| Ultimate compressive strength $q_u$ | 227,14 [kPa]  |            |
| Undrained shear strength $S_u$      | 113,57 [kPa]  |            |
| Failure strain $\epsilon_v$         | 4,04 [%]      |            |
| Estimated stiffness $E_{50}$        | 8179,96 [kPa] |            |
| Dotted line max.                    | 0,00 [%]      |            |
| Dotted line min.                    | 9,95 [%]      |            |





| Sample ID                           | Curing time    | Test date  |
|-------------------------------------|----------------|------------|
| WET.8.5.3                           | 28 Days        | 28.03.2023 |
| Sample height                       | 100,00 [mm]    |            |
| Sample diameter                     | 54,00 [mm]     |            |
| Ultimate compressive strength $q_u$ | 348,97 [kPa]   |            |
| Undrained shear strength $S_u$      | 174,49 [kPa]   |            |
| Failure strain $\epsilon_v$         | 4,03 [%]       |            |
| Estimated stiffness $E_{50}$        | 10178,12 [kPa] |            |
| Dotted line max.                    | 0,00 [%]       |            |
| Dotted line min.                    | 9,91 [%]       |            |

# APPENDIX B.1 SAMPLE IMAGES AND UNCONFINED COMPRESSION TEST RESULTS



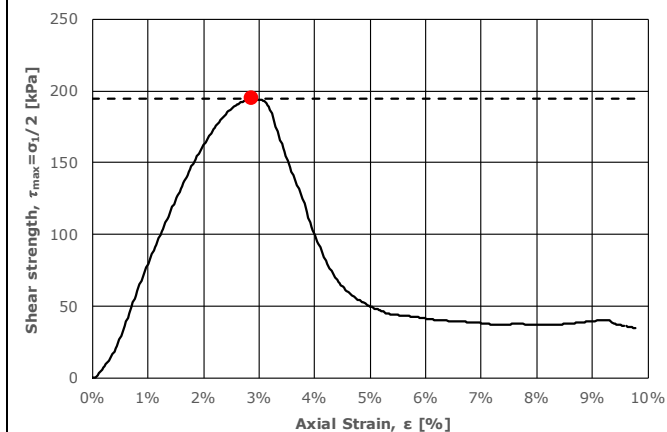
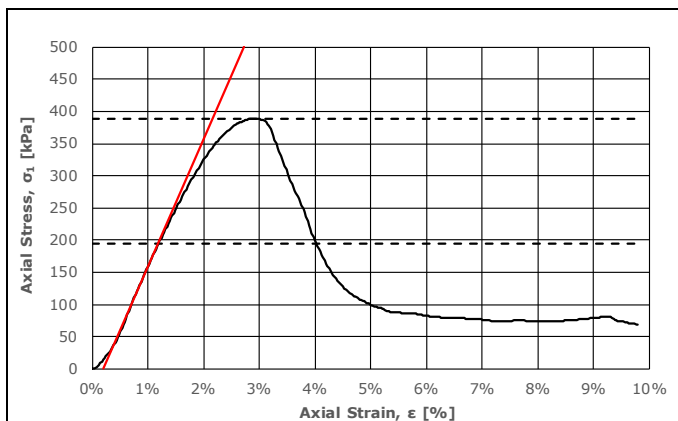
|   |                                     |           |             |         |           |            |
|---|-------------------------------------|-----------|-------------|---------|-----------|------------|
|  | Sample ID                           | WET.8.6.1 | Curing time | 28 Days | Test date | 29.03.2023 |
|   | Sample height                       | 100,00    | [mm]        |         |           |            |
|   | Sample diameter                     | 54,00     | [mm]        |         |           |            |
|   | Ultimate compressive strength $q_u$ | 253,71    | [kPa]       |         |           |            |
|   | Undrained shear strength $S_u$      | 126,86    | [kPa]       |         |           |            |
|   | Failure strain $\epsilon_v$         | 5,39      | [%]         |         |           |            |
|   | Estimated stiffness $E_{50}$        | 6339,14   | [kPa]       |         |           |            |
|   | Dotted line max.                    | 0,00      | [%]         |         |           |            |
| Dotted line min.  | 9,96                                | [%]       |             |         |           |            |

|   |                                     |           |             |         |           |            |
|---|-------------------------------------|-----------|-------------|---------|-----------|------------|
|  | Sample ID                           | WET.8.6.2 | Curing time | 28 Days | Test date | 29.03.2023 |
|   | Sample height                       | 100,00    | [mm]        |         |           |            |
|   | Sample diameter                     | 54,00     | [mm]        |         |           |            |
|   | Ultimate compressive strength $q_u$ | 308,65    | [kPa]       |         |           |            |
|   | Undrained shear strength $S_u$      | 154,32    | [kPa]       |         |           |            |
|   | Failure strain $\epsilon_v$         | 4,96      | [%]         |         |           |            |
|   | Estimated stiffness $E_{50}$        | 7736,94   | [kPa]       |         |           |            |
|   | Dotted line max.                    | 0,00      | [%]         |         |           |            |
| Dotted line min.  | 9,91                                | [%]       |             |         |           |            |

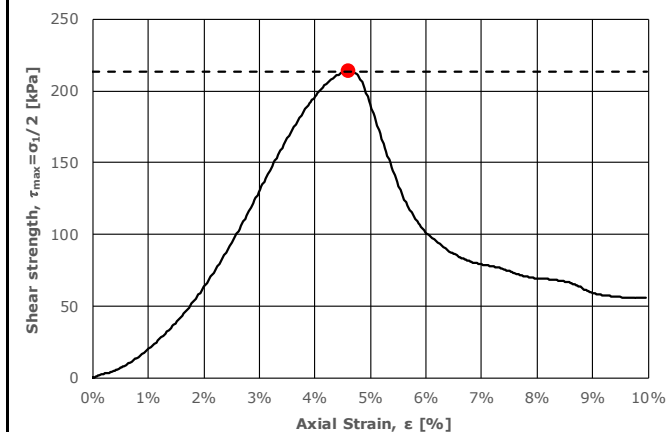
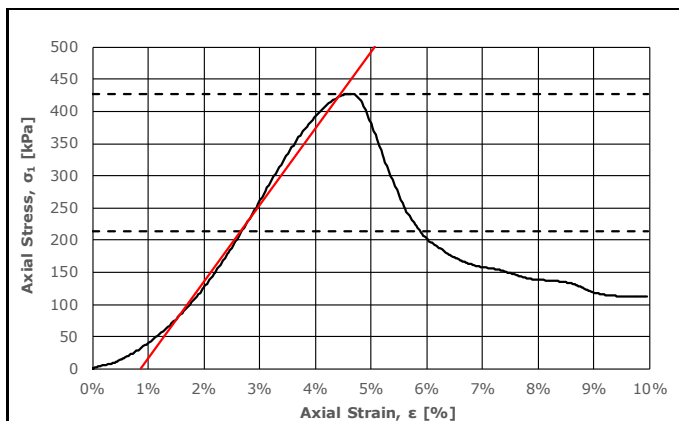
|   |                                     |           |             |         |           |            |
|---|-------------------------------------|-----------|-------------|---------|-----------|------------|
|  | Sample ID                           | WET.8.6.3 | Curing time | 28 Days | Test date | 29.03.2023 |
|   | Sample height                       | 100,00    | [mm]        |         |           |            |
|   | Sample diameter                     | 54,00     | [mm]        |         |           |            |
|   | Ultimate compressive strength $q_u$ | 267,29    | [kPa]       |         |           |            |
|   | Undrained shear strength $S_u$      | 133,65    | [kPa]       |         |           |            |
|   | Failure strain $\epsilon_v$         | 4,41      | [%]         |         |           |            |
|   | Estimated stiffness $E_{50}$        | 7233,27   | [kPa]       |         |           |            |
|   | Dotted line max.                    | 0,00      | [%]         |         |           |            |
| Dotted line min.  | 9,63                                | [%]       |             |         |           |            |



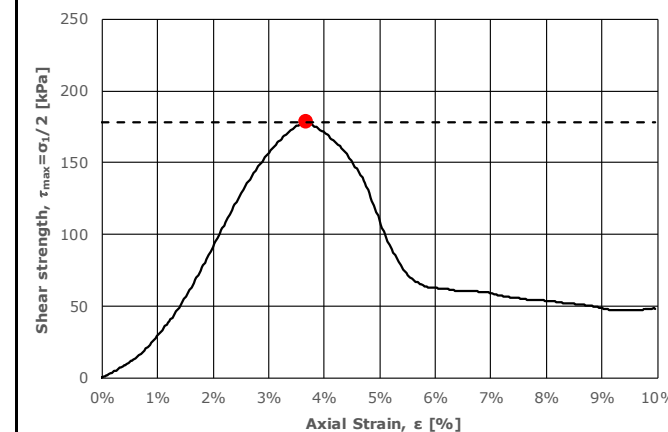
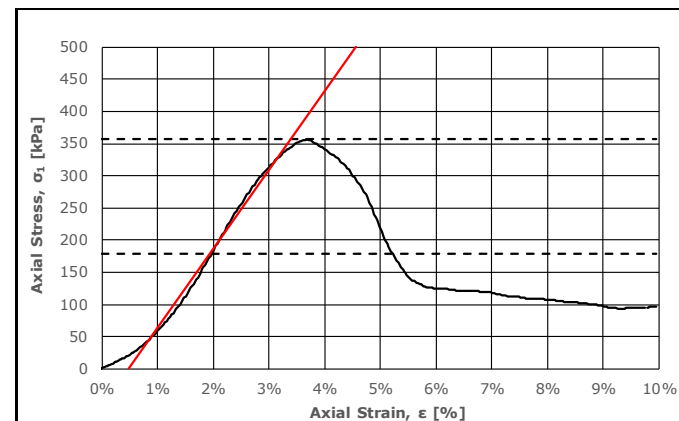
# APPENDIX B.1 SAMPLE IMAGES AND UNCONFINED COMPRESSION TEST RESULTS



| Sample ID                           | Curing time | Test date  |
|-------------------------------------|-------------|------------|
| WET.8.7.1                           | 28 Days     | 29.03.2023 |
| Sample height                       | 100,00      | [mm]       |
| Sample diameter                     | 54,00       | [mm]       |
| Ultimate compressive strength $q_u$ | 388,74      | [kPa]      |
| Undrained shear strength $S_u$      | 194,37      | [kPa]      |
| Failure strain $\epsilon_v$         | 2,88        | [%]        |
| Estimated stiffness $E_{50}$        | 19841,27    | [kPa]      |
| Dotted line max.                    | 0,00        | [%]        |
| Dotted line min.                    | 9,78        | [%]        |

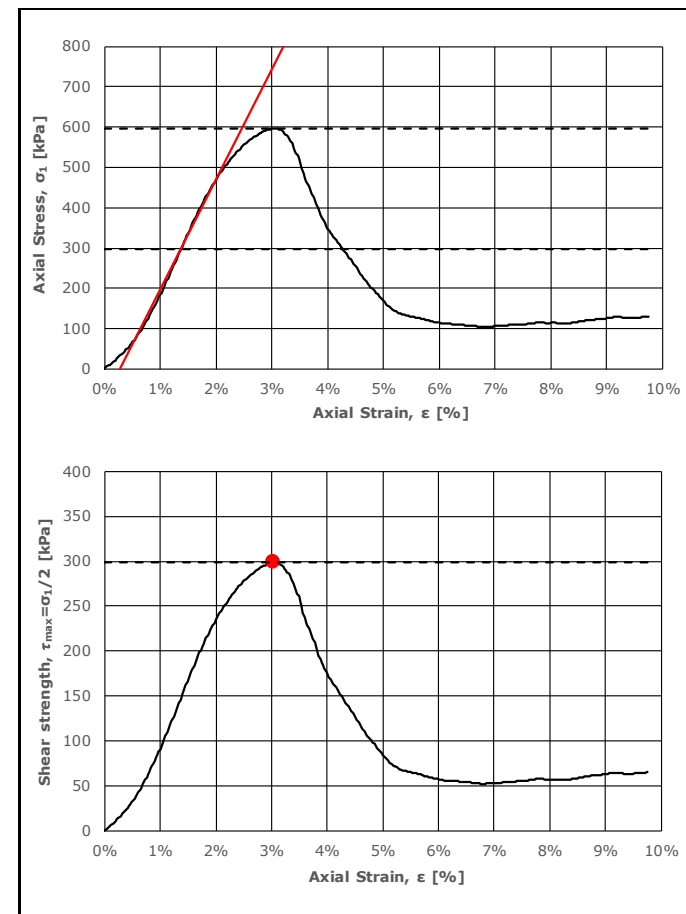
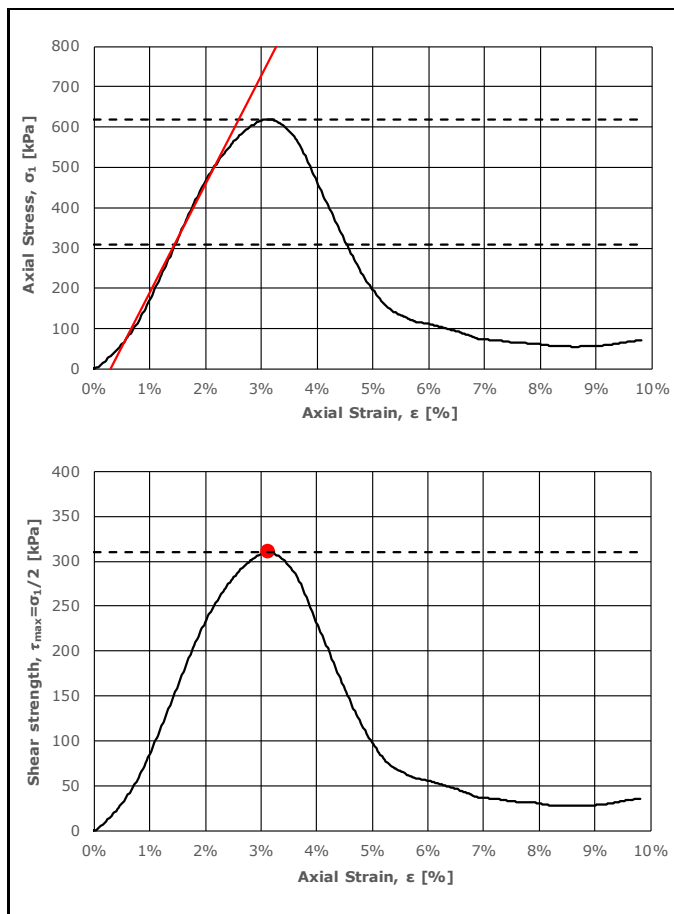
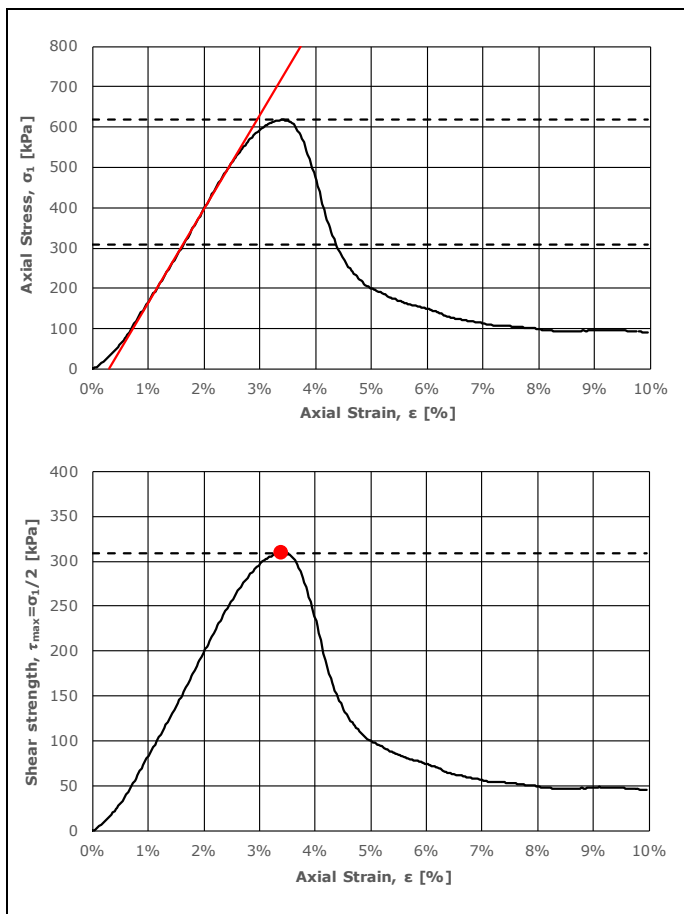



| Sample ID                           | Curing time | Test date  |
|-------------------------------------|-------------|------------|
| WET.8.7.2                           | 28 Days     | 29.03.2023 |
| Sample height                       | 100,00      | [mm]       |
| Sample diameter                     | 54,00       | [mm]       |
| Ultimate compressive strength $q_u$ | 427,45      | [kPa]      |
| Undrained shear strength $S_u$      | 213,72      | [kPa]      |
| Failure strain $\epsilon_v$         | 4,62        | [%]        |
| Estimated stiffness $E_{50}$        | 11933,17    | [kPa]      |
| Dotted line max.                    | 0,00        | [%]        |
| Dotted line min.                    | 9,98        | [%]        |





| Sample ID                           | Curing time | Test date  |
|-------------------------------------|-------------|------------|
| WET.8.7.3                           | 28 Days     | 29.03.2023 |
| Sample height                       | 100,00      | [mm]       |
| Sample diameter                     | 54,00       | [mm]       |
| Ultimate compressive strength $q_u$ | 356,32      | [kPa]      |
| Undrained shear strength $S_u$      | 178,16      | [kPa]      |
| Failure strain $\epsilon_v$         | 3,68        | [%]        |
| Estimated stiffness $E_{50}$        | 12254,90    | [kPa]      |
| Dotted line max.                    | 0,00        | [%]        |
| Dotted line min.                    | 9,95        | [%]        |

# APPENDIX B.1 SAMPLE IMAGES AND UNCONFINED COMPRESSION TEST RESULTS

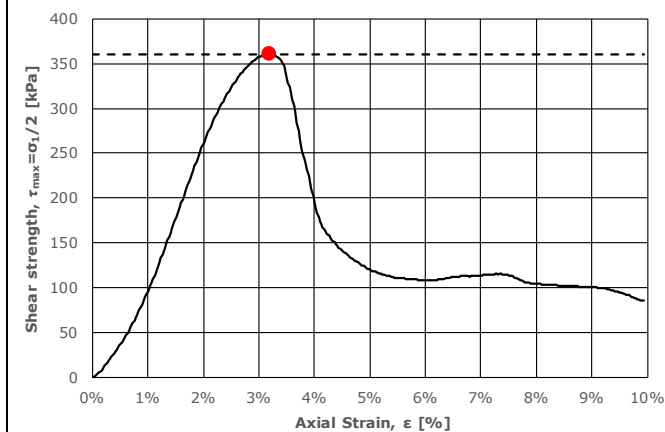
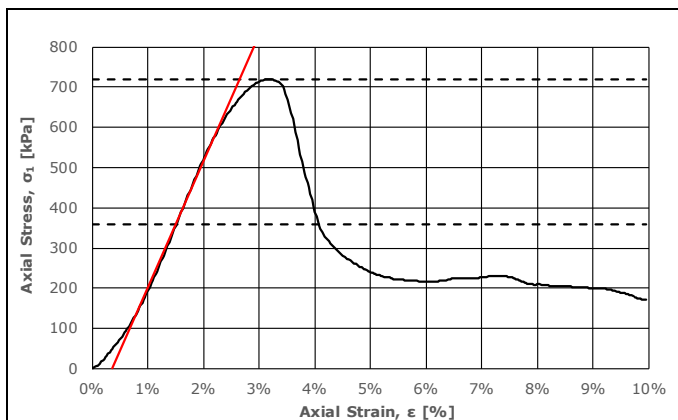


|   |                                     |           |             |         |           |            |
|---|-------------------------------------|-----------|-------------|---------|-----------|------------|
|  | Sample ID                           | WET.8.8.1 | Curing time | 28 Days | Test date | 29.03.2023 |
|   | Sample height                       | 100,00    | [mm]        |         |           |            |
|   | Sample diameter                     | 54,00     | [mm]        |         |           |            |
|   | Ultimate compressive strength $q_u$ | 618,03    | [kPa]       |         |           |            |
|   | Undrained shear strength $S_u$      | 309,01    | [kPa]       |         |           |            |
|   | Failure strain $\epsilon_v$         | 3,41      | [%]         |         |           |            |
|   | Estimated stiffness $E_{50}$        | 23323,62  | [kPa]       |         |           |            |
|   | Dotted line max.                    | 0,00      | [%]         |         |           |            |
|   | Dotted line min.                    | 9,96      | [%]         |         |           |            |

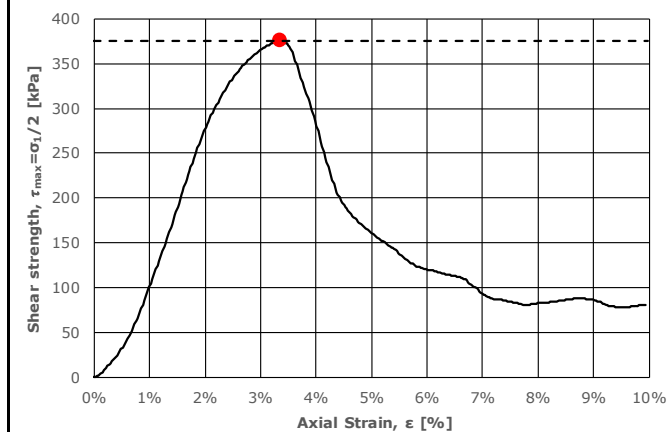
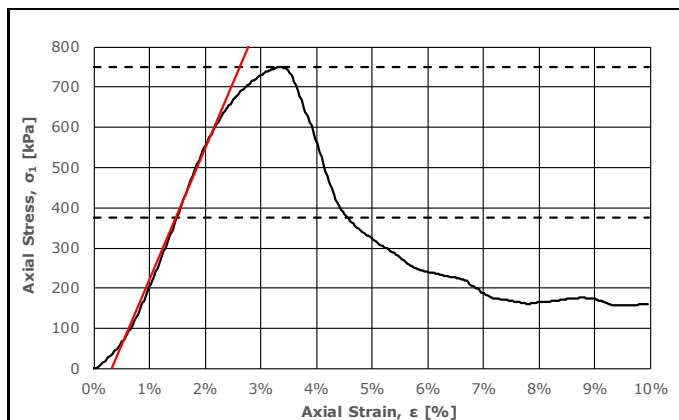
|   |                                     |           |             |         |           |            |
|---|-------------------------------------|-----------|-------------|---------|-----------|------------|
|  | Sample ID                           | WET.8.8.2 | Curing time | 28 Days | Test date | 29.03.2023 |
|   | Sample height                       | 100,00    | [mm]        |         |           |            |
|   | Sample diameter                     | 54,00     | [mm]        |         |           |            |
|   | Ultimate compressive strength $q_u$ | 619,59    | [kPa]       |         |           |            |
|   | Undrained shear strength $S_u$      | 309,79    | [kPa]       |         |           |            |
|   | Failure strain $\epsilon_v$         | 3,13      | [%]         |         |           |            |
|   | Estimated stiffness $E_{50}$        | 27027,03  | [kPa]       |         |           |            |
|   | Dotted line max.                    | 0,00      | [%]         |         |           |            |
|   | Dotted line min.                    | 9,81      | [%]         |         |           |            |

|   |                                     |           |             |         |           |            |
|---|-------------------------------------|-----------|-------------|---------|-----------|------------|
|  | Sample ID                           | WET.8.8.3 | Curing time | 28 Days | Test date | 29.03.2023 |
|   | Sample height                       | 100,00    | [mm]        |         |           |            |
|   | Sample diameter                     | 54,00     | [mm]        |         |           |            |
|   | Ultimate compressive strength $q_u$ | 597,14    | [kPa]       |         |           |            |
|   | Undrained shear strength $S_u$      | 298,57    | [kPa]       |         |           |            |
|   | Failure strain $\epsilon_v$         | 3,03      | [%]         |         |           |            |
|   | Estimated stiffness $E_{50}$        | 27397,26  | [kPa]       |         |           |            |
|   | Dotted line max.                    | 0,00      | [%]         |         |           |            |
|   | Dotted line min.                    | 9,75      | [%]         |         |           |            |

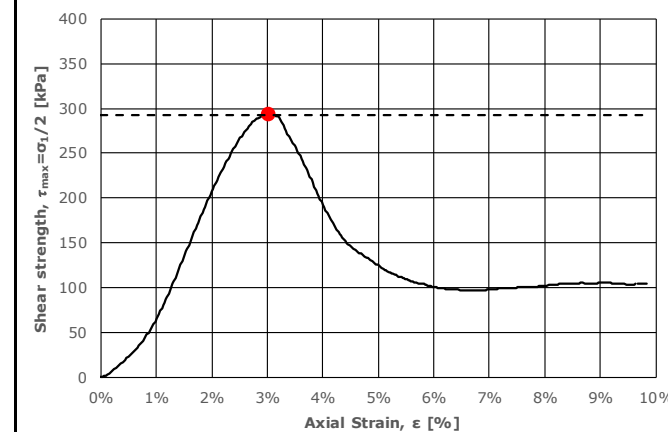
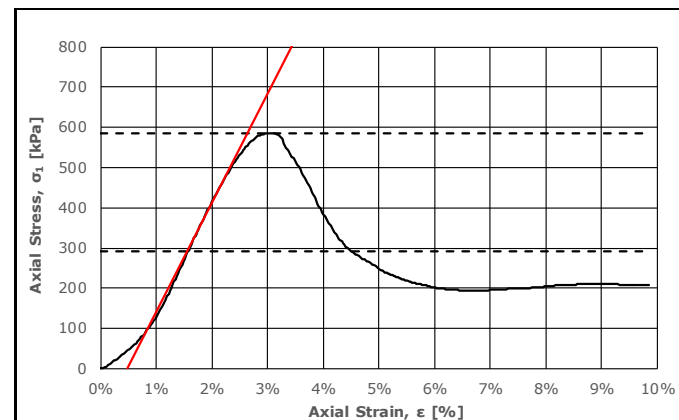
# APPENDIX B.1 SAMPLE IMAGES AND UNCONFINED COMPRESSION TEST RESULTS



| Sample ID                           | Curing time    | Test date  |
|-------------------------------------|----------------|------------|
| WET.8.9.1                           | 28 Days        | 29.03.2023 |
| Sample height                       | 100,00 [mm]    |            |
| Sample diameter                     | 54,00 [mm]     |            |
| Ultimate compressive strength $q_u$ | 719,47 [kPa]   |            |
| Undrained shear strength $S_u$      | 359,74 [kPa]   |            |
| Failure strain $\epsilon_v$         | 3,20 [%]       |            |
| Estimated stiffness $E_{50}$        | 31496,06 [kPa] |            |
| Dotted line max.                    | 0,00 [%]       |            |
| Dotted line min.                    | 9,94 [%]       |            |

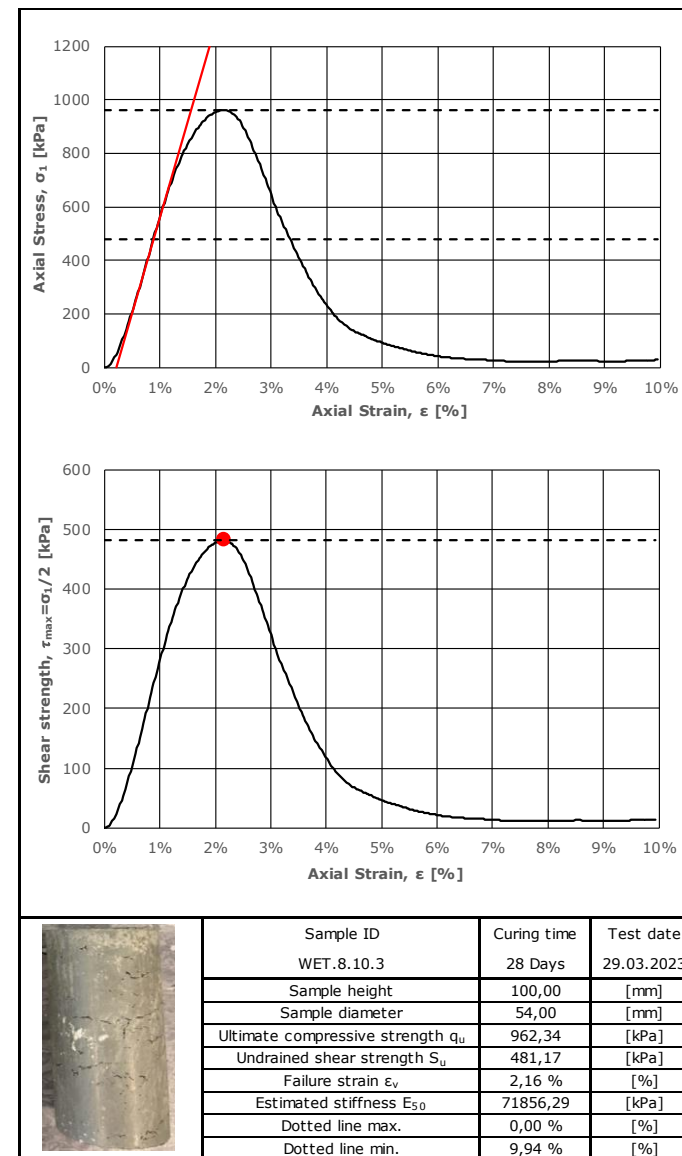
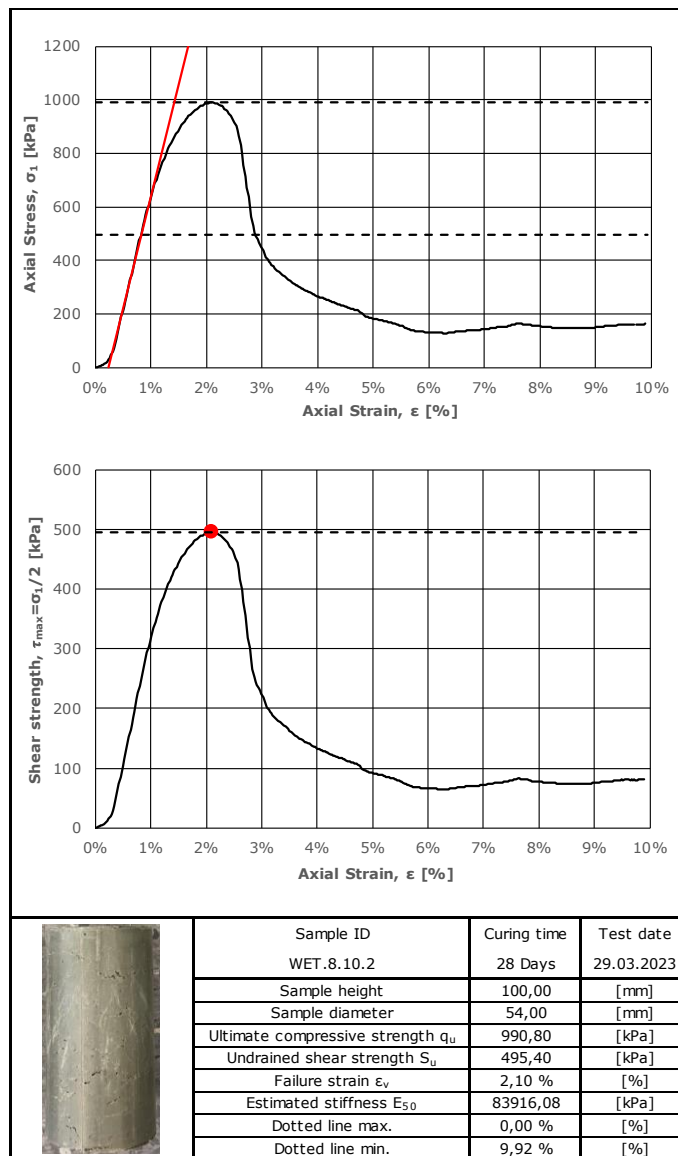
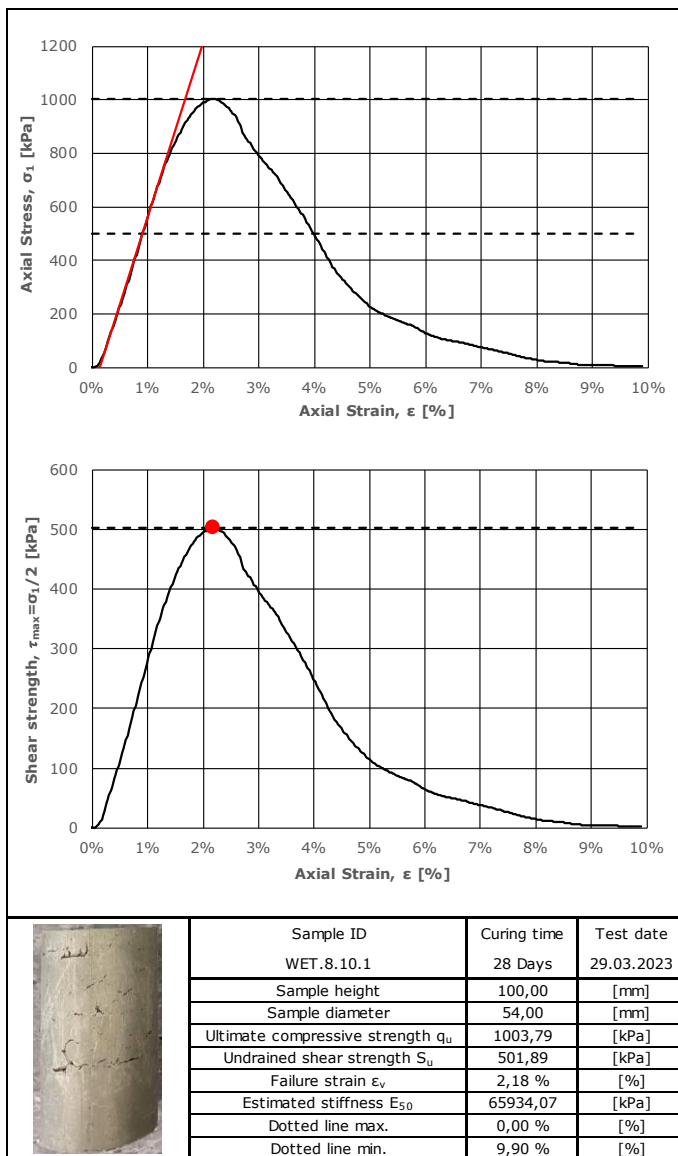


| Sample ID                           | Curing time    | Test date  |
|-------------------------------------|----------------|------------|
| WET.8.9.2                           | 28 Days        | 29.03.2023 |
| Sample height                       | 100,00 [mm]    |            |
| Sample diameter                     | 54,00 [mm]     |            |
| Ultimate compressive strength $q_u$ | 749,78 [kPa]   |            |
| Undrained shear strength $S_u$      | 374,89 [kPa]   |            |
| Failure strain $\epsilon_v$         | 3,35 [%]       |            |
| Estimated stiffness $E_{50}$        | 32586,56 [kPa] |            |
| Dotted line max.                    | 0,00 [%]       |            |
| Dotted line min.                    | 9,97 [%]       |            |

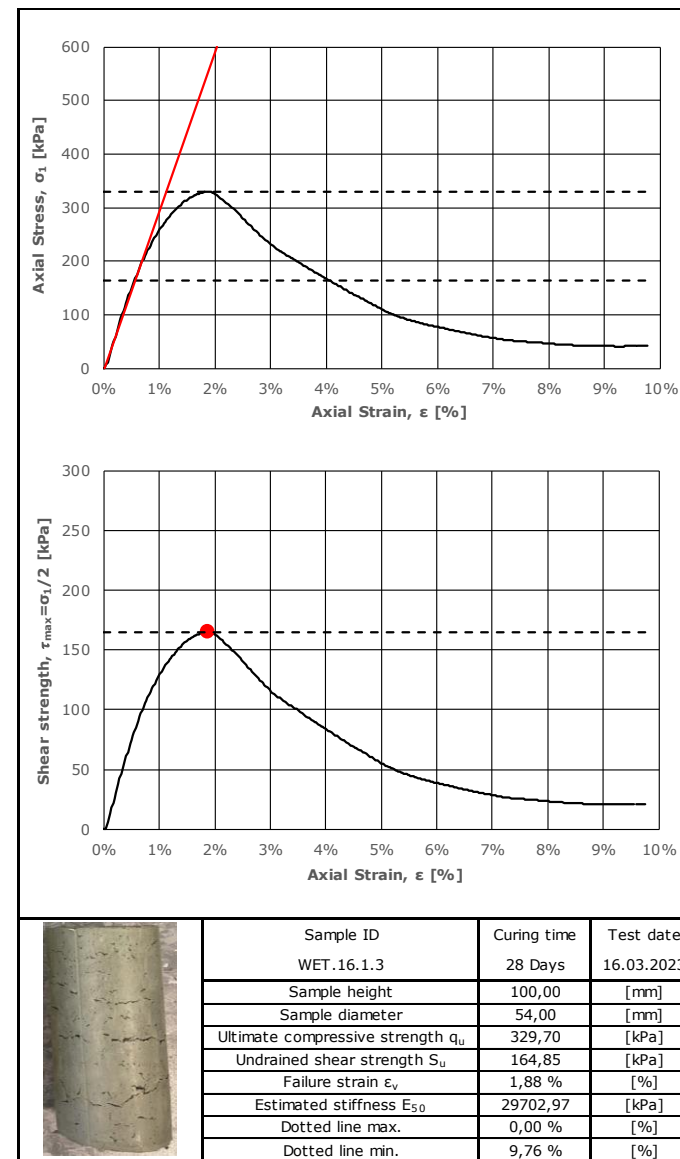
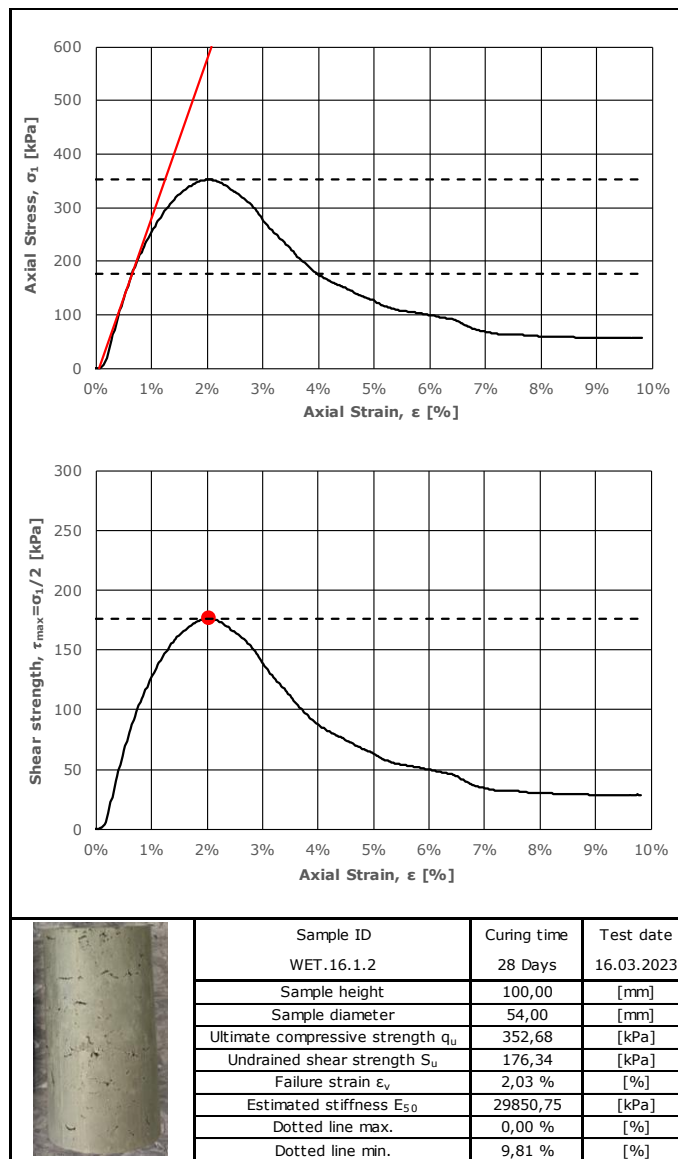
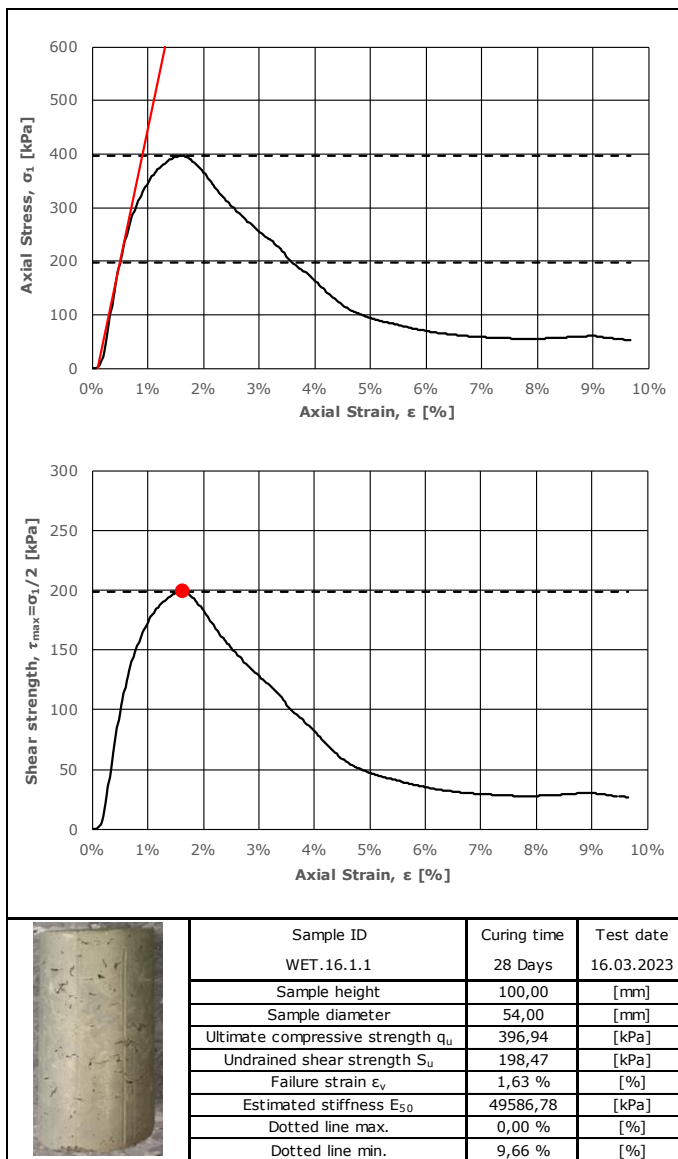


| Sample ID                           | Curing time    | Test date  |
|-------------------------------------|----------------|------------|
| WET.8.9.3                           | 28 Days        | 29.03.2023 |
| Sample height                       | 100,00 [mm]    |            |
| Sample diameter                     | 54,00 [mm]     |            |
| Ultimate compressive strength $q_u$ | 585,65 [kPa]   |            |
| Undrained shear strength $S_u$      | 292,82 [kPa]   |            |
| Failure strain $\epsilon_v$         | 3,03 [%]       |            |
| Estimated stiffness $E_{50}$        | 27164,69 [kPa] |            |
| Dotted line max.                    | 0,00 [%]       |            |
| Dotted line min.                    | 9,87 [%]       |            |

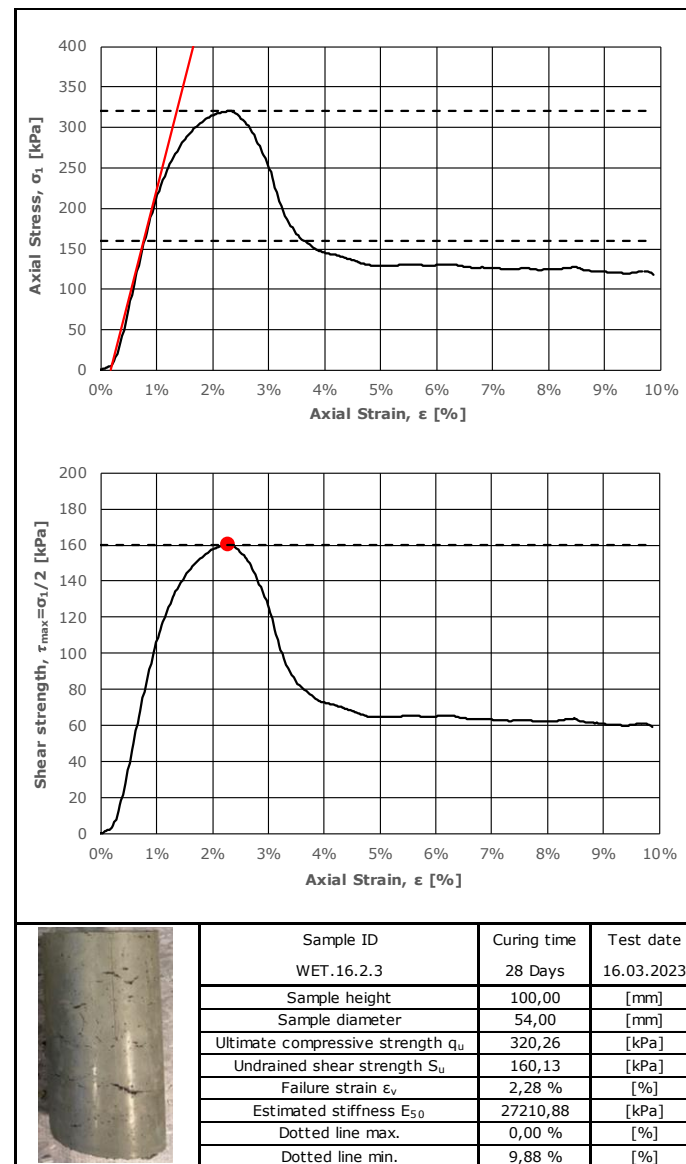
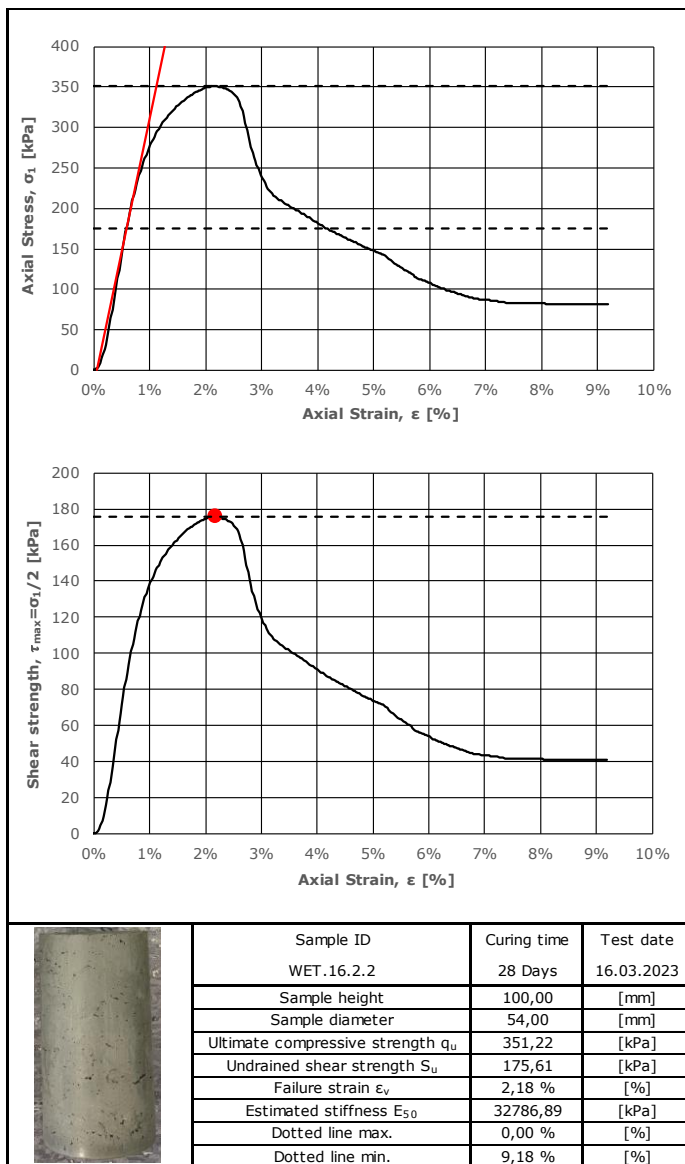
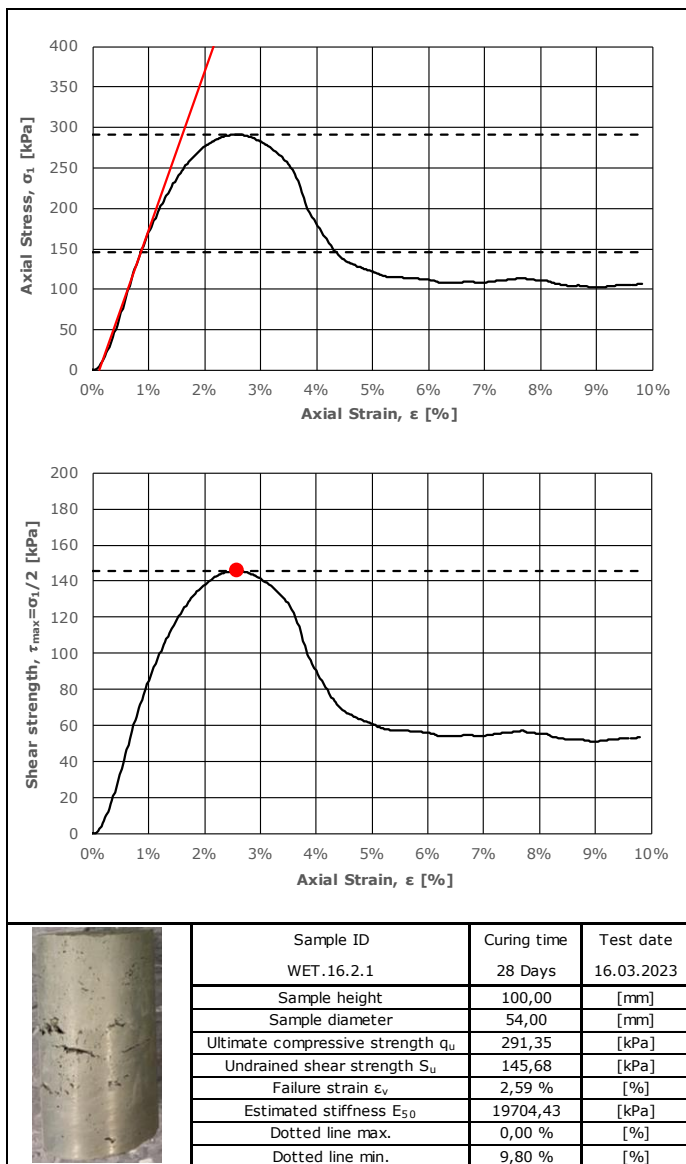
# APPENDIX B.1 SAMPLE IMAGES AND UNCONFINED COMPRESSION TEST RESULTS



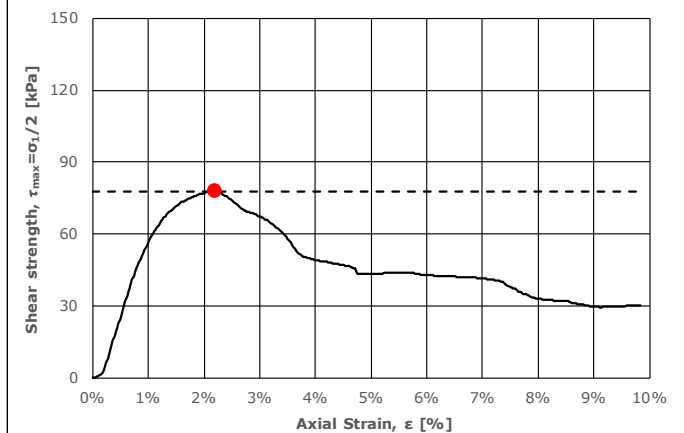
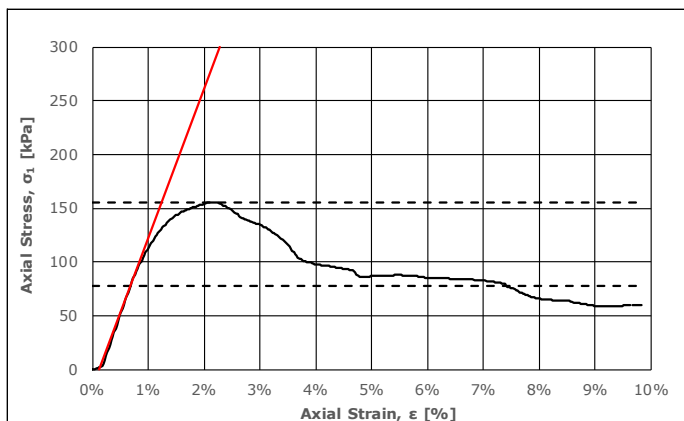
# APPENDIX B.1 SAMPLE IMAGES AND UNCONFINED COMPRESSION TEST RESULTS



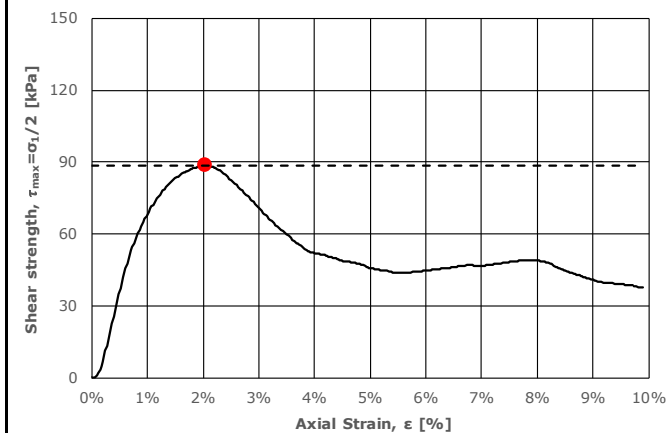
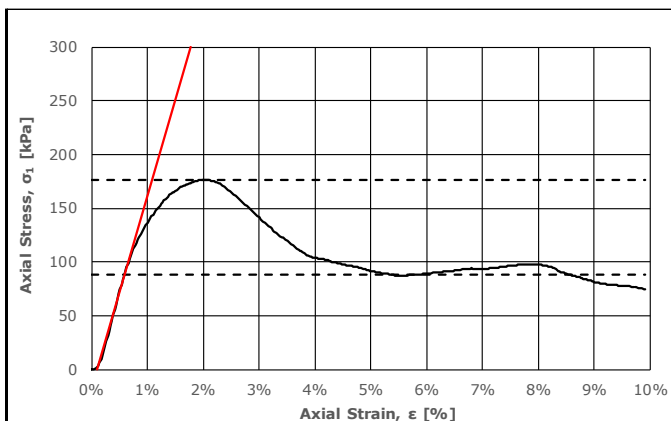
# APPENDIX B.1 SAMPLE IMAGES AND UNCONFINED COMPRESSION TEST RESULTS



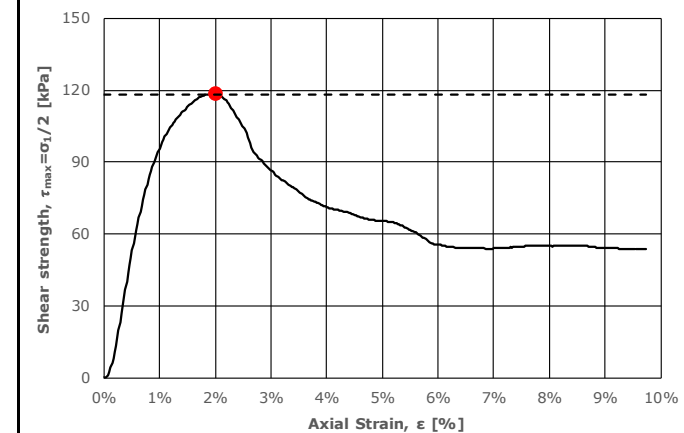
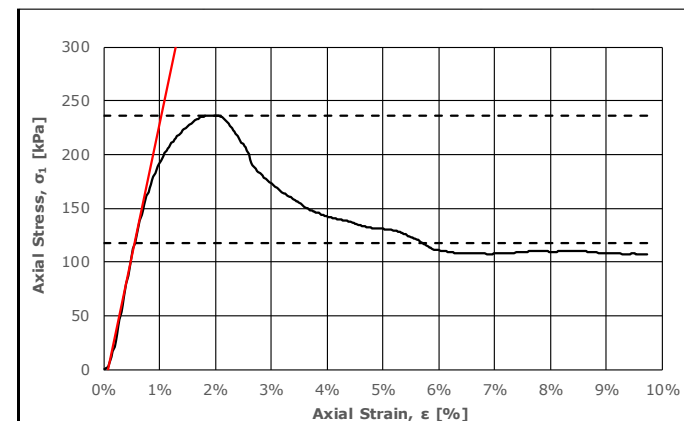
# APPENDIX B.1 SAMPLE IMAGES AND UNCONFINED COMPRESSION TEST RESULTS



| Sample ID                           | Curing time    | Test date  |
|-------------------------------------|----------------|------------|
| WET.16.3.1                          | 28 Days        | 17.03.2023 |
| Sample height                       | 100,00 [mm]    |            |
| Sample diameter                     | 54,00 [mm]     |            |
| Ultimate compressive strength $q_u$ | 155,80 [kPa]   |            |
| Undrained shear strength $S_u$      | 77,90 [kPa]    |            |
| Failure strain $\epsilon_v$         | 2,20 [%]       |            |
| Estimated stiffness $E_{50}$        | 13953,49 [kPa] |            |
| Dotted line max.                    | 0,00 [%]       |            |
| Dotted line min.                    | 9,83 [%]       |            |

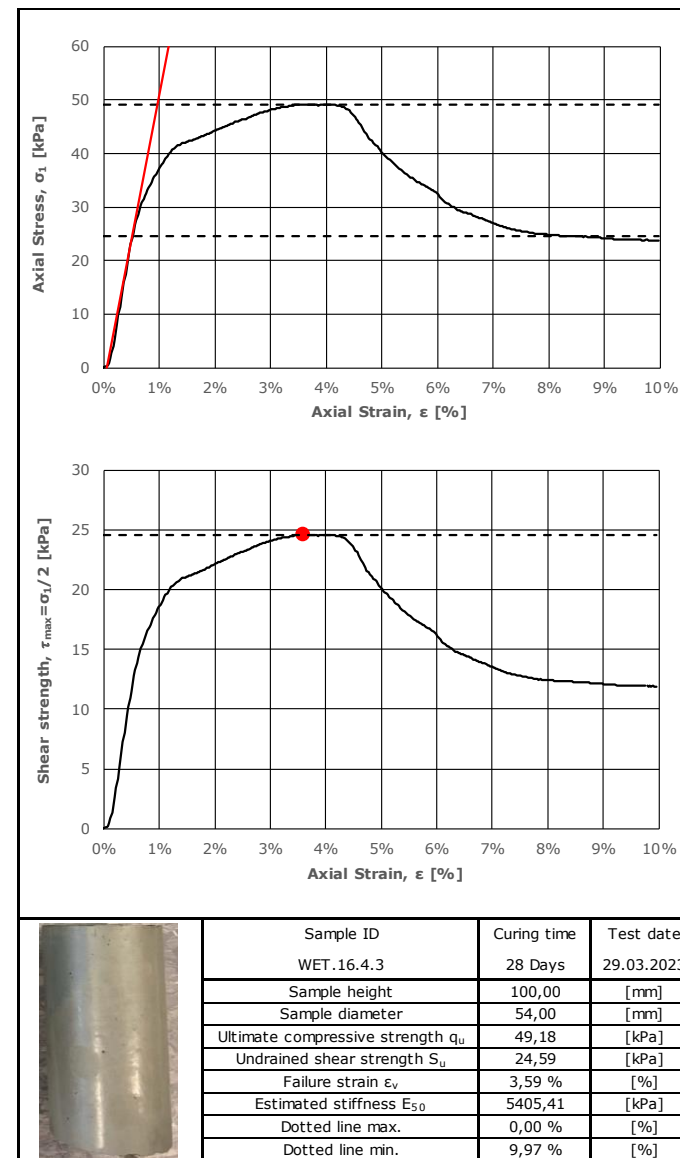
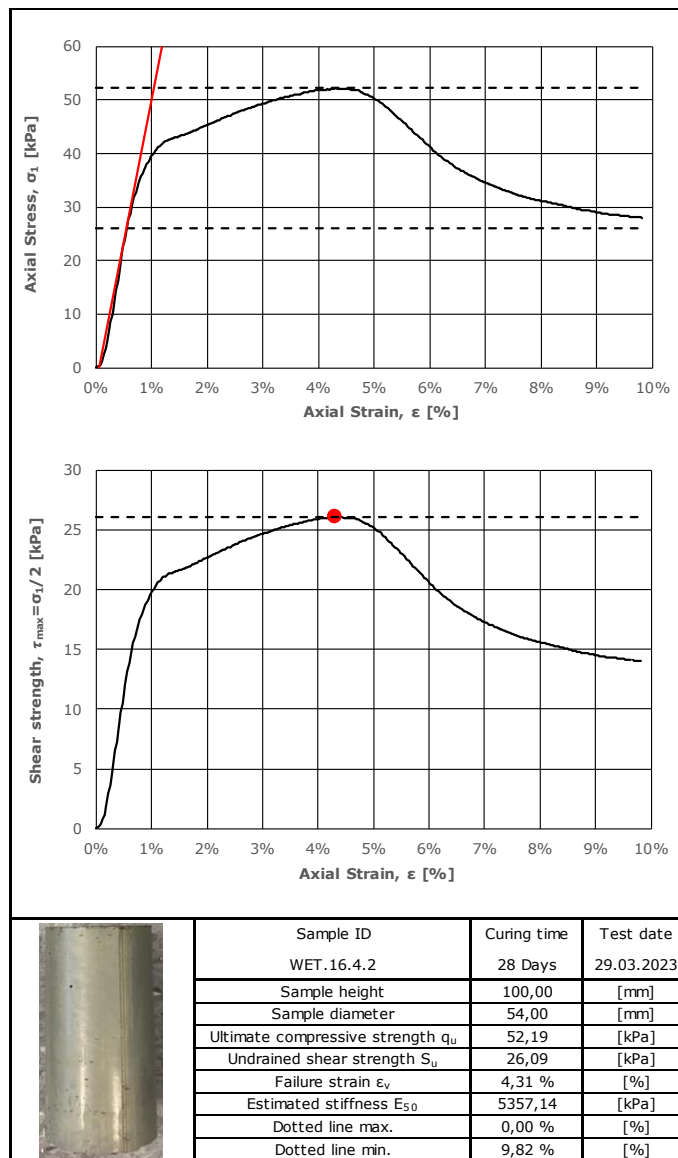
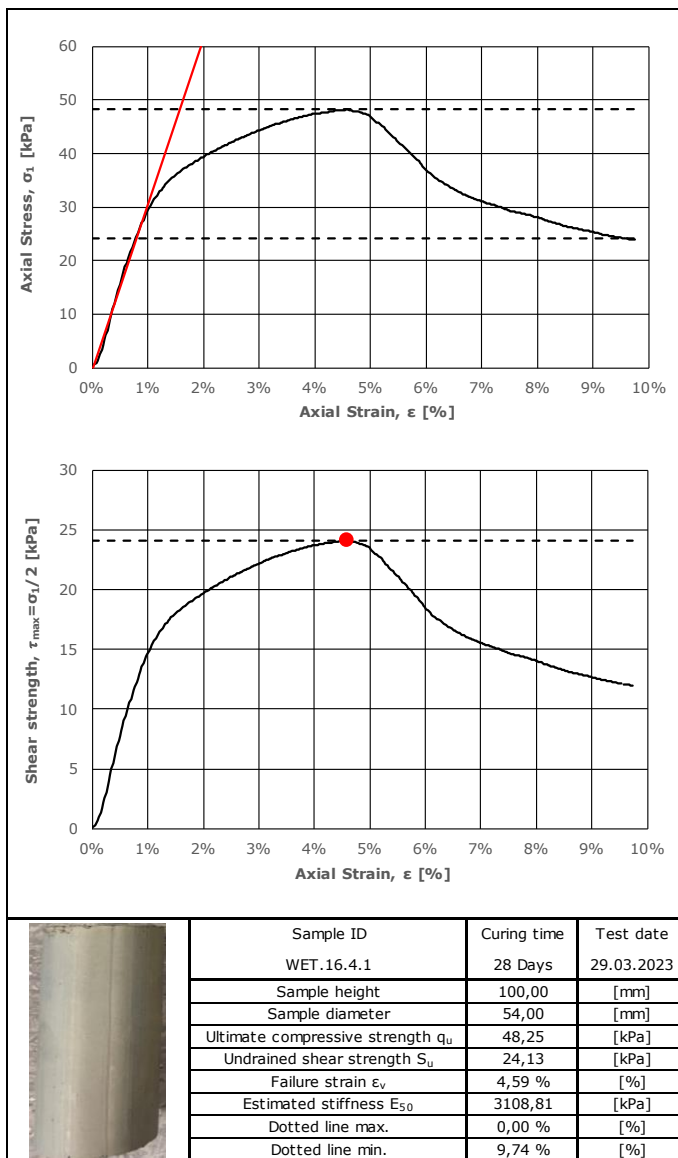


| Sample ID                           | Curing time    | Test date  |
|-------------------------------------|----------------|------------|
| WET.16.3.2                          | 28 Days        | 17.03.2023 |
| Sample height                       | 100,00 [mm]    |            |
| Sample diameter                     | 54,00 [mm]     |            |
| Ultimate compressive strength $q_u$ | 176,65 [kPa]   |            |
| Undrained shear strength $S_u$      | 88,33 [kPa]    |            |
| Failure strain $\epsilon_v$         | 2,05 [%]       |            |
| Estimated stiffness $E_{50}$        | 17964,07 [kPa] |            |
| Dotted line max.                    | 0,00 [%]       |            |
| Dotted line min.                    | 9,91 [%]       |            |



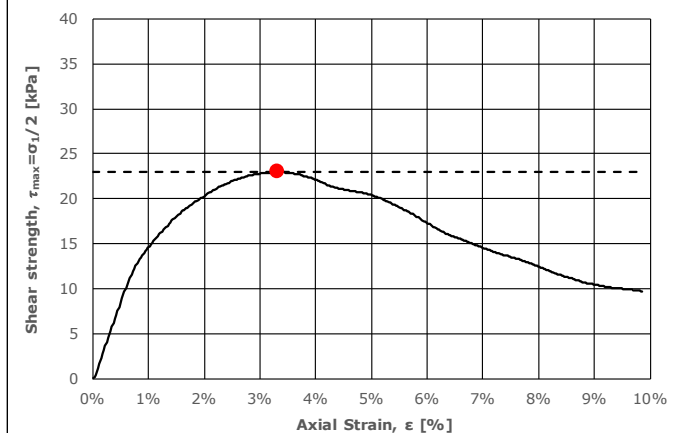
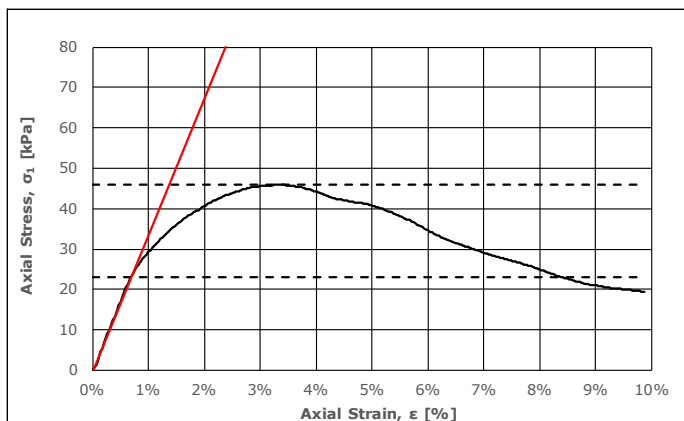
| Sample ID                           | Curing time    | Test date  |
|-------------------------------------|----------------|------------|
| WET.16.3.3                          | 28 Days        | 17.03.2023 |
| Sample height                       | 100,00 [mm]    |            |
| Sample diameter                     | 54,00 [mm]     |            |
| Ultimate compressive strength $q_u$ | 236,56 [kPa]   |            |
| Undrained shear strength $S_u$      | 118,28 [kPa]   |            |
| Failure strain $\epsilon_v$         | 2,02 [%]       |            |
| Estimated stiffness $E_{50}$        | 24590,16 [kPa] |            |
| Dotted line max.                    | 0,00 [%]       |            |
| Dotted line min.                    | 9,73 [%]       |            |

# APPENDIX B.1 SAMPLE IMAGES AND UNCONFINED COMPRESSION TEST RESULTS

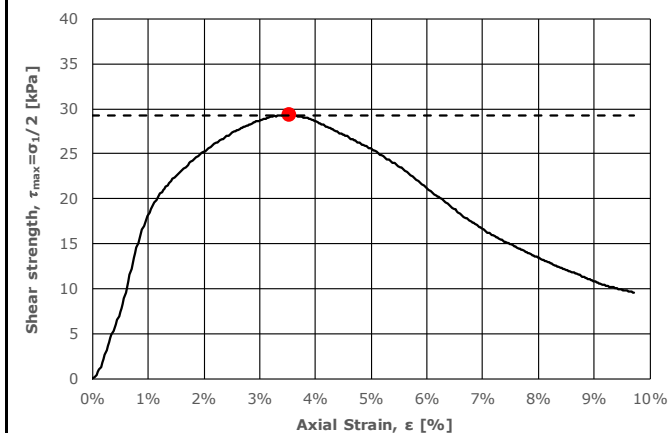
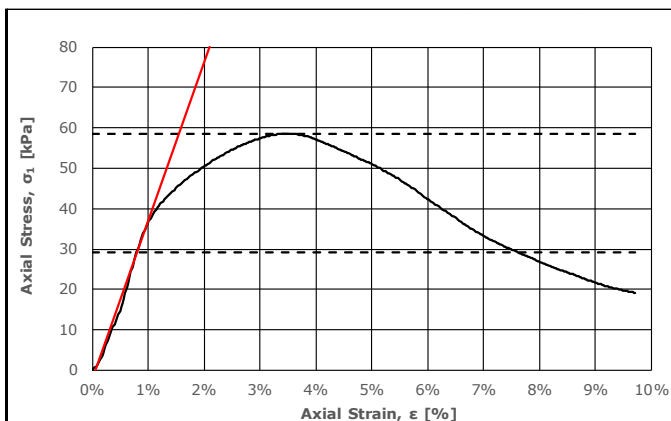




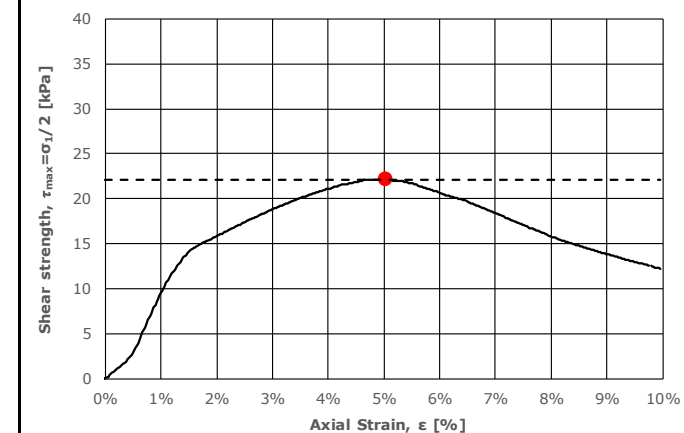
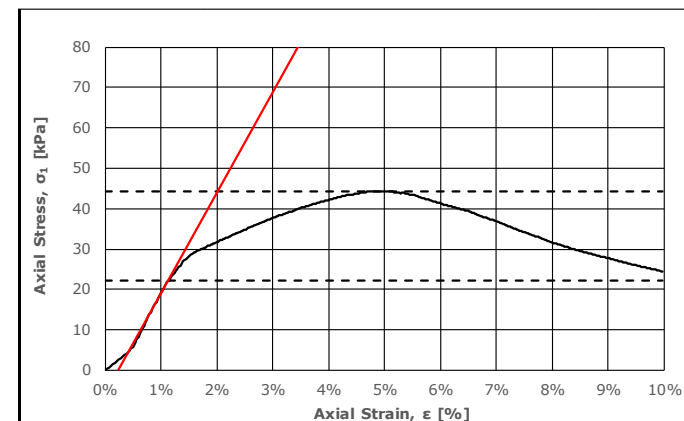
# APPENDIX B.1 SAMPLE IMAGES AND UNCONFINED COMPRESSION TEST RESULTS



| Sample ID                           | Curing time   | Test date  |
|-------------------------------------|---------------|------------|
| WET.16.5.1                          | 28 Days       | 29.03.2023 |
| Sample height                       | 100,00 [mm]   |            |
| Sample diameter                     | 54,00 [mm]    |            |
| Ultimate compressive strength $q_u$ | 45,96 [kPa]   |            |
| Undrained shear strength $S_u$      | 22,98 [kPa]   |            |
| Failure strain $\epsilon_v$         | 3,31 [%]      |            |
| Estimated stiffness $E_{50}$        | 3361,34 [kPa] |            |
| Dotted line max.                    | 0,00 [%]      |            |
| Dotted line min.                    | 9,87 [%]      |            |

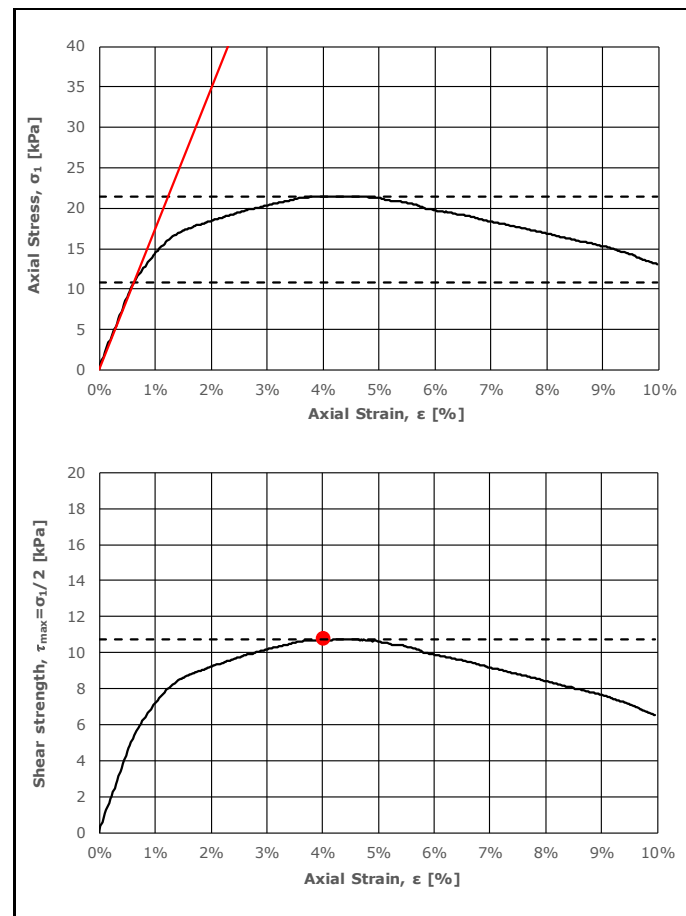
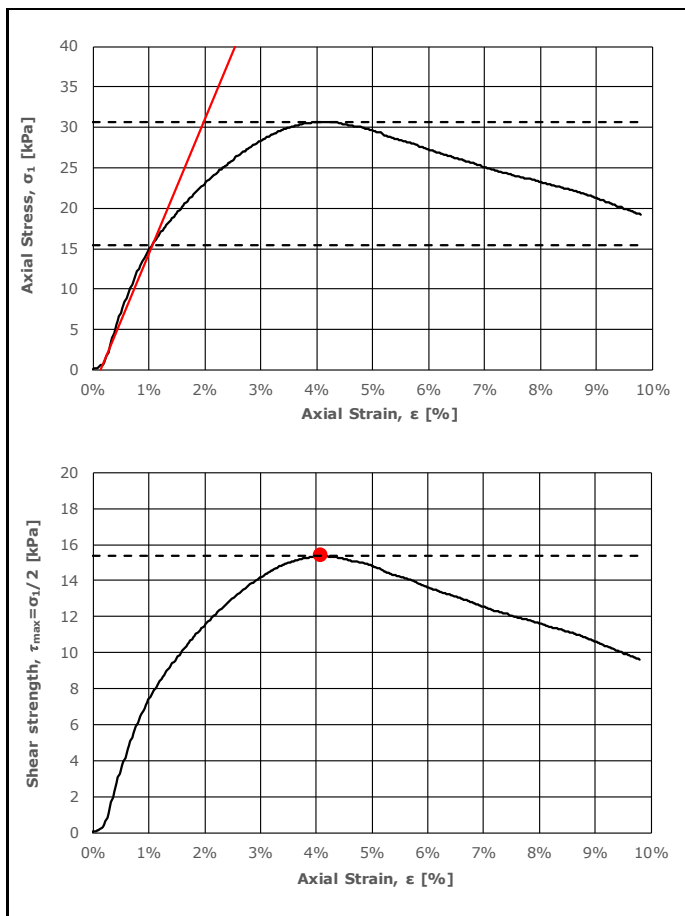
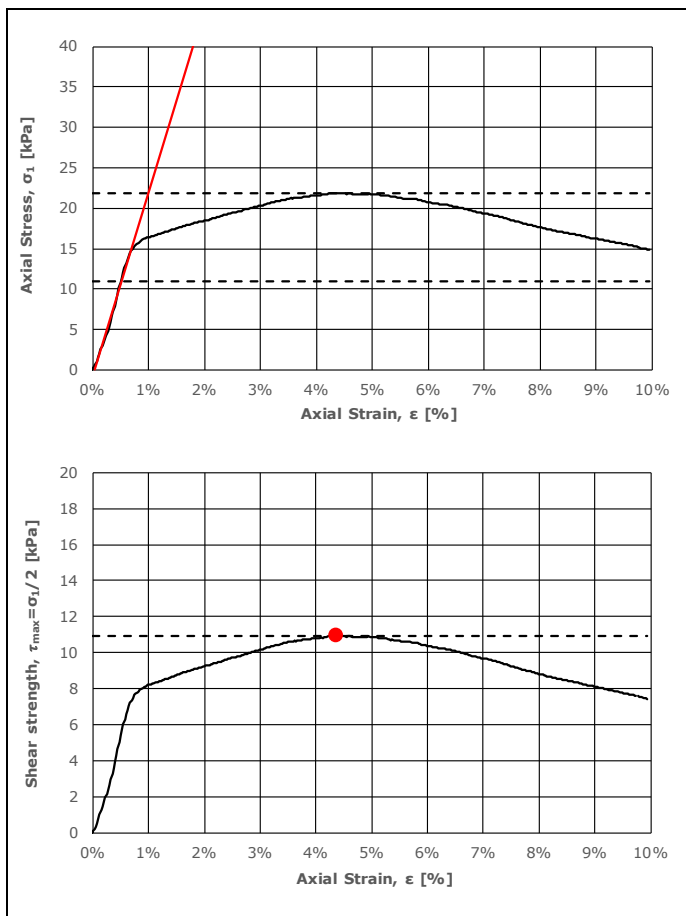


| Sample ID                           | Curing time   | Test date  |
|-------------------------------------|---------------|------------|
| WET.16.5.2                          | 28 Days       | 29.03.2023 |
| Sample height                       | 100,00 [mm]   |            |
| Sample diameter                     | 54,00 [mm]    |            |
| Ultimate compressive strength $q_u$ | 58,54 [kPa]   |            |
| Undrained shear strength $S_u$      | 29,27 [kPa]   |            |
| Failure strain $\epsilon_v$         | 3,54 [%]      |            |
| Estimated stiffness $E_{50}$        | 3940,89 [kPa] |            |
| Dotted line max.                    | 0,00 [%]      |            |
| Dotted line min.                    | 9,72 [%]      |            |



| Sample ID                           | Curing time   | Test date  |
|-------------------------------------|---------------|------------|
| WET.16.5.3                          | 28 Days       | 29.03.2023 |
| Sample height                       | 100,00 [mm]   |            |
| Sample diameter                     | 54,00 [mm]    |            |
| Ultimate compressive strength $q_u$ | 44,31 [kPa]   |            |
| Undrained shear strength $S_u$      | 22,15 [kPa]   |            |
| Failure strain $\epsilon_v$         | 5,04 [%]      |            |
| Estimated stiffness $E_{50}$        | 2492,21 [kPa] |            |
| Dotted line max.                    | 0,00 [%]      |            |
| Dotted line min.                    | 9,97 [%]      |            |

# APPENDIX B.1 SAMPLE IMAGES AND UNCONFINED COMPRESSION TEST RESULTS

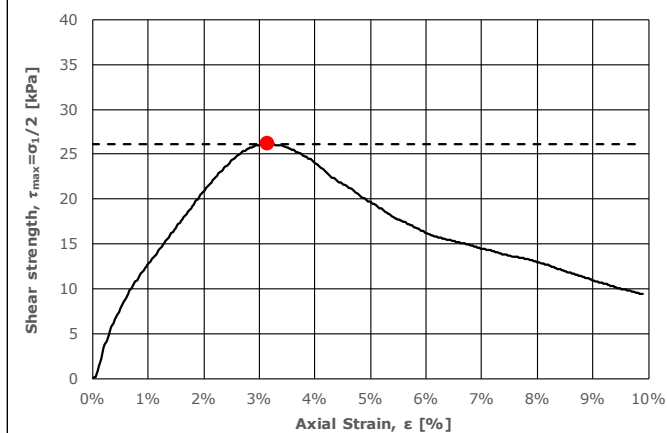
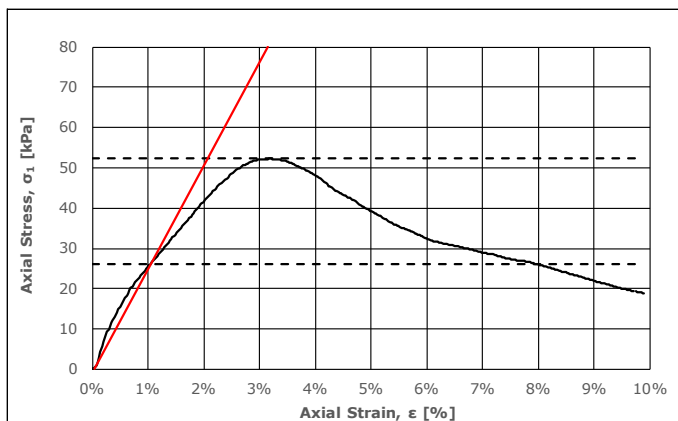


|  |                                     |            |             |         |           |            |
|--|-------------------------------------|------------|-------------|---------|-----------|------------|
|  | Sample ID                           | WET.16.6.1 | Curing time | 28 Days | Test date | 29.03.2023 |
|  | Sample height                       | 100,00     | [mm]        |         |           |            |
|  | Sample diameter                     | 54,00      | [mm]        |         |           |            |
|  | Ultimate compressive strength $q_u$ | 21,89      | [kPa]       |         |           |            |
|  | Undrained shear strength $S_u$      | 10,94      | [kPa]       |         |           |            |
|  | Failure strain $\epsilon_v$         | 4,37       | [%]         |         |           |            |
|  | Estimated stiffness $E_{50}$        | 2285,71    | [kPa]       |         |           |            |
|  | Dotted line max.                    | 0,00       | [%]         |         |           |            |
|  | Dotted line min.                    | 9,94       | [%]         |         |           |            |

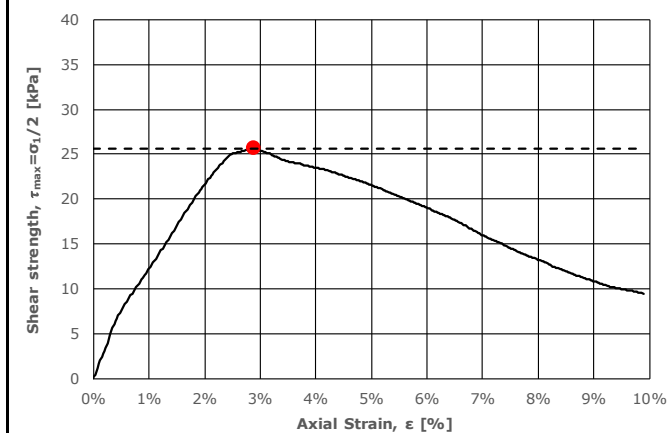
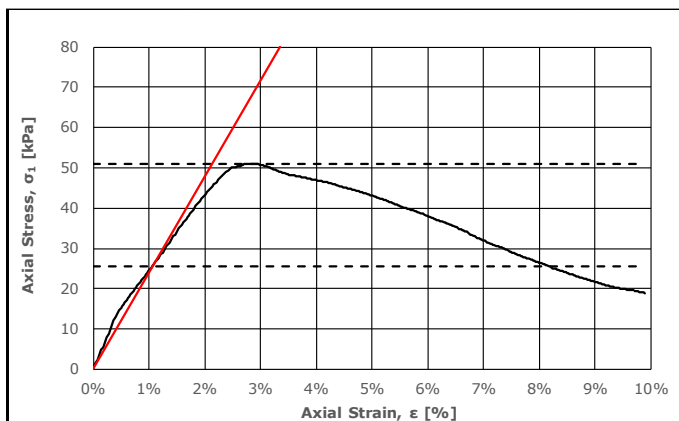
|  |                                     |            |             |         |           |            |
|--|-------------------------------------|------------|-------------|---------|-----------|------------|
|  | Sample ID                           | WET.16.6.2 | Curing time | 28 Days | Test date | 29.03.2023 |
|  | Sample height                       | 100,00     | [mm]        |         |           |            |
|  | Sample diameter                     | 54,00      | [mm]        |         |           |            |
|  | Ultimate compressive strength $q_u$ | 30,72      | [kPa]       |         |           |            |
|  | Undrained shear strength $S_u$      | 15,36      | [kPa]       |         |           |            |
|  | Failure strain $\epsilon_v$         | 4,09       | [%]         |         |           |            |
|  | Estimated stiffness $E_{50}$        | 1659,75    | [kPa]       |         |           |            |
|  | Dotted line max.                    | 0,00       | [%]         |         |           |            |
|  | Dotted line min.                    | 9,79       | [%]         |         |           |            |

|  |                                     |            |             |         |           |            |
|--|-------------------------------------|------------|-------------|---------|-----------|------------|
|  | Sample ID                           | WET.16.6.3 | Curing time | 28 Days | Test date | 29.03.2023 |
|  | Sample height                       | 100,00     | [mm]        |         |           |            |
|  | Sample diameter                     | 54,00      | [mm]        |         |           |            |
|  | Ultimate compressive strength $q_u$ | 21,51      | [kPa]       |         |           |            |
|  | Undrained shear strength $S_u$      | 10,75      | [kPa]       |         |           |            |
|  | Failure strain $\epsilon_v$         | 4,02       | [%]         |         |           |            |
|  | Estimated stiffness $E_{50}$        | 1739,13    | [kPa]       |         |           |            |
|  | Dotted line max.                    | 0,00       | [%]         |         |           |            |
|  | Dotted line min.                    | 9,97       | [%]         |         |           |            |

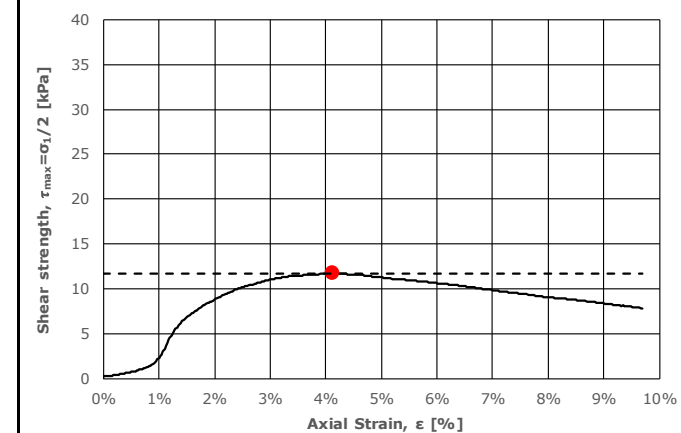
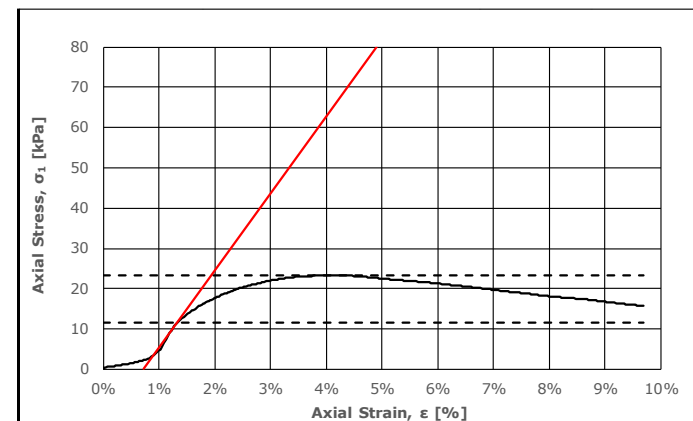
## APPENDIX B.1 SAMPLE IMAGES AND UNCONFINED COMPRESSION TEST RESULTS



| Sample ID                           | Curing time   | Test date  |
|-------------------------------------|---------------|------------|
| WET.16.7.1                          | 28 Days       | 30.03.2023 |
| Sample height                       | 100,00 [mm]   |            |
| Sample diameter                     | 54,00 [mm]    |            |
| Ultimate compressive strength $q_u$ | 52,29 [kPa]   |            |
| Undrained shear strength $S_u$      | 26,15 [kPa]   |            |
| Failure strain $\epsilon_v$         | 3,16 [%]      |            |
| Estimated stiffness $E_{50}$        | 2580,65 [kPa] |            |
| Dotted line max.                    | 0,00 [%]      |            |
| Dotted line min.                    | 9,89 [%]      |            |

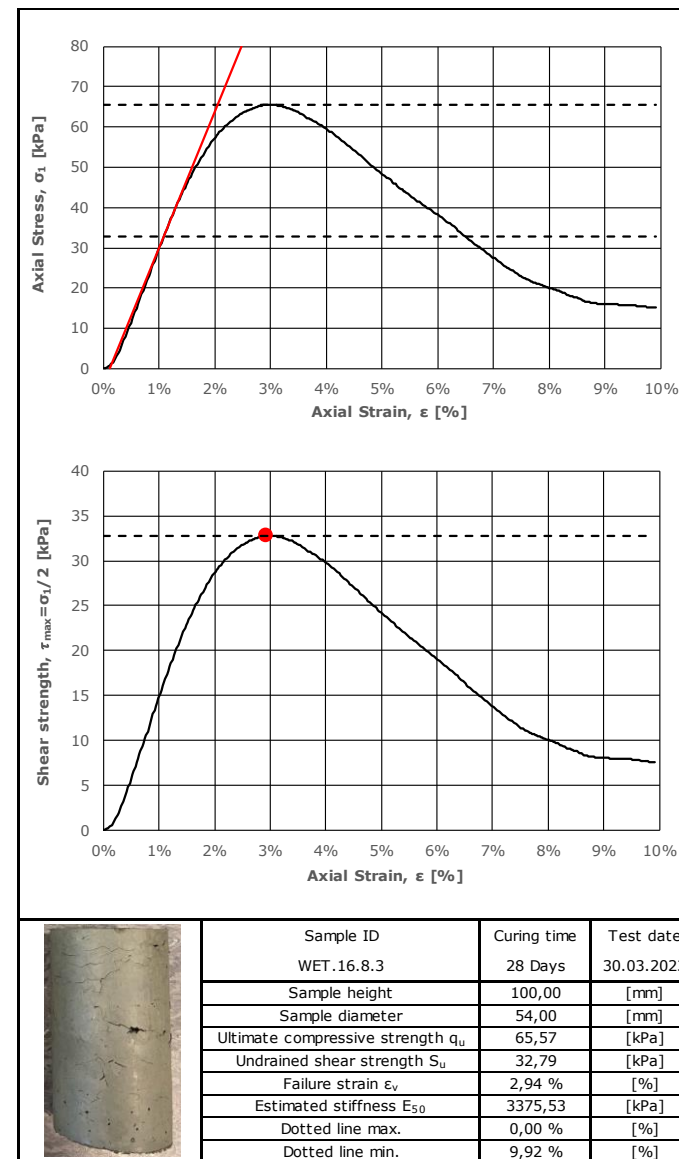
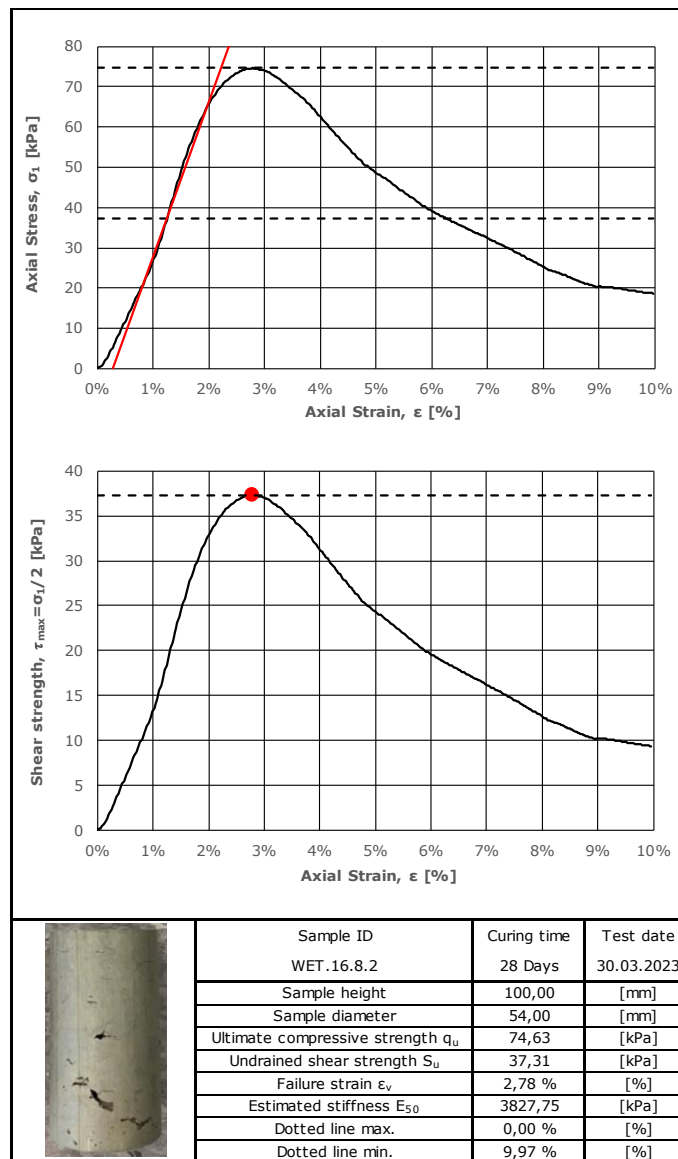
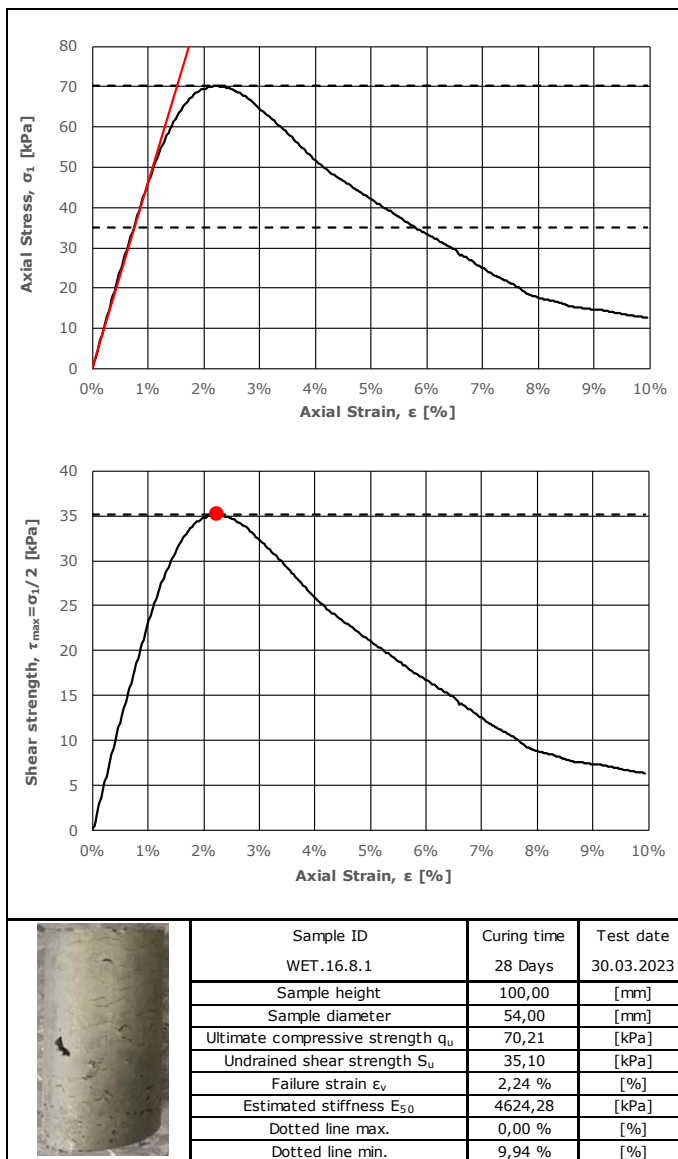


| Sample ID                           | Curing time   | Test date  |
|-------------------------------------|---------------|------------|
| WET.16.7.2                          | 28 Days       | 30.03.2023 |
| Sample height                       | 100,00 [mm]   |            |
| Sample diameter                     | 54,00 [mm]    |            |
| Ultimate compressive strength $q_u$ | 51,11 [kPa]   |            |
| Undrained shear strength $S_u$      | 25,55 [kPa]   |            |
| Failure strain $\epsilon_v$         | 2,89 [%]      |            |
| Estimated stiffness $E_{50}$        | 2395,21 [kPa] |            |
| Dotted line max.                    | 0,00 [%]      |            |
| Dotted line min.                    | 9,89 [%]      |            |

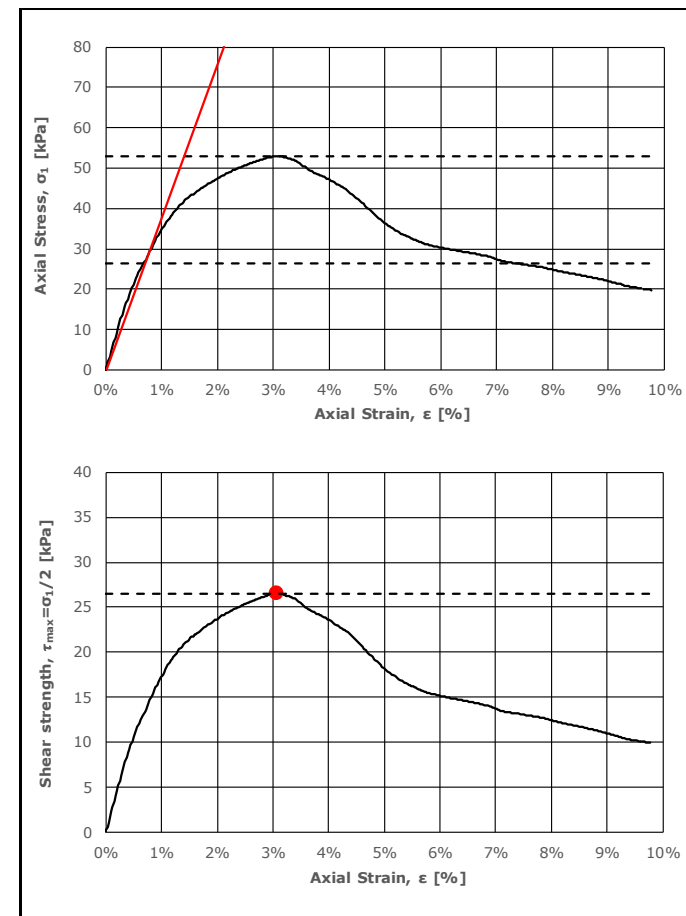
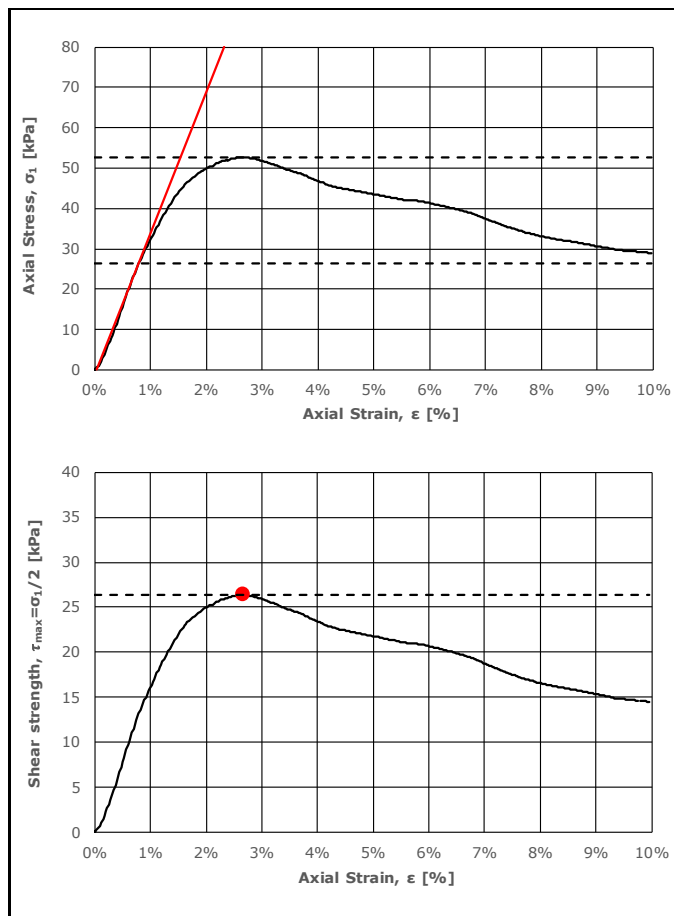
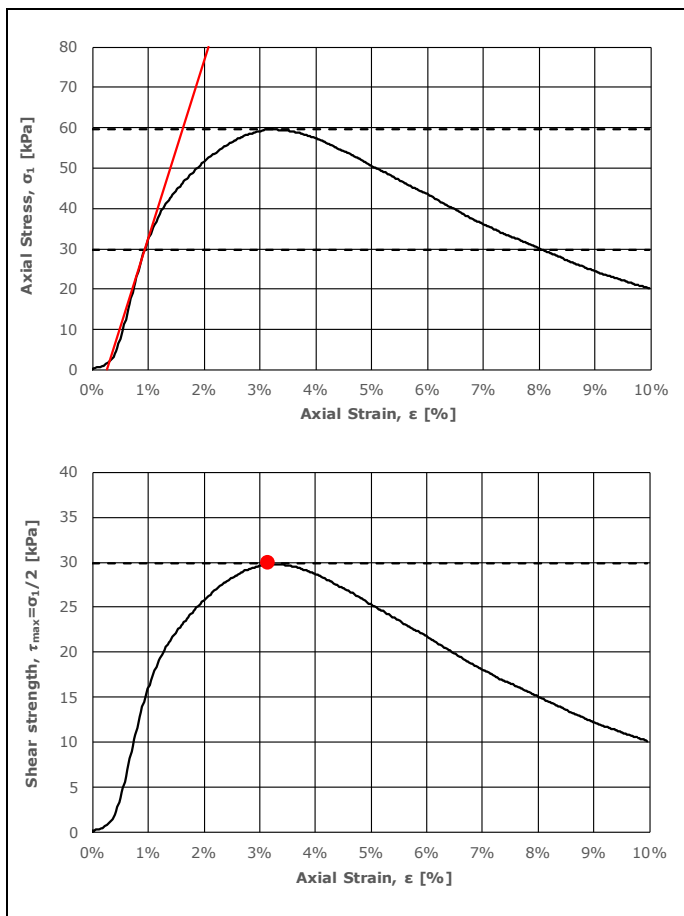


| Sample ID                           | Curing time   | Test date  |
|-------------------------------------|---------------|------------|
| WET.16.7.3                          | 28 Days       | 30.03.2023 |
| Sample height                       | 100,00 [mm]   |            |
| Sample diameter                     | 54,00 [mm]    |            |
| Ultimate compressive strength $q_u$ | 23,37 [kPa]   |            |
| Undrained shear strength $S_u$      | 11,68 [kPa]   |            |
| Failure strain $\epsilon_v$         | 4,12 [%]      |            |
| Estimated stiffness $E_{50}$        | 1913,88 [kPa] |            |
| Dotted line max.                    | 0,00 [%]      |            |
| Dotted line min.                    | 9,69 [%]      |            |

# APPENDIX B.1 SAMPLE IMAGES AND UNCONFINED COMPRESSION TEST RESULTS



# APPENDIX B.1 SAMPLE IMAGES AND UNCONFINED COMPRESSION TEST RESULTS



| Sample ID                           | Curing time   | Test date  |
|-------------------------------------|---------------|------------|
| WET.16.9.1                          | 28 Days       | 30.03.2023 |
| Sample height                       | 100,00 [mm]   |            |
| Sample diameter                     | 54,00 [mm]    |            |
| Ultimate compressive strength $q_u$ | 59,63 [kPa]   |            |
| Undrained shear strength $S_u$      | 29,82 [kPa]   |            |
| Failure strain $\epsilon_v$         | 3,16 [%]      |            |
| Estimated stiffness $E_{50}$        | 4395,60 [kPa] |            |
| Dotted line max.                    | 0,00 [%]      |            |
| Dotted line min.                    | 9,97 [%]      |            |

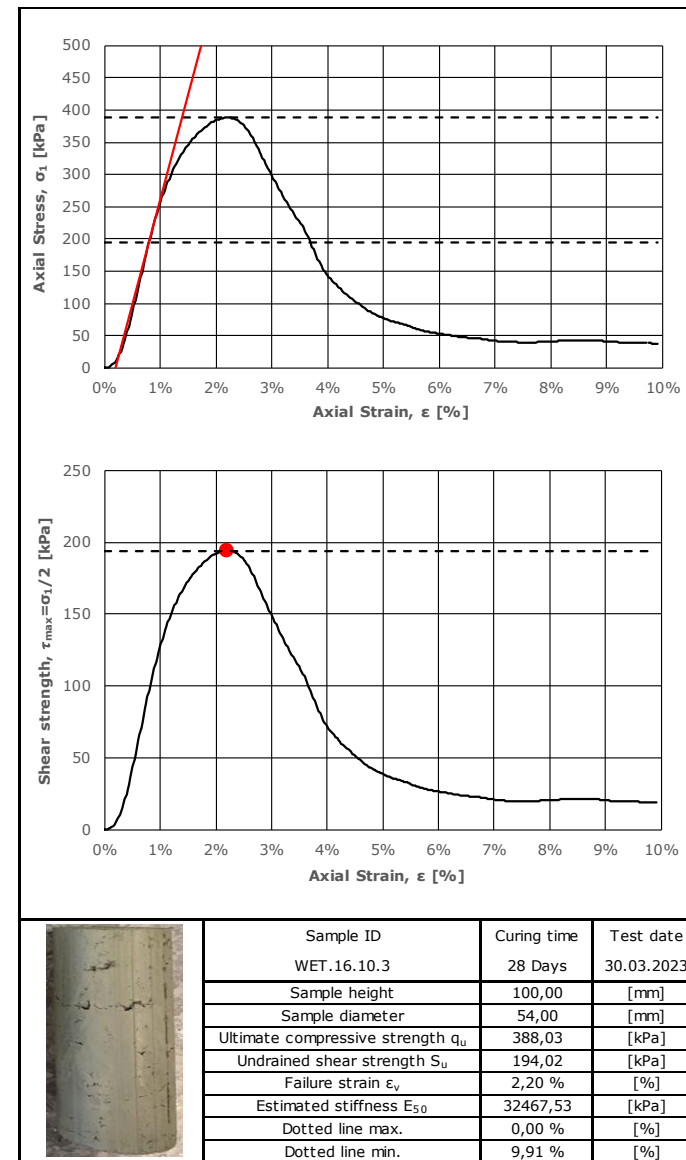
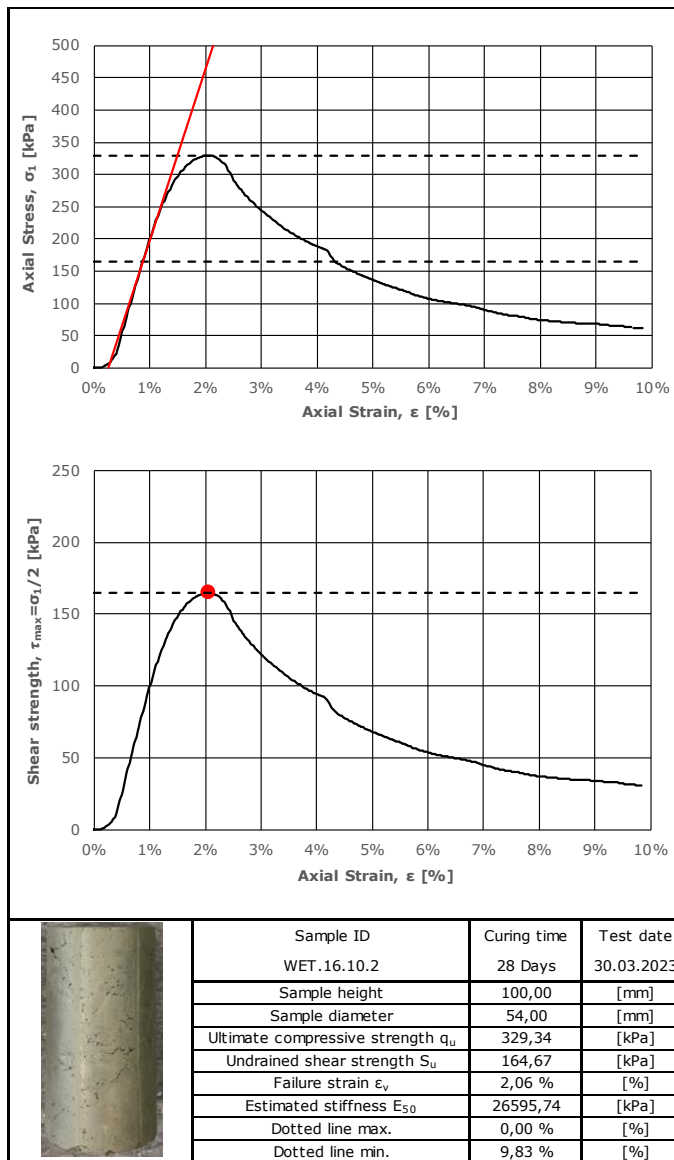
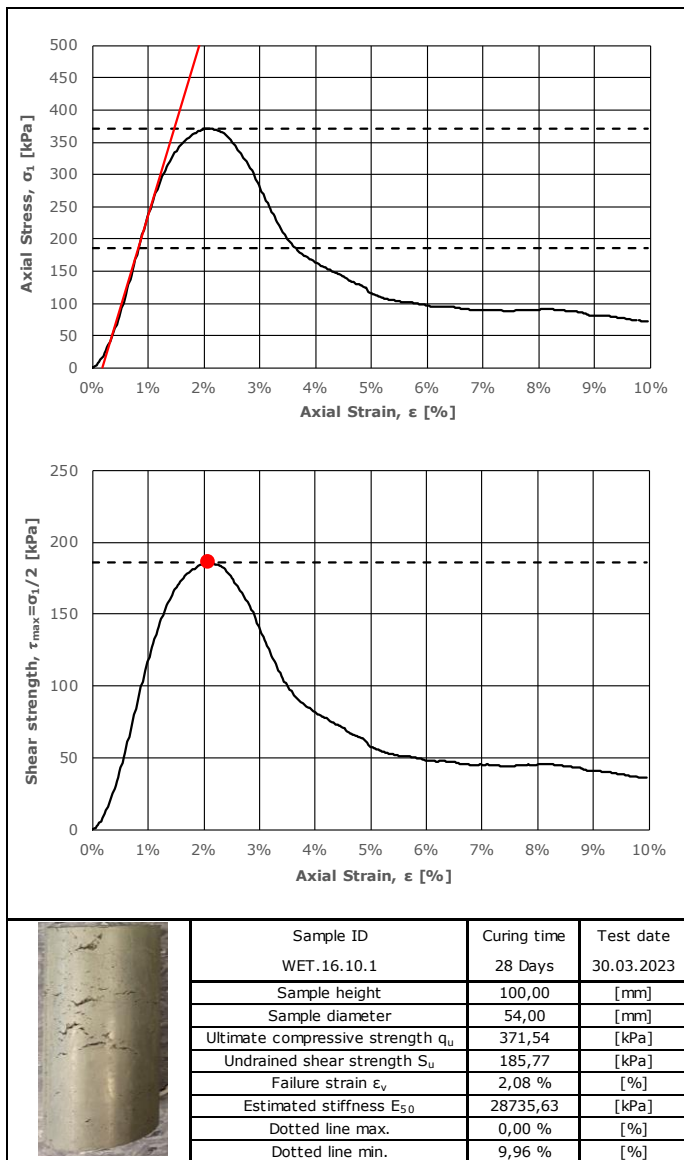


| Sample ID                           | Curing time   | Test date  |
|-------------------------------------|---------------|------------|
| WET.16.9.2                          | 28 Days       | 30.03.2023 |
| Sample height                       | 100,00 [mm]   |            |
| Sample diameter                     | 54,00 [mm]    |            |
| Ultimate compressive strength $q_u$ | 52,79 [kPa]   |            |
| Undrained shear strength $S_u$      | 26,40 [kPa]   |            |
| Failure strain $\epsilon_v$         | 2,66 [%]      |            |
| Estimated stiffness $E_{50}$        | 3508,77 [kPa] |            |
| Dotted line max.                    | 0,00 [%]      |            |
| Dotted line min.                    | 9,96 [%]      |            |



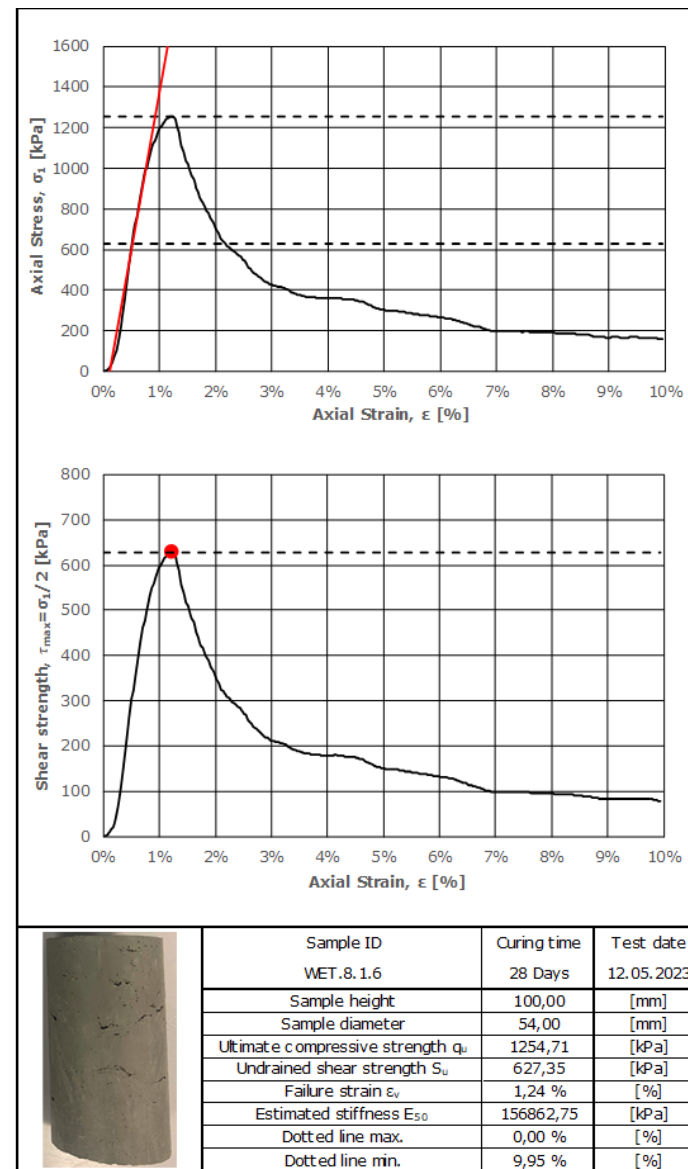
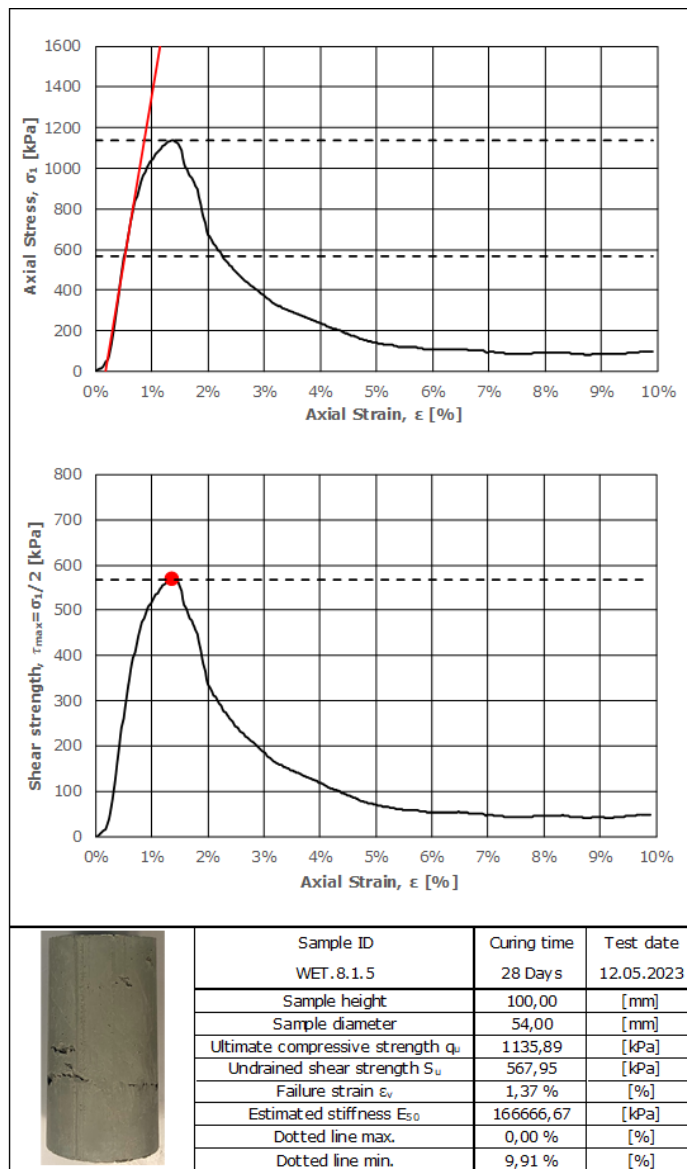
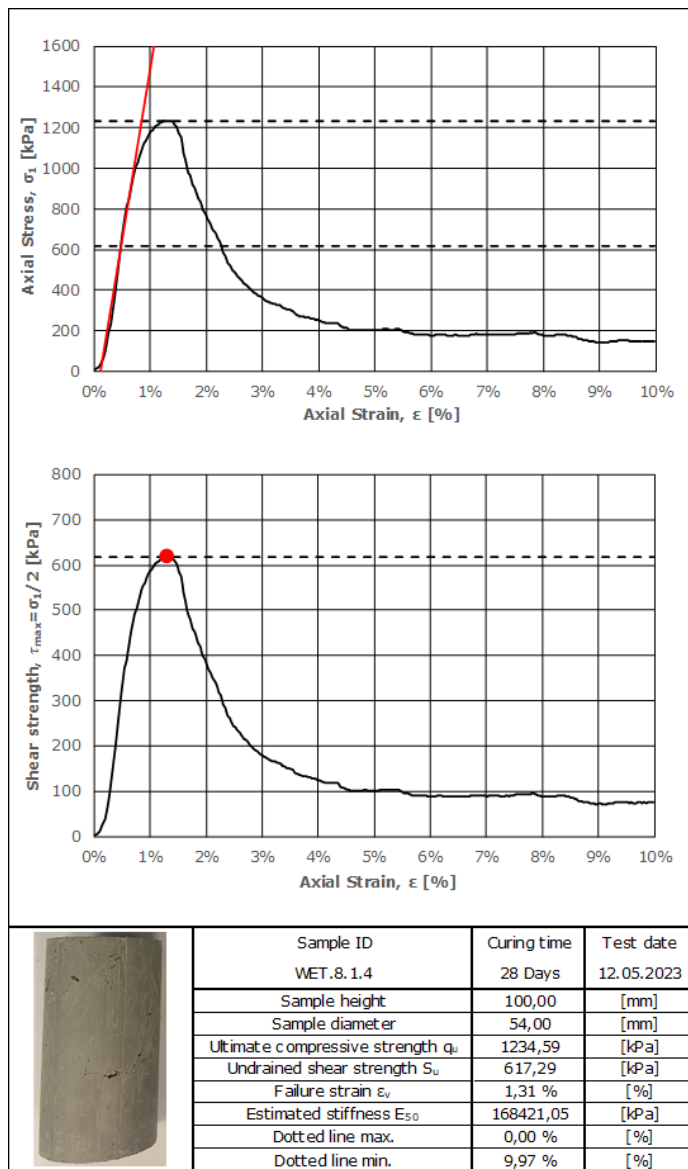
| Sample ID                           | Curing time   | Test date  |
|-------------------------------------|---------------|------------|
| WET.16.9.3                          | 28 Days       | 30.03.2023 |
| Sample height                       | 100,00 [mm]   |            |
| Sample diameter                     | 54,00 [mm]    |            |
| Ultimate compressive strength $q_u$ | 52,96 [kPa]   |            |
| Undrained shear strength $S_u$      | 26,48 [kPa]   |            |
| Failure strain $\epsilon_v$         | 3,06 [%]      |            |
| Estimated stiffness $E_{50}$        | 3791,47 [kPa] |            |
| Dotted line max.                    | 0,00 [%]      |            |
| Dotted line min.                    | 9,77 [%]      |            |

# APPENDIX B.1 SAMPLE IMAGES AND UNCONFINED COMPRESSION TEST RESULTS



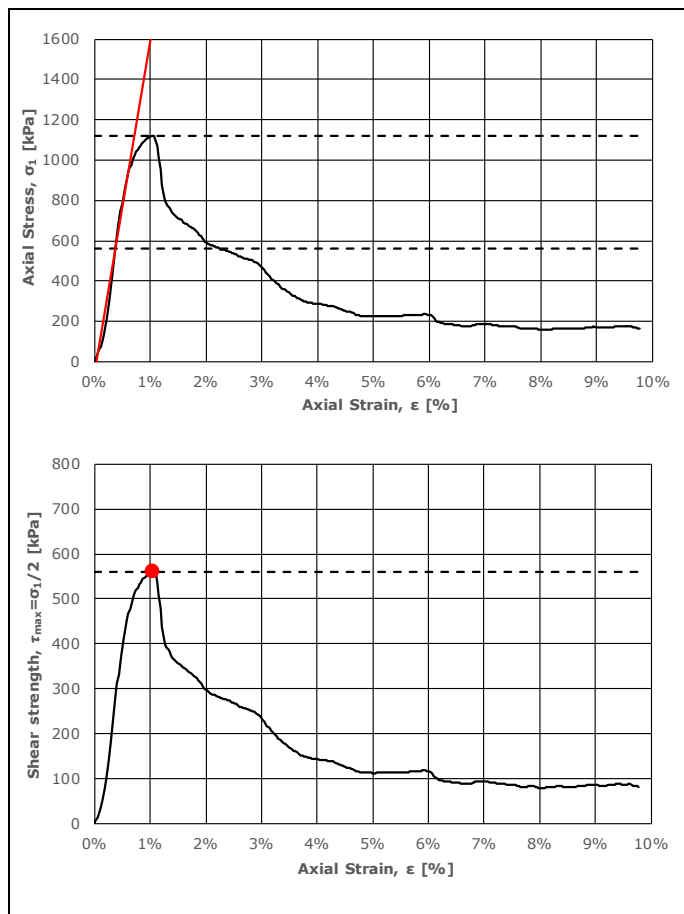
**B.2 SAMPLE IMAGES AND UNCONFINED COMPRESSION  
TEST RESULTS FOR SINGLE MIXING METHOD  
EVALUATION**

APPENDIX B.2 SAMPLE IMAGES AND UNCONFINED COMPRESSION TEST RESULTS FOR SINGLE MIXING METHOD EVALUATION

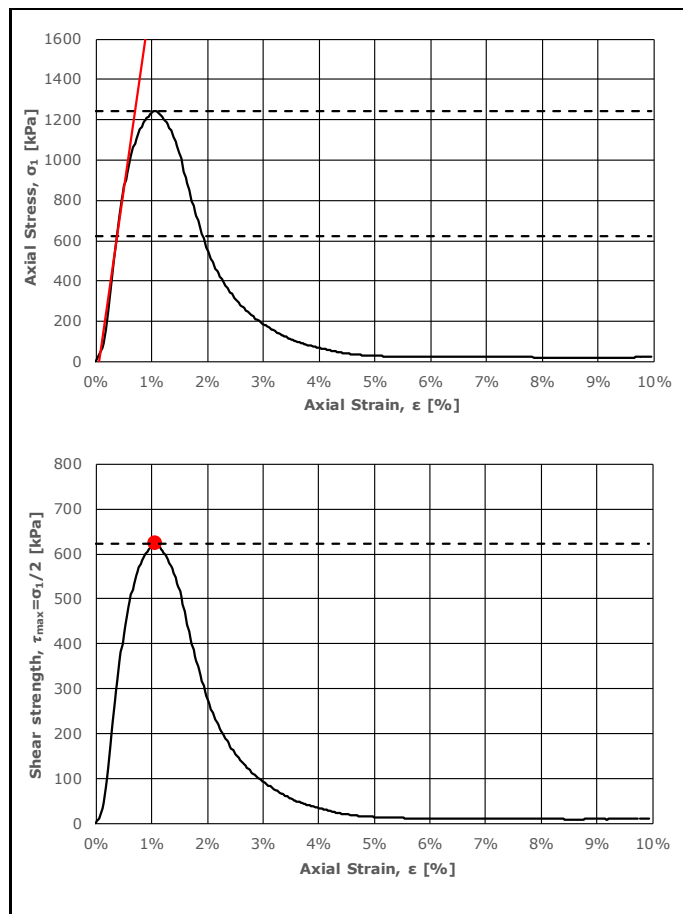




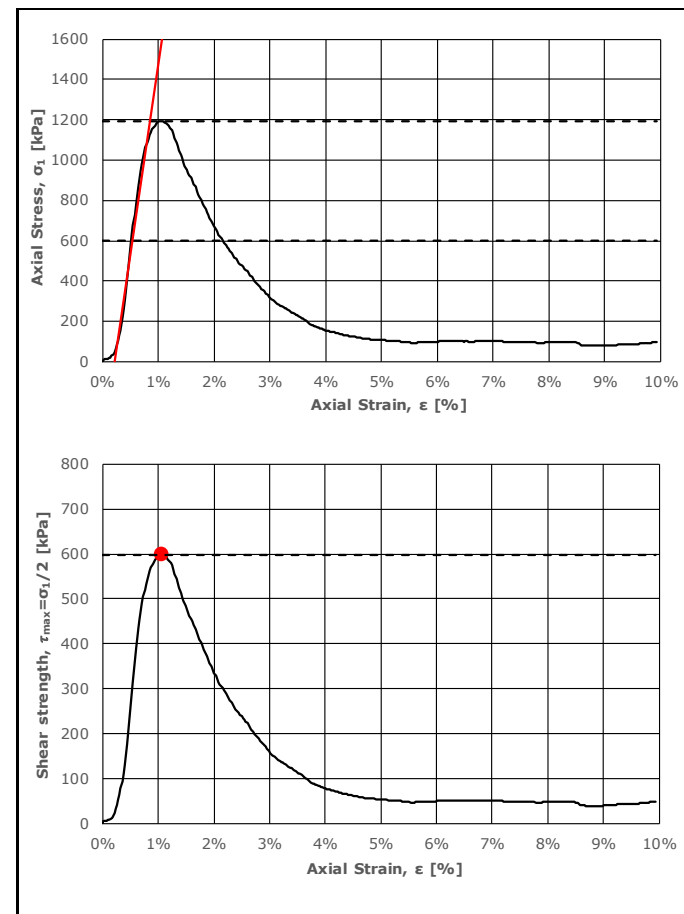
## APPENDIX B.2 SAMPLE IMAGES AND UNCONFINED COMPRESSION TEST RESULTS FOR SINGLE MIXING METHOD EVALUATION



| Sample ID                           | Curing time     | Test date  |
|-------------------------------------|-----------------|------------|
| MDM.8.1.1                           | 28 Days         | 12.05.2023 |
| Sample height                       | 100,00 [mm]     |            |
| Sample diameter                     | 54,00 [mm]      |            |
| Ultimate compressive strength $q_u$ | 1120,63 [kPa]   |            |
| Undrained shear strength $S_u$      | 560,32 [kPa]    |            |
| Failure strain $\epsilon_v$         | 1,05 [%]        |            |
| Estimated stiffness $E_{50}$        | 166666,67 [kPa] |            |
| Dotted line max.                    | 0,00 [%]        |            |
| Dotted line min.                    | 9,77 [%]        |            |

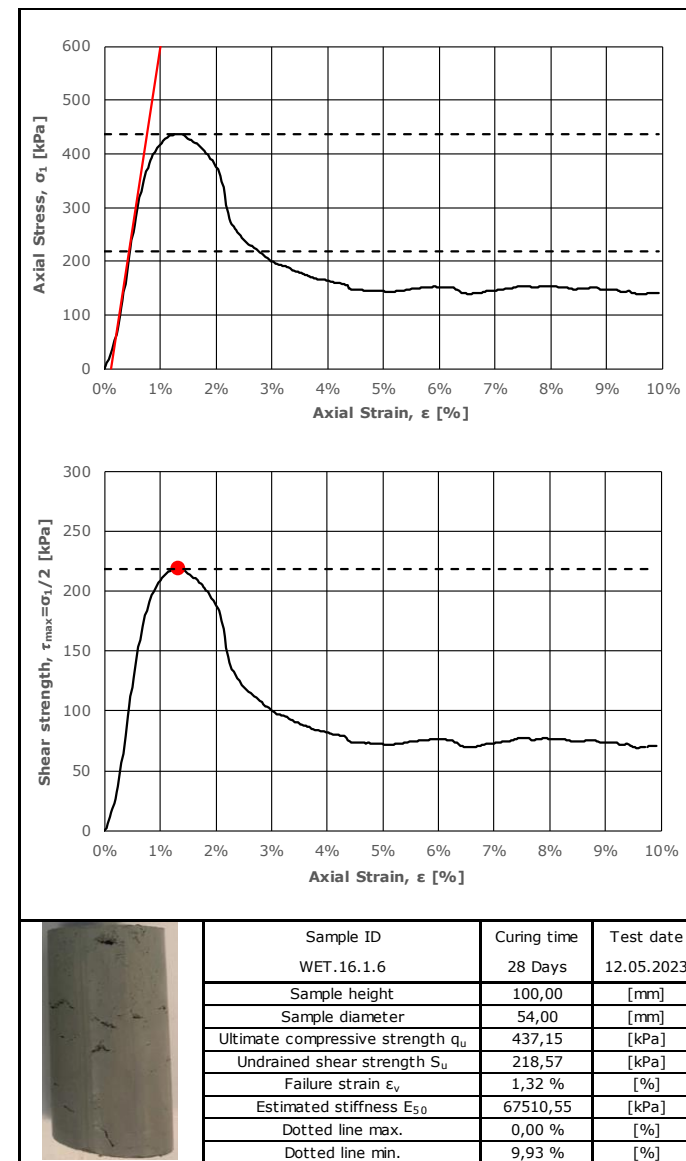
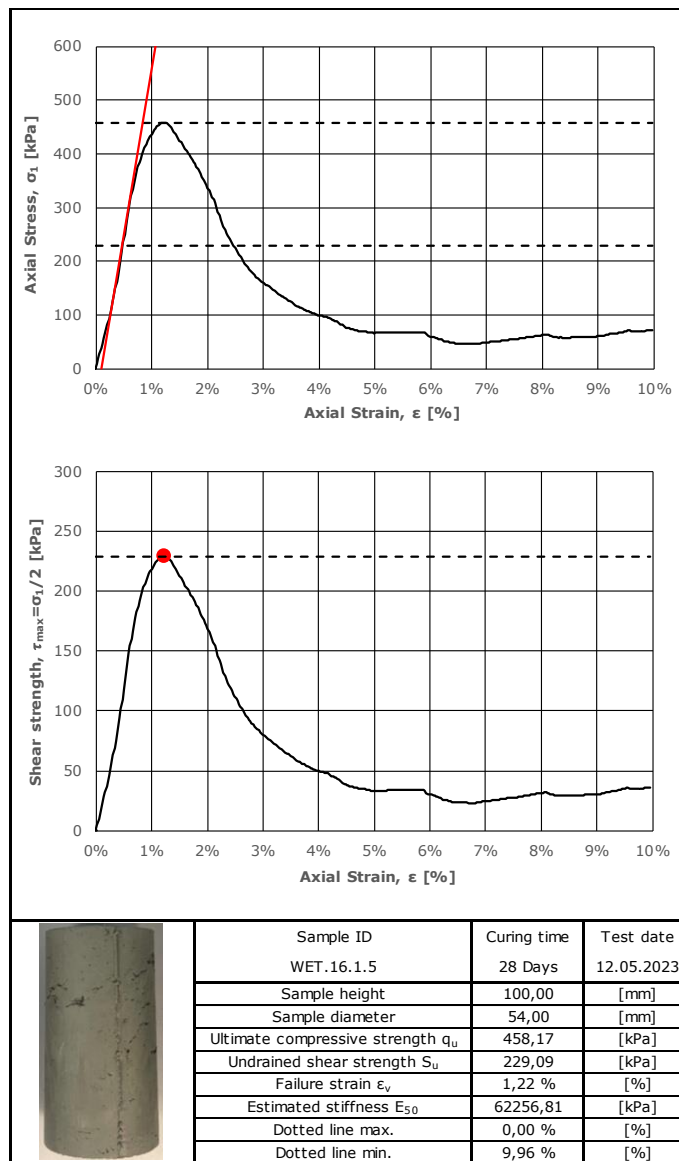
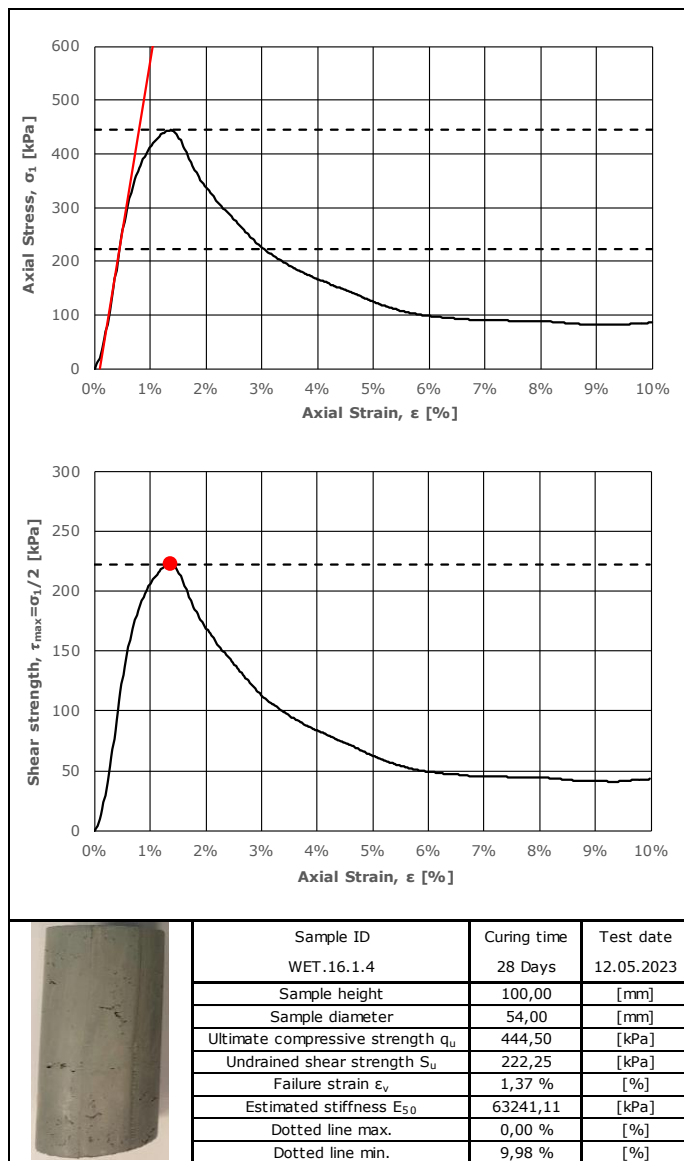


| Sample ID                           | Curing time     | Test date  |
|-------------------------------------|-----------------|------------|
| MDM.8.1.2                           | 28 Days         | 12.05.2023 |
| Sample height                       | 100,00 [mm]     |            |
| Sample diameter                     | 54,00 [mm]      |            |
| Ultimate compressive strength $q_u$ | 1243,78 [kPa]   |            |
| Undrained shear strength $S_u$      | 621,89 [kPa]    |            |
| Failure strain $\epsilon_v$         | 1,06 [%]        |            |
| Estimated stiffness $E_{50}$        | 195121,95 [kPa] |            |
| Dotted line max.                    | 0,00 [%]        |            |
| Dotted line min.                    | 9,94 [%]        |            |

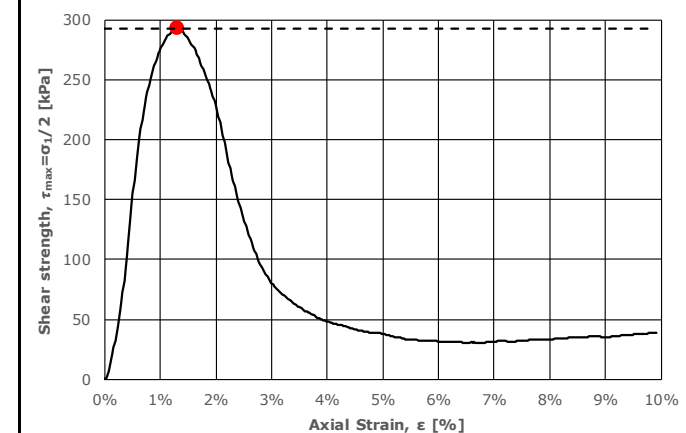
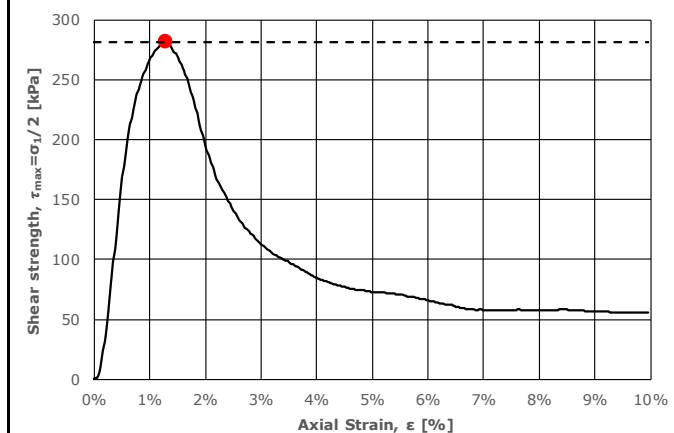
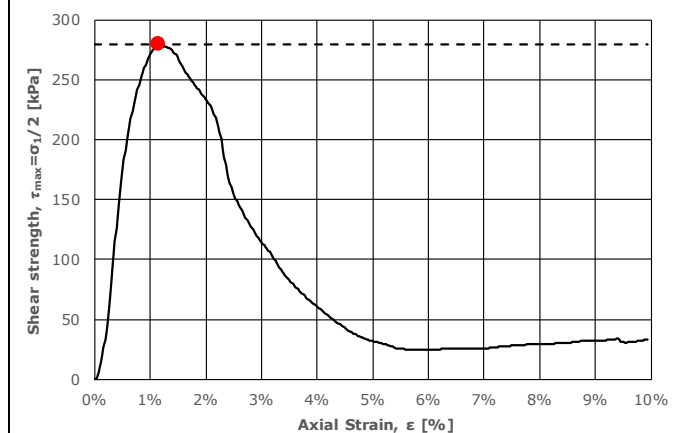
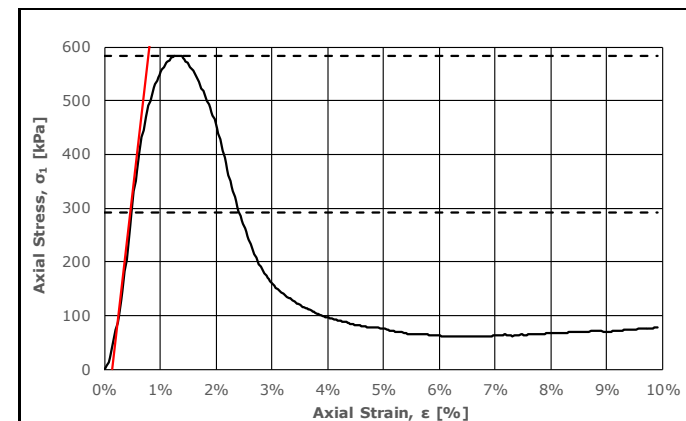
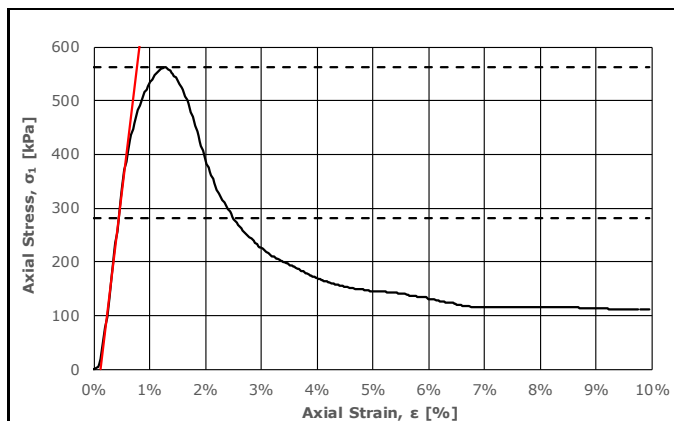
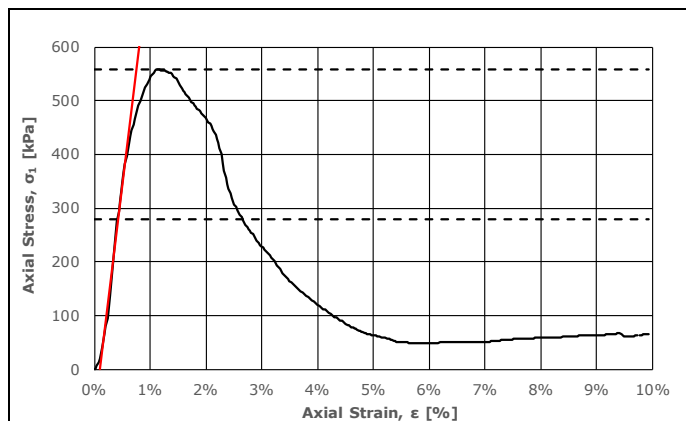


| Sample ID                           | Curing time     | Test date  |
|-------------------------------------|-----------------|------------|
| MDM.8.1.3                           | 28 Days         | 12.05.2023 |
| Sample height                       | 100,00 [mm]     |            |
| Sample diameter                     | 54,00 [mm]      |            |
| Ultimate compressive strength $q_u$ | 1195,50 [kPa]   |            |
| Undrained shear strength $S_u$      | 597,75 [kPa]    |            |
| Failure strain $\epsilon_v$         | 1,07 [%]        |            |
| Estimated stiffness $E_{50}$        | 192771,08 [kPa] |            |
| Dotted line max.                    | 0,00 [%]        |            |
| Dotted line min.                    | 9,93 [%]        |            |

## APPENDIX B.2 SAMPLE IMAGES AND UNCONFINED COMPRESSION TEST RESULTS FOR SINGLE MIXING METHOD EVALUATION



## APPENDIX B.2 SAMPLE IMAGES AND UNCONFINED COMPRESSION TEST RESULTS FOR SINGLE MIXING METHOD EVALUATION



| Sample ID                           | Curing time    | Test date  |
|-------------------------------------|----------------|------------|
| MDM.16.1.1                          | 28 Days        | 12.05.2023 |
| Sample height                       | 100,00 [mm]    |            |
| Sample diameter                     | 54,00 [mm]     |            |
| Ultimate compressive strength $q_u$ | 558,74 [kPa]   |            |
| Undrained shear strength $S_u$      | 279,37 [kPa]   |            |
| Failure strain $\epsilon_v$         | 1,14 [%]       |            |
| Estimated stiffness $E_{50}$        | 85561,50 [kPa] |            |
| Dotted line max.                    | 0,00 [%]       |            |
| Dotted line min.                    | 9,93 [%]       |            |



| Sample ID                           | Curing time    | Test date  |
|-------------------------------------|----------------|------------|
| MDM.16.1.2                          | 28 Days        | 12.05.2023 |
| Sample height                       | 100,00 [mm]    |            |
| Sample diameter                     | 54,00 [mm]     |            |
| Ultimate compressive strength $q_u$ | 562,10 [kPa]   |            |
| Undrained shear strength $S_u$      | 281,05 [kPa]   |            |
| Failure strain $\epsilon_v$         | 1,29 [%]       |            |
| Estimated stiffness $E_{50}$        | 86956,52 [kPa] |            |
| Dotted line max.                    | 0,00 [%]       |            |
| Dotted line min.                    | 9,95 [%]       |            |



| Sample ID                           | Curing time    | Test date  |
|-------------------------------------|----------------|------------|
| MDM.16.1.3                          | 28 Days        | 12.05.2023 |
| Sample height                       | 100,00 [mm]    |            |
| Sample diameter                     | 54,00 [mm]     |            |
| Ultimate compressive strength $q_u$ | 584,72 [kPa]   |            |
| Undrained shear strength $S_u$      | 292,36 [kPa]   |            |
| Failure strain $\epsilon_v$         | 1,31 [%]       |            |
| Estimated stiffness $E_{50}$        | 90395,48 [kPa] |            |
| Dotted line max.                    | 0,00 [%]       |            |
| Dotted line min.                    | 9,91 [%]       |            |

## **B.3 LABORATORY RESULT OVERVIEW**

### **B.3.1. WATER CONTENT, ENTRAPPED AIR AND CORRECTED WBR**

APPENDIX B.3.1. WATER CONTENT, ENTRAPPED AIR AND CORRECTED WBR

Table 43: Corrected wbr, entrapped air and water content for samples prepared with the dry mixing method and a wbr of 8.

| Sample ID <sup>[1]</sup> | Initial clay water content, $w_{stab}$ | Corrected wbr, $wbr_{corr}$ | Water content after UCT, $w_{UCT}$ | Measured density, $\rho_{stab}$ [ $t/m^3$ ] | Theoretical density, $\rho_{theor.}$ [ $t/m^3$ ] | Entrapped air, $n_{air}$ |
|--------------------------|--|-----------------------------|------------------------------------|---|--|--------------------------|
| DRY.8.1.1                | 42.5 %                                 | 7.56                        | 43.1 %                             | 1.76  | 1.82   | 3.23 %                   |
| DRY.8.1.2                |  |                             |                                    | 1.76  |  | 3.40 %                   |
| DRY.8.1.3                |  |                             |                                    | 1.75  |  | 3.89 %                   |
| DRY.8.2.1                | 42.5 %                                 | 7.56                        | 39.2 %                             | 1.78  | 1.82   | 2.45 %                   |
| DRY.8.2.2                |  |                             |                                    | 1.78  |  | 2.04 %                   |
| DRY.8.2.3                |  |                             |                                    | 1.79  |  | 1.69 %                   |
| DRY.8.3.1                | 45.4 %                                 | 8.07                        | 40.2 %                             | 1.77  | 1.79   | 1.35 %                   |
| DRY.8.3.2                |  |                             |                                    | 1.78  |  | 0.86 %                   |
| DRY.8.3.3                |  |                             |                                    | 1.81  |  | -0.88 %                  |
| DRY.8.4.1                | 38.1 %                                 | 6.77                        | 33.6 %                             | 1.86  | 1.87   | 0.83 %                   |
| DRY.8.4.2                |  |                             |                                    | 1.87  |  | -0.01 %                  |
| DRY.8.4.3                |  |                             |                                    | 1.86  |  | 0.61 %                   |
| DRY.8.5.1                | 38.1 %                                 | 6.77                        | 38.4 %                             | 1.83  | 1.87   | 2.11 %                   |
| DRY.8.5.2                |  |                             |                                    | 1.83  |  | 2.22 %                   |
| DRY.8.5.3                |  |                             |                                    | 1.83  |  | 2.37 %                   |
| DRY.8.6.1                | 38.1 %                                 | 6.77                        | 39.9 %                             | 1.82  | 1.87   | 2.59 %                   |
| DRY.8.6.2                |  |                             |                                    | 1.81  |  | 3.23 %                   |
| DRY.8.6.3                |  |                             |                                    | 1.81  |  | 3.06 %                   |
| DRY.8.7.1                | 38.1 %                                 | 6.77                        | 39.7 %                             | 1.80  | 1.87   | 3.80 %                   |
| DRY.8.7.2                |  |                             |                                    | 1.81  |  | 3.21 %                   |
| DRY.8.7.3                |  |                             |                                    | 1.82  |  | 2.48 %                   |
| DRY.8.8.1                | 38.1 %                                 | 6.77                        | 38.6 %                             | 1.84  | 1.87   | 1.89 %                   |
| DRY.8.8.2                |  |                             |                                    | 1.83  |  | 2.41 %                   |
| DRY.8.8.3                |  |                             |                                    | 1.82  |  | 2.56 %                   |
| DRY.8.9.1                | 38.1 %                                 | 6.77                        | 41.0 %                             | 1.81  | 1.87   | 3.24 %                   |
| DRY.8.9.2                |  |                             |                                    | 1.81  |  | 3.08 %                   |
| DRY.8.9.3                |  |                             |                                    | 1.80  |  | 3.87 %                   |
| DRY.8.10.1               | 38.1 %                                 | 6.77                        | 36.5 %                             | 1.84  | 1.87   | 1.89 %                   |
| DRY.8.10.2               |  |                             |                                    | 1.86  |  | 0.37 %                   |
| DRY.8.10.3               |  |                             |                                    | 1.85  |  | 0.96 %                   |

[1] Sample ID explanation: DRY.8.1.2 = Dry mixing method, water to binder ratio of 8, lattice point 1, sample number 2

APPENDIX B.3.1. WATER CONTENT, ENTRAPPED AIR AND CORRECTED WBR

Table 44: Corrected wbr, entrapped air and water content for samples prepared with the dry mixing method and a wbr of 16.

| Sample ID <sup>[1]</sup> | Initial clay water content, $w_{stab}$ | Corrected wbr, $wbr_{corr}$ | Water content after UCT, $w_{UCT}$ | Measured density, $\rho_{stab}$ [t/m <sup>3</sup> ] | Theoretical density, $\rho_{theor.}$ [t/m <sup>3</sup> ] | Entrapped air, $n_{air}$ |
|--------------------------|--|-----------------------------|------------------------------------|---|--|--------------------------|
| DRY.16.1.1               | 42.5 %                                 | 15.12                       | 41.0 %                             | 1.78  | 1.82   | 2.20 %                   |
| DRY.16.1.2               |  |                             |                                    | 1.77  |  | 2.92 %                   |
| DRY.16.1.3               |  |                             |                                    | 1.77  |  | 3.00 %                   |
| DRY.16.2.1               | 42.5 %                                 | 15.12                       | 44.7 %                             | 1.75  | 1.82   | 3.70 %                   |
| DRY.16.2.2               |  |                             |                                    | 1.77  |  | 2.60 %                   |
| DRY.16.2.3               |  |                             |                                    | 1.76  |  | 3.20 %                   |
| DRY.16.3.1               | 45.4 %                                 | 16.14                       | 41.7 %                             | 1.80  | 1.79   | -0.41 %                  |
| DRY.16.3.2               |  |                             |                                    | 1.79  |  | 0.37 %                   |
| DRY.16.3.3               |  |                             |                                    | 1.78  |  | 0.46 %                   |
| DRY.16.4.1               | 38.1 %                                 | 13.54                       | 40.9 %                             | 1.85  | 1.87   | 1.14 %                   |
| DRY.16.4.2               |  |                             |                                    | 1.84  |  | 1.42 %                   |
| DRY.16.4.3               |  |                             |                                    | 1.85  |  | 0.87 %                   |
| DRY.16.5.1               | 42.0 %                                 | 15.65                       | 39.0 %                             | 1.82  | 1.83   | 0.10 %                   |
| DRY.16.5.2               |  |                             |                                    | 1.83  |  | -0.11 %                  |
| DRY.16.5.3               |  |                             |                                    | 1.83  |  | -0.12 %                  |
| DRY.16.6.1               | 42.0 %                                 | 15.65                       | 38.6 %                             | 1.81  | 1.83   | 0.67 %                   |
| DRY.16.6.2               |  |                             |                                    | 1.81  |  | 0.96 %                   |
| DRY.16.6.3               |  |                             |                                    | 1.82  |  | 0.15 %                   |
| DRY.16.7.1               | 45.4 %                                 | 16.16                       | 42.1 %                             | 1.79  | 1.79   | 0.08 %                   |
| DRY.16.7.2               |  |                             |                                    | 1.78  |  | 0.51 %                   |
| DRY.16.7.3               |  |                             |                                    | 1.75  |  | 2.14 %                   |
| DRY.16.8.1               | 45.4 %                                 | 16.16                       | 40.6 %                             | 1.76  | 1.79   | 1.66 %                   |
| DRY.16.8.2               |  |                             |                                    | 1.78  |  | 0.81 %                   |
| DRY.16.8.3               |  |                             |                                    | 1.80  |  | -0.25 %                  |
| DRY.16.9.1               | 43.0 %                                 | 15.29                       | 39.0 %                             | 1.80  | 1.82   | 1.08 %                   |
| DRY.16.9.2               |  |                             |                                    | 1.79  |  | 1.72 %                   |
| DRY.16.9.3               |  |                             |                                    | 1.82  |  | -0.08 %                  |
| DRY.16.10.1              | 43.0 %                                 | 15.29                       | 39.5 %                             | 1.83  | 1.82   | -0.76 %                  |
| DRY.16.10.2              |  |                             |                                    | 1.78  |  | 2.13 %                   |
| DRY.16.10.3              |  |                             |                                    | 1.80  |  | 0.94 %                   |

[1] Sample ID explanation: DRY.16.1.2 = Dry mixing method, water to binder ratio of 16, lattice point 1, sample number 2

APPENDIX B.3.1. WATER CONTENT, ENTRAPPED AIR AND CORRECTED WBR

Table 45: Corrected wbr, entrapped air and water content for samples prepared with the wet mixing method and a wbr of 8.

| Sample ID <sup>[1]</sup> | Initial clay water content, $w_{stab}$ | Corrected wbr, $wbr_{corr}$ | Water content after UCT, $w_{UCT}$ | Measured density, $\rho_{stab} [t/m^3]$ | Theoretical density, $\rho_{theor.} [t/m^3]$ | Entrapped air, $n_{air}$ |
|--------------------------|--|-----------------------------|------------------------------------|---|--|--------------------------|
| WET.8.1.1                | 42.5 %                                 | 7.62                        | 41.7 %                             | 1.76                                    | 1.82   | 3.19 %                   |
| WET.8.1.2                |  |                             |                                    | 1.78                                    |  | 2.05 %                   |
| WET.8.1.3                |  |                             |                                    | 1.77                                    |  | 3.08 %                   |
| WET.8.1.4 <sup>[2]</sup> | 35.7 %                                 | 6.55                        | 43.6 %                             | 1.77                                    | 1.90   | 7.09 %                   |
| WET.8.1.5 <sup>[2]</sup> |  |                             |                                    | 1.76                                    |  | 7.53 %                   |
| WET.8.1.6 <sup>[2]</sup> |  |                             |                                    | 1.77                                    |  | 6.77 %                   |
| MDM.8.1.1 <sup>[2]</sup> | 44.2 %                                 | 7.87                        | 43.6 %                             | 1.76                                    | 1.80   | 2.68 %                   |
| MDM.8.1.2 <sup>[2]</sup> |  |                             |                                    | 1.76                                    |  | 2.51 %                   |
| MDM.8.1.3 <sup>[2]</sup> |  |                             |                                    | 1.76                                    |  | 2.24 %                   |
| WET.8.2.1                | 43.8 %                                 | 8.14                        | 44.1 %                             | 1.77                                    | 1.81   | 1.93 %                   |
| WET.8.2.2                |  |                             |                                    | 1.78                                    |  | 1.32 %                   |
| WET.8.2.3                |  |                             |                                    | 1.74                                    |  | 4.01 %                   |
| WET.8.3.1                | 40.6 %                                 | 7.60                        | 41.2 %                             | 1.80                                    | 1.84   | 2.09 %                   |
| WET.8.3.2                |  |                             |                                    | 1.80                                    |  | 2.49 %                   |
| WET.8.3.3                |  |                             |                                    | 1.81                                    |  | 1.67 %                   |
| WET.8.4.1                | 43.8 %                                 | 7.82                        | 44.1 %                             | 1.76                                    | 1.81   | 2.60 %                   |
| WET.8.4.2                |  |                             |                                    | 1.76                                    |  | 2.64 %                   |
| WET.8.4.3                |  |                             |                                    | 1.77                                    |  | 2.01 %                   |
| WET.8.5.1                | 43.8 %                                 | 7.82                        | 45.8 %                             | 1.76                                    | 1.81   | 2.63 %                   |
| WET.8.5.2                |  |                             |                                    | 1.77                                    |  | 2.38 %                   |
| WET.8.5.3                |  |                             |                                    | 1.76                                    |  | 2.61 %                   |
| WET.8.6.1                | 51.3 %                                 | 8.98                        | 43.6 %                             | 1.74                                    | 1.74   | 0.18 %                   |
| WET.8.6.2                |  |                             |                                    | 1.79                                    |  | -2.70 %                  |
| WET.8.6.3                |  |                             |                                    | 1.77                                    |  | -1.63 %                  |
| WET.8.7.1                | 51.3 %                                 | 8.98                        | 44.4 %                             | 1.78                                    | 1.74   | -2.28 %                  |
| WET.8.7.2                |  |                             |                                    | 1.78                                    |  | -2.14 %                  |
| WET.8.7.3                |  |                             |                                    | 1.78                                    |  | -2.09 %                  |
| WET.8.8.1                | 40.1 %                                 | 7.23                        | 40.9 %                             | 1.81                                    | 1.85   | 1.98 %                   |
| WET.8.8.2                |  |                             |                                    | 1.80                                    |  | 2.43 %                   |
| WET.8.8.3                |  |                             |                                    | 1.82                                    |  | 1.70 %                   |
| WET.8.9.1                | 40.1 %                                 | 7.23                        | 43.1 %                             | 1.78                                    | 1.85   | 3.70 %                   |
| WET.8.9.2                |  |                             |                                    | 1.78                                    |  | 3.89 %                   |
| WET.8.9.3                |  |                             |                                    | 1.78                                    |  | 3.55 %                   |
| WET.8.10.1               | 41.2 %                                 | 7.70                        | 41.7 %                             | 1.80                                    | 1.84   | 2.00 %                   |
| WET.8.10.2               |  |                             |                                    | 1.80                                    |  | 2.14 %                   |
| WET.8.10.3               |  |                             |                                    | 1.75                                    |  | 4.48 %                   |

[1] Sample ID explanation: WET.8.1.2 = Wet mixing method, MDM.8.1.2 = Modified dry mixing method, water to binder ratio of 8, lattice point 1, sample number 2

[2] Additional points for single wet mixing method evaluation

APPENDIX B.3.1. WATER CONTENT, ENTRAPPED AIR AND CORRECTED WBR

Table 46: Corrected wbr, entrapped air and water content for samples prepared with the wet mixing method and a wbr of 16.

| Sample ID <sup>[1]</sup>  | Initial clay water content, $w_{stab}$ | Corrected wbr, $wbr_{corr}$ | Water content after UCT, $w_{UCT}$ | Measured density, $\rho_{stab}$ [ $t/m^3$ ] | Theoretical density, $\rho_{theor.}$ [ $t/m^3$ ] | Entrapped air, $n_{air}$ |
|---------------------------|--|-----------------------------|------------------------------------|---|--|--------------------------|
| WET.16.1.1                | 42.5 %                                 | 15.18                       | 41.8 %                             | 1.80  | 1.82   | 1.36 %                   |
| WET.16.1.2                |  |                             |                                    | 1.80  |  | 1.43 %                   |
| WET.16.1.3                |  |                             |                                    | 1.79  |  | 1.54 %                   |
| WET.16.1.4 <sup>[2]</sup> | 46.6 %                                 | 16.54                       | 45.4 %                             | 1.77  | 1.78   | 0.53 %                   |
| WET.16.1.5 <sup>[2]</sup> |  |                             |                                    | 1.76  |  | 1.19 %                   |
| WET.16.1.6 <sup>[2]</sup> |  |                             |                                    | 1.77  |  | 0.79 %                   |
| MDM.16.1.1 <sup>[2]</sup> | 44.9 %                                 | 15.98                       | 43.0 %                             | 1.78  | 1.80   | 1.09 %                   |
| MDM.16.1.2 <sup>[2]</sup> |  |                             |                                    | 1.78  |  | 0.73 %                   |
| MDM.16.1.3 <sup>[2]</sup> |  |                             |                                    | 1.78  |  | 0.71 %                   |
| WET.16.2.1                | 43.8 %                                 | 16.29                       | 40.1 %                             | 1.78  | 1.81   | 1.64 %                   |
| WET.16.2.2                |  |                             |                                    | 1.77  |  | 1.92 %                   |
| WET.16.2.3                |  |                             |                                    | 1.80  |  | 0.28 %                   |
| WET.16.3.1                | 40.6 %                                 | 15.14                       | 41.7 %                             | 1.77  | 1.84   | 3.99 %                   |
| WET.16.3.2                |  |                             |                                    | 1.78  |  | 3.61 %                   |
| WET.16.3.3                |  |                             |                                    | 1.81  |  | 2.04 %                   |
| WET.16.4.1                | 41.2 %                                 | 15.36                       | 41.3 %                             | 1.82  | 1.84   | 0.80 %                   |
| WET.16.4.2                |  |                             |                                    | 1.87  |  | -2.02 %                  |
| WET.16.4.3                |  |                             |                                    | 1.84  |  | -0.10 %                  |
| WET.16.5.1                | 43.7 %                                 | 15.55                       | 42.3 %                             | 1.85  | 1.81   | -1.95 %                  |
| WET.16.5.2                |  |                             |                                    | 1.82  |  | -0.68 %                  |
| WET.16.5.3                |  |                             |                                    | 1.82  |  | -0.62 %                  |
| WET.16.6.1                | 43.7 %                                 | 15.55                       | 43.3 %                             | 1.77  | 1.81   | 2.06 %                   |
| WET.16.6.2                |  |                             |                                    | 1.82  |  | -0.59 %                  |
| WET.16.6.3                |  |                             |                                    | 1.79  |  | 1.28 %                   |
| WET.16.7.1                | 46.2 %                                 | 15.42                       | 45.6 %                             | 1.75  | 1.79   | 1.75 %                   |
| WET.16.7.2                |  |                             |                                    | 1.77  |  | 0.58 %                   |
| WET.16.7.3                |  |                             |                                    | 1.78  |  | 0.21 %                   |
| WET.16.8.1                | 46.2 %                                 | 15.42                       | 45.2 %                             | 1.77  | 1.79   | 0.91 %                   |
| WET.16.8.2                |  |                             |                                    | 1.78  |  | 0.15 %                   |
| WET.16.8.3                |  |                             |                                    | 1.79  |  | -0.41 %                  |
| WET.16.9.1                | 44.6 %                                 | 14.94                       | 43.3 %                             | 1.78  | 1.80   | 1.02 %                   |
| WET.16.9.2                |  |                             |                                    | 1.73  |  | 3.84 %                   |
| WET.16.9.3                |  |                             |                                    | 1.73  |  | 3.92 %                   |
| WET.16.10.1               | 44.6 %                                 | 14.94                       | 43.8 %                             | 1.79  | 1.80   | 0.69 %                   |
| WET.16.10.2               |  |                             |                                    | 1.79  |  | 0.60 %                   |
| WET.16.10.3               |  |                             |                                    | 1.78  |  | 1.20 %                   |

[1] Sample ID explanation: WET.16.1.2 = Wet mixing method, MDM.16.1.2 = Modified dry mixing method, water to binder ratio of 16, lattice point 1, sample number 2

[2] Additional points for single wet mixing method evaluation



### **B.3.2. STRENGTH, STIFFNESS AND STRAIN**

APPENDIX B.3.2. STRENGTH, STIFFNESS AND STRAIN

Table 47: UCT results for samples prepared with the dry mixing method and a wbr of 8.

| Sample ID <sup>[1]</sup> | Ultimate compressive strength, $q_u$ [kPa] | Undrained shear strength, $S_u$ [kPa] | Failure strain, $\varepsilon_v$ | Estimated stiffness, $E_{50}$ [kPa] |
|--------------------------|--|---------------------------------------|---------------------------------|-------------------------------------|
| DRY.8.1.1                | 857  | 428                                   | 2.51 %                          | 57 971                              |
| DRY.8.1.2                | 747  | 374                                   | 2.97 %                          | 36 254                              |
| DRY.8.1.3                | 989  | 494                                   | 2.52 %                          | 57 143                              |
| DRY.8.2.1                | 1117                                       | 558                                   | 1.67 %                          | 98 765                              |
| DRY.8.2.2                | 1333                                       | 667                                   | 2.08 %                          | 101 266                             |
| DRY.8.2.3                | 1231                                       | 616                                   | 2.14 %                          | 93 023                              |
| DRY.8.3.1                | 1137                                       | 569                                   | 1.64 %                          | 116 667                             |
| DRY.8.3.2                | 1029                                       | 515                                   | 1.83 %                          | 100 719                             |
| DRY.8.3.3                | 632  | 316                                   | 2.08 %                          | 51 095                              |
| DRY.8.4.1                | 167  | 83                                    | 2.92 %                          | 7 576                               |
| DRY.8.4.2                | 177  | 88                                    | 3.40 %                          | 7 109                               |
| DRY.8.4.3                | 137  | 68                                    | 3.48 %                          | 5 988                               |
| DRY.8.5.1                | 532  | 266                                   | 5.21 %                          | 13 115                              |
| DRY.8.5.2                | 544  | 272                                   | 5.06 %                          | 11 561                              |
| DRY.8.5.3                | 424  | 212                                   | 4.27 %                          | 12 140                              |
| DRY.8.6.1                | 350  | 175                                   | 4.70 %                          | 9 975                               |
| DRY.8.6.2                | 287  | 144                                   | 4.41 %                          | 10 101                              |
| DRY.8.6.3                | 195  | 98                                    | 3.67 %                          | 7 477                               |
| DRY.8.7.1                | 443  | 222                                   | 4.75 %                          | 12 821                              |
| DRY.8.7.2                | 415  | 208                                   | 3.90 %                          | 15 544                              |
| DRY.8.7.3                | 305  | 153                                   | 3.66 %                          | 11 673                              |
| DRY.8.8.1                | 574  | 287                                   | 4.23 %                          | 18 265                              |
| DRY.8.8.2                | 585  | 292                                   | 4.21 %                          | 18 648                              |
| DRY.8.8.3                | 565  | 283                                   | 3.68 %                          | 19 802                              |
| DRY.8.9.1                | 586  | 293                                   | 3.81 %                          | 19 512                              |
| DRY.8.9.2                | 657  | 329                                   | 3.88 %                          | 19 324                              |
| DRY.8.9.3                | 644  | 322                                   | 3.83 %                          | 19 753                              |
| DRY.8.10.1               | 1182                                       | 591                                   | 1.87 %                          | 97 902                              |
| DRY.8.10.2               | 1162                                       | 581                                   | 2.09 %                          | 89 172                              |
| DRY.8.10.3               | 1045                                       | 523                                   | 1.83 %                          | 90 909                              |

[1] Sample ID explanation: DRY.8.1.2 = Dry mixing method, water to binder ratio of 8, lattice point 1, sample number 2

APPENDIX B.3.2. STRENGTH, STIFFNESS AND STRAIN

Table 48: UCT results for samples prepared with the dry mixing method and a wbr of 16.

| Sample ID <sup>[1]</sup> | Ultimate compressive strength, $q_u$ [kPa] | Undrained shear strength, $S_u$ [kPa] | Failure strain, $\epsilon_v$ | Estimated stiffness, $E_{50}$ [kPa] |
|--------------------------|--|---------------------------------------|------------------------------|-------------------------------------|
| DRY.16.1.1               | 436  | 218                                   | 2.35 %                       | 29 557                              |
| DRY.16.1.2               | 451  | 226                                   | 2.30 %                       | 33 708                              |
| DRY.16.1.3               | 434  | 217                                   | 2.27 %                       | 33 708                              |
| DRY.16.2.1               | 256  | 128                                   | 2.19 %                       | 22 599                              |
| DRY.16.2.2               | 263  | 132                                   | 2.39 %                       | 26 846                              |
| DRY.16.2.3               | 261  | 130                                   | 2.19 %                       | 22 472                              |
| DRY.16.3.1               | 167  | 84                                    | 2.57 %                       | 12 195                              |
| DRY.16.3.2               | 161  | 80                                    | 2.37 %                       | 11 111                              |
| DRY.16.3.3               | 148  | 74                                    | 2.78 %                       | 8 850                               |
| DRY.16.4.1               | 50   | 25                                    | 2.81 %                       | 4 188                               |
| DRY.16.4.2               | 56   | 28                                    | 4.04 %                       | 3 433                               |
| DRY.16.4.3               | 52   | 26                                    | 3.21 %                       | 3 902                               |
| DRY.16.5.1               | 136  | 68                                    | 3.28 %                       | 9 662                               |
| DRY.16.5.2               | 142  | 71                                    | 3.25 %                       | 9 479                               |
| DRY.16.5.3               | 124  | 62                                    | 2.85 %                       | 9 390                               |
| DRY.16.6.1               | 112  | 56                                    | 6.38 %                       | 2 597                               |
| DRY.16.6.2               | 114  | 57                                    | 6.78 %                       | 2 581                               |
| DRY.16.6.3               | 102  | 51                                    | 5.58 %                       | 2 873                               |
| DRY.16.7.1               | 122  | 61                                    | 4.80 %                       | 3 837                               |
| DRY.16.7.2               | 130  | 65                                    | 5.33 %                       | 3 883                               |
| DRY.16.7.3               | 119  | 60                                    | 5.20 %                       | 3 441                               |
| DRY.16.8.1               | 246  | 123                                   | 4.19 %                       | 8 902                               |
| DRY.16.8.2               | 266  | 133                                   | 4.11 %                       | 8 219                               |
| DRY.16.8.3               | 230  | 115                                   | 4.39 %                       | 7 075                               |
| DRY.16.9.1               | 197  | 98                                    | 3.69 %                       | 9 288                               |
| DRY.16.9.2               | 215  | 108                                   | 3.77 %                       | 9 772                               |
| DRY.16.9.3               | 177  | 89                                    | 3.00 %                       | 8 287                               |
| DRY.16.10.1              | 294  | 147                                   | 2.11 %                       | 25 478                              |
| DRY.16.10.2              | 330  | 165                                   | 2.43 %                       | 20 942                              |
| DRY.16.10.3              | 351  | 176                                   | 2.10 %                       | 29 197                              |

[1] Sample ID explanation: DRY.16.1.2 = Dry mixing method, water to binder ratio of 16, lattice point 1, sample number 2

APPENDIX B.3.2. STRENGTH, STIFFNESS AND STRAIN

Table 49: UCT results for samples prepared with the wet mixing method and a wbr of 8.

| Sample ID <sup>[1]</sup>   | Ultimate compressive strength, $q_u$ [kPa] | Undrained shear strength, $S_u$ [kPa] | Failure strain, $\epsilon_v$ | Estimated stiffness, $E_{50}$ [kPa] |
|--|--|---------------------------------------|------------------------------|-------------------------------------|
| WET.8.1.1  | 1090                                       | 545                                   | 1.57 %                       | 118 644                             |
| WET.8.1.2  | 1081                                       | 540                                   | 1.67 %                       | 112 903                             |
| WET.8.1.3  | 949  | 474                                   | 1.71 %                       | 84 848                              |
| WET.8.1.4 <sup>[2]</sup>   | 1235                                       | 617                                   | 1.31 %                       | 168 421                             |
| WET.8.1.5 <sup>[2]</sup>   | 1136                                       | 568                                   | 1.37 %                       | 166 667                             |
| WET.8.1.6 <sup>[2]</sup>   | 1255                                       | 627                                   | 1.24 %                       | 156 863                             |
| MDM.8.1.1 <sup>[2]</sup>   | 1121                                       | 560                                   | 1.05 %                       | 166 667                             |
| MDM.8.1.2 <sup>[2]</sup>   | 1244                                       | 622                                   | 1.06 %                       | 195 122                             |
| MDM.8.1.3 <sup>[2]</sup>   | 1196                                       | 598                                   | 1.07 %                       | 192 771                             |
| WET.8.2.1  | 1316                                       | 658                                   | 1.33 %                       | 130 081                             |
| WET.8.2.2  | 1225                                       | 613                                   | 1.66 %                       | 104 575                             |
| WET.8.2.3  | 1357                                       | 678                                   | 1.30 %                       | 170 213                             |
| WET.8.3.1  | 857  | 429                                   | 1.99 %                       | 95 238                              |
| WET.8.3.2  | 991  | 496                                   | 1.85 %                       | 74 534                              |
| WET.8.3.3  | 898  | 449                                   | 1.61 %                       | 94 488                              |
| WET.8.4.1  | 174  | 87                                    | 2.50 %                       | 9 009                               |
| WET.8.4.2  | 169  | 85                                    | 2.75 %                       | 9 050                               |
| WET.8.4.3  | 183  | 92                                    | 2.60 %                       | 9 756                               |
| WET.8.5.1  | 270  | 135                                   | 4.31 %                       | 8 529                               |
| WET.8.5.2  | 227  | 114                                   | 4.04 %                       | 8 180                               |
| WET.8.5.3  | 349  | 174                                   | 4.03 %                       | 10 178                              |
| WET.8.6.1  | 254  | 127                                   | 5.39 %                       | 6 339                               |
| WET.8.6.2  | 309  | 154                                   | 4.96 %                       | 7 737                               |
| WET.8.6.3  | 267  | 134                                   | 4.41 %                       | 7 233                               |
| WET.8.7.1  | 389  | 194                                   | 2.88 %                       | 19 841                              |
| WET.8.7.2  | 427  | 214                                   | 4.62 %                       | 11 933                              |
| WET.8.7.3  | 356  | 178                                   | 3.68 %                       | 12 255                              |
| WET.8.8.1  | 618  | 309                                   | 3.41 %                       | 23 324                              |
| WET.8.8.2  | 620  | 310                                   | 3.13 %                       | 27 027                              |
| WET.8.8.3  | 597  | 299                                   | 3.03 %                       | 27 397                              |
| WET.8.9.1  | 719  | 360                                   | 3.20 %                       | 31 496                              |
| WET.8.9.2  | 750  | 375                                   | 3.35 %                       | 32 587                              |
| WET.8.9.3  | 586  | 293                                   | 3.03 %                       | 27 165                              |
| WET.8.10.1   | 1004                                       | 502                                   | 2.18 %                       | 65 934                              |
| WET.8.10.2   | 991  | 495                                   | 2.10 %                       | 83 916                              |
| WET.8.10.3   | 962  | 481                                   | 2.16 %                       | 71 856                              |
| [1] Sample ID explanation: WET.8.1.2 = Wet mixing method, MDM.8.1.2 = Modified dry mixing method, water to binder ratio of 8, lattice point 1, sample number 2 |  |                                       |                              |                                     |
| [2] Additional points for single wet mixing method evaluation  |  |                                       |                              |                                     |

APPENDIX B.3.2. STRENGTH, STIFFNESS AND STRAIN

Table 50: UCT results for samples prepared with the wet mixing method and a wbr of 16.

| Sample ID <sup>[1]</sup>  | Ultimate compressive strength, $q_u$ [kPa] | Undrained shear strength, $S_u$ [kPa] | Failure strain, $\epsilon_v$ | Estimated stiffness, $E_{50}$ [kPa] |
|---|--|---------------------------------------|------------------------------|-------------------------------------|
| WET.16.1.1  | 397  | 198                                   | 1.63 %                       | 49 587                              |
| WET.16.1.2  | 353  | 176                                   | 2.03 %                       | 29 851                              |
| WET.16.1.3  | 330  | 165                                   | 1.88 %                       | 29 703                              |
| WET.16.1.4 <sup>[2]</sup>   | 444  | 222                                   | 1.37 %                       | 63 241                              |
| WET.16.1.5 <sup>[2]</sup>   | 458  | 229                                   | 1.22 %                       | 62 257                              |
| WET.16.1.6 <sup>[2]</sup>   | 437  | 219                                   | 1.32 %                       | 67 511                              |
| MDM.16.1.1 <sup>[2]</sup>   | 559  | 279                                   | 1.14 %                       | 85 561                              |
| MDM.16.1.2 <sup>[2]</sup>   | 562  | 281                                   | 1.29 %                       | 86 957                              |
| MDM.16.1.3 <sup>[2]</sup>   | 585  | 292                                   | 1.31 %                       | 90 395                              |
| WET.16.2.1  | 291  | 146                                   | 2.59 %                       | 19 704                              |
| WET.16.2.2  | 351  | 176                                   | 2.18 %                       | 32 787                              |
| WET.16.2.3  | 320  | 160                                   | 2.28 %                       | 27 211                              |
| WET.16.3.1  | 156  | 78                                    | 2.20 %                       | 13 953                              |
| WET.16.3.2  | 177  | 88                                    | 2.05 %                       | 17 964                              |
| WET.16.3.3  | 237  | 118                                   | 2.02 %                       | 24 590                              |
| WET.16.4.1  | 48   | 24                                    | 4.59 %                       | 3 109                               |
| WET.16.4.2  | 52   | 26                                    | 4.31 %                       | 5 357                               |
| WET.16.4.3  | 49   | 25                                    | 3.59 %                       | 5 405                               |
| WET.16.5.1  | 46   | 23                                    | 3.31 %                       | 3 361                               |
| WET.16.5.2  | 59   | 29                                    | 3.54 %                       | 3 941                               |
| WET.16.5.3  | 44   | 22                                    | 5.04 %                       | 2 492                               |
| WET.16.6.1  | 22   | 11                                    | 4.37 %                       | 2 286                               |
| WET.16.6.2  | 31   | 15                                    | 4.09 %                       | 1 660                               |
| WET.16.6.3  | 22   | 11                                    | 4.02 %                       | 1 739                               |
| WET.16.7.1  | 52   | 26                                    | 3.16 %                       | 2 581                               |
| WET.16.7.2  | 51   | 26                                    | 2.89 %                       | 2 395                               |
| WET.16.7.3  | 23   | 12                                    | 4.12 %                       | 1 914                               |
| WET.16.8.1  | 70   | 35                                    | 2.24 %                       | 4 624                               |
| WET.16.8.2  | 75   | 37                                    | 2.78 %                       | 3 828                               |
| WET.16.8.3  | 66   | 33                                    | 2.94 %                       | 3 376                               |
| WET.16.9.1  | 60   | 30                                    | 3.16 %                       | 4 396                               |
| WET.16.9.2  | 53   | 26                                    | 2.66 %                       | 3 509                               |
| WET.16.9.3  | 53   | 26                                    | 3.06 %                       | 3 791                               |
| WET.16.10.1   | 372  | 186                                   | 2.08 %                       | 28 736                              |
| WET.16.10.2   | 329  | 165                                   | 2.06 %                       | 26 596                              |
| WET.16.10.3   | 388  | 194                                   | 2.20 %                       | 32 468                              |
| [1] Sample ID explanation: WET.16.1.2 = Wet mixing method, MDM.16.1.2 = Modified dry mixing method, water to binder ratio of 16, lattice point 1, sample number 2 |  |                                       |                              |                                     |
| [2] Additional points for single wet mixing method evaluation   |  |                                       |                              |                                     |

### **B.3.3. P-WAVE VELOCITY**

APPENDIX B.3.3. P-WAVE VELOCITY

Table 51: P-wave test results for samples prepared with the dry mixing method.

| wbr=8                    |             |                              | wbr=16      |             |                              |
|--------------------------|-------------|------------------------------|-------------|-------------|------------------------------|
| Sample ID <sup>[1]</sup> | Voltage [V] | P-wave velocity, $V_p$ [m/s] | Sample ID   | Voltage [V] | P-wave velocity, $V_p$ [m/s] |
| DRY.8.1.1                | 250         | 1250                         | DRY.16.1.1  | 250         | 1017                         |
| DRY.8.1.2                | 400         | 1150                         | DRY.16.1.2  | 250         | 950                          |
| DRY.8.1.3                | 300         | 1220                         | DRY.16.1.3  | 350         | 995                          |
| DRY.8.2.1                | 250         | 1550                         | DRY.16.2.1  | 250         | 1040                         |
| DRY.8.2.2                | 300         | 1460                         | DRY.16.2.2  | 350         | 935                          |
| DRY.8.2.3                | 350         | 1500                         | DRY.16.2.3  | 250         | 970                          |
| DRY.8.3.1                | 250         | 1465                         | DRY.16.3.1  | 350         | 1300                         |
| DRY.8.3.2                | 300         | 1395                         | DRY.16.3.2  | 250         | 1350                         |
| DRY.8.3.3                | 300         | 1060                         | DRY.16.3.3  | 250         | 1380                         |
| DRY.8.4.1                | 250         | 270                          | DRY.16.4.1  | 250         | 1510                         |
| DRY.8.4.2                | 250         | 280                          | DRY.16.4.2  | 300         | 1515                         |
| DRY.8.4.3                | 400         | 275                          | DRY.16.4.3  | 250         | 1510                         |
| DRY.8.5.1                | 400         | 335                          | DRY.16.5.1  | 300         | 475                          |
| DRY.8.5.2                | 300         | 315                          | DRY.16.5.2  | 300         | 545                          |
| DRY.8.5.3                | 250         | 320                          | DRY.16.5.3  | 300         | 490                          |
| DRY.8.6.1                | 300         | 295                          | DRY.16.6.1  | 400         | 285                          |
| DRY.8.6.2                | 350         | 300                          | DRY.16.6.2  | 400         | 270                          |
| DRY.8.6.3                | 350         | 310                          | DRY.16.6.3  | 400         | 260                          |
| DRY.8.7.1                | 300         | 300                          | DRY.16.7.1  | 300         | 285                          |
| DRY.8.7.2                | 300         | 385                          | DRY.16.7.2  | 300         | 280                          |
| DRY.8.7.3                | 350         | 380                          | DRY.16.7.3  | 300         | 280                          |
| DRY.8.8.1                | 300         | 550                          | DRY.16.8.1  | 250         | 290                          |
| DRY.8.8.2                | 300         | 430                          | DRY.16.8.2  | 250         | 285                          |
| DRY.8.8.3                | 300         | 490                          | DRY.16.8.3  | 350         | 285                          |
| DRY.8.9.1                | 250         | 470                          | DRY.16.9.1  | 350         | 290                          |
| DRY.8.9.2                | 250         | 480                          | DRY.16.9.2  | 300         | 310                          |
| DRY.8.9.3                | 250         | 460                          | DRY.16.9.3  | 300         | 300                          |
| DRY.8.10.1               | 250         | 1260                         | DRY.16.10.1 | 300         | 875                          |
| DRY.8.10.2               | 300         | 1160                         | DRY.16.10.2 | 300         | 790                          |
| DRY.8.10.3               | 250         | 1310                         | DRY.16.10.3 | 300         | 870                          |

[1] Sample ID explanation: DRY.8.1.2 = Dry mixing method, water to binder ratio of 8, lattice point 1, sample number 2

APPENDIX B.3.3. P-WAVE VELOCITY

Table 52: P-wave test results for samples prepared with the wet mixing method.

| wbr=8                    |             |                              | wbr=16      |             |                              |
|--------------------------|-------------|------------------------------|-------------|-------------|------------------------------|
| Sample ID <sup>[1]</sup> | Voltage [V] | P-wave velocity, $V_p$ [m/s] | Sample ID   | Voltage [V] | P-wave velocity, $V_p$ [m/s] |
| WET.8.1.1                | 250         | 1510                         | WET.16.1.1  | 250         | 1170                         |
| WET.8.1.2                | 300         | 1420                         | WET.16.1.2  | 250         | 1080                         |
| WET.8.1.3                | 250         | 1500                         | WET.16.1.3  | 250         | 1135                         |
| WET.8.2.1                | 250         | 1650                         | WET.16.2.1  | 250         | 1090                         |
| WET.8.2.2                | 300         | 1600                         | WET.16.2.2  | 250         | 1050                         |
| WET.8.2.3                | 250         | 1670                         | WET.16.2.3  | 250         | 1085                         |
| WET.8.3.1                | 250         | 1620                         | WET.16.3.1  | 250         | 1160                         |
| WET.8.3.2                | 250         | 1545                         | WET.16.3.2  | 300         | 1145                         |
| WET.8.3.3                | 250         | 1570                         | WET.16.3.3  | 250         | 1225                         |
| WET.8.4.1                | 300         | 310                          | WET.16.4.1  | 250         | 1500                         |
| WET.8.4.2                | 300         | 300                          | WET.16.4.2  | 250         | 1505                         |
| WET.8.4.3                | 300         | 330                          | WET.16.4.3  | 250         | 1490                         |
| WET.8.5.1                | 300         | 365                          | WET.16.5.1  | 300         | 1330                         |
| WET.8.5.2                | 300         | 265                          | WET.16.5.2  | 250         | 570                          |
| WET.8.5.3                | 300         | 340                          | WET.16.5.3  | 250         | 1535                         |
| WET.8.6.1                | 300         | 275                          | WET.16.6.1  | 250         | 1510                         |
| WET.8.6.2                | 250         | 290                          | WET.16.6.2  | 350         | 290                          |
| WET.8.6.3                | 300         | 335                          | WET.16.6.3  | 300         | 1515                         |
| WET.8.7.1                | 300         | 425                          | WET.16.7.1  | 300         | 270                          |
| WET.8.7.2                | 300         | 330                          | WET.16.7.2  | 300         | 265                          |
| WET.8.7.3                | 300         | 340                          | WET.16.7.3  | 300         | 1250                         |
| WET.8.8.1                | 250         | 490                          | WET.16.8.1  | 300         | 245                          |
| WET.8.8.2                | 250         | 465                          | WET.16.8.2  | 350         | 265                          |
| WET.8.8.3                | 250         | 460                          | WET.16.8.3  | 350         | 240                          |
| WET.8.9.1                | 250         | 480                          | WET.16.9.1  | 300         | 405                          |
| WET.8.9.2                | 250         | 425                          | WET.16.9.2  | 350         | 395                          |
| WET.8.9.3                | 250         | 475                          | WET.16.9.3  | 300         | 615                          |
| WET.8.10.1               | 250         | 930                          | WET.16.10.1 | 250         | 490                          |
| WET.8.10.2               | 250         | 850                          | WET.16.10.2 | 250         | 515                          |
| WET.8.10.3               | 350         | 870                          | WET.16.10.3 | 250         | 525                          |

[1] Sample ID explanation: WET.8.1.2 = Wet mixing method, MDM.8.1.2 = Modified dry mixing method, water to binder ratio of 8, lattice point 1, sample number 2



## **B.4 DESIGN EXPERT RESULTS**

### **B.4.1. DRY AND WET MIXING METHOD WITH WBR=8**

# R1: Ultimate compressive strength, $q_u$

## DRY.8

Configure Fit Summary Model ANOVA Diagnostics Model Graphs

Fit Summary Sequential Model Sum of Squares [Type I] Model Summary Statistics

**Fit Summary**

Response 1: Ultimate compressive strength

Mixture Component Coding is L\_Pseudo.

| Source        | Sequential p-value | Lack of Fit p-value | Adjusted R <sup>2</sup> | Predicted R <sup>2</sup> |                  |
|---------------|--------------------|---------------------|-------------------------|--------------------------|------------------|
| Linear        | 0,0001             |                     | 0,5130                  | 0,2740                   |                  |
| Quadratic     | < 0,0001           |                     | <b>0,8917</b>           | <b>0,8294</b>            | <b>Suggested</b> |
| Special Cubic | 0,5666             |                     | 0,8878                  | 0,8142                   |                  |
| Cubic         | 0,0126             |                     | 0,9270                  | 0,8742                   | <b>Aliased</b>   |

Configure Fit Summary Model ANOVA Diagnostics Model Graphs

Mixture Order: Modified Auto Select...

Model Type: Scheffe Add Term

|          |  |
|----------|--|
| <b>m</b> | The term will be included in the model.  |
| <b>!</b> | Indicates the term is aliased with another term, or was not estimated in the Fit Summary calculations. Including the term in the model is not recommended. |
| <b>🔒</b> | A user-forced term. Automatic model selection will always produce a model that includes this term.   |
| <b>🔒</b> | Indicates that the term is required to be in the model by the program.   |

- 🔒** A-CEM I
- 🔒** B-GGBS
- 🔒** C-PSA
- m** AB
- AC
- m** BC
- ABC
- AB(A-B)
- AC(A-C)
- !** BC(B-C)
- A<sup>2</sup>BC
- AB<sup>2</sup>C
- !** ABC<sup>2</sup>
- !** AB(A-B)<sup>2</sup>
- !** AC(A-C)<sup>2</sup>
- !** BC(B-C)<sup>2</sup>

## WET.8

Configure Fit Summary Model ANOVA Diagnostics Model Graphs

Fit Summary Sequential Model Sum of Squares [Type I] Model Summary Statistics

**Fit Summary**

Response 1: Ultimate compressive strength

Mixture Component Coding is L\_Pseudo.

| Source        | Sequential p-value | Lack of Fit p-value | Adjusted R <sup>2</sup> | Predicted R <sup>2</sup> |                  |
|---------------|--------------------|---------------------|-------------------------|--------------------------|------------------|
| Linear        | < 0,0001           |                     | 0,6802                  | 0,5561                   |                  |
| Quadratic     | < 0,0001           |                     | <b>0,9704</b>           | <b>0,9540</b>            | <b>Suggested</b> |
| Special Cubic | 0,3599             |                     | 0,9702                  | 0,9510                   |                  |
| Cubic         | 0,0533             |                     | 0,9761                  | 0,9589                   | <b>Aliased</b>   |

Configure Fit Summary Model ANOVA Diagnostics Model Graphs

Mixture Order: Quadratic Auto Select...

Model Type: Scheffe Add Term

|          |  |
|----------|--|
| <b>m</b> | The term will be included in the model.  |
| <b>!</b> | Indicates the term is aliased with another term, or was not estimated in the Fit Summary calculations. Including the term in the model is not recommended. |
| <b>🔒</b> | A user-forced term. Automatic model selection will always produce a model that includes this term.   |
| <b>🔒</b> | Indicates that the term is required to be in the model by the program.   |

- 🔒** A-CEM I
- 🔒** B-GGBS
- 🔒** C-PSA
- m** AB
- m** AC
- m** BC
- ABC
- AB(A-B)
- AC(A-C)
- !** BC(B-C)
- A<sup>2</sup>BC
- AB<sup>2</sup>C
- !** ABC<sup>2</sup>
- !** AB(A-B)<sup>2</sup>
- !** AC(A-C)<sup>2</sup>
- !** BC(B-C)<sup>2</sup>

# DRY.8

Configure Fit Summary Model ANOVA Diagnostics Model Graphs

Analysis of Variance Fit Statistics Model Comparison Statistics Coefficients Coded Equation Real Equation Actual Equation

**ANOVA for Reduced Quadratic model**

Response 1: Ultimate compressive strength

| Source                        | Sum of Squares | df | Mean Square | F-value | p-value  |             |
|-------------------------------|----------------|----|-------------|---------|----------|-------------|
| Block                         | 3335,40        | 2  | 1667,70     |         |          |             |
| Model                         | 3,042E+06      | 4  | 7,606E+05   | 51,71   | < 0.0001 | significant |
| <sup>(1)</sup> Linear Mixture | 1,847E+06      | 2  | 9,235E+05   | 62,79   | < 0.0001 |             |
| AB                            | 8,096E+05      | 1  | 8,096E+05   | 55,04   | < 0.0001 |             |
| BC                            | 75655,66       | 1  | 75655,66    | 5,14    | 0,0346   |             |
| Residual                      | 2,942E+05      | 20 | 14709,09    |         |          |             |
| Cor Total                     | 3,340E+06      | 26 |             |         |          |             |

Configure Fit Summary Model ANOVA Diagnostics Model Graphs

Analysis of Variance Fit Statistics Model Comparison Statistics Coefficients Coded Equation Real Equation Actual Equation

**Fit Statistics**

|           |        |                          |         |
|-----------|--------|--------------------------|---------|
| Std. Dev. | 121,28 | R <sup>2</sup>           | 0,9118  |
| Mean      | 700,56 | Adjusted R <sup>2</sup>  | 0,8942  |
| C.V. %    | 17,31  | Predicted R <sup>2</sup> | 0,8385  |
|           |        | Adeq Precision           | 18,3636 |

Configure Fit Summary Model ANOVA Diagnostics Model Graphs

Analysis of Variance Fit Statistics Model Comparison Statistics Coefficients Coded Equation Real Equation Actual Equation

**Final Equation in Terms of L\_Pseudo Components**

|                               |               |
|-------------------------------|---------------|
| Ultimate compressive strength | =             |
|                               | +878,20 * A   |
|                               | +398,83 * B   |
|                               | +361,47 * C   |
|                               | +2711,57 * AB |
|                               | -1060,17 * BC |

# WET.8

Configure Fit Summary Model ANOVA Diagnostics Model Graphs

Analysis of Variance Fit Statistics Model Comparison Statistics Coefficients Coded Equation Real Equation Actual Equation

**ANOVA for Quadratic model**

Response 1: Ultimate compressive strength

| Source                        | Sum of Squares | df | Mean Square | F-value | p-value  |             |
|-------------------------------|----------------|----|-------------|---------|----------|-------------|
| Block                         | 31661,89       | 2  | 15830,95    |         |          |             |
| Model                         | 3,708E+06      | 5  | 7,417E+05   | 171,60  | < 0.0001 | significant |
| <sup>(1)</sup> Linear Mixture | 2,677E+06      | 2  | 1,339E+06   | 309,74  | < 0.0001 |             |
| AB                            | 6,153E+05      | 1  | 6,153E+05   | 142,35  | < 0.0001 |             |
| AC                            | 55682,68       | 1  | 55682,68    | 12,88   | 0,0017   |             |
| BC                            | 1,192E+05      | 1  | 1,192E+05   | 27,57   | < 0.0001 |             |
| Residual                      | 90765,94       | 21 | 4322,19     |         |          |             |
| Cor Total                     | 3,831E+06      | 28 |             |         |          |             |

Configure Fit Summary Model ANOVA Diagnostics Model Graphs

Analysis of Variance Fit Statistics Model Comparison Statistics Coefficients Coded Equation Real Equation Actual Equation

**Fit Statistics**

|           |        |                          |         |
|-----------|--------|--------------------------|---------|
| Std. Dev. | 65,74  | R <sup>2</sup>           | 0,9761  |
| Mean      | 681,33 | Adjusted R <sup>2</sup>  | 0,9704  |
| C.V. %    | 9,65   | Predicted R <sup>2</sup> | 0,9540  |
|           |        | Adeq Precision           | 33,9195 |

Configure Fit Summary Model ANOVA Diagnostics Model Graphs

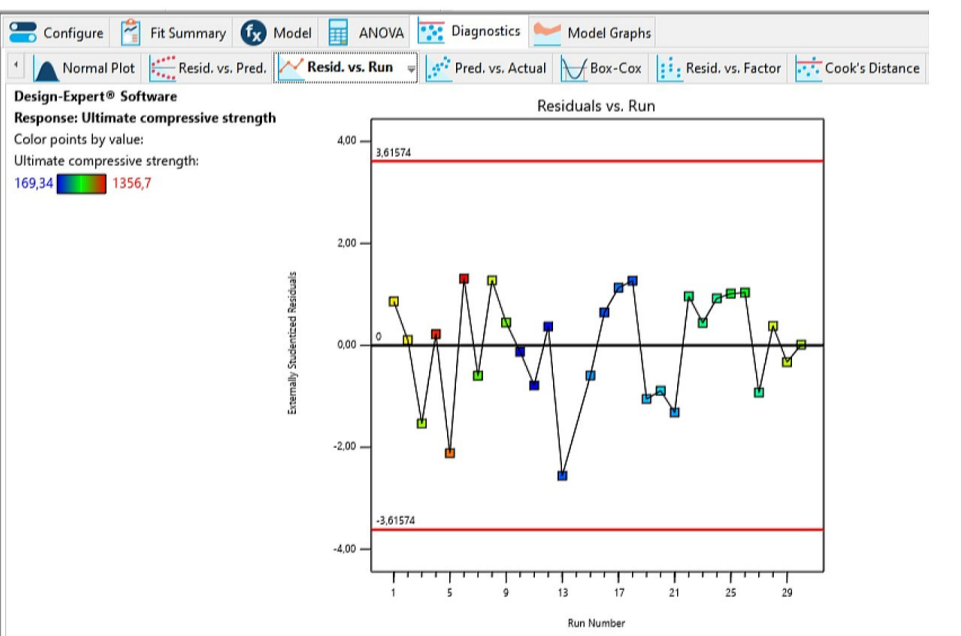
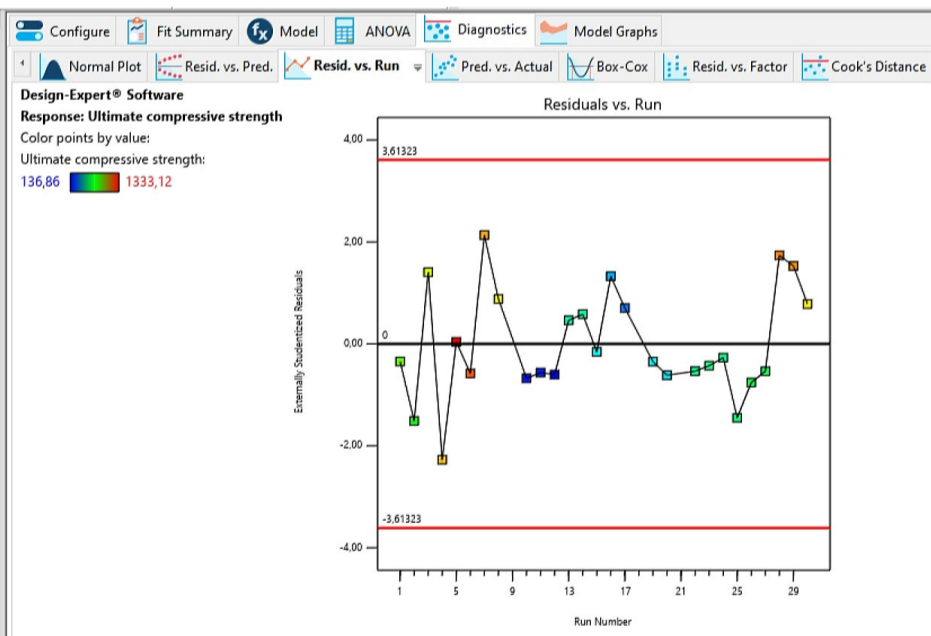
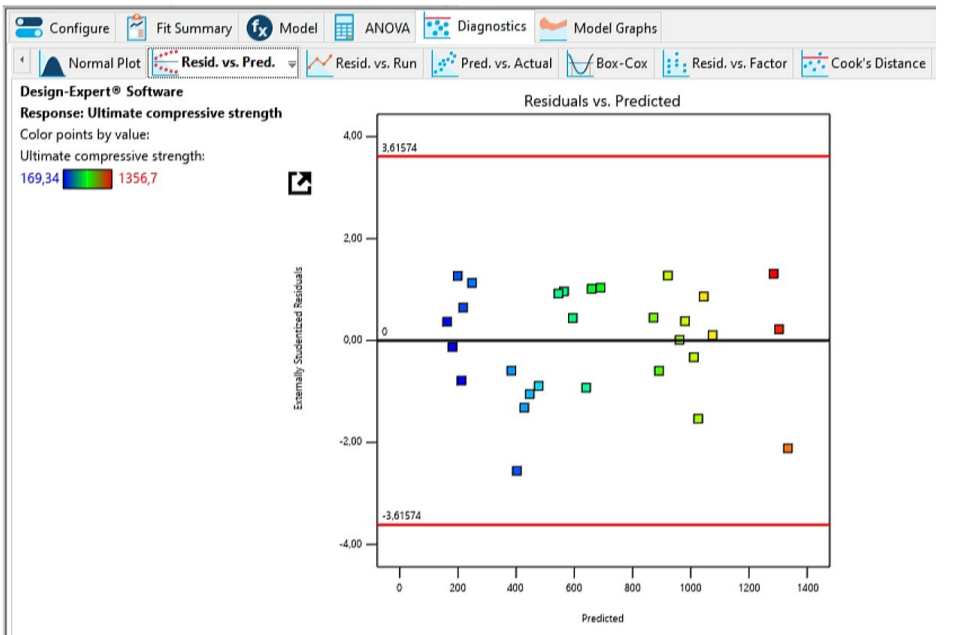
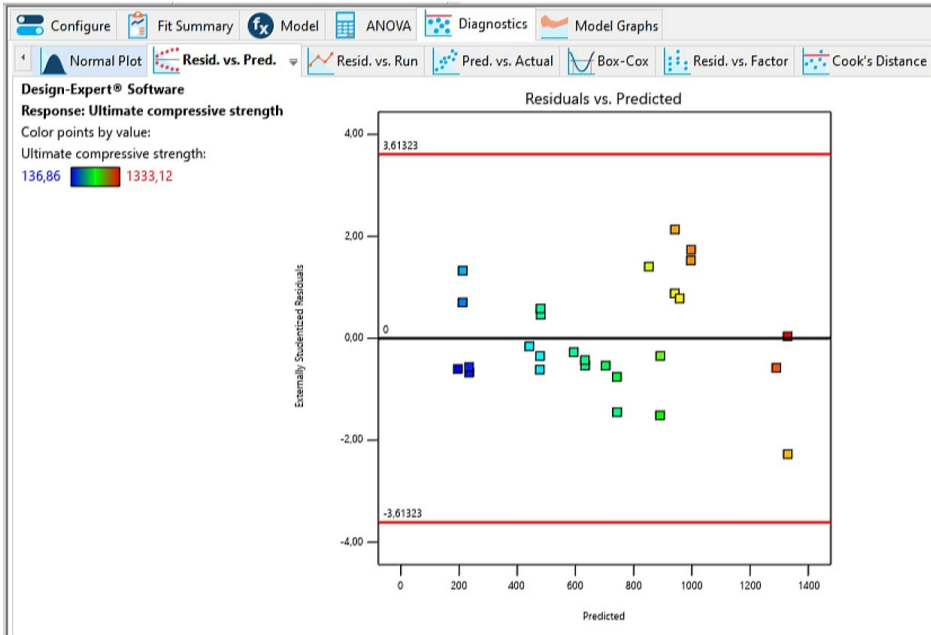
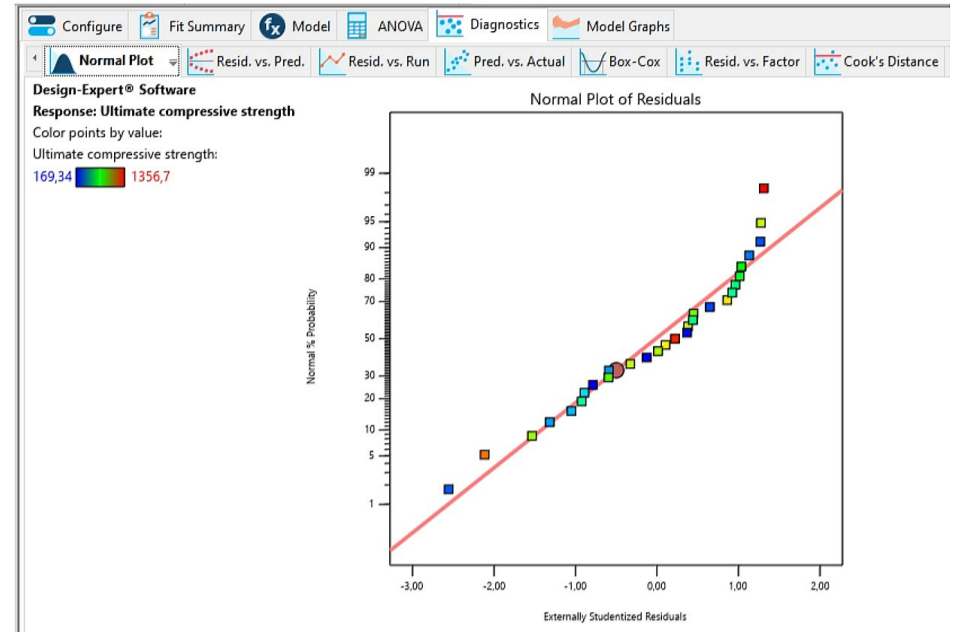
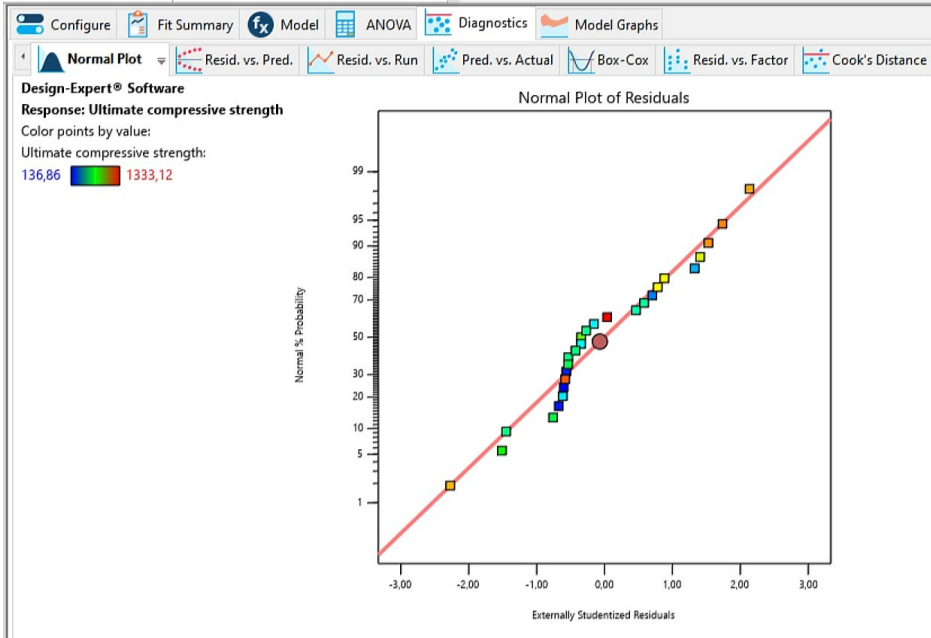
Analysis of Variance Fit Statistics Model Comparison Statistics Coefficients Coded Equation Real Equation Actual Equation

**Final Equation in Terms of L\_Pseudo Components**

|                               |               |
|-------------------------------|---------------|
| Ultimate compressive strength | =             |
|                               | +1048,46 * A  |
|                               | +383,00 * B   |
|                               | +443,70 * C   |
|                               | +2366,77 * AB |
|                               | -712,02 * AC  |
|                               | -1311,20 * BC |

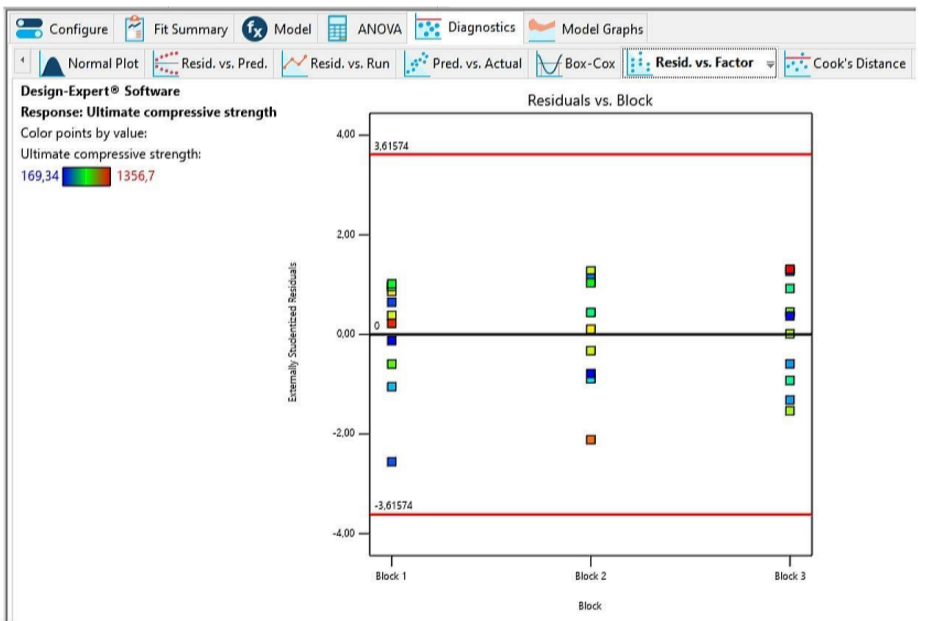
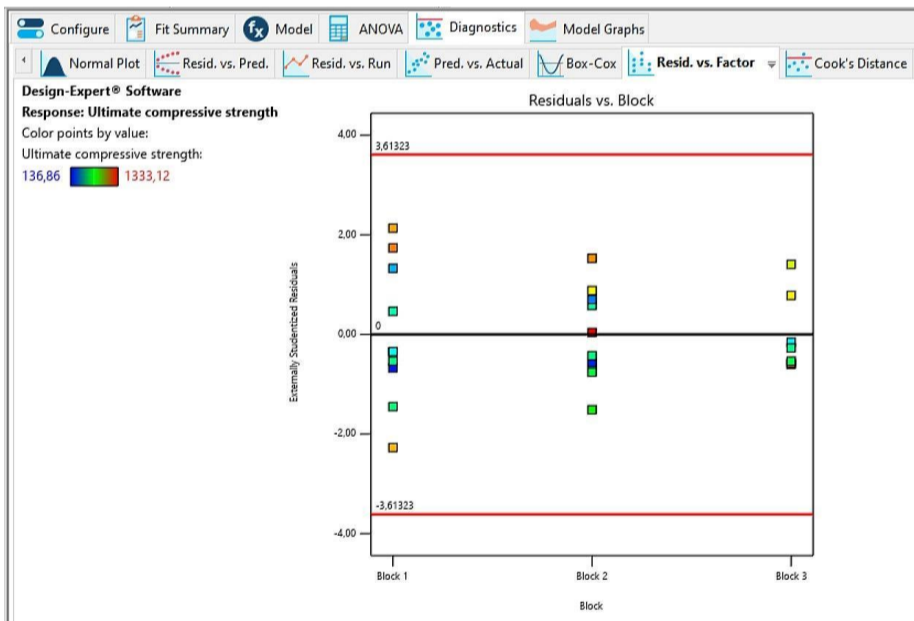
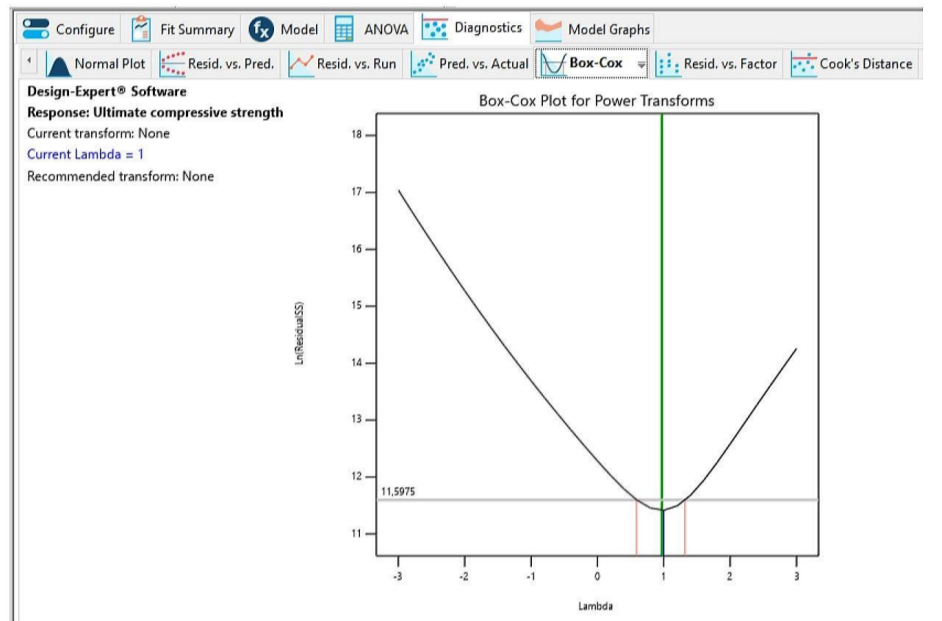
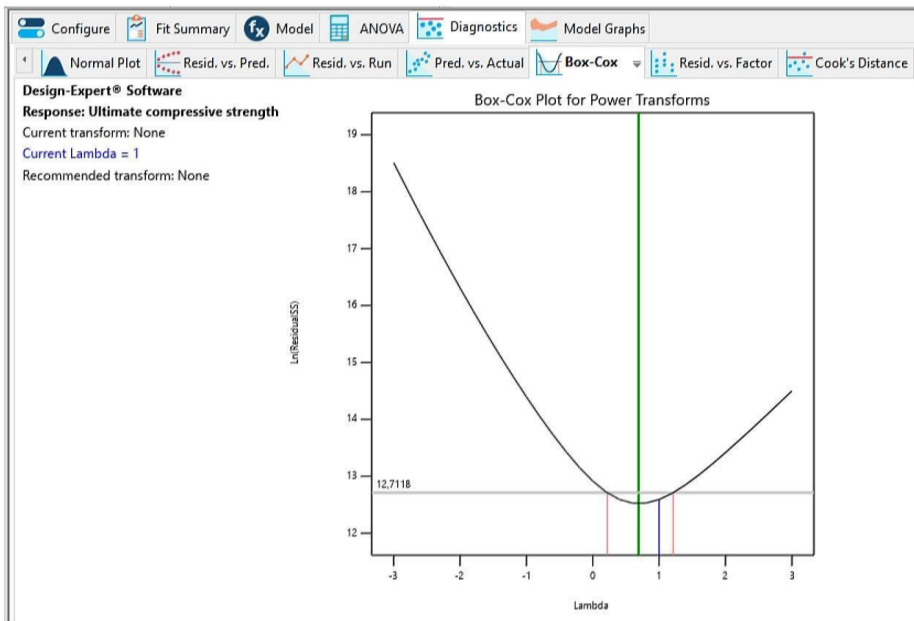
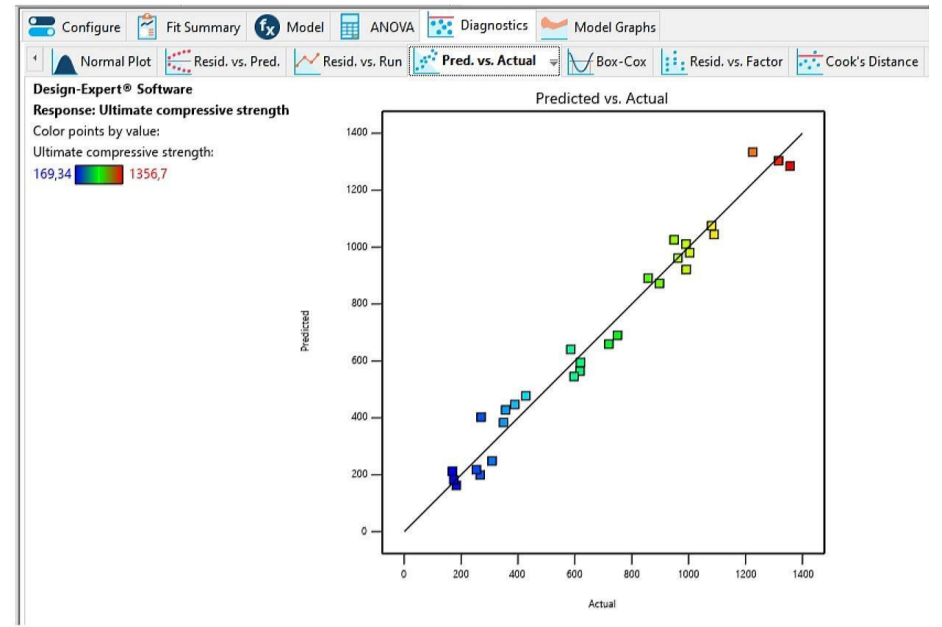
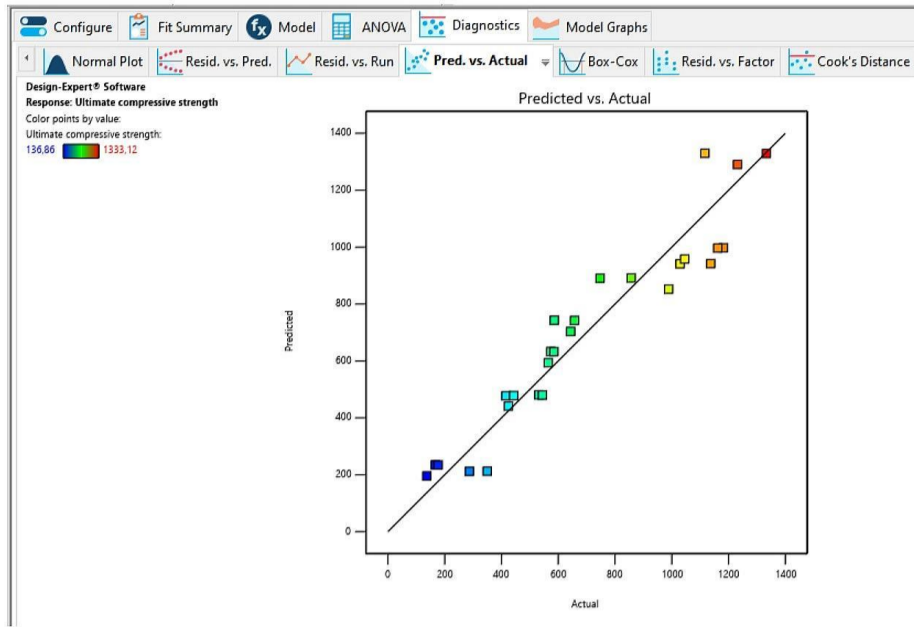
**DRY.8**

**WET.8**



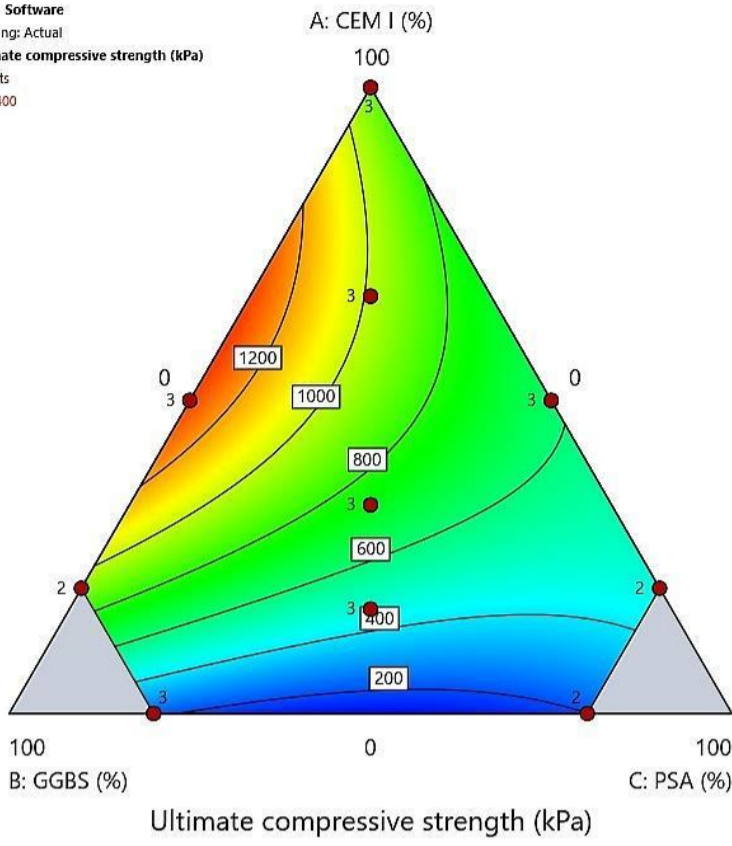
**DRY.8**

**WET.8**



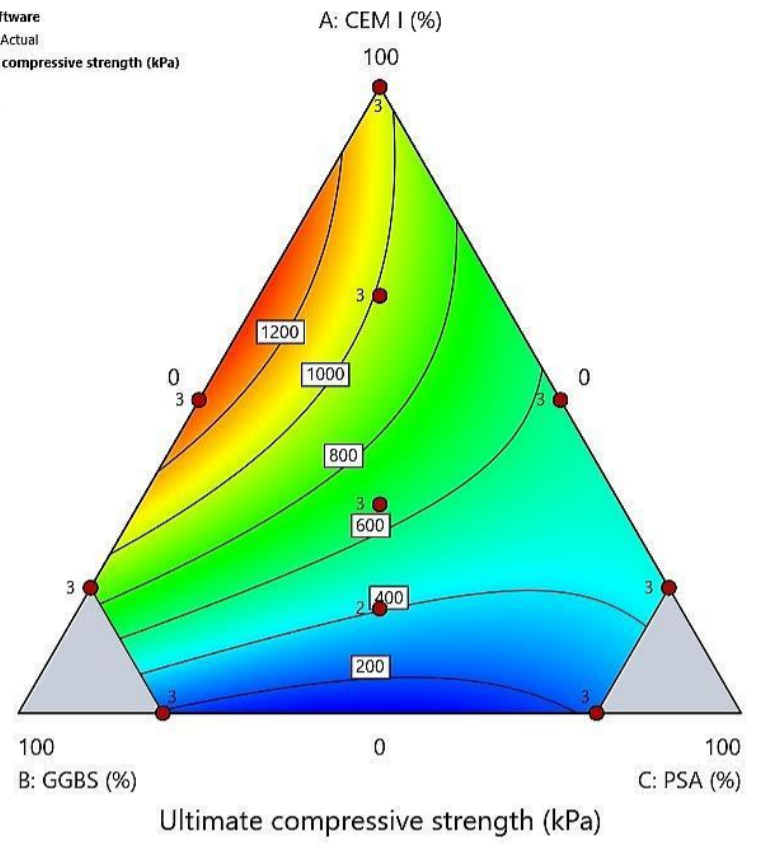
# DRY.8

Design-Expert® Software  
 Component Coding: Actual  
 Response: Ultimate compressive strength (kPa)  
 Design Points  
 100 1400

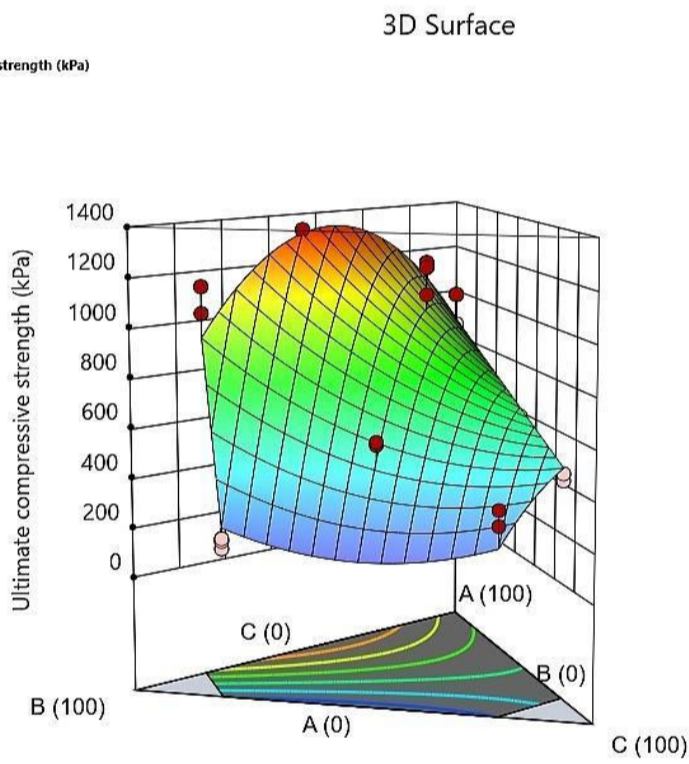


# WET.8

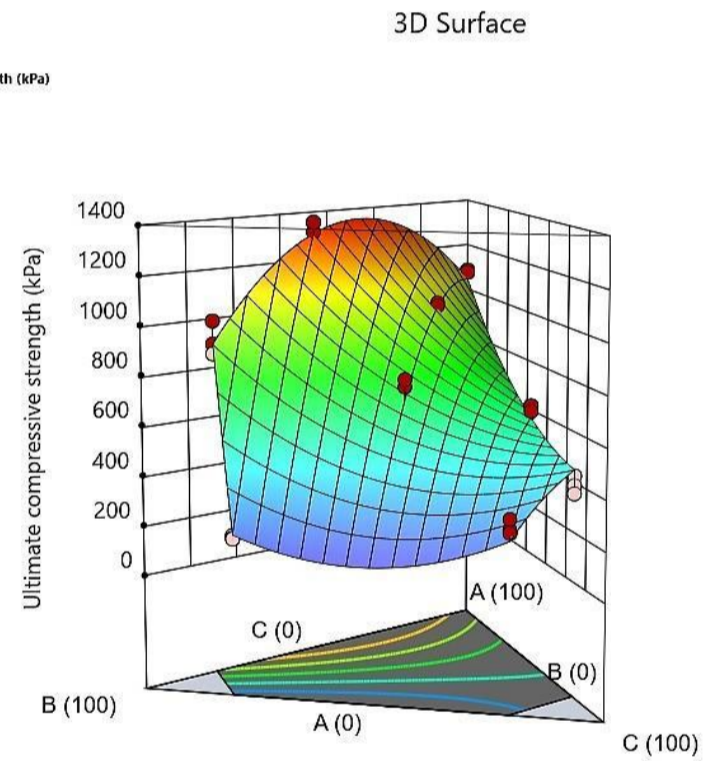
Design-Expert® Software  
 Component Coding: Actual  
 Response: Ultimate compressive strength (kPa)  
 Design Points  
 100 1400



Design-Expert® Software  
 Component Coding: Actual  
 Response: Ultimate compressive strength (kPa)  
 Design Points:  
 Above Surface  
 Below Surface  
 100 1400



Design-Expert® Software  
 Component Coding: Actual  
 Response: Ultimate compressive strength (kPa)  
 Design Points:  
 Above Surface  
 Below Surface  
 100 1400



# R2: Undrained shear strength, $S_u$

## DRY.8

| Source           | Sequential p-value | Lack of Fit p-value | Adjusted R <sup>2</sup> | Predicted R <sup>2</sup> |                  |
|------------------|--------------------|---------------------|-------------------------|--------------------------|------------------|
| Linear           | 0,0001             |                     | 0,5130                  | 0,2740                   |                  |
| <b>Quadratic</b> | <b>&lt; 0.0001</b> |                     | <b>0,8917</b>           | <b>0,8294</b>            | <b>Suggested</b> |
| Special Cubic    | 0,5667             |                     | 0,8878                  | 0,8143                   |                  |
| Cubic            | 0,0126             |                     | 0,9270                  | 0,8742                   | <b>Aliased</b>   |

Mixture Order: Modified Auto Select...

Model Type: Scheffe Add Term

| Term                 | Status |
|----------------------|--------|
| A-CEM I              | L      |
| B-GGBS               | L      |
| C-PSA                | L      |
| AB                   | m      |
| AC                   | m      |
| BC                   | m      |
| ABC                  |        |
| AB(A-B)              |        |
| AC(A-C)              |        |
| BC(B-C)              | !      |
| A <sup>2</sup> BC    |        |
| AB <sup>2</sup> C    |        |
| ABC <sup>2</sup>     | !      |
| AB(A-B) <sup>2</sup> | !      |
| AC(A-C) <sup>2</sup> | !      |
| BC(B-C) <sup>2</sup> | !      |

Legend:

- m: The term will be included in the model.
- !: Indicates the term is aliased with another term, or was not estimated in the Fit Summary calculations. Including the term in the model is not recommended.
- L: A user-forced term. Automatic model selection will always produce a model that includes this term.
- L: Indicates that the term is required to be in the model by the program.

## WET.8

| Source           | Sequential p-value | Lack of Fit p-value | Adjusted R <sup>2</sup> | Predicted R <sup>2</sup> |                  |
|------------------|--------------------|---------------------|-------------------------|--------------------------|------------------|
| Linear           | < 0.0001           |                     | 0,6802                  | 0,5561                   |                  |
| <b>Quadratic</b> | <b>&lt; 0.0001</b> |                     | <b>0,9704</b>           | <b>0,9540</b>            | <b>Suggested</b> |
| Special Cubic    | 0,3599             |                     | 0,9702                  | 0,9510                   |                  |
| Cubic            | 0,0533             |                     | 0,9761                  | 0,9589                   | <b>Aliased</b>   |

Mixture Order: Quadratic Auto Select...

Model Type: Scheffe Add Term

| Term                 | Status |
|----------------------|--------|
| A-CEM I              | L      |
| B-GGBS               | L      |
| C-PSA                | L      |
| AB                   | m      |
| AC                   | m      |
| BC                   | m      |
| ABC                  |        |
| AB(A-B)              |        |
| AC(A-C)              |        |
| BC(B-C)              | !      |
| A <sup>2</sup> BC    |        |
| AB <sup>2</sup> C    |        |
| ABC <sup>2</sup>     | !      |
| AB(A-B) <sup>2</sup> | !      |
| AC(A-C) <sup>2</sup> | !      |
| BC(B-C) <sup>2</sup> | !      |

Legend:

- m: The term will be included in the model.
- !: Indicates the term is aliased with another term, or was not estimated in the Fit Summary calculations. Including the term in the model is not recommended.
- L: A user-forced term. Automatic model selection will always produce a model that includes this term.
- L: Indicates that the term is required to be in the model by the program.

# DRY.8

Configure Fit Summary Model ANOVA Diagnostics Model Graphs

Analysis of Variance Fit Statistics Model Comparison Statistics Coefficients Coded Equation Real Equation Actual Equation

### ANOVA for Reduced Quadratic model

Response 2: Undrained shear strength

| Source            | Sum of Squares | df | Mean Square | F-value | p-value  |             |
|-------------------|----------------|----|-------------|---------|----------|-------------|
| Block             | 833,89         | 2  | 416,94      |         |          |             |
| Model             | 7,606E+05      | 4  | 1,902E+05   | 51,71   | < 0.0001 | significant |
| (1)Linear Mixture | 4,618E+05      | 2  | 2,309E+05   | 62,79   | < 0.0001 |             |
| AB                | 2,024E+05      | 1  | 2,024E+05   | 55,04   | < 0.0001 |             |
| BC                | 18915,47       | 1  | 18915,47    | 5,14    | 0,0346   |             |
| Residual          | 73543,58       | 20 | 3677,18     |         |          |             |
| Cor Total         | 8,350E+05      | 26 |             |         |          |             |

Configure Fit Summary Model ANOVA Diagnostics Model Graphs

Analysis of Variance Fit Statistics Model Comparison Statistics Coefficients Coded Equation Real Equation Actual Equation

### Fit Statistics

|           |        |                          |         |
|-----------|--------|--------------------------|---------|
| Std. Dev. | 60,64  | R <sup>2</sup>           | 0,9118  |
| Mean      | 350,28 | Adjusted R <sup>2</sup>  | 0,8942  |
| C.V. %    | 17,31  | Predicted R <sup>2</sup> | 0,8385  |
|           |        | Adeq Precision           | 18,3639 |

Configure Fit Summary Model ANOVA Diagnostics Model Graphs

Analysis of Variance Fit Statistics Model Comparison Statistics Coefficients Coded Equation Real Equation Actual Equation

### Final Equation in Terms of L\_Pseudo Components

|                          |   |               |
|--------------------------|---|---------------|
| Undrained shear strength | = |               |
|                          |   | +439,10 * A   |
|                          |   | +199,42 * B   |
|                          |   | +180,74 * C   |
|                          |   | +1355,78 * AB |
|                          |   | -530,11 * BC  |

# WET.8

Configure Fit Summary Model ANOVA Diagnostics Model Graphs

Analysis of Variance Fit Statistics Model Comparison Statistics Coefficients Coded Equation Real Equation Actual Equation

### ANOVA for Quadratic model

Response 2: Undrained shear strength

| Source            | Sum of Squares | df | Mean Square | F-value | p-value  |             |
|-------------------|----------------|----|-------------|---------|----------|-------------|
| Block             | 7914,60        | 2  | 3957,30     |         |          |             |
| Model             | 9,271E+05      | 5  | 1,854E+05   | 171,59  | < 0.0001 | significant |
| (1)Linear Mixture | 6,694E+05      | 2  | 3,347E+05   | 309,73  | < 0.0001 |             |
| AB                | 1,538E+05      | 1  | 1,538E+05   | 142,35  | < 0.0001 |             |
| AC                | 13921,67       | 1  | 13921,67    | 12,88   | 0,0017   |             |
| BC                | 29787,59       | 1  | 29787,59    | 27,57   | < 0.0001 |             |
| Residual          | 22692,05       | 21 | 1080,57     |         |          |             |
| Cor Total         | 9,577E+05      | 28 |             |         |          |             |

Configure Fit Summary Model ANOVA Diagnostics Model Graphs

Analysis of Variance Fit Statistics Model Comparison Statistics Coefficients Coded Equation Real Equation Actual Equation

### Fit Statistics

|           |        |                          |         |
|-----------|--------|--------------------------|---------|
| Std. Dev. | 32,87  | R <sup>2</sup>           | 0,9761  |
| Mean      | 340,66 | Adjusted R <sup>2</sup>  | 0,9704  |
| C.V. %    | 9,65   | Predicted R <sup>2</sup> | 0,9540  |
|           |        | Adeq Precision           | 33,9190 |

Configure Fit Summary Model ANOVA Diagnostics Model Graphs

Analysis of Variance Fit Statistics Model Comparison Statistics Coefficients Coded Equation Real Equation Actual Equation

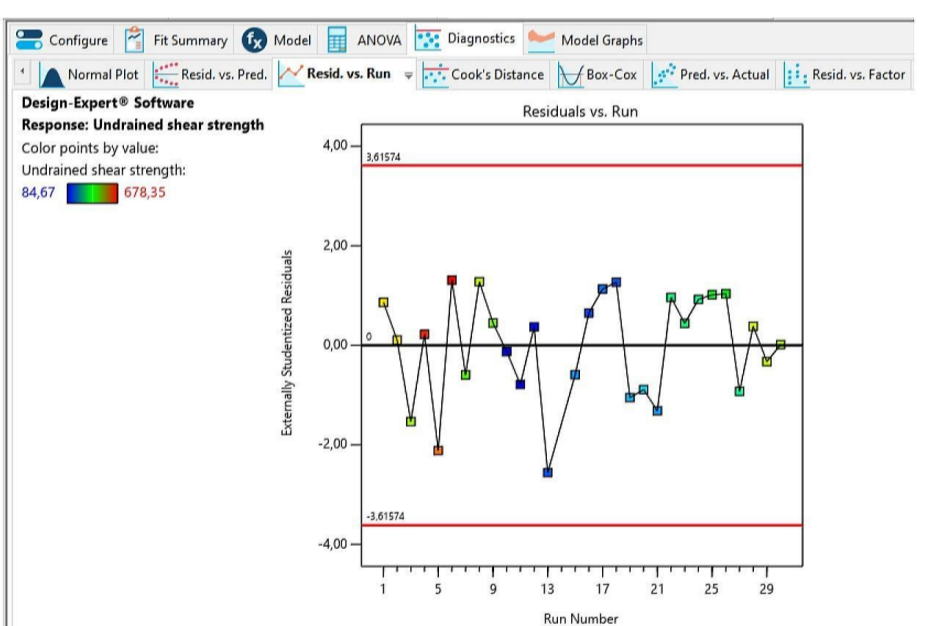
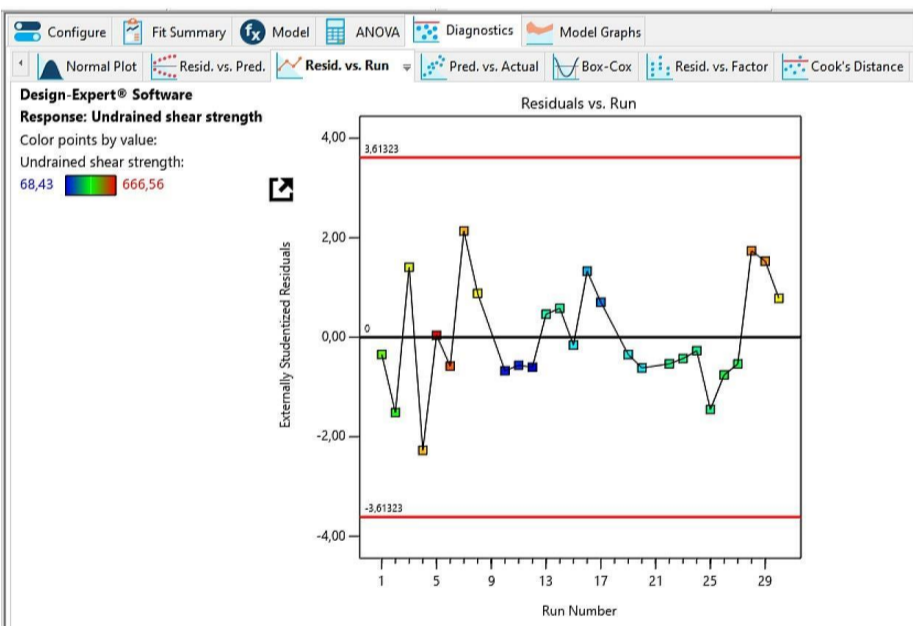
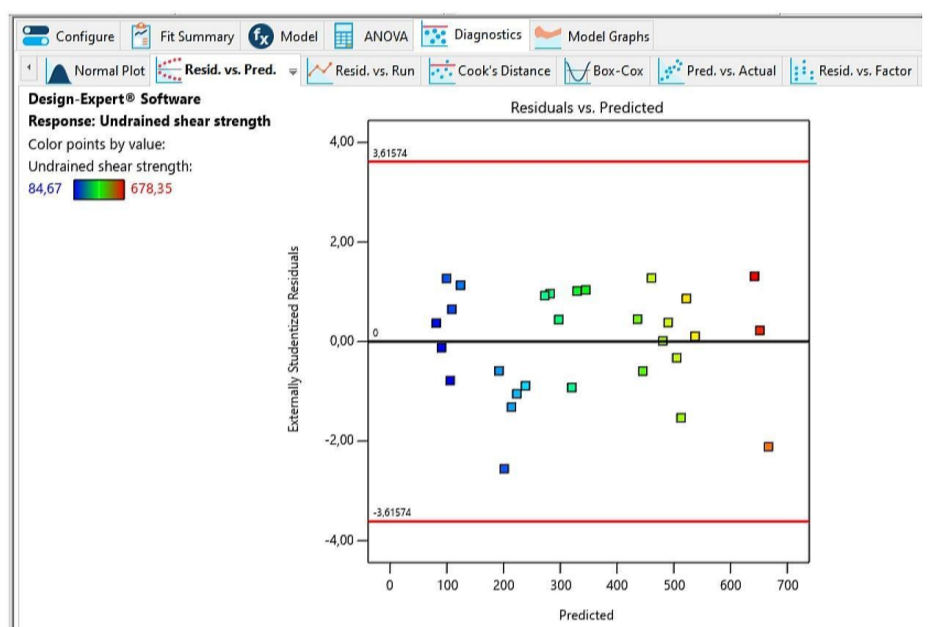
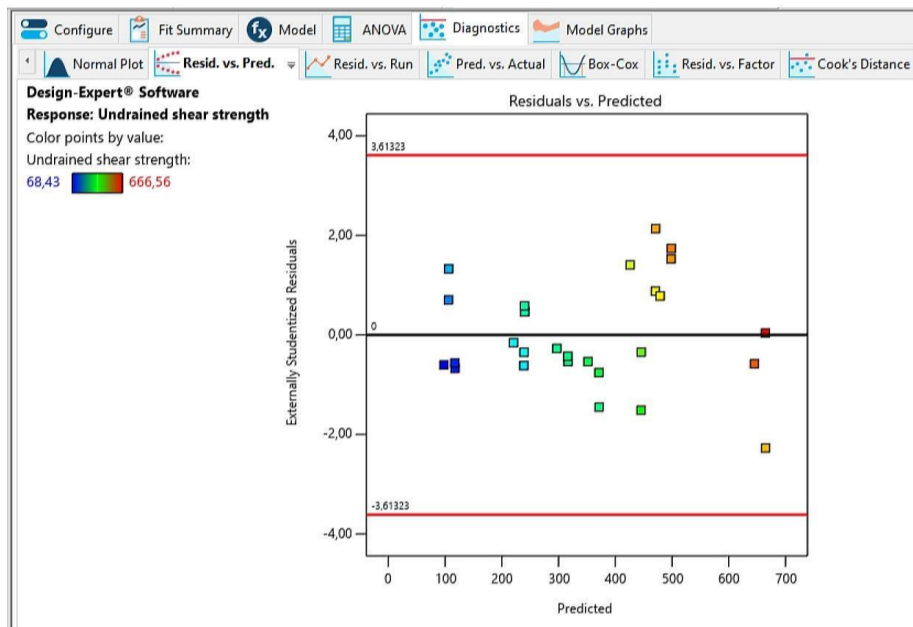
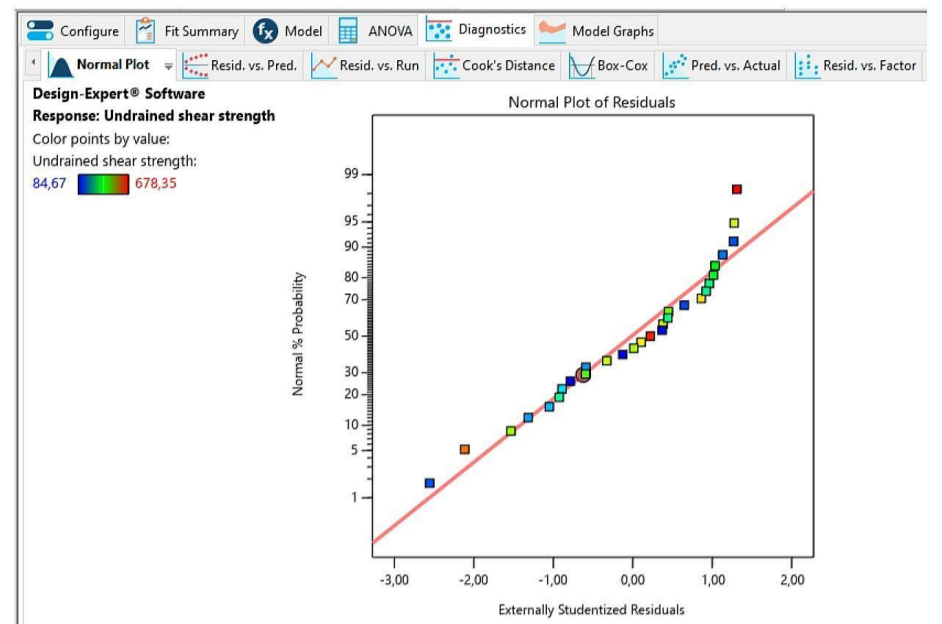
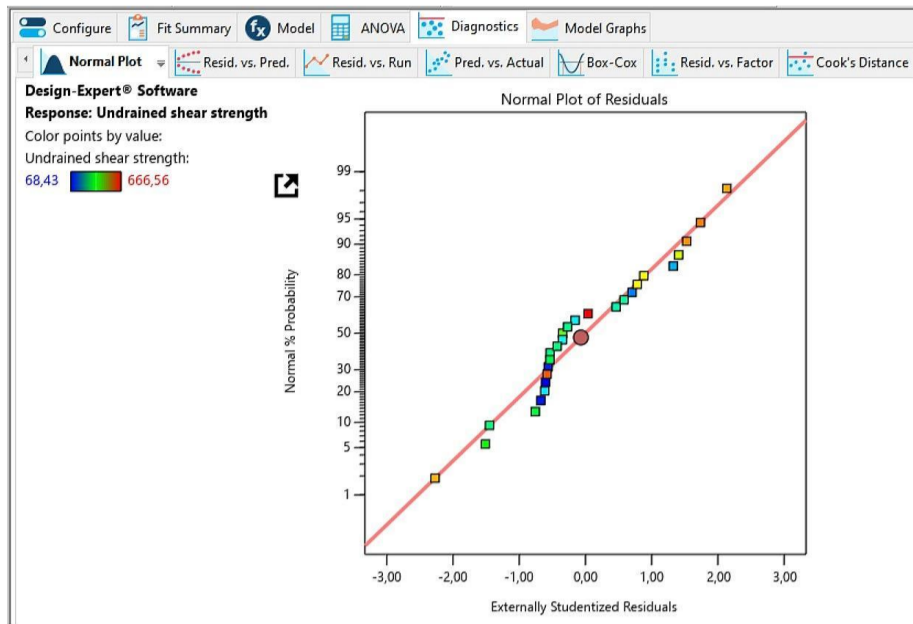
### Final Equation in Terms of L\_Pseudo Components

|                          |   |               |
|--------------------------|---|---------------|
| Undrained shear strength | = |               |
|                          |   | +524,23 * A   |
|                          |   | +191,50 * B   |
|                          |   | +221,85 * C   |
|                          |   | +1183,39 * AB |
|                          |   | -356,02 * AC  |
|                          |   | -655,58 * BC  |



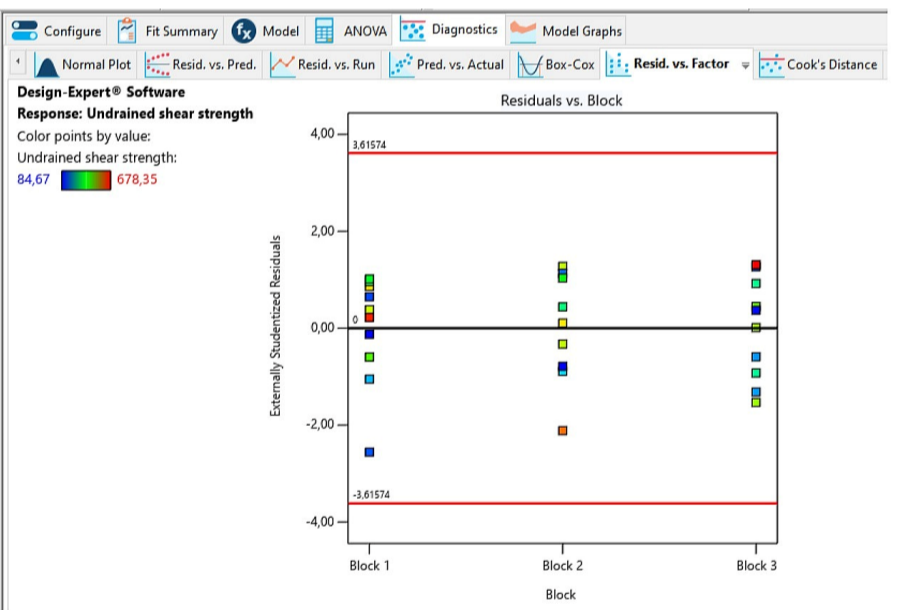
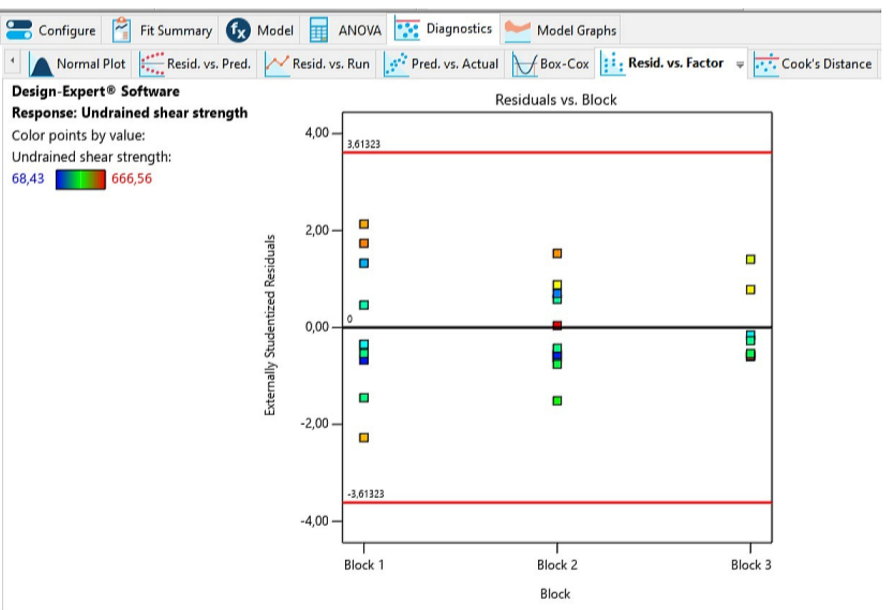
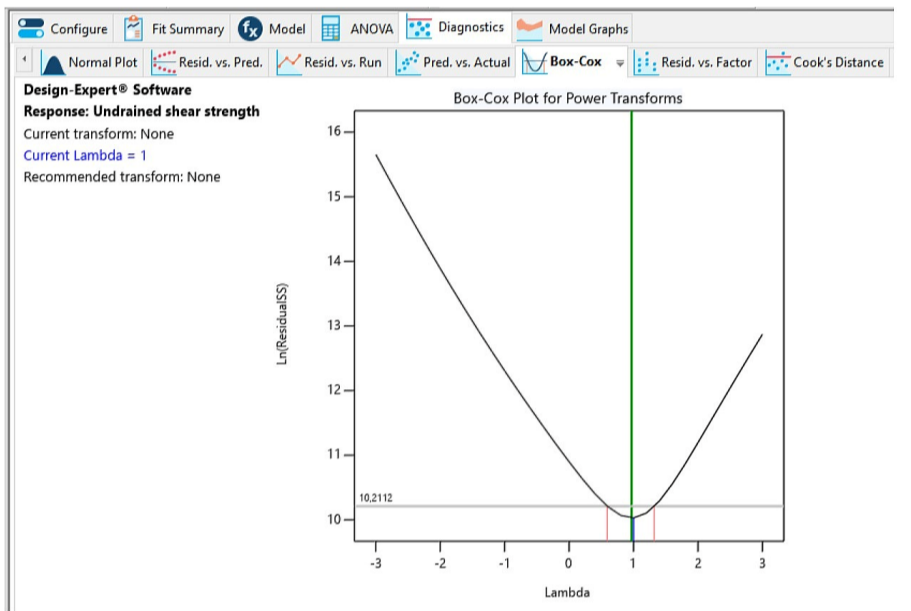
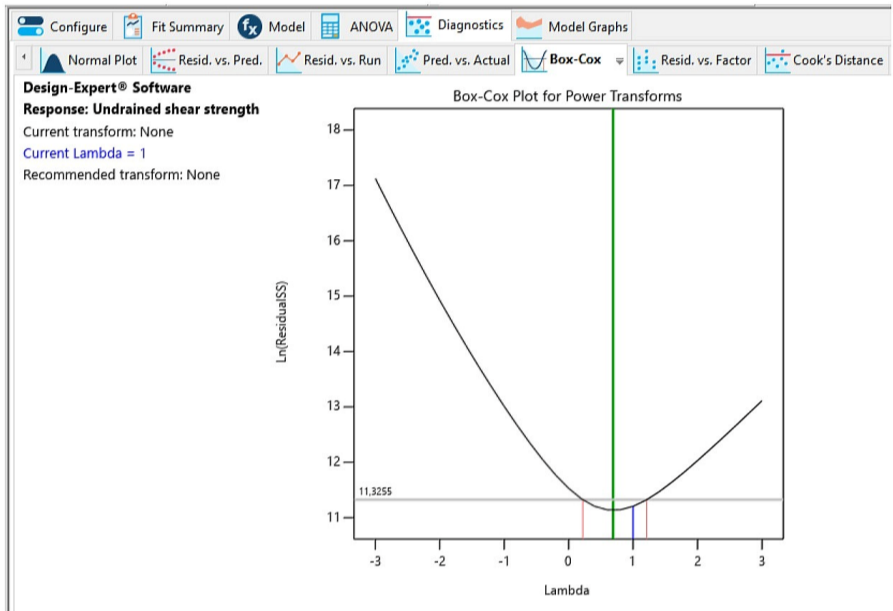
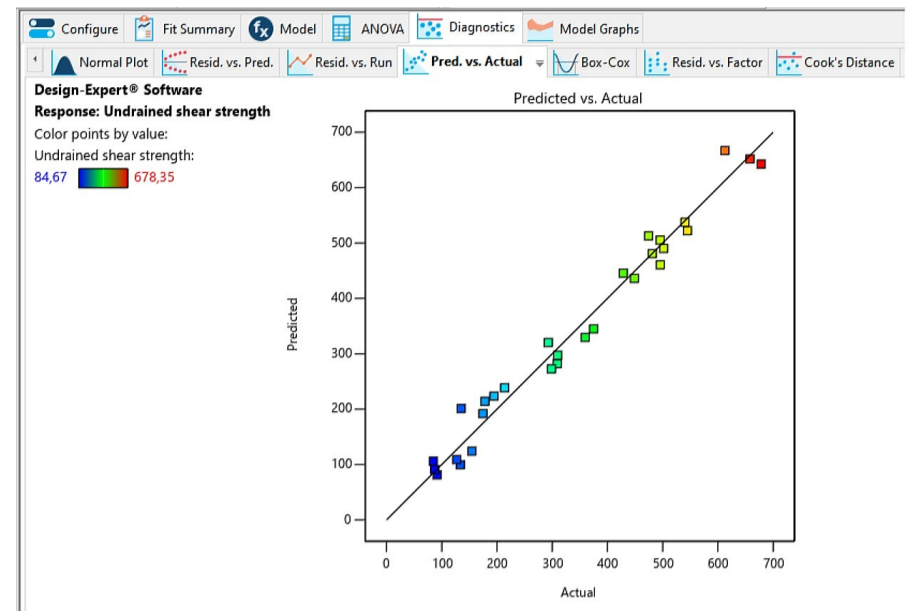
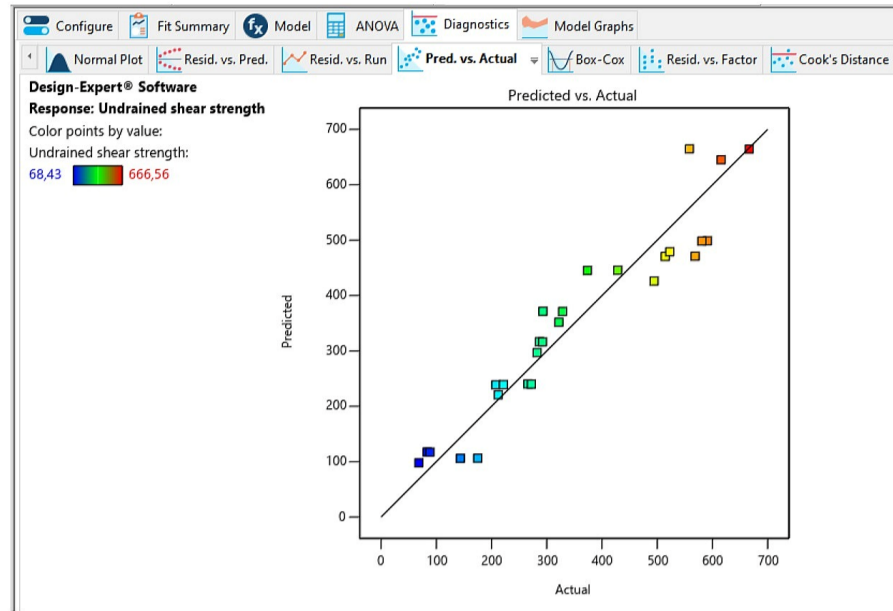
**DRY.8**

**WET.8**

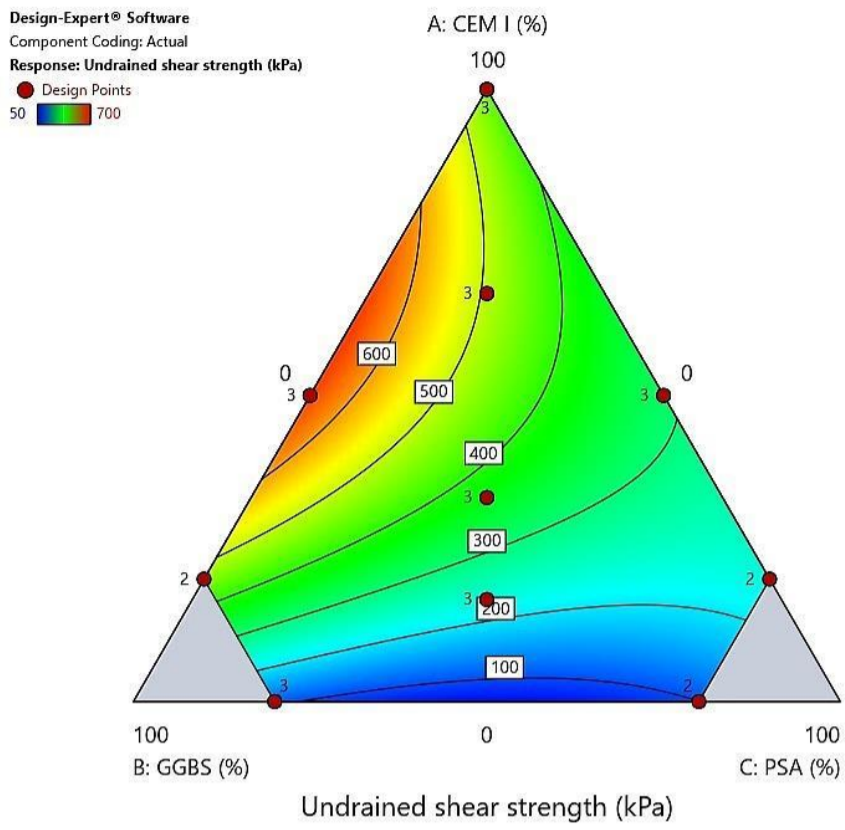


**DRY.8**

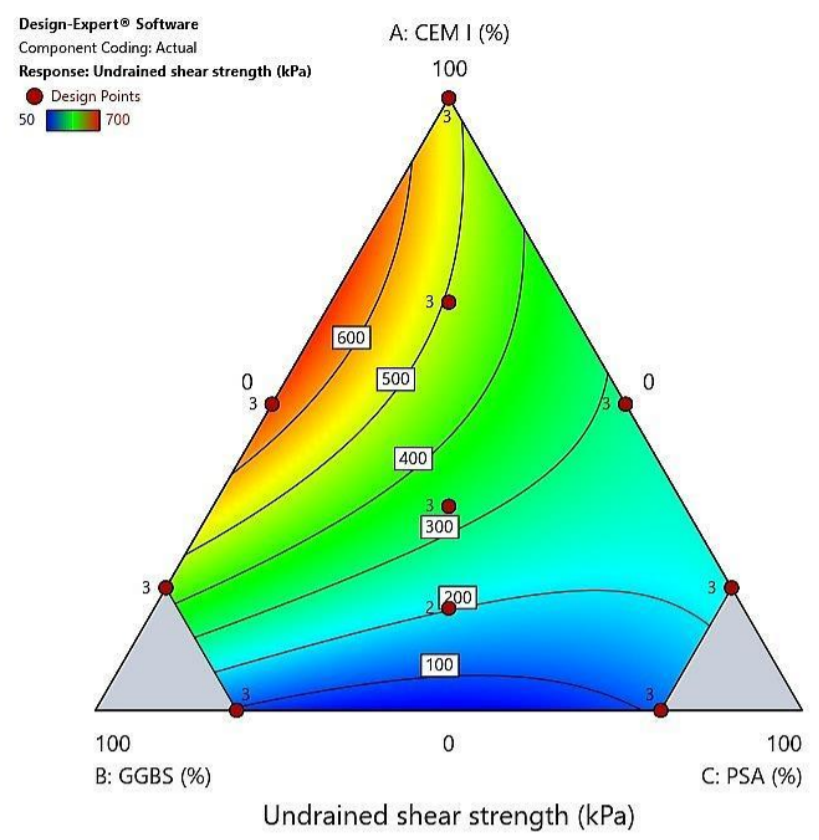
**WET.8**



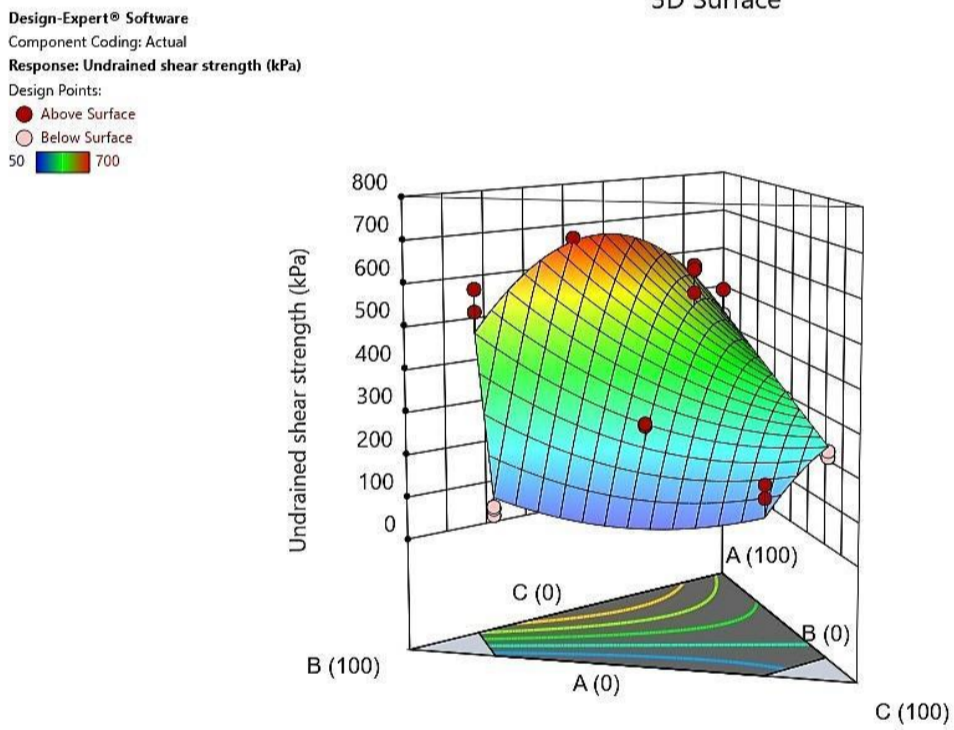
# DRY.8



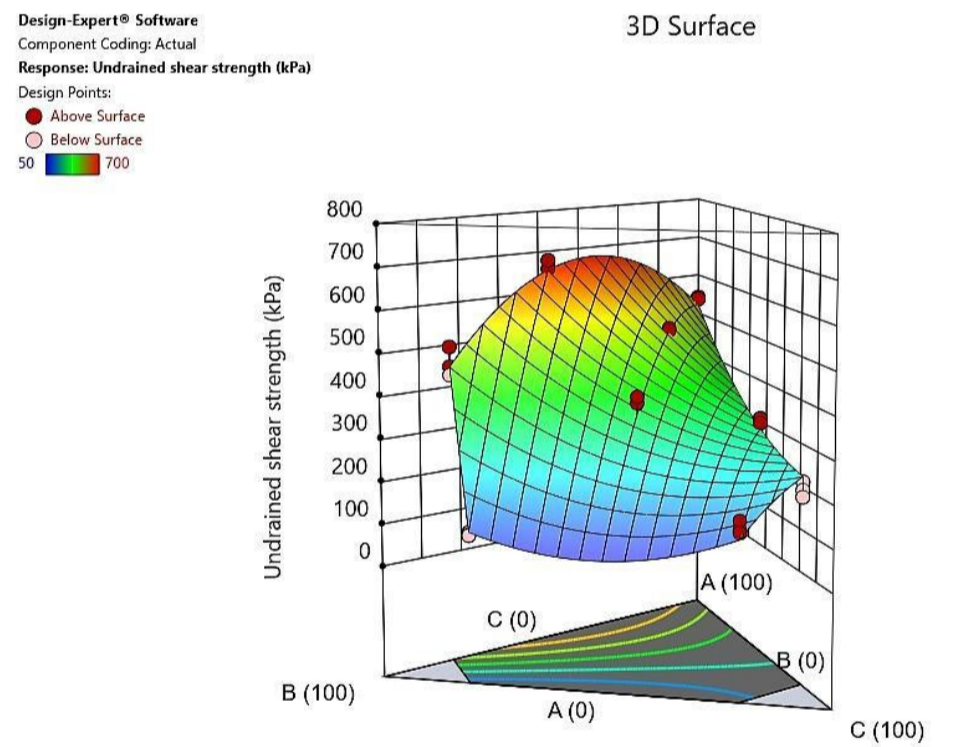
# WET.8



3D Surface



3D Surface



# R3: Failure strain, $\epsilon_v$

## DRY.8

Configure Fit Summary Model ANOVA Diagnostics Model Graphs

Fit Summary Sequential Model Sum of Squares [Type I] Model Summary Statistics

**Fit Summary**

Response 3: Failure strain

Mixture Component Coding is L\_Pseudo.

| Source        | Sequential p-value | Lack of Fit p-value | Adjusted R <sup>2</sup> | Predicted R <sup>2</sup> |           |
|---------------|--------------------|---------------------|-------------------------|--------------------------|-----------|
| Linear        | < 0.0001           |                     | 0,6279                  | 0,5054                   |           |
| Quadratic     | 0,0092             |                     | 0,7615                  | 0,6561                   | Suggested |
| Special Cubic | 0,9000             |                     | 0,7485                  | 0,6372                   |           |
| Cubic         | < 0.0001           |                     | 0,9330                  | 0,8538                   | Aliased   |

## WET.8

Configure Fit Summary Model ANOVA Diagnostics Model Graphs

Fit Summary Sequential Model Sum of Squares [Type I] Model Summary Statistics

**Fit Summary**

Response 3: Failure strain

Mixture Component Coding is L\_Pseudo.

| Source        | Sequential p-value | Lack of Fit p-value | Adjusted R <sup>2</sup> | Predicted R <sup>2</sup> |           |
|---------------|--------------------|---------------------|-------------------------|--------------------------|-----------|
| Linear        | < 0.0001           |                     | 0,8960                  | 0,8615                   |           |
| Quadratic     | 0,0051             |                     | 0,9360                  | 0,8966                   | Suggested |
| Special Cubic | 0,1002             |                     | 0,9417                  | 0,9033                   |           |
| Cubic         | 0,0299             |                     | 0,9569                  | 0,9097                   | Aliased   |

Configure Fit Summary Model ANOVA Diagnostics Model Graphs

Mixture Order: Modified Auto Select...

Model Type: Scheffe Add Term

|  |                      |  |  |
|--|----------------------|--|--|
|  | A-CEM I              |  | The term will be included in the model.  |
|  | B-GGBS               |  | Indicates the term is aliased with another term, or was not estimated in the Fit Summary calculations. Including the term in the model is not recommended. |
|  | C-PSA                |  | A user-forced term. Automatic model selection will always produce a model that includes this term.   |
|  | AB                   |  | Indicates that the term is required to be in the model by the program.   |
|  | AC                   |  |  |
|  | BC                   |  |  |
|  | ABC                  |  |  |
|  | AB(A-B)              |  |  |
|  | AC(A-C)              |  |  |
|  | BC(B-C)              |  |  |
|  | A <sup>2</sup> BC    |  |  |
|  | AB <sup>2</sup> C    |  |  |
|  | ABC <sup>2</sup>     |  |  |
|  | AB(A-B) <sup>2</sup> |  |  |
|  | AC(A-C) <sup>2</sup> |  |  |
|  | BC(B-C) <sup>2</sup> |  |  |

Configure Fit Summary Model ANOVA Diagnostics Model Graphs

Mixture Order: Modified Auto Select...

Model Type: Scheffe Add Term

|  |                      |  |  |
|--|----------------------|--|--|
|  | A-CEM I              |  | The term will be included in the model.  |
|  | B-GGBS               |  | Indicates the term is aliased with another term, or was not estimated in the Fit Summary calculations. Including the term in the model is not recommended. |
|  | C-PSA                |  | A user-forced term. Automatic model selection will always produce a model that includes this term.   |
|  | AB                   |  | Indicates that the term is required to be in the model by the program.   |
|  | AC                   |  |  |
|  | BC                   |  |  |
|  | ABC                  |  |  |
|  | AB(A-B)              |  |  |
|  | AC(A-C)              |  |  |
|  | BC(B-C)              |  |  |
|  | A <sup>2</sup> BC    |  |  |
|  | AB <sup>2</sup> C    |  |  |
|  | ABC <sup>2</sup>     |  |  |
|  | AB(A-B) <sup>2</sup> |  |  |
|  | AC(A-C) <sup>2</sup> |  |  |
|  | BC(B-C) <sup>2</sup> |  |  |

# DRY.8

Configure Fit Summary Model ANOVA Diagnostics Model Graphs

Analysis of Variance Fit Statistics Model Comparison Statistics Coefficients Coded Equation Real Equation Actual Equation

### ANOVA for Reduced Quadratic model

Response 3: Failure strain

| Source                        | Sum of Squares | df | Mean Square | F-value | p-value  |             |
|-------------------------------|----------------|----|-------------|---------|----------|-------------|
| Block                         | 0,3372         | 2  | 0,1686      |         |          |             |
| Model                         | 26,86          | 4  | 6,71        | 20,78   | < 0.0001 | significant |
| <sup>(1)</sup> Linear Mixture | 21,96          | 2  | 10,98       | 33,97   | < 0.0001 |             |
| AC                            | 0,5638         | 1  | 0,5638      | 1,74    | 0,2015   |             |
| BC                            | 4,90           | 1  | 4,90        | 15,17   | 0,0009   |             |
| Residual                      | 6,46           | 20 | 0,3232      |         |          |             |
| Cor Total                     | 33,66          | 26 |             |         |          |             |

Configure Fit Summary Model ANOVA Diagnostics Model Graphs

Analysis of Variance Fit Statistics Model Comparison Statistics Coefficients Coded Equation Real Equation Actual Equation

### Fit Statistics

|           |        |                          |         |
|-----------|--------|--------------------------|---------|
| Std. Dev. | 0,5685 | R <sup>2</sup>           | 0,8060  |
| Mean      | 3,29   | Adjusted R <sup>2</sup>  | 0,7672  |
| C.V. %    | 17,27  | Predicted R <sup>2</sup> | 0,6655  |
|           |        | Adeq Precision           | 11,6355 |

Configure Fit Summary Model ANOVA Diagnostics Model Graphs

Analysis of Variance Fit Statistics Model Comparison Statistics Coefficients Coded Equation Real Equation Actual Equation

### Final Equation in Terms of L\_Pseudo Components

|                |            |
|----------------|------------|
| Failure strain | =          |
|                | +2,27 * A  |
|                | +1,46 * B  |
|                | +4,10 * C  |
|                | +2,44 * AC |
|                | +8,55 * BC |

# WET.8

Configure Fit Summary Model ANOVA Diagnostics Model Graphs

Analysis of Variance Fit Statistics Model Comparison Statistics Coefficients Coded Equation Real Equation Actual Equation

### ANOVA for Reduced Quadratic model

Response 3: Failure strain

| Source                        | Sum of Squares | df | Mean Square | F-value | p-value  |             |
|-------------------------------|----------------|----|-------------|---------|----------|-------------|
| Block                         | 0,1131         | 2  | 0,0566      |         |          |             |
| Model                         | 34,90          | 3  | 11,63       | 133,57  | < 0.0001 | significant |
| <sup>(1)</sup> Linear Mixture | 33,29          | 2  | 16,65       | 191,13  | < 0.0001 |             |
| BC                            | 1,61           | 1  | 1,61        | 18,45   | 0,0003   |             |
| Residual                      | 1,92           | 22 | 0,0871      |         |          |             |
| Cor Total                     | 36,93          | 27 |             |         |          |             |

Configure Fit Summary Model ANOVA Diagnostics Model Graphs

Analysis of Variance Fit Statistics Model Comparison Statistics Coefficients Coded Equation Real Equation Actual Equation

### Fit Statistics

|           |        |                          |         |
|-----------|--------|--------------------------|---------|
| Std. Dev. | 0,2951 | R <sup>2</sup>           | 0,9480  |
| Mean      | 2,84   | Adjusted R <sup>2</sup>  | 0,9409  |
| C.V. %    | 10,39  | Predicted R <sup>2</sup> | 0,9107  |
|           |        | Adeq Precision           | 26,7036 |

Configure Fit Summary Model ANOVA Diagnostics Model Graphs

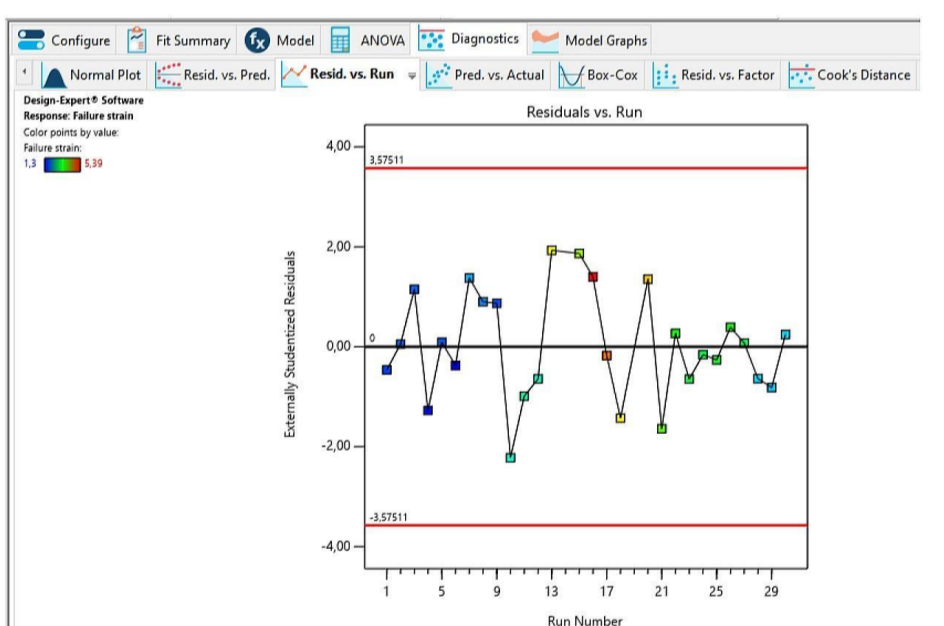
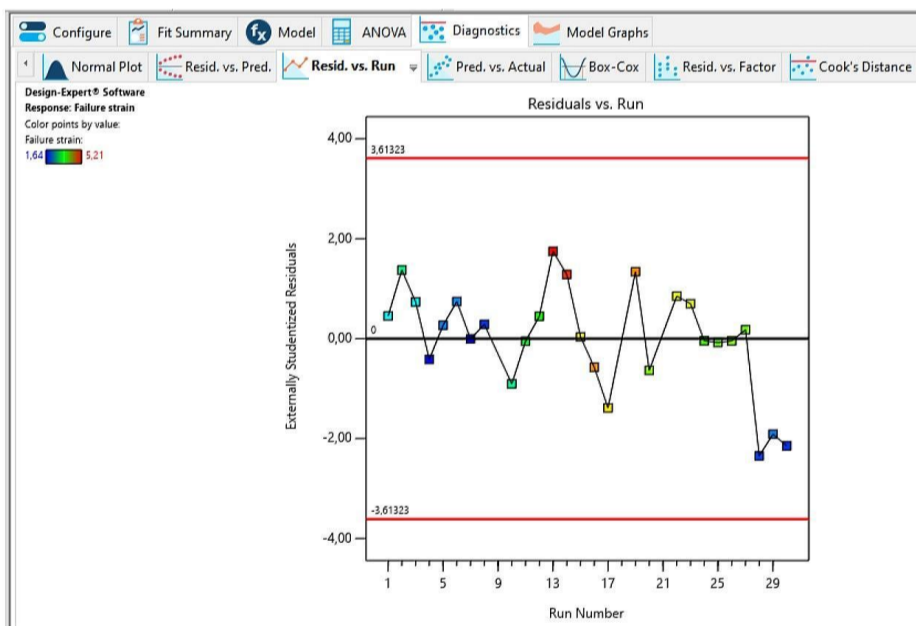
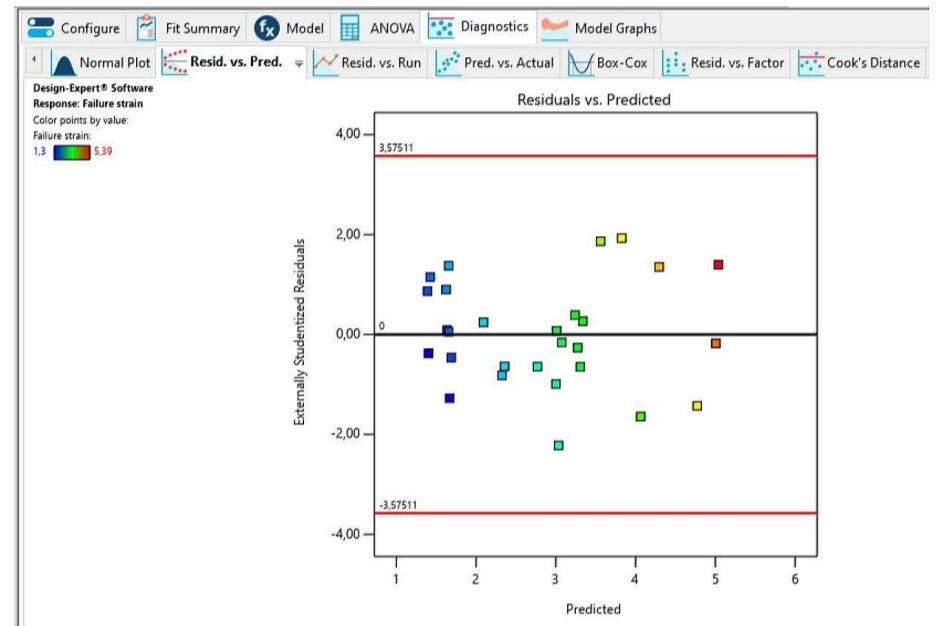
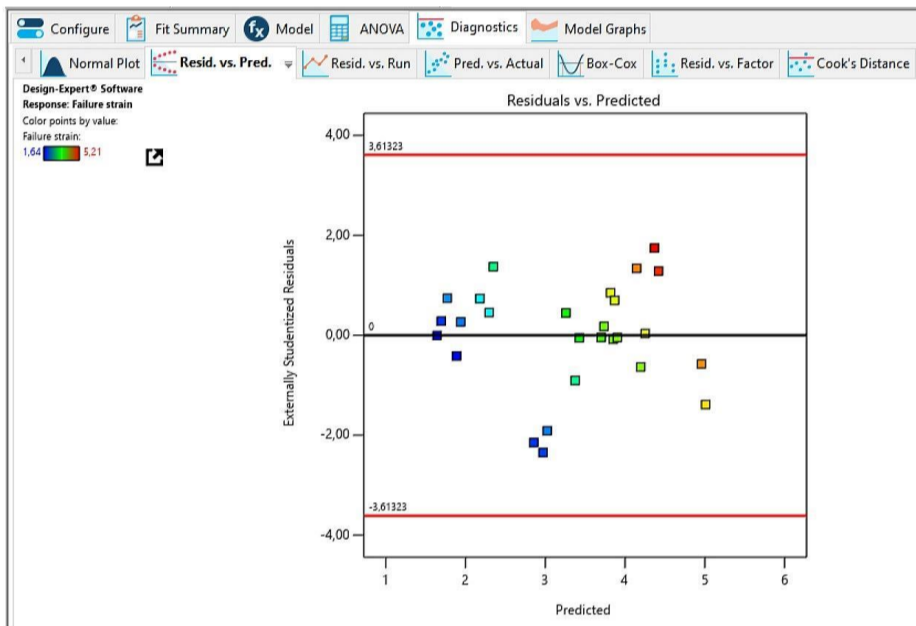
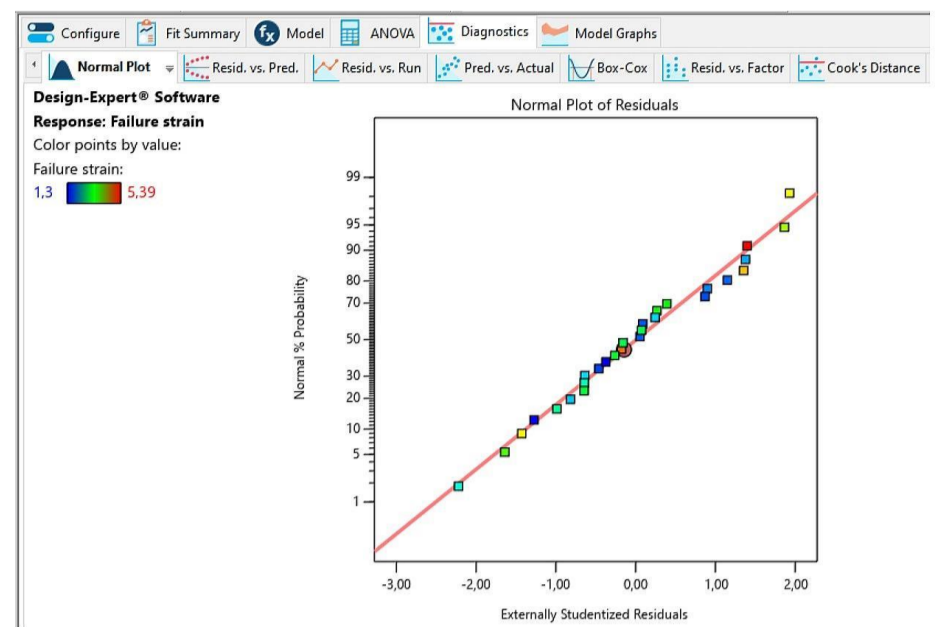
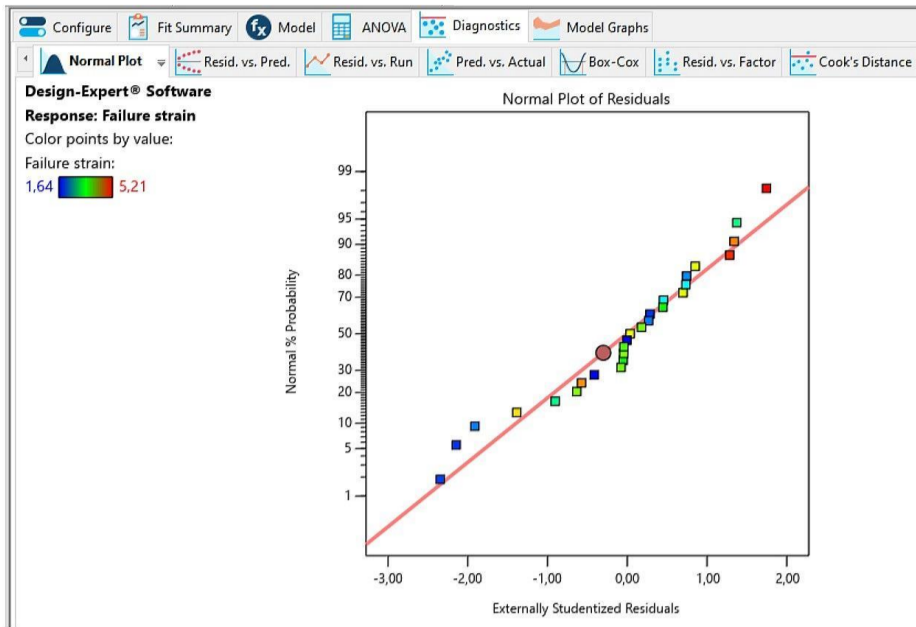
Analysis of Variance Fit Statistics Model Comparison Statistics Coefficients Coded Equation Real Equation Actual Equation

### Final Equation in Terms of L\_Pseudo Components

|                |            |
|----------------|------------|
| Failure strain | =          |
|                | +1,59 * A  |
|                | +1,55 * B  |
|                | +4,89 * C  |
|                | +4,49 * BC |

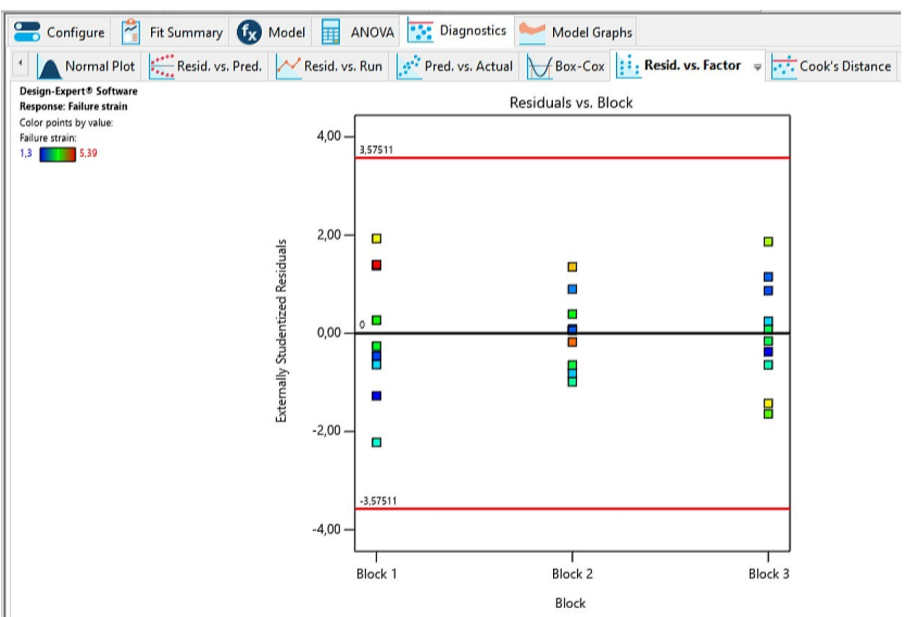
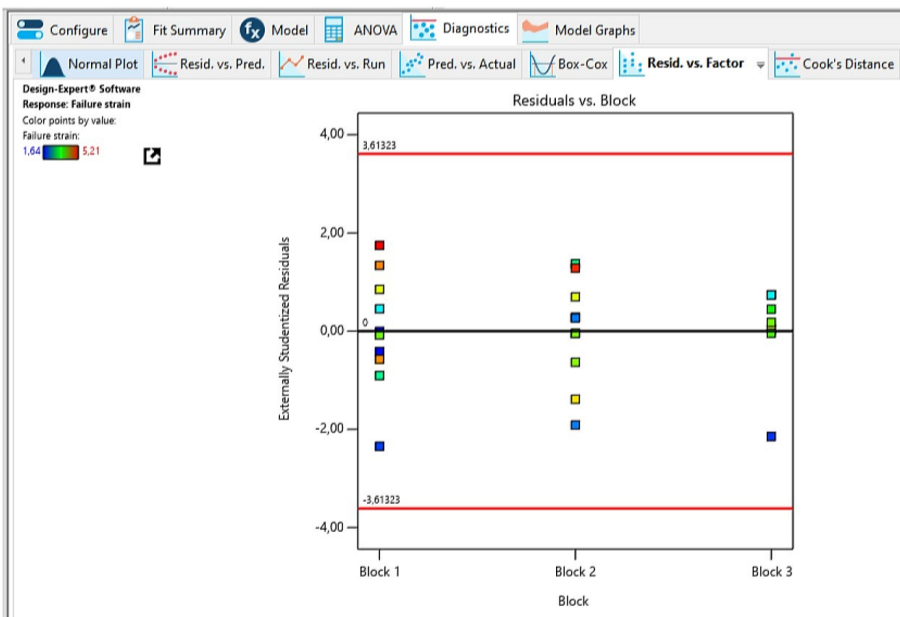
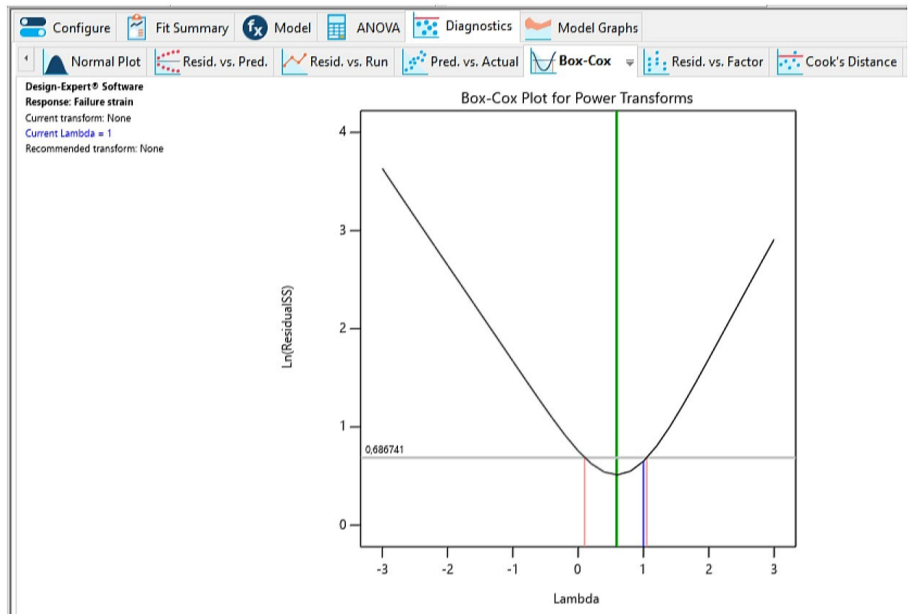
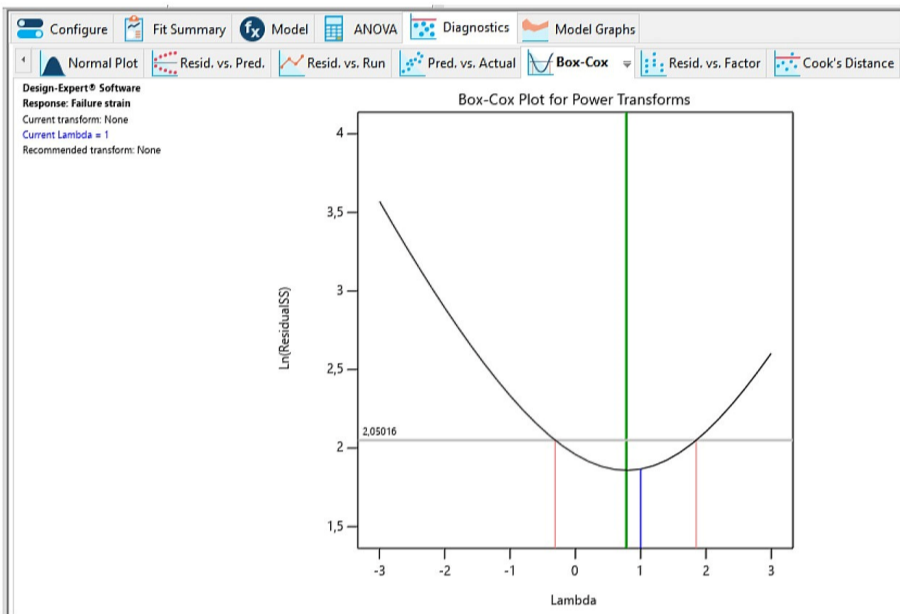
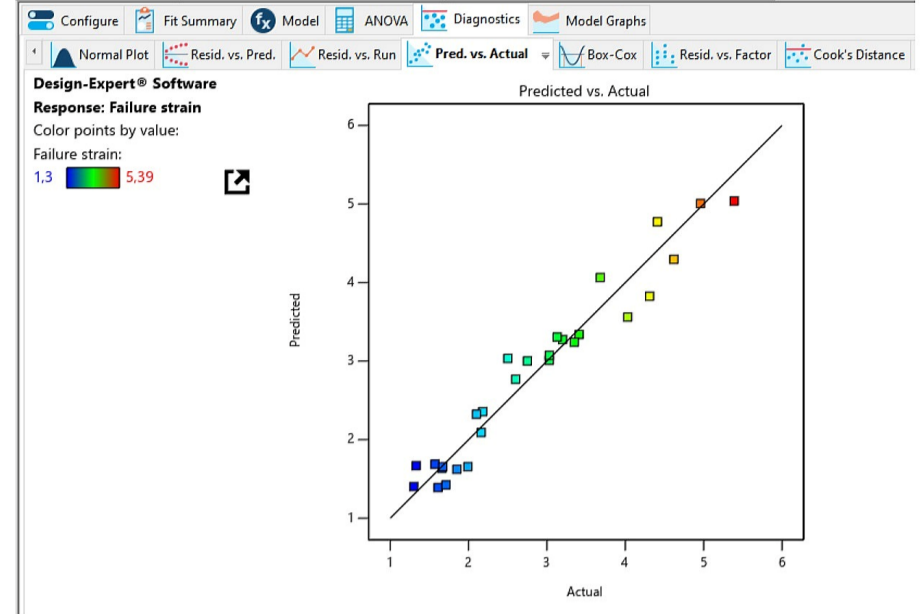
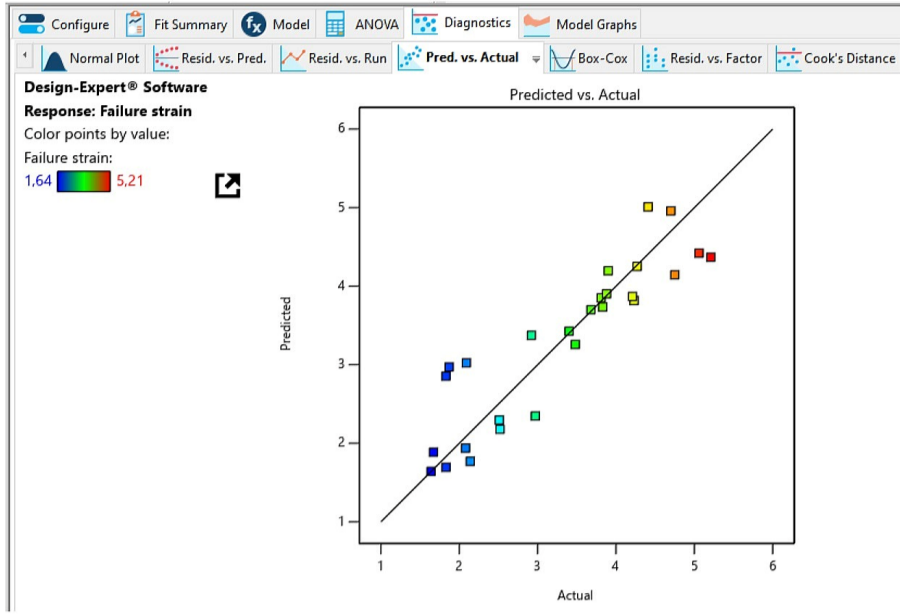
**DRY.8**

**WET.8**



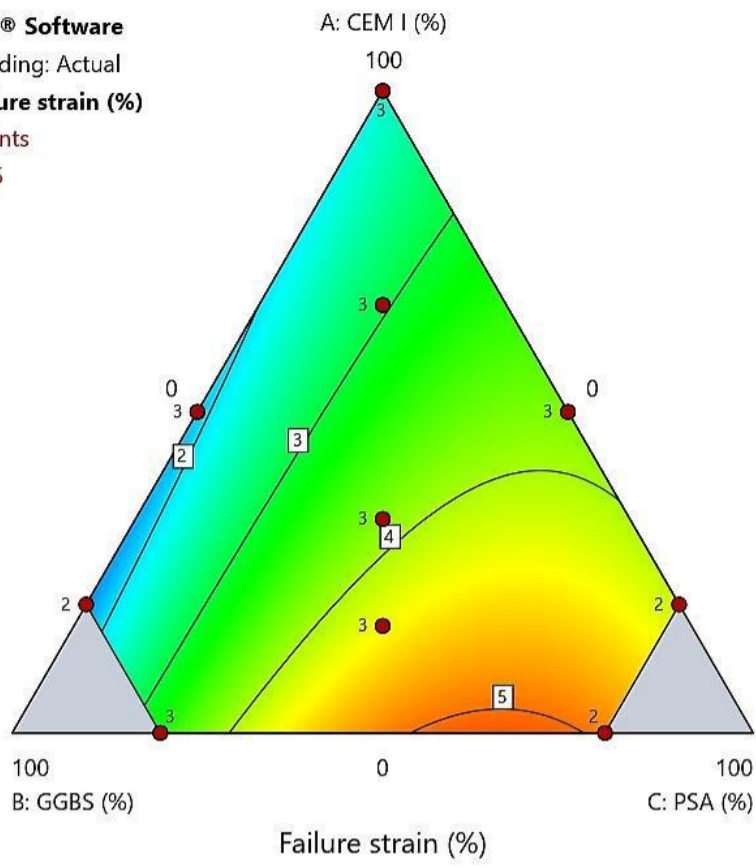
**DRY.8**

**WET.8**



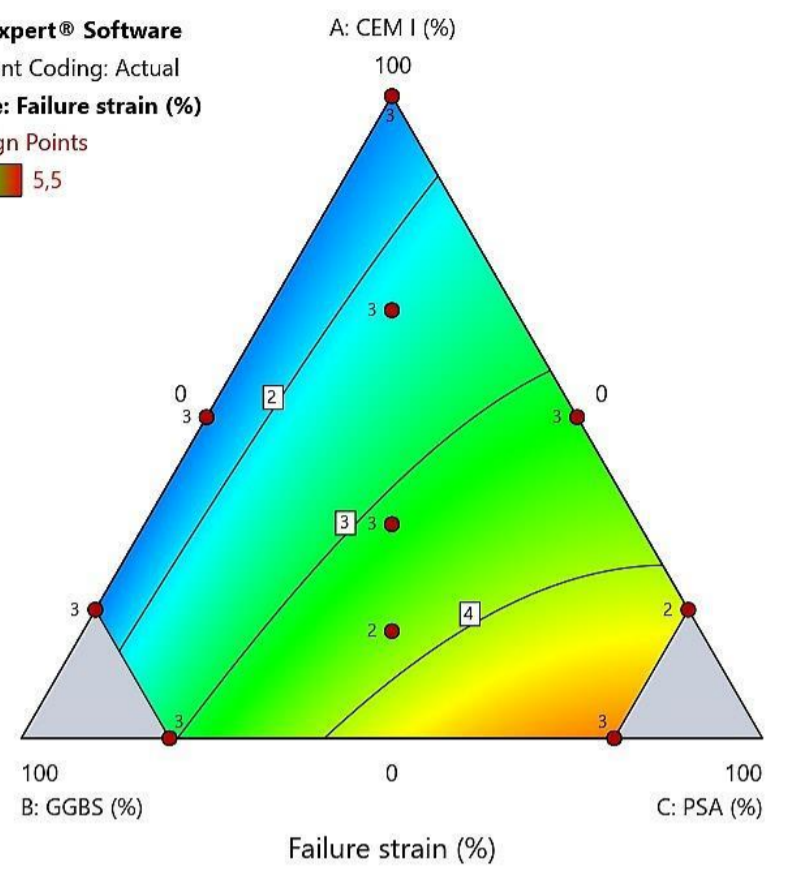
# DRY.8

Design-Expert® Software  
 Component Coding: Actual  
**Response: Failure strain (%)**  
 ● Design Points  
 1 5,5

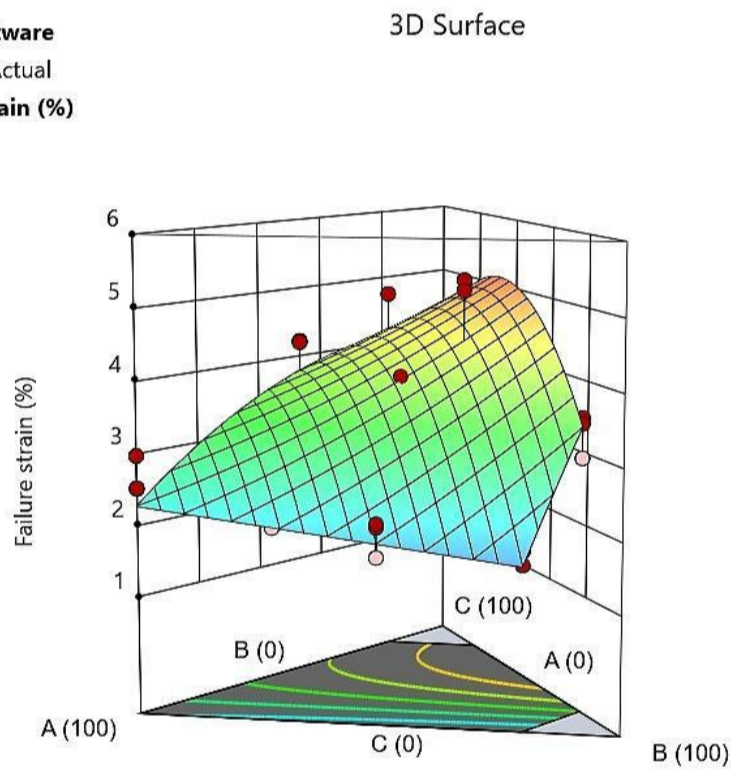


# WET.8

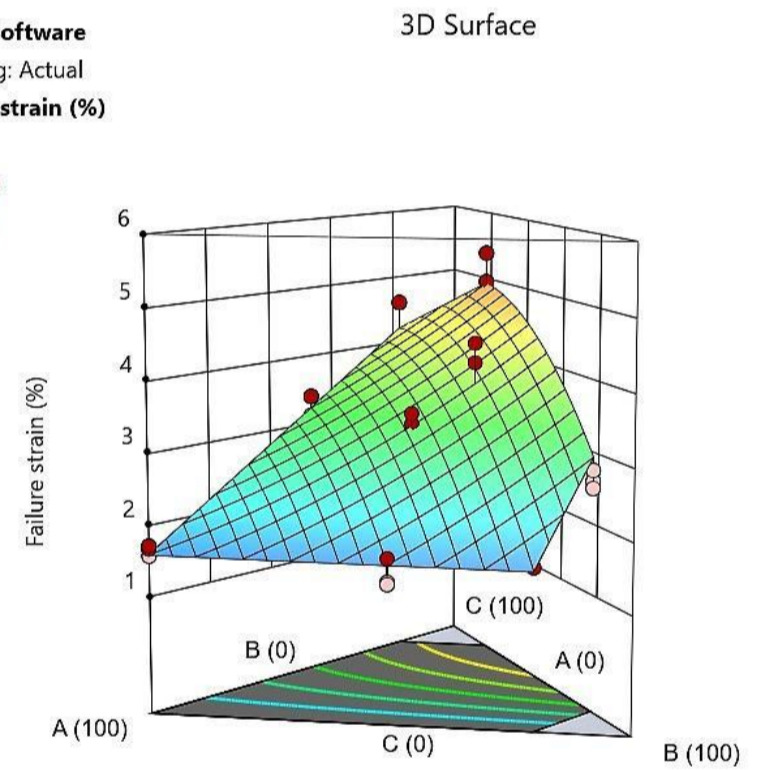
Design-Expert® Software  
 Component Coding: Actual  
**Response: Failure strain (%)**  
 ● Design Points  
 1 5,5



Design-Expert® Software  
 Component Coding: Actual  
**Response: Failure strain (%)**  
 Design Points:  
 ● Above Surface  
 ○ Below Surface  
 1 5,5



Design-Expert® Software  
 Component Coding: Actual  
**Response: Failure strain (%)**  
 Design Points:  
 ● Above Surface  
 ○ Below Surface  
 1 5,5





# R4: Estimated stiffness, $E_{50}$

## DRY.8

Configure Fit Summary Model ANOVA Diagnostics Model Graphs

Fit Summary Sequential Model Sum of Squares [Type I] Model Summary Statistics

**Fit Summary**

Response 4: Estimated stiffness

Mixture Component Coding is L\_Pseudo.

| Source        | Sequential p-value | Lack of Fit p-value | Adjusted R <sup>2</sup> | Predicted R <sup>2</sup> |                  |
|---------------|--------------------|---------------------|-------------------------|--------------------------|------------------|
| Linear        | 0,0001             |                     | 0,5455                  | 0,3219                   |                  |
| Quadratic     | <b>0,0003</b>      |                     | <b>0,8159</b>           | <b>0,7176</b>            | <b>Suggested</b> |
| Special Cubic | 0,7972             |                     | 0,8053                  | 0,6901                   |                  |
| Cubic         | 0,0008             |                     | 0,9192                  | 0,8678                   | <b>Aliased</b>   |

Configure Fit Summary Model ANOVA Diagnostics Model Graphs

Mixture Order: Quadratic Auto Select...

Model Type: Scheffe Add Term

|  |                      |
|--|----------------------|
|  | A-CEM I              |
|  | B-GGBS               |
|  | C-PSA                |
|  | AB                   |
|  | AC                   |
|  | BC                   |
|  | ABC                  |
|  | AB(A-B)              |
|  | AC(A-C)              |
|  | BC(B-C)              |
|  | A <sup>2</sup> BC    |
|  | AB <sup>2</sup> C    |
|  | ABC <sup>2</sup>     |
|  | AB(A-B) <sup>2</sup> |
|  | AC(A-C) <sup>2</sup> |
|  | BC(B-C) <sup>2</sup> |

|  |  |
|--|--|
|  | The term will be included in the model.  |
|  | Indicates the term is aliased with another term, or was not estimated in the Fit Summary calculations. Including the term in the model is not recommended. |
|  | A user-forced term. Automatic model selection will always produce a model that includes this term.   |
|  | Indicates that the term is required to be in the model by the program.   |

## WET.8

Configure Fit Summary Model ANOVA Diagnostics Model Graphs

Fit Summary Sequential Model Sum of Squares [Type I] Model Summary Statistics

**Fit Summary**

Response 4: Estimated stiffness

Mixture Component Coding is L\_Pseudo.

| Source        | Sequential p-value | Lack of Fit p-value | Adjusted R <sup>2</sup> | Predicted R <sup>2</sup> |                  |
|---------------|--------------------|---------------------|-------------------------|--------------------------|------------------|
| Linear        | < 0.0001           |                     | 0,7166                  | 0,6119                   |                  |
| Quadratic     | < <b>0.0001</b>    |                     | <b>0,9710</b>           | <b>0,9555</b>            | <b>Suggested</b> |
| Special Cubic | 0,2914             |                     | 0,9713                  | 0,9496                   |                  |
| Cubic         | 0,3082             |                     | 0,9721                  | 0,9390                   | <b>Aliased</b>   |

Configure Fit Summary Model ANOVA Diagnostics Model Graphs

Mixture Order: Quadratic Auto Select...

Model Type: Scheffe Add Term

|  |                      |
|--|----------------------|
|  | A-CEM I              |
|  | B-GGBS               |
|  | C-PSA                |
|  | AB                   |
|  | AC                   |
|  | BC                   |
|  | ABC                  |
|  | AB(A-B)              |
|  | AC(A-C)              |
|  | BC(B-C)              |
|  | A <sup>2</sup> BC    |
|  | AB <sup>2</sup> C    |
|  | ABC <sup>2</sup>     |
|  | AB(A-B) <sup>2</sup> |
|  | AC(A-C) <sup>2</sup> |
|  | BC(B-C) <sup>2</sup> |

|  |  |
|--|--|
|  | The term will be included in the model.  |
|  | Indicates the term is aliased with another term, or was not estimated in the Fit Summary calculations. Including the term in the model is not recommended. |
|  | A user-forced term. Automatic model selection will always produce a model that includes this term.   |
|  | Indicates that the term is required to be in the model by the program.   |

# DRY.8

Configure Fit Summary Model ANOVA Diagnostics Model Graphs

Analysis of Variance Fit Statistics Model Comparison Statistics Coefficients Coded Equation Real Equation Actual Equation

### ANOVA for Quadratic model

Response 4: Estimated stiffness

| Source                        | Sum of Squares | df | Mean Square | F-value | p-value  |             |
|-------------------------------|----------------|----|-------------|---------|----------|-------------|
| Block                         | 1,962E+08      | 2  | 9,808E+07   |         |          |             |
| Model                         | 3,257E+10      | 5  | 6,514E+09   | 20,51   | < 0.0001 | significant |
| <sup>(1)</sup> Linear Mixture | 2,228E+10      | 2  | 1,114E+10   | 35,07   | < 0.0001 |             |
| AB                            | 3,236E+09      | 1  | 3,236E+09   | 10,19   | 0,0053   |             |
| AC                            | 1,092E+09      | 1  | 1,092E+09   | 3,44    | 0,0811   |             |
| BC                            | 3,791E+09      | 1  | 3,791E+09   | 11,94   | 0,0030   |             |
| Residual                      | 5,400E+09      | 17 | 3,176E+08   |         |          |             |
| Cor Total                     | 3,816E+10      | 24 |             |         |          |             |

Configure Fit Summary Model ANOVA Diagnostics Model Graphs

Analysis of Variance Fit Statistics Model Comparison Statistics Coefficients Coded Equation Real Equation Actual Equation

### Fit Statistics

|           |          |                          |         |
|-----------|----------|--------------------------|---------|
| Std. Dev. | 17822,55 | R <sup>2</sup>           | 0,8578  |
| Mean      | 44751,27 | Adjusted R <sup>2</sup>  | 0,8159  |
| C.V. %    | 39,83    | Predicted R <sup>2</sup> | 0,7176  |
|           |          | Adeq Precision           | 11,5186 |

Configure Fit Summary Model ANOVA Diagnostics Model Graphs

Analysis of Variance Fit Statistics Model Comparison Statistics Coefficients Coded Equation Real Equation Actual Equation

### Final Equation in Terms of L\_Pseudo Components

|                     |            |      |
|---------------------|------------|------|
| Estimated stiffness | =          |      |
|                     | +69252,99  | * A  |
|                     | +58792,74  | * B  |
|                     | +31052,32  | * C  |
|                     | +1,903E+05 | * AB |
|                     | -1,106E+05 | * AC |
|                     | -2,516E+05 | * BC |

# WET.8

Configure Fit Summary Model ANOVA Diagnostics Model Graphs

Analysis of Variance Fit Statistics Model Comparison Statistics Coefficients Coded Equation Real Equation Actual Equation

### ANOVA for Quadratic model

Response 4: Estimated stiffness

| Source                        | Sum of Squares | df | Mean Square | F-value | p-value  |             |
|-------------------------------|----------------|----|-------------|---------|----------|-------------|
| Block                         | 1,961E+09      | 2  | 9,807E+08   |         |          |             |
| Model                         | 4,163E+10      | 5  | 8,326E+09   | 161,94  | < 0.0001 | significant |
| <sup>(1)</sup> Linear Mixture | 3,154E+10      | 2  | 1,577E+10   | 306,71  | < 0.0001 |             |
| AB                            | 1,549E+09      | 1  | 1,549E+09   | 30,14   | < 0.0001 |             |
| AC                            | 5,052E+09      | 1  | 5,052E+09   | 98,27   | < 0.0001 |             |
| BC                            | 4,115E+09      | 1  | 4,115E+09   | 80,04   | < 0.0001 |             |
| Residual                      | 9,768E+08      | 19 | 5,141E+07   |         |          |             |
| Cor Total                     | 4,457E+10      | 26 |             |         |          |             |

Configure Fit Summary Model ANOVA Diagnostics Model Graphs

Analysis of Variance Fit Statistics Model Comparison Statistics Coefficients Coded Equation Real Equation Actual Equation

### Fit Statistics

|           |          |                          |         |
|-----------|----------|--------------------------|---------|
| Std. Dev. | 7170,20  | R <sup>2</sup>           | 0,9771  |
| Mean      | 45667,64 | Adjusted R <sup>2</sup>  | 0,9710  |
| C.V. %    | 15,70    | Predicted R <sup>2</sup> | 0,9555  |
|           |          | Adeq Precision           | 30,0072 |

Configure Fit Summary Model ANOVA Diagnostics Model Graphs

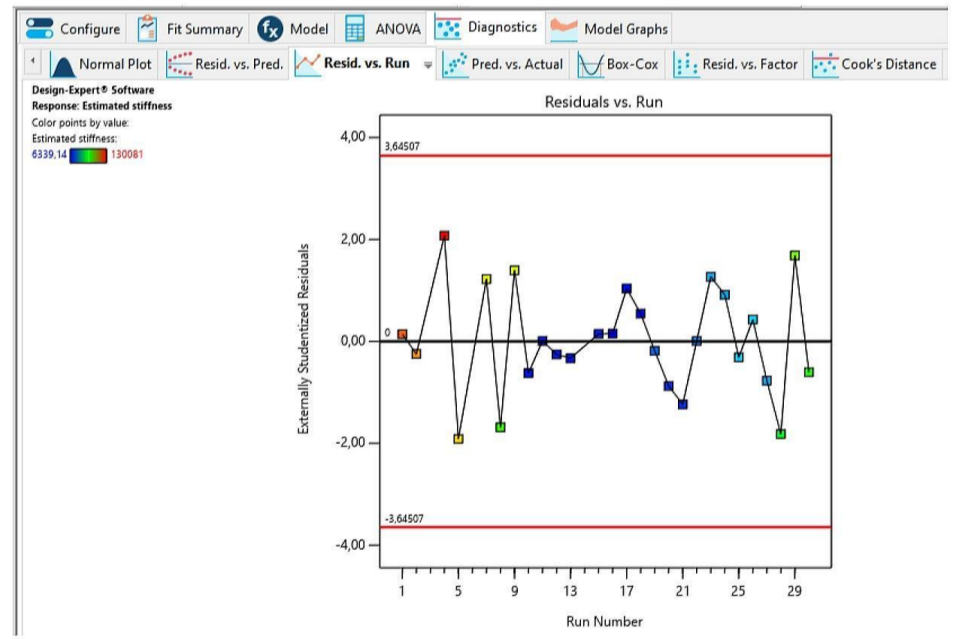
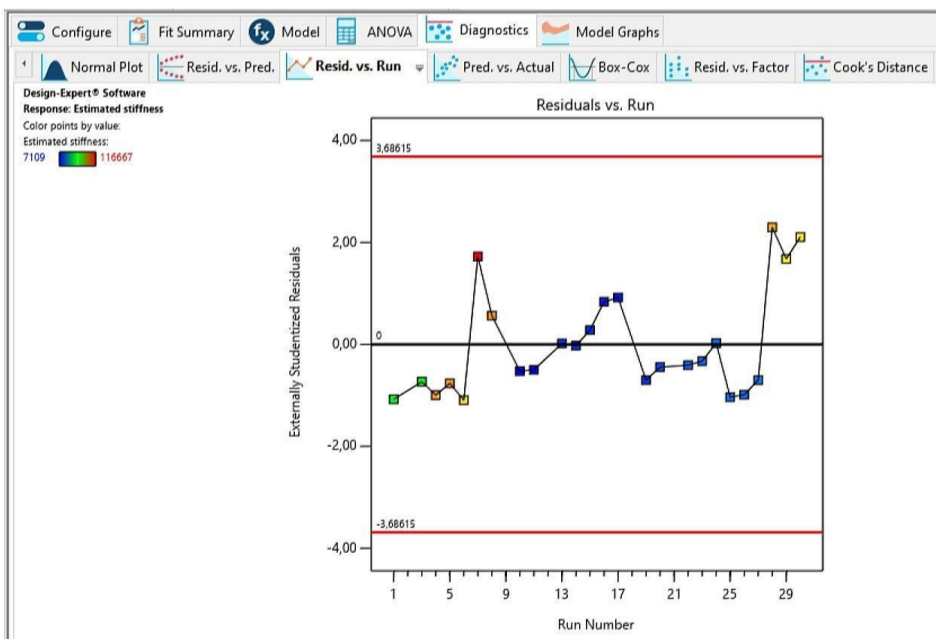
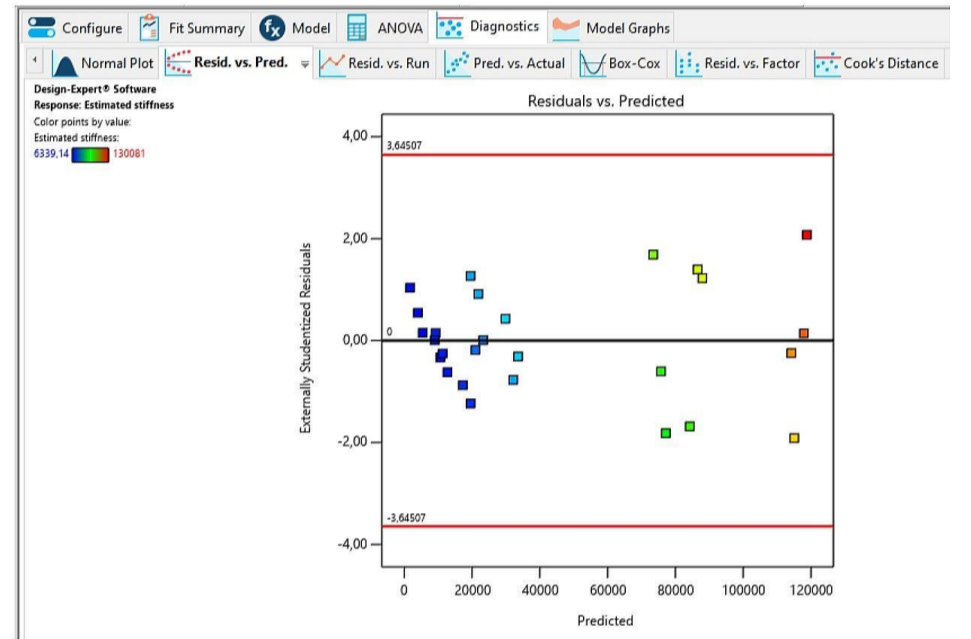
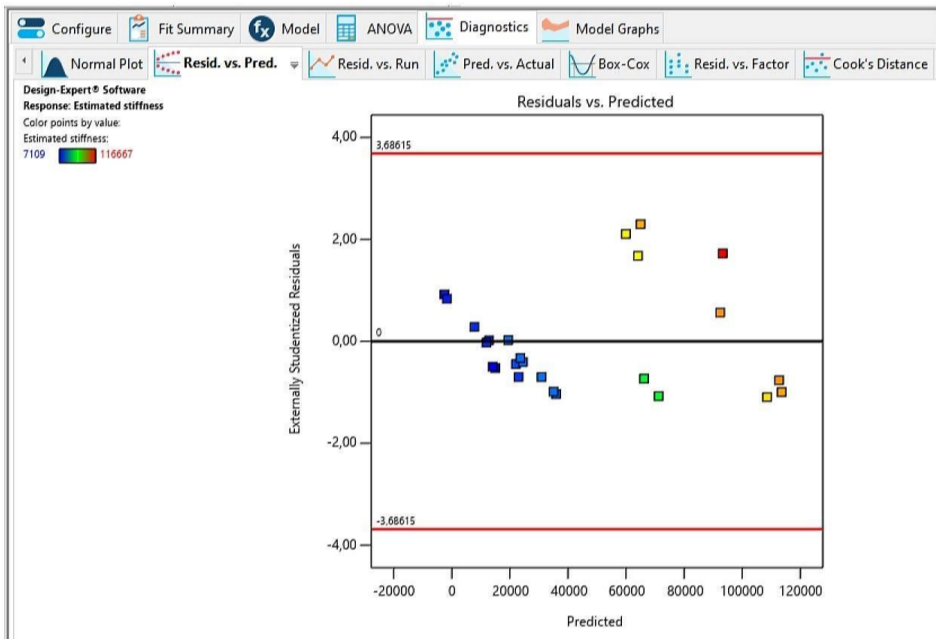
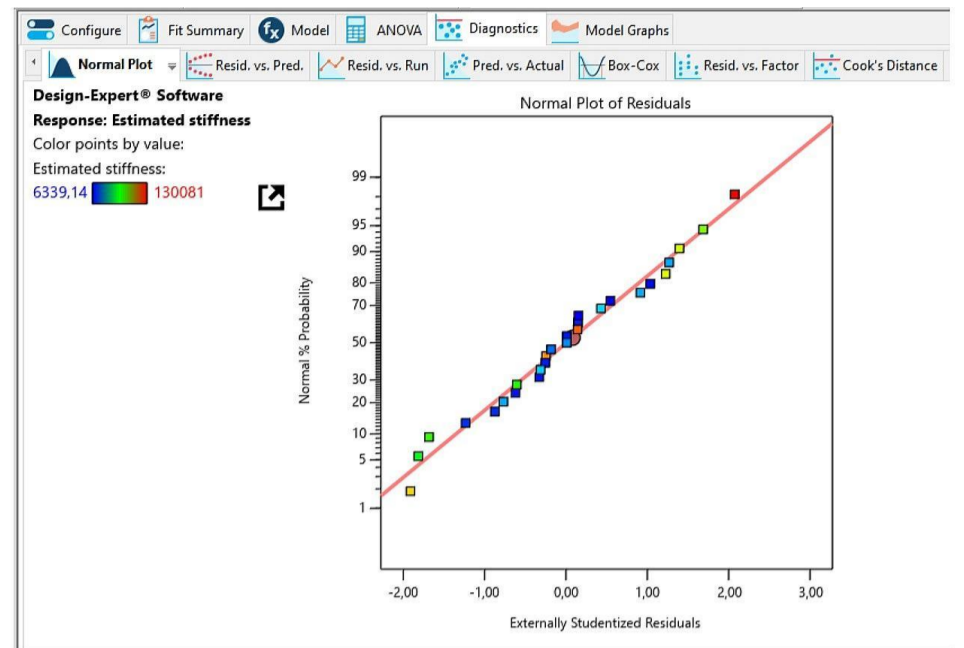
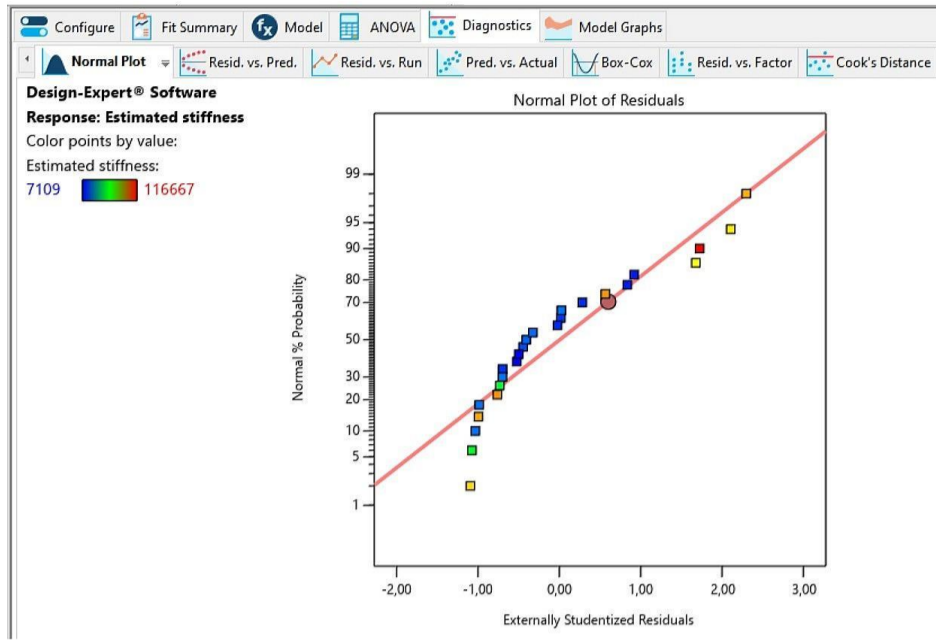
Analysis of Variance Fit Statistics Model Comparison Statistics Coefficients Coded Equation Real Equation Actual Equation

### Final Equation in Terms of L\_Pseudo Components

|                     |            |      |
|---------------------|------------|------|
| Estimated stiffness | =          |      |
|                     | +1,162E+05 | * A  |
|                     | +52622,49  | * B  |
|                     | +40446,88  | * C  |
|                     | +1,307E+05 | * AB |
|                     | -2,271E+05 | * AC |
|                     | -2,449E+05 | * BC |

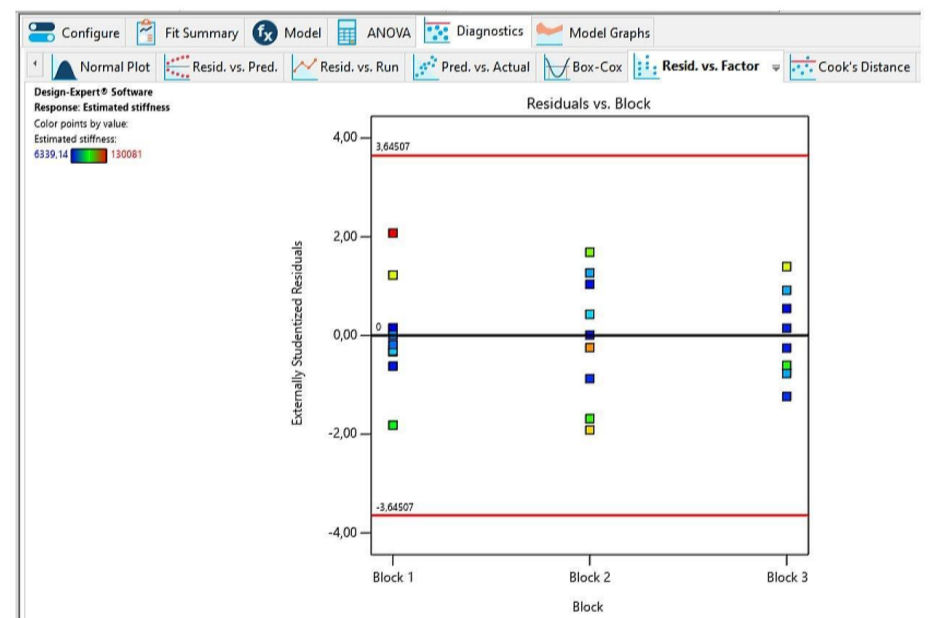
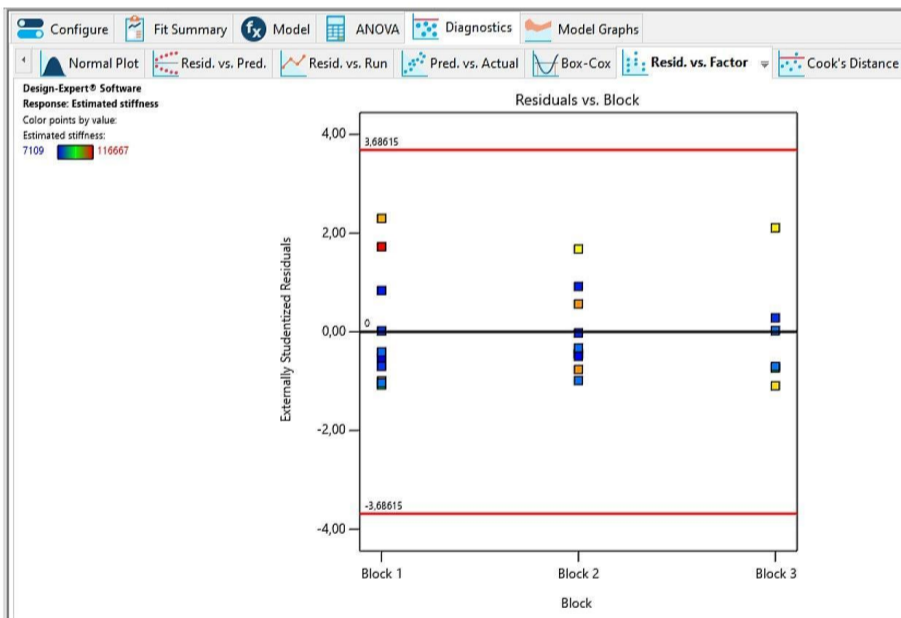
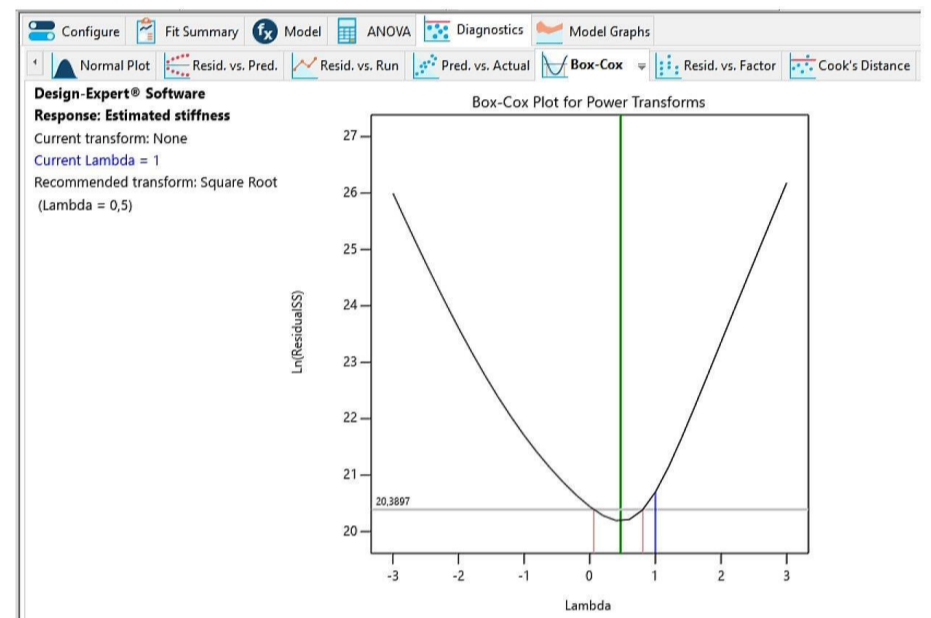
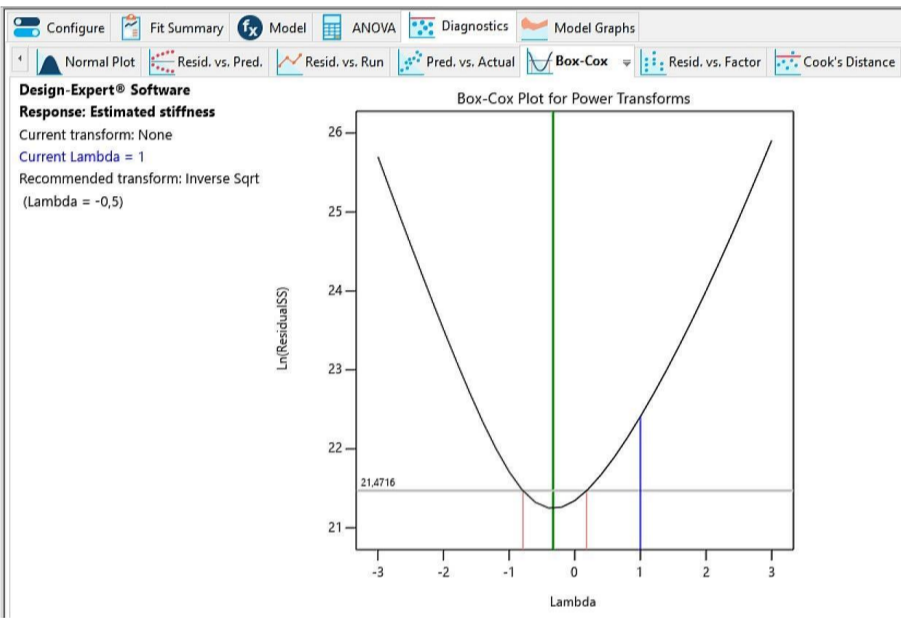
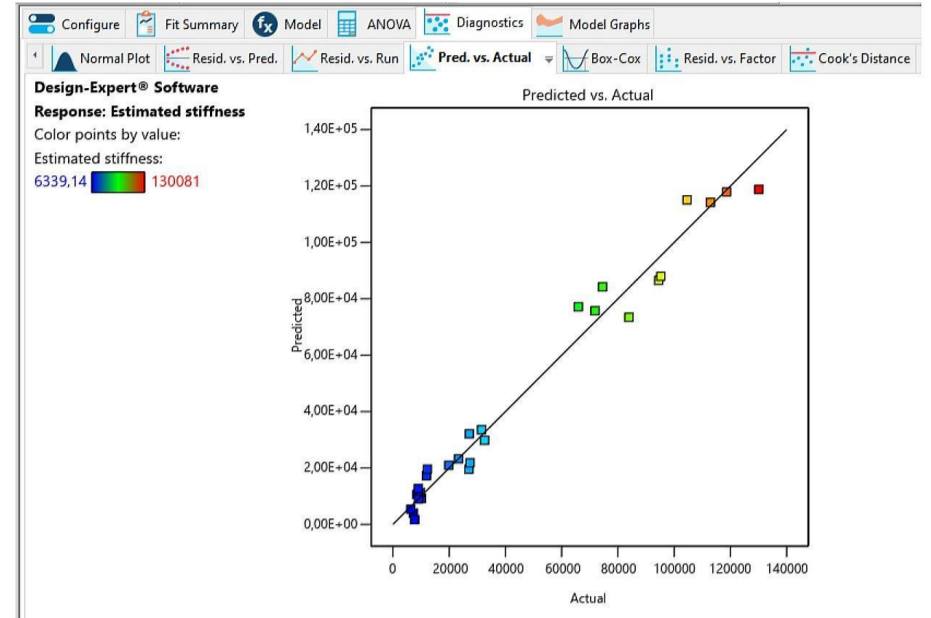
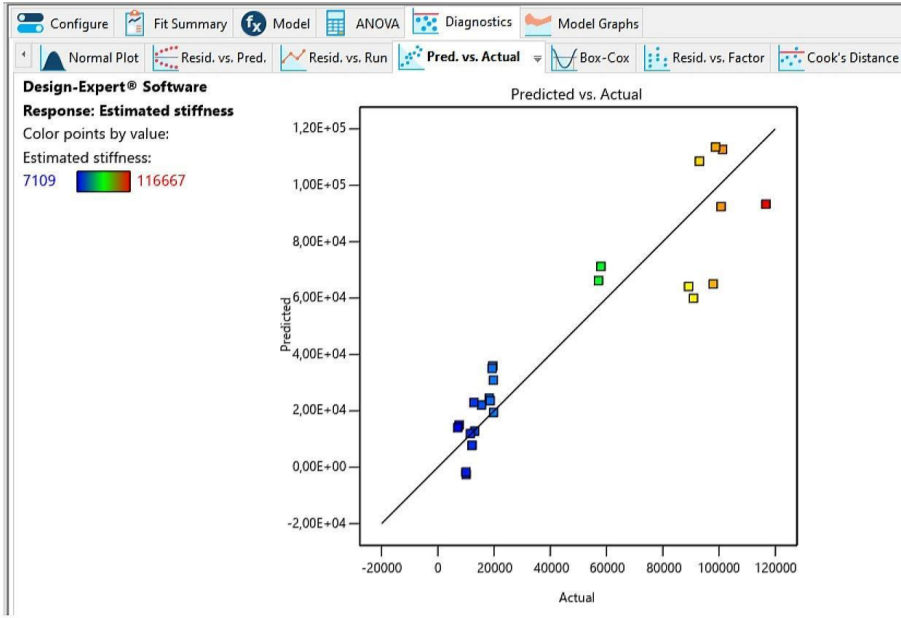
**DRY.8**

**WET.8**



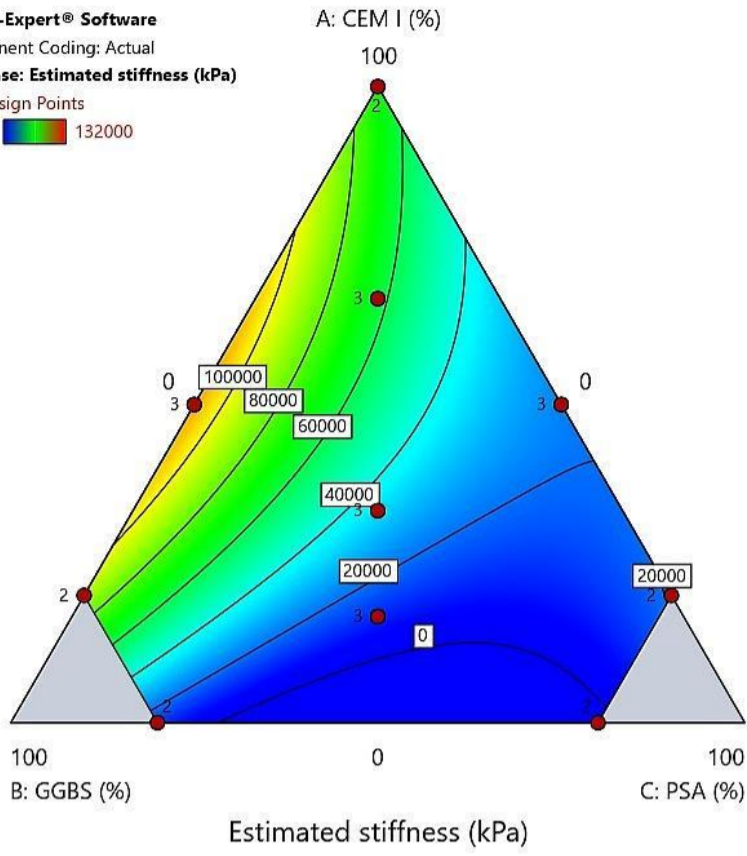
**DRY.8**

**WET.8**



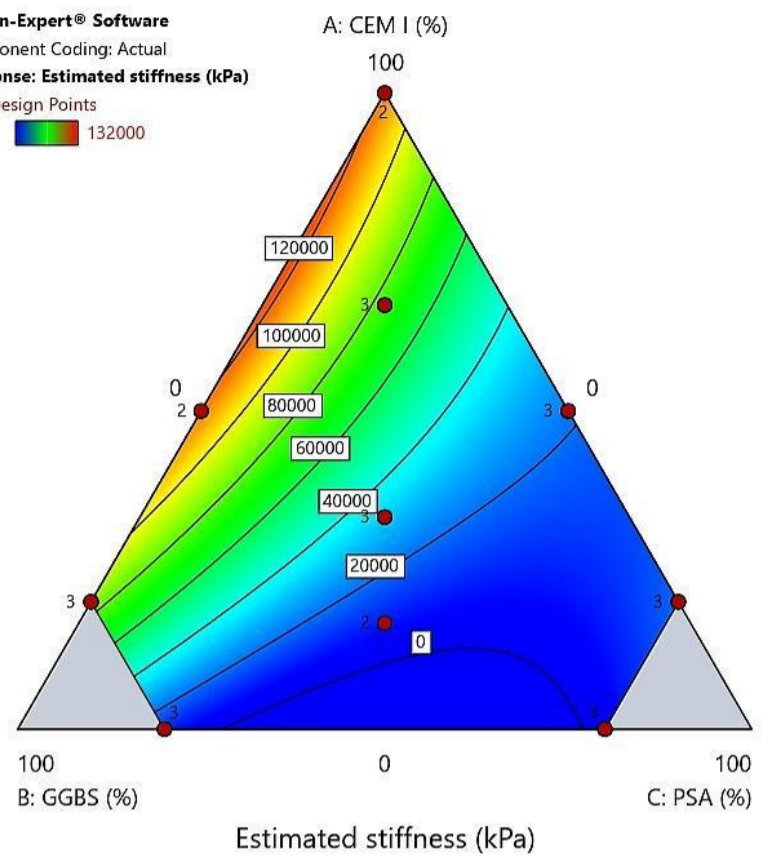
# DRY.8

Design-Expert® Software  
 Component Coding: Actual  
 Response: Estimated stiffness (kPa)  
 ● Design Points  
 6000 132000

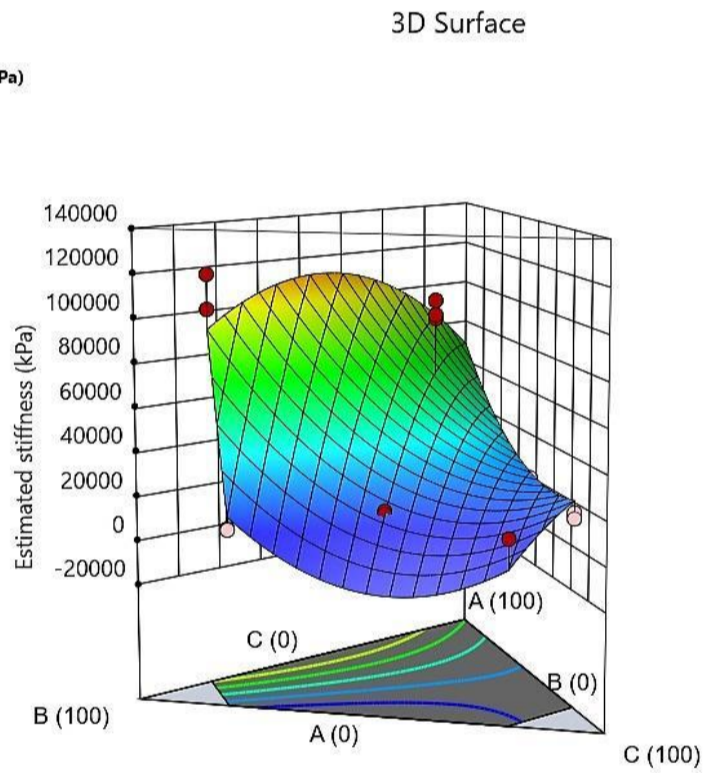


# WET.8

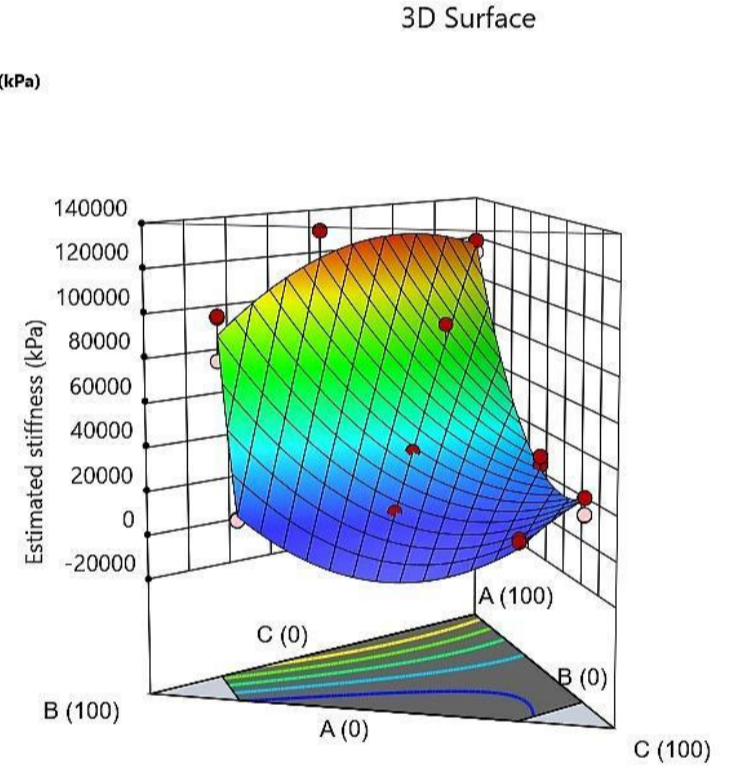
Design-Expert® Software  
 Component Coding: Actual  
 Response: Estimated stiffness (kPa)  
 ● Design Points  
 6000 132000



Design-Expert® Software  
 Component Coding: Actual  
 Response: Estimated stiffness (kPa)  
 Design Points:  
 ● Above Surface  
 ○ Below Surface  
 6000 132000



Design-Expert® Software  
 Component Coding: Actual  
 Response: Estimated stiffness (kPa)  
 Design Points:  
 ● Above Surface  
 ○ Below Surface  
 6000 132000



# R5: P-wave velocity, $V_p$

## DRY.8

Configure Fit Summary Model ANOVA Diagnostics Model Graphs

Fit Summary Sequential Model Sum of Squares [Type I] Model Summary Statistics

**Fit Summary**  
Response 5: P-wave velocity  
Mixture Component Coding is L\_Pseudo.

| Source        | Sequential p-value | Lack of Fit p-value | Adjusted R <sup>2</sup> | Predicted R <sup>2</sup> |                  |
|---------------|--------------------|---------------------|-------------------------|--------------------------|------------------|
| Linear        | < 0.0001           |                     | 0,6602                  | 0,5170                   |                  |
| Quadratic     | < 0.0001           |                     | <b>0,9310</b>           | <b>0,8968</b>            | <b>Suggested</b> |
| Special Cubic | 0,7658             |                     | 0,9275                  | 0,8846                   |                  |
| Cubic         | 0,0002             |                     | 0,9711                  | 0,9516                   | <b>Aliased</b>   |

Configure Fit Summary Model ANOVA Diagnostics Model Graphs

Mixture Order: Quadratic Auto Select...

Model Type: Scheffe Add Term

|          |  |
|----------|--|
| <b>m</b> | The term will be included in the model.  |
| <b>!</b> | Indicates the term is aliased with another term, or was not estimated in the Fit Summary calculations. Including the term in the model is not recommended. |
| <b>!</b> | A user-forced term. Automatic model selection will always produce a model that includes this term.   |
| <b>!</b> | Indicates that the term is required to be in the model by the program.   |

- A-CEM I
- B-GGBS
- C-PSA
- m** AB
- m** AC
- m** BC
- ABC
- AB(A-B)
- AC(A-C)
- !** BC(B-C)
- A<sup>2</sup>BC
- AB<sup>2</sup>C
- !** ABC<sup>2</sup>
- !** AB(A-B)<sup>2</sup>
- !** AC(A-C)<sup>2</sup>
- !** BC(B-C)<sup>2</sup>

## WET.8

Configure Fit Summary Model ANOVA Diagnostics Model Graphs

Fit Summary Sequential Model Sum of Squares [Type I] Model Summary Statistics

**Fit Summary**  
Response 5: P-wave velocity  
Mixture Component Coding is L\_Pseudo.

| Source        | Sequential p-value | Lack of Fit p-value | Adjusted R <sup>2</sup> | Predicted R <sup>2</sup> |                  |
|---------------|--------------------|---------------------|-------------------------|--------------------------|------------------|
| Linear        | < 0.0001           |                     | 0,6450                  | 0,5185                   |                  |
| Quadratic     | < 0.0001           |                     | <b>0,9645</b>           | <b>0,9457</b>            | <b>Suggested</b> |
| Special Cubic | 0,6275             |                     | 0,9632                  | 0,9417                   |                  |
| Cubic         | < 0.0001           |                     | 0,9973                  | 0,9952                   | <b>Aliased</b>   |

Configure Fit Summary Model ANOVA Diagnostics Model Graphs

Mixture Order: Quadratic Auto Select...

Model Type: Scheffe Add Term

|          |  |
|----------|--|
| <b>m</b> | The term will be included in the model.  |
| <b>!</b> | Indicates the term is aliased with another term, or was not estimated in the Fit Summary calculations. Including the term in the model is not recommended. |
| <b>!</b> | A user-forced term. Automatic model selection will always produce a model that includes this term.   |
| <b>!</b> | Indicates that the term is required to be in the model by the program.   |

- A-CEM I
- B-GGBS
- C-PSA
- m** AB
- m** AC
- m** BC
- ABC
- AB(A-B)
- AC(A-C)
- !** BC(B-C)
- A<sup>2</sup>BC
- AB<sup>2</sup>C
- !** ABC<sup>2</sup>
- !** AB(A-B)<sup>2</sup>
- !** AC(A-C)<sup>2</sup>
- !** BC(B-C)<sup>2</sup>

# DRY.8

Configure Fit Summary Model ANOVA Diagnostics Model Graphs

Analysis of Variance Fit Statistics Model Comparison Statistics Coefficients Coded Equation Real Equation Actual Equation

**ANOVA for Quadratic model**  
Response 5: P-wave velocity

| Source                        | Sum of Squares | df | Mean Square | F-value | p-value  |             |
|-------------------------------|----------------|----|-------------|---------|----------|-------------|
| Block                         | 16504,47       | 2  | 8252,24     |         |          |             |
| Model                         | 6,048E+06      | 5  | 1,210E+06   | 65,72   | < 0.0001 | significant |
| <sup>(1)</sup> Linear Mixture | 4,405E+06      | 2  | 2,202E+06   | 119,66  | < 0.0001 |             |
| AB                            | 4,920E+05      | 1  | 4,920E+05   | 26,73   | < 0.0001 |             |
| AC                            | 3,229E+05      | 1  | 3,229E+05   | 17,55   | 0,0005   |             |
| BC                            | 5,982E+05      | 1  | 5,982E+05   | 32,50   | < 0.0001 |             |
| Residual                      | 3,497E+05      | 19 | 18404,79    |         |          |             |
| Cor Total                     | 6,414E+06      | 26 |             |         |          |             |

Configure Fit Summary Model ANOVA Diagnostics Model Graphs

Analysis of Variance Fit Statistics Model Comparison Statistics Coefficients Coded Equation Real Equation Actual Equation

**Fit Statistics**

|           |        |                          |         |
|-----------|--------|--------------------------|---------|
| Std. Dev. | 135,66 | R <sup>2</sup>           | 0,9453  |
| Mean      | 765,74 | Adjusted R <sup>2</sup>  | 0,9310  |
| C.V. %    | 17,72  | Predicted R <sup>2</sup> | 0,8968  |
|           |        | Adeq Precision           | 19,9102 |

Configure Fit Summary Model ANOVA Diagnostics Model Graphs

Analysis of Variance Fit Statistics Model Comparison Statistics Coefficients Coded Equation Real Equation Actual Equation

**Final Equation in Terms of L\_Pseudo Components**

|                 |               |
|-----------------|---------------|
| P-wave velocity | =             |
|                 | +1264,13 * A  |
|                 | +878,22 * B   |
|                 | +620,97 * C   |
|                 | +2114,02 * AB |
|                 | -1847,77 * AC |
|                 | -3150,25 * BC |

# WET.8

Configure Fit Summary Model ANOVA Diagnostics Model Graphs

Analysis of Variance Fit Statistics Model Comparison Statistics Coefficients Coded Equation Real Equation Actual Equation

**ANOVA for Quadratic model**  
Response 5: P-wave velocity

| Source                        | Sum of Squares | df | Mean Square | F-value | p-value  |             |
|-------------------------------|----------------|----|-------------|---------|----------|-------------|
| Block                         | 1550,91        | 2  | 775,45      |         |          |             |
| Model                         | 8,208E+06      | 5  | 1,642E+06   | 142,46  | < 0.0001 | significant |
| <sup>(1)</sup> Linear Mixture | 5,681E+06      | 2  | 2,840E+06   | 246,49  | < 0.0001 |             |
| AB                            | 2,196E+05      | 1  | 2,196E+05   | 19,05   | 0,0003   |             |
| AC                            | 1,119E+06      | 1  | 1,119E+06   | 97,07   | < 0.0001 |             |
| BC                            | 1,333E+06      | 1  | 1,333E+06   | 115,63  | < 0.0001 |             |
| Residual                      | 2,420E+05      | 21 | 11523,80    |         |          |             |
| Cor Total                     | 8,452E+06      | 28 |             |         |          |             |

Configure Fit Summary Model ANOVA Diagnostics Model Graphs

Analysis of Variance Fit Statistics Model Comparison Statistics Coefficients Coded Equation Real Equation Actual Equation

**Fit Statistics**

|           |        |                          |         |
|-----------|--------|--------------------------|---------|
| Std. Dev. | 107,35 | R <sup>2</sup>           | 0,9714  |
| Mean      | 798,97 | Adjusted R <sup>2</sup>  | 0,9645  |
| C.V. %    | 13,44  | Predicted R <sup>2</sup> | 0,9457  |
|           |        | Adeq Precision           | 26,6538 |

Configure Fit Summary Model ANOVA Diagnostics Model Graphs

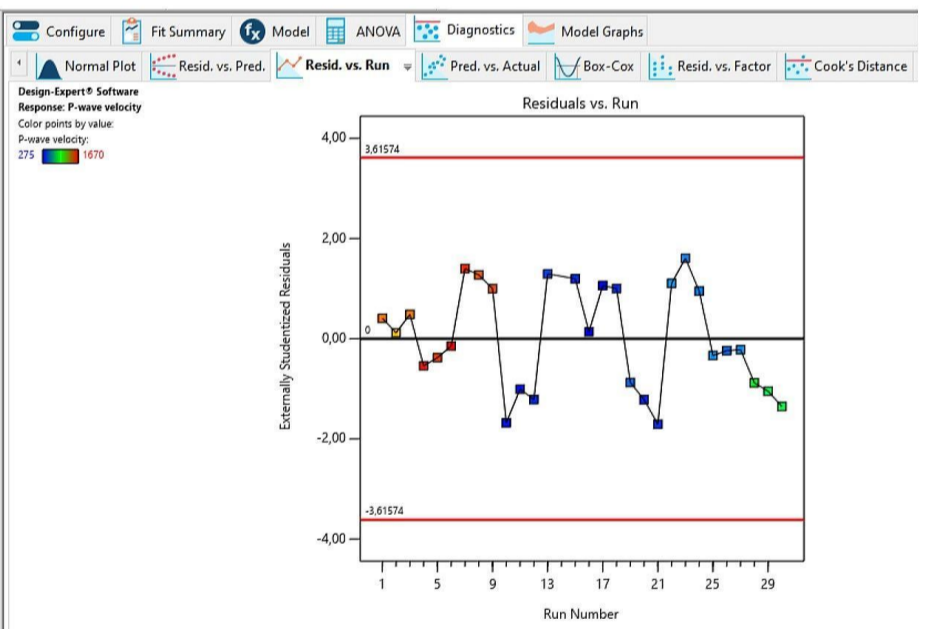
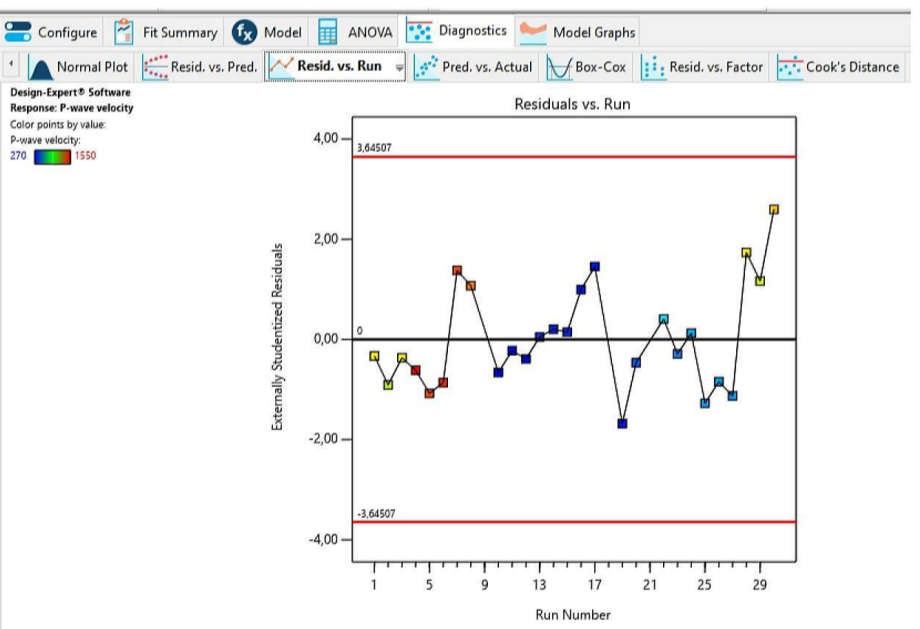
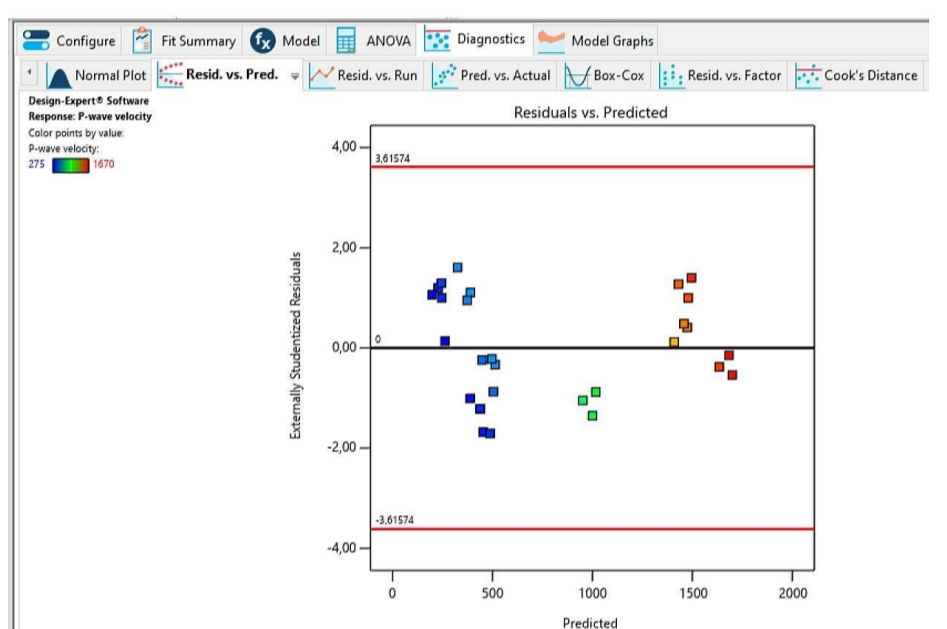
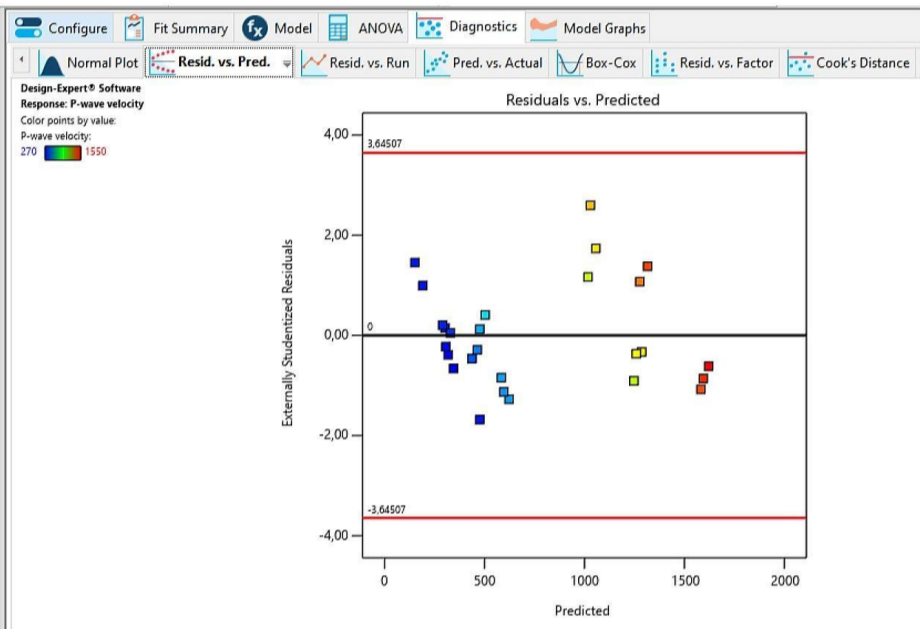
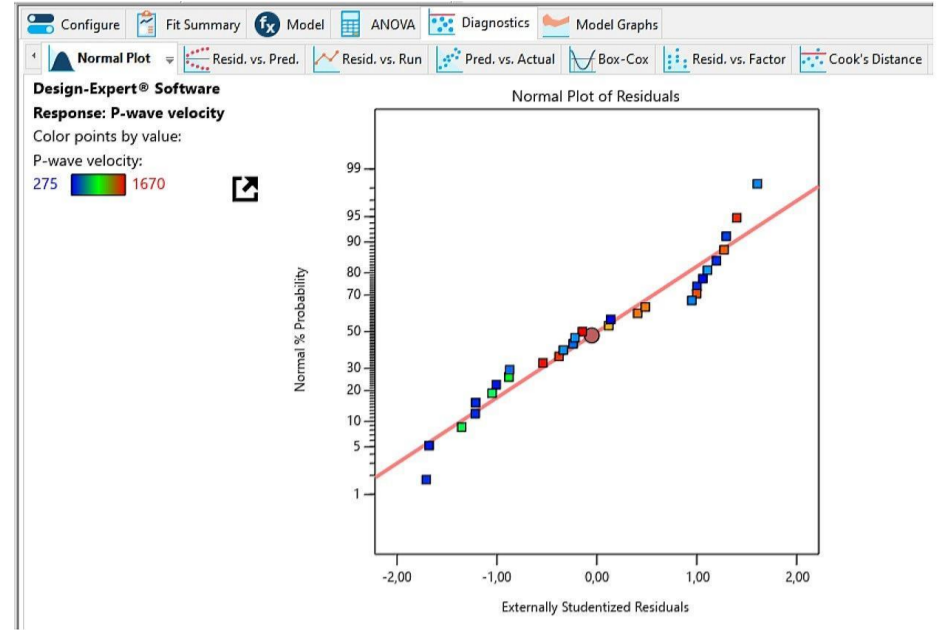
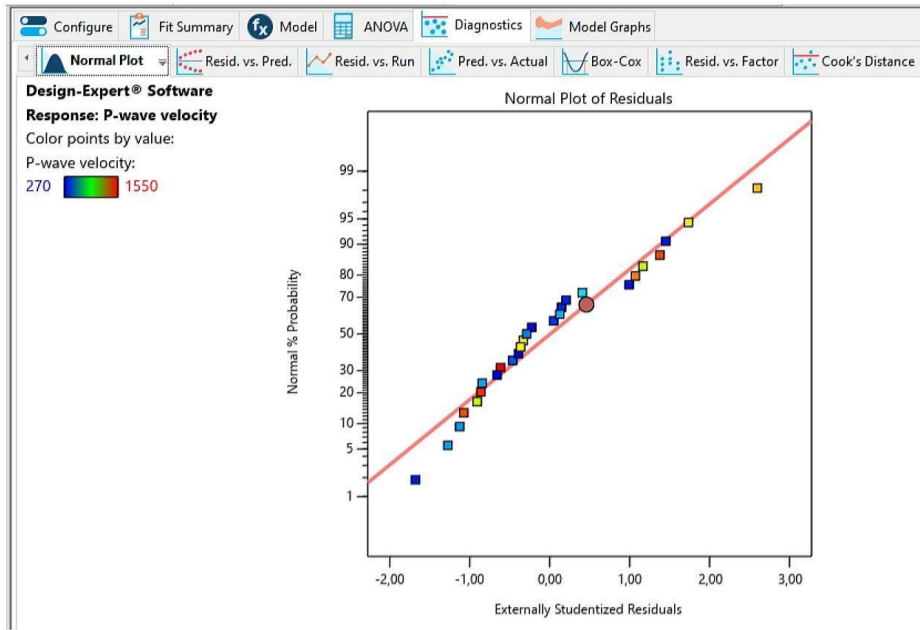
Analysis of Variance Fit Statistics Model Comparison Statistics Coefficients Coded Equation Real Equation Actual Equation

**Final Equation in Terms of L\_Pseudo Components**

|                 |               |
|-----------------|---------------|
| P-wave velocity | =             |
|                 | +1447,58 * A  |
|                 | +1191,29 * B  |
|                 | +873,12 * C   |
|                 | +1413,83 * AB |
|                 | -3191,38 * AC |
|                 | -4384,72 * BC |

**DRY.8**

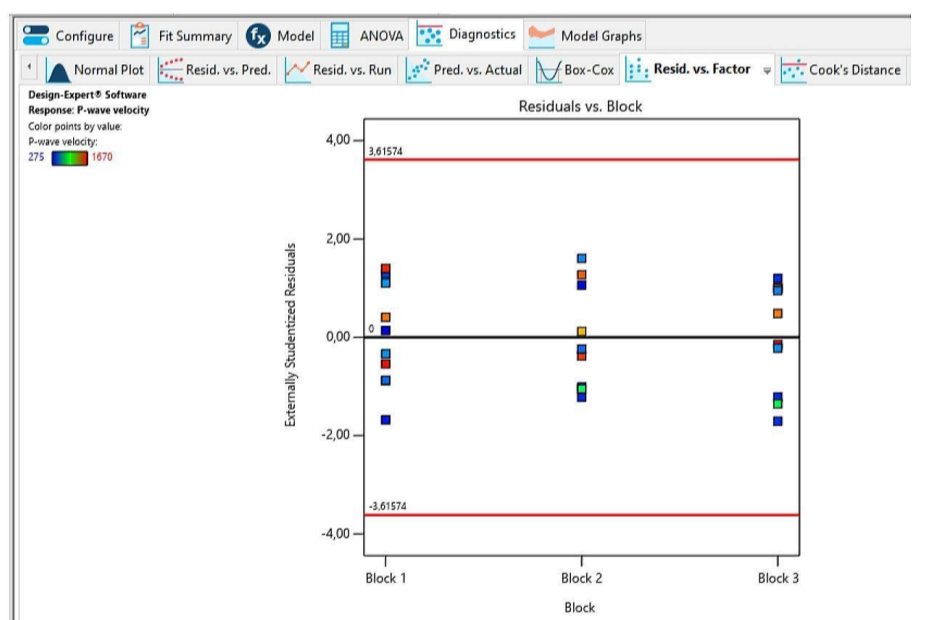
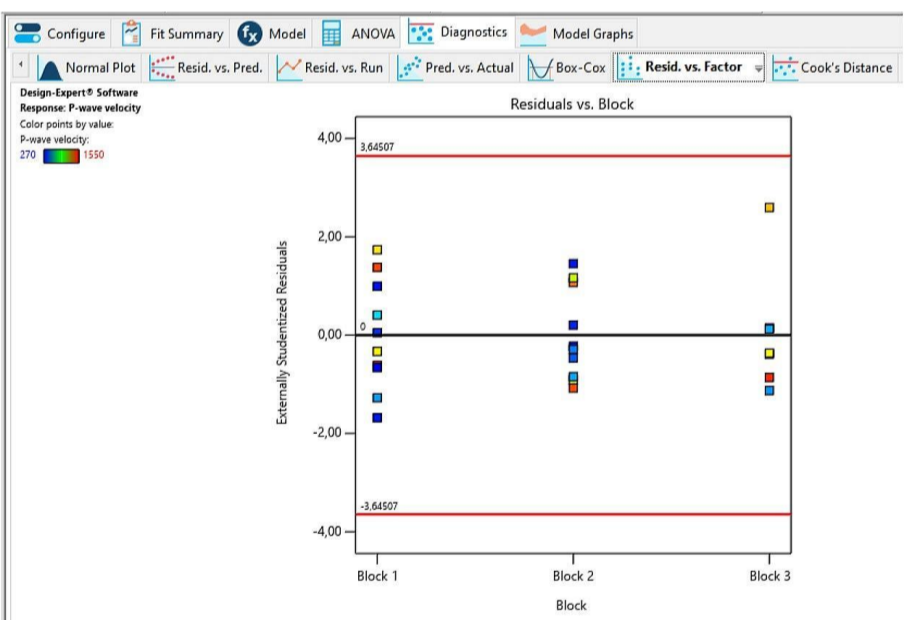
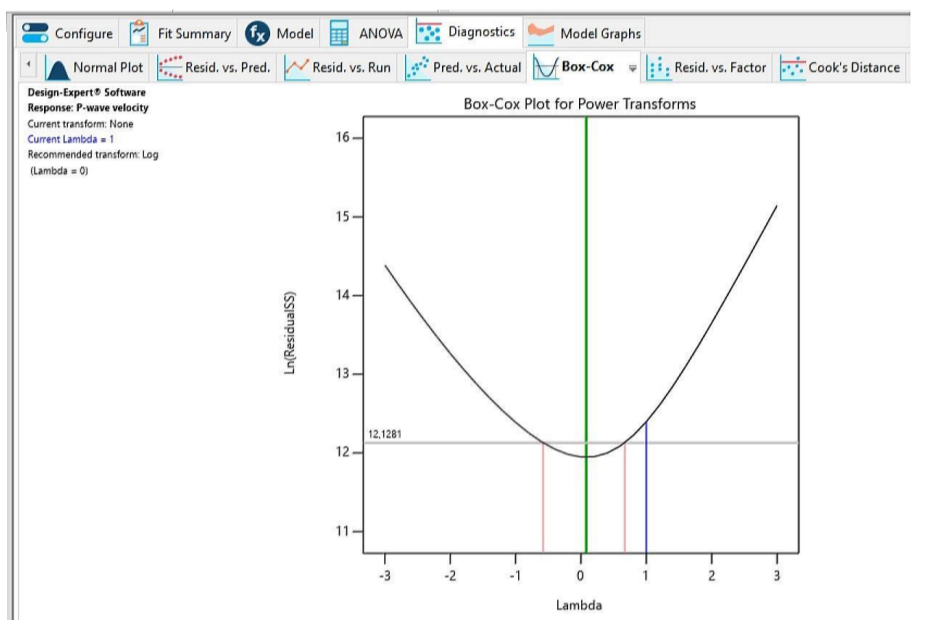
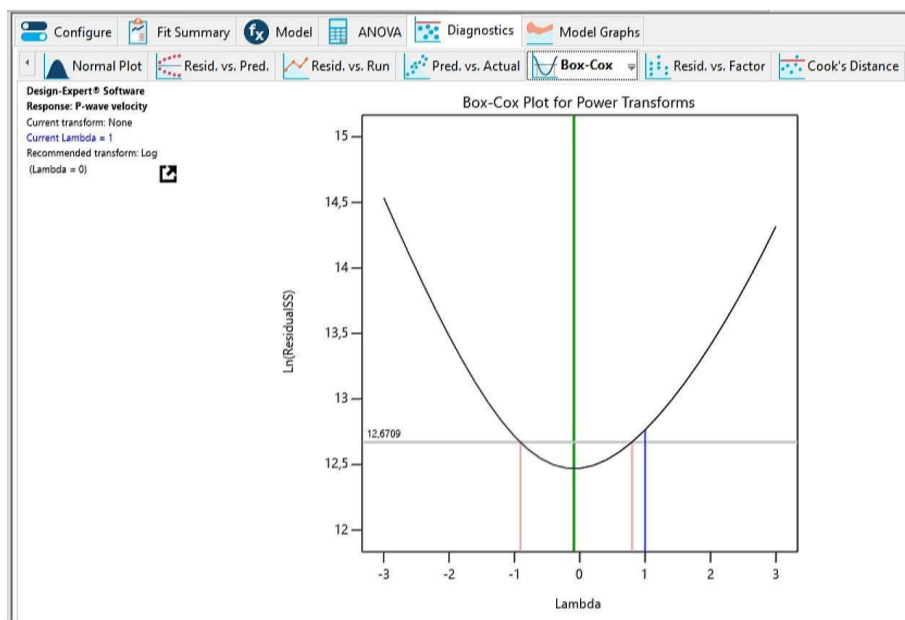
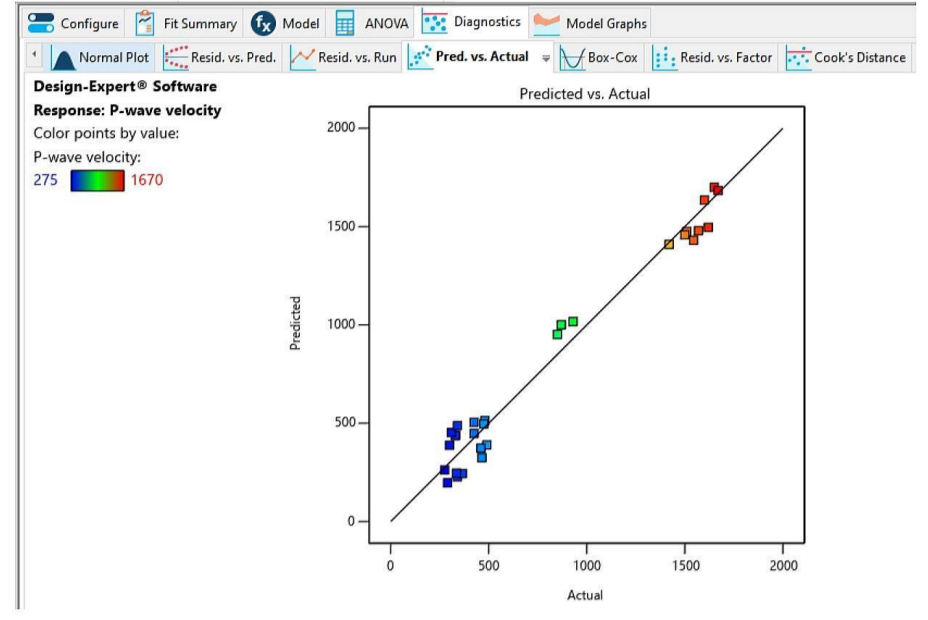
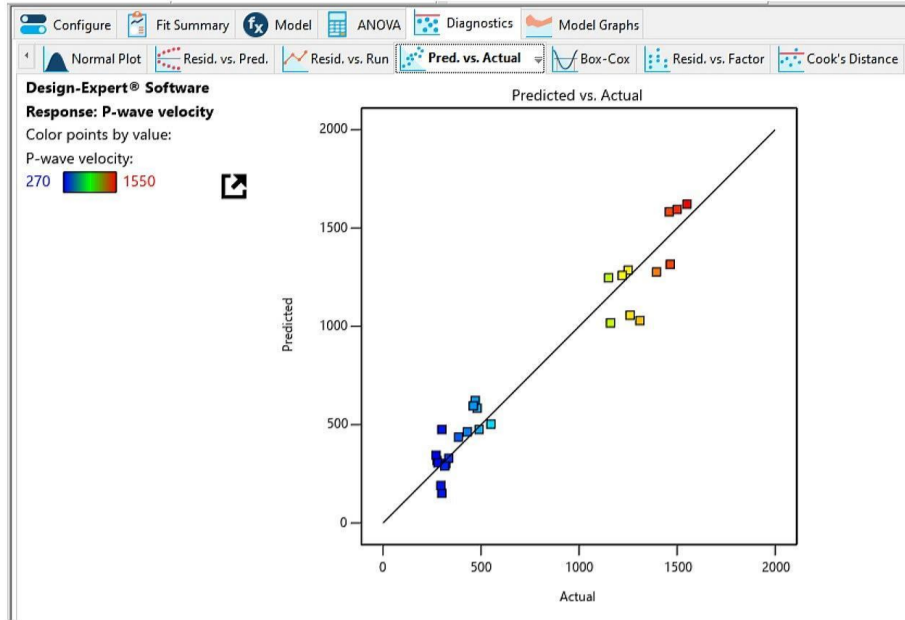
**WET.8**





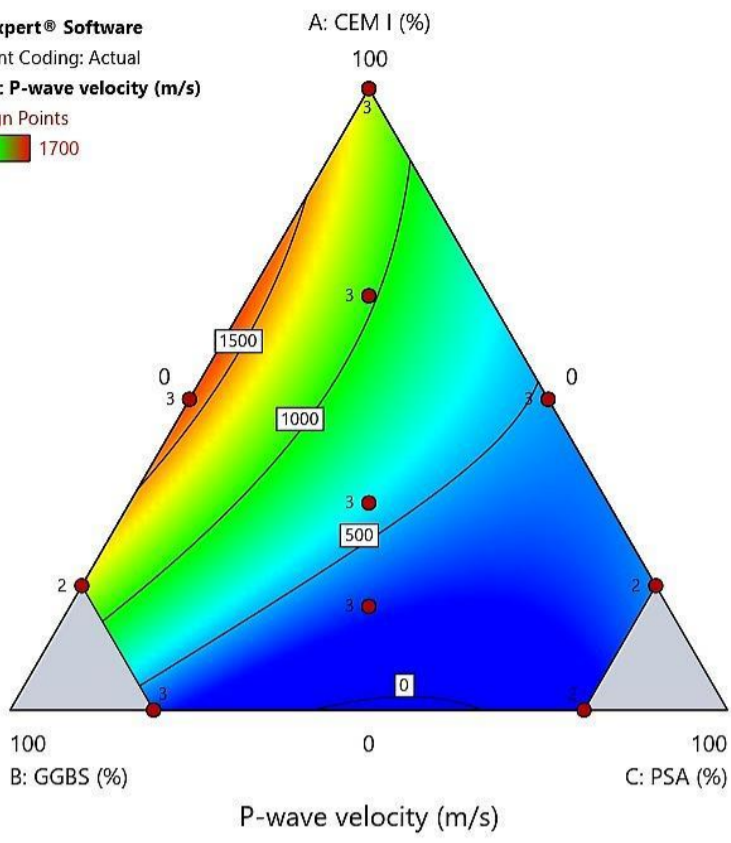
**DRY.8**

**WET.8**



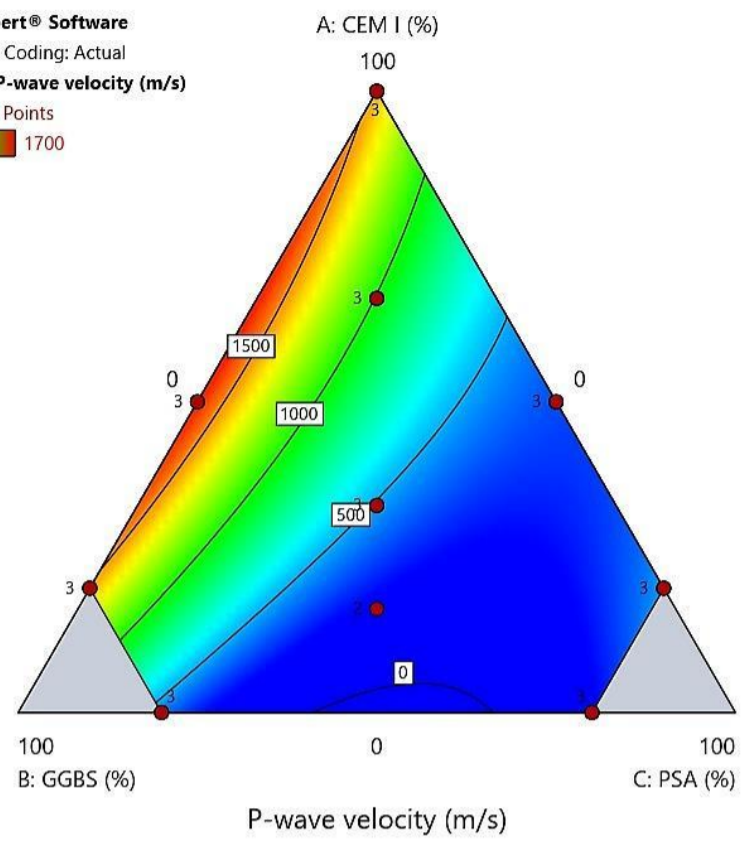
# DRY.8

Design-Expert® Software  
 Component Coding: Actual  
 Response: P-wave velocity (m/s)  
 ● Design Points  
 250 1700

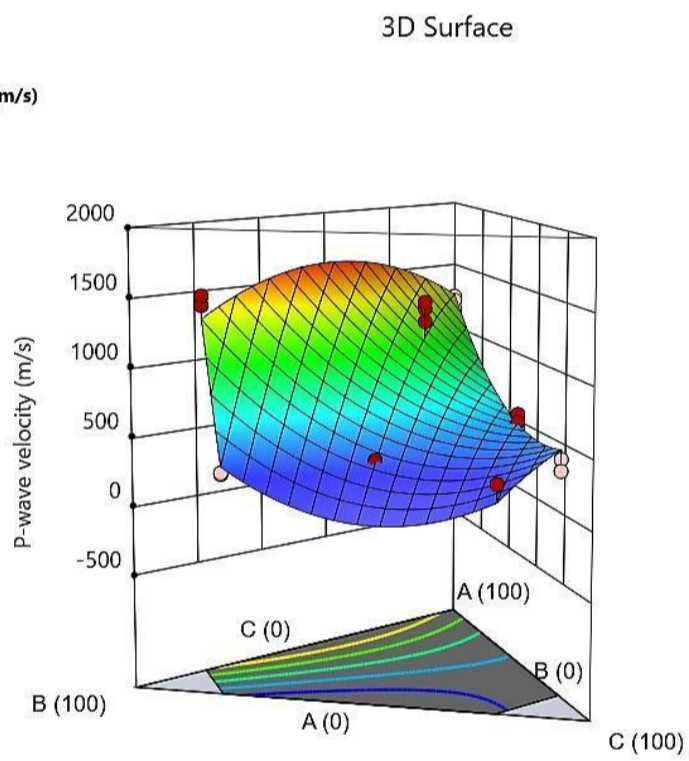


# WET.8

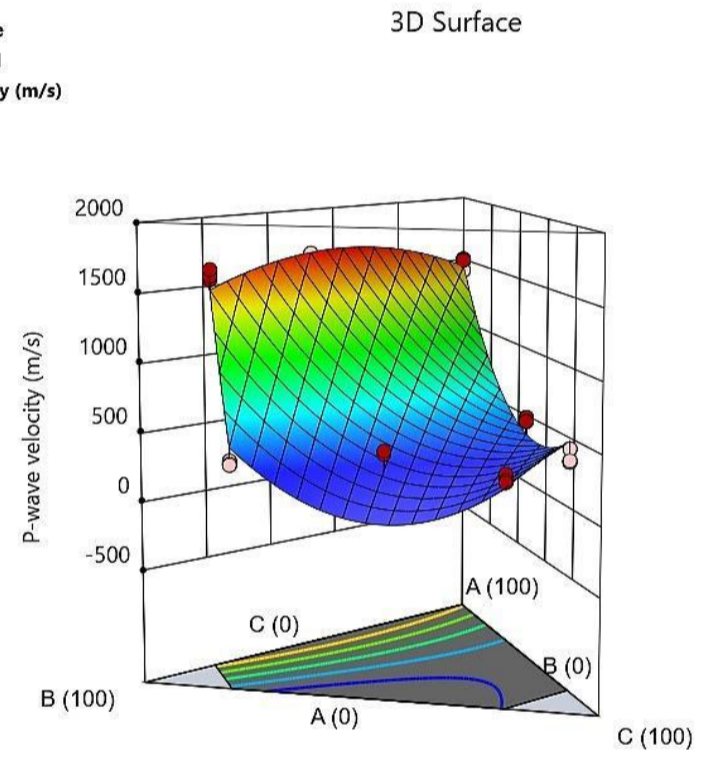
Design-Expert® Software  
 Component Coding: Actual  
 Response: P-wave velocity (m/s)  
 ● Design Points  
 250 1700



Design-Expert® Software  
 Component Coding: Actual  
 Response: P-wave velocity (m/s)  
 Design Points:  
 ● Above Surface  
 ○ Below Surface  
 250 1700



Design-Expert® Software  
 Component Coding: Actual  
 Response: P-wave velocity (m/s)  
 Design Points:  
 ● Above Surface  
 ○ Below Surface  
 250 1700



**B.4.2. DRY AND WET MIXING METHOD WITH WBR=16**

# R1: Ultimate compressive strength, $q_u$

## DRY.16

**Fit Summary**  
Response 1: Ultimate compressive strength  
Mixture Component Coding is L\_Pseudo.

| Source        | Sequential p-value | Lack of Fit p-value | Adjusted R <sup>2</sup> | Predicted R <sup>2</sup> |                  |
|---------------|--------------------|---------------------|-------------------------|--------------------------|------------------|
| Linear        | < 0.0001           |                     | 0,9692                  | 0,9577                   |                  |
| Quadratic     | <b>0,0296</b>      |                     | <b>0,9766</b>           | <b>0,9656</b>            | <b>Suggested</b> |
| Special Cubic | 0,7503             |                     | 0,9756                  | 0,9627                   |                  |
| Cubic         | 0,0002             |                     | 0,9891                  | 0,9817                   | <b>Aliased</b>   |

## WET.16

**Fit Summary**  
Response 1: Ultimate compressive strength  
Mixture Component Coding is L\_Pseudo.

| Source        | Sequential p-value | Lack of Fit p-value | Adjusted R <sup>2</sup> | Predicted R <sup>2</sup> |                  |
|---------------|--------------------|---------------------|-------------------------|--------------------------|------------------|
| Linear        | < 0.0001           |                     | 0,7593                  | 0,6875                   |                  |
| Quadratic     | <b>0,0042</b>      |                     | <b>0,8513</b>           | <b>0,8036</b>            | <b>Suggested</b> |
| Special Cubic | 0,3742             |                     | 0,8501                  | 0,7962                   |                  |
| Cubic         | 0,0012             |                     | 0,9210                  | 0,8740                   | <b>Aliased</b>   |

Mixture Order: Modified  
Model Type: Scheffe

| Icon | Description  |
|------|--|
| m    | The term will be included in the model.  |
| !    | Indicates the term is aliased with another term, or was not estimated in the Fit Summary calculations. Including the term in the model is not recommended. |
| 🔒    | A user-forced term. Automatic model selection will always produce a model that includes this term.   |
| 🔒    | Indicates that the term is required to be in the model by the program.   |

Mixture Order: Quadratic  
Model Type: Scheffe

| Icon | Description  |
|------|--|
| m    | The term will be included in the model.  |
| !    | Indicates the term is aliased with another term, or was not estimated in the Fit Summary calculations. Including the term in the model is not recommended. |
| 🔒    | A user-forced term. Automatic model selection will always produce a model that includes this term.   |
| 🔒    | Indicates that the term is required to be in the model by the program.   |

# DRY.16

Configure Fit Summary Model ANOVA Diagnostics Model Graphs

Analysis of Variance Fit Statistics Model Comparison Statistics Coefficients Coded Equation Real Equation Actual Equation

**ANOVA for Reduced Quadratic model**

Response 1: Ultimate compressive strength

| Source             | Sum of Squares | df | Mean Square | F-value | p-value  |             |
|--------------------|----------------|----|-------------|---------|----------|-------------|
| Block              | 980,40         | 2  | 490,20      |         |          |             |
| Model              | 3,585E+05      | 4  | 89626,82    | 286,74  | < 0.0001 | significant |
| (1) Linear Mixture | 3,553E+05      | 2  | 1,776E+05   | 568,31  | < 0.0001 |             |
| AB                 | 1073,72        | 1  | 1073,72     | 3,44    | 0,0767   |             |
| AC                 | 2494,79        | 1  | 2494,79     | 7,98    | 0,0096   |             |
| Residual           | 7189,18        | 23 | 312,57      |         |          |             |
| Cor Total          | 3,667E+05      | 29 |             |         |          |             |

Configure Fit Summary Model ANOVA Diagnostics Model Graphs

Analysis of Variance Fit Statistics Model Comparison Statistics Coefficients Coded Equation Real Equation Actual Equation

**Fit Statistics**

|           |        |                          |         |
|-----------|--------|--------------------------|---------|
| Std. Dev. | 17,68  | R <sup>2</sup>           | 0,9803  |
| Mean      | 204,70 | Adjusted R <sup>2</sup>  | 0,9769  |
| C.V. %    | 8,64   | Predicted R <sup>2</sup> | 0,9674  |
|           |        | Adeq Precision           | 46,0365 |

Configure Fit Summary Model ANOVA Diagnostics Model Graphs

Analysis of Variance Fit Statistics Model Comparison Statistics Coefficients Coded Equation Real Equation Actual Equation

**Final Equation in Terms of L\_Pseudo Components**

|                               |              |
|-------------------------------|--------------|
| Ultimate compressive strength | =            |
|                               | +443,68 * A  |
|                               | +53,91 * B   |
|                               | +101,17 * C  |
|                               | +93,17 * AB  |
|                               | -142,02 * AC |

# WET.16

Configure Fit Summary Model ANOVA Diagnostics Model Graphs

Analysis of Variance Fit Statistics Model Comparison Statistics Coefficients Coded Equation Real Equation Actual Equation

**ANOVA for Quadratic model**

Response 1: Ultimate compressive strength

| Source             | Sum of Squares | df | Mean Square | F-value | p-value  |             |
|--------------------|----------------|----|-------------|---------|----------|-------------|
| Block              | 1480,63        | 2  | 740,32      |         |          |             |
| Model              | 4,753E+05      | 5  | 95065,32    | 30,78   | < 0.0001 | significant |
| (1) Linear Mixture | 4,201E+05      | 2  | 2,101E+05   | 68,01   | < 0.0001 |             |
| AB                 | 14650,68       | 1  | 14650,68    | 4,74    | 0,0410   |             |
| AC                 | 34553,84       | 1  | 34553,84    | 11,19   | 0,0031   |             |
| BC                 | 8218,78        | 1  | 8218,78     | 2,66    | 0,1178   |             |
| Residual           | 64863,35       | 21 | 3088,73     |         |          |             |
| Cor Total          | 5,417E+05      | 28 |             |         |          |             |

Configure Fit Summary Model ANOVA Diagnostics Model Graphs

Analysis of Variance Fit Statistics Model Comparison Statistics Coefficients Coded Equation Real Equation Actual Equation

**Fit Statistics**

|           |        |                          |         |
|-----------|--------|--------------------------|---------|
| Std. Dev. | 55,58  | R <sup>2</sup>           | 0,8799  |
| Mean      | 156,96 | Adjusted R <sup>2</sup>  | 0,8513  |
| C.V. %    | 35,41  | Predicted R <sup>2</sup> | 0,8036  |
|           |        | Adeq Precision           | 13,0372 |

Configure Fit Summary Model ANOVA Diagnostics Model Graphs

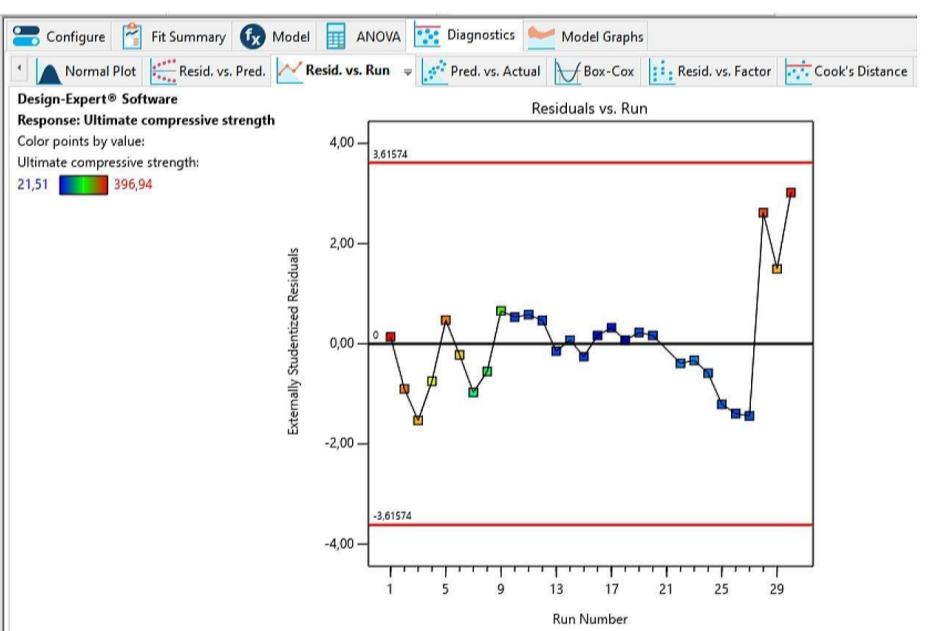
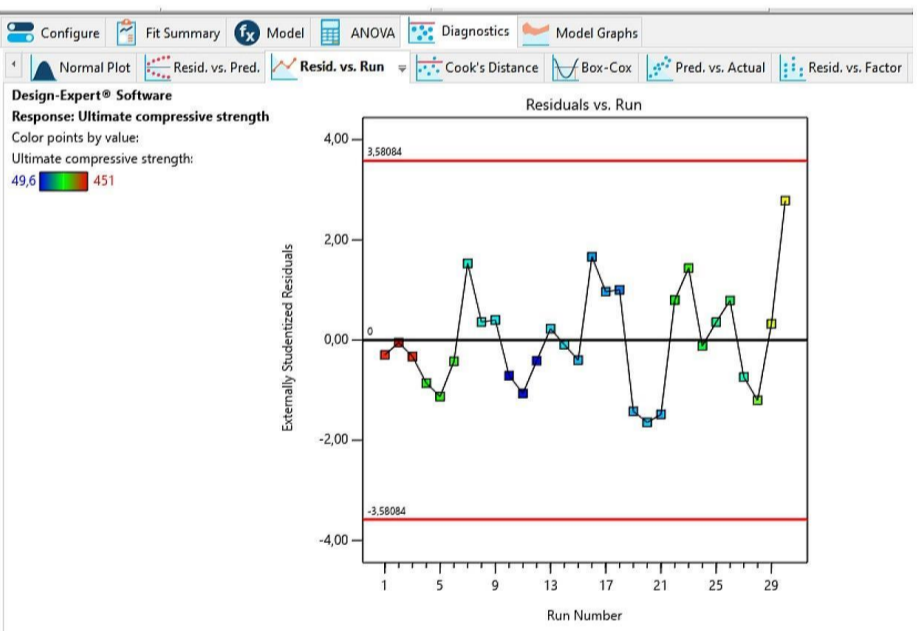
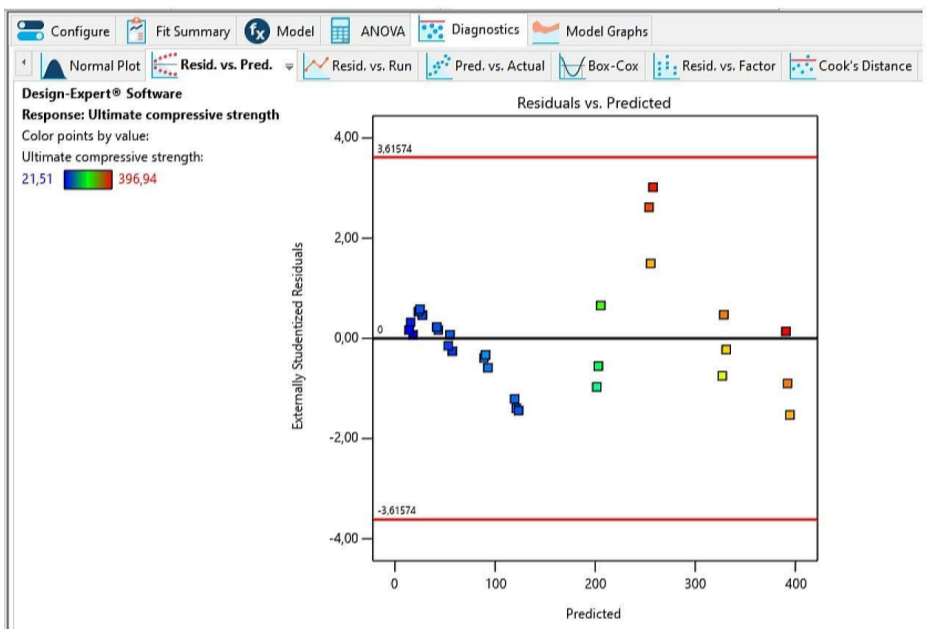
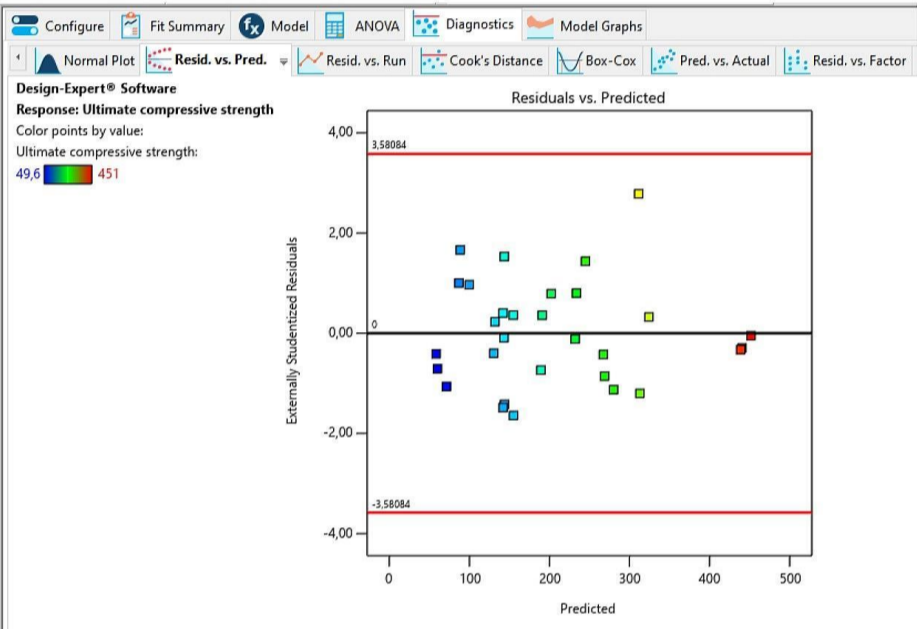
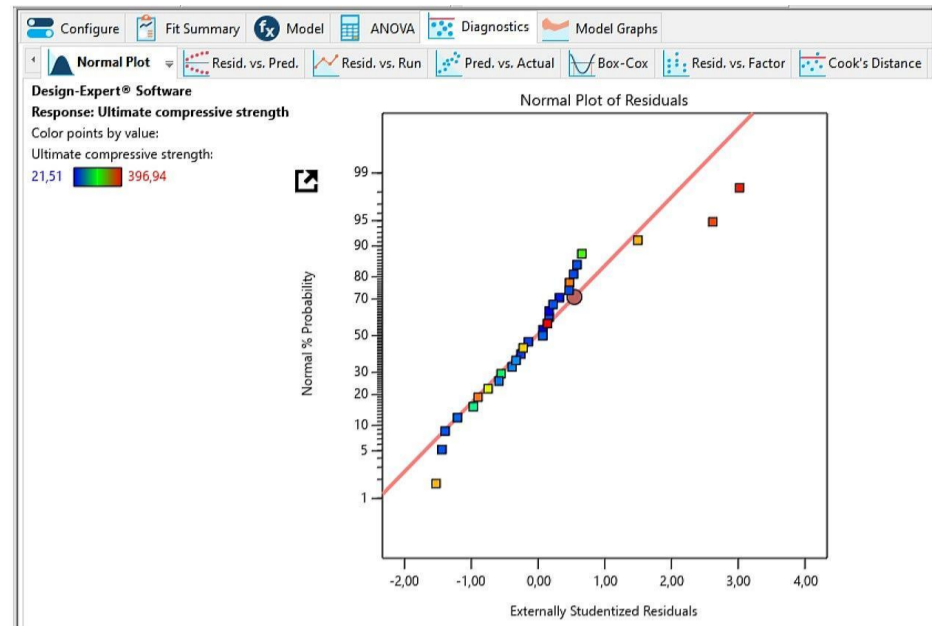
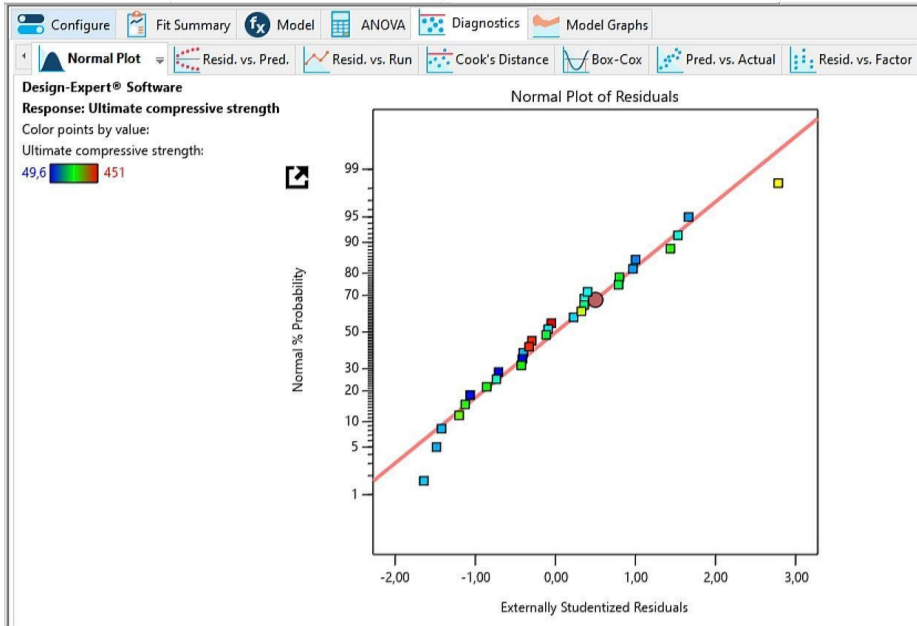
Analysis of Variance Fit Statistics Model Comparison Statistics Coefficients Coded Equation Real Equation Actual Equation

**Final Equation in Terms of L\_Pseudo Components**

|                               |              |
|-------------------------------|--------------|
| Ultimate compressive strength | =            |
|                               | +392,51 * A  |
|                               | +83,50 * B   |
|                               | +68,03 * C   |
|                               | +363,29 * AB |
|                               | -558,17 * AC |
|                               | -344,87 * BC |

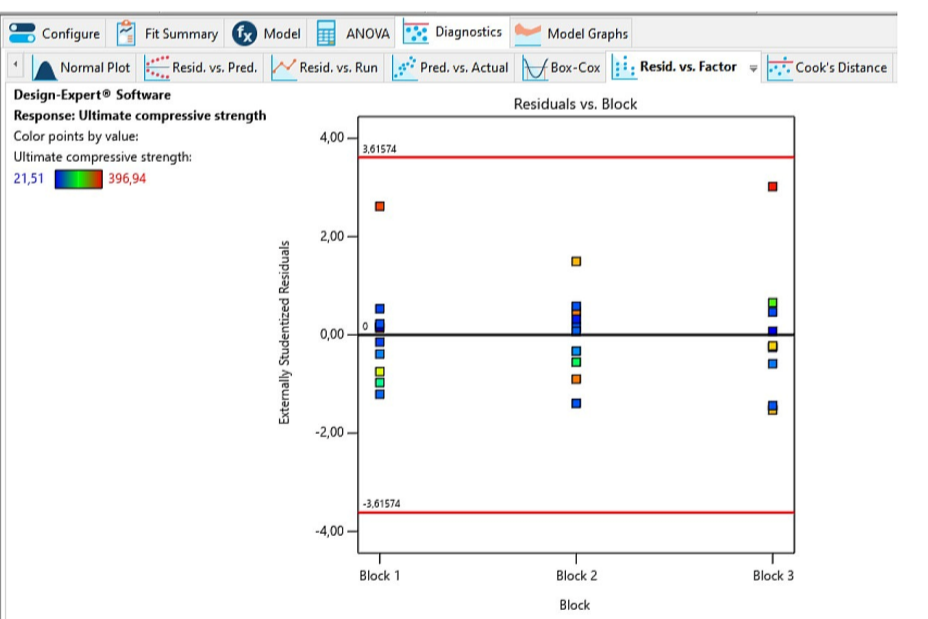
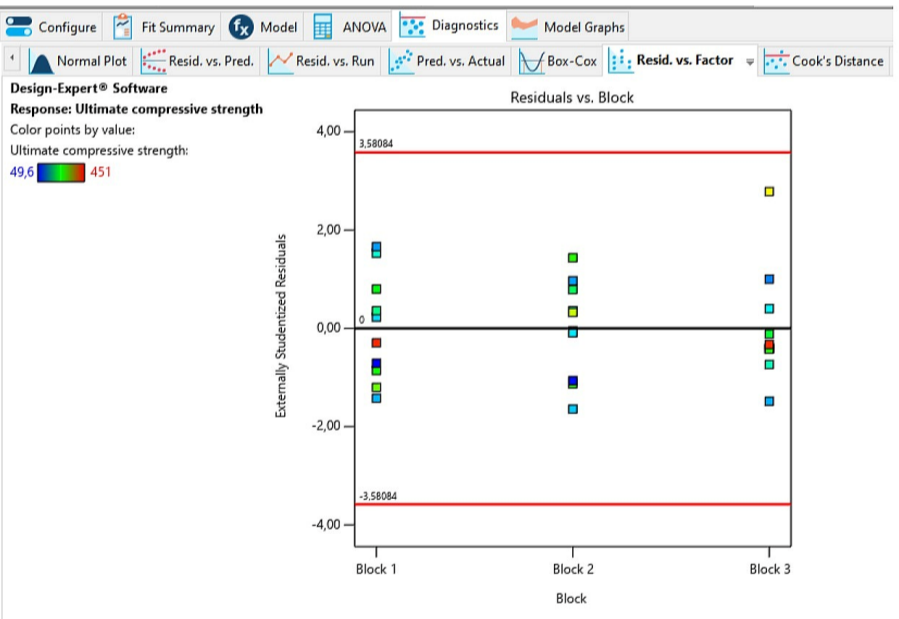
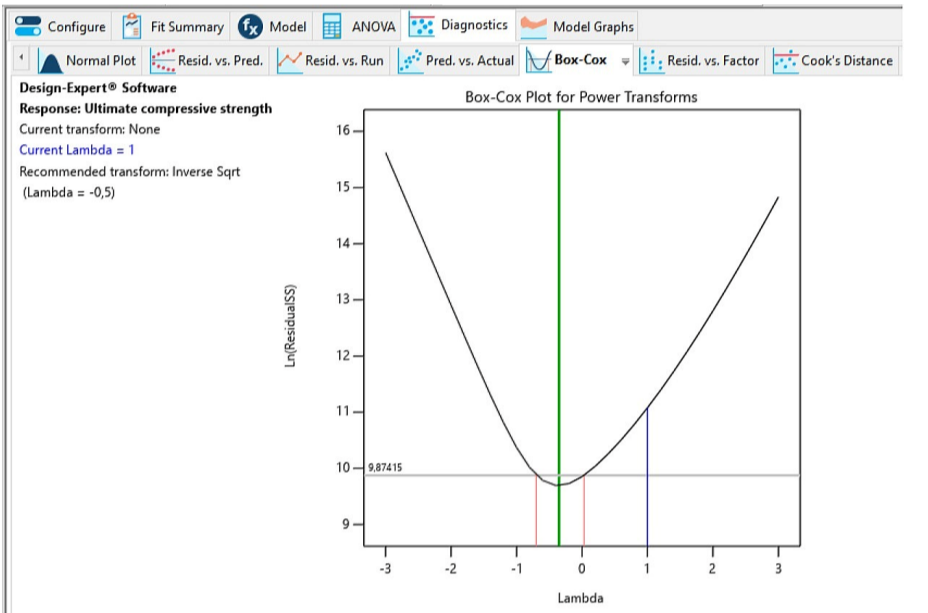
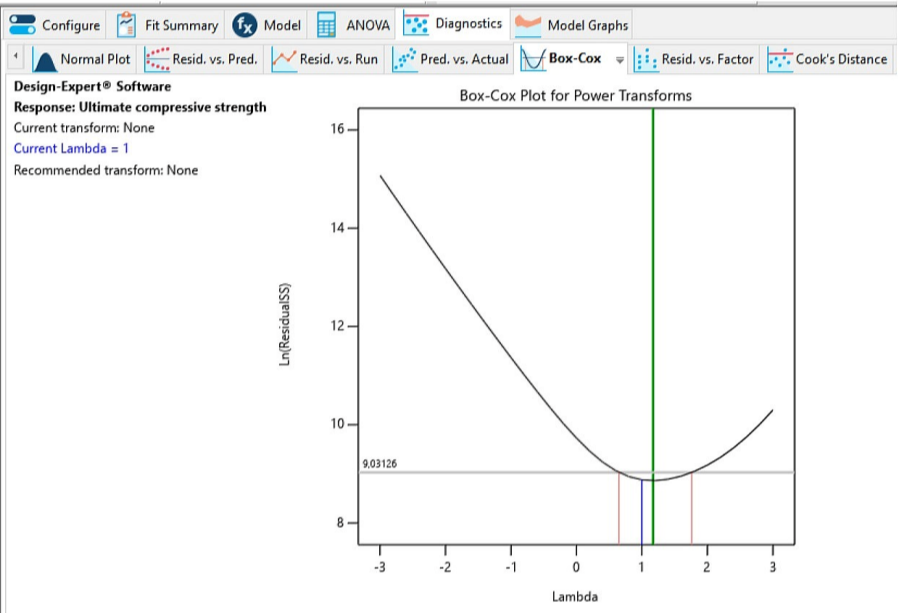
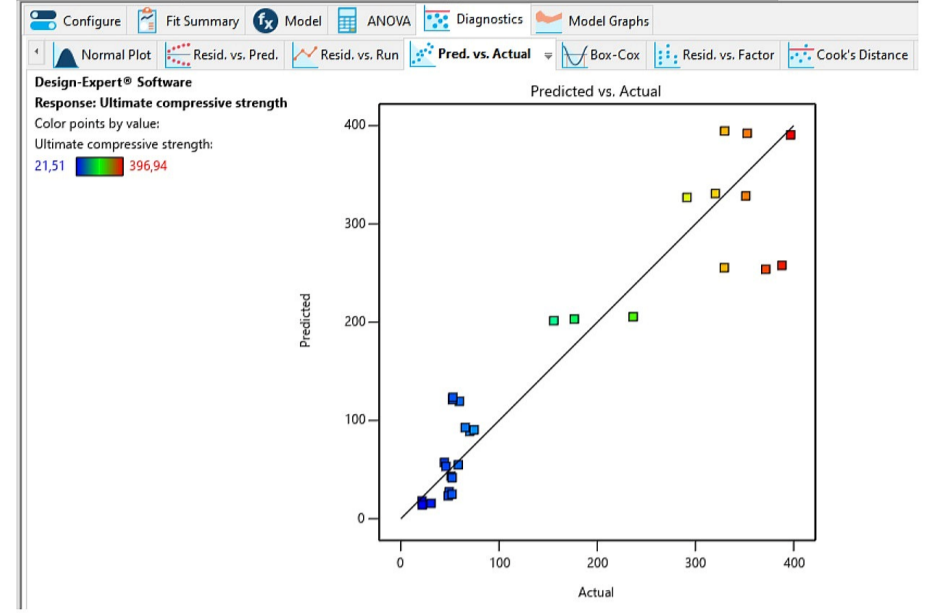
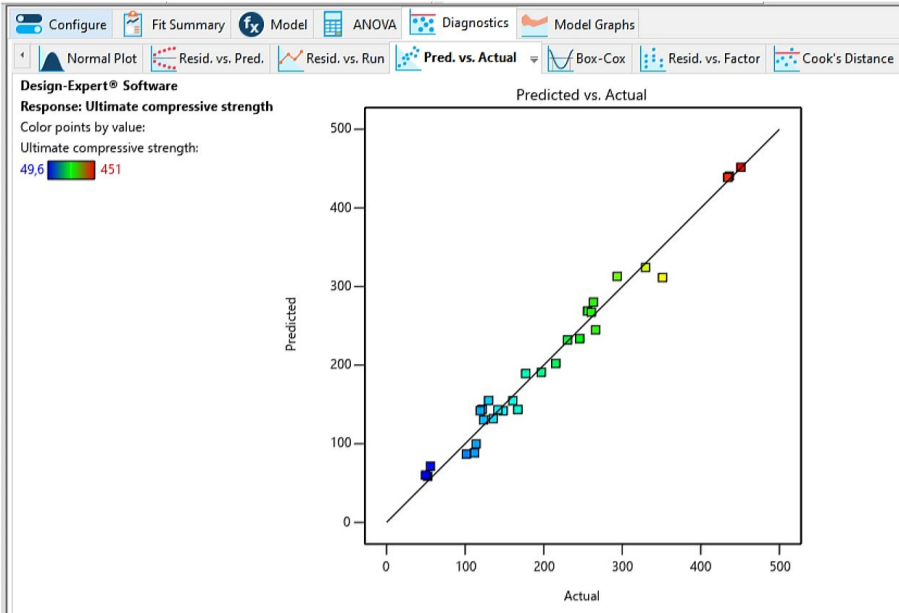
**DRY.16**

**WET.16**



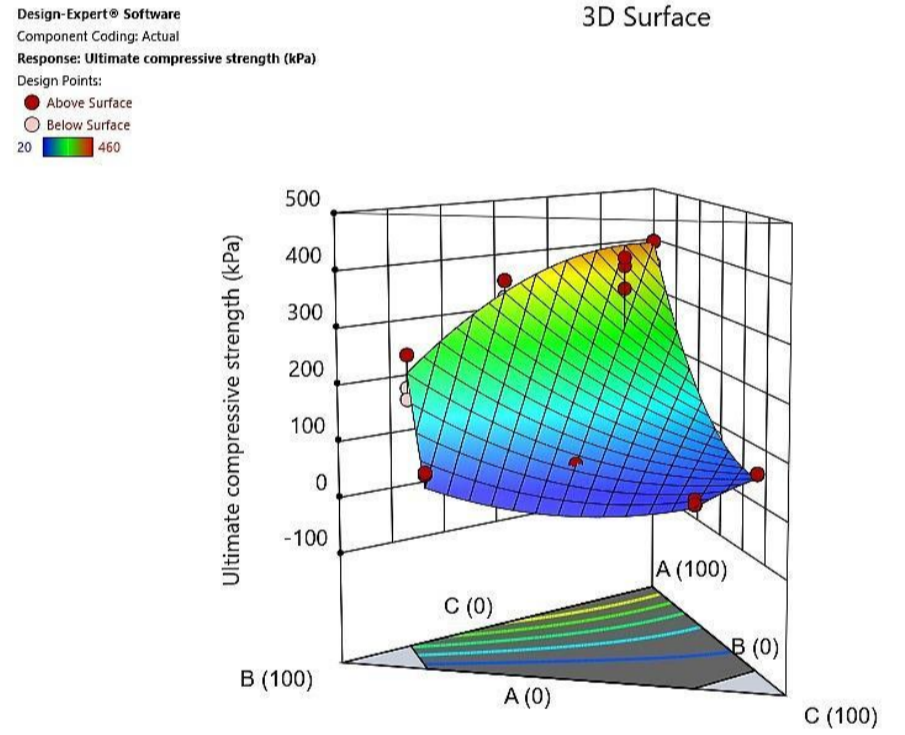
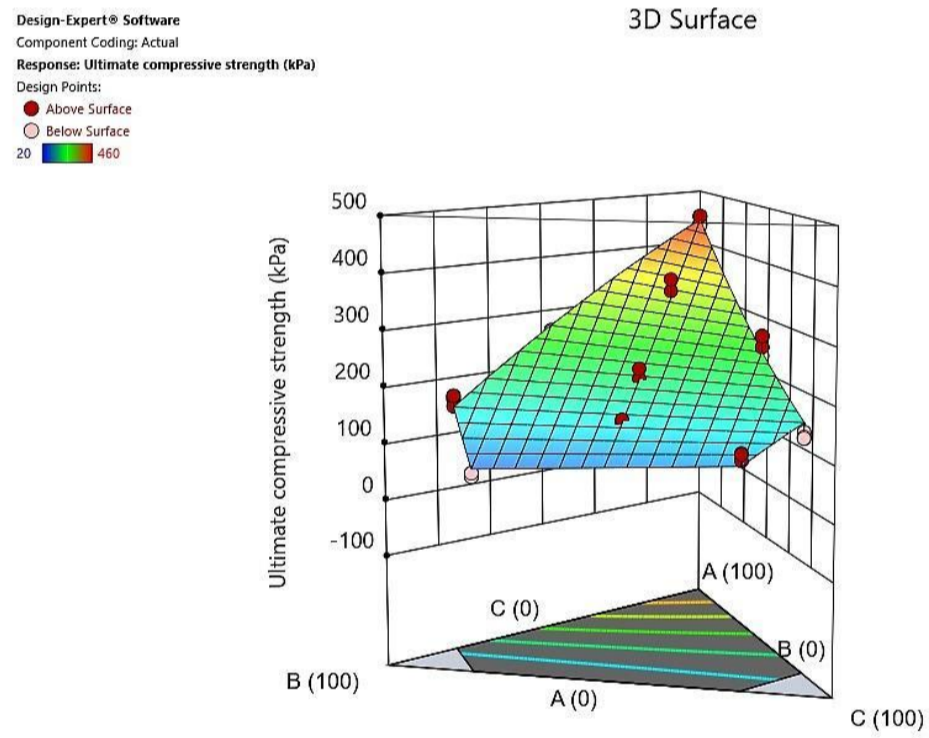
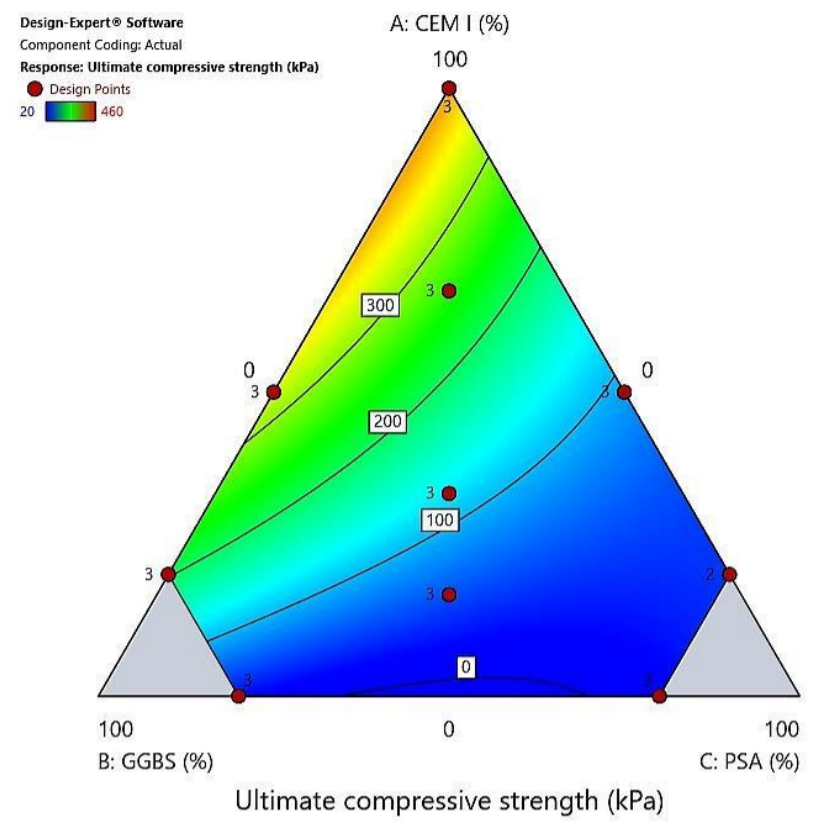
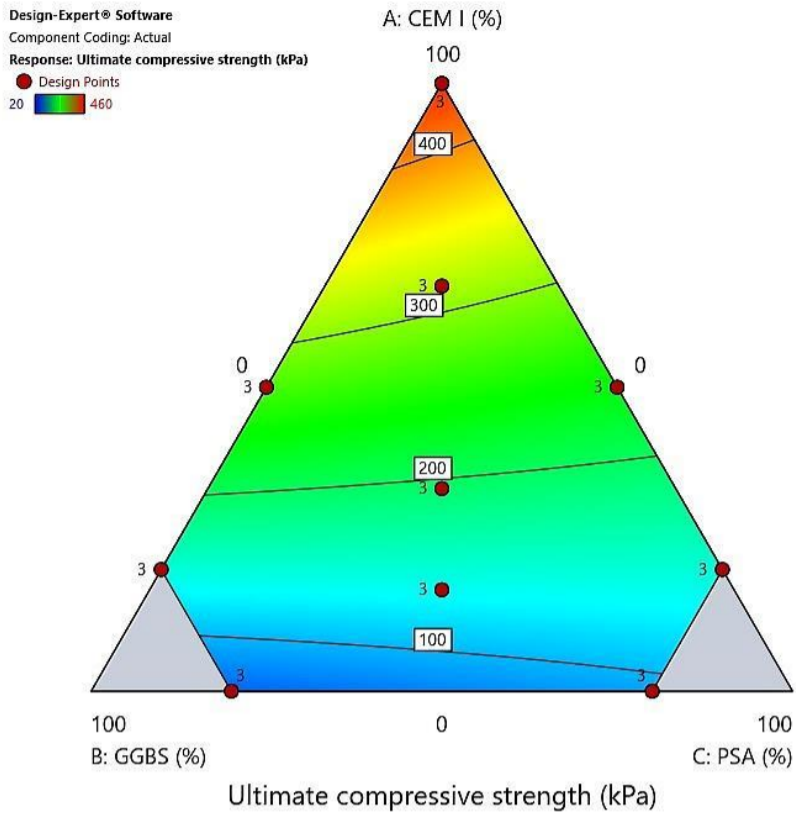
**DRY.16**

**WET.16**



# DRY.16

# WET.16





# R2: Undrained shear strength, $S_u$

## DRY.16

Configure Fit Summary Model ANOVA Diagnostics Model Graphs

Fit Summary Sequential Model Sum of Squares [Type I] Model Summary Statistics

**Fit Summary**  
Response 2: Undrained shear strength  
Mixture Component Coding is L\_Pseudo.

| Source        | Sequential p-value | Lack of Fit p-value | Adjusted R <sup>2</sup> | Predicted R <sup>2</sup> |                  |
|---------------|--------------------|---------------------|-------------------------|--------------------------|------------------|
| Linear        | < 0,0001           |                     | 0,9692                  | 0,9577                   |                  |
| Quadratic     | <b>0,0296</b>      |                     | <b>0,9766</b>           | <b>0,9656</b>            | <b>Suggested</b> |
| Special Cubic | 0,7500             |                     | 0,9756                  | 0,9627                   |                  |
| Cubic         | 0,0002             |                     | 0,9891                  | 0,9817                   | <b>Aliased</b>   |

Configure Fit Summary Model ANOVA Diagnostics Model Graphs

Mixture Order: Modified Auto Select...

Model Type: Scheffe Add Term

|  |                      |  |
|--|----------------------|--|
|  | A-CEM I              |  |
|  | B-GGBS               |  |
|  | C-PSA                |  |
|  | AB                   | The term will be included in the model.  |
|  | AC                   | The term will be included in the model.  |
|  | BC                   |  |
|  | ABC                  |  |
|  | AB(A-B)              |  |
|  | AC(A-C)              |  |
|  | BC(B-C)              | Indicates the term is aliased with another term, or was not estimated in the Fit Summary calculations. Including the term in the model is not recommended. |
|  | A <sup>2</sup> BC    |  |
|  | AB <sup>2</sup> C    |  |
|  | ABC <sup>2</sup>     | A user-forced term. Automatic model selection will always produce a model that includes this term.   |
|  | AB(A-B) <sup>2</sup> | Indicates that the term is required to be in the model by the program.   |
|  | AC(A-C) <sup>2</sup> |  |
|  | BC(B-C) <sup>2</sup> |  |

## WET.16

Configure Fit Summary Model ANOVA Diagnostics Model Graphs

Fit Summary Sequential Model Sum of Squares [Type I] Model Summary Statistics

**Fit Summary**  
Response 2: Undrained shear strength  
Mixture Component Coding is L\_Pseudo.

| Source        | Sequential p-value | Lack of Fit p-value | Adjusted R <sup>2</sup> | Predicted R <sup>2</sup> |                  |
|---------------|--------------------|---------------------|-------------------------|--------------------------|------------------|
| Linear        | < 0,0001           |                     | 0,7593                  | 0,6875                   |                  |
| Quadratic     | <b>0,0042</b>      |                     | <b>0,8513</b>           | <b>0,8036</b>            | <b>Suggested</b> |
| Special Cubic | 0,3743             |                     | 0,8501                  | 0,7962                   |                  |
| Cubic         | 0,0012             |                     | 0,9210                  | 0,8740                   | <b>Aliased</b>   |

Configure Fit Summary Model ANOVA Diagnostics Model Graphs

Mixture Order: Quadratic Auto Select...

Model Type: Scheffe Add Term

|  |                      |  |
|--|----------------------|--|
|  | A-CEM I              |  |
|  | B-GGBS               |  |
|  | C-PSA                |  |
|  | AB                   | The term will be included in the model.  |
|  | AC                   | The term will be included in the model.  |
|  | BC                   | The term will be included in the model.  |
|  | ABC                  |  |
|  | AB(A-B)              |  |
|  | AC(A-C)              |  |
|  | BC(B-C)              | Indicates the term is aliased with another term, or was not estimated in the Fit Summary calculations. Including the term in the model is not recommended. |
|  | A <sup>2</sup> BC    |  |
|  | AB <sup>2</sup> C    |  |
|  | ABC <sup>2</sup>     | A user-forced term. Automatic model selection will always produce a model that includes this term.   |
|  | AB(A-B) <sup>2</sup> | Indicates that the term is required to be in the model by the program.   |
|  | AC(A-C) <sup>2</sup> |  |
|  | BC(B-C) <sup>2</sup> |  |

# DRY.16

Configure Fit Summary Model ANOVA Diagnostics Model Graphs

Analysis of Variance Fit Statistics Model Comparison Statistics Coefficients Coded Equation Real Equation Actual Equation

**ANOVA for Reduced Quadratic model**  
Response 2: Undrained shear strength

| Source                        | Sum of Squares | df | Mean Square | F-value | p-value  |             |
|-------------------------------|----------------|----|-------------|---------|----------|-------------|
| Block                         | 245,14         | 2  | 122,57      |         |          |             |
| Model                         | 89628,94       | 4  | 22407,24    | 286,80  | < 0.0001 | significant |
| <sup>(1)</sup> Linear Mixture | 88821,73       | 2  | 44410,87    | 568,44  | < 0.0001 |             |
| AB                            | 268,59         | 1  | 268,59      | 3,44    | 0,0766   |             |
| AC                            | 623,66         | 1  | 623,66      | 7,98    | 0,0096   |             |
| Residual                      | 1796,95        | 23 | 78,13       |         |          |             |
| Cor Total                     | 91671,03       | 29 |             |         |          |             |

Configure Fit Summary Model ANOVA Diagnostics Model Graphs

Analysis of Variance Fit Statistics Model Comparison Statistics Coefficients Coded Equation Real Equation Actual Equation

**Fit Statistics**

|           |        |                          |         |
|-----------|--------|--------------------------|---------|
| Std. Dev. | 8,84   | R <sup>2</sup>           | 0,9803  |
| Mean      | 102,35 | Adjusted R <sup>2</sup>  | 0,9769  |
| C.V. %    | 8,64   | Predicted R <sup>2</sup> | 0,9675  |
|           |        | Adeq Precision           | 46,0415 |

Configure Fit Summary Model ANOVA Diagnostics Model Graphs

Analysis of Variance Fit Statistics Model Comparison Statistics Coefficients Coded Equation Real Equation Actual Equation

**Final Equation in Terms of L\_Pseudo Components**

|                          |             |
|--------------------------|-------------|
| Undrained shear strength | =           |
|                          | +221,84 * A |
|                          | +26,95 * B  |
|                          | +50,58 * C  |
|                          | +46,60 * AB |
|                          | -71,01 * AC |

# WET.16

Configure Fit Summary Model ANOVA Diagnostics Model Graphs

Analysis of Variance Fit Statistics Model Comparison Statistics Coefficients Coded Equation Real Equation Actual Equation

**ANOVA for Quadratic model**  
Response 2: Undrained shear strength

| Source                        | Sum of Squares | df | Mean Square | F-value | p-value  |             |
|-------------------------------|----------------|----|-------------|---------|----------|-------------|
| Block                         | 370,12         | 2  | 185,06      |         |          |             |
| Model                         | 1,188E+05      | 5  | 23767,03    | 30,78   | < 0.0001 | significant |
| <sup>(1)</sup> Linear Mixture | 1,050E+05      | 2  | 52520,33    | 68,02   | < 0.0001 |             |
| AB                            | 3663,06        | 1  | 3663,06     | 4,74    | 0,0409   |             |
| AC                            | 8638,00        | 1  | 8638,00     | 11,19   | 0,0031   |             |
| BC                            | 2054,68        | 1  | 2054,68     | 2,66    | 0,1177   |             |
| Residual                      | 16215,59       | 21 | 772,17      |         |          |             |
| Cor Total                     | 1,354E+05      | 28 |             |         |          |             |

Configure Fit Summary Model ANOVA Diagnostics Model Graphs

Analysis of Variance Fit Statistics Model Comparison Statistics Coefficients Coded Equation Real Equation Actual Equation

**Fit Statistics**

|           |       |                          |         |
|-----------|-------|--------------------------|---------|
| Std. Dev. | 27,79 | R <sup>2</sup>           | 0,8799  |
| Mean      | 78,48 | Adjusted R <sup>2</sup>  | 0,8513  |
| C.V. %    | 35,41 | Predicted R <sup>2</sup> | 0,8036  |
|           |       | Adeq Precision           | 13,0374 |

Configure Fit Summary Model ANOVA Diagnostics Model Graphs

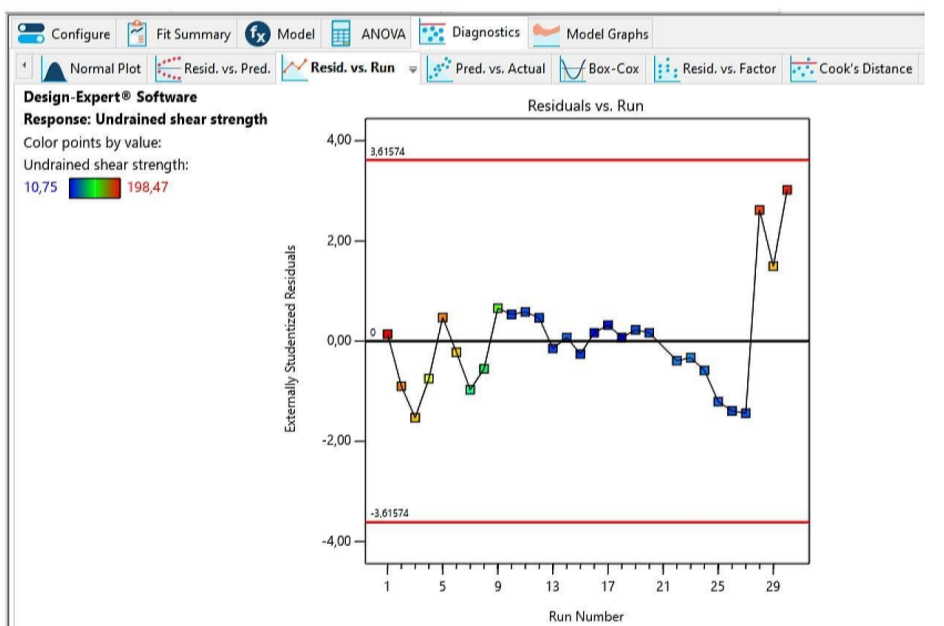
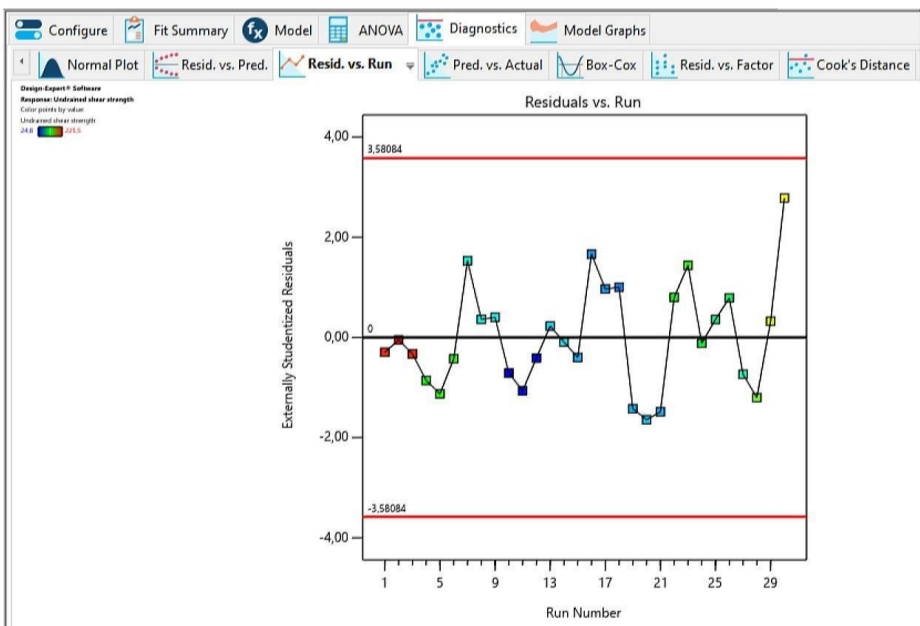
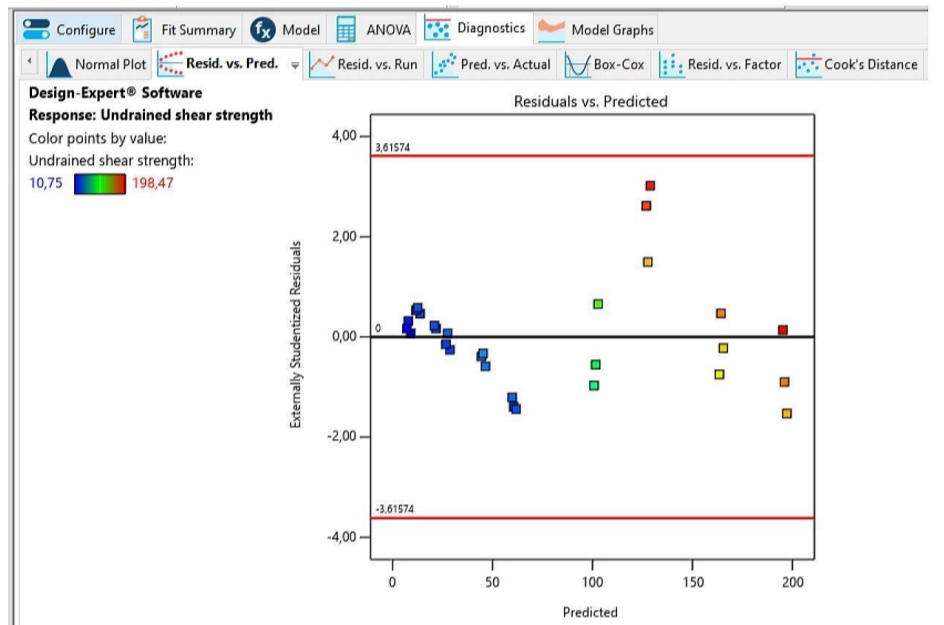
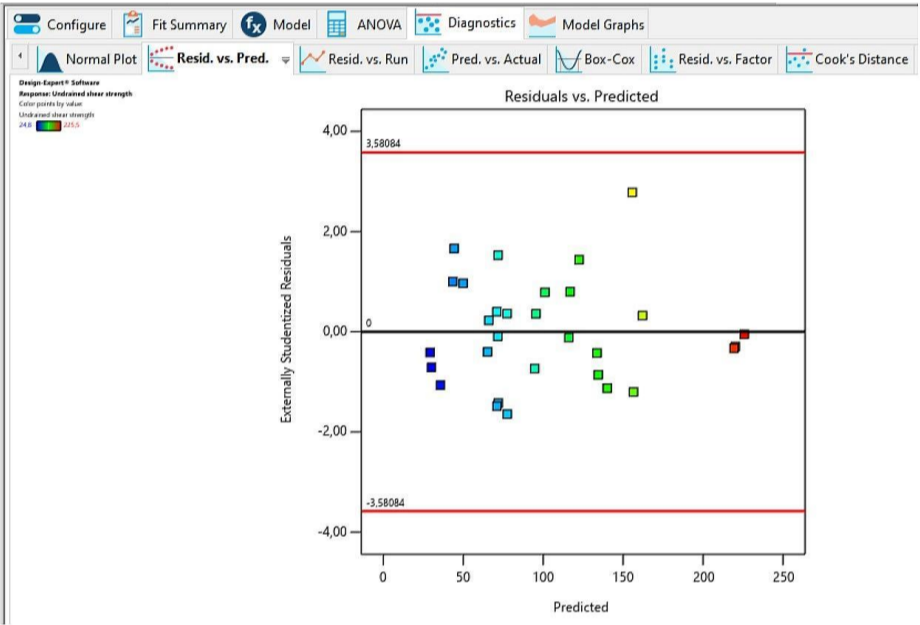
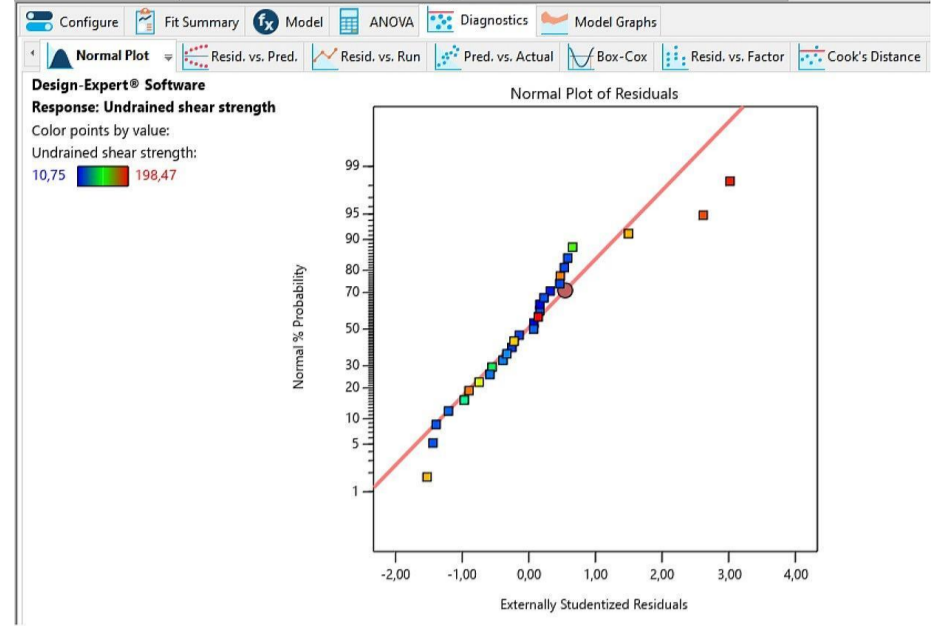
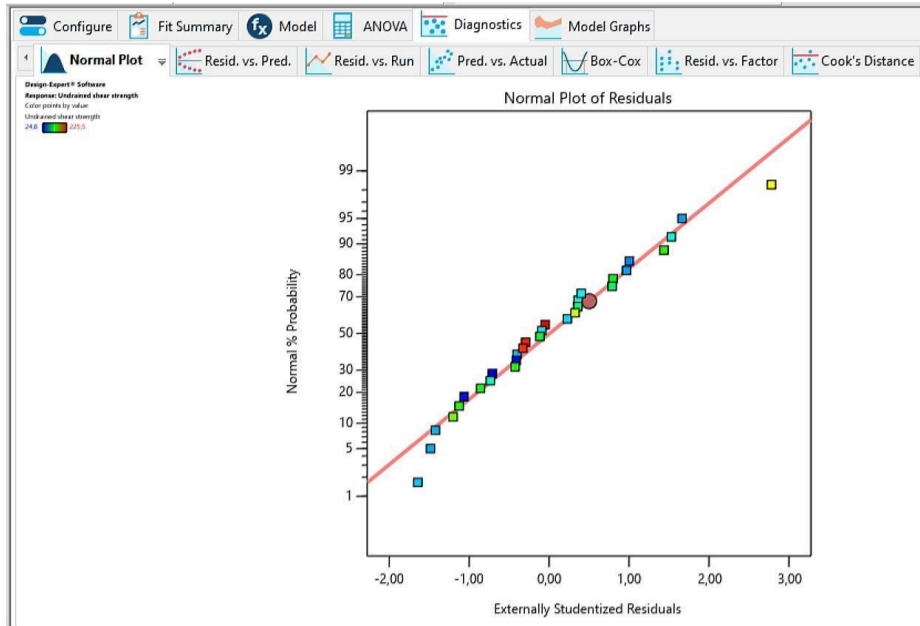
Analysis of Variance Fit Statistics Model Comparison Statistics Coefficients Coded Equation Real Equation Actual Equation

**Final Equation in Terms of L\_Pseudo Components**

|                          |              |
|--------------------------|--------------|
| Undrained shear strength | =            |
|                          | +196,25 * A  |
|                          | +41,75 * B   |
|                          | +34,01 * C   |
|                          | +181,65 * AB |
|                          | -279,08 * AC |
|                          | -172,44 * BC |

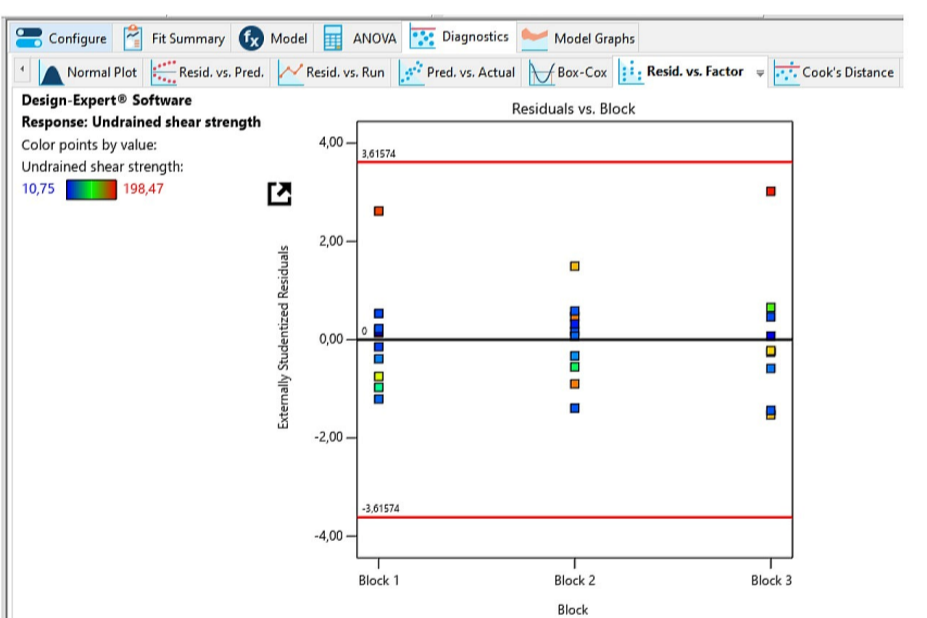
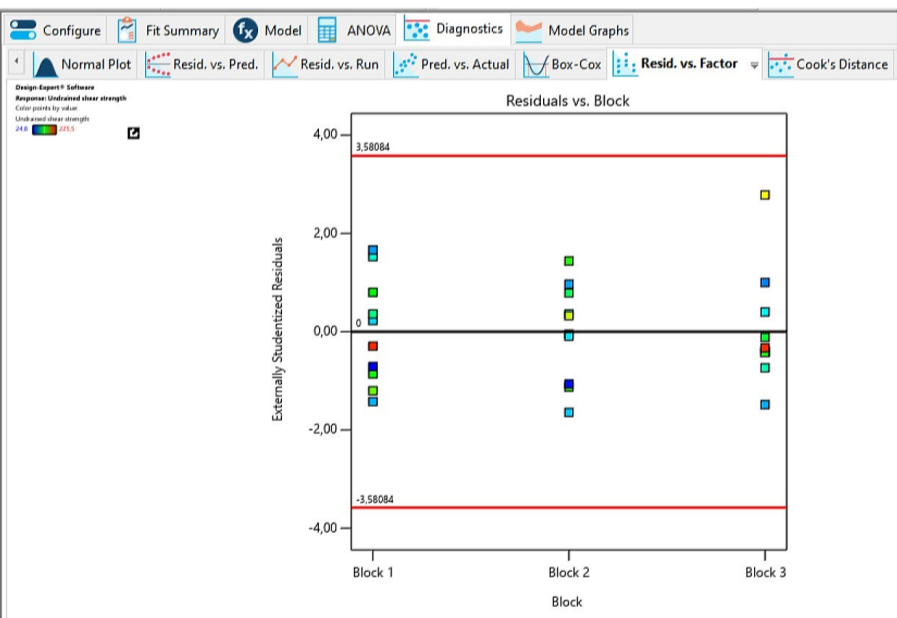
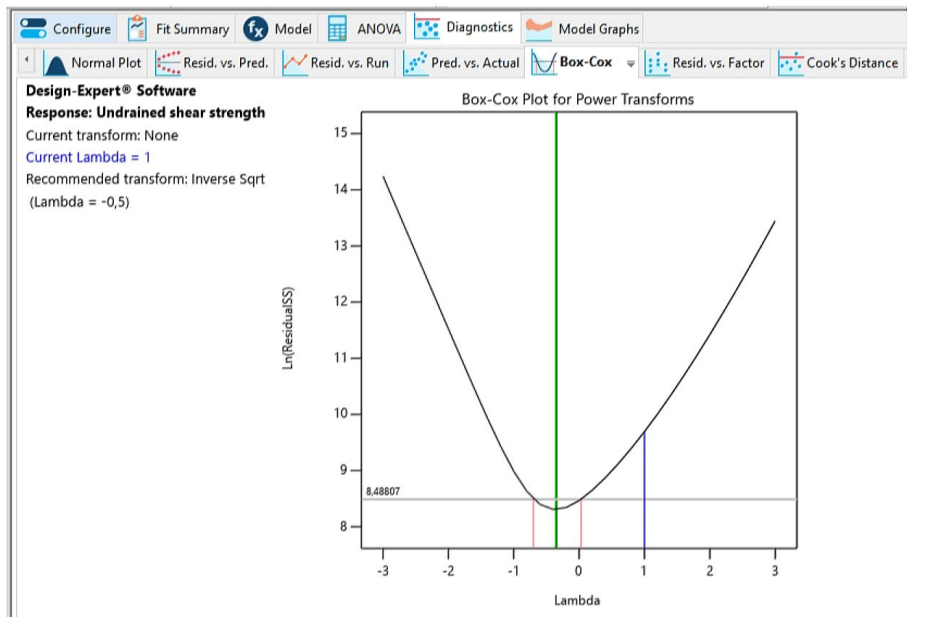
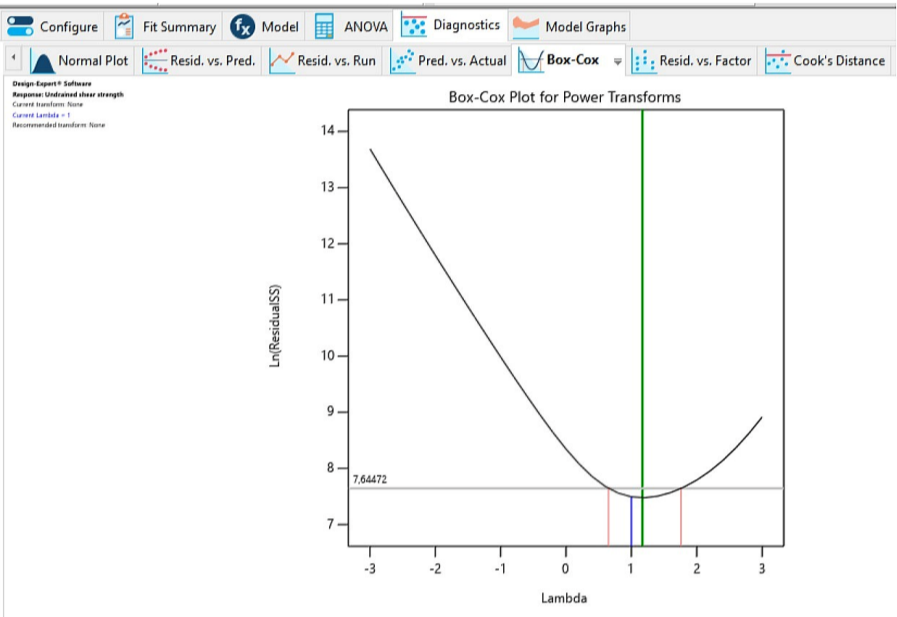
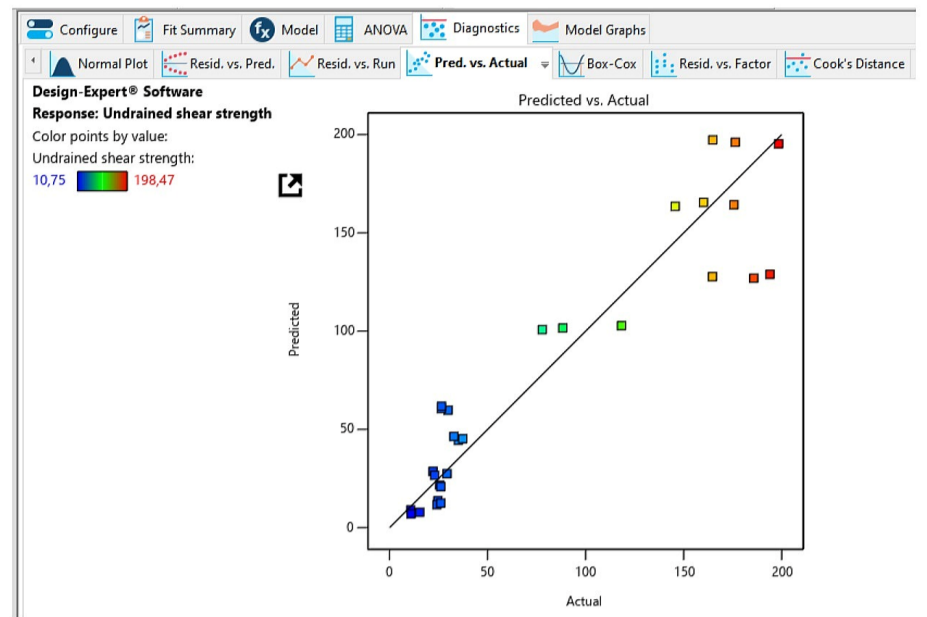
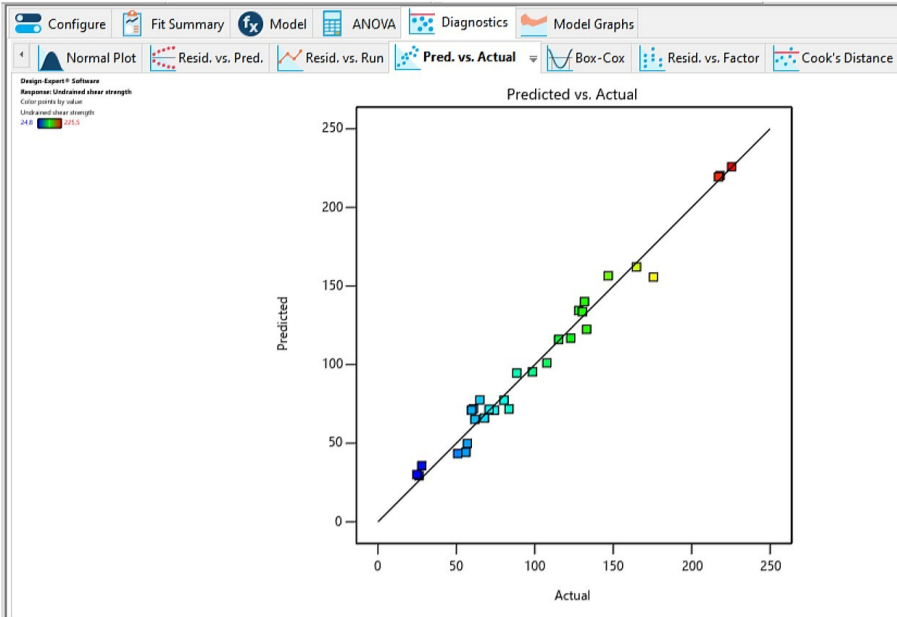
**DRY.16**

**WET.16**



**DRY.16**

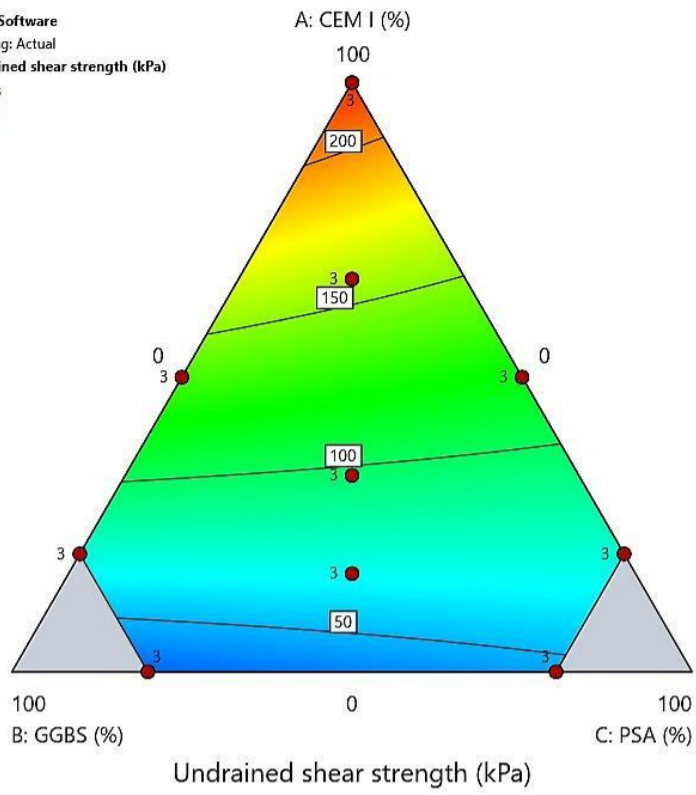
**WET.16**



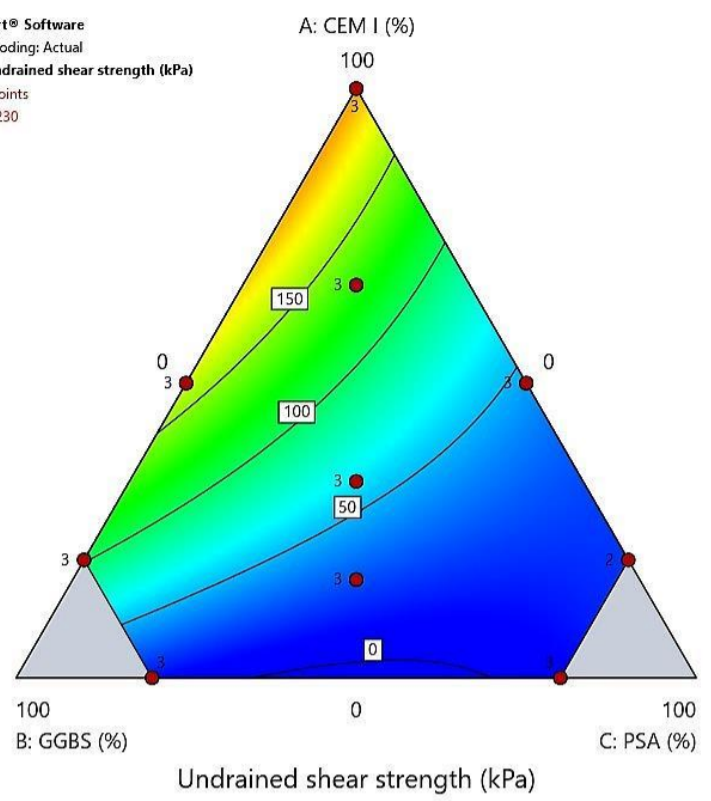
# DRY.16

# WET.16

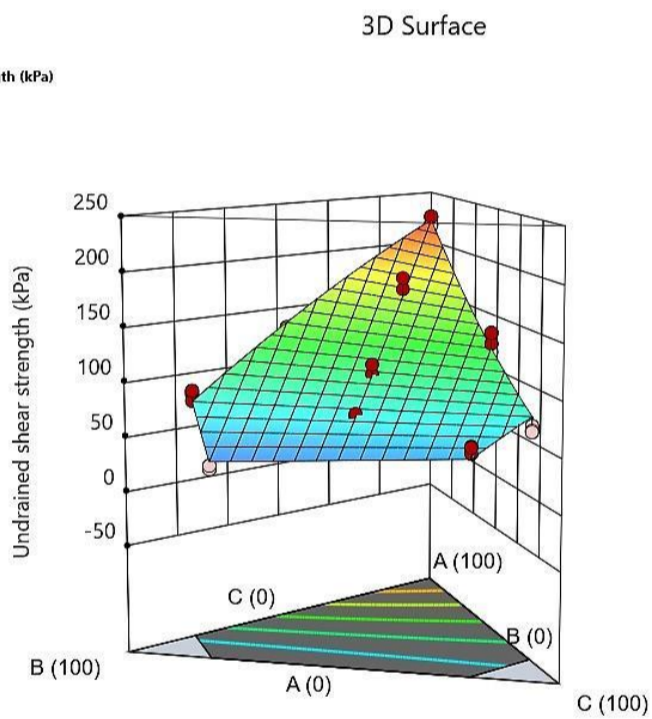
Design-Expert® Software  
Component Coding: Actual  
Response: Undrained shear strength (kPa)  
Design Points  
10 230



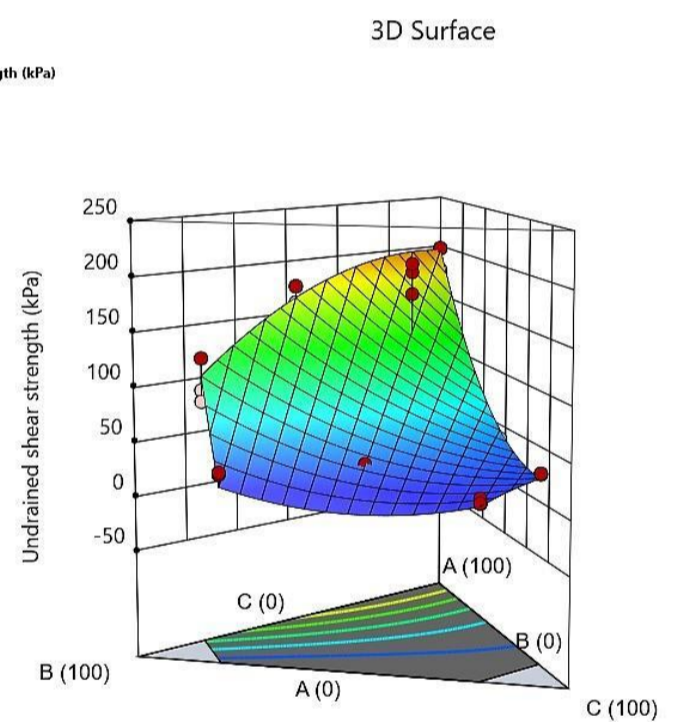
Design-Expert® Software  
Component Coding: Actual  
Response: Undrained shear strength (kPa)  
Design Points  
10 230



Design-Expert® Software  
Component Coding: Actual  
Response: Undrained shear strength (kPa)  
Design Points:  
● Above Surface  
○ Below Surface  
10 230

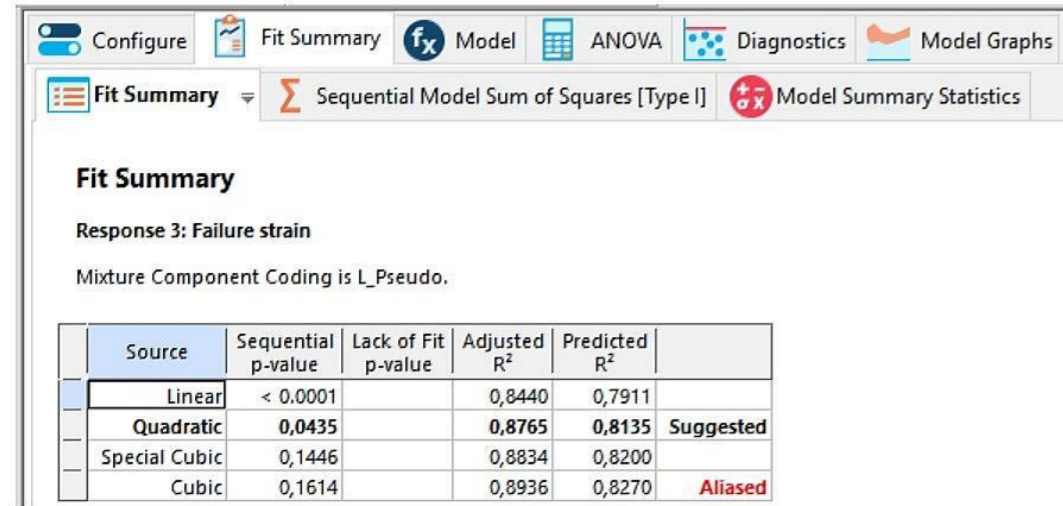


Design-Expert® Software  
Component Coding: Actual  
Response: Undrained shear strength (kPa)  
Design Points:  
● Above Surface  
○ Below Surface  
10 230



# R3: Failure strain, $\epsilon_v$

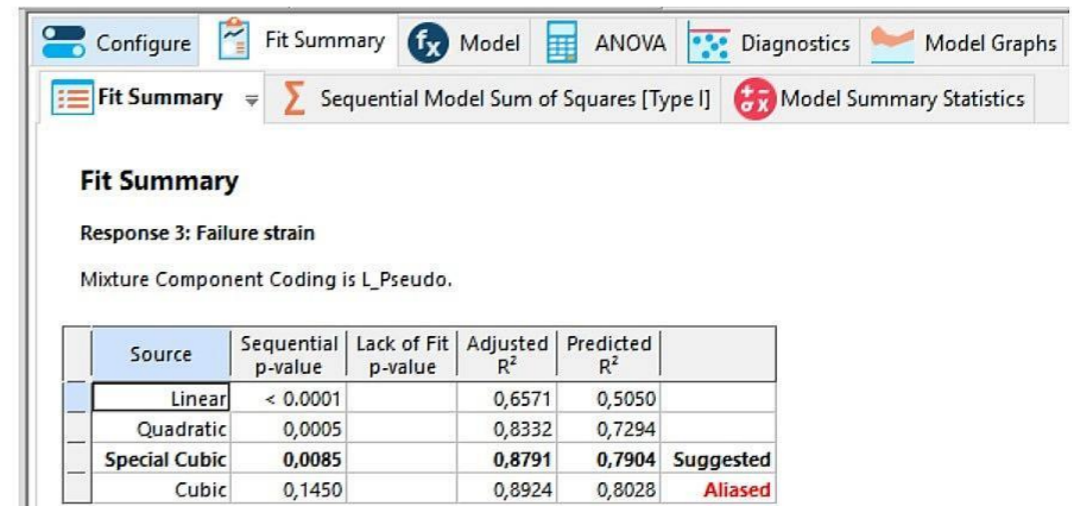
## DRY.16



**Fit Summary**  
Response 3: Failure strain  
Mixture Component Coding is L\_Pseudo.

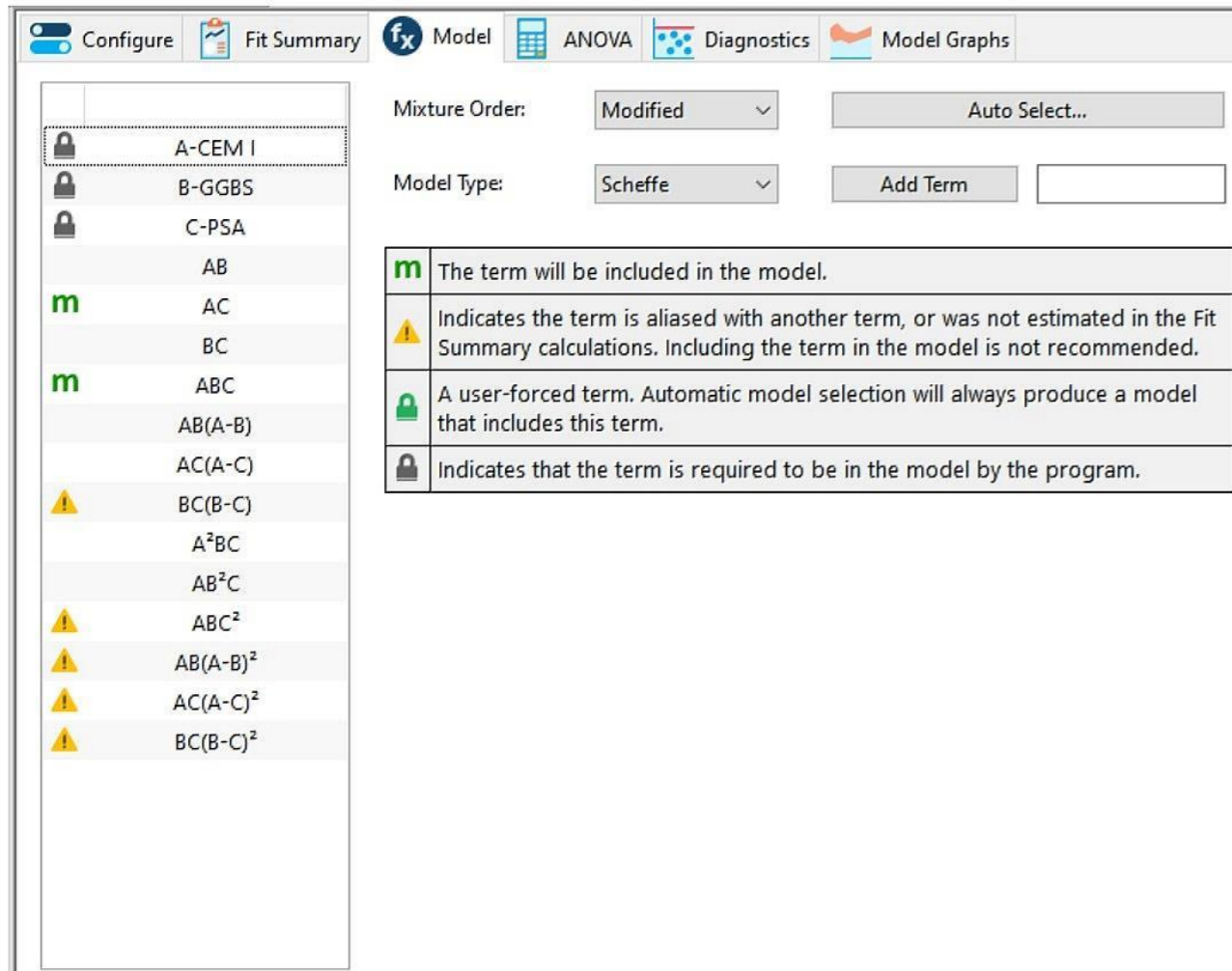
| Source        | Sequential p-value | Lack of Fit p-value | Adjusted R <sup>2</sup> | Predicted R <sup>2</sup> |                  |
|---------------|--------------------|---------------------|-------------------------|--------------------------|------------------|
| Linear        | < 0.0001           |                     | 0,8440                  | 0,7911                   |                  |
| Quadratic     | <b>0,0435</b>      |                     | <b>0,8765</b>           | <b>0,8135</b>            | <b>Suggested</b> |
| Special Cubic | 0,1446             |                     | 0,8834                  | 0,8200                   |                  |
| Cubic         | 0,1614             |                     | 0,8936                  | 0,8270                   | <b>Aliased</b>   |

## WET.16



**Fit Summary**  
Response 3: Failure strain  
Mixture Component Coding is L\_Pseudo.

| Source        | Sequential p-value | Lack of Fit p-value | Adjusted R <sup>2</sup> | Predicted R <sup>2</sup> |                  |
|---------------|--------------------|---------------------|-------------------------|--------------------------|------------------|
| Linear        | < 0.0001           |                     | 0,6571                  | 0,5050                   |                  |
| Quadratic     | 0,0005             |                     | 0,8332                  | 0,7294                   |                  |
| Special Cubic | <b>0,0085</b>      |                     | <b>0,8791</b>           | <b>0,7904</b>            | <b>Suggested</b> |
| Cubic         | 0,1450             |                     | 0,8924                  | 0,8028                   | <b>Aliased</b>   |

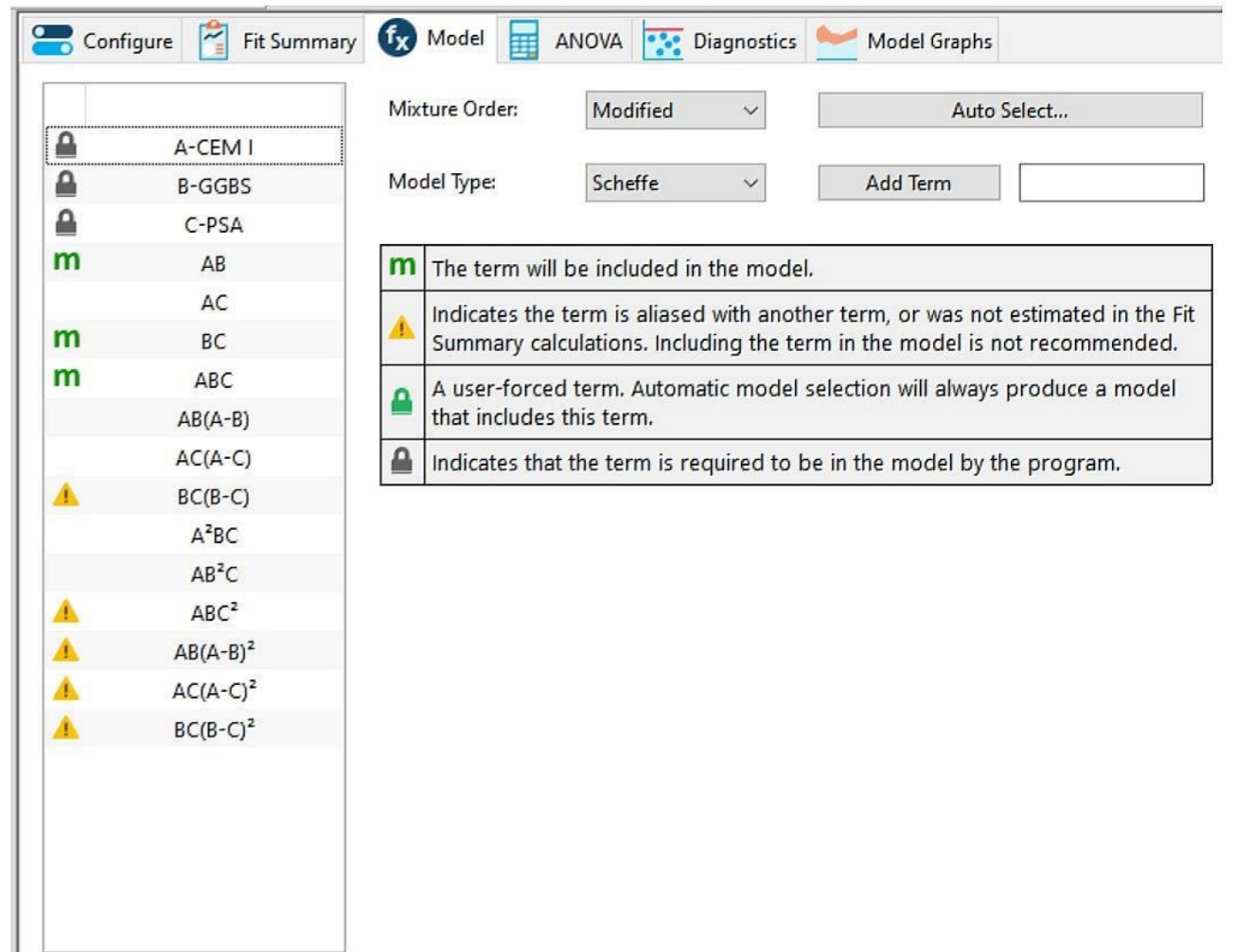


Mixture Order: Modified

Model Type: Scheffe

|  |  |
|--|--|
|  | The term will be included in the model.  |
|  | Indicates the term is aliased with another term, or was not estimated in the Fit Summary calculations. Including the term in the model is not recommended. |
|  | A user-forced term. Automatic model selection will always produce a model that includes this term.   |
|  | Indicates that the term is required to be in the model by the program.   |

- A-CEM I
- B-GGBS
- C-PSA
- AB
- AC
- BC
- ABC
- AB(A-B)
- AC(A-C)
- BC(B-C)
- A<sup>2</sup>BC
- AB<sup>2</sup>C
- ABC<sup>2</sup>
- AB(A-B)<sup>2</sup>
- AC(A-C)<sup>2</sup>
- BC(B-C)<sup>2</sup>



Mixture Order: Modified

Model Type: Scheffe

|  |  |
|--|--|
|  | The term will be included in the model.  |
|  | Indicates the term is aliased with another term, or was not estimated in the Fit Summary calculations. Including the term in the model is not recommended. |
|  | A user-forced term. Automatic model selection will always produce a model that includes this term.   |
|  | Indicates that the term is required to be in the model by the program.   |

- A-CEM I
- B-GGBS
- C-PSA
- AB
- AC
- BC
- ABC
- AB(A-B)
- AC(A-C)
- BC(B-C)
- A<sup>2</sup>BC
- AB<sup>2</sup>C
- ABC<sup>2</sup>
- AB(A-B)<sup>2</sup>
- AC(A-C)<sup>2</sup>
- BC(B-C)<sup>2</sup>

# DRY.16

Configure | Fit Summary | Model | ANOVA | Diagnostics | Model Graphs

Analysis of Variance | Fit Statistics | Model Comparison Statistics | Coefficients | Coded Equation | Actual Equation

### ANOVA for Reduced Special Cubic model

Response 3: Failure strain

| Source                        | Sum of Squares | df | Mean Square | F-value | p-value  |             |
|-------------------------------|----------------|----|-------------|---------|----------|-------------|
| Block                         | 0,5547         | 2  | 0,2773      |         |          |             |
| Model                         | 46,12          | 4  | 11,53       | 57,04   | < 0.0001 | significant |
| <sup>(1)</sup> Linear Mixture | 43,44          | 2  | 21,72       | 107,44  | < 0.0001 |             |
| AC                            | 0,5862         | 1  | 0,5862      | 2,90    | 0,1021   |             |
| ABC                           | 1,44           | 1  | 1,44        | 7,12    | 0,0137   |             |
| Residual                      | 4,65           | 23 | 0,2022      |         |          |             |
| Cor Total                     | 51,33          | 29 |             |         |          |             |

Configure | Fit Summary | Model | ANOVA | Diagnostics | Model Graphs

Analysis of Variance | Fit Statistics | Model Comparison Statistics | Coefficients | Coded Equation | Actual Equation

### Fit Statistics

|           |        |                          |         |
|-----------|--------|--------------------------|---------|
| Std. Dev. | 0,4496 | R <sup>2</sup>           | 0,9084  |
| Mean      | 3,49   | Adjusted R <sup>2</sup>  | 0,8925  |
| C.V. %    | 12,88  | Predicted R <sup>2</sup> | 0,8396  |
|           |        | Adeq Precision           | 18,4469 |

Configure | Fit Summary | Model | ANOVA | Diagnostics | Model Graphs

Analysis of Variance | Fit Statistics | Model Comparison Statistics | Coefficients | Coded Equation | Actual Equation

### Final Equation in Terms of L\_Pseudo Components

|                |       |
|----------------|-------|
| Failure strain | =     |
| +2,24          | * A   |
| +2,52          | * B   |
| +6,78          | * C   |
| -2,24          | * AC  |
| -16,73         | * ABC |

# WET.16

Configure | Fit Summary | Model | ANOVA | Diagnostics | Model Graphs

Analysis of Variance | Fit Statistics | Model Comparison Statistics | Coefficients | Coded Equation | Actual Equation

### ANOVA for Reduced Special Cubic model

Response 3: Failure strain

| Source                        | Sum of Squares | df | Mean Square | F-value | p-value  |             |
|-------------------------------|----------------|----|-------------|---------|----------|-------------|
| Block                         | 0,1513         | 2  | 0,0756      |         |          |             |
| Model                         | 17,45          | 5  | 3,49        | 34,86   | < 0.0001 | significant |
| <sup>(1)</sup> Linear Mixture | 13,32          | 2  | 6,66        | 66,50   | < 0.0001 |             |
| AB                            | 0,0023         | 1  | 0,0023      | 0,0226  | 0,8819   |             |
| BC                            | 2,60           | 1  | 2,60        | 25,94   | < 0.0001 |             |
| ABC                           | 0,6355         | 1  | 0,6355      | 6,35    | 0,0204   |             |
| Residual                      | 2,00           | 20 | 0,1001      |         |          |             |
| Cor Total                     | 19,60          | 27 |             |         |          |             |

Configure | Fit Summary | Model | ANOVA | Diagnostics | Model Graphs

Analysis of Variance | Fit Statistics | Model Comparison Statistics | Coefficients | Coded Equation | Actual Equation

### Fit Statistics

|           |        |                          |         |
|-----------|--------|--------------------------|---------|
| Std. Dev. | 0,3164 | R <sup>2</sup>           | 0,8971  |
| Mean      | 2,85   | Adjusted R <sup>2</sup>  | 0,8713  |
| C.V. %    | 11,09  | Predicted R <sup>2</sup> | 0,7918  |
|           |        | Adeq Precision           | 14,6023 |

Configure | Fit Summary | Model | ANOVA | Diagnostics | Model Graphs

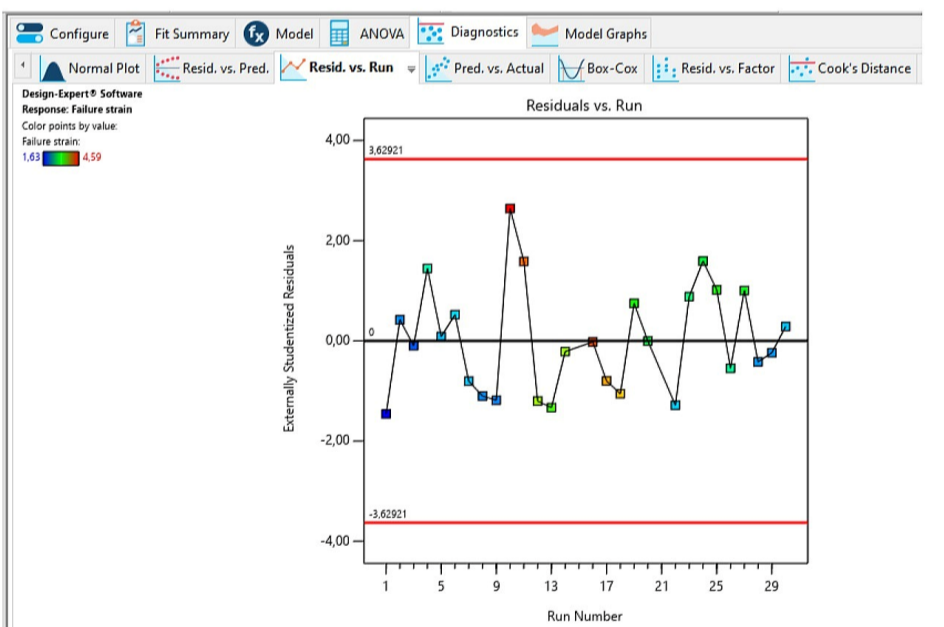
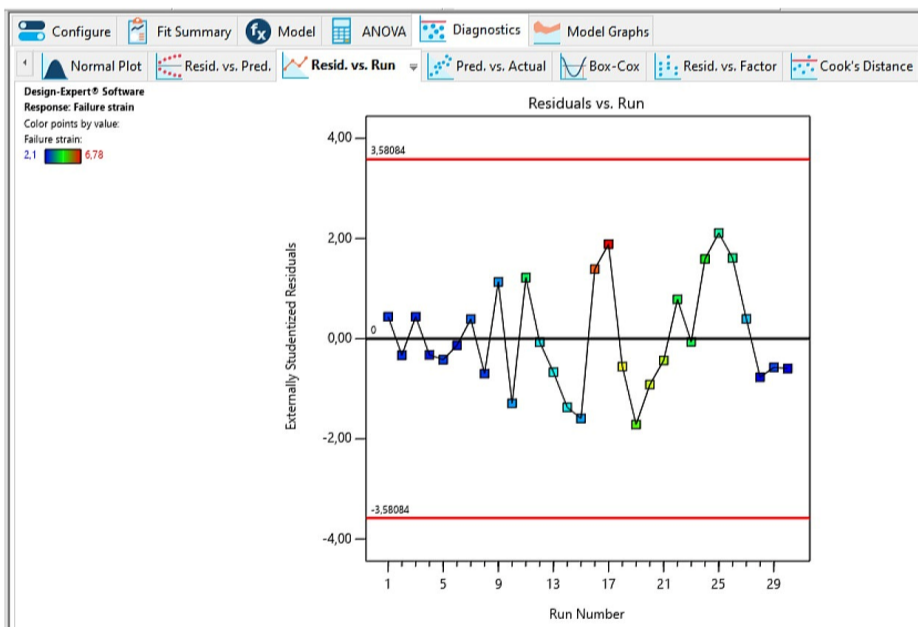
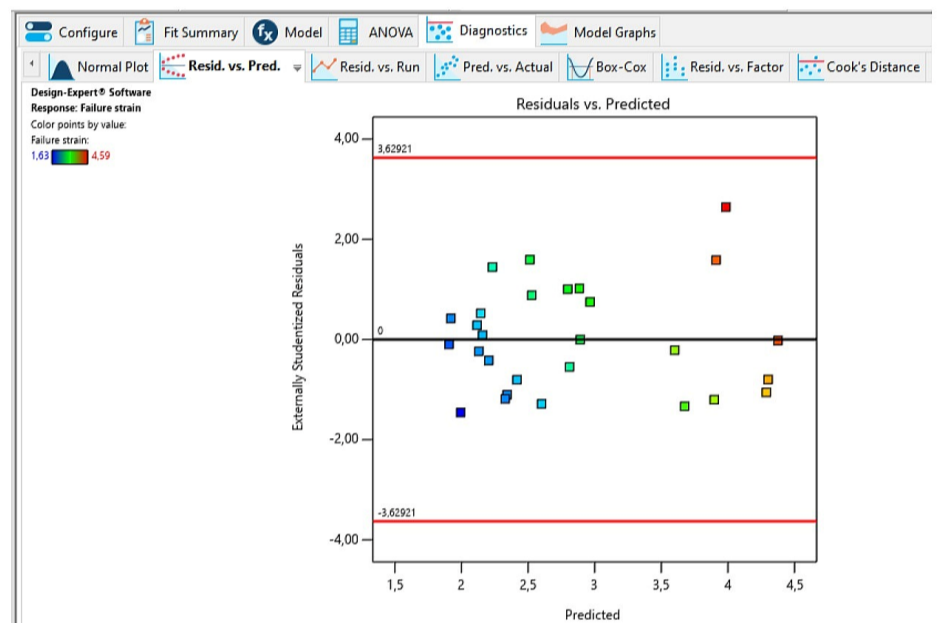
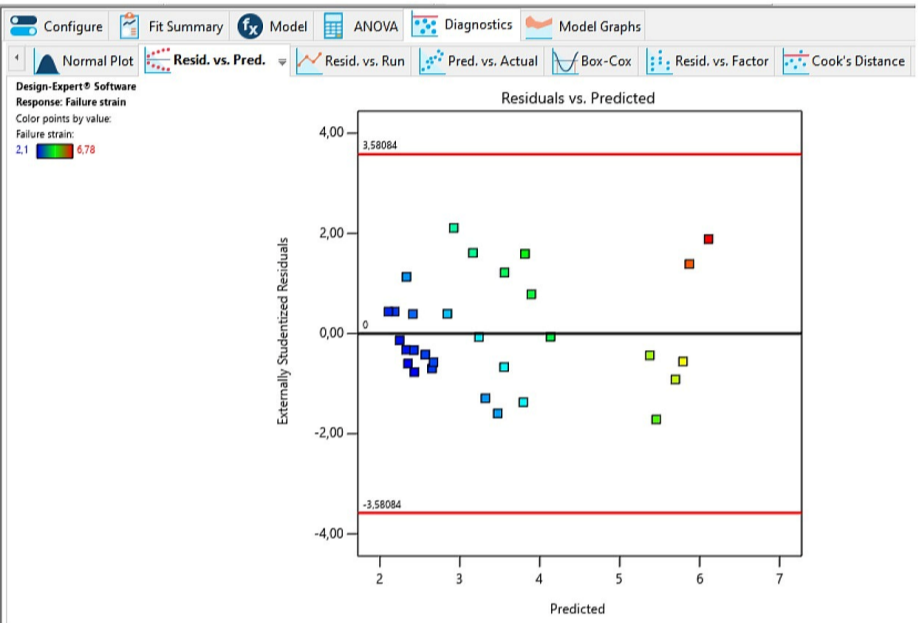
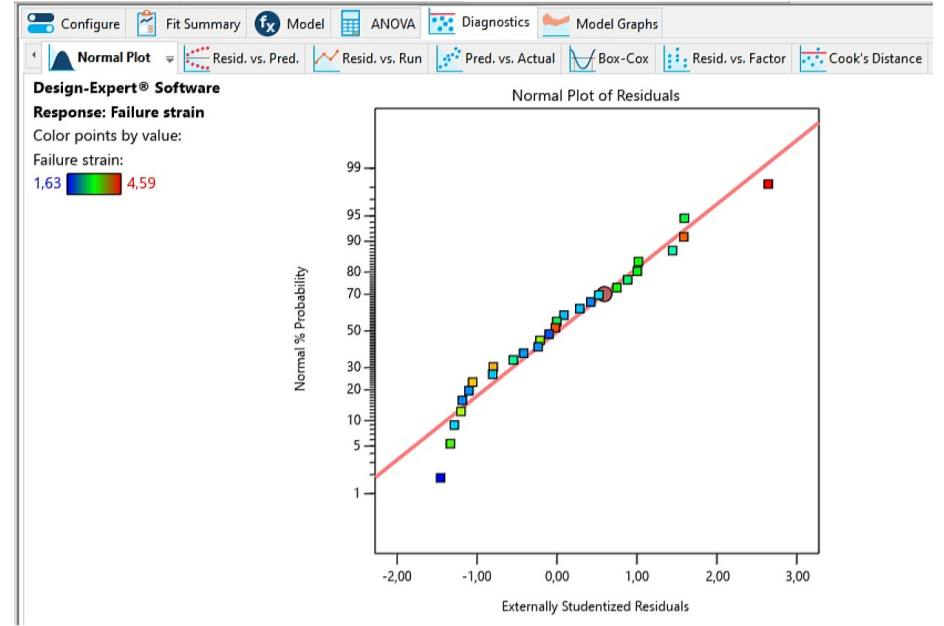
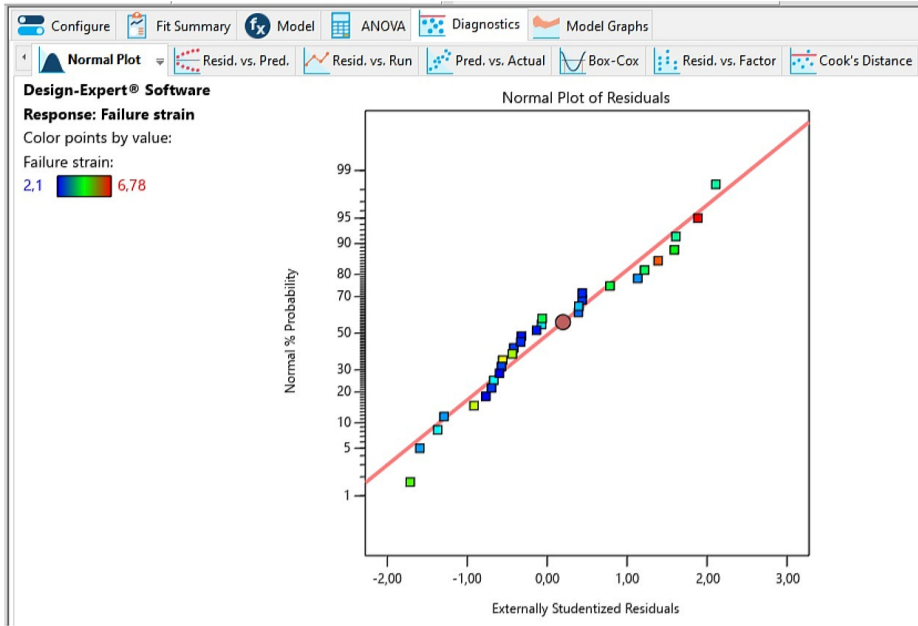
Analysis of Variance | Fit Statistics | Model Comparison Statistics | Coefficients | Coded Equation | Actual Equation

### Final Equation in Terms of L\_Pseudo Components

|                |       |
|----------------|-------|
| Failure strain | =     |
| +1,94          | * A   |
| +2,50          | * B   |
| +3,15          | * C   |
| -0,1734        | * AB  |
| +8,11          | * BC  |
| -15,75         | * ABC |

### DRY.16

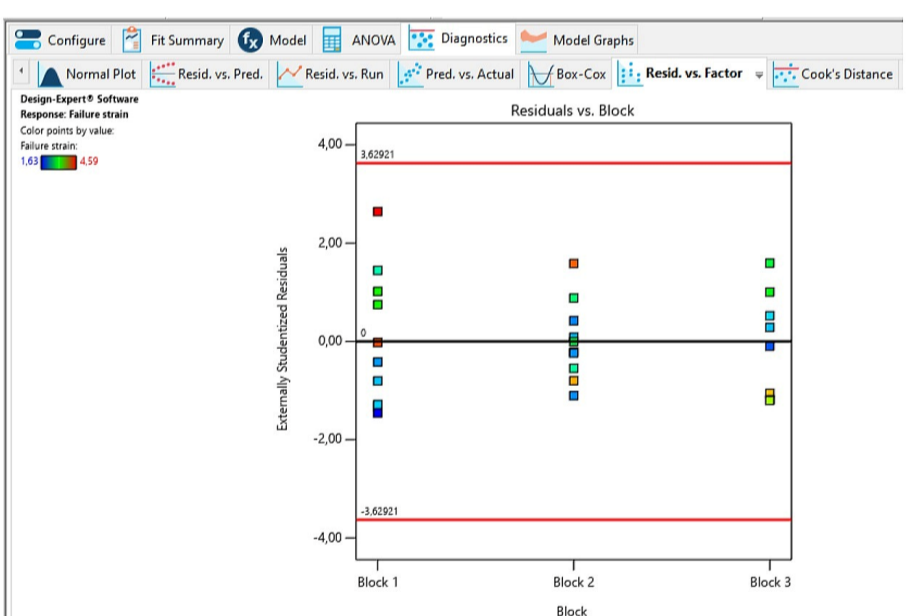
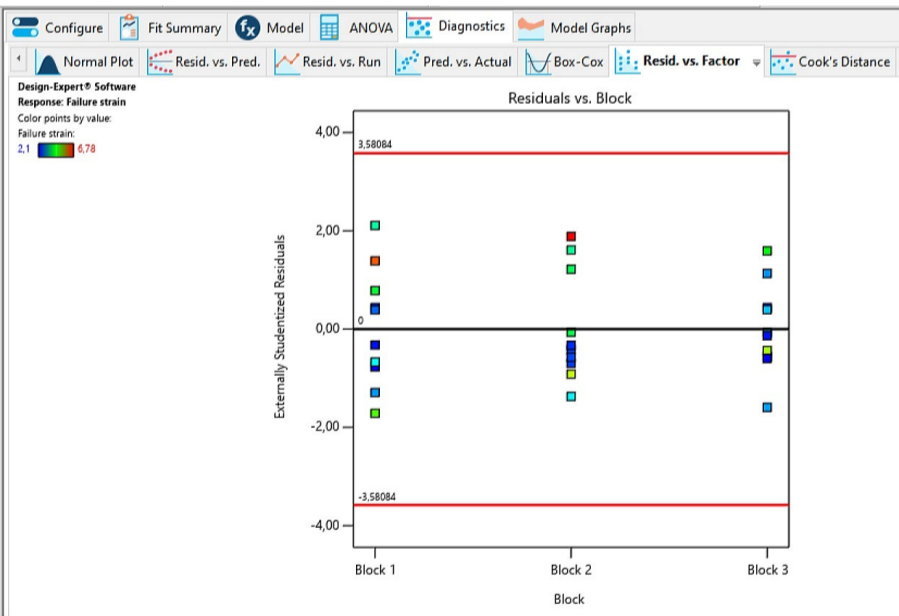
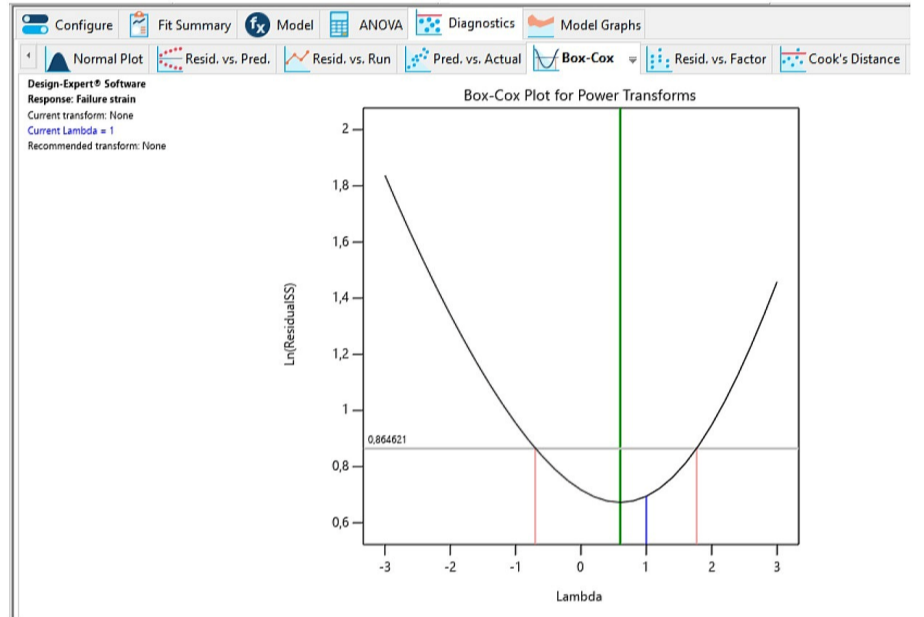
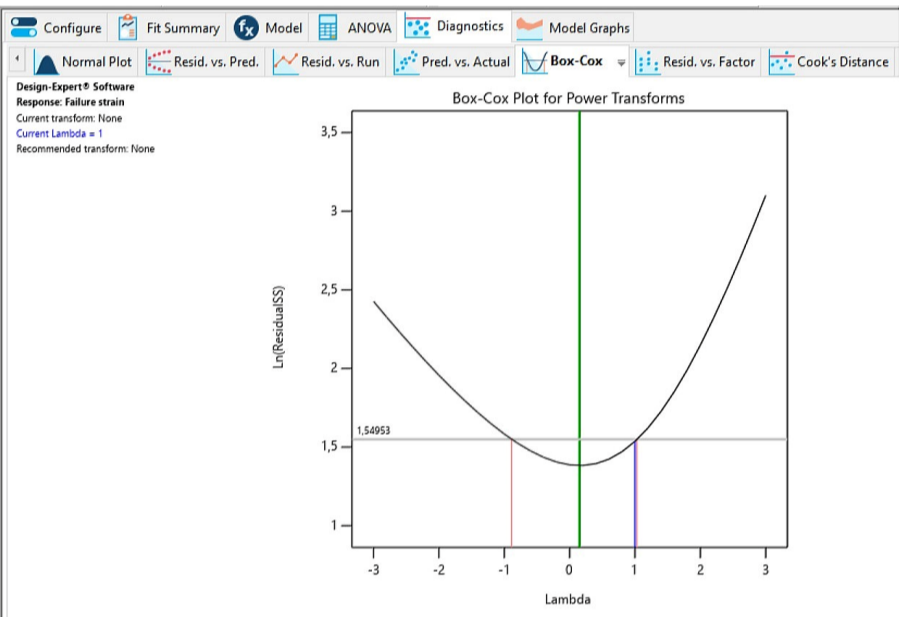
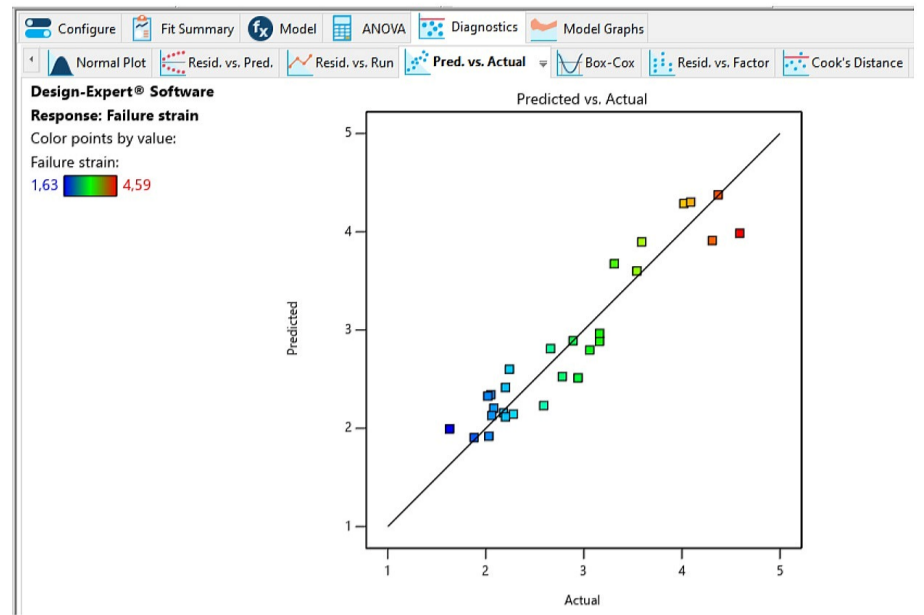
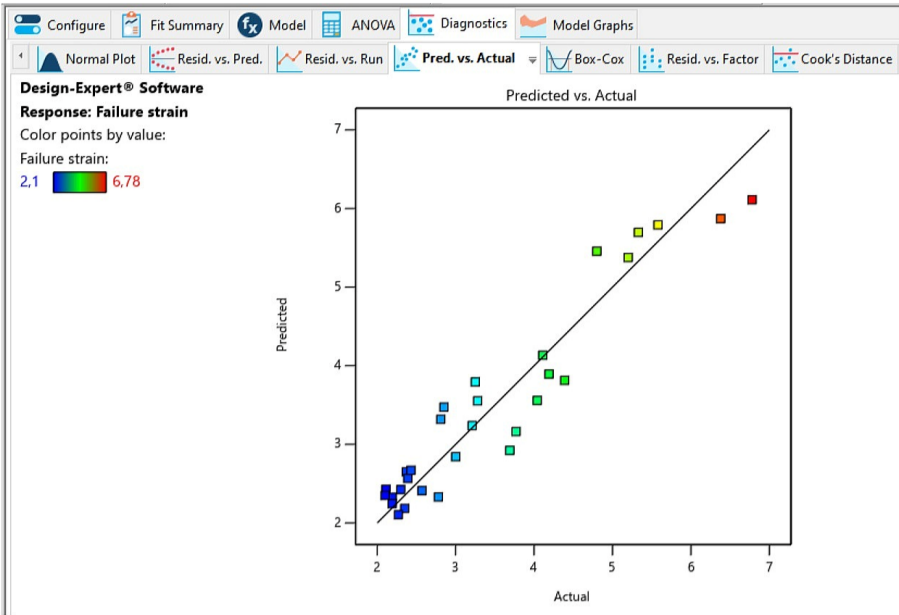
### WET.16





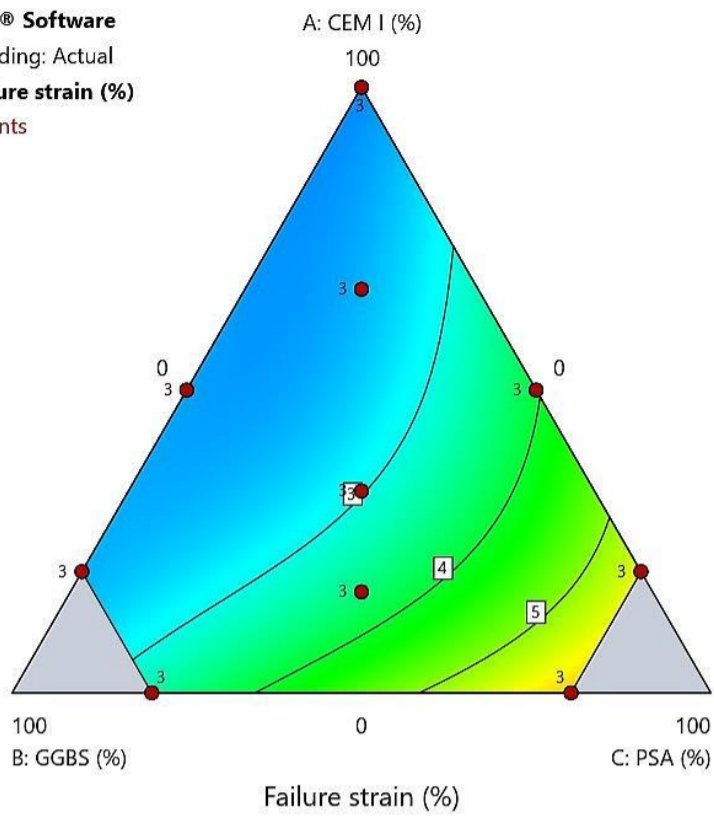
**DRY.16**

**WET.16**



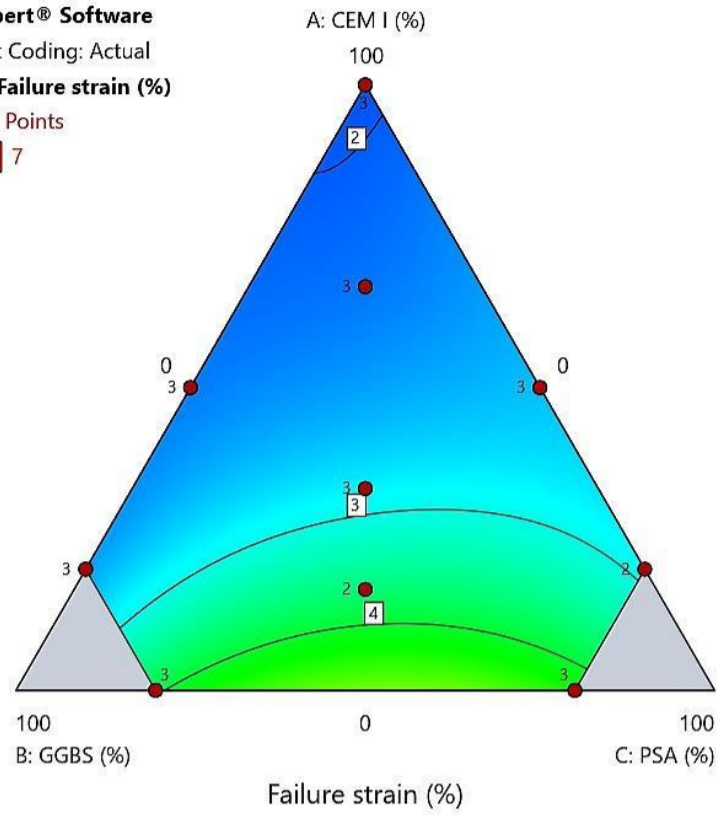
# DRY.16

**Design-Expert® Software**  
 Component Coding: Actual  
**Response: Failure strain (%)**  
 ● Design Points  
 1,5 7

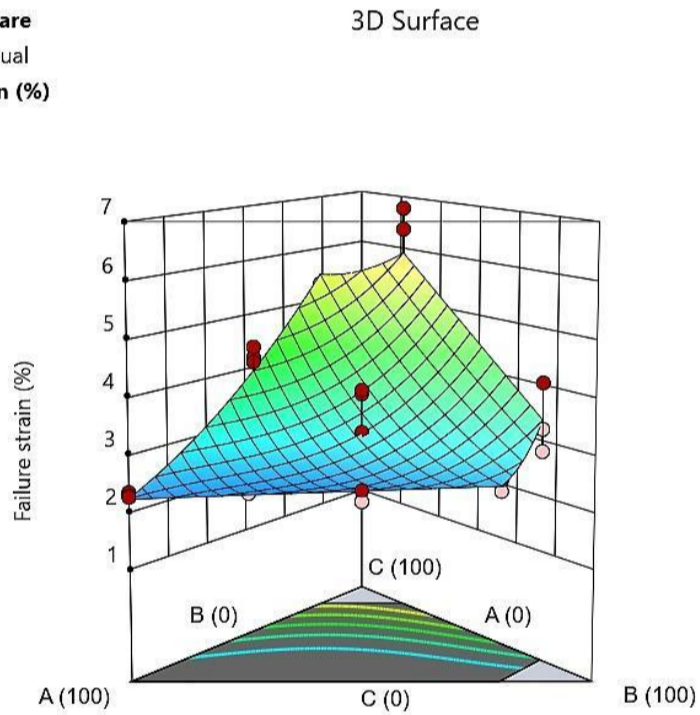


# WET.16

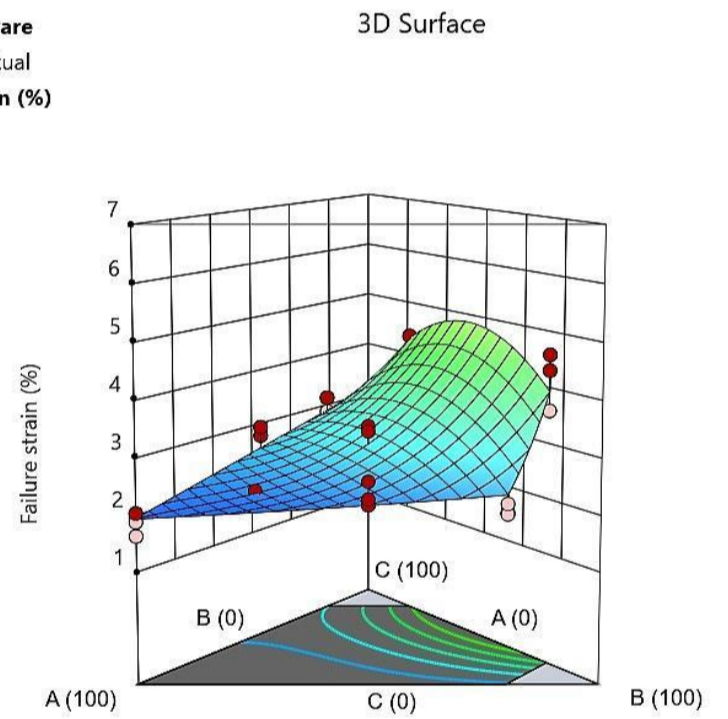
**Design-Expert® Software**  
 Component Coding: Actual  
**Response: Failure strain (%)**  
 ● Design Points  
 1,5 7



**Design-Expert® Software**  
 Component Coding: Actual  
**Response: Failure strain (%)**  
 Design Points:  
 ● Above Surface  
 ○ Below Surface  
 1,5 7



**Design-Expert® Software**  
 Component Coding: Actual  
**Response: Failure strain (%)**  
 Design Points:  
 ● Above Surface  
 ○ Below Surface  
 1,5 7



# R4: Estimated stiffness, $E_{50}$

## DRY.16

Configure Fit Summary Model ANOVA Diagnostics Model Graphs

Fit Summary Sequential Model Sum of Squares [Type I] Model Summary Statistics

**Fit Summary**  
Response 4: Estimated stiffness  
Mixture Component Coding is L\_Pseudo.

| Source        | Sequential p-value | Lack of Fit p-value | Adjusted R <sup>2</sup> | Predicted R <sup>2</sup> |           |
|---------------|--------------------|---------------------|-------------------------|--------------------------|-----------|
| Linear        | < 0.0001           |                     | 0,8741                  | 0,8341                   |           |
| Quadratic     | < 0.0001           |                     | 0,9587                  | 0,9389                   | Suggested |
| Special Cubic | 0,3173             |                     | 0,9588                  | 0,9356                   |           |
| Cubic         | 0,2442             |                     | 0,9608                  | 0,9286                   | Aliased   |

## WET.16

Configure Fit Summary Model ANOVA Diagnostics Model Graphs

Fit Summary Sequential Model Sum of Squares [Type I] Model Summary Statistics

**Fit Summary**  
Response 4: Estimated stiffness  
Mixture Component Coding is L\_Pseudo.

| Source        | Sequential p-value | Lack of Fit p-value | Adjusted R <sup>2</sup> | Predicted R <sup>2</sup> |           |
|---------------|--------------------|---------------------|-------------------------|--------------------------|-----------|
| Linear        | < 0.0001           |                     | 0,7032                  | 0,6087                   |           |
| Quadratic     | 0,0036             |                     | 0,8239                  | 0,7485                   | Suggested |
| Special Cubic | 0,6447             |                     | 0,8168                  | 0,7265                   |           |
| Cubic         | 0,0069             |                     | 0,8860                  | 0,8102                   | Aliased   |

Configure Fit Summary Model ANOVA Diagnostics Model Graphs

Mixture Order: Modified Auto Select...

Model Type: Scheffe Add Term

|          |  |
|----------|--|
| <b>m</b> | The term will be included in the model.  |
| <b>!</b> | Indicates the term is aliased with another term, or was not estimated in the Fit Summary calculations. Including the term in the model is not recommended. |
| <b>!</b> | A user-forced term. Automatic model selection will always produce a model that includes this term.   |
| <b>!</b> | Indicates that the term is required to be in the model by the program.   |

- A-CEM I
- B-GGBS
- C-PSA
- m** AB
- m** AC
- BC
- ABC
- AB(A-B)
- AC(A-C)
- !** BC(B-C)
- A<sup>2</sup>BC
- AB<sup>2</sup>C
- !** ABC<sup>2</sup>
- !** AB(A-B)<sup>2</sup>
- !** AC(A-C)<sup>2</sup>
- !** BC(B-C)<sup>2</sup>

Configure Fit Summary Model ANOVA Diagnostics Model Graphs

Mixture Order: Modified Auto Select...

Model Type: Scheffe Add Term

|          |  |
|----------|--|
| <b>m</b> | The term will be included in the model.  |
| <b>!</b> | Indicates the term is aliased with another term, or was not estimated in the Fit Summary calculations. Including the term in the model is not recommended. |
| <b>!</b> | A user-forced term. Automatic model selection will always produce a model that includes this term.   |
| <b>!</b> | Indicates that the term is required to be in the model by the program.   |

- A-CEM I
- B-GGBS
- C-PSA
- AB
- m** AC
- m** BC
- ABC
- AB(A-B)
- AC(A-C)
- !** BC(B-C)
- A<sup>2</sup>BC
- AB<sup>2</sup>C
- !** ABC<sup>2</sup>
- !** AB(A-B)<sup>2</sup>
- !** AC(A-C)<sup>2</sup>
- !** BC(B-C)<sup>2</sup>

# DRY.16

Configure Fit Summary Model ANOVA Diagnostics Model Graphs

Analysis of Variance Fit Statistics Model Comparison Statistics Coefficients Coded Equation Real Equation Actual Equation

### ANOVA for Reduced Quadratic model

Response 4: Estimated stiffness

| Source                        | Sum of Squares | df | Mean Square | F-value | p-value  |             |
|-------------------------------|----------------|----|-------------|---------|----------|-------------|
| Block                         | 2,032E+07      | 2  | 1,016E+07   |         |          |             |
| Model                         | 2,606E+09      | 4  | 6,514E+08   | 150,88  | < 0.0001 | significant |
| <sup>(1)</sup> Linear Mixture | 2,387E+09      | 2  | 1,193E+09   | 276,41  | < 0.0001 |             |
| AB                            | 5,683E+07      | 1  | 5,683E+07   | 13,16   | 0,0015   |             |
| AC                            | 1,818E+08      | 1  | 1,818E+08   | 42,10   | < 0.0001 |             |
| Residual                      | 9,498E+07      | 22 | 4,317E+06   |         |          |             |
| Cor Total                     | 2,721E+09      | 28 |             |         |          |             |

Configure Fit Summary Model ANOVA Diagnostics Model Graphs

Analysis of Variance Fit Statistics Model Comparison Statistics Coefficients Coded Equation Real Equation Actual Equation

### Fit Statistics

|           |          |                          |         |
|-----------|----------|--------------------------|---------|
| Std. Dev. | 2077,80  | R <sup>2</sup>           | 0,9648  |
| Mean      | 12354,31 | Adjusted R <sup>2</sup>  | 0,9584  |
| C.V. %    | 16,82    | Predicted R <sup>2</sup> | 0,9408  |
|           |          | Adeq Precision           | 29,9356 |

Configure Fit Summary Model ANOVA Diagnostics Model Graphs

Analysis of Variance Fit Statistics Model Comparison Statistics Coefficients Coded Equation Real Equation Actual Equation

### Final Equation in Terms of L\_Pseudo Components

|                     |      |
|---------------------|------|
| Estimated stiffness | =    |
| +32718,75           | * A  |
| +2962,63            | * B  |
| +3705,37            | * C  |
| +21510,07           | * AB |
| -38470,19           | * AC |

# WET.16

Configure Fit Summary Model ANOVA Diagnostics Model Graphs

Analysis of Variance Fit Statistics Model Comparison Statistics Coefficients Coded Equation Real Equation Actual Equation

### ANOVA for Reduced Quadratic model

Response 4: Estimated stiffness

| Source                        | Sum of Squares | df | Mean Square | F-value | p-value  |             |
|-------------------------------|----------------|----|-------------|---------|----------|-------------|
| Block                         | 1,336E+08      | 2  | 6,682E+07   |         |          |             |
| Model                         | 3,032E+09      | 4  | 7,581E+08   | 27,69   | < 0.0001 | significant |
| <sup>(1)</sup> Linear Mixture | 2,622E+09      | 2  | 1,311E+09   | 47,89   | < 0.0001 |             |
| AC                            | 3,445E+08      | 1  | 3,445E+08   | 12,58   | 0,0019   |             |
| BC                            | 1,791E+08      | 1  | 1,791E+08   | 6,54    | 0,0183   |             |
| Residual                      | 5,749E+08      | 21 | 2,738E+07   |         |          |             |
| Cor Total                     | 3,741E+09      | 27 |             |         |          |             |

Configure Fit Summary Model ANOVA Diagnostics Model Graphs

Analysis of Variance Fit Statistics Model Comparison Statistics Coefficients Coded Equation Real Equation Actual Equation

### Fit Statistics

|           |          |                          |         |
|-----------|----------|--------------------------|---------|
| Std. Dev. | 5232,23  | R <sup>2</sup>           | 0,8406  |
| Mean      | 12193,29 | Adjusted R <sup>2</sup>  | 0,8103  |
| C.V. %    | 42,91    | Predicted R <sup>2</sup> | 0,7247  |
|           |          | Adeq Precision           | 14,1067 |

Configure Fit Summary Model ANOVA Diagnostics Model Graphs

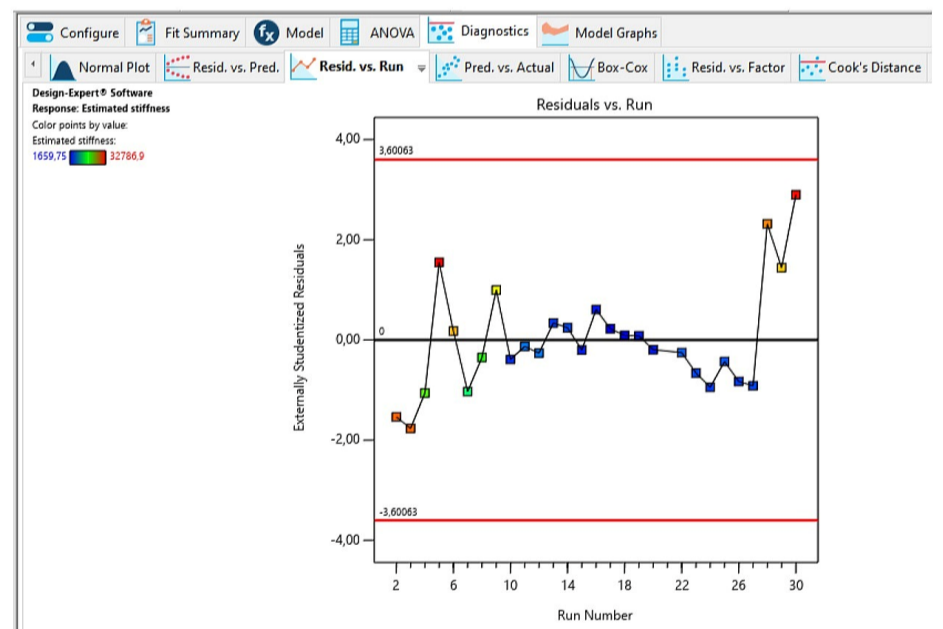
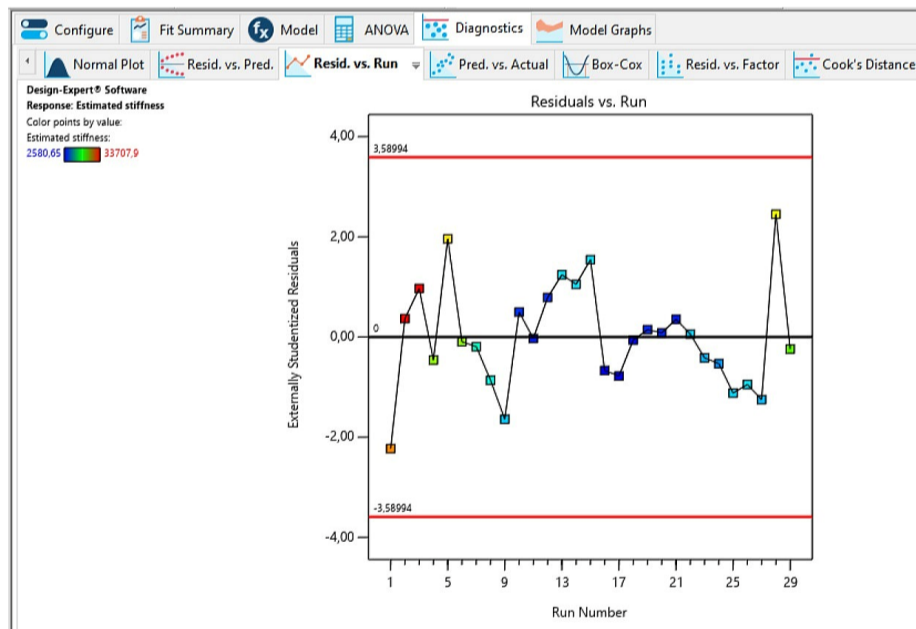
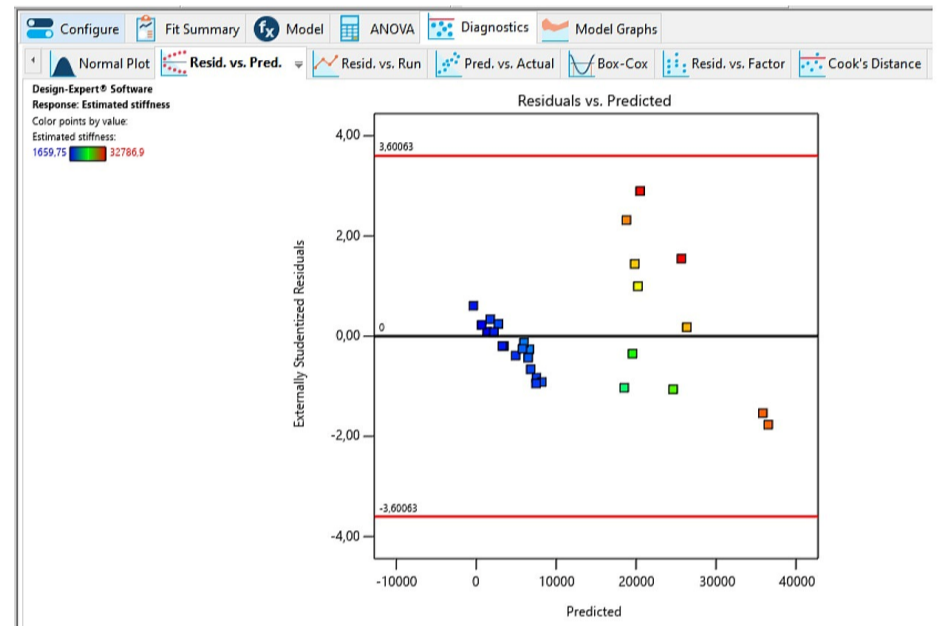
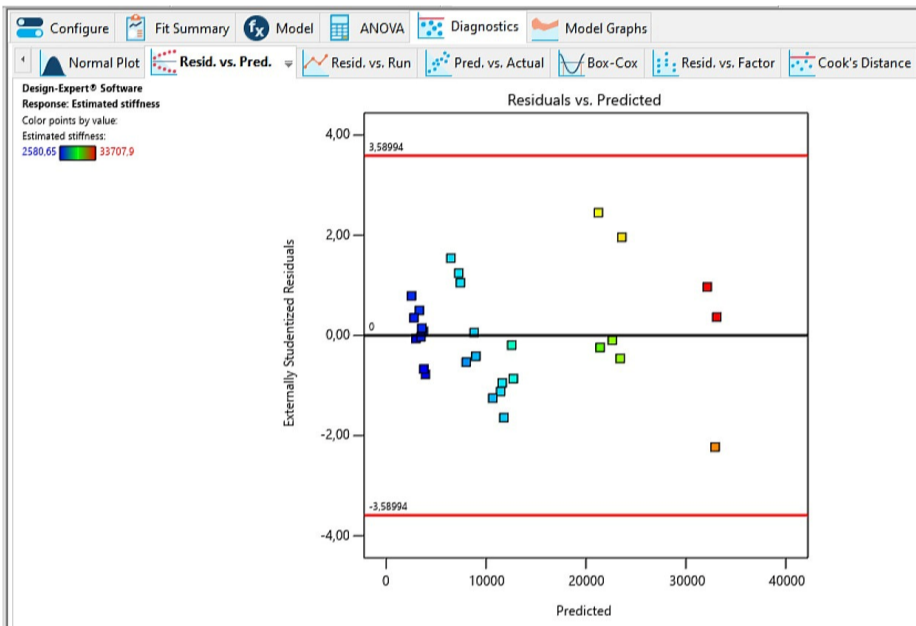
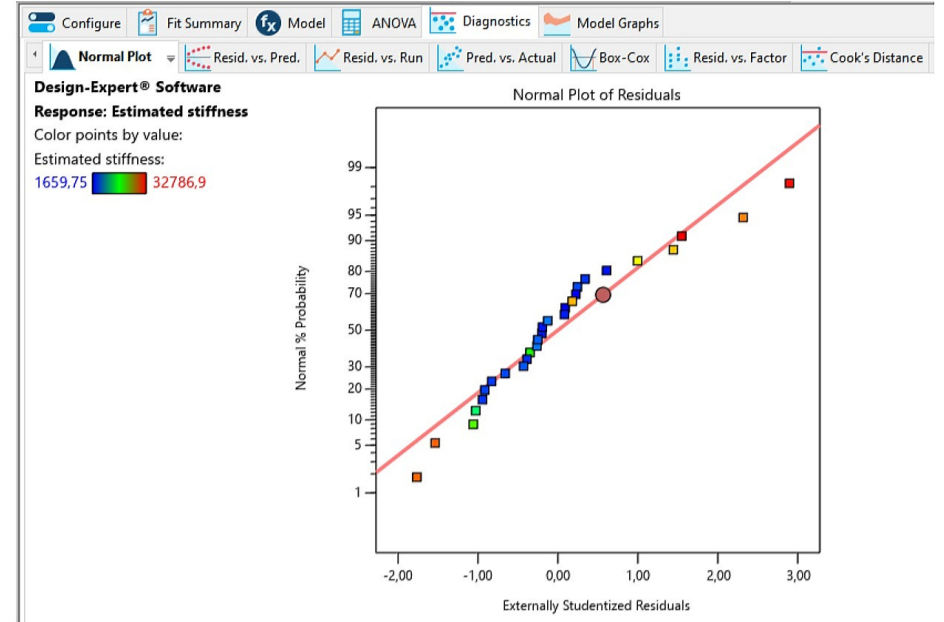
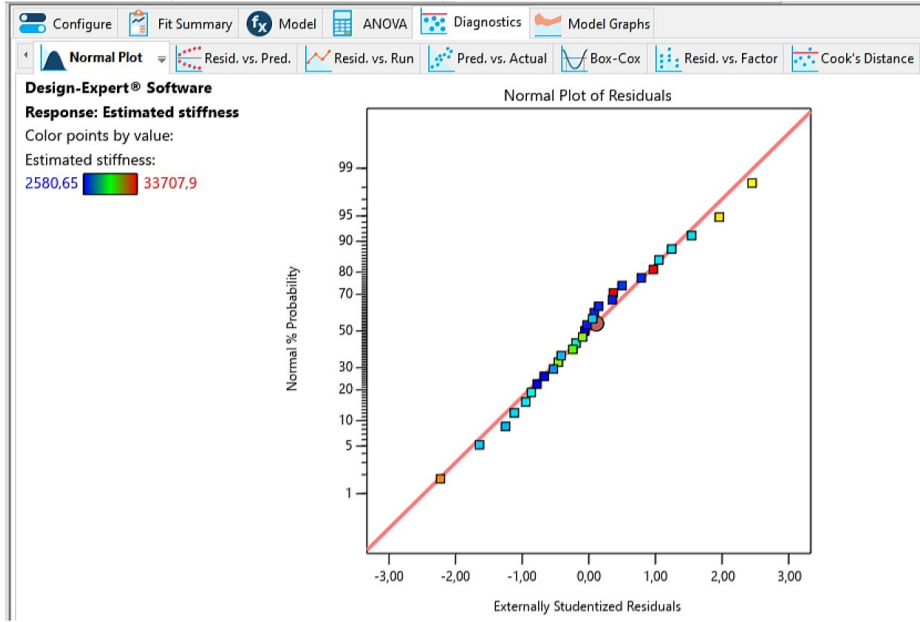
Analysis of Variance Fit Statistics Model Comparison Statistics Coefficients Coded Equation Real Equation Actual Equation

### Final Equation in Terms of L\_Pseudo Components

|                     |      |
|---------------------|------|
| Estimated stiffness | =    |
| +35743,96           | * A  |
| +15352,93           | * B  |
| +6533,04            | * C  |
| -57783,98           | * AC |
| -48408,52           | * BC |

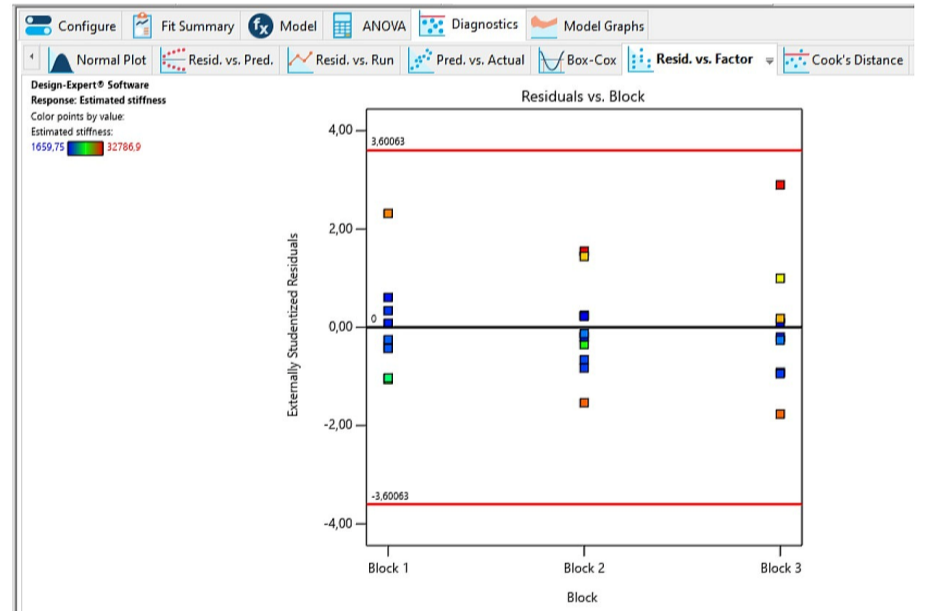
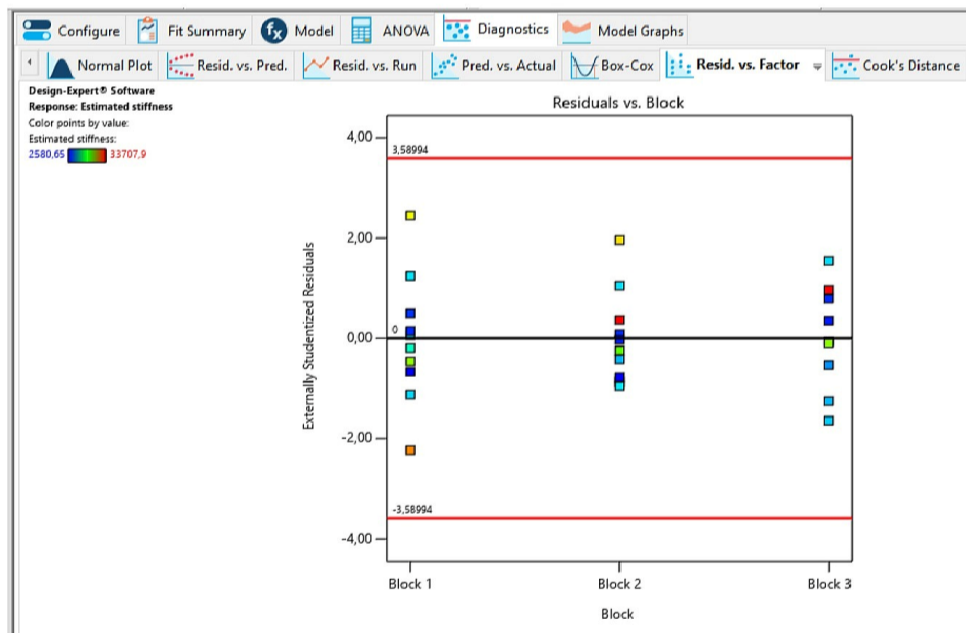
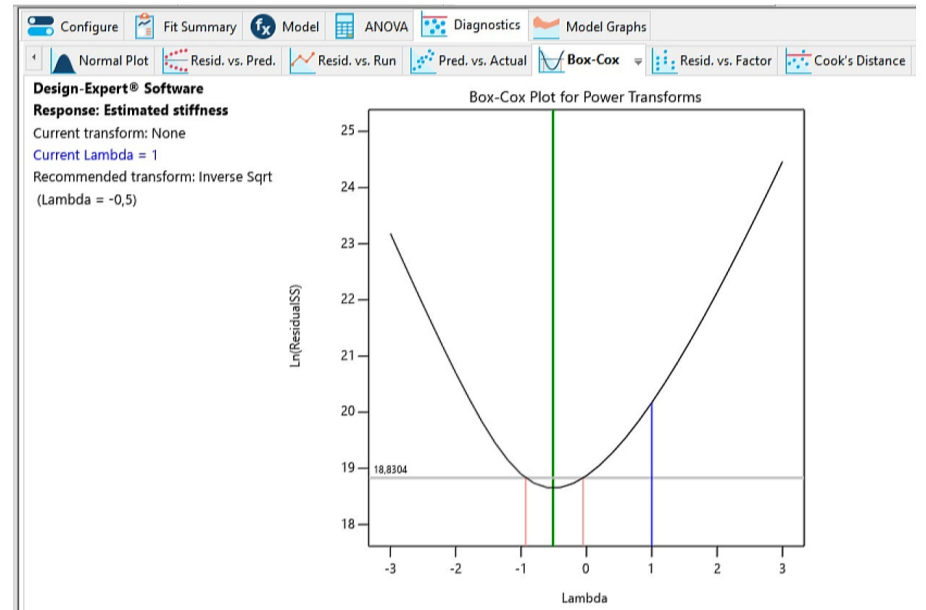
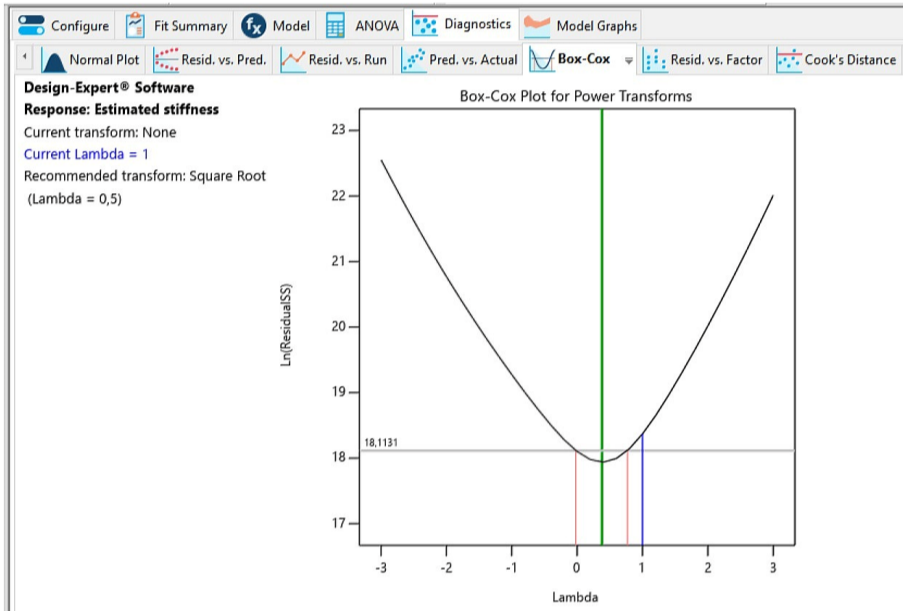
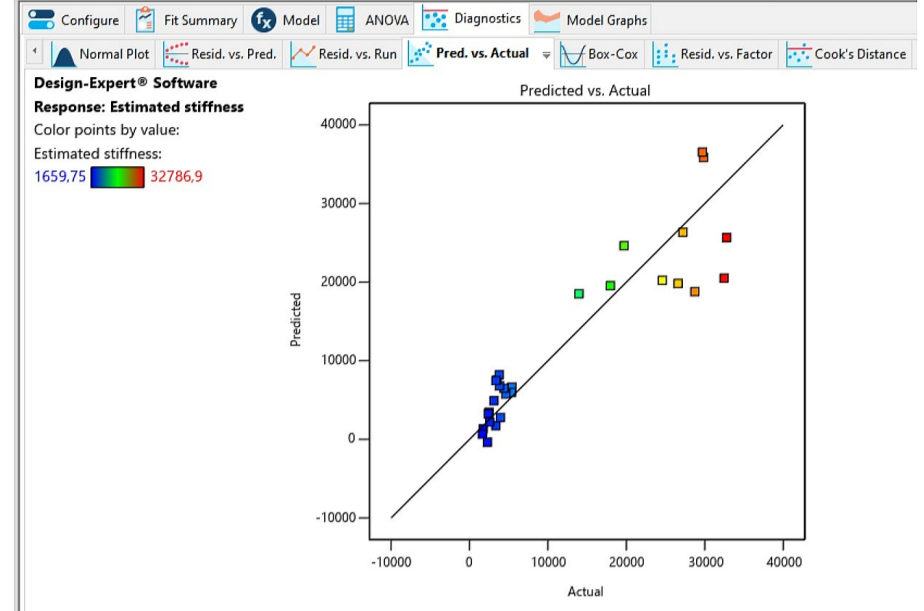
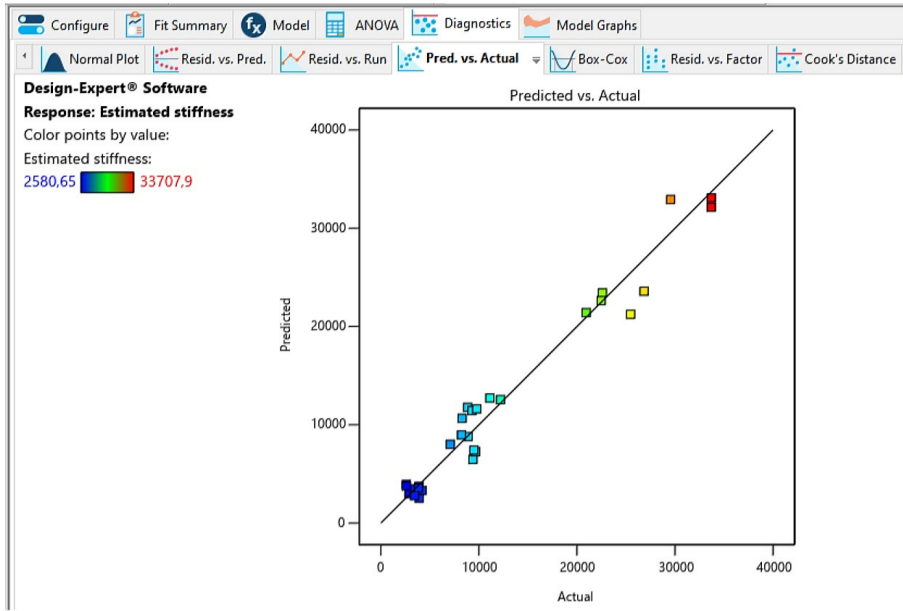
**DRY.16**

**WET.16**

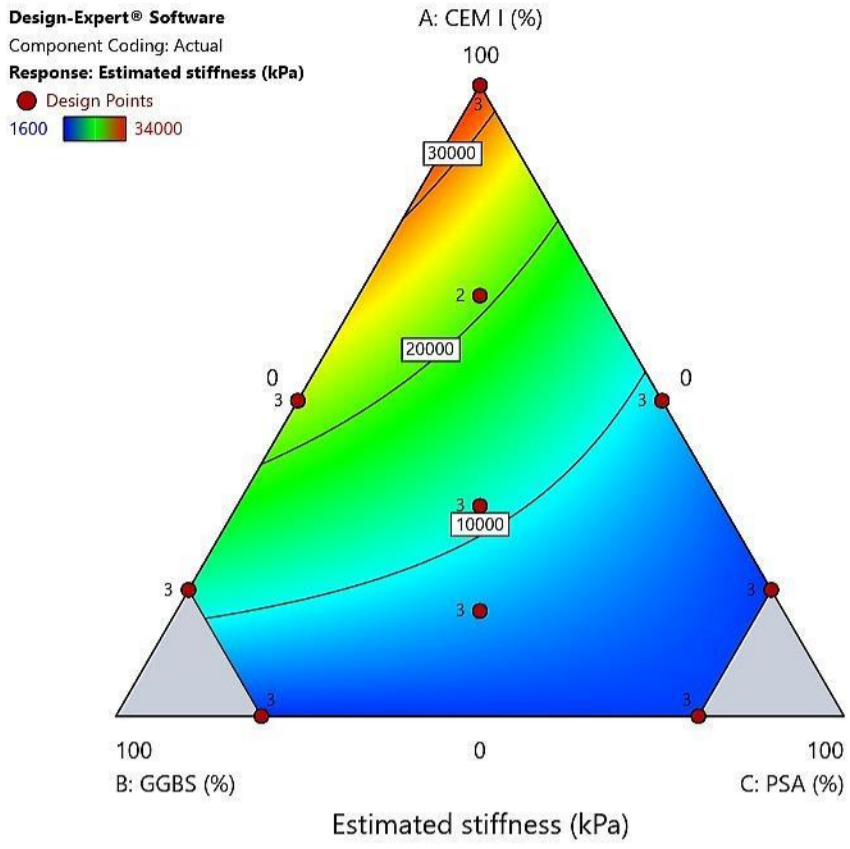


**DRY.16**

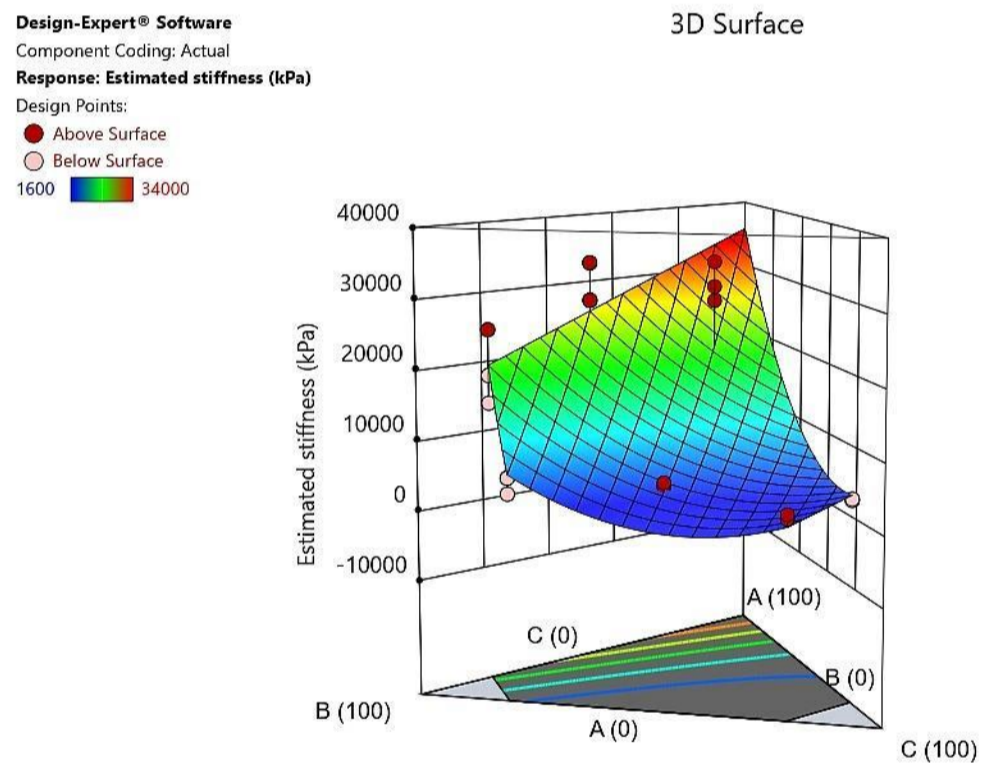
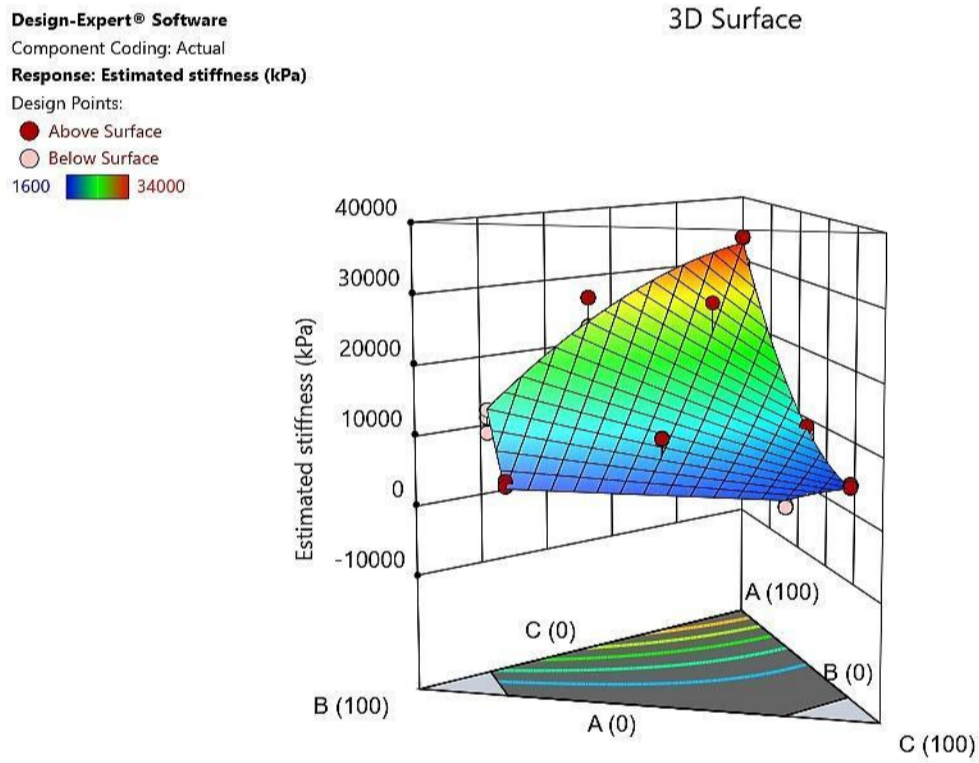
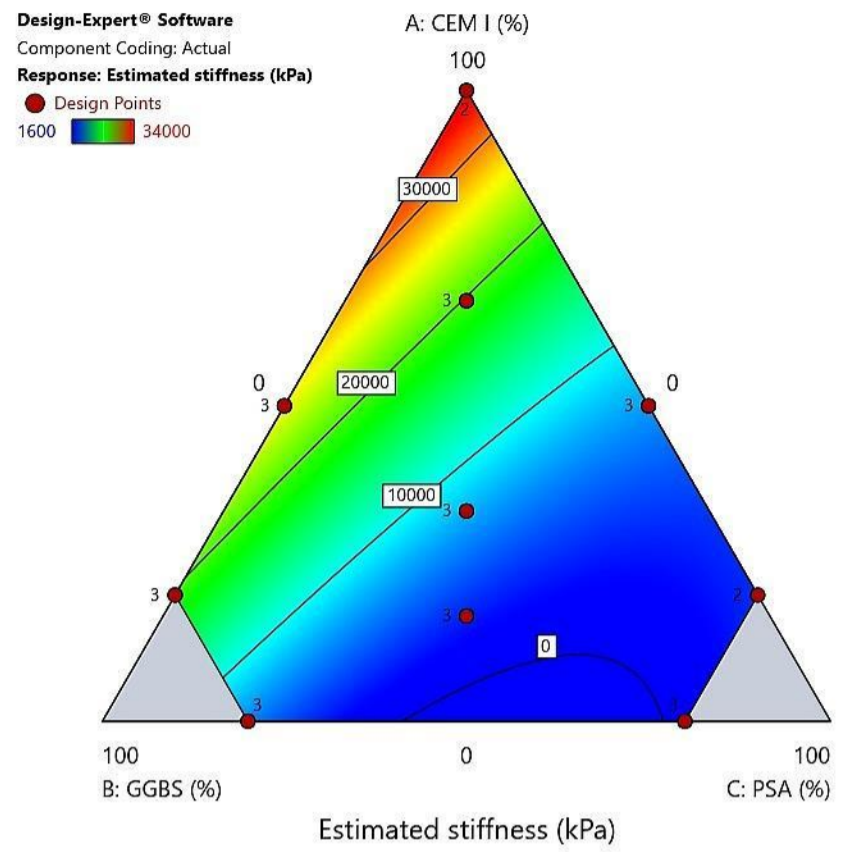
**WET.16**



# DRY.16



# WET.16



# R5: P-wave velocity, $V_p$

## DRY.16

Configure Fit Summary Model ANOVA Diagnostics Model Graphs

Fit Summary Sequential Model Sum of Squares [Type I] Model Summary Statistics

**Fit Summary**  
Response 5: P-wave velocity  
Mixture Component Coding is L\_Pseudo.

| Source        | Sequential p-value | Lack of Fit p-value | Adjusted R <sup>2</sup> | Predicted R <sup>2</sup> |                  |
|---------------|--------------------|---------------------|-------------------------|--------------------------|------------------|
| Linear        | < 0.0001           |                     | 0,7464                  | 0,6710                   |                  |
| Quadratic     | < 0.0001           |                     | <b>0,9141</b>           | <b>0,8824</b>            | <b>Suggested</b> |
| Special Cubic | 0,1096             |                     | 0,9206                  | 0,8878                   |                  |
| Cubic         | < 0.0001           |                     | 0,9734                  | 0,9606                   | <b>Aliased</b>   |

Configure Fit Summary Model ANOVA Diagnostics Model Graphs

Mixture Order: Quadratic Auto Select...

Model Type: Scheffe Add Term

|  |                      |
|--|----------------------|
|  | A-CEM I              |
|  | B-GGBS               |
|  | C-PSA                |
|  | AB                   |
|  | AC                   |
|  | BC                   |
|  | ABC                  |
|  | AB(A-B)              |
|  | AC(A-C)              |
|  | BC(B-C)              |
|  | A <sup>2</sup> BC    |
|  | AB <sup>2</sup> C    |
|  | ABC <sup>2</sup>     |
|  | AB(A-B) <sup>2</sup> |
|  | AC(A-C) <sup>2</sup> |
|  | BC(B-C) <sup>2</sup> |

|  |  |
|--|--|
|  | The term will be included in the model.  |
|  | Indicates the term is aliased with another term, or was not estimated in the Fit Summary calculations. Including the term in the model is not recommended. |
|  | A user-forced term. Automatic model selection will always produce a model that includes this term.   |
|  | Indicates that the term is required to be in the model by the program.   |

## WET.16

Configure Fit Summary Model ANOVA Diagnostics Model Graphs

Fit Summary Sequential Model Sum of Squares [Type I] Model Summary Statistics

**Fit Summary**  
Response 5: P-wave velocity  
Mixture Component Coding is L\_Pseudo.

| Source        | Sequential p-value | Lack of Fit p-value | Adjusted R <sup>2</sup> | Predicted R <sup>2</sup> |                  |
|---------------|--------------------|---------------------|-------------------------|--------------------------|------------------|
| Linear        | 0,0061             |                     | 0,3022                  | -0,0036                  |                  |
| Quadratic     | < 0.0001           |                     | 0,8047                  | 0,7225                   |                  |
| Special Cubic | <b>0,0107</b>      |                     | <b>0,8554</b>           | <b>0,8014</b>            | <b>Suggested</b> |
| Cubic         | 0,1380             |                     | 0,8719                  | 0,8124                   | <b>Aliased</b>   |

Configure Fit Summary Model ANOVA Diagnostics Model Graphs

Mixture Order: Modified Auto Select...

Model Type: Scheffe Add Term

|  |                      |
|--|----------------------|
|  | A-CEM I              |
|  | B-GGBS               |
|  | C-PSA                |
|  | AB                   |
|  | AC                   |
|  | BC                   |
|  | ABC                  |
|  | AB(A-B)              |
|  | AC(A-C)              |
|  | BC(B-C)              |
|  | A <sup>2</sup> BC    |
|  | AB <sup>2</sup> C    |
|  | ABC <sup>2</sup>     |
|  | AB(A-B) <sup>2</sup> |
|  | AC(A-C) <sup>2</sup> |
|  | BC(B-C) <sup>2</sup> |

|  |  |
|--|--|
|  | The term will be included in the model.  |
|  | Indicates the term is aliased with another term, or was not estimated in the Fit Summary calculations. Including the term in the model is not recommended. |
|  | A user-forced term. Automatic model selection will always produce a model that includes this term.   |
|  | Indicates that the term is required to be in the model by the program.   |



# DRY.16

Configure Fit Summary Model ANOVA Diagnostics Model Graphs

Analysis of Variance Fit Statistics Model Comparison Statistics Coefficients Coded Equation Real Equation Actual Equation

### ANOVA for Quadratic model

Response 5: P-wave velocity

| Source            | Sum of Squares | df | Mean Square | F-value | p-value  |             |
|-------------------|----------------|----|-------------|---------|----------|-------------|
| Block             | 1053,27        | 2  | 526,63      |         |          |             |
| Model             | 5,524E+06      | 5  | 1,105E+06   | 58,48   | < 0.0001 | significant |
| (1)Linear Mixture | 4,545E+06      | 2  | 2,272E+06   | 120,29  | < 0.0001 |             |
| AB                | 7,579E+05      | 1  | 7,579E+05   | 40,12   | < 0.0001 |             |
| AC                | 1,809E+05      | 1  | 1,809E+05   | 9,58    | 0,0053   |             |
| BC                | 3,348E+05      | 1  | 3,348E+05   | 17,72   | 0,0004   |             |
| Residual          | 4,156E+05      | 22 | 18891,19    |         |          |             |
| Cor Total         | 5,941E+06      | 29 |             |         |          |             |

Configure Fit Summary Model ANOVA Diagnostics Model Graphs

Analysis of Variance Fit Statistics Model Comparison Statistics Coefficients Coded Equation Real Equation Actual Equation

### Fit Statistics

|           |        |                          |         |
|-----------|--------|--------------------------|---------|
| Std. Dev. | 137,45 | R <sup>2</sup>           | 0,9300  |
| Mean      | 731,23 | Adjusted R <sup>2</sup>  | 0,9141  |
| C.V. %    | 18,80  | Predicted R <sup>2</sup> | 0,8824  |
|           |        | Adeq Precision           | 17,7298 |

Configure Fit Summary Model ANOVA Diagnostics Model Graphs

Analysis of Variance Fit Statistics Model Comparison Statistics Coefficients Coded Equation Real Equation Actual Equation

### Final Equation in Terms of L\_Pseudo Components

|                 |               |
|-----------------|---------------|
| P-wave velocity | =             |
|                 | +1067,48 * A  |
|                 | +2084,41 * B  |
|                 | +261,78 * C   |
|                 | -2607,99 * AB |
|                 | -1274,18 * AC |
|                 | -2083,68 * BC |

# WET.16

Configure Fit Summary Model ANOVA Diagnostics Model Graphs

Analysis of Variance Fit Statistics Model Comparison Statistics Coefficients Coded Equation Real Equation Actual Equation

### ANOVA for Reduced Quadratic model

Response 5: P-wave velocity

| Source            | Sum of Squares | df | Mean Square | F-value | p-value  |             |
|-------------------|----------------|----|-------------|---------|----------|-------------|
| Block             | 3,708E+05      | 2  | 1,854E+05   |         |          |             |
| Model             | 4,818E+06      | 4  | 1,204E+06   | 27,34   | < 0.0001 | significant |
| (1)Linear Mixture | 2,056E+06      | 2  | 1,028E+06   | 23,34   | < 0.0001 |             |
| AB                | 2,837E+05      | 1  | 2,837E+05   | 6,44    | 0,0192   |             |
| AC                | 2,226E+06      | 1  | 2,226E+06   | 50,52   | < 0.0001 |             |
| Residual          | 9,251E+05      | 21 | 44052,92    |         |          |             |
| Cor Total         | 6,114E+06      | 27 |             |         |          |             |

Configure Fit Summary Model ANOVA Diagnostics Model Graphs

Analysis of Variance Fit Statistics Model Comparison Statistics Coefficients Coded Equation Real Equation Actual Equation

### Fit Statistics

|           |        |                          |         |
|-----------|--------|--------------------------|---------|
| Std. Dev. | 209,89 | R <sup>2</sup>           | 0,8389  |
| Mean      | 904,46 | Adjusted R <sup>2</sup>  | 0,8082  |
| C.V. %    | 23,21  | Predicted R <sup>2</sup> | 0,7514  |
|           |        | Adeq Precision           | 15,4760 |

Configure Fit Summary Model ANOVA Diagnostics Model Graphs

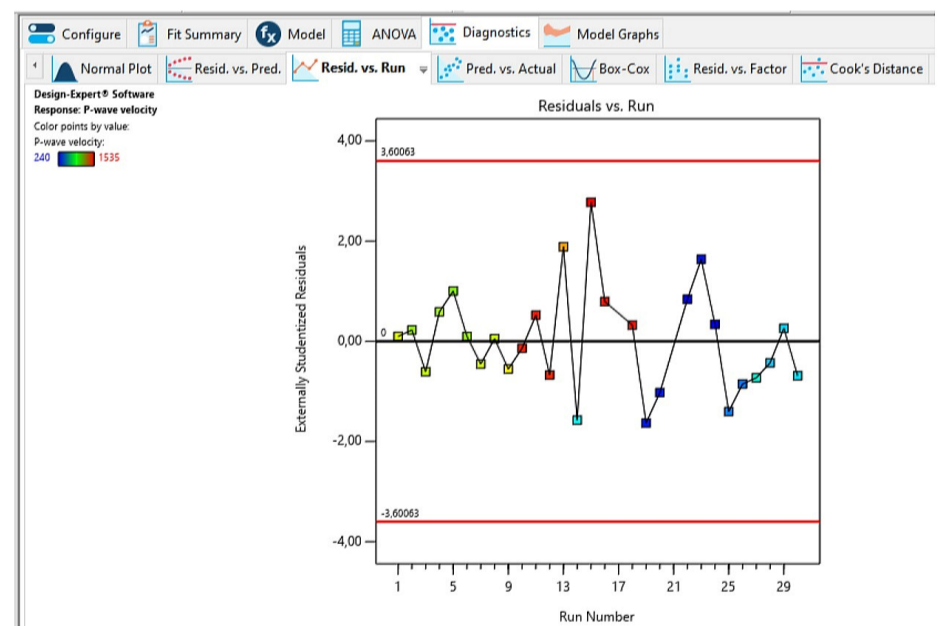
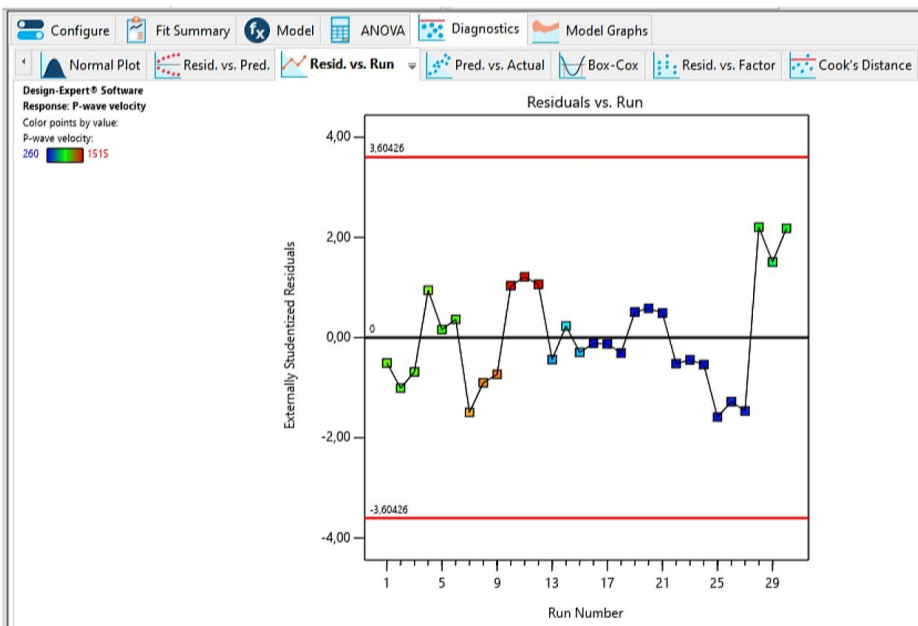
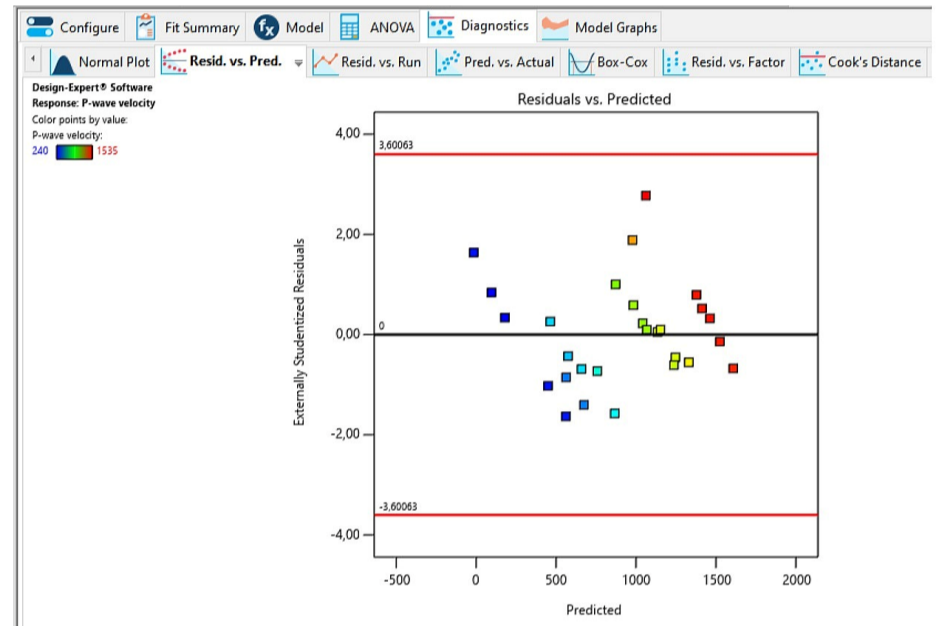
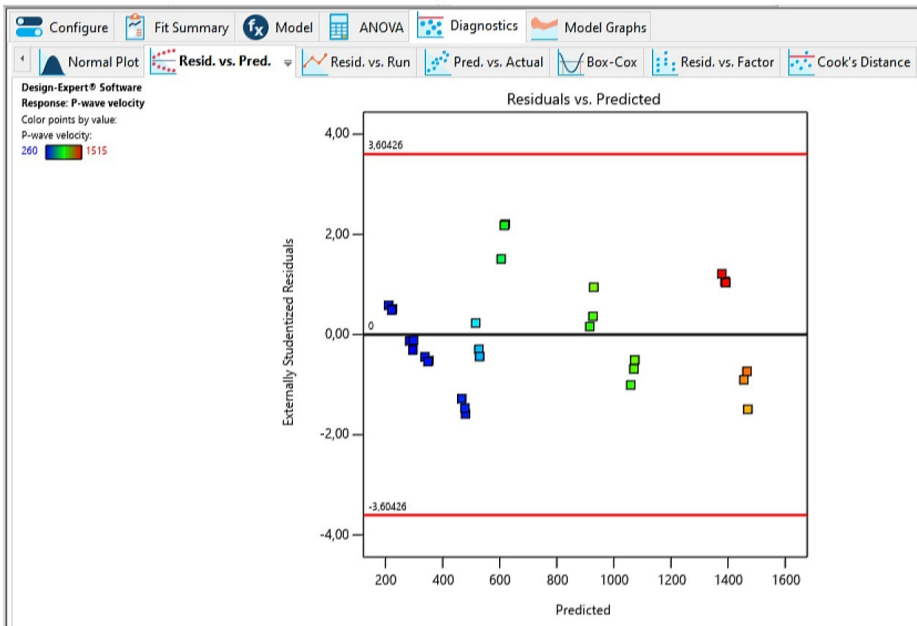
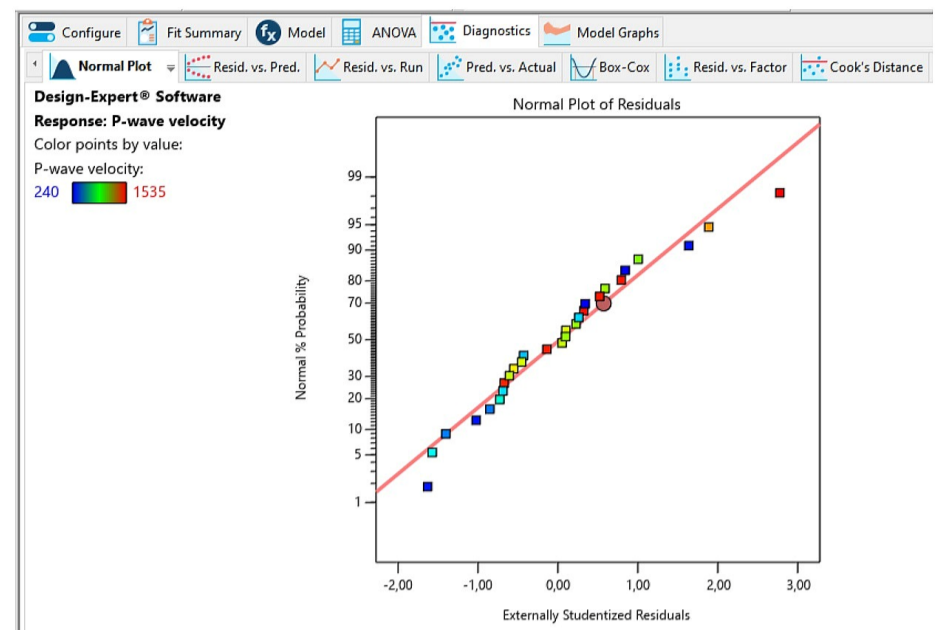
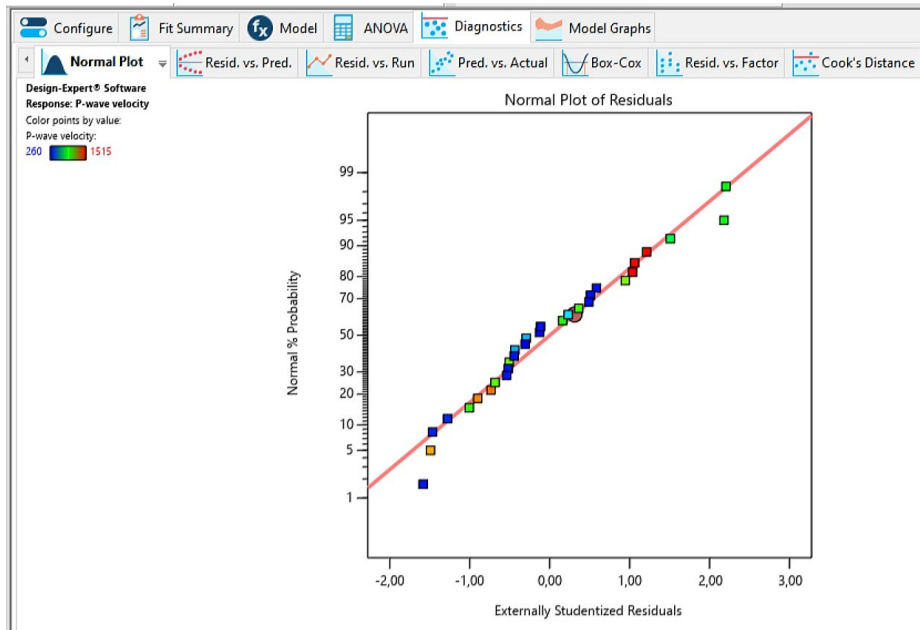
Analysis of Variance Fit Statistics Model Comparison Statistics Coefficients Coded Equation Real Equation Actual Equation

### Final Equation in Terms of L\_Pseudo Components

|                 |               |
|-----------------|---------------|
| P-wave velocity | =             |
|                 | +1144,20 * A  |
|                 | +1564,20 * B  |
|                 | +1320,63 * C  |
|                 | -1518,83 * AB |
|                 | -4582,97 * AC |

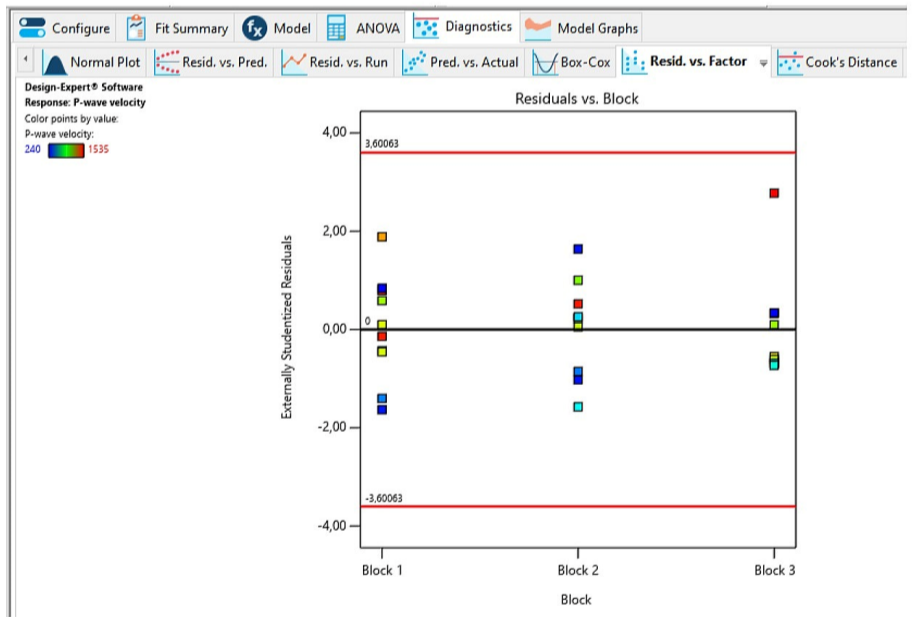
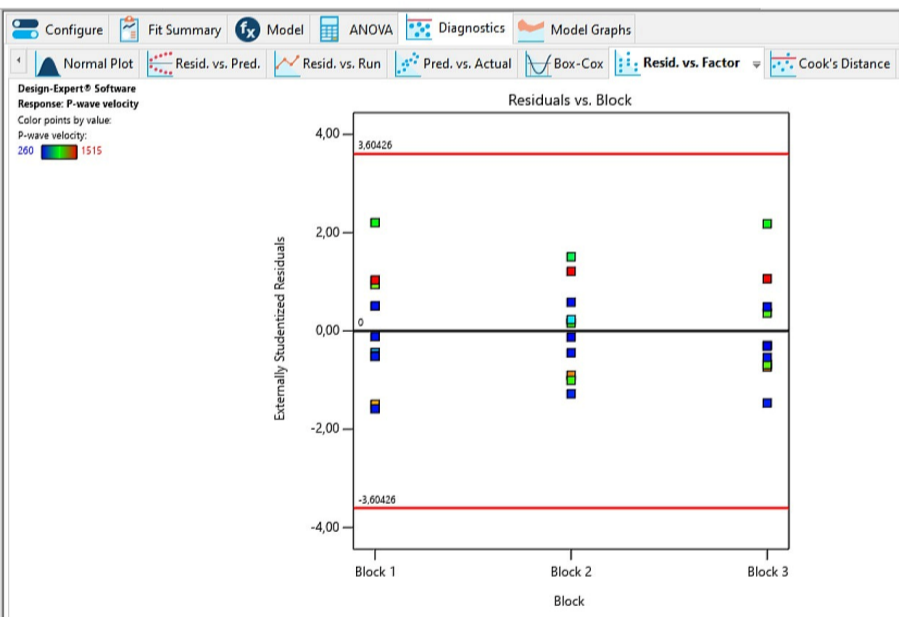
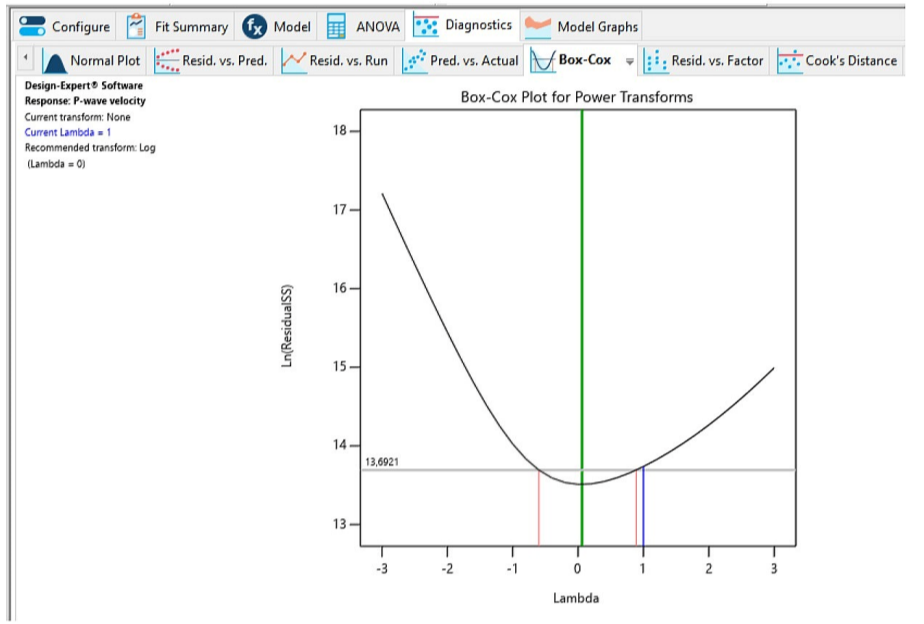
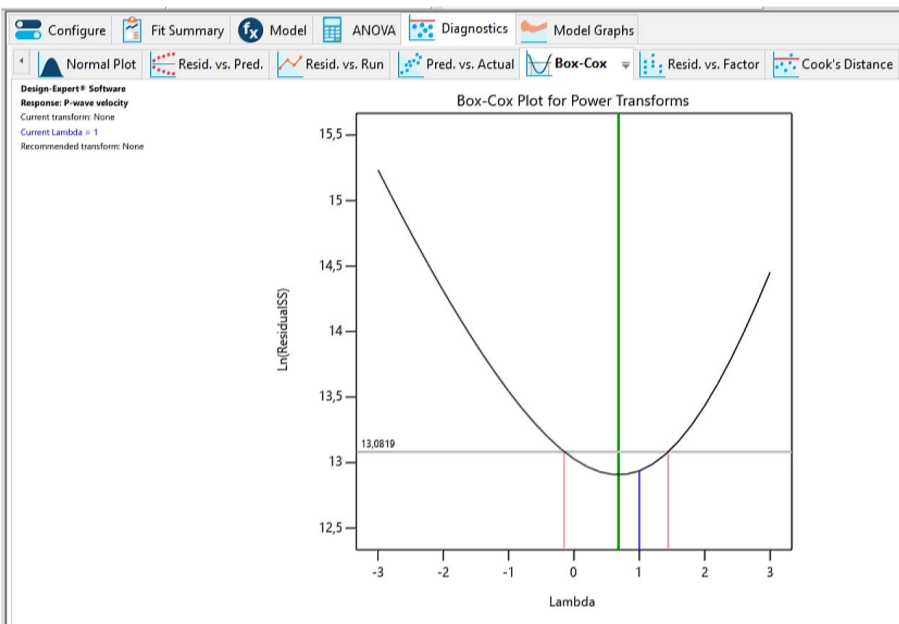
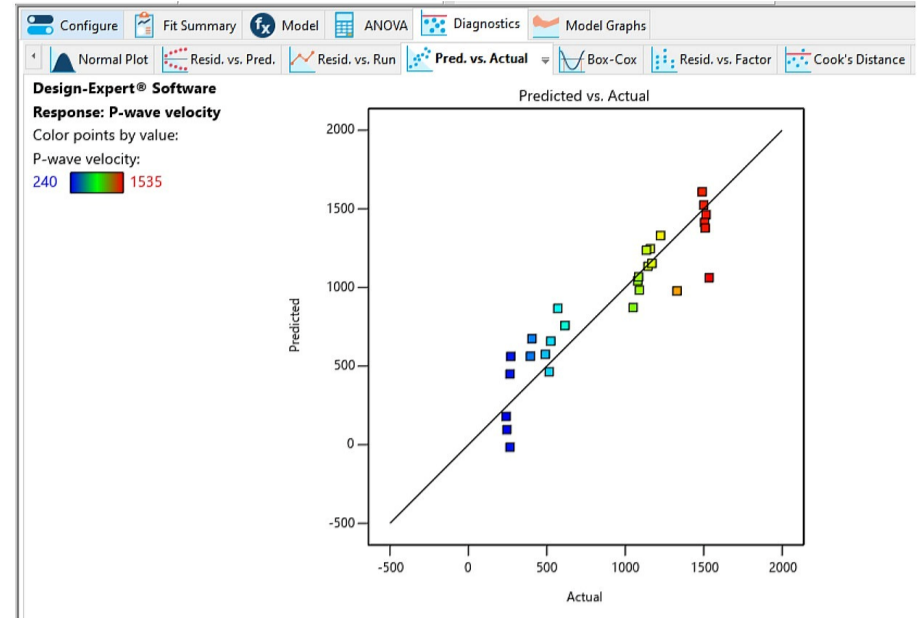
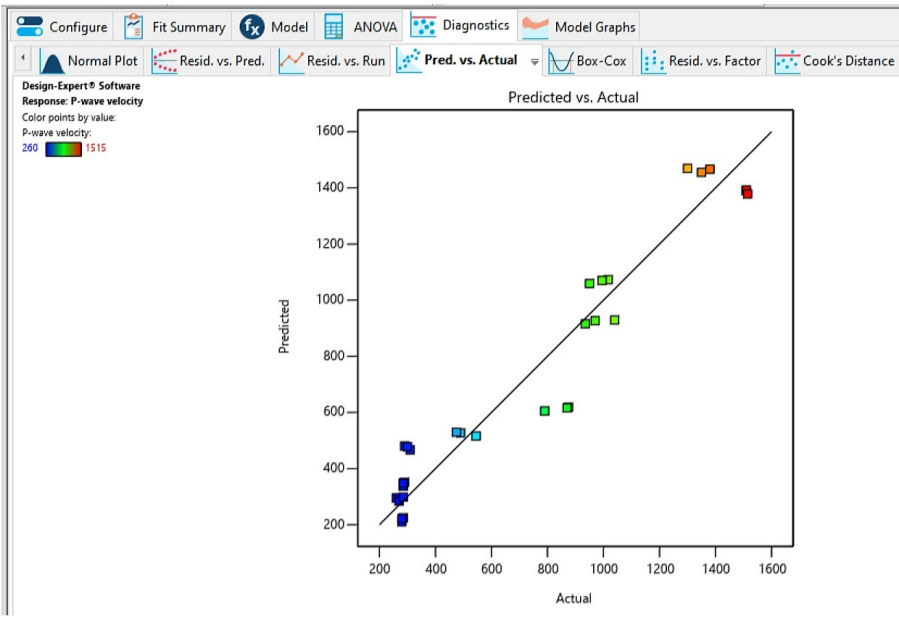
**DRY.16**

**WET.16**



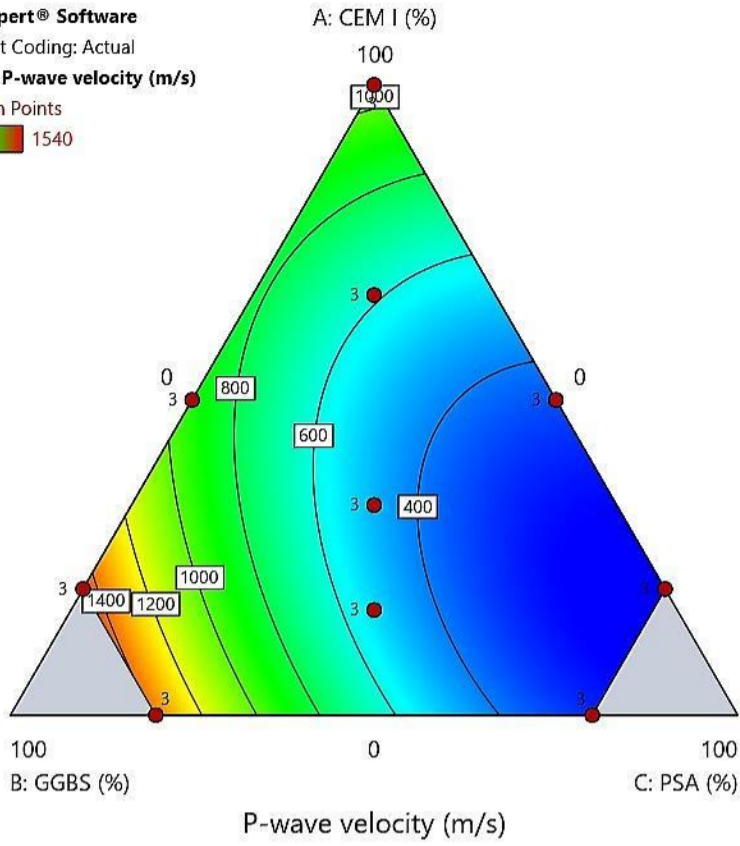
**DRY.16**

**WET.16**



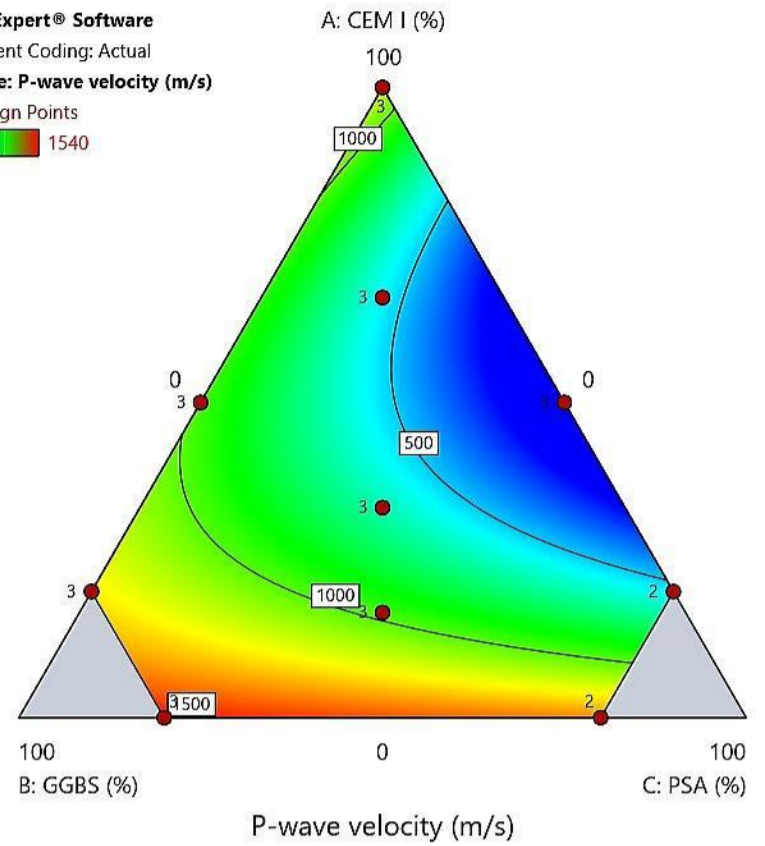
# DRY.16

Design-Expert® Software  
 Component Coding: Actual  
 Response: P-wave velocity (m/s)  
 ● Design Points  
 240 1540



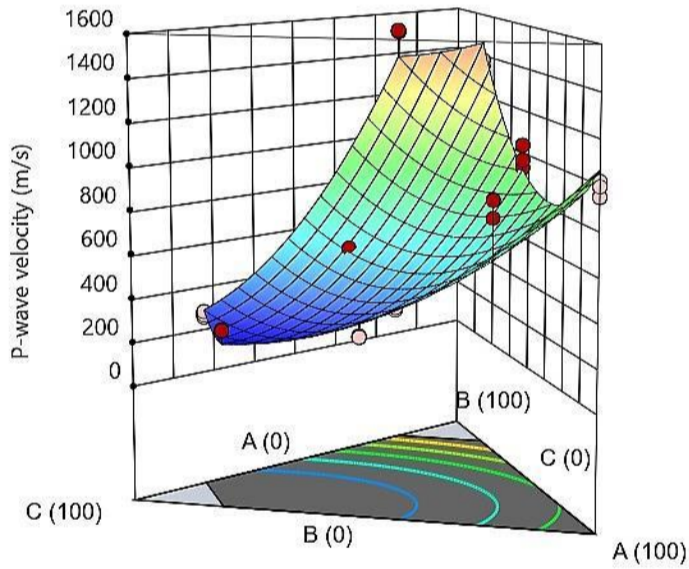
# WET.16

Design-Expert® Software  
 Component Coding: Actual  
 Response: P-wave velocity (m/s)  
 ● Design Points  
 240 1540



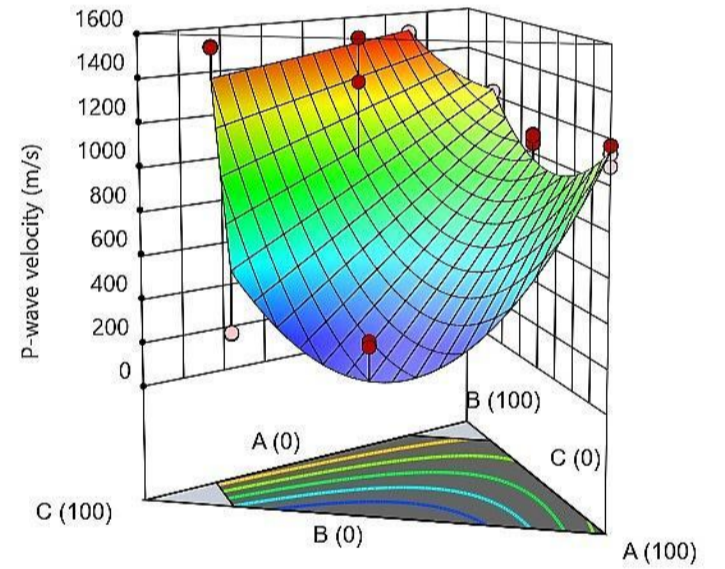
3D Surface

Design-Expert® Software  
 Component Coding: Actual  
 Response: P-wave velocity (m/s)  
 ● Above Surface  
 ○ Below Surface  
 240 1540



3D Surface

Design-Expert® Software  
 Component Coding: Actual  
 Response: P-wave velocity (m/s)  
 ● Above Surface  
 ○ Below Surface  
 240 1540





 **NTNU**

Norwegian University of  
Science and Technology